DIVERSITY ORIENTED SYNTHESIS

EDITED BY: Andrea Basso, Seung Bum Park and Lisa Moni
PUBLISHED IN: Frontiers in Chemistry

frontiers Research Topics

ISSN 1664-8714
ISBN 978-2-88945-788-5
DOI 10.3389/978-2-88945-788-5

About Frontiers

Frontiers is more than just an open-access publisher of scholarly articles: it is a pioneering approach to the world of academia, radically improving the way scholarly research is managed. The grand vision of Frontiers is a world where all people have an equal opportunity to seek, share and generate knowledge. Frontiers provides immediate and permanent online open access to all its publications, but this alone is not enough to realize our grand goals.

Frontiers Journal Series

The Frontiers Journal Series is a multi-tier and interdisciplinary set of open-access, online journals, promising a paradigm shift from the current review, selection and dissemination processes in academic publishing. All Frontiers journals are driven by researchers for researchers; therefore, they constitute a service to the scholarly community. At the same time, the Frontiers Journal Series operates on a revolutionary invention, the tiered publishing system, initially addressing specific communities of scholars, and gradually climbing up to broader public understanding, thus serving the interests of the lay society, too.

Dedication to Quality

Each Frontiers article is a landmark of the highest quality, thanks to genuinely collaborative interactions between authors and review editors, who include some of the world's best academicians. Research must be certified by peers before entering a stream of knowledge that may eventually reach the public - and shape society; therefore, Frontiers only applies the most rigorous and unbiased reviews.
Frontiers revolutionizes research publishing by freely delivering the most outstanding research, evaluated with no bias from both the academic and social point of view. By applying the most advanced information technologies, Frontiers is catapulting scholarly publishing into a new generation.

What are Frontiers Research Topics?

Frontiers Research Topics are very popular trademarks of the Frontiers Journals Series: they are collections of at least ten articles, all centered on a particular subject. With their unique mix of varied contributions from Original Research to Review Articles, Frontiers Research Topics unify the most influential researchers, the latest key findings and historical advances in a hot research area! Find out more on how to host your own Frontiers Research Topic or contribute to one as an author by contacting the Frontiers Editorial Office: researchtopics@frontiersin.org

DIVERSITY ORIENTED SYNTHESIS

Topic Editors:
Andrea Basso, University of Genova, Italy
Seung Bum Park, Seoul National University, South Korea
Lisa Moni, University of Genova, Italy

Has the concept of Diversity Oriented Synthesis remained unchanged over these two decades, or do we observe improvements or deviations from the original guidelines drawn by the pioneers?

The aim of this Research Topic is to collect contributions on the state-of-the-art and progress of Diversity Oriented Synthesis, and to foresee its shape in the next decade.

Citation: Basso, A., Park, S. B., Moni, L., eds. (2019). Diversity Oriented Synthesis. Lausanne: Frontiers Media. doi: 10.3389/978-2-88945-788-5

Table of Contents

frontiers in Chemistry

EDITORIAL
published: 24 January 2019
doi: 10.3389/fchem.2018.00668

Editorial: Diversity Oriented Synthesis

Andrea Basso[1]*, *Seung Bum Park*[2]* and *Lisa Moni*[1]*

[1] *Dipartimento di Chimica e Chimica Industriale, Università degli Studi di Genova, Genova, Italy,* [2] *Department of Chemistry, CRI Center for Chemical Proteomics, Seoul National University, Seoul, South Korea*

Keywords: diversity orientated synthesis, multicomponent reactions (MCRs), fragment based drug design, chemoimformatics, principal component analysis—PCA, heterocycles

Editorial on the Research Topic

Diversity Oriented Synthesis

Small molecules play an essential role in the field of drug discovery and chemical biology. It is therefore fundamental to have synthetic methodologies capable of assembling molecules characterized by innovative molecular frameworks, both in terms of skeleton and of stereochemistry. Diversity-oriented synthesis (DOS) aims to explore, through rapid and efficient synthetic methodologies, unexplored areas of the biology-relevant chemical space, to find new bioactive molecules, possibly aimed toward new biological targets (Burke and Schreiber, 2004; Galloway et al., 2010).

One of the most successful approaches applied in DOS is the build/couple/pair approach. This approach has been used efficiently in the past by numerous research groups, and several success stories. Yi et al. in their short review illustrate how the build/couple/pair approach can be applied to the synthesis of natural product-like compounds and macrocycles. Since this thematic issue looks more to the future than to the past, Yi also illustrates a more recent strategy, ring-distortion, which aims to achieve molecular diversity by altering pre-existing cyclic systems, through ring closures or openings, ring expansions or contractions, and other transformations. Through this approach the synthesis of natural product-like molecules, as well as macrocycles and benzannulated compounds, can be achieved.

Within this context, Kidd et al. demonstrated that the typical and well-tested build/couple/pair approach is currently used to produce DOS libraries as part of the fragment-based drug discovery (FBDD) (Erlanson and Jahnke, 2016), as opposed to the past, where DOS libraries were almost exclusively analyzed through HT screenings. Particularly interesting are those cases where new synthetic methodologies are introduced in the DOS strategy, as for example the C–H activation or the site-selective late-stage modifications of complex scaffolds. In fact, the use of these methodologies meets one of the requirements necessary for such molecules to be efficiently exploited in the FBDD, which is also one of the stated objectives of DOS, i.e., to *escape from flatland* (Lovering et al., 2009) and therefore to generate 3-dimensionally diversified molecules with a globular structure and abundance of chiral centers and sp3 carbons.

Other ways to assemble 3-dimensionally complex structures were presented by Lenci et al., who exploited morpholine skeletons rich in sp3 carbon atoms, derived from sugars and amino acids, and by Moni et al., who exploited spiro-fused ring systems as scaffolds for the generation of three DOS libraries. Both groups benefitted from chemoinformatic analysis of chemical space, to gain insight into the detailed structure of the molecular scaffolds and to verify the validity of synthetic strategy. Specifically, calculation of the Principal Component Analysis was used by Lenci and Trabocchi to group the synthetized molecules into four main clusters, depending on both their main skeletons and side-chain properties.

Edited and reviewed by:
Iwao Ojima,
Stony Brook University, United States

***Correspondence:**
Andrea Basso
andrea.basso@unige.it
Seung Bum Park
sbpark@snu.ac.kr
Lisa Moni
lisa.moni@unige.it

Specialty section:
This article was submitted to Organic Chemistry, a section of the journal Frontiers in Chemistry

Received: *11 December 2018*
Accepted: *21 December 2018*
Published: *24 January 2019*

Citation:
Basso A, Park SB and Moni L (2019) Editorial: Diversity Oriented Synthesis. Front. Chem. 6:668. doi: 10.3389/fchem.2018.00668

The work by Moni et al. reveals, among other things, how multicomponent reactions, combining three or more diversomers in a single step, are useful to assemble DOS libraries in a straightforward manner. Along the same lines is the report by Maskrey et al. which, exploiting one of the oldest multicomponent reactions, the Biginelli reaction, manages to obtain fused polyheterocycles, through a cascade process involving a hetero Diels-Alder reaction, in a stereoselective fashion.

The possibility to use the multicomponent Ugi reaction, followed by post-condensation cyclizations, to obtain polyheterocyclic systems, was analyzed in detail by Bariwal et al., who explored the various synthetic routes of assembling small/medium-sized rings, taking examples from recent literature.

A comprehensive review was also published by Murlykina et al. who, taking advantage of their expertise on the properties and reactivity of amino-azole derivatives, illustrate the strategies that can lead to DOS libraries from these compounds, both by exploiting two-component reactions as well as multicomponent processes. The synthesis of nitrogen-containing polyheterocycles, useful both in the field of drug-like substances and functional materials, is the subject of the article by Wu et al. The authors show how the DOS approach can be used to generate imidazothiazole-based chemical probes capable of identifying the biological targets implied in epigenetic processes.

As was the case for combinatorial chemistry, which was initially developed in the field of drug discovery, but then found wide application in other fields, such as materials science, the same phenomenon is happening for DOS, and Grotkopp et al. demonstrated this with their studies on luminescent materials. The DOS approach developed herein enables a rapid assembly of dual emissive bichromophores, to be employed for accessing unimolecular white light emitters for OLED and biophysical analytics.

In conclusion, going back to the question made at the beginning of this thematic issue, i.e., whether the diversity-oriented synthesis approach is still valid or is experiencing a contraction, we can now answer that the concept of DOS is still validly applicable, and improvements and deviations from its original guidelines are taking DOS in new directions, already showing very interesting results in various research fields.

AUTHOR CONTRIBUTIONS

All authors listed have made a substantial, direct and intellectual contribution to the work, and approved it for publication.

REFERENCES

Burke, M. D., and Schreiber, S. L. (2004). A planning strategy for diversity-oriented synthesis. *Angew. Chem. Int. Ed.* 43, 46–58. doi: 10.1002/anie.200300626

Erlanson, D. A., and Jahnke, W. (2016). *Fragment-Based Drug Discovery Lessons and Outlook*. Weinhein: Wiley-VCH Verlang GmbH and Co.

Galloway, W. R., Isidro-Llobet, A., and Spring, D. R. (2010). Diversity-oriented synthesis as a tool for the discovery of novel biologically active small molecules. *Nat. Commun.* 1, 80–92. doi: 10.1038/ncomms1081

Lovering, F., Bikker, J., and Humblet, C. (2009). Escape from flatland: increasing saturation as an approach to improving clinical success. *J. Med. Chem.* 52, 6752–6756. doi: 10.1021/jm901241e

Conflict of Interest Statement: The authors declare that the research was conducted in the absence of any commercial or financial relationships that could be construed as a potential conflict of interest.

frontiers in Chemistry

MINI REVIEW
published: 22 October 2018
doi: 10.3389/fchem.2018.00507

A Brief Overview of Two Major Strategies in Diversity-Oriented Synthesis: Build/Couple/Pair and Ring-Distortion

*Sihyeong Yi†, Begur Vasanthkumar Varun†, Yoona Choi† and Seung Bum Park**

Department of Chemistry, CRI Center for Chemical Proteomics, Seoul National University, Seoul, South Korea

In the interdisciplinary research field of chemical biology and drug discovery, diversity-oriented synthesis (DOS) has become indispensable in the construction of novel small-molecule libraries rich in skeletal and stereochemical diversity. DOS aims to populate the unexplored chemical space with new potential bioactive molecules via forward synthetic analysis. Since the introduction of this concept by Schreiber, DOS has evolved along with many significant breakthroughs. It is therefore important to understand the key DOS strategies to build molecular diversity with maximized biological relevancy. Due to the length limitations of this mini review, we briefly discuss the recent DOS plans using build/couple/pair (B/C/P) and ring-distortion strategies for the synthesis of major biologically relevant target molecules like natural products and their related compounds, macrocycles, and privileged structures.

Keywords: diversity-oriented synthesis, build/couple/pair, ring-distortion, natural product, macrocycle, privileged structure

OPEN ACCESS

Edited by:
Gwilherm Evano,
Free University of Brussels, Belgium

Reviewed by:
Raphaël Frédérick,
Université Catholique de Louvain, Belgium
Steven Ballet,
Vrije Universiteit Brussel, Belgium
Laurent Commeiras,
Aix-Marseille Université, France

***Correspondence:**
Seung Bum Park
sbpark@snu.ac.kr

†These authors have contributed equally to this work

Specialty section:
This article was submitted to Organic Chemistry, a section of the journal Frontiers in Chemistry

Received: *08 August 2018*
Accepted: *03 October 2018*
Published: *22 October 2018*

Citation:
Yi S, Varun BV, Choi Y and Park SB (2018) A Brief Overview of Two Major Strategies in Diversity-Oriented Synthesis: Build/Couple/Pair and Ring-Distortion. Front. Chem. 6:507. doi: 10.3389/fchem.2018.00507

INTRODUCTION

Small molecules play an indispensable role in the fields of drug discovery and chemical biology due to their unique features compared to biologics, polymers, and nanoparticles (Samanen, 2013). However, while the knowledge of biological systems has grown in the post-genomic era, the discovery of novel small molecular therapeutics or bioprobes has become more complicated. This can be attributed to advances in chemical biology and drug discovery disclosing novel targets beyond conventional druggable proteins, such as DNA (Hurley, 2002), RNA (Lieberman, 2018; Warner et al., 2018), protein–protein interactions (PPIs) (Scott et al., 2016), and protein–RNA interactions (PRIs) (Hentze et al., 2018), among others. Furthermore, a lack of information regarding the structures and modes of action of these novel targets renders rational drug discovery challenging.

The development of high-throughput screening (HTS) and high-content screening (HCS) enabled rapid and efficient investigation of biological activities to yield existing drug-like compound libraries constructed by combinatorial synthesis (Schreiber, 2000; Tan, 2005; Basso, 2012). However, contrary to expectations, extensive screening exercises against huge compound libraries delivered a relatively small number of new chemical entities, particularly in the case of bioassays for novel undruggable targets or unbiased phenotypic screenings, where rational ligand design is challenging (Burke and Schreiber, 2004; Galloway et al., 2010; Garcia-Castro et al., 2016). This may be due to the limited diversity of conventional drug-like compound libraries, especially

in terms of skeletal and stereochemical diversity. Indeed, it should be noted that skeletal diversity is essential for specific binding events with diverse biopolymers bearing three-dimensional (3D) unique binding sites and structural diversity (Kim et al., 2014). In fact, it is not the size of a chemical library that is most important, but the skeletal and stereochemical diversity of its core structures. Thus, there is a huge demand for high-quality compound collections through the efficient construction of drug-like small molecule libraries enriched with molecular diversity, and particularly, skeletal and stereochemical diversity (Spring, 2003).

To meet such demands in molecular diversity, Schreiber et al. introduced the concept of diversity-oriented synthesis (DOS) (Schreiber, 2000). The aim of DOS as a synthetic strategy is to occupy the unexplored parts of chemical space via the efficient synthesis of unique compound collections bearing diversity and complexity in their scaffolds. DOS involves "forward synthetic analysis," where the products of each step become the branching substrates for subsequent steps (Tan, 2005). Hence, the DOS approach leads to an exponential increase in the molecular diversity of chemical libraries through multiple systematic branching sequences. Indeed, the DOS strategy has attested its capacity and value through the development of various novel therapeutic agents and biological modulators and through advancing biological understandings (Kuruvilla et al., 2002; Kuo et al., 2015; Schreiber et al., 2015; Hideshima et al., 2016; Kato et al., 2016; Plouffe et al., 2016; Wellington et al., 2017; Gerry and Schreiber, 2018). For example, Schreiber *et al.* discovered a novel multistage antimalarial inhibitor, BRD7929, through the extensive screening of their compound library constructed by DOS strategy (Kato et al., 2016), while Park et al. reported a novel leucyl-tRNA synthetase/RagD PPI inhibitor discovered from DOS library (Kim et al., 2016).

Since the DOS concept was introduced, many synthetic pathways have been developed by various research groups to construct efficient chemical libraries (Nielsen and Schreiber, 2008). Among them, the build/couple/pair (B/C/P) strategy is the most widely followed and commonly applicable synthetic strategy. This strategy involves 3 synthetic phases, namely a build phase, a couple phase, and a pair phase (**Figure 1A**; Burke and Schreiber, 2004). More specifically, the build phase involves the synthesis of a single or multiple key building blocks embedded with suitable functional groups for later-stage coupling reactions. In the couple phase, a variety of intermolecular coupling reactions can be employed to generate a dense array of reactive sites and functional groups on the key building blocks installed during the build phase. Finally, in the pair phase, the intermediates constructed through the build and couple phases take part in intramolecular pairing reactions to yield an array of final products with the desired skeletal and stereochemical diversity (Nielsen and Schreiber, 2008; Kim et al., 2016).

Recently, the ring-distortion strategy has also been developed as a distinctive DOS strategy for the systematic construction of novel small-molecule collections with high structural diversity and complexity. In contrast to the B/C/P strategy, the ring-distortion strategy is distinct in that it pursues molecular diversity via distortion of the existing ring systems through ring-cleavage, ring-expansion, ring-contraction, ring-fusion, ring-rearrangement, ring-aromatization, and combinations of the above (**Figure 2A**; Huigens et al., 2013).

However, in any DOS strategy, the common structural features of existing bioactive molecules have been widely investigated to grant sufficient biological relevancy to the resulting compounds (Kim et al., 2014). As such, natural products are commonly investigated, and their structural features are considered to be potent sources of information in drug discovery. In addition, macrocycles have received a significant amount of attention in the field of drug discovery due to distinguishable structural features compared to other small molecules. Furthermore, privileged structures, which are common structural motifs in a vast number of bioactive natural products and therapeutic agents, contain novel structural features that secure a high biological relevancy (Evans et al., 1988).

Thus, in this mini review, we present recent advancements in the B/C/P and ring-distortion DOS approaches in the context of natural products, natural product-like compounds, macrocycles, and privileged structures.

THE BUILD/COUPLE/PAIR (B/C/P) STRATEGY

Synthesis of Natural Products and Natural Product-Like Compounds via the B/C/P Strategy

Natural products play a pivotal role in the search of novel therapeutics. Bioactive natural products tend to have complex 3D polycyclic structures rich in sp^3 carbons and stereogenic centers, and their inherent bioactivities may provide clues for the design of novel core skeletons with high biological relevancy (Wipf, 2012; Shimokawa, 2014; Chen et al., 2015). Therefore, the efficient construction of natural product libraries and their unnatural analogs can be considered an important DOS strategy.

A team led by Lei proposed that complex molecules such as bioactive natural products can be synthesized via the B/C/P strategy through the pairing of various functional groups present in their structures (Zhang et al., 2014). Selecting lycopodium alkaloids as a model system, they reported the total syntheses of four lycopodium alkaloids and six related unnatural scaffolds. In contrast to other total synthetic approaches, the reported DOS approach allowed the parallel synthesis of unnatural scaffolds, thereby increasing the population of "lycopodium-like" natural products in the unexplored chemical space (Harayama et al., 1974; Ma and Gang, 2004; Chandra et al., 2009). As shown in **Figure 1B**, chiral intermediate **1** was formed through the build and couple phases, while intermediate **2** was prepared by means of the early pairing phase, which was crucial to the overall synthetic protocol. By encompassing double pairing processes in a sequential manner, the "later pairing phase" allowed the efficient construction of unique core skeletons. To illustrate the power of this B/C/P strategy, stepwise double pairing procedures, such as B–C pairing and E–F pairing in **Figure 1B** led to the total synthesis of (+)-serratezomine A (6/6/6/5 system) and an

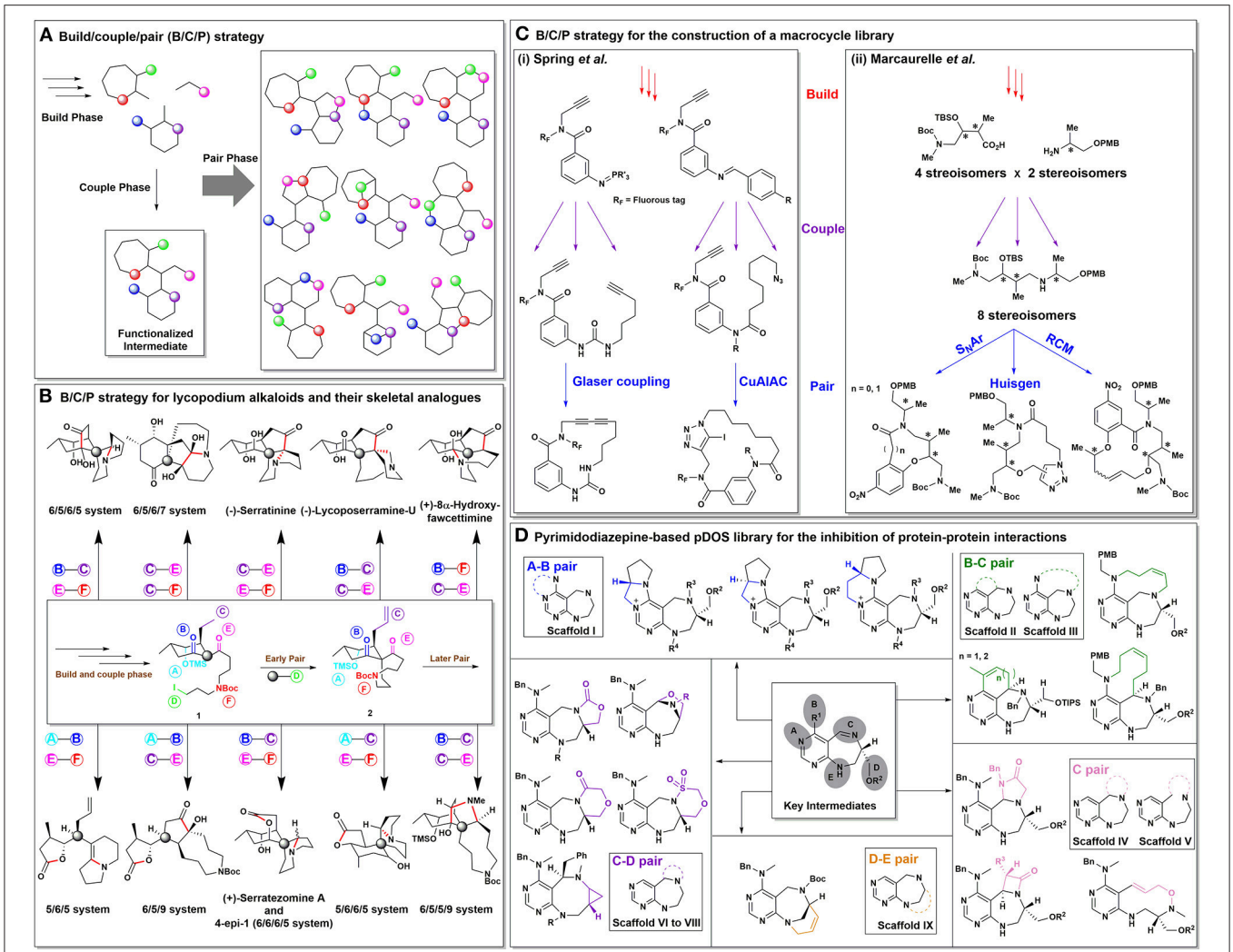

FIGURE 1 | (A) A schematic representation of the B/C/P strategy. **(B)** Outline of lycopodium alkaloids and their unnatural scaffolds with their respective pairing patterns. **(C)** Outline of the B/C/P strategy for the construction of libraries consisting of macrocycles and medium-sized rings. **(D)** A pDOS library established via the B/C/P strategy for the inhibition of protein–protein interactions.

unnatural skeletal analog (6/5/6/5 system) of (–)-serratinine. In addition, the double pairing pattern involving A–B pairing followed by C–E or E–F pairing led to the formation of tricyclic compounds (6/5/9 or 5/6/5 systems, respectively). Other pairing patterns leading to the total syntheses of (–)-serratinine, (+)-8α-hydroxyfawcettimine, (–)-lycoposerramine-U, and three tetracyclic unnatural scaffolds were also examined. Overall, this work demonstrated a unique and efficient route to the synthesis of complex natural product-like molecules using the B/C/P strategy.

Synthesis of Macrocycles via the B/C/P Strategy

Although various macrocycle-based natural products are known to exhibit therapeutic potential, as a sole structural unit, macrocycles have not been traditionally considered as suitable small molecules for drug discovery screening processes (Schreiber, 2000). However, recent reports have claimed that macrocyclic structures can pre-organize their conformations, which allows improved interactions with extended protein surfaces and subsequent high biological activities (Driggers et al., 2008; Villar et al., 2014). As such, numerous DOS strategies have been pursued to construct structurally and functionally diverse macrocycles (Madsen and Clausen, 2011; Collins et al., 2016).

For the efficient construction of libraries containing a diverse array of macrocycles, Spring et al. developed advanced B/C/P approaches (Beckmann et al., 2013; Nie et al., 2016). These B/C/P approaches not only allowed diversification in the multi-dimensional pattern, but also resulted in the judicious modification of the chemical structures following the pairing phase (**Figure 1Ci**). Using an advanced B/C/P approach, they also reported the synthesis of a library containing 73 macrocycles having 59 different scaffolds (Beckmann et al., 2013). In this case, the build phase involved the synthesis of fluorous-tagged azido

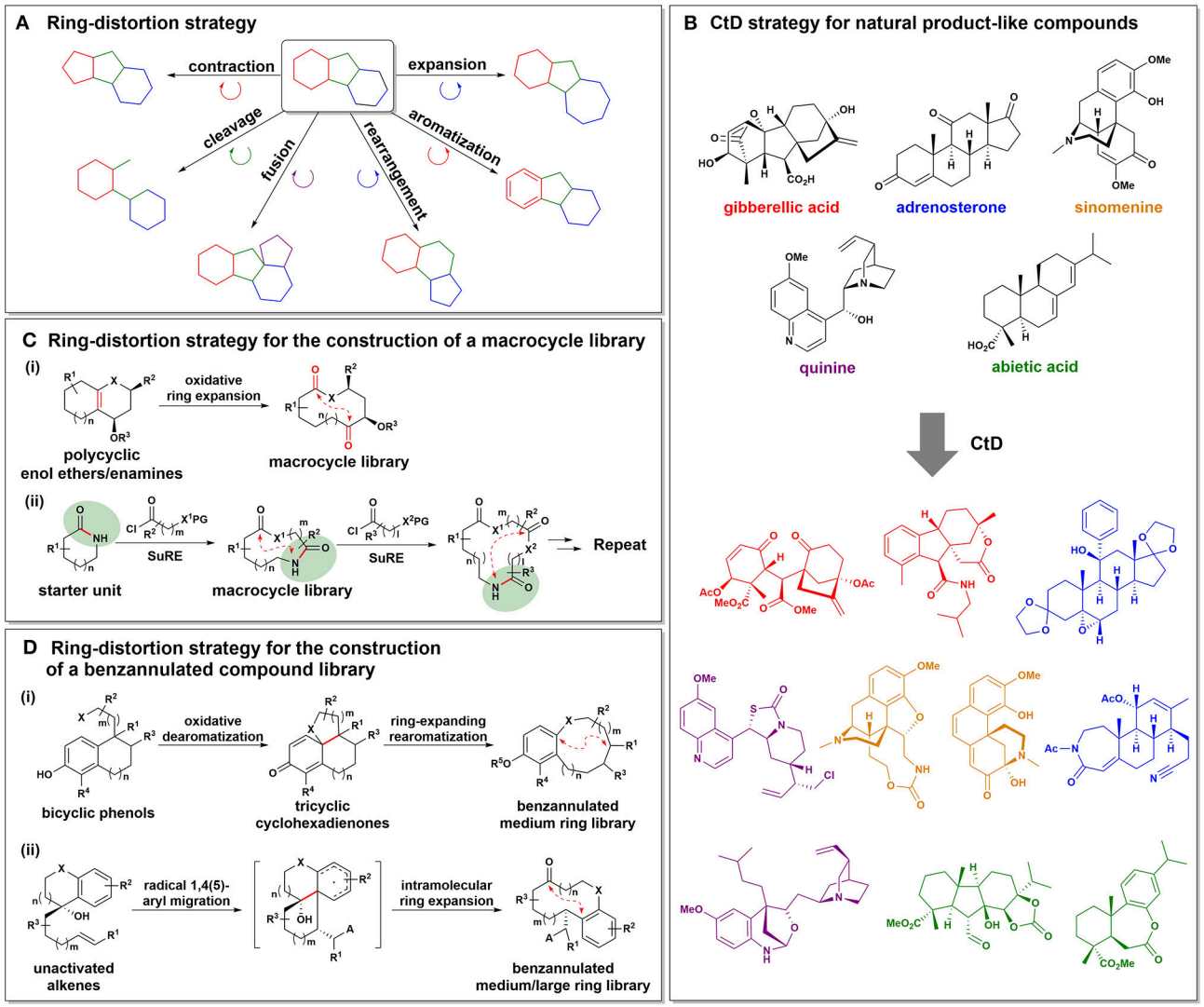

FIGURE 2 | (A) Schematic representation of the ring-distortion strategy. **(B)** The complexity-to-diversity (CtD) strategy for the construction of diverse and complex compounds starting from readily available natural products. **(C)** The ring-distortion strategy for the construction of macrocyclic lactone and lactam libraries. **(D)** The ring-distortion strategy for the construction of biologically relevant benzannulated small molecules.

compounds, which were converted *in situ* into the corresponding pluripotent aza-ylides. These aza-ylides were then coupled with suitable appendages to facilitate the subsequent pairing reactions. Similarly, in 2016, they reported the synthesis of 45 diverse macrocyclic compounds of various sizes, ranging from 15- to 33-membered rings (Nie et al., 2016). In this case, the imine moieties branching out from the aza-ylides served as second-line building blocks for diversification of the macrocycle library. The introduction and subsequent modification of the fluorous tag and other reactive sites in these macrocycles could therefore improve the efficiency as well as skeletal diversity of the library synthesis.

Moreover, Marcaurelle et al. utilized an aldol-based B/C/P strategy to construct a library containing in excess of 30,000 compounds, which were based on a variety of skeletons ranging from 8- to 14-membered rings, of which 14,400 compounds were macrolactams aimed at the discovery of novel histone deacetylase inhibitors (**Figure 1Cii**; Marcaurelle et al., 2010). Notably, this study presented an excellent example of the DOS strategy to demonstrate its power and efficiency for the highly systematic construction of small-molecule libraries with maximized architectural complexity.

The B/C/P Strategy in the pDOS Pathway

A clear definition of privileged structures was made in a seminal article on drug discovery methods reported by Evans et al. (1988). More specifically, they stated that "privileged structures are capable of providing useful ligands for more than one receptor and that judicious modification of such structures could

be a viable alternative in the search for new receptor agonists and antagonists." Based on the concept of modification around privileged structures, a number of groups have reported various bio-relevant compounds, with many successfully delivering clinical candidates as well as FDA-approved drugs (Mason et al., 1999; Nicolaou et al., 2000a,b,c; Brohm et al., 2002; Kissau et al., 2003; Newman, 2008). For example, Nicolaou et al. published a series of articles on the combinatorial library syntheses of natural product-like compounds in which the benzopyran skeleton was employed as a privileged structure (Nicolaou et al., 2000a,b,c). In this context, the construction of a DOS library derived from privileged structures can be considered crucial to accessing highly biologically relevant molecular diversity (Kim et al., 2014).

We envisioned that incorporating these privileged structures into polyheterocycles enhances the biological relevancy of the resulting compounds with pre-defined conformations, which may be beneficial for specific binding with biopolymers due to the prepaid entropic penalty (Oh and Park, 2011; Kim et al., 2014; Lenci et al., 2016). Hence, within the theme of DOS, our group introduced a novel design strategy, namely "privileged substructure-based diversity-oriented synthesis" (pDOS), which aims to populate the chemical space with privileged substructure-embedded polyheterocycles (An et al., 2008; Oh and Park, 2011; Zhu et al., 2012; Kim et al., 2013, 2014). In particular, the systematic construction of diverse sp^3-rich 3D polyheterocycles containing privileged substructures has been emphasized since their rigid and diverse frameworks can selectively bind with biopolymers to induce conformational changes and subsequent functional modulation. Thus, a small-molecule library constructed by the pDOS strategy could be considered an excellent resource for the discovery of specific modulators of protein–protein and protein–DNA/RNA interactions.

In addition, we recently reported a pDOS library in which pyrimidodiazepines were employed as the privileged substructure (Kim et al., 2016). We found that the 6/7-bicyclic pyrimidodiazepine system demonstrated a significantly higher conformational flexibility with more reactive sites compared to those of pyrimidine-embedded 6/6 or 6/5 systems. In this case, the build and couple phases produced key pyrimidodiazepine-based intermediates containing five orthogonal reactive sites. In the pair phase, each reactive site was paired to produce 16 different polyheterocycles containing the pyrimidodiazepine substructure and with a high degree of 3D skeletal complexity in nine distinct scaffolds. As shown in **Figure 1D**, A–B pairing and B–C pairing led to the synthesis of tetracyclic and tricyclic compounds, respectively (scaffolds I–III). Due to the dual (i.e., electrophilic and nucleophilic) nature of the imine moiety, the C pairing allowed the synthesis of scaffolds IV and V. Using the C–D and D–E pairing combinations, scaffolds VI–IX were also constructed. Based on our HTS screening endeavors against this pDOS library, we identified aziridine-containing pyrimidodiazepines from scaffold VIII (constructed through C–D pairing) as a novel small-molecule inhibitor of the leucine tRNA synthetase (LRS)–RagD protein–protein interaction.

THE RING-DISTORTION STRATEGY

Synthesis of Natural Product-Like Compounds via the Ring-Distortion Strategy

For the construction of natural product-like compound collections, Hergenrother et al. developed a novel approach starting from natural products, known as the complexity-to-diversity (CtD) strategy (Huigens et al., 2013; Rafferty et al., 2014; Garcia et al., 2016). In this approach, the molecular frameworks of readily available natural products were converted into structurally complex and diverse core skeletons through various chemoselective ring-distortion reactions (**Figure 2B**). As natural products exhibit an inherent structural complexity with defined stereochemistry (Clardy and Walsh, 2004), the resulting core skeletons derived from natural products tend to be structurally and stereochemically more complex and distinct compared to existing compound collections. In their initial report on the CtD strategy, gibberellic acid, quinine, and adrenosterone were employed as synthetic starting points, and were transformed into 19, 12, and 18 different scaffolds, respectively, through various ring-distortion reactions (3 reaction steps on average; Huigens et al., 2013). The subsequent application of traditional diversification strategies to final scaffolds therefore allowed the construction of a 119-membered highly complex compound library. They also applied the CtD strategy to other readily available natural products such as abietic acid and sinomenine, which afforded 84 and 65 complex compounds, respectively (Rafferty et al., 2014; Garcia et al., 2016). Chemoinformatic analysis of the resulting compound collections obtained using the CtD strategy demonstrated a higher skeletal complexity compared to conventional compound collections in terms of higher fractions of sp^3-hybridized carbon atoms (F_{sp3}), lower clogP values, and greater numbers of stereocenters.

Synthesis of Macrocycles via the Ring-Distortion Strategy

For the systematic construction of diverse macrocycles, several DOS approaches utilizing ring-distortion reactions (and in particular, ring-expansion reactions) have been pursued (Kopp et al., 2012; Kitsiou et al., 2015; Stephens et al., 2017, 2018). For example, Tan et al. reported an efficient oxidative ring-expansion strategy for the construction of diverse macrocyclic small molecule collections (**Figure 2Ci**; Kopp et al., 2012). Interestingly, easily accessible polycyclic enol ethers or enamines containing bridging double bonds were found to smoothly undergo oxidative cleavage to generate various macrolactones and macrolactams, regardless of substrate effects, such as ring size, substituents, and stereochemistry. Subsequent transformations using functional handles in the macrocyclic scaffolds afforded additional structural diversity. In addition, the chemoinformatic analysis of 32 unprecedented macrocyclic compounds using principal component analysis (PCA) and principal moments of inertia (PMI) analysis

illustrated the possibilities of the resulting macrocycles to modulate novel biological targets through occupying unique chemical space distinct from the current synthetic drugs.

Moreover, the successive ring-expansion (SuRE) strategy described by Unsworth et al. led to the generation of structurally diverse macrocyclic lactams and lactones in a sequential manner (Kitsiou et al., 2015; Stephens et al., 2017, 2018). As shown in **Figure 2Cii**, the amide functionality present in the cyclic starter unit enabled coupling with the linear fragment via an acylation reaction, and subsequent deprotection and ring-opening along with chain incorporation yielded the ring-expanded product. The key strength of the SuRE method is that the same coupling and ring-expansion sequence can be repeated as the reactive amide functionality is regenerated in the product. Using this simple SuRE strategy, a functionalized macrocycle library was successfully constructed.

Synthesis of Biologically Relevant Benzannulated Compounds via the Ring-Distortion Strategy

Benzannulated medium/macro- or bridged rings are common structural moieties in a number of bioactive natural products and pharmacologically significant synthetic compounds such as penicillide, zeranol, and rifampin (Salituro et al., 1993; Fürstner et al., 1999; Yu and Sun, 2013; Hussain et al., 2014). In this context, Tan et al. developed an efficient biomimetic ring-expansion approach to construct diverse benzannulated medium-sized rings via an oxidative dearomatization and ring-expanding rearomatization sequence (**Figure 2Di**; Bauer et al., 2013). This strategy involves the oxidative dearomatization of bicyclic phenol precursors to provide polycyclic cyclohexadienones and a subsequent ring-expansion driven by rearomatization of the phenol ring to afford benzannulated medium-sized rings. The structural and physicochemical similarities between the resulting 47 scaffolds and benzannulated medium ring-based natural products were confirmed by PCA analysis.

Furthermore, Liu et al. reported a radical-based diversity-oriented synthetic approach for the fabrication of 37 discrete benzannulated medium/macro- or bridged-rings in a stereoselective manner (**Figure 2Dii**; Li et al., 2016). In this strategy, the radical 1,4- or 1,5-aryl migration of unactivated alkenes and subsequent intramolecular ring-expansion provided benzannulated medium or large rings. Additional ring-distortion reactions of the resulting core skeletons afforded novel medium-sized and medium-bridged rings with high regio- and stereoselectivities. PCA analysis and preliminary biological studies confirmed the significant biological relevance of this compound collection.

CONCLUSION

In this mini review, we briefly emphasized the important roles of diversity-oriented synthesis (DOS) in the field of drug discovery and chemical biology, and introduced the most common DOS strategies for the construction of novel small molecule libraries with maximized molecular diversity. We also discussed two key diversity-oriented synthetic approaches (i.e., the build/couple/pair (B/C/P) strategy and the ring-distortion strategy) and visualized how each strategy allows design of the resulting scaffolds with high biological relevancy via the incorporation of key structural elements such as bioactive natural products, macrocycles, and privileged structures. We concluded that both the B/C/P strategy and the ring-distortion strategy are powerful approaches for the creation of a number of diverse and complex scaffolds in an efficient manner. The combination of DOS-based molecular diversity and unbiased phenotypic screening may shed light on the unraveled signaling pathways and other intricate biological processes by allowing the sustainable supply of new drug candidates and chemical probes.

AUTHOR CONTRIBUTIONS

SY, BV, and YC contributed equally to this manuscript. SY, BV, and YC collected the related references and prepared the manuscript. SP directed the preparation of this manuscript. All authors critically reviewed the text and figures prior to submission.

FUNDING

This work was supported by the Creative Research Initiative Grant (2014R1A3A2030423), Bio & Medical Technology Development Program (2012M3A9C4048780), and A3 Foresight International Cooperation Program (2016K2A9A2A10005504) through the National Research Foundation of Korea (NRF) funded by the Korean Government (Ministry of Science & ICT).

ACKNOWLEDGMENTS

We appreciate Mr. Chanwoo Kim and Miss Jaeyoung Koo of our laboratory at Seoul National University for their helpful discussion about this manuscript. SY is grateful for the NRF-2017-Fostering Core Leaders of the Future Basic Science Program/Global Ph.D. Fellowship Program (2017H1A2A1045200).

REFERENCES

An, H., Eum, S.-J., Koh, M., Lee, S. K., and Park, S. B. (2008). Diversity-oriented synthesis of privileged benzopyranyl heterocycles from s-*cis*-enones. *J. Org. Chem.* 73, 1752–1761. doi: 10.1021/jo702196f

Basso, A. (2012). Diversity oriented synthesis: how and why? Diversity Oriented Synthesis. *Nat. Commun.* 1, 1–5. doi: 10.2478/dos-2012-0001

Bauer, R. A., Wenderski, T. A., and Tan, D. S. (2013). Biomimetic diversity-oriented synthesis of benzannulated medium rings via ring expansion. *Nat. Chem. Biol.* 9, 21–29. doi: 10.1038/nchembio.1130

Beckmann, H. S. G., Nie, F., Hagerman, C. E., Johansson, H., Tan, Y. S., Wilcke, D., et al. (2013). A strategy for the diversity-oriented synthesis of macrocyclic scaffolds using multidimensional coupling. *Nat. Chem.* 5, 861–867. doi: 10.1038/nchem.1729

Brohm, D., Philippe, N., Metzger, S., Bhargavba, A., Müller, O., Lieb, F., et al. (2002). Solid-phase synthesis of dysidiolide-derived protein phosphatase inhibitors. *J. Am. Chem. Soc*. 124, 13171–13178. doi: 10.1021/ja027609f

Burke, M. D., and Schreiber, S. L. (2004). A planning strategy for diversity-oriented synthesis. *Angew. Chem. Int. Ed.* 43, 46–58. doi: 10.1002/anie.200300626

Chandra, A., Pigza, J. A., Han, J.-S., Mutnick, D., and Johnston, J. N. (2009). Total synthesis of the Lycopodium alkaloid (+)-serratezomine A. *J. Am. Chem. Soc.* 131, 3470–3471. doi: 10.1021/ja900536d

Chen, Q.-F., Wang, F.-P., and Liu, X.-Y. (2015). Generating skeletal diversity from the C_{19}-diterpenoid alkaloid deltaline: a ring-distortion approach. *Chem. Eur. J.* 21, 8946–8950. doi: 10.1002/chem.201500839

Clardy, J., and Walsh, C. (2004). Lessons from natural molecules. *Nature* 432, 829–837. doi: 10.1038/nature03194

Collins, S., Bartlett, S., Nie, F., Sore, H. F., and Spring, D. R. (2016). Diversity-oriented synthesis of macrocycle libraries for drug discovery and chemical biology. *Synthesis* 48, 1457–1473. doi: 10.1055/s-0035-1561414

Driggers, E. M., Hale, S. P., Lee, J., and Terrett, N. K. (2008). The exploration of macrocycles for drug discovery–an underexploited structural class. *Nat. Rev. Drug Discov.* 7, 608–624. doi: 10.1038/nrd2590

Evans, B. E., Rittle, K. E., Bock, M. G., Dipardo, R. M., Freidinger, R. M., Whitter, W. L., et al. (1988). Methods for drug discovery: development of potent, selective, orally effective cholecystokinin antagonists. *J. Med. Chem.* 31, 2235–2246. doi: 10.1021/jm00120a002

Fürstner, A., Seidel, G., and Kindler, N. (1999). Macrocycles by ring-closing-metathesis, XI: syntheses of (R)-(+)-lasiodiplodin, zeranol, and truncated salicylihalamides. *Tetrahedron* 55, 8215–8230. doi: 10.1016/S0040-4020(99)00302-6

Galloway, W. R. J. D., Isidro-Llobet, A., and Spring, D. R. (2010). Diversity-oriented synthesis as a tool for the discovery of novel biologically active small molecules. *Nat. Commun.* 1, 80–92. doi: 10.1038/ncomms1081

Garcia, A., Drown, B. S., and Hergenrother, P. J. (2016). Access to a structurally complex compound collection via ring distortion of the alkaloid sinomenine. *Org. Lett.* 18, 4852–4855. doi: 10.1021/acs.orglett.6b02333

Garcia-Castro, M., Zimmermann, S., Sankar, M. G., and Kumar, K. (2016). Scaffold diversity synthesis and its application in probe and drug discovery. *Angew. Chem. Int. Ed.* 55, 7586–7605. doi: 10.1002/anie.201508818

Gerry, C. J., and Schreiber, S. L. (2018). Chemical probes and drug leads from advances in synthetic planning and methodology. *Nat. Rev. Drug Discov.* 17, 333–352. doi: 10.1038/nrd.2018.53

Harayama, T., Ohtani, M., Oki, M., and Inubushi, Y. (1974). Total synthesis of the lycopodium alkaloid (±)-serratinine. *J. Chem. Soc., Chem. Commun.* 827–828.

Hentze, M. W., Castello, A., Schwarzl, T., and Preiss, T. (2018). A brave new world of RNA-binding proteins. *Nat. Rev. Mol. Cell Biol.* 19, 327–341. doi: 10.1038/nrm.2017.130

Hideshima, T., Qi, J., Paranal, R. M., Tang, W., Greenberg, E., West, N., et al. (2016). Discovery of selective small-molecule HDAC6 inhibitor for overcoming proteasome inhibitor resistance in multiple myeloma. *Proc. Natl. Acad. Sci. U.S.A.*113, 13162–13167. doi: 10.1073/pnas.1608067113

Huigens, R. W. I. I. I., Morrison, K. C., Hicklin, R. W., Flood, T. A. Jr., Richter, M. F., and Hergenrother, P. J. (2013). A ring-distortion strategy to construct stereochemically complex and structurally diverse compounds from natural products. *Nat. Chem.* 5, 195–202. doi: 10.1038/nchem.1549

Hurley, L. H. (2002). DNA and its associated processes as targets for cancer therapy. *Nat. Rev. Cancer* 2, 188–200. doi: 10.1038/nrc749

Hussain, A., Yousuf, S. K., and Mukherjee, D. (2014). Importance and synthesis of benzannulated medium-sized and macrocyclic rings (BMRs). *RSC Adv.* 4, 43241–43257. doi: 10.1039/C4RA07434C

Kato, N., Comer, E., Sakata-Kato, T., Sharma, A., Sharma, M., Maetani, M., et al. (2016). Diversity-oriented synthesis yields novel multistage antimalarial inhibitors. *Nature* 538, 344–349. doi: 10.1038/nature19804

Kim, H., Tung, T. T., and Park, S. B. (2013). Privileged substructure-based diversity-oriented synthesis pathway for diverse pyrimidine-embedded polyheterocycles. *Org. Lett.* 15, 5814–5817. doi: 10.1021/ol402872b

Kim, J., Jung, J., Koo, J., Cho, W., Lee, W. S., Kim, C., et al. (2016). Diversity-oriented synthetic strategy for developing a chemical modulator of protein–protein interaction. *Nat. Commun.* 7, 13196–13205. doi: 10.1038/ncomms13196

Kim, J., Kim, H., and Park, S. B. (2014). Privileged structures: efficient chemical "navigators" toward unexplored biologically relevant chemical spaces. *J. Am. Chem. Soc.* 136, 14629–14638. doi: 10.1021/ja508343a

Kissau, L., Stahl, P., Mazitschek, R., Giannis, A., and Waldmann, H. (2003). Development of natural product-derived receptor tyrosine kinase inhibitors based on conservation of protein domain fold. *J. Med. Chem.* 46, 2917–2931. doi: 10.1021/jm0307943

Kitsiou, C., Hindes, J. J., I'Anson, P., Jackson, P., Wilson, T. C., Daly, E. K., et al. (2015). The synthesis of structurally diverse macrocycles by successive ring expansion. *Angew. Chem. Int. Ed.* 54, 15794–15798. doi: 10.1002/anie.201509153

Kopp, F., Stratton, C. F., Akella, L. B., and Tan, D. S. (2012). A diversity-oriented synthesis approach to macrocycles via oxidative ring expansion. *Nat. Chem. Biol.* 8, 358–365. doi: 10.1038/nchembio.911

Kuo, S.-Y., Castoreno, A. B., Aldrich, L. N., Lassen, K. G., Goel, G., Dantik, V., et al. (2015). Small-molecule enhancers of autophagy modulate cellular disease phenotypes suggested by human genetics. *Proc. Natl. Acad. Sci. U.S.A.*112, E4281–E4287. doi: 10.1073/pnas.1512289112

Kuruvilla, F. G., Shamji, A. F., Sternson, S. M., Hergenrother, P. J., and Schreiber, S. L. (2002). Dissecting glucose signaling with diversity-oriented synthesis and small-molecule microarrays. *Nature* 416, 653–657. doi: 10.1038/416653a

Lenci, E., Menchi, G., and Trabocchi, A. (2016). Carbohydrates in diversity-oriented synthesis: challenges and opportunities. *Org. Biomol. Chem.* 14, 808–825. doi: 10.1039/C5OB02253C

Li, L., Li, Z.-L., Wang, F.-L., Guo, Z., Cheng, Y.-F., Wang, N., et al. (2016). Radical aryl migration enables diversity-oriented synthesis of structurally diverse medium/macro- or bridged-rings. *Nat. Commun.* 7, 13852–13862. doi: 10.1038/ncomms13852

Lieberman, J. (2018). Tapping the RNA world for therapeutics. *Nat. Struct. Mol. Biol.* 25, 357–364. doi: 10.1038/s41594-018-0054-4

Ma,. X., and Gang, D. R. (2004). The Lycopodium alkaloids. *Nat. Prod. Rep.* 21, 752–772. doi: 10.1039/b409720n

Madsen, C. M., and Clausen, M. H. (2011). Biologically active macrocyclic compounds – from natural products to diversity-oriented synthesis. *Eur. J. Org. Chem.* 3107–3115. doi: 10.1002/ejoc.201001715

Marcaurelle, L. A., Comer, E., Dandapani, S., Duvall, J. R., Gerard, B., Kesavan, S., et al. (2010). An aldol-based build/couple/pair strategy for the synthesis of medium- and large-sized rings: discovery of macrocyclic histone deacetylase inhibitors. *J. Am. Chem. Soc.* 132, 16962–16976. doi: 10.1021/ja105119r

Mason, J. S., Morize, I., Menard, P. R., Cheney, D. L., Hulme, C., and Labaudiniere, R. F. (1999). New 4-point pharmacophore method for molecular similarity and diversity applications: overview of the method and applications, including a novel approach to the design of combinatorial libraries containing privileged substructures. *J. Med. Chem.* 42, 3251–3264. doi: 10.1021/jm9806998

Newman, D. J. (2008). Natural products as leads to potential drugs: an old process or the new hope for drug discovery? *J. Med. Chem.* 51, 2589–2599. doi: 10.1021/jm0704090

Nicolaou, K. C., Pfefferkorn, J. A., Barluenga, S., Mitchell, H. J., Roecker, A. J., and Cao, G.-Q. (2000c). Natural product-like combinatorial libraries based on privileged structures. 3. The "libraries from libraries" principle for diversity enhancement of benzopyran libraries. *J. Am. Chem. Soc.* 122, 9968–9976. doi: 10.1021/ja0020355

Nicolaou, K. C., Pfefferkorn, J. A., Mitchell, H. J., Roecker, A. J., Barluenga, S., Cao, G.-Q., et al. (2000b). Natural product-like combinatorial libraries based on privileged structures. 2. Construction of a 10,000-membered benzopyran library by directed split-and-pool chemistry using nanokans and optical encoding. *J. Am. Chem. Soc*. 122, 9954–9967. doi: 10.1021/ja002034c

Nicolaou, K. C., Pfefferkorn, J. A., Roecker, A. J., Cao, G.-Q., Barluenga, S., and Mitchell, H. J. (2000a). Natural product-like combinatorial libraries based on privileged structures. 1. General principles and solid-phase synthesis of benzopyrans. *J. Am. Chem. Soc.* 122, 9939–9953. doi: 10.1021/ja002033k

Nie, F., Kunciw, D. L., Wilcke, D., Stokes, J. E., Galloway, W. R. J. D., Bartlett, S., et al. (2016). A multidimensional diversity-oriented synthesis strategy for

structurally diverse and complex macrocycles. *Angew. Chem. Int. Ed.* 55, 11139–11143. doi: 10.1002/anie.201605460

Nielsen, T. E., and Schreiber, S. L. (2008). Towards the optimal screening collection: a synthesis strategy. *Angew. Chem. Int. Ed.* 47, 48–56. doi: 10.1002/anie.200703073

Oh, S., and Park, S. B. (2011). A design strategy for drug-like polyheterocycles with privileged substructures for discovery of specific small-molecule modulators. *Chem. Commun.* 47, 12754–12761. doi: 10.1039/c1cc14042f

Plouffe, D. M., Wree, M., Du, A. Y., Meister, S., Li, F., Patra, K., et al. (2016). High-throughput assay and discovery of small molecules that interrupt malaria transmission. *Cell Host Microbe* 19, 114–126. doi: 10.1016/j.chom.2015.12.001

Rafferty, R. J., Hicklin, R. W., Maloof, K. A., and Hergenrother, P. J. (2014). Synthesis of complex and diverse compounds through ring distortion of abietic acid. *Angew. Chem. Int. Ed.* 53, 220–224. doi: 10.1002/anie.201308743

Salituro, G. M., Pettibone, D. J., Clineschmidt, B. V., Williamson, J. M., and Zink, D. L. (1993). Potent, non-peptidic oxytocin receptor antagonists from a natural source. *Bioorg. Med. Chem. Lett.* 3, 337–340. doi: 10.1016/S0960-894X(01)80905-7

Samanen, J. (2013). "How do SMDs differ from biomolecular drugs?" in: *Introduction to Biological and Small Molecule Drug Research and Development: Theory and Case Studies,* eds R. Jefferis, S. Roberts, and R. Ganellin (Waltham, MA: Elsevier), 169–176.

Schreiber, S. L. (2000). Target-oriented and diversity-oriented organic synthesis in drug discovery. *Science* 287, 1964–1969. doi: 10.1126/science.287.5460.1964

Schreiber, S. L., Kotz, J. D., Li, M., Aubé, J., Austin, C. P., Reed, J. C., et al. (2015). Advancing biological understanding and therapeutics discovery with small-molecule probes. *Cell* 161, 1252–1265. doi: 10.1016/j.cell.2015.05.023

Scott, D. E., Bayly, A. R., Abell, C., and Skidmore, J. (2016). Small molecules, big targets: drug discovery faces the protein-protein interaction challenge. *Nat. Rev. Drug Discov.* 15, 533–550. doi: 10.1038/nrd.2016.29

Shimokawa, J. (2014). Divergent strategy in natural product total synthesis. *Tetrahedron Lett.* 55, 6156–6162. doi: 10.1016/j.tetlet.2014.09.078

Spring, D. R. (2003). Diversity-oriented synthesis; a challenge for synthetic chemists. *Org. Biomol. Chem.* 1, 3867–3870. doi: 10.1039/b310752n

Stephens, T. C., Lawer, A., French, T., and Unsworth, W. P. (2018). Iterative assembly of macrocyclic lactones using successive ring expansion reactions. *Chem. Eur. J.* 24, 13947-13953 doi: 10.1002/chem.201803064

Stephens, T. C., Lodi, M., Steer, A. M., Lin, Y., Gill, M. T., and Unsworth, W. P. (2017). Synthesis of cyclic peptide mimetics by the successive ring expansion of lactams. *Chem. Eur. J.* 23, 13314–13318. doi: 10.1002/chem.201703316

Tan, D. S. (2005). Diversity-oriented synthesis: exploring the intersections between chemistry and biology. *Nat. Chem. Biol.* 1, 74–84. doi: 10.1038/nchembio0705-74

Villar, E. A., Beglov, D., Chennamadhavuni, S., Porco, J. A. Jr., Kozakov, D., Vajda, S., et al. (2014). How proteins bind macrocycles. *Nat. Chem. Biol.* 10, 723–731. doi: 10.1038/nchembio.1584

Warner, K. D., Hajdin, C. E., and Weeks, K. M. (2018). Principles for targeting RNA with drug-like small molecules. *Nat. Rev. Drug Discov.* 17, 547–558. doi: 10.1038/nrd.2018.93

Wellington, S., Nag, P. P., Michalska, K., Johnston, S. E., Jedrzejczak, R. P., Kaushik, V. K., et al. (2017). A small-molecule allosteric inhibitor of *Mycobacterium tuberculosis* tryptophan synthase. *Nat. Chem. Biol.* 13, 943–950. doi: 10.1038/nchembio.2420

Wipf, P. (2012). Diversity-oriented synthesis of peptidomimetics: how and why. *Diver. Orient. Synthes.* 1, 6–10. doi: 10.2478/dos-2012-0002

Yu, X., and Sun, D. (2013). Macrocyclic drugs and synthetic methodologies toward macrocycles. *Molecules* 18, 6230–6268. doi: 10.3390/molecules18066230

Zhang, J., Wu, J., Hong, B., Ai, W., Wang, X., Li, H., et al. (2014). Diversity-oriented synthesis of Lycopodium alkaloids inspired by the hidden functional group pairing pattern. *Nat. Commun.* 5, 4614–4622. doi: 10.1038/ncomms5614

Zhu, M., Lim, B. J., Koh, M., and Park, S. B. (2012). Construction of polyheterocyclic benzopyran library with diverse core skeletons through diversity-oriented synthesis pathway: part II. *ACS Comb. Sci.* 14, 124–134. doi: 10.1021/co2001907

Conflict of Interest Statement: The authors declare that the research was conducted in the absence of any commercial or financial relationships that could be construed as a potential conflict of interest.

frontiers in Chemistry

MINI REVIEW
published: 16 October 2018
doi: 10.3389/fchem.2018.00460

Recent Applications of Diversity-Oriented Synthesis Toward Novel, 3-Dimensional Fragment Collections

*Sarah L. Kidd, Thomas J. Osberger, Natalia Mateu, Hannah F. Sore and David R. Spring**

Department of Chemistry, University of Cambridge, Cambridge, United Kingdom

Fragment-based drug discovery (FBDD) is a well-established approach for the discovery of novel medicines, illustrated by the approval of two FBBD-derived drugs. This methodology is based on the utilization of small "fragment" molecules (<300 Da) as starting points for drug discovery and optimization. Organic synthesis has been identified as a significant obstacle in FBDD, however, in particular owing to the lack of novel 3-dimensional (3D) fragment collections that feature useful synthetic vectors for modification of hit compounds. Diversity-oriented synthesis (DOS) is a synthetic strategy that aims to efficiently produce compound collections with high levels of structural diversity and three-dimensionality and is therefore well-suited for the construction of novel fragment collections. This Mini-Review highlights recent studies at the intersection of DOS and FBDD aiming to produce novel libraries of diverse, polycyclic, fragment-like compounds, and their application in fragment-based screening projects.

Keywords: fragment-based drug discovery, diversity-oriented synthesis, medicinal chemistry, organic synthesis, compound collections

OPEN ACCESS

Edited by:
Seung Bum Park,
Seoul National University, South Korea

Reviewed by:
Wei Zhang,
University of Massachusetts Boston, United States
Yu Zhou,
Shanghai Institute of Materia Medica (CAS), China

****Correspondence:***
David R. Spring
spring@ch.cam.ac.uk

Specialty section:
This article was submitted to Organic Chemistry, a section of the journal Frontiers in Chemistry

Received: *30 June 2018*
Accepted: *14 September 2018*
Published: *16 October 2018*

Citation:
Kidd SL, Osberger TJ, Mateu N, Sore HF and Spring DR (2018) Recent Applications of Diversity-Oriented Synthesis Toward Novel, 3-Dimensional Fragment Collections. Front. Chem. 6:460. doi: 10.3389/fchem.2018.00460

INTRODUCTION

Within the biomedical community there remains a pressing need for new molecules to seed early stage drug discovery programs. Diversity-oriented synthesis (DOS) emerged in the early 2000s in response to this challenge, a strategy which involves the efficient and deliberate construction of multiple scaffolds in a divergent manner (Lee et al., 2000; Schreiber, 2000; Spring, 2003; Burke and Schreiber, 2004). Nowadays, applications of this methodology span much of the spectrum of chemical space with examples describing the synthesis of fragment(Hung et al., 2011), small molecule (Wyatt et al., 2008; Lenci et al., 2015; Caputo et al., 2017), peptide (Kotha et al., 2013; Contreras-Cruz et al., 2017; Zhang et al., 2017) and macrocyclic (Isidro-Llobet et al., 2011; Kopp et al., 2012; Beckmann et al., 2013; Dow et al., 2017) collections all abundant within the literature. Furthermore, as the field of DOS has evolved, research themes have focused on addressing key calls from within the drug discovery community, namely the deficiencies within compound screening libraries (Lipkus et al., 2008; Dow et al., 2012), the identification of new bioactive molecules against challenging biological targets (Stanton et al., 2009; Kato et al., 2016; Kim et al., 2016) and populating underexplored areas of chemical space with novel structural entities (Thomas et al., 2008; Morton et al., 2009; Pizzirani et al., 2010). Until recently, however, the majority of DOS successes have been achieved in high-throughput screening (HTS) contexts (Chou et al., 2011; Laraia et al., 2014; Aldrich et al., 2015; Kuo et al., 2015).

Recent applications of DOS, however, exemplify how this methodology can be utilized to address significant challenges currently faced within the field of fragment-based drug discovery (FBDD). FBDD is now a widely adopted technique across both industry and academia, with two marketed drugs having emerged from this methodology [vemurafenib (Bollag et al., 2012), venetoclax (Souers et al., 2013)] and dozens of clinical candidates (Erlanson et al., 2016). This process involves the screening of small "fragment" molecule libraries (<300 Da) to identify efficient, but none the less weakly binding molecules, which are in turn subsequently elaborated to generate potent lead compounds (Erlanson and Jahnke, 2016). "Rule of three" guidelines are commonly employed within FBDD and library construction, relating to a molecular weight <300 Da, the number of hydrogen and acceptors/donors ≤3 and a cLogP ≤3 (Congreve et al., 2003). Importantly, due to the additional physicochemical constraints imposed on these screening libraries compared to traditional HTS approaches, it is broadly accepted that this method allows far more efficient sampling of chemical space, since there are far fewer possible fragment-sized molecules (Murray and Rees, 2009; Hall et al., 2014).

Despite significant advances in the foundational technologies of FBDD which have aided its implementation, reports associated with the synthetic intractability of hit fragments support the view that organic synthesis may be a rate-limiting step in the FBDD cycle, and in fact across drug discovery as a whole (Murray and Rees, 2016; Blakemore et al., 2018). In a similar vein to traditional drug discovery, deficiencies in commercially available fragment screening collections have been noted, in particular relating to the overrepresentation of sp^2-rich flat molecules (Hajduk et al., 2011; Hung et al., 2011) that feature limited numbers of synthetic handles for fragment elaboration. This latter feature is especially important within FBDD since this process relies on the merging, growth or linkage of small fragment molecules to develop initial weak hits (typically μM or mM range) hits into potent lead compounds. Without these vital functional handles, this process is significantly more time consuming, requiring the development of new synthetic routes to modify relatively simple fragment scaffolds. Furthermore, the incompatibility of many existing synthetic methodologies with amines, heterocycles, and unprotected polar functionalities limits their utilization. Consequently, there is a need for new strategies and technologies that enable non-traditional disconnections, late-stage functionalization as well as the incorporation of 3D elements into drug-like scaffolds.

Thus, appeals from within scientific community have been made for the development of novel and flexible synthetic methodologies that enable access to new fragments and their derivatives, including those with increased 3-dimensionality and heterocyclic architecture (Keseru et al., 2016; Murray and Rees, 2016). Despite the debates within the literature on the requirements of 3D character within fragment libraries, population of these underrepresented areas can be considered to complement existing flatter libraries, whilst providing access to alternative growth vectors, and therefore remains an important avenue of research (Morley et al., 2013; Fuller et al., 2016). From the perspective of library construction, the 3D character of the resulting libraries is commonly judged by the number of chiral centers and the fraction of sp^3 carbons (Fsp^3) within a molecule (Lovering et al., 2009), in addition to visual representations of the molecular shape space distribution using principal moment of inertia (PMI) analysis (Sauer and Schwarz, 2003; Kopp et al., 2012).

With a growing demand for novel heterocycles and 3D-shaped molecules for use within FBDD campaigns, many studies centering on the synthesis of 3D fragments around single heterocycles have been reported, for example using C-H activation methodologies (Davis et al., 2015; Palmer et al., 2016; Antermite et al., 2018). This mini-review aims to highlight the suitability of DOS approaches for addressing these challenges through the production of multiple scaffolds with a broader coverage of chemical space. One important feature of this strategy is the utilization of highly efficient and modular synthetic routes, commonly in the form of a build/couple/pair (B/C/P) algorithm (Nielsen and Schreiber, 2008). This involves (1) *the build phase*—construction of common starting materials, (2) *the couple phase*—intermolecular coupling of the building blocks with readily synthesized or commercial materials to form reactive intermediates and (3) *the pair phase*—intramolecular reaction or cyclisation of these precursors to afford distinct scaffolds. Thus, the flexibility of these strategies often results in methodologies that can provide efficient access to analogs of a desired scaffold. Herein, we discuss recent applications of the DOS strategy to the construction of novel and diverse 3D fragment collections and their applications in FBDD.

THE APPLICATION OF DOS TO ACCESS NOVEL FRAGMENTS WITH MULTIPLE GROWTH VECTORS

The first publication conceptually merging DOS and FBDD appeared in 2011 in which Hung et al. (2011) described the application of DOS for the generation of a 3D fragment collection utilizing allyl proline-based precursors as the basis for library design. The researchers exploited three proline-derived building blocks in a B/C/P sequence to facilitate the formation of a series of fused and spiro bicyclic compounds (**Figure 1B**). This was achieved through installation of a second olefin *via N*-substitution using a variety of linker types, furnishing distinct linear precursors**.** Subsequently subjecting these intermediates to various intramolecular cyclizations such as ring closing metathesis (RCM) and oxo-Michael reactions, yielded 20 compounds based on 12 frameworks. Furthermore, due to the modular nature of this approach a complete matrix of stereoisomers of the 5–6, 5–7, 5–8, and 5–9 bicyclic frameworks could be constructed. Finally, the scaffolds were derivatized in a post-pair phase manner through functional group interconversion or olefin reduction to increase the diversity and the saturation, affording a total of 35 fragments.

Importantly, polar functional handles were installed throughout the library, enabling potential fragment growth from different vectors during hit-to-lead efforts. The applicability of the resultant library to FBDD was demonstrated *via*

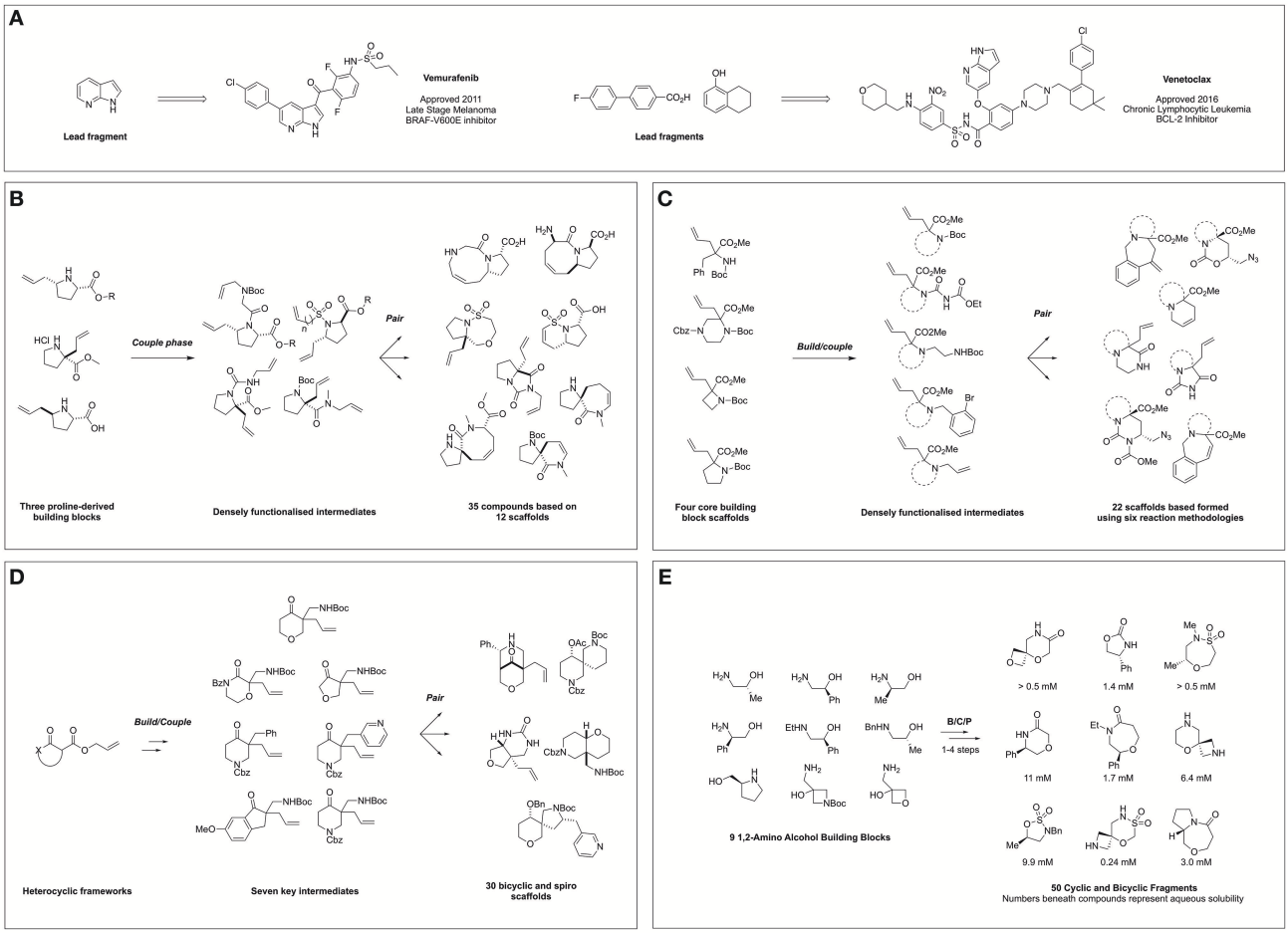

FIGURE 1 | FBDD-derived drugs and diversity-oriented synthesis of novel fragment libraries. **(A)** Clinically approved drugs derived from FBDD and their lead fragments. **(B)** Hung et al. (2011) Report on DOS of fragment-like molecules. **(C)** Foley et al. (2015) Lead-like modular route to novel scaffolds. **(D)** Mayol-Llinàs et al. (2017) Lead-like scaffold DOS for CNS and FBDD. **(E)** Haftchenary et al. (2016) DOS of aqueous soluble fragments from 1,2-amino alcohols.

chemoinformatic analysis, which highlighted rule of three compliance whilst principle moment of inertia (PMI) plots suggested a broad coverage of 3D molecular shape space.

Amino acid-derived reagents represent valuable building blocks for use within DOS methodologies owing to their polar and chiral nature, and their exploitation within these techniques has become more prevalent within the field. Work by Foley et al. (2015) described the application of four α,α-amino acid derived building blocks to generate a library of diverse bicyclic and tricyclic fragments (Foley et al., 2015). Through variation in the building block structure and the nature of the pair-phase cyclisation the researchers constructed 22 different heterocyclic scaffolds in a synthetically efficient manner (**Figure 1C**). Firstly, five different nitrogen substituents were installed on the four amino acid building blocks: a *tert*-butyl carbamate, an acyl urea, a 1,2-diamine, a *o*-bromobenzylamine or a second allyl olefin. In turn, pair phase reactions were then explored through reactivity of these functionalities with either the preinstalled ester or allyl moieties. This included iodine-mediated cyclisation followed by azide addition and reactivity of the electrophillic ester moiety with *N*-based nucleophiles. Finally, ring closure *via* either Pd-mediated Heck reaction or Ru-mediated metathesis afforded further tri- and bicyclic fragments. The final collection of 22 scaffolds featured biologically relevant moieties such as ureas, hydantoins, and lactams, in addition to multiple functional synthetic handles. Subsequent virtual enumeration led to a library of 1,110 compounds that were predicted to possess lead-like properties and with considerable 3D character, (average Fsp^3 = 0.57) and several examples meeting the criteria for FBDD.

In a similar vein, Mayol-Llinàs and co-workers also explored the use of cyclic α-allyl quaternary ketones in a divergent and modular synthetic process to generate a library of 30 structurally distinct scaffolds featuring spiro, fused and bridged architectures (**Figure 1D**) (Mayol-Llinàs et al., 2017). Instead of amino acid-based precursors, Tsuji-type decarboxylative allylation was utilized to generate seven quaternary allylated building blocks. One example was selected for pilot studies, during which a variety of transformations were applied in a

reagent-based approach to yield 12 different scaffolds through exploitation of four key reactive moieties within the intermediate. This included an intramolecular Mannich reaction, a sequence of hydroboration-oxidation followed by either reduction or sulfonylation and then cyclisation, base-mediated cyclisation and Pd-catalyzed aminoarylation. Then, the remaining six precursors were subjected to the most promising conditions, yielding an additional 18 scaffolds. Virtual library enumeration was also conducted using six synthetic transformations, including reductive amination, urea formation and sulfonylation using 98 medicinal chemistry relevant capping groups. Multiparameter optimization analysis (Wager et al., 2010) was used to assess the amenability of this work to a CNS-based drug discovery context. In addition, it was noted the resulting library possessed lead-like properties (Doveston et al., 2014) and that many of the compounds and derivatives would be applicable to a FBDD setting.

A recent report from Haftchenary at the Broad Institute detailed the synthesis of a fragment collection based on chiral 1,2-amino alcohols (**Figure 1E**) (Haftchenary et al., 2016). Beginning from a library of nine readily available amino alcohols, a range of 5-, 6-, and 7-membered scaffolds were synthesized in 1–4 steps using established synthetic procedures. The resulting fragment collection included medicinally important heterocycles such as oxazolidinones, morpholinones, and sulfamidate and sultam-based rings, along with fused and spiro-bicyclic compounds.

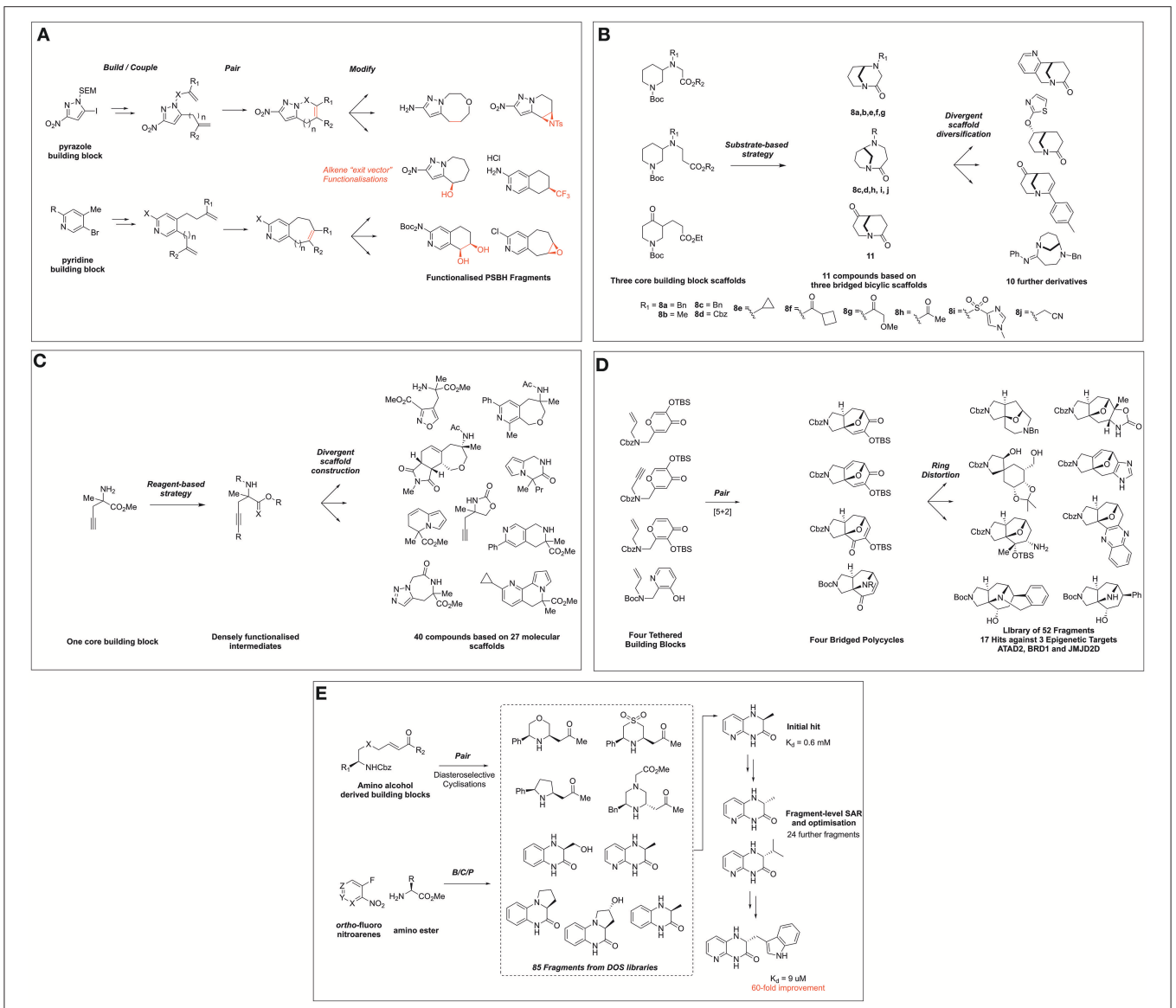

FIGURE 2 | Fragment collections derived from DOS and their application to FBDD. **(A)** Twigg et al. (2016) DOS of partially saturated bicyclic heteroaromatic fragments. **(B)** Hassan et al. (2018) DOS fragment library based on twisted amides. **(C)** Mateu et al. (2018) DOS fragment library based on α,α-disubstituted amino esters. **(D)** Foley et al. (2017) synthesis of scaffolds distantly related to natural products. **(E)** Wang et al. (2016) DOS fragment evolution strategy against GSK3.

Importantly for a screening context, the aqueous solubility of each of the 50 final fragments was measured, with values ranging from 0.085 to >15 mM, within the range for many fragment screening techniques.

Further to the goal of populating fragment space with sp^3-enriched compound collections that possess favorable fragment-like properties and synthetic exit vectors, Spring and coworkers disclosed a DOS-related approach to the synthesis of partially saturated bicyclic heteraromatic (PSBH) molecules (**Figure 2A**) (Twigg et al., 2016). The synthetic route centered on the functionalization of pyrazole and pyridine-based building blocks featuring possessing amino-, or nitro groups, which were incorporated as potential solubilizing moieties; alternatively, a chloro substituent was incorporated as a hydrophobic element. The build and couple stages comprised of Suzuki cross coupling and alkylations to install various alkene functionalities, which were paired using RCM to afford bicyclic scaffolds, each featuring a positionally defined endocyclic alkene vector for further functionalization.

The endocyclic alkene was then modified in a post-pairing event to exemplify its utility as a synthetic growth vector in these fragments. A variety of alkene transformations, including dihalogenation, epoxidation, aziridination, cyclopropanation, halohydrin formation, and hydroboration-oxidation, were performed to yield a range of further functionalized scaffolds. The resulting library of compounds was then subjected to analysis of its physicochemical properties, which compared favorably to commercial screening libraries in relation to key properties such as number of chiral centers (0.88 vs. 0.27 or 0.18) and fraction aromatic (0.43 vs. 0.42 and 0.52), while maintaining rule of three compliance.

Hassan et al. recently disclosed an interesting example via the exploitation of twisted bicyclic amide compounds for the generation of a 3D fragment screening library (Hassan et al., 2018). In this work five 3-(ω-carboxylate)-substituted piperidine starting materials were manipulated to produce a 22-member polycyclic library (**Figure 2B**). Using substrate-based DOS methodology, five analogous starting materials based on three common structures were constructed and *via* Bu_2SnO-mediated cyclisation these were transformed to afford bicyclo[4.3.1]decane and bicyclo[3.3.1]nonane scaffolds in moderate yield. The generality of this methodology was exemplified through the synthesis of six further compounds through modification of the *N*-substituent the bicyclic ring systems.

In turn, these three key scaffolds were ultimately then divergently modified through manipulation of either the ketone or amide functionalities to generate a further nine compounds. The ketone moiety within the bicyclo[3.3.1]nonane was first modified by the use of either gold- or palladium-mediated reactions to afford tetra- or tricyclic heteroaromoatic fused motifs. Alternatively, this moiety could also be reduced and a variety of heteroaromatics or alkyl moiety installed *via* either S_NAr or alkylation conditions in a diastereoselective fashion. Finally, the twisted amide within these scaffolds could also be manipulated to form either a chloroenamine intermediate, followed by Suzuki-coupling to install an aryl substituent or simply by amidine formation. The resultant library was shown to possess fragment lead-like properties with a high Fsp^3 (0.63) and generally 17 or fewer heavy atoms and a clogP < 2.5. Furthermore, PMI analysis of the shape distribution suggested the library possessed significant 3D character to complement existing fragment collections for screening purposes.

The most recent and final example of synthetic efforts within this field by Mateu et al. (2018) report the use of α,α-disubstituted amino esters for the DOS of fragments incorporating a *N*-substituted quaternary carbon, an important and underrepresented motif within screening collections (**Figure 2C**). Using a single building block, 40 structurally diverse molecules based on 27 molecular frameworks were constructed in a synthetically efficient manner using an average of only three synthetic steps to access the entire library. This involved exploiting the three reactive handles within the building block in different combinations and utilizing a broad range of chemistries such as [2+2+2] cyclotrimiserizations, Au-, Ru-, and Cu- mediated cyclizations and regioselective click chemistry to afford mono-, bi-, and tri-fused heterocycles featuring this important motif. Importantly, the authors also demonstrated the versatility of this synthetic methodology through the synthesis of an alternative quaternary *R*-substituent and the asymmetric synthesis of one library member.

Subsequent computational assessment of the resulting library *via* PMI analysis revealed a broad distribution of molecular shape space, in addition to favorable comparisons to a commercially available fragment collection in terms of 3-dimensional shape space coverage. Additionally, the mean values of the physicochemical properties of the library demonstrated the compatibility of the library for fragment screening, falling within the Rule of three guidelines, whilst exhibiting more favorable properties when again compared to existing commercial libraries. The authors note promising hits identified by X-ray fragment screening at the XChem screening facility, against proteins from three distinct families (a hydrolase, a TGF β growth factor, and a peptidase).

DEMONSTRATION OF DOS METHODOLOGIES FOR THE IDENTIFICATION OF NOVEL BINDERS FOR CHALLENGING BIOLOGICAL TARGETS

In addition to populating new areas of fragment chemical space, DOS-derived fragment libraries can play a significant role in the identification of novel binders to seed future FBDD programs. Recent work by Foley et al. (2017) demonstrated the application of DOS-derived fragment libraries in the identification of novel hits against three epigenetic proteins from two distinct mechanistic classes (ATAD2, BRD1, and JMJD2D), *via* X-ray crystallographic screening methods. The researchers took inspiration from natural product frameworks, utilizing intramolecular [5+2] cyclizations to forge bridged structures incorporating natural product-related heteroaromatic frameworks (**Figure 2D**). Ring distortion reactions on these four initial structures using either expansion, cleavage, annulation, or substitution methodologies, were performed to divergently

modify the precursors, ultimately affording a library of 52 fragments based on 23 different scaffolds with bridged architectures and a high sp^3 content. Interestingly, when this library was screened against the three epigenetic targets *via* high-throughput X-ray crystallography methods, 17 hits were identified against the three proteins, including those binding in novel regions of the proteins to those described previously. Moreover, comparisons could be drawn between the natural product-like fragment library and that obtained from commercial sources, whereby a significantly higher hit rate against ATAD2 was observed with the 3D fragments synthesized where seven hits were identified from a 52-member library vs. the commercially available fragment library where nine hits were identified from a 700-member library. Although the authors did not report any biophysical data for the fragments, the identification of novel X-ray hits from these efforts demonstrate the promise of a merged DOS-FBDD approach.

Finally, Young and co-workers recently demonstrated the successful use of the DOS strategy to optimize fragments against the serine/theronine kinase GSK3β (Wang et al., 2016), which is overexpressed in cancer and Alzheimer's disease (Luo, 2009; Hernandez et al., 2012). To initiate the investigation, a set of 86 fragments was compiled from DOS libraries constructed *via* three distinct B/C/P pathways (**Figure 2E**). The first DOS fragment library utilized allylproline building blocks and has been previously discussed in this review (**Figure 1A**). The second DOS library coupled enones with amino alcohol and related building blocks. The final scaffolds were accessed *via* catalytic, diastereoselective aza-Michael additions to afford stereochemically diverse disubstituted heterocycles. The third DOS library incorporated into this study was generated from *ortho*-nitrofluoro arenes and α-amino ester building blocks. Intermolecular coupling products were obtained *via* S_NAr, and pairing products were accessed by reduction of the nitro group followed by spontaneous cyclisation onto the ester functionality. This modular approach yielded a small collection of enantiomerically enriched bicyclic piperazinone compounds.

Using this fragment collection, screening against GSK3β was performed using differential scanning fluorimetry (DSF) to detect fragment binding. Initial results identified a benzopiperizinone-library member to exhibit good thermal stabilization and subsequent assays showed 46% inhibition of GSK3β at 1 mM concentration. A library of derivatives based on this initial hit were then synthesized using the modular and rapid DOS chemistry initially developed. Thus, the single enantiomer variants and other derivatives could easily be constructed to generate structure-activity relationships (SAR). Preliminary fragment-level SAR indicated the *(R)*-enantiomer of the chiral center to be more potent, and further studies identified the substituent at this site as an important potential growth vector. Fragment growth by incorporating large aryl groups into the scaffold *via* the same B/C/P pathway yielded the lead compound, with a large indolyl unit connected to the core heterocycle. This fragment exhibited a $K_d = 9\,\mu M$, a 60-fold improvement over the initial fragment hit. Ultimately an X-ray crystal structure of the lead compound with GSK3β was obtained, revealing it binds in the ATP pocket of this kinase.

This study demonstrated the successful implementation of a DOS-based FBDD workflow to evolve fragments against an important kinase target. Key to the success of this project was the utility of the DOS concept as a tool to generate skeletally and stereochemically diverse initial libraries, and later as an efficient, modular route to analogs for SAR and fragment growth.

FUTURE PERSPECTIVES

The studies discussed herein have demonstrated the utility of DOS as an effective approach for populating new areas of fragment space, in areas largely complementary to existing fragment collections. In each case, the resulting libraries featured high structural and shape diversity, increased 3D character and exemplified synthetic vectors for fragment growth. The latter two examples discussed detail applications of these libraries for the identification of novel fragment binders and inhibitors against challenging protein targets, ultimately demonstrating the utility of DOS within drug discovery efforts.

It is worth noting the increasing application of computational virtual library enumeration, an element of which has featured in several of the publications discussed. It is envisioned that these methodologies will only increase in their utility when coupled to *in silico*-based screening techniques to guide library design and prioritization of synthesis. Moreover, a focus on applications of newly developed methodologies to DOS, for example C-H activation, and site selective late-stage modifications of complex scaffolds would enable population of underexplored areas of chemical space and further derivatization of the resulting scaffolds. Finally, an outstanding requirement within this field is the establishment of new translational collaborations between academic and industrial groups to enable the routine screening of the novel libraries.

AUTHOR CONTRIBUTIONS

SLK and TJO conceived and wrote the manuscript. All other authors (NM, HFS and DRS) provided comments and discussion on the manuscript to aid its preparation.

FUNDING

Our research is supported by the EPSRC, BBSRC, MRC, Wellcome Trust, and ERC (FP7/2007-2013; 279337/DOS). SK thanks AstraZeneca for funding.

ACKNOWLEDGMENTS

The authors would like to thank Dr D. Twigg from Astex for useful discussions on the topic.

REFERENCES

Aldrich, L. N., Kuo, S. Y., Castoreno, A. B., Goel, G., Kuballa, P., Rees, M. G., et al. (2015). Discovery of a small-molecule probe for V-ATPase function. *J. Am. Chem. Soc.* 137, 5563–5568. doi: 10.1021/jacs.5b02150

Antermite, D., Dominic, P. A., and Bull, J. A. (2018). Regio- and stereoselective palladium-catalyzed C(sp3)–H arylation of pyrrolidines and piperidines with C(3) directing groups. *Organ. Lett.* 20, 3948–3952. doi: 10.1021/acs.orglett.8b01521

Beckmann, H. S., Nie, F., Hagerman, C. E., Johansson, H., Tan, Y. S., Wilcke, D., et al. (2013). A strategy for the diversity-oriented synthesis of macrocyclic scaffolds using multidimensional coupling. *Nat. Chem.* 5, 861–867. doi: 10.1038/nchem.1729

Blakemore, D. C., Castro, L., Churcher, I., Rees, D. C., Thomas, A. W., Wilson, D. M., et al. (2018). Organic synthesis provides opportunities to transform drug discovery. *Nat. Chem.* 10, 383–394. doi: 10.1038/s41557-018-0021-z

Bollag, G., Tsai, J., Zhang, J., Zhang, C., Ibrahim, P., Nolop, K., et al. (2012). Vemurafenib: the first drug approved for BRAF-mutant cancer. *Nat. Rev. Drug Discov.* 11, 873–886. doi: 10.1038/nrd3847

Burke, M. D., and Schreiber, S. L. (2004). A planning strategy for diversity-oriented synthesis. *Angew. Chem. Int. Ed.* 43, 46–58. doi: 10.1002/anie.200300626

Caputo, S., Banfi, L., Basso, A., Galatini, A., Moni, L., Riva, R., et al. (2017). Diversity-oriented synthesis of various enantiopure heterocycles by coupling organocatalysis with multicomponent reactions. *Eur. J. Organ. Chem.* 2017, 6619–6628. doi: 10.1002/ejoc.201701328

Chou, D. H. C., Duvall, J. R., Gerard, B., Liu, H., Pandya, B. A., Suh, B. C., et al. (2011). Synthesis of a novel suppressor of β-cell apoptosis via diversity-oriented synthesis. *ACS Med. Chem. Lett.* 2, 698–702. doi: 10.1021/ml200120m

Congreve, M., Carr, R., Murray, C., and Jhoti, H. (2003). A 'rule of three' for fragment-based lead discovery? *Drug Discov. Today* 8, 876–877. doi: 10.1016/S1359-6446(03)02831-9

Contreras-Cruz, D. A., Sánchez-Carmona, M. A., Vengoechea-Gómez, F. A., Peña-Ortíz, D., and Miranda, L. D. (2017). Diversity-oriented synthesis of cyclopropyl peptides from Ugi-derived dehydroalanines. *Tetrahedron* 73, 6146–6156. doi: 10.1016/j.tet.2017.09.005

Davis, O. A., Croft, R. A., and Bull, J. A. (2015). Synthesis of diversely functionalised 2,2-disubstituted oxetanes: fragment motifs in new chemical space. *Chem. Commun.* 51, 15446–15449. doi: 10.1039/C5CC05740J

Doveston, R., Marsden, S., and Nelson, A. (2014). Towards the realisation of lead-oriented synthesis. *Drug Discov. Today* 19, 813–819. doi: 10.1016/j.drudis.2013.11.006

Dow, M., Fisher, M., James, T., Marchetti, F., and Nelson, A. (2012). Towards the systematic exploration of chemical space. *Organ. Biomol. Chem.* 10, 17–28. doi: 10.1039/C1OB06098H

Dow, M., Marchetti, F., Abrahams, K. A., Vaz, L., Besra, G. S., Warriner, S., et al. (2017). Modular synthesis of diverse natural product-like macrocycles: discovery of hits with antimycobacterial activity. *Chem. A Eur. J.* 23, 7207–7211. doi: 10.1002/chem.201701150

Erlanson, D. A., Fesik, S. W., Hubbard, R. E., Jahnke, W., and Jhoti, H., (2016). Twenty years on: the impact of fragments on drug discovery. *Nat. Rev. Drug Discov.* 15, 605–619. doi: 10.1038/nrd.2016.109

Erlanson, D. A., and Jahnke, W. (2016). *Fragment-Based Drug Discovery Lessons and Outlook*. Weinhein: Wiley-VCH Verlang GmbH and Co.

Foley, D., Doveston, R., Churcher, I., Nelson, A., and Marsden, S. P. (2015). A systematic approach to diverse, lead-like scaffolds from α,α-disubstituted amino acids. *Chem. Commun.* 51, 11174–11177. doi: 10.1039/C5CC03002A

Foley, D. J., Craven, P. G. E., Collins, P. M., Doveston, R. G., Aimon, A., Talon, R., et al. (2017). Synthesis and demonstration of the biological relevance of *sp*3rich Scaffolds distantly related to natural product frameworks. *Chem. A Eur. J.* 23, 15227–15232. doi: 10.1002/chem.201704169

Fuller, N., Spadola, L., Cowen, S., Patel, J., Schonherr, H., Cao, Q., et al. (2016). An improved model for fragment-based lead generation at AstraZeneca. *Drug Discov. Today* 21, 1272–1283. doi: 10.1016/j.drudis.2016.04.023

Haftchenary, S., Nelson, S. D., Furst, L., Dandapani, S., Ferrara, S. J., Bošković, Ž. V., et al. (2016). Efficient routes to a diverse array of amino alcohol-derived chiral fragments. *Comb. Sci.* 18, 569–574. doi: 10.1021/acscombsci.6b00050

Hajduk, P. J., Galloway, W. R., and Spring, D. R. (2011). Drug discovery: a question of library design. *Nature* 470, 42–43. doi: 10.1038/470042a

Hall, R. J., Mortenson, P. N., and Murray, C. W. (2014). Efficient exploration of chemical space by fragment-based screening. *Prog. Biophys. Mol. Biol.* 116, 82–91. doi: 10.1016/j.pbiomolbio.2014.09.007

Hassan, H., Marsden, S. P., and Nelson, A. (2018). Design and synthesis of a fragment set based on twisted bicyclic lactams. *Bioorgan. Med. Chem.* 26, 3030–3033. doi: 10.1016/j.bmc.2018.02.027

Hernandez, F., Lucas, J. J., and Avila, J. (2012). GSK3 and tau: two convergence points in Alzheimer's disease. *J. Alzheimer's Dis.* 33, S141–S144. doi: 10.3233/JAD-2012-129025

Hung, A. W., Ramek, A., Wang, Y., Kaya, T., Wilson, J. A., Clemons, P. A., et al. (2011). Route to three-dimensional fragments using diversity-oriented synthesis. *Proc. Natl. Acad. Sci. U.S.A.* 108, 6799–6804. doi: 10.1073/pnas.1015271108

Isidro-Llobet, A., Murillo, T., Bello, P., Cilibrizzi, A., Hodgkinson, J. T., Galloway, W. R. J. D., et al. (2011). Diversity-oriented synthesis of macrocyclic peptidomimetics. *Proc. Natl. Acad. Sci. U.S.A.* 108, 6793–6798. doi: 10.1073/pnas.1015267108

Kato, N., Comer, E., Sakata-Kato, T., Sharma, A., Sharma,. M., Maetani, M., et al. (2016). Diversity-oriented synthesis yields novel multistage antimalarial inhibitors. *Nature* 538, 344–349. doi: 10.1038/nature19804

Keseru, G. M., Erlanson, D. A., Ferenczy, G. G., Hann, M. M., Murray, C. W., and Pickett, S. D. (2016). Design principles for fragment libraries: maximizing the value of learnings from pharma Fragment-Based Drug Discovery (FBDD) programs for use in academia. *J. Med. Chem.* 59, 8189–8206. doi: 10.1021/acs.jmedchem.6b00197

Kim, J., Jung, J., Koo, J., Cho, W., Lee, W. S., Kim, C., et al. (2016). Diversity-oriented synthetic strategy for developing a chemical modulator of protein–protein interaction. *Nat. Commun.* 7:13196. doi: 10.1038/ncomms13196

Kopp, F., Stratton, C. F., Akella, L. B., and Tan, D. S. (2012). A diversity-oriented synthesis approach to macrocycles via oxidative ring expansion. *Nat. Chem. Biol.* 8, 358–365. doi: 10.1038/nchembio.911

Kotha, S., Goyal, D., and Chavan, A. S. (2013). Diversity-oriented approaches to unusual α-amino acids and peptides: step economy, atom economy, redox economy, and beyond. *J. Organ. Chem.* 78, 12288–12313. doi: 10.1021/jo4020722

Kuo, S.-Y., Castoreno, A. B., Aldrich, L. N., Lassen, K. G., Goel, G., Dančík, V., et al. (2015). Small-molecule enhancers of autophagy modulate cellular disease phenotypes suggested by human genetics. *Proc. Natl. Acad. Sci. U.S.A.* 112, 4281–e4287. doi: 10.1073/pnas.1512289112

Laraia, L., Stokes, J., Emery, A., McKenzie, G. J., Venkitaraman, A. R., and Spring, D. R. (2014). High content screening of diverse compound libraries identifies potent modulators of tubulin dynamics. *ACS Med. Chem. Lett.* 5, 598–603. doi: 10.1021/ml5000564

Lee, D., Sello, J. K., and Schreiber, S. L. (2000). Pairwise use of complexity-generating reactions in diversity-oriented organic synthesis. *Organ. Lett.* 2, 709–712. doi: 10.1021/ol005574n

Lenci, E., Menchi, G., Guarna, A., and Trabocchi, A. (2015). Skeletal diversity from carbohydrates: use of mannose for the diversity-oriented synthesis of polyhydroxylated compounds. *J. Organ. Chem.* 80, 2182–2191. doi: 10.1021/jo502701c

Lipkus, A. H., Yuan, Q., Lucas, K. A., Funk, S. A., Bartelt, W. F., Schenck, R. J., et al. (2008). Structural diversity of organic chemistry. A Scaffold Analysis of the CAS Registry. *Organ. Chem.* 73, 4443–4451. doi: 10.1021/jo8001276

Lovering, F., Bikker, J., and Humblet, C. (2009). Escape from flatland: increasing saturation as an approach to improving clinical success. *J. Med. Chem.* 52, 6752–6756. doi: 10.1021/jm901241e

Luo, J. (2009). Glycogen synthase kinase 3beta (GSK3beta) in tumorigenesis and cancer chemotherapy. *Cancer Lett.* 273, 194–200. doi: 10.1016/j.canlet.2008.05.045

Mateu, N., Kidd, S. L., Kalash, L., Sore, H. F., Madin, A., Bender, A., et al. (2018). Synthesis of structurally diverse N-substituted quaternary-carbon-containing small molecules from α,α-disubstituted propargyl amino esters. *Chem. Eur. J.* 24, 13681–13687. doi: 10.1002/chem.201803143.

Mayol-Llinàs, J., Farnaby, W., and Nelson, A. (2017). Modular synthesis of thirty lead-like scaffolds suitable for CNS drug discovery. *Chem. Commun.* 53, 12345–12348. doi: 10.1039/C7CC06078E

Morley, A. D., Pugliese, A., Birchall, K., Bower, J., Brennan, P., Brown, N., et al. (2013). Fragment-based hit identification: thinking in 3D. *Drug Discov. Today* 18, 1221–1227. doi: 10.1016/j.drudis.2013.07.011

Morton, D., Leach, S., Cordier, C., Warriner, S., and Nelson, A. (2009). Synthesis of natural-product-like molecules with over eighty distinct scaffolds. *Angew. Chem. Int. Ed.* 48, 104–109. doi: 10.1002/anie.200804486

Murray, C. W., and Rees, D. C. (2009). The rise of fragment-based drug discovery. *Nat. Chem.* 1, 187–192. doi: 10.1038/nchem.217

Murray, C. W., and Rees, D. C. (2016). Opportunity knocks: organic chemistry for Fragment-Based Drug Discovery (FBDD). *Angew. Chem. Int. Ed*. 55, 488–492. doi: 10.1002/anie.201506783

Nielsen, T. E., and Schreiber, S. L. (2008). Towards the optimal screening collection: a synthesis strategy. *Angew. Chem. Int. Ed.* 47, 48–56. doi: 10.1002/anie.200703073

Palmer, N., Peakman, T. M., Norton, D., and Rees, D. C. (2016). Design and synthesis of dihydroisoquinolones for fragment-based drug discovery (FBDD). *Organ. Biomol. Chem*. 14, 1599–1610. doi: 10.1039/C5OB02461G

Pizzirani, D., Kaya, T., Clemons, P. A., and Schreiber, S. L. (2010). Stereochemical and skeletal diversity arising from amino propargylic alcohols. *Organ. Lett.* 12, 2822–2825. doi: 10.1021/ol100914b

Sauer, W. H. B., and Schwarz, M. K. (2003). Molecular shape diversity of combinatorial libraries: a prerequisite for broad bioactivity. *J. Chem. Inf. Comput. Sci.* 43, 987–1003. doi: 10.1021/ci025599w

Schreiber, S. L. (2000). Target-oriented and diversity-oriented organic synthesis in drug discovery. *Science* 287, 1964–1969. doi: 10.1126/science.287.5460.1964

Souers, A. J., Leverson, J. D., Boghaert, E. R., Ackler, S. L., Catron, N. D., Chen, J., et al. (2013). ABT-199, a potent and selective BCL-2 inhibitor, achieves antitumor activity while sparing platelets. *Nat. Med*. 19, 202–208. doi: 10.1038/nm.3048

Spring, D. R. (2003). Diversity-oriented synthesis; a challenge for synthetic chemists. *Organ. Biomol. Chem.* 1, 3867–3870. doi: 10.1039/b310752n

Stanton, B. Z., Peng, L. F., Maloof, N., Nakai, K., Wang, X., Duffner, J. L., et al. (2009). A small molecule that binds Hedgehog and blocks its signaling in human cells. *Nat. Chem. Biol.* 5, 154–156. doi: 10.1038/nchembio.142

Thomas, G. L., Spandl, R. J., Glansdorp, F. G., Welch, M., Bender, A., Cockfield, J., et al. (2008). Anti-MRSA agent discovery using diversity-oriented synthesis. *Angew. Chem. Int. Ed.* 47, 2808–2812. doi: 10.1002/anie.200705415

Twigg, D. G., Kondo, N., Mitchell, S. L., Galloway, W. R. J. D., Sore, H. F., Madin, A., et al. (2016). Partially saturated bicyclic heteroaromatics as an sp^3-enriched fragment collection. *Angew. Chem. Int. Ed.* 55, 12479–12483. doi: 10.1002/anie.201606496

Wager, T. T., Hou, X., Verhoest, P. R., and Villalobos, A. (2010). Moving beyond rules: the development of a central nervous system multiparameter optimization (CNS MPO) approach to enable alignment of druglike properties. *ACS Chem. Neurosci.* 1, 435–449. doi: 10.1021/cn100008c

Wang, Y., Wach, J. Y., Sheehan, P., Zhong, C., Zhan, C., Harris, R., et al. (2016). Diversity-oriented synthesis as a strategy for fragment evolution against GSK3β. *ACS Med. Chem. Lett*. 7, 852–856. doi: 10.1021/acsmedchemlett.6b00230

Wyatt, E., Galloway, W. R. J. D., Thomas, G., Welch, M., Loiseleur, O., Plowright, A., et al. (2008). Identification of an anti-MRSA dihydrofolate reductase inhibitor from a diversity-oriented synthesis. *Chem. Commun*. 40, 4962–4964. doi: 10.1039/b812901k

Zhang, J., Mulumba, M., Ong, H., and Lubell, W. D. (2017). Diversity-oriented synthesis of cyclic azapeptides by A3 -macrocyclization provides high-affinity CD36-modulating peptidomimetics. *Angew. Chem. Int. Ed.* 56, 6284–6288. doi: 10.1002/anie.201611685

Conflict of Interest Statement: The authors declare that the research was conducted in the absence of any commercial or financial relationships that could be construed as a potential conflict of interest.

frontiers in Chemistry

ORIGINAL RESEARCH
published: 30 October 2018
doi: 10.3389/fchem.2018.00522

Diversity-Oriented Synthesis and Chemoinformatic Analysis of the Molecular Diversity of sp^3-Rich Morpholine Peptidomimetics

Elena Lenci, Riccardo Innocenti, Gloria Menchi and Andrea Trabocchi**

Department of Chemistry "Ugo Schiff", University of Florence, Florence, Italy

Diversity-Oriented Synthesis (DOS) consists of generating structurally diverse compounds from a complexity-generating reaction followed by cyclization steps and appendage diversity. DOS has gathered interest to systematically explore the chemical space by generating high-quality small-molecule collections as probes to investigate biological pathways. The generation of heterocycles using amino acid and sugar derivatives as building blocks is a powerful approach to access chemical and geometrical diversity thanks to the high number of stereocenters and the polyfunctionality of such compounds. Our efforts in this field are focused on the generation of diversity-oriented molecules of peptidomimetic nature as a tool addressing protein-protein interactions, taking advantage of amino acid- and sugar-derived polyfunctional building blocks to be applied in couple-pair synthetic approaches. In this paper, the combination of diversity-oriented synthesis and chemoinformatics analysis of chemical space and molecular diversity of heterocyclic peptidomimetics are reported, with particular interest toward carbohydrate- and amino acid-derived morpholine scaffolds with a higher fraction of sp^3 carbon atoms. Also, the chemoinformatic analysis of chemical space and molecular diversity of 186 morpholine peptidomimetics is outlined.

Keywords: chemical diversity, heterocycles, amino acids, carbohydrates, small molecules, building blocks, spiro-lactam

OPEN ACCESS

Edited by:
Andrea Basso,
Università di Genova, Italy

Reviewed by:
Mads Hartvig Clausen,
Technical University of Denmark, Denmark
Bruno Linclau,
University of Southampton, United Kingdom

****Correspondence:***
Elena Lenci
elena.lenci@unifi.it
Andrea Trabocchi
andrea.trabocchi@unifi.it

Specialty section:
This article was submitted to Organic Chemistry, a section of the journal Frontiers in Chemistry

Received: *29 June 2018*
Accepted: *10 October 2018*
Published: *30 October 2018*

Citation:
Lenci E, Innocenti R, Menchi G and Trabocchi A (2018) Diversity-Oriented Synthesis and Chemoinformatic Analysis of the Molecular Diversity of sp^3-Rich Morpholine Peptidomimetics. Front. Chem. 6:522. doi: 10.3389/fchem.2018.00522

INTRODUCTION

When the molecular targets behind a disease are poorly characterized or difficult to identify, the screening of small-molecule libraries is a powerful starting point for drug discovery programmes (Gerry and Schreiber, 2018). This is especially true considering that many biological mechanisms, such as signal transduction or gene expression, are regulated by protein-protein interaction (PPI), "undruggable" targets that cannot be addressed with existing chemical tools (Wells and McClendon, 2007). Even though many synthetic efforts have given a great advance in improving peptide druggability, this class of compounds covers only 2% of the worldwide drug market (Sun, 2013) and the development of new peptidomimetic scaffolds is still a growing field of medicinal chemistry and chemical biology (Kaminker et al., 2018; Ramaswamy et al., 2018). In this context, Diversity-Oriented Synthesis (DOS) (Trabocchi, 2013; Chauhan et al., 2017; Zeng et al., 2017), where many different molecular scaffolds possessing a high structural complexity are developed

using short synthetic strategies, is a convenient approach for the generation of large sets of small molecule peptidomimetics. In particular, in view of creating sp^3-rich molecular entities, with polyfunctional and stereochemically dense characteristics, building blocks from the chiral pool are increasingly used in DOS, as showed by the relevance recently gained by the biosynthetically inspired divergent approach (Yang et al., 2014; Bender et al., 2018), or the diversity-oriented synthesis of natural-product inspired libraries (Huigens et al., 2013; McLeod et al., 2014; Annamalai et al., 2017; Saleeb et al., 2018). Our efforts in this field are focused on the exploitation of amino acid and sugar derivatives for the generation of peptidomimetic libraries around the morpholine skeleton, as this key nucleus is contained in many natural products and drugs (**Figure 1**) (Wijtmans et al., 2004; Pal'chikov, 2013).

Over the years, we reported the synthesis of many different bicyclic compounds **3** based on the 6,8-dioxa-3-azabicyclo[3.2.1]octane core, an atom-by-atom dipeptide isostere. They proved to be active as aspartyl protease inhibitors (SAP2: Trabocchi et al., 2010; Calugi et al., 2012; HIV: Calugi et al., 2014; BACE1: Innocenti et al., 2017) and as RGD integrin ligands (Cini et al., 2009; Bianchini et al., 2012). The short and convenient synthetic strategies consist of combining two key components from the chiral pool, an amino carbonyl derivative **1** and a diol species **2**, followed by the acid-catalyzed acetalization of the resulting coupling intermediate (**Scheme 1A**) (Trabocchi et al., 2006). Representative follow-up chemistry was achieved generating spirocylic scaffolds **4** (Trabocchi et al., 2007). This couple/pair approach proved to be even more interesting in a diversity-oriented point of view when α-amino acid derivatives **6** were combined with dimethoxyacetaldehyde **5**, as morpholine acetal scaffold **7** was a good starting point for the generation of many bi- and tricyclic compounds, such as diketopiperazines **8** and 2-oxa-5-azabicyclo[4.1.0]heptanes **9** (Sladojevich et al., 2008; Lalli et al., 2009; Lenci et al., 2015a) (**Scheme 1B**). Also, bicyclic morpholine lactone **12**, coming from aminoacetaldehyde dimethylacetal **10** and protected methyl threonate derivative **11**, gave structures **13**, taking advantage of lactone aminolysis, and structures **14**, when the aminolysis was combined with diketopiperazine synthesis (Lalli et al., 2009; Ciofi et al., 2010) (**Scheme 1C**).

Also, the combination of mannose **15** with aminoacetaldehyde **10** allowed to obtain morpholine-derived compounds enriched with polyhydroxylated chains (compounds **16**–**19**, **Scheme 2a**) exploiting the reactivity of sugar hydroxyl groups toward the acetal moiety (Lenci et al., 2015b, 2016). Similarly, the application of lactone formation and *trans*-acetalization pairing reactions were used in the synthesis of **21**–**22** starting from the Petasis coupling intermediate obtained by glycolaldehyde **20** (**Scheme 2b**) (Lenci et al., 2017).

Considering that a higher scaffold complexity is generally associated with a more successful outcome in drug discovery and development (Clemons et al., 2010; Galloway et al., 2011; Flagstad et al., 2016; Stotani et al., 2016), we recently turned our attention on exploiting the chemistry useful to develop skeletally complex sp^3-rich morpholines, for example by using multicomponent reactions. In this work, as a further improvement in this direction, we envisioned to install quaternary stereocenters on this nucleus, as they are often present in the structure of many biologically active compounds and pharmaceutical agents (Christoffers and Baro, 2006; Hawner and Alexakis, 2010). This was envisaged by transforming the sp^3 carbon atom in α-position of the carbomethoxy group of different morpholin-3-one starting materials, by means of the Staudinger reaction, to generate morpholinone-derived spiro-β-lactams (**Scheme 3A**), and by different alkylation strategies (**Scheme 3B**).

Finally, the exploration of the chemical space accessed by these new compounds was analyzed using PCA (Principal Component Analysis) and PMI (Principal Moment of Inertia) graphical representation in relation to our in-house library of more than 170 morpholine compounds developed over the years in our laboratory. The entire collection of morpholines was also studied using different chemoinformatic approaches (Colomer et al., 2016) by characterizing the degree of complexity of each library

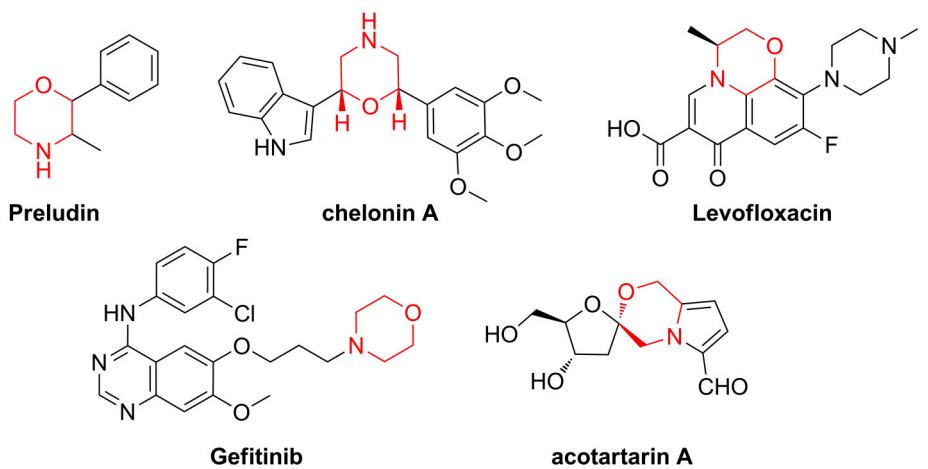

FIGURE 1 | Representative examples of natural products and drugs containing a morpholine ring.

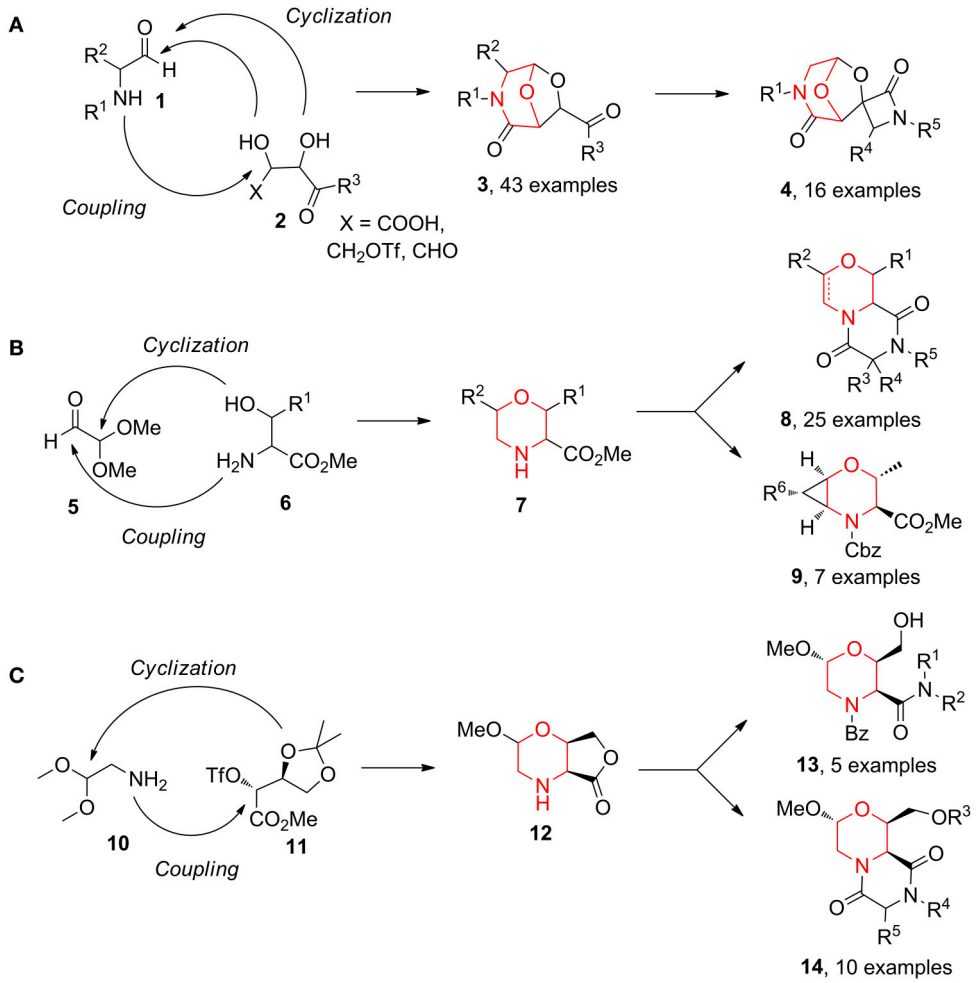

SCHEME 1 | Representative diversity-oriented synthesis of morpholines, starting from amino carbonyl derivative **1** and diol **2 (A)**; from dimethoxyacetaldehyde **5** and amino acid derivative **6 (B)**; and from aminoacetaldehyde **10** and threonate derivative **11 (C)**.

member, by using the Fsp^3 definition (Lovering et al., 2009), and through the relationship between different drug- and lead-like properties.

MATERIALS AND METHODS

Chemistry

Experimental procedures, compound characterization data for newly synthesized compounds **35–38** and **42** and NOESY 1D spectra for compounds **37** and **42**, are reported in the **Supplementary Material**. NMR spectra were collected on a Varian INOVA 400 spectrometer operating at 400 MHz for 1 H. The spectra were obtained in $CDCl_3$ solutions. Proton signals were assigned via TOCSY spectra, and NOESY spectra provided the data used in the conformational analyses. TOCSY spectra were recorded with 2,048 points in t1, 200 points in t2, and 8 scans per t2 increment, and 80 ms as mixing time. NOESY spectra were recorded with a similar number of t1 and t2 points unless otherwise noted, 32 per t2 increment, and 500 ms as mixing time. 1D NOESY experiments were carried out using 64 increments and 500 ms as mixing time.

Molecular Modeling Methods

Molecular modeling calculations were carried out on compounds **35–38** and compound **42** so as to assess the global minimum conformer and to gain insight into the detailed structure of the molecular scaffolds. Energy-minimized conformations of **35–38** and compound **42** were achieved using SPARTAN Version 5.1 (Wavefunction, Inc., Irvine, C). Conformational searches were carried out using Monte Carlo method within MMFF94 force field (Halgren, 1996) and the AM1 semiempirical method (Dewar et al., 1985) was used to optimize the global minimum conformer.

Chemoinformatics Analysis

PCA Analysis

The web-based public tool ChemGPS-NP (http://chemgps.bmc.uu.se/) was used for the PCA analysis of compounds **35–38** and compound **42**, to compare their chemical properties with those of an in-house library of morpholine-derived compounds.

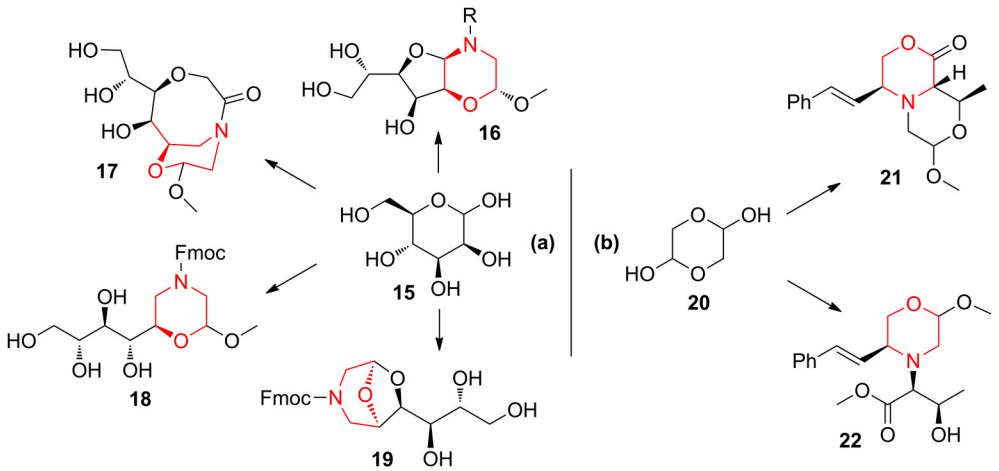

SCHEME 2 | Representative syntheses of morpholine-derived compounds starting from mannose **15 (a)** and from glycolaldehyde **20 (b)**.

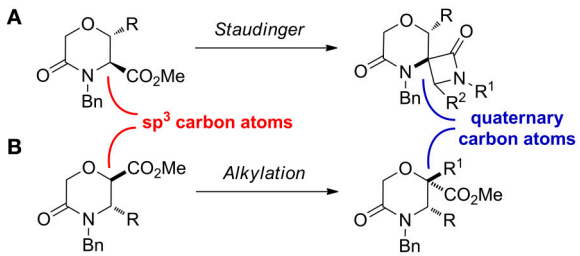

SCHEME 3 | Synthetic approaches exploited to install quaternary carbon atoms on morpholine-3-one. **(A)** the Staudinger ketene-imine reaction on methyl 5-oxomorpholine-3-carboxylate and **(B)** alkylation reaction on methyl 5-oxomorpholine-2-carboxylate.

ChemGPS-NP can be applied for comprehensive chemical space navigation and exploration in terms of global mapping on to a consistent 8-dimensional map of structural characteristics. The first four dimensions of the ChemGPS-NP map capture 77% of data variance. Chemical compounds were positioned onto this map using interpolation in terms of PCA score prediction. SMILES codes for all compounds were retrieved using ChemBioDraw Ultra 12.0 and submitted to ChemGPS-NP for achieving the corresponding PC scores. The PCA data were then used for the construction of PC1 (representing size, shape, and polarizability) vs. PC2 (representing aromatic and conjugation related properties).

PMI Analysis

Principal moments of inertia analysis was carried out by calculating the lowest energy conformation of compounds **35**–**38** and compound **42**, and each compound from an in-house library of morpholine-derived compounds. The conformational search was performed using the built-in AMMP molecular mechanics algorithm with default parameters of the VEGA ZZ molecular modeling software package v.3.0.1 (Pedretti et al., 2002). Once the lowest energy conformer was calculated, the three principal moments of inertia (Ixx, Iyy, Izz) and the normalized principal moments of inertia were determined. Specifically, the three calculated principal moments of inertia were sorted by ascending magnitude I_1, I_2, and I_3. Subsequently, in order to eliminate completely the dependency of the chosen representation on the size of the molecules, normalization was performed by dividing the two lower PMI-values (I_1 and I_2) by the highest value (I_3), generating two characteristic values of normalized PMI ratios (NPRs) for each compound (I_1/I_3 and I_2/I_3). Then, NPR1 (I_1/I_3) and NPR2 (I_2/I_3) were plotted on a triangular graph with the vertices (0,1), (0.5,0.5), and (1,1) representing a perfect rod, disc and sphere, respectively.

Calculation of Medicinally-Relevant Molecular Properties

Molecular weight, cLogP, and the number of sp^3 carbon atoms, stereogenic centers, rotatable bonds, hydrogen bond acceptors and donors were calculated using the web-based public tool FAFDrugs (Free ADME-Tox Filtering Tool), developed at the Paris Diderot University (Lagorce et al., 2015). LogP values are computed by using the xLogP3 program (Cheng et al., 2007), enhanced by employing an in-house library of experimental logP-values from the PHYSPROP database (Lobell et al., 2006) as several models showed that xLogP3 and cLogP methods give similar results (Mannhold et al., 2009). Fsp^3 was calculated as the number of sp^3 hybridized carbon atoms vs. the total carbon count. FC* was calculated as the number of stereocenters vs. the total carbon count. Rotatable bonds were defined as any single bond, not in a ring, bound to a non-terminal heavy (i.e., non-hydrogen) atom, excluding amide C-N bonds. Hydrogen bond donors were taken as the sum of all OHs and NHs, and hydrogen bond acceptors were taken as the sum of all oxygen and nitrogen atoms without a formal positive charge, excluding pyrrole nitrogen, heteroaromatic oxygen and higher oxidation states of nitrogen, in agreement with the Lipinski definition (Lipinski, 1997).

RESULTS AND DISCUSSION

Synthesis

As case study to install quaternary stereocenters on the morpholine nucleus, we explored simple synthetic methodologies capable of transforming the sp^3 carbon atom in the α-position of the carbomethoxy group of different morpholin-3-one compounds. In particular, we selected methyl 5-oxomorpholine-2-carboxylate **25** derived by the application of the Castagnoli-Cushman reaction (Dar'in et al., 2015) between imine **23** and 1,4-dioxane-2,6-dione (**24**), and methyl 5-oxomorpholine-3-carboxylates **28** and **29**, obtained respectively from serine and threonine derivatives **26**-**27** after the acylation with α-bromoacetylbromide and subsequent NaH-mediated intramolecular cyclization reaction (**Scheme 4**). To improve the scaffold complexity and to install quaternary stereocenters on these compounds, we firstly studied the Staudinger reaction (Alcaide et al., 2007; Cossío et al., 2008; Omidvari and Zarei, 2018) with different aromatic imines to generate polycyclic spiro-β-lactams, in agreement with previous studies on 3-aza-6,8-dioxabicyclo[3.2.1]octane bicycles giving compounds **4** (Trabocchi et al., 2007). In particular, compounds **28** and **29** were transformed into the more reactive acyl chloride derivatives **30**–**31** in order to generate the intermediate ketene more easily and to avoid the formation of amide by-products (**Scheme 4**).

However, after refluxing the acyl chloride **30**-**31** in the presence of triethylamine as a base and aromatic imines **32**–**34** in toluene for 16 h, the spiro-β-lactams **35**–**38**, characterized by the 8-oxa-2,5-diazaspiro[3.5]nonane-1,6-dione molecular framework, were obtained in moderate yields, as a consequence of the formation of amide by-products **39**–**41** (**Table 1**).

Considering that the nucleophilicity of the amine derivatives comprising the imine proved to affect the yields, only aromatic imines were taken into account. Also, as shown in **Table 1**, the steric hindrance of both imine and morpholine counterparts resulted in reducing drastically the yield. In particular, best results were obtained starting from serine-derived morpholine **30** using *N*-benzylidene-1-phenylmethanamine **32** and *N*-(4-methoxybenzylidene)-4-methylaniline **33**, even though the higher steric hindrance of this second imine resulted in the achievement of compound **36** in lower yield (35% instead of 52%, **Table 1**, entry 1 and 2). On the other hand, threonine-derived morpholine **31** was found to be less reactive and unstable, as a consequence of the presence of the methyl group adjacent to the ketene functionality. In fact, no reaction was observed with imine **33** (**Table 1**, entry 3), whereas the use of *N*-benzylidene-1-phenylmethanamine **32** and *N*-(4-methoxybenzylidene)-4-phenylmethanamine **34** yielded the spiro compounds **37** and **38** in low yields (**Table 1**, entry 4 and 5, respectively) and with many degradation products, confirming the difficulty in achieving highly substituted spiro-β-lactams, as also reported (Bari and Bhalla, 2010).

Nevertheless, interesting results were obtained as regarding the diastereoselectivity. In fact, despite the four theoretically possible diastereomers, in all cases the *cis*-products were obtained as a major or single stereoisomer, as shown by 1D and 2D NOESY experiments carried out on spiro compound **37** and **35** (see **Figures S13**, **S14**). In particular, the existence of a NOESY peak between H-3 and the methyl group at C-9 for compound **37** proved the relative configuration as reported in **Figure 2**. The absence of any correlation between the methyl group and H-7 suggested that the methyl group is oriented in equatorial position. Although purely indicative, this observation was found to be reasonable for such a constrained structure and was in agreement with the global minimum conformer resulting from molecular modeling calculations (**Figure 2**, right). Specifically, the calculated distance between H-3 and the CH_3 atoms was 2.1 Å, whereas for the other possible diastereomer

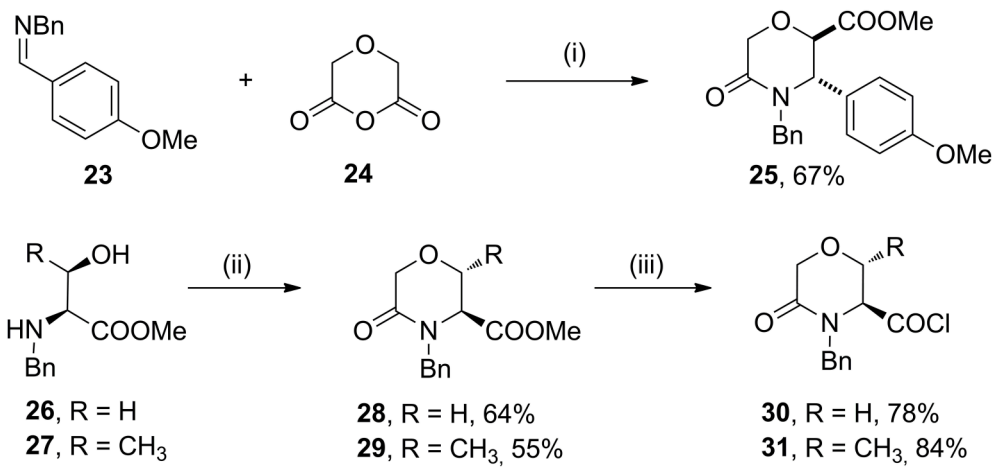

SCHEME 4 | Synthesis of methyl 5-oxomorpholine-2-carboxylate **25** and methyl 5-oxomorpholine-3-carboxylates **28** and **29** and preparation of acyl chloride derivatives **30** and **31**. Reagents and conditions: (i) dry toluene, 80°C, 4 h; then $SOCl_2$, MeOH, reflux, 2 h; (ii) $BrCOCH_2Br$, Et_3N, dry CH_2Cl_2, −15°C, 1 h; then NaH, THF dry, 0 °C - r. t., 1 h; (iii) LiOH, H_2O/THF, r. t., 16 h; then $SOCl_2$, reflux, 2 h.

TABLE 1 | Synthesis of spiro-β-lactams **35**–**38** from serine and threonine-derived morpholine derivatives **30** and **31**.

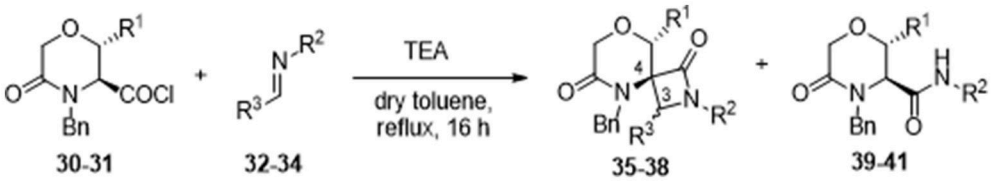

Entry	Imine	R^1	R^2	R^3	Yield (Product)	Diastereomer
1	**32**	H	CH_2Ph	Ph	52% (**35**) + 25% (**39**)	(3,4)-*cis*
2	**33**	H	*p*-CH_3Ph	*p*-OMePh	35% (**36**) + 33% (**40**)	3:1 (3,4)-*cis*/ (3,4)-*trans*
3	**33**	CH_3	*p*-CH_3Ph	*p*-OMePh	–	–
4	**32**	CH_3	CH_2Ph	Ph	15% (**37**)	(3,4)-*cis*
5	**34**	CH_3	CH_2Ph	*p*-OMePh	19% (**38**) + 11% (**41**)	(3,4)-*cis*

at the spiro position this distance was found being more than 4 Å. Similar structural arrangement was ascertained for compound **35**, with the C-1 carbonyl group pointing toward C-9 and the H-3 showing a strong NOESY correlation with H-9 protons, whereas the same *cis*-configuration was evinced for the other compounds by comparing the diagnostic signal of the H-3 proton, which appeared as a singlet in an unambiguous region of ^{1}H-NMR spectrum between 4.74 and 4.84 ppm. This diastereoselectivity is in agreement with what observed for similar spiro-β-lactams obtained starting from proline-derived ketenes (Khasanov et al., 2004) and 6,8-dioxabicyclo[3.2.1]octane-derived ketenes (Trabocchi et al., 2007), as the widely accepted mechanism of the reaction involves the nucleophilic attack of the imine on the ketene species to give a zwitterionic intermediate, which preferentially undergoes an outward conrotatory ring closure, due to stabilizing stereoelectronic effects.

Unfortunately, when the Staudinger reaction was performed between the acid chloride of methyl 5-oxomorpholine-2-carboxylate **25** and aromatic imines **32**–**34**, only degradation products were observed. Thus, in order to install a quaternary stereocenter on this morpholin-3-one, we explored a complementary approach based on an alkylation strategy, and in particular, as a case study, we performed the methylation of the α-carbon of the carbomethoxy group of **25** using NaHDMS as a strong base to generate the intermediate carbanion (**Scheme 5**).

Compound **42** was obtained with 72% yield as a single stereoisomer, showing inversion of the configuration at the α-carbon. Structure analysis performed by NMR and molecular modeling calculations showed a half-chair conformation for the morpholinone scaffold possessing both the methyl and aryl groups in axial position and with a *trans* geometry. Specifically, the *trans* arrangement was ascertained by key NOESY peaks between H-3 and CH_3 at C-2, and a strong NOESY interaction between H-6 and the methyl group at C-2, suggesting the methyl group being positioned in axial orientation (**Figure 3**).

Chemoinformatic Analysis

The exploration of the chemical space accessed by newly synthesized compounds **35**–**42**, in relation to the pool of 176 morpholine-derived small molecules previously synthesized in our laboratories, was then studied by using different chemoinformatic approaches (see **Figure 4** for a scaffold tree composed by all the 16 different molecular frameworks present in this library).

Firstly, Principal Component Analysis (PCA), performed using the web-based public tool ChemGPS-NP, was used to simplify the comparison of all these molecules on the basis of different chemical properties (Xue et al., 2004; Tan, 2005). A pool of 186 compounds was analyzed, focusing in particular on principal component one (PC1), representing size, shape and polarizability, and the principal component two (PC2), that is a direct expression of aromatic and conjugation related properties, and plotted in a graph (**Figure 5**), where compounds **35**–**42** are shown as red diamonds, their parent analogs **25**, **28,** and **29** as blue diamonds, and the previously synthesized morpholines as black squares. All the library members were found being grouped in four different clusters (**Figure 5**, I–IV), depending on both the structure of the skeletons and side chain properties. As regarding to the introduction of quaternary stereocenters in the morpholine nucleus, a peculiar effect was found for the Staudinger reaction products. In fact, although the methylation did not induce any movement within the chemical space, as both compounds **25** and **42** reside in the second cluster, the Staudinger chemistry proved to shift the serine and threonine-derived morpholinone compounds **28**–**29** from the third cluster to the first one (**Figure 5**, red arrow), being populated also by spiro-β-lactams derived from the bicycle 3-aza-6,8-dioxabicyclo[3.2.1]octane, possibly due to the contribution to aromaticity given by the Staudinger reaction with aromatic imines.

This significant movement in the chemical space achieved by the Staudinger chemistry was also observed in the Principal

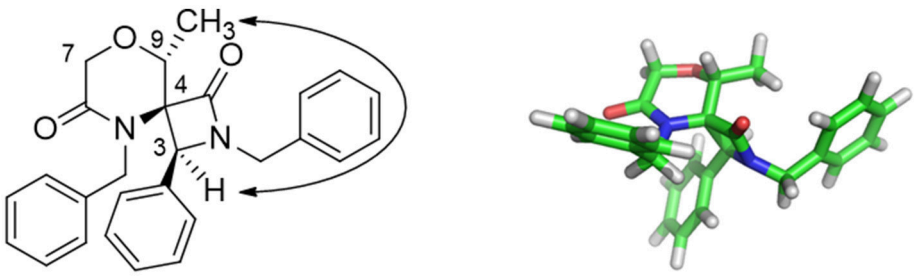

FIGURE 2 | Key NOESY peak **(Left)**, and lowest energy conformer **(Right)** of compound **37** showing the major stereoisomer resulting from the two newly-generated stereocenters at C-3 and C-4.

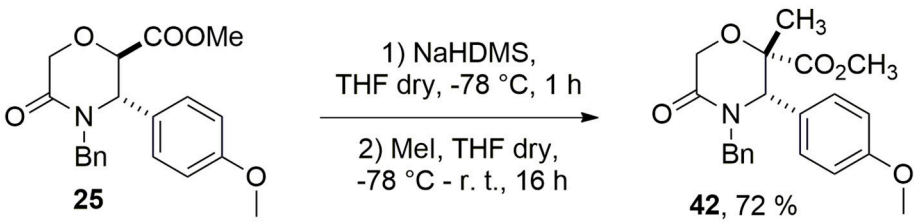

SCHEME 5 | Methylation of 5-oxomorpholine-2-carboxylate **25**.

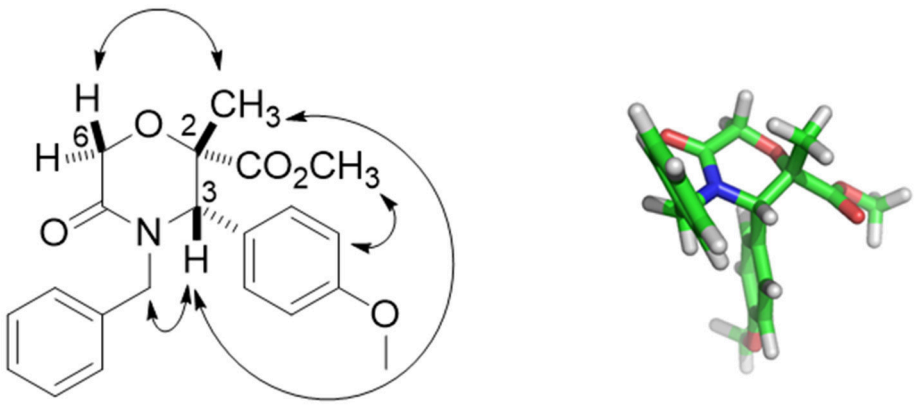

FIGURE 3 | Key NOESY peaks **(Left)**, and lowest energy conformer **(Right)** of compound **42** showing the aryl and methyl groups in axial positions.

Moment of Inertia (PMI) analysis graph (**Figure 6**), obtained by calculating the three principal moments of inertia (I_{xx}, I_{yy}, I_{zz}) and plotting their corresponding normalized values (I_1/I_3 and I_2/I_3) on a triangular graph, where the vertices (0,1), (0.5,0.5), and (1,1) represent a perfect rod (acetylene), disc (benzene) and sphere (adamantane), respectively (Sauer and Schwarz, 2003). As evinced from this graph, morpholine-derived compounds were found to lie along the center-left side of the triangle, as usually observed in the PMI analysis of small molecules. However, while the Staudinger chemistry performed on bicyclic 3-aza-6,8-dioxabicyclo[3.2.1]octanes did not result in a relevant shift in the PMI graph (**Figure 6**, green arrow), the installation of spiro-β-lactams on the morpholin-3-ones **28**–**29** proved to modulate significantly the three-dimensional complexity of these molecular frameworks. Compounds **28**–**29** were found to move from the center of the graph toward the rod-sphere axis (as for spiro-β-lactams **35**, **37, 38**) or the disc corner (as for spiro-β-lactam **36** that contains a *N*-*p*-tolyl group instead of a *N*-benzyl group) (**Figure 6**, red arrows). Also, amide by-products **39**–**41** were found lying closer to the rod-disc axis, as a result of the less three-dimensional character possessed by these structures, when compared to **28**–**29**. On the contrary, the effect of the extra methyl group in compound **42** did not prove to change significantly the shape of the morpholine nucleus, as this compound was found to be close to its parent **25** in the PMI plot. Interestingly, the bicyclic compounds based on

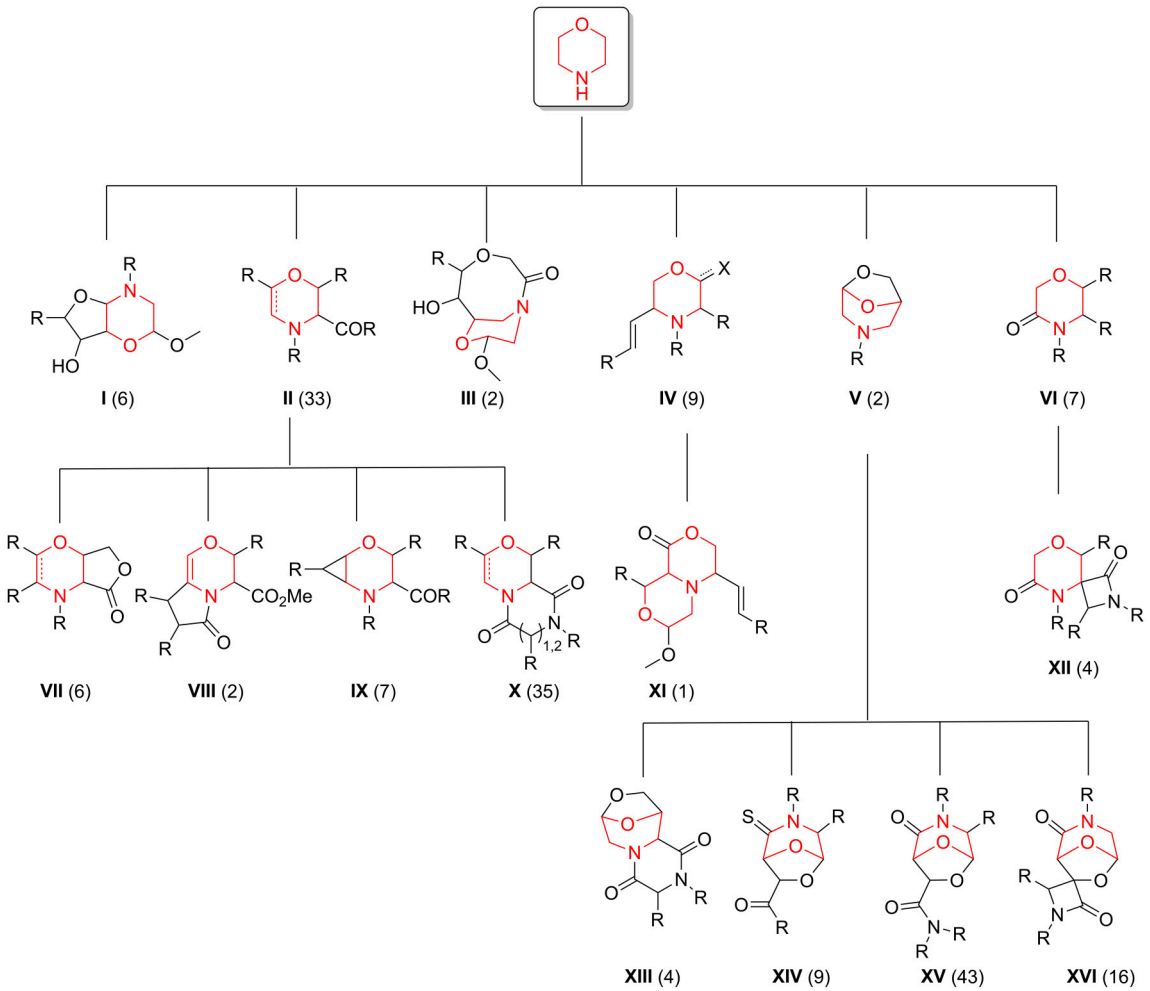

FIGURE 4 | Morpholine-containing molecular scaffolds of our in-house library. The number of compounds in the library representing each scaffold is displayed in brackets.

the 6,8-dioxa-3-azabicyclo[3.2.1]octane core were found to be not close to the sphere region, as expected, possibly due to the major contribution in exploring the space toward the sphere-disc axis given by the side chains, as in the case of some dihydro-1,4-oxazine compounds with peculiar functional groups like the myristoyl chain.

To gain insight into a chemoinformatic evaluation of our in-house morpholine library, we calculated the saturation index (Fsp^3) of each compound collection, as a measure of the molecular complexity (Lovering et al., 2009). This value was calculated as the ratio between the number of sp^3 hybridized carbons in the molecule vs. the total carbon count and compared with those of a reference set of 40 brand-name blockbuster (BB) drugs as reported by Tan (Bauer et al., 2010; Kopp et al., 2012) (**Figure 7**, left). A similar approach was applied also to quantify the presence of stereocenters (**Figure 7**, right), by defining FC* as the ratio of stereogenic center vs. the total carbon count. These two parameters (Fsp^3 and FC*) allow to evaluate the quality of small molecule collections as regarding to the ability of both accessing new areas of the chemical space and giving successful results in drug discovery programmes. Sp^3-rich DOS-derived small molecule collections proved to be more selective and more effective in binding to specific targets, as compared to analog small molecule libraries with lower Fsp^3 ratio (Clemons et al., 2010), although the hit rate trend was found to be opposite in fragment-based screening (Hall et al., 2014). The analysis of the Fsp^3 and FC* parameters revealed that our library possesses higher frequency of molecules with a Fsp^3 in the range between 0.4 and 0.6, as compared to the drugs, and also higher mean value of Fsp^3 (Fsp^3 morpholines = 0.52, Fsp^3 BB drugs = 0.40) and FC* ratio (FC* morpholines = 0.19, FC* BB drugs = 0.05). However, the Staudinger ketene-imine reaction, despite the possibility to introduce a quaternary stereocenter in the molecule, proved not to be a good strategy in terms of improving the Fsp^3 ratio of the overall molecule, since it introduced a high number of sp^2 carbon atoms due to the presence of aromatic appendages. In fact, the Fsp^3 of starting compounds **28** and **29** (respectively 0.38 and 0.43) were reduced dramatically after

the reaction to a mean value of 0.26 for the spiro-β-lactams **35**–**38**.

Finally, the investigation of small molecule physicochemical properties was carried out in order to establish the "druggability" and "lead-likeness" of our library, according to Lipinski's "rule of five" (Lipinski, 1997, 2004; Lipinski and Hopkins, 2004) and Congreve's "rule of three" (Congreve et al., 2003), respectively. In particular, we evaluated the lipophilicity and the molecular weight as key parameters to achieve good solubility, membrane permeability and subsequent oral bioavailability, by plotting clogP values (calculated as the logarithm of the partition coefficient between n-octanol and water) and the molecular weight of each library member in a graph (**Figure 8**, left). Only 12 out of 186 compounds were not compliant with Lipinski's "rule of five," as they showed cLogP values higher than 5 and molecular weight higher than 500. This was evinced for compounds where morpholine was installed in a pentapeptide, or in the case of few bicyclic or morpholines characterized by a large number of aromatic substituents. Forty-five of these compounds were found following the restricted "lead-likeness" filters as proposed by the Congreve's "rule of three," too, proving to be good starting points for potential drug optimization (Teague et al., 1999). Similarly, Veber et al. (2002) have proposed that the number of rotatable bonds (RB), together with the number of hydrogen bond donors (HBD) and hydrogen bond acceptors (HBA), can give another good criteria for predicting oral bioavailability. According to such structural parameters, only 8 compounds of

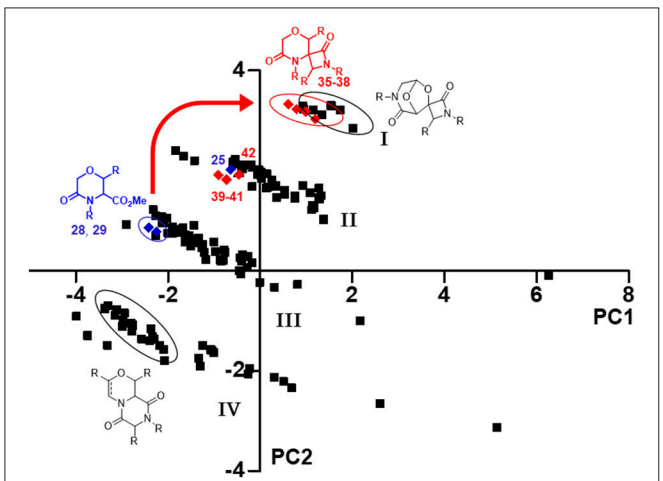

FIGURE 5 | PCA plot resulting from the correlation between PC1 vs. PC2, showing the positioning in the chemical space of compounds **35**–**42** (red diamonds) and their parent analog **25**, **28,** and **29** (blue diamonds), in relation to an in-house library of 176 morpholine compounds (black squares). The thick red arrow indicates the shift in the chemical space induced by Staudinger chemistry from compounds **28–29** to spiro-β-lactams **35**–**38**. The ellipses highlight the various compounds subclasses; the compound clusters are numbered as **I**–**IV**.

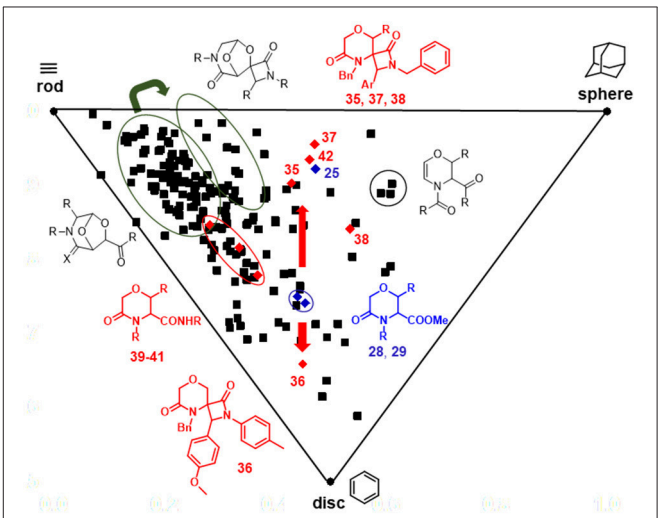

FIGURE 6 | PMI plot showing the skeletal diversity of compounds **35–42** and their parent analogs **25**, **28,** and **29** (red diamonds), in relation to an in-house library of 176 morpholine compounds (black squares). The thick red arrows indicate the shift in the chemical space induced by Staudinger chemistry from compounds **28, 29** to spiro-β-lactams **35**–**38**, whereas the green arrow indicates the shift induced by the same chemistry performed on 6,8-dioxa-3-azabicyclo[3.2.1]octane core. The ellipses highlight the various compounds subclasses.

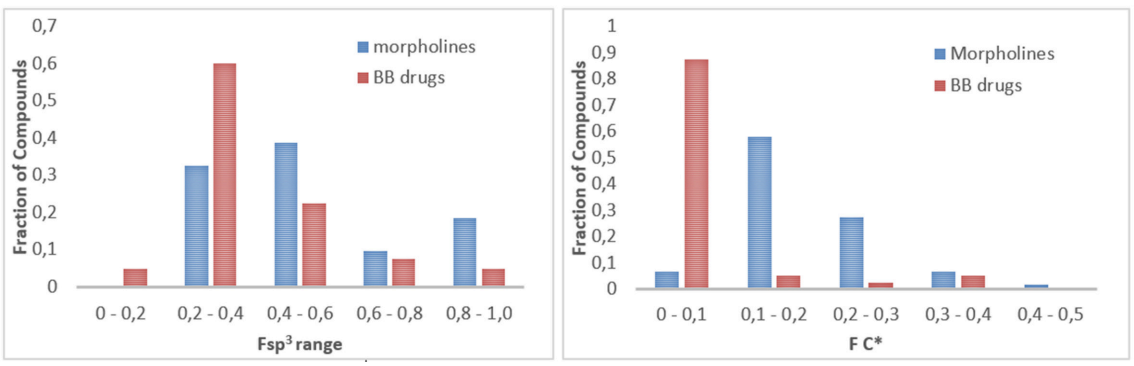

FIGURE 7 | (**Left**) Fraction of compounds (morpholines in blue, blockbuster drugs in red) with different Fsp^3 value, subdivided into 5 different ranges. (**Right**) Fraction of compounds (morpholines in blue, blockbuster drugs in red) with different FC* value, subdivided into 5 different ranges.

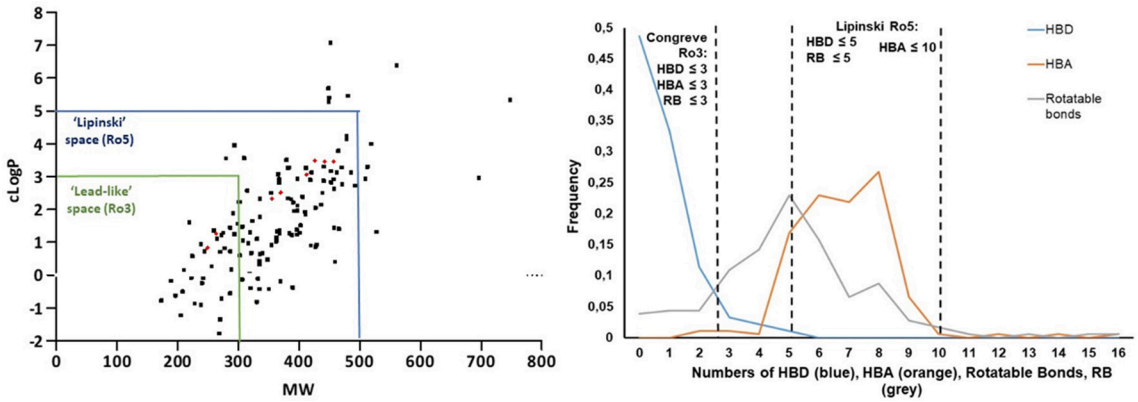

FIGURE 8 | (**Left**) cLogP vs. molecular weight plot highlights all the compounds that follow Lipinski's "rule of five" (Lipiski space, blue box) and lead-likeness "rule of three" (Lead-like space, green box). (**Right**) Fraction of compounds with different number of hydrogen bond donors (HBD, blue line), hydrogen bond acceptors (HBA, orange line) and rotatable bonds (RB, gray line).

our library were found not following the Veber's rule (RB $\leq$ 10 and (HBA + HBD) $\leq$ 12) for a good bioavailability. The graph reported in **Figure 8**, right can easily show that most of the morpholine compounds are within the cut-off values of drug-like Lipinski's "rule of five" (HBA $\leq$ 10, HBD $\leq$ 5, RB $\leq$ 5), whereas only for the number of HBD (blue line) the Congreve lead-like "rule of three" is satisfied (HBD $\leq$ 3, HBA $\leq$ 3, RB $\leq$ 3) (**Figure 8**, right). As expected, no particular changing in the Lipinski drug-like properties were observed for the spiro-β-lactams **35–38** derived from the Staudinger reaction, since the molecular weight and the cLogP values increased significantly, but still remained under the cut-off values of Lipinski's "rule of five," as well as the number of HBA, HBD and rotatable bonds. In particular, the introduction of the nitrogen atom brought another hydrogen bond acceptor to the molecule (moving from 5 to 6) and the number of rotatable bonds increased from 4 to 5 or 6, depending on the imine counterpart.

CONCLUSIONS

The development of new peptidomimetic scaffolds useful to address protein-protein interactions is still a growing field of medicinal chemistry and chemical biology. This approach requires efficient synthetic processes able to produce high-quality small molecule collections, as in the case of the use of Diversity Oriented Synthesis (DOS) strategies, especially starting from amino acid and sugar derivatives, to produce polyfunctional and sp^3-rich building blocks. Our efforts in this field are focused on the generation of different peptidomimetic compounds around the morpholine nucleus, as this heterocycle is contained in many different bioactive molecules.

In order to increase the complexity and the sp^3 character of this important nucleus, we studied different build/couple/pair strategies that exploit complexity-generating reactions. In this work, as a further improvement in this direction, we envisioned to transform the sp^3 carbon atom in α-position of the carbomethoxy group of selected morpholin-3-one starting materials, by means of the Staudinger reaction, to generate morpholinone-derived spiro-β-lactams and of different alkylation strategies. This approach proved to be valuable, especially when assessing the structural diversity and complexity of these new compounds in comparison with 176 morpholine-derived small molecules previously synthesized in our laboratories, by analyzing the populated chemical space. In fact, both PCA (Principal Component Analysis) and PMI (Principal Moment of Inertia) analysis revealed that the Staudinger ketene-imine reaction proved to shift the serine and threonine-derived morpholine-3-one compounds in new areas of the chemical space, assessing a relevant change of positions, hardly achieved by using other synthetic approaches. Finally, we also investigated different small-molecule physicochemical parameters (cLogP, molecular weight, number of rotatable bonds, hydrogen bond acceptors, hydrogen bond donators, Fsp^3, FC*) of all the 186 morpholines of the library in comparison with a reference set of 40 brand-name blockbuster (BB) drugs. These analyses revealed that only few compounds did not show "drug-like" values, as defined by the Lipinski rule of five, whereas most of the compounds showed higher Fsp^3 and FC* values as compared to the drugs. Indeed, several applications in medicinal chemistry projects demonstrated over the years the value of morpholine as a scaffold for peptidomimetic design and drug discovery.

AUTHOR CONTRIBUTIONS

AT and EL conceived the research. EL and RI carried out the synthesis. EL carried out the chemoinformatics analyses. AT carried out the molecular modeling calculations. AT and GM supervised the work. EL and AT wrote the paper. All the authors revised the manuscript.

FUNDING

Financial support from MIUR PRIN2015 (cod. 20157WW5EH), Fondazione CR Firenze and University of Florence are acknowledged.

SUPPLEMENTARY MATERIAL

The Supplementary Material for this article can be found online at: https://www.frontiersin.org/articles/10.3389/fchem.2018.00522/full#supplementary-material

REFERENCES

Alcaide, B., Almendros, P., and Aragoncillo, C. (2007). *Chem. Rev.* 107, 4437–4492. doi: 10.1021/cr0307300

Annamalai, M., Kumar, K., Hristeva, S., Bielska, M., and Ortega, R. (2017). Highly stereoselective synthesis of a compound collection based on the bicyclic scaffolds of natural products. *Molecules* 22:827. doi: 10.3390/molecules22050827

Bari, S. S., and Bhalla, A. (2010). Spirocyclic β-Lactams: synthesis and biological evaluation of novel heterocycles. *Top. Heterocycl. Chem.* 22, 49–99. doi: 10.1007/7081_2009_8

Bauer, R. A., Wurst, J. M., and Tan, D. S. (2010). Expanding the range of 'druggable' targets with natural product-based libraries: an academic perspective. *Curr. Opin. Chem. Biol.* 14, 308–314. doi: 10.1016/j.cbpa.2010.02.001

Bender, C. F., Paradise, C. L., Lynch, V. M., Yoshimoto, F. K., and De Brabander, J. K. (2018). A biosynthetically inspired synthesis of (-)-berkelic acid and analogs, *Tetrahedron* 74, 909–919. doi: 10.1016/j.tet.2018.01.021

Bianchini, F., Cini, N., Trabocchi, A., Bottoncetti, A., Raspanti, S., Vanzi, E., et al. (2012). ^{125}I-Radiolabelled morpholine-containing Arg-Gly-Asp-ligand of $\alpha_v\beta_3$ integrin as a molecular imaging probe for angiogenesis. *J. Med. Chem.* 55, 5024–5033. doi: 10.1021/jm2016232

Calugi, C., Guarna, A., and Trabocchi, A. (2014). Identification of constrained peptidomimetic chemotypes as HIV protease inhibitors. *Eur. J. Med. Chem.* 84, 444–453. doi: 10.1016/j.ejmech.2014.07.049

Calugi, C., Trabocchi, A., De Bernardis, F., Arancia, S., Navarra, P., Cauda, R., et al. (2012). Bicyclic Peptidomimetics targeting secreted aspartic Protease 2 (SAP2) from *Candida albicans* reveal a constrained inhibitory chemotype. *Bioorg. Med. Chem.* 20, 7206–7213. doi: 10.1016/j.bmc.2012.09.031

Chauhan, J., Luthra, T., Gundla, R., Ferraro, A., Holzgrabe, U., and Sen, S. (2017). A Diversity oriented synthesis of natural product inspired molecular libraries. *Org. Biomol. Chem.* 15, 9108–9120. doi: 10.1039/C7OB02230A

Cheng, T., Zhao, Y., Li, X., Lin, F., Xu, Y., Zhang, X., et al. (2007). Computation of octanol-water partition coefficients by guiding an additive model with knowledge. *J. Chem. Inf. Model.* 47, 2140–2148. doi: 10.1021/ci700257y

Christoffers, J., and Baro, A. (2006). *Quaternary Stereocenters: Challenges and Solutions for Organic Synthesis*. Hoboken, NJ: John Wiley & Sons.

Cini, N., Trabocchi, A., Menchi, G., Bottoncetti, A., Raspanti, S., Pupi, A., et al. (2009). Morpholine-based RGD-cyclopentapeptides as $\alpha_v\beta_3/\alpha_v\beta_5$ integrin ligands: role of configuration towards receptor binding affinity. *Bioorg. Med. Chem.* 17, 1542–1549. doi: 10.1016/j.bmc.2009.01.006

Ciofi, L., Morvillo, M., Sladojevich, F., Guarna, A., and Trabocchi, A. (2010). Skeletal diversity by sequential one-pot and stepwise routes using morpholine ester scaffolds. *Tetrahedron Lett.* 51, 6282–6285. doi: 10.1016/j.tetlet.2010.09.103

Clemons, P. A., Bodycombe, N. E., Carrinski, H. A., Wilson, J. A., Shamji, A. F., Wagner, B. K., et al. (2010). Small molecules of different origins have distinct distributions of structural complexity that correlate with protein-binding profiles. *Proc. Natl. Acad. Sci. U.S.A.* 107, 18787–18792. doi: 10.1073/pnas.1012741107

Colomer, I., Empson, C. J., Craven, P., Owen, Z., Doveston, R. G., Churcher, I., et al. (2016). A divergent synthetic approach to diverse molecular scaffolds: assessment of lead-likeness using LLAMA, an open-access computational tool. *Chem. Commun.* 52, 7209–7212. doi: 10.1039/C6CC03244C

Congreve, M., Carr, R., Murray, C., and Jhoti, H. (2003). A 'rule of three' for fragment-based lead discovery? *Drug Discov. Today* 8, 876–877. doi: 10.1016/S1359-6446(03)02831-9

Cossío, F. P., Arrieta, A., and Sierra, M. A. (2008). The mechanism of the Ketene–Imine (Staudinger) reaction in its centennial: still an unsolved problem? *Acc. Chem. Res.* 41, 925–936. doi: 10.1021/ar800033j

Dar'in, D., Bakulina, O., Chizhova, M., and Krasavin, M. (2015). New heterocyclic product space for the Castagnoli–Cushman three-component reaction. *Org. Lett.* 17, 3930–3933. doi: 10.1021/acs.orglett.5b02014

Dewar, M. J. S., Zoebisch, E. G., Healy, E. F., and Stewart, J. J. P. (1985). Development and use of quantum mechanical molecular models. 76. AM1: a new general purpose quantum mechanical molecular model. *J. Am. Chem. Soc.* 107, 3902 – 3909. doi: 10.1021/ja00299a024

Flagstad, T., Min, G., Bonnet, K., Morgentin, R., Roche, D., Clausen, M. H., et al. (2016). Synthesis of sp3-rich scaffolds for molecular libraries through complexity-generating cascade reactions. *Org. Biomol. Chem.* 14, 4943–4946. doi: 10.1039/C6OB00961A

Galloway, W. R. J. D., Isidro-Llobet, A., and Spring, D. R. (2011). Diversity-oriented synthesis as a tool for the discovery of novel biologically active small molecules. *Nat. Commun.* 1:80. doi: 10.1038/ncomms1081

Gerry, C. J., and Schreiber, S. L. (2018). Chemical probes and drug leads from advances in synthetic planning and methodology. *Nat. Rev. Drug Discov.* 17, 333–352. doi: 10.1038/nrd.2018.53

Halgren, T. A. (1996). Merck molecular force field. I. Basis, form, scope, parameterization, and performance of MMFF94. *J. Comput. Chem.* 17, 490–519. doi: 10.1002/(SICI)1096-987X(199604)17:5/6<490::AID-JCC1>3.0.CO;2-P

Hall, R. J., Mortenson, P. N., and Murray, C. W. (2014). Efficient exploration of chemical space by fragment-based screening. *Prog. Biophys. Mol. Biol.* 116, 82–91. doi: 10.1016/j.pbiomolbio.2014.09.007

Hawner, C., and Alexakis, A. (2010). Metal-catalyzed asymmetric conjugate addition reaction: formation of quaternary stereocenters. *Chem. Commun.* 46, 7295–7306. doi: 10.1039/c0cc02309d

Huigens, R. W., Morrison, K. C., Hicklin, R. W., Flood, T. A., Richter, M. F., and Hergenrother, P. J. (2013). A ring-distortion strategy to construct stereochemically complex and structurally diverse compounds from natural products. *Nat. Chem.* 5, 195–202. doi: 10.1038/nchem.1549

Innocenti, R., Lenci, E., Menchi, G., Pupi, A., and Trabocchi, A. (2017). Design and synthesis of bicyclic acetals as Beta Secretase (BACE1) inhibitors. *Bioorg. Med. Chem.* 25, 5077–5083. doi: 10.1016/j.bmc.2017.03.030

Kaminker, R., Kaminker, I., Gutekunst, W. R., Luo, Y., Lee, S., Niu, J., et al. (2018). Tuning conformation and properties of peptidomimetic backbones through dual N/Cα-substitution, *Chem. Commun.* 54, 5237–5240. doi: 10.1039/C8CC01356J

Khasanov, A. B., Ramirez-Weinhouse, M. M., Webb, T. R., and Thiruvazhi, M. (2004). Novel asymmetric approach to proline-derived Spiro-β-lactams. *J. Org. Chem.* 69, 5766–5769. doi: 10.1021/jo049430o

Kopp, F., Stratton, C. F., Akella, L. B., and Tan, D. S. (2012). A diversity-oriented synthesis approach to macrocycles via oxidative ring expansion. *Nat. Chem. Biol.* 2012, 358–365. doi: 10.1038/nchembio.911.

Lagorce, D., Sperandio, O., Baell, J. B., Miteva, M. A., and Villoutreix, B. O. (2015). FAF-Drugs3: a web server for compound property calculation and chemical library design. *Nucleic Acids Res.* 1, 200–207. doi: 10.1093/nar/gkv353

Lalli, C., Trabocchi, A., Sladojevich, F., Menchi, G., and Guarna, A. (2009). Diversity-oriented synthesis of morpholine-containing molecular scaffolds. *Chem. Eur. J.* 5, 7871–7875. doi: 10.1002/chem.200900744

Lenci, E., Innocenti, R., Biagioni, A., Menchi, G., Bianchini, F., and Trabocchi, A. (2016). Identification of novel human breast Carcinoma (MDA-MB-231) cell growth modulators from a carbohydrate-based diversity oriented synthesis library. *Molecules* 21:1405. doi: 10.3390/molecules21101405

Lenci, E., Innocenti, R., Menchi, G., Faggi, C., and Trabocchi, A. (2015a). Two-step one-pot synthesis of dihydropyrazinones as Xaa-Ser dipeptide isosteres through morpholine acetal rearrangement. *Org. Biomol. Chem.* 13, 7013–7019. doi: 10.1039/C5OB00783F

Lenci, E., Menchi, G., Guarna, A., and Trabocchi, A. (2015b). Skeletal diversity from Carbohydrates: use of mannose for the diversity-oriented synthesis of Polyhydroxylated compounds. *J. Org. Chem.* 80, 2182–2191. doi: 10.1021/jo502701c

Lenci, E., Rossi, A., Menchi, G., and Trabocchi, A. (2017). Short synthesis of polyfunctional sp3-rich threonine-derived morpholine scaffolds. *Org. Biomol. Chem.* 15, 9710–9717. doi: 10.1039/C7OB02454A

Lipinski, C., and Hopkins, A. (2004). Navigating chemical space for biology and medicine. *Nature* 432, 855–861. doi: 10.1038/nature03193

Lipinski, C. A. (1997). Experimental and computational approaches to estimate solubility and permeability in drug discovery and development settings. *Adv. Drug Deliv. Rev.* 46, 3–26. doi: 10.1016/S0169-409X(96)00423-1

Lipinski, C. A. (2004). Lead- and drug-like compounds: the rule-of-five revolution. *Drug Discov. Today* 1, 337–341. doi: 10.1016/j.ddtec.2004.11.007

Lobell, M., Hendrix, M., Hinzen, B., Keldenich, J., Meier, H., Schmeck, C., et al. (2006). *In silico* ADMET traffic lights as a tool for the prioritization of HTS hits. *ChemMedChem* 1, 1229–1236. doi: 10.1002/cmdc.200600168

Lovering, F., Bikker, J., and Humblet, C. (2009). Escape from Flatland: increasing saturation as an approach to improving clinical success. *J. Med. Chem.* 2009, 6752–6756. doi: 10.1021/jm901241e

Mannhold, R., Poda, G. I., Ostermann, C., and Tetko, I. V. (2009). Calculation of molecular lipophilicity: state-of-the-art and comparison of logP methods on more than 96,000 compounds. *J. Pharm. Sci.* 98, 861–893. doi: 10.1002/jps.21494

McLeod, M. C., Singh, G., Plampin, J. N., Rane, D., Wang, J. L., Day, V. W., et al. (2014). Probing chemical space with alkaloid-inspired libraries. *Nat. Chem.* 6, 133–140. doi: 10.1038/nchem.1844

Omidvari, Z., and Zarei, M. (2018). Synthesis of novel β-Lactams from Phenothiazin-10-ylacetic acid. *J. Heterocyclic Chem.* 55, 1085–1091. doi: 10.1002/jhet.3138

Pal'chikov, V. A. (2013). Morpholines. Synthesis and biological activity. *Russ. J. Org. Chem.* 49, 787–814. doi: 10.1134/S1070428013060018

Pedretti, A., Villa, L., and Vistoli, G. (2002). VEGA: a versatile program to convert, handle and visualize molecular structure on Windows-based PCs. *J. Mol. Graph.* 21, 47–49. doi: 10.1016/S1093-3263(02)00123-7

Ramaswamy, K., Forbes, L., Minuesa, G., Gindin, T., Brown, F., Kharas, M. G., et al. (2018). Peptidomimetic blockade of MYB in acute myeloid leukemia. *Nat. Commun.* 9, 1–13. doi: 10.1038/s41467-017-02618-6

Saleeb, M., Mojica, S., Eriksson, A. U., Andersson, C. D., Gylfe, A., and Elofsson, M. (2018). Natural product inspired library synthesis - Identification of 2,3-diarylbenzofuran and 2,3-dihydrobenzofuran based inhibitors of *Chlamydia trachomatis*. *Eur. J. Med. Chem.* 143, 1077–1089. doi: 10.1016/j.ejmech.2017.11.099

Sauer, W. H. B., and Schwarz, M. K. (2003). Molecular shape diversity of combinatorial libraries: a prerequisite for broad bioactivity. *J. Chem. Inf. Comput. Sci.* 43, 987–1003. doi: 10.1021/ci025599w

Sladojevich, F., Trabocchi, A., and Guarna, A. (2008). Stereoselective cyclopropanation of serine- and threonine-derived oxazines to access new morpholine-based scaffolds. *Org. Biomol. Chem.* 6, 3328–3336. doi: 10.1039/b808895k

Stotani, S., Lorenz, C., Winkler, M., Medda, F., Picazo, E., Martinez, R. O., et al. (2016). Design and synthesis of Fsp3-Rich, Bis-Spirocyclic-based compound libraries for biological screening. *ACS Comb. Sci.* 18, 330–336. doi: 10.1021/acscombsci.6b00005

Sun, L. (2013). Peptide-based drug development. *Mod. Chem. Appl.* 1:e103. doi: 10.4172/2329-6798.1000e103

Tan, D. S. (2005). Diversity-oriented synthesis: exploring the intersections between chemistry and biology. *Nat. Chem. Biol.* 1, 74–84. doi: 10.1038/nchembio0705-74

Teague, S. J., Davis, A. M., Leeson, P. D., and Oprea, T. (1999). The design of leadlike combinatorial libraries. *Angew. Chem. Int. Ed.* 38, 3743–3748. doi: 10.1002/(SICI)15213773(19991216)38:24 <3743::AID-ANIE3743>3.0.CO;2-U

Trabocchi, A. (2013). *Diversity-Oriented Synthesis: Basics and Applications in Organic Synthesis, Drug Discovery, and Chemical Biology*. Hoboken, NJ: John Wiley & Sons.

Trabocchi, A., Lalli, C., Guarna, F., and Guarna, A. (2007). Diastereoselective synthesis of highly constrained Spiro-β-Lactams by the Staudinger reaction using an unsymmetrical bicyclic ketene. *Eur. J. Org. Chem.* 16, 4594–4599. doi: 10.1002/ejoc.200700260

Trabocchi, A., Mannino, C., Machetti, F., De Bernardis, F., Arancia, S., Cauda, R., et al. (2010). Identification of inhibitors of drug-resistant *Candida albicans* strains from a library of bicyclic peptidomimetic compounds. *J. Med. Chem.* 53, 2502–2509. doi: 10.1021/jm901734u

Trabocchi, A., Menchi, G., Guarna, F., Machetti, F., Scarpi, D., and Guarna, A. (2006). Design, synthesis and applications of aza 6,8-dioxa-bicyclo[3.2.1]octane-based scaffolds for peptidominetic chemistry. *Synlett* 3, 331–353. doi: 10.1055/s-2006-926249

Veber, D. F., Johnson, S. R., Cheng, H. Y., Smith, B. R., Ward, K. W., and Kopple, K. D. (2002). Molecular properties that influence the oral bioavailability of drug candidates. *J. Med. Chem.* 6, 2615–2623. doi: 10.1021/jm020017n

Wells, J. A., and McClendon, C. L. (2007). Reaching for high-hanging fruit in drug discovery at protein–protein interfaces. *Nature* 450, 1001–1009. doi: 10.1038/nature06526

Wijtmans, R., Vink, M. K. S., Schoemaker, H. E., van Delft, F. L., Blaauw, R. H., and Rutjes, F. P. J. T. (2004). Biological relevance and synthesis of C-substituted morpholine derivatives. *Synthesis* 5, 641–662. doi: 10.1055/s-2004-816003

Xue, L., Stahura, F., and Bajorath, J. (2004). "Cell-based partitioning," in *Chemoinformatics,* ed J. Bajorath (Totowa, NJ: Humana Press), 279–289

Yang, Y., Bai, Y., Sun, S., and Dai, M. (2014). Biosynthetically inspired divergent approach to Monoterpene Indole alkaloids: total synthesis of Mersicarpine, Leuconodines, B., and D, Leuconoxine, Melodinine, E., Leuconolam, and Rhazinilam. *Org. Lett.* 16, 6216–6219. doi: 10.1021/ol503150c

Zeng, J., Sun, G., Yao, W., Zhu, Y., Wang, R., Cai, L., et al. (2017). 3-Aminodeoxypyranoses in Glycosylation: diversity-oriented synthesis and assembly in Oligosaccharides. *Angew. Chem. Int. Ed.* 56, 5227–5231. doi: 10.1002/anie.201700178

Conflict of Interest Statement: The authors declare that the research was conducted in the absence of any commercial or financial relationships that could be construed as a potential conflict of interest.

frontiers in Chemistry

ORIGINAL RESEARCH
published: 06 September 2018
doi: 10.3389/fchem.2018.00369

Exploitation of the Ugi 5-Center-4-Component Reaction (U-5C-4CR) for the Generation of Diverse Libraries of Polycyclic (Spiro)Compounds

Lisa Moni[1], *Fabio De Moliner*[1], *Silvia Garbarino*[1], *Jörn Saupe*[2], *Christian Mang*[2]* *and Andrea Basso*[1]*

[1] Dipartimento di Chimica e Chimica Industriale, Università degli Studi di Genova, Genova, Italy, [2] AnalytiCon Discovery GmbH, Potsdam, Germany

OPEN ACCESS

Edited by:
Ramon Rios,
University of Southampton,
United Kingdom

Reviewed by:
Jung Woon Yang,
Sungkyunkwan University, South Korea
Sami Lakhdar,
École Nationale Supérieure d'Ingénieurs De Caen, France

***Correspondence:**
Christian Mang
c.mang@ac-discovery.com
Andrea Basso
andrea.basso@unige.it

Specialty section:
This article was submitted to Organic Chemistry, a section of the journal Frontiers in Chemistry

Received: 18 June 2018
Accepted: 02 August 2018
Published: 06 September 2018

Citation:
Moni L, De Moliner F, Garbarino S, Saupe J, Mang C and Basso A (2018) Exploitation of the Ugi 5-Center-4-Component Reaction (U-5C-4CR) for the Generation of Diverse Libraries of Polycyclic (Spiro)Compounds. Front. Chem. 6:369. doi: 10.3389/fchem.2018.00369

An Ugi multicomponent reaction with chiral cyclic amino acids, benzyl isocyanide and cyclic ketones (or acetone) has been exploited as key step for the generation of peptidomimetics. After a straightforward set of elaborations, the peptidomimetics were converted into polycyclic scaffolds displaying two orthogonally protected secondary amines. Libraries of compounds were obtained decorating the molecules through acylation/reductive amination reactions on these functional groups.

Keywords: multicomponent reactions, diversity oriented synthesis, scaffold diversity, combinatorial libraries, isocyanides

INTRODUCTION

Drug research is nowadays suffering from the relatively low number of newly approved medicines with a clear health benefit for patients. One of the pitfalls has been recognized in the inadequate availability of potential new starting points for library generation. Structurally novel scaffolds with new modes of action are therefore highly desirable, and the possibility to assemble them through straightforward, yet complexity generating, procedures is a major challenge.

Multicomponent reactions (MCRs) (Orru and de Greef, 2003; Touré and Hall, 2009) are a very powerful tool in the hands of organic chemists, enabling them to assemble complex scaffolds from relatively simple building blocks in just one synthetic step. Among MCRs, isocyanide (Koopmanschap et al., 2014; Giustiniano et al., 2017)-based ones, and specifically the Ugi reaction (U-4CR) (Dömling and Ugi, 2000; Dömling, 2006), are by far the most versatile and exploited ones, also because different variants are available. One of these is the so-called Ugi-5-center-4-component reaction (U-5C-4CR) that, employing α (Demharter et al., 1996; Ugi et al., 1996; Park et al., 1998; Kim et al., 2001; Zimmer et al., 2001; Liu and Dömling, 2009; Mandai et al., 2011; Mimura et al., 2015)- or β (Basso et al., 2004, 2005, 2010)-amino acids as bifunctional reagents, generates α,α′-imino dicarboxylic acid derivatives **A** according to the general mechanism depicted in **Scheme 1**.

The U-5C-4CR has been recently used by Dawidowski (Dawidowski et al., 2012) to prepare 2,6-diketopiperazines **B** starting from proline as aminoacid component, exploiting an intramolecular transamidation between the primary amido group deriving from the cleavage of the *tert*-butyl isocyanide side-chain and the methyl ester group generated during

the multicomponent step (**Scheme 2**). In our hands, when the carbonyl component of the multicomponent step was a ketone, cyclization of **A** to imide **C** partially occurred during the Ugi reaction, even on the secondary amide deriving from unhindered isocyanides (**Scheme 2**; Dawidowski et al., 2014). With the aim to expand the scope of this chemistry, and due to overexploited synthesis of diketopiperazine libraries for biological applications (Perrotta et al., 2001; Fischer, 2003), we envisioned the possibility to further elaborate structures **C**, through a set of transformations amenable to afford original scaffolds, in optically pure form, with additional reactive groups amenable of selective functionalizations. In this paper we report our results.

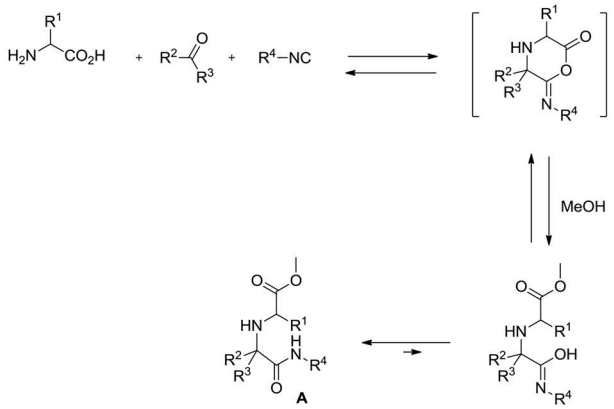

SCHEME 1 | Mechanism of the Ugi 5-center-4-component reaction (U-5C-4CR).

RESULTS AND DISCUSSION

Our studies started by investigating the reactivity of *trans*-4-hydroxy-L-proline with *N*-Boc-azetidinone and benzyl isocyanide in methanol (**Scheme 3**). Different reasons were at the basis of the choice of the carbonyl component: first of all, by using a symmetrical ketone, no additional stereocenters were generated during the Ugi reaction (often showing poor

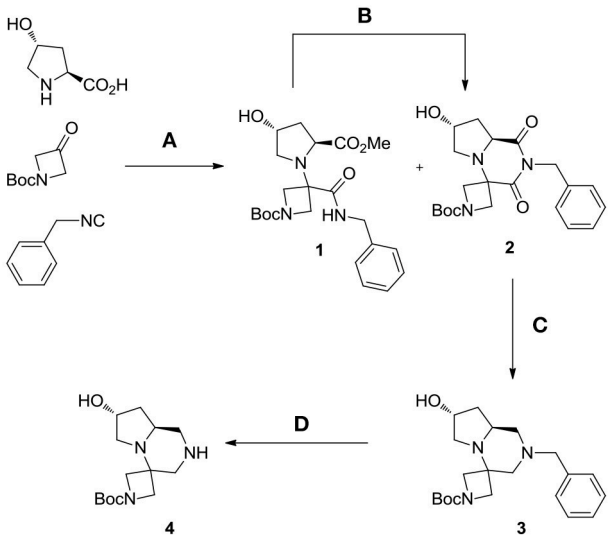

SCHEME 3 | Synthesis of spiro tricyclic scaffold **4**. Reagents and conditions: **(A)** MeOH, 65°C, sealed tube; **(B)** DBU, acetonitrile, rt, 47%; **(C)** borane-Me_2S complex, THF, 60°C, then MeOH, rt, 76%; **(D)** H_2 (55 psi), EtOH, rt, quantitative.

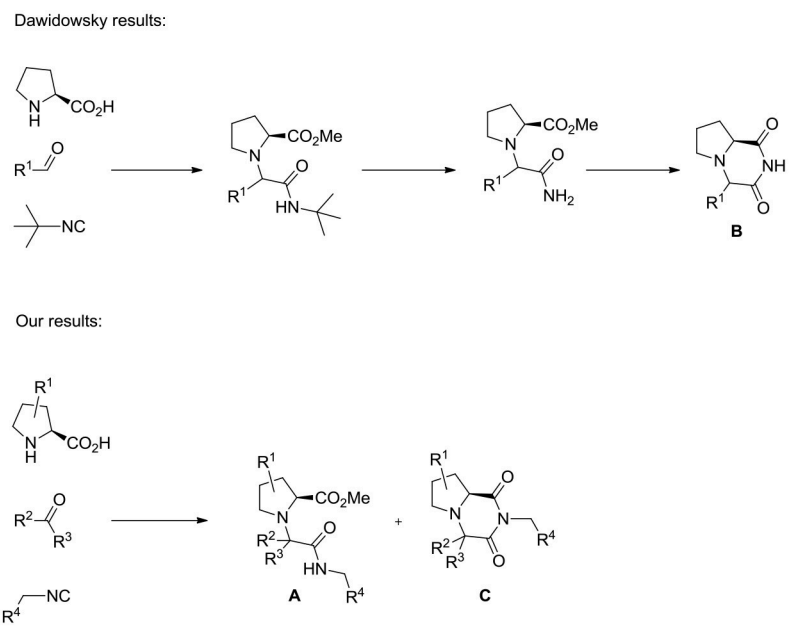

SCHEME 2 | Different outcomes of the reaction between proline derivatives, carbonyl compounds and isocyanides.

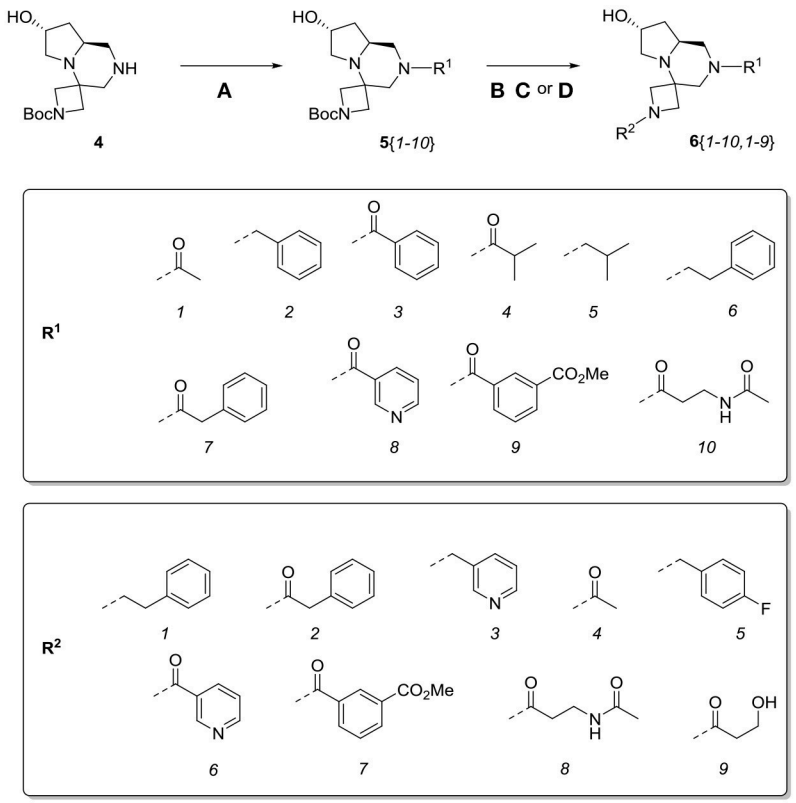

SCHEME 4 | Library generation starting from scaffold **4**. Reagents and conditions: **(A)** acyl chloride, Et_3N, DCM, rt or carboxylic acid, TBTU, DIPEA, DCM, rt; **(B)** acyl chloride or sulfonyl chloride, Et_3N, DCM or **(C)** isocyanate, DCM or **(D)** aldehyde/ketone, borane-Me_2S complex, DCM.

stereoselectivity); then the use of a cyclic ketone allowed us to obtain spiro compounds, privileged structures characterized by high conformational stability; finally, the employment of an *N*-protected azetidinone could be straightforwardly exploited for further functionalizations.

The contemporary presence of a secondary amino group and a cyclic ketone kinetically disfavored the Ugi reaction, which did not proceed at room temperature, even with the addition of a Lewis acid as previously reported by Dawidowski for other substrates (Dawidowski et al., 2014). However, by performing it in a sealed tube at 65°C, a mixture of Ugi adduct **1** and cyclic imide **2** was isolated after 6 days. This mixture was subjected to complete cyclization by addition of a catalytic amount of DBU in acetonitrile. The overall yield after the two steps was an acceptable 47% and remarkably, under these conditions, no epimerization was observed at the L-proline a-carbon, thus allowing us to obtain compound **2** in enantiomerically and diastereomerically pure form.

The subsequent step was the conversion of imide **2** into tertiary amine **3**, exploiting a borane-mediated reduction developed in our laboratories. After careful optimization of the reaction conditions, it was found that, by employing a large excess of borane-dimethylsulfide complex and by heating the mixture at 60°C for 24 h, complete conversion was obtained. From a practical point of view the addition of borane was best performed at 0°C in two aliquots, a white flocculate was observed with the reaction proceeding. Upon completion, slow addition of methanol at 0°C resulted in decomposition of excess borane; however, in order to break complexes between boron and the basic nitrogen atoms of the product, the methanolic solution was left stirring at room temperature overnight.

The crude material was purified by flash chromatography, yielding the desired product **3** in 76% yield. The spiro tricyclic system obtained was the starting point for the generation of a library of compounds. The library generation contemplated the successive deprotection and acylation of the benzyl- and Boc-protected nitrogen atoms, respectively.

Deprotection of the benzyl group was found more difficult than expected and only after 2 days under H_2 pressure (55 psi) with one replacement of the catalyst (10% Pd/C) after the first day the desired compound **4** was obtained upon filtration, without need of further purification (**Scheme 3**).

At this stage, reaction with various acyl chlorides or activated carboxylic acids afforded a first set of compounds. No acylation of the secondary alcohol moiety was observed and reactions proceeded usually with 70–80% yield for compounds **5**{*1,3,4,7–10*} (**Scheme 4**). In order to introduce a higher degree of diversification between the library members, alkylated products **5**{2,5–6} were also included. Compounds **5**{*5–6*} were prepared with an alternative strategy that involved the use, respectively

TABLE 1 | HPLC-UV purities of library members **6**{*1–10,1–9*}.

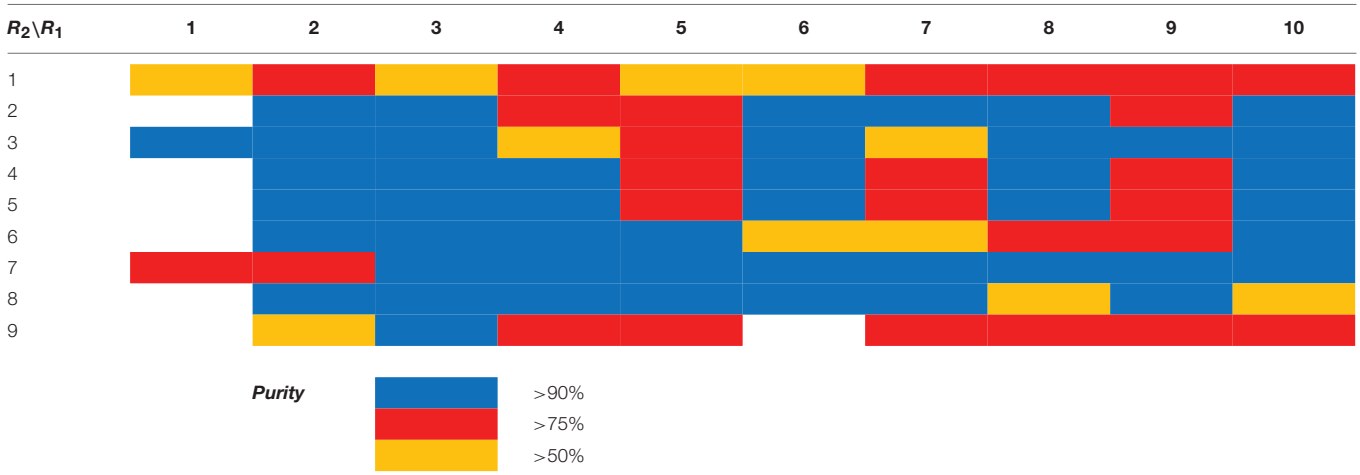

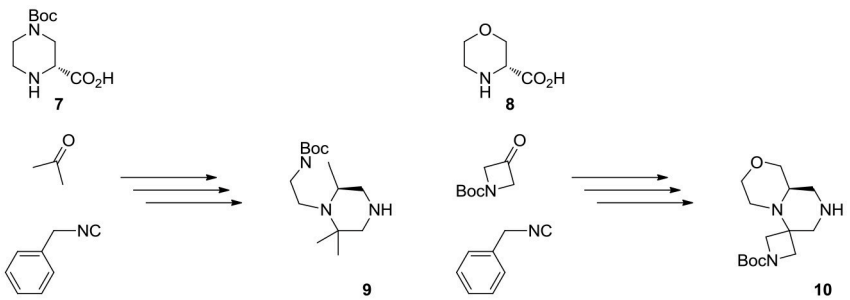

SCHEME 5 | Multicomponent approach to the synthesis of scaffolds **9** and **10**. See experimental part for details.

of phenetyl or isobutyl isonitrile in the initial Ugi reaction with hydroxyproline and *N*-Boc-azetidinone. The multicomponent adducts followed the same sequence of transamidation and imide reduction affording directly **5**{*5–6*}. Compound **5**{*2*}, on the other hand, already derived from the same sequence with benzyl isocyanide. All compounds were fully characterized (see experimental part and **Data Sheet 1**).

With the diversomers **5**{*1–10*} in hand in multigram scale, we proceeded with the introduction of the second diversity input, by cleavage of the Boc group (HCl/MeOH) and elaboration of the free secondary amino group. This was carried out by decoration with acid chlorides, sulfonyl chlorides, isocyanates, aldehydes and ketones using standard conditions affording compound library **6**{*1–10,1–9*} (**Scheme 4**). The final compounds were obtained in 50–100 mg scale, usually with purities higher than 75% (**Table 1**).

The overall synthetic methodology was extended to other two enantiomerically pure cyclic amino acids, namely (R)-4-(*tert*-butoxycarbonyl)piperazine-2-carboxylic acid **7** and (R)-morpholine-2-carboxylic acid **8** (**Scheme 5**). In the first instance, the piperazine ring already possessed an additional Boc-protected amino group, therefore the Ugi reaction was performed with acetone, affording scaffold **9**. In the second case, *N*-Boc-azetidinone was used instead, in analogy with the first library described in this paper.

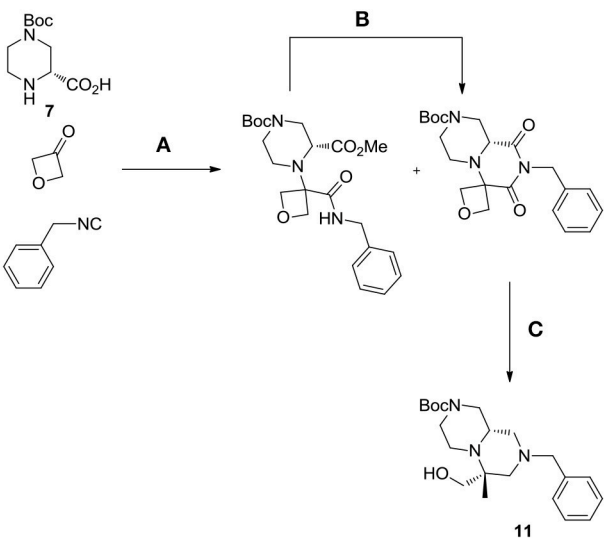

SCHEME 6 | Unexpected outcome of the reaction with oxetanone as carbonyl component. Reagents and conditions: **(A)** MeOH, 65°C, sealed tube; **(B)** DBU, acetonitrile, rt, 54%; **(C)** borane-Me_2S complex, THF, 60°C, then MeOH, rt, 57%.

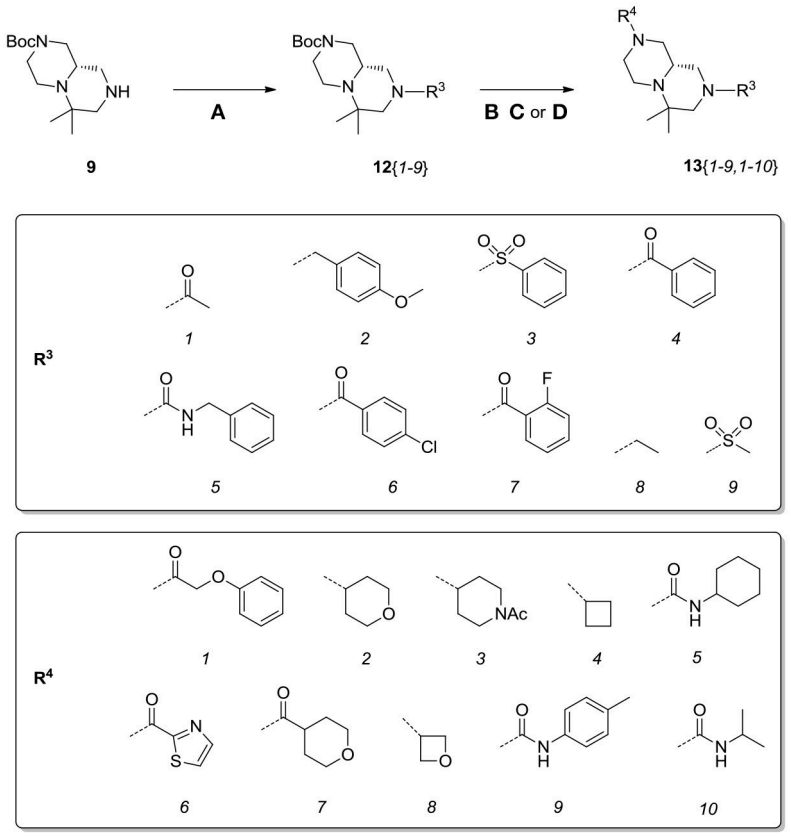

SCHEME 7 | Synthesis of library **13**. Reagents and conditions: **(A)** acyl chloride (or sulfonyl chloride or isocyanate), Et_3N, DCM, rt; **(B)** acyl chloride or sulfonyl chloride, Et_3N, DCM or **(C)** isocyanate, DCM or **(D)** aldehyde/ketone, borane-Me_2S complex, DCM.

Interestingly, in the case of piperazine-2-carboxylic acid **7**, also oxetanone was used as carbonyl component in the Ugi reaction, however, during borane reduction of the imide intermediate, the oxetanone ring was stereoselectively opened, affording derivative **11** (**Scheme 6**).

Scaffolds **9** and **10** were then subjected to the same decorations procedures of compound **4**, affording libraries **13**{*1–9,1–10*} (**Scheme 7** and **Table 2**) and **15**{*1–11,1–11*} (**Scheme 8** and **Table 3**).

The library compounds were analyzed using Lead Likeness And Molecular Analysis (Llama) (Colomer et al., 2016). Analyzing the library members revealed that all compound show a molecular weight below 500 g/mol (**Figure 1**) as well as a partition coefficient AlogP between −3 and 5, with the majority of compounds having a AlogP between −1 and 3 (**Figure 2**). These values perfectly fit into the Lipinski rule of five, which is an important benchmark to obtain orally available compounds (Lipinski et al., 2001). Also the degree of carbon sp^3 fraction was analyzed (**Figure 3**). The remarkably high amount of saturation is translated into a sp^3 fraction of carbon in the range of 0.3 to 1 with the majority of compounds showing values between 0.4 and 1.

For the visualization of the diversity generated with this library, a principal moments of inertia (PMI) analysis was performed (**Figure 4**). It shows the actual synthesized compounds of the three scaffolds; library 15 in blue, library 10 in red and library 6 in yellow. A broad distribution with the majority of compounds being in the region between rod- and disc-like and a certain portion of library members in the sphere-like region was observed. The library 15 has fewer compounds in the disc like region, compared to the two other libraries 16 and 17. However, the PMI analysis proofs that the Ugi 5-center-4-component reaction allows the generation of compound libraries with a good three-dimensional distribution of compounds.

CONCLUSIONS

In conclusion, we have demonstrated that diverse libraries of polycyclic (spiro)compounds can be efficiently assembled in a straightforward manner, exploiting a multicomponent approach. The potential of the Ugi reaction as a versatile tool for parallel chemistry, even beyond explicitly peptidic space, has been once more evidenced. Parameter analysis of the structurally new libraries described in this work shows that PhysChem values are in a perfect range for pharmacological applications. Moreover, Fsp^3—a parameter of growing interest in recent years—is addressed in an exemplary fashion.

TABLE 2 | HPLC-UV purities of library members **13**{*1–9,1–10*}.

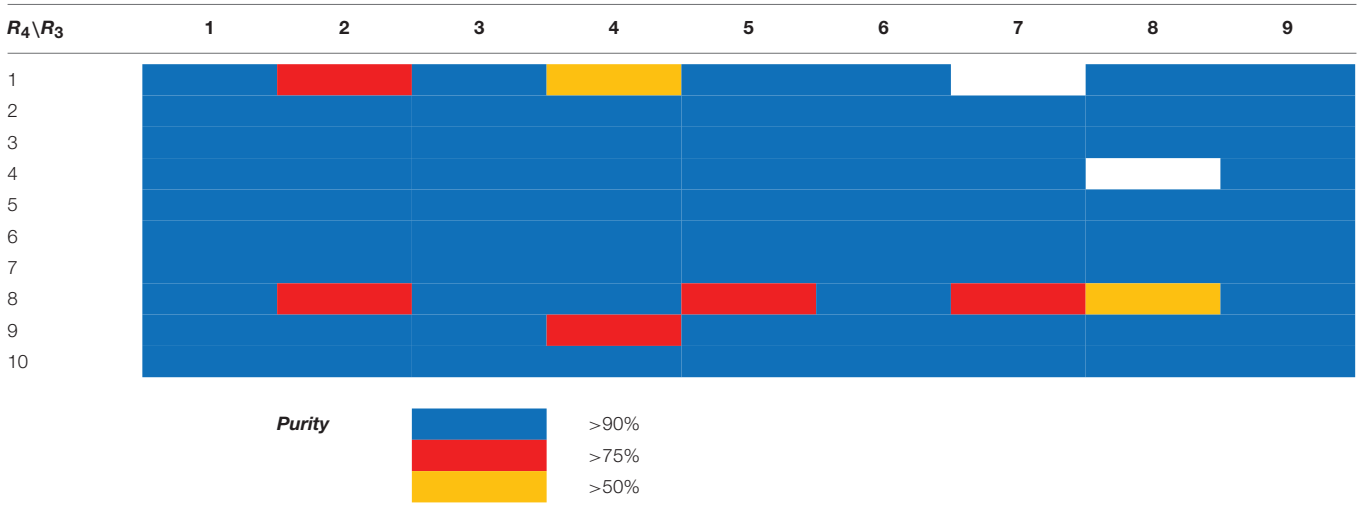

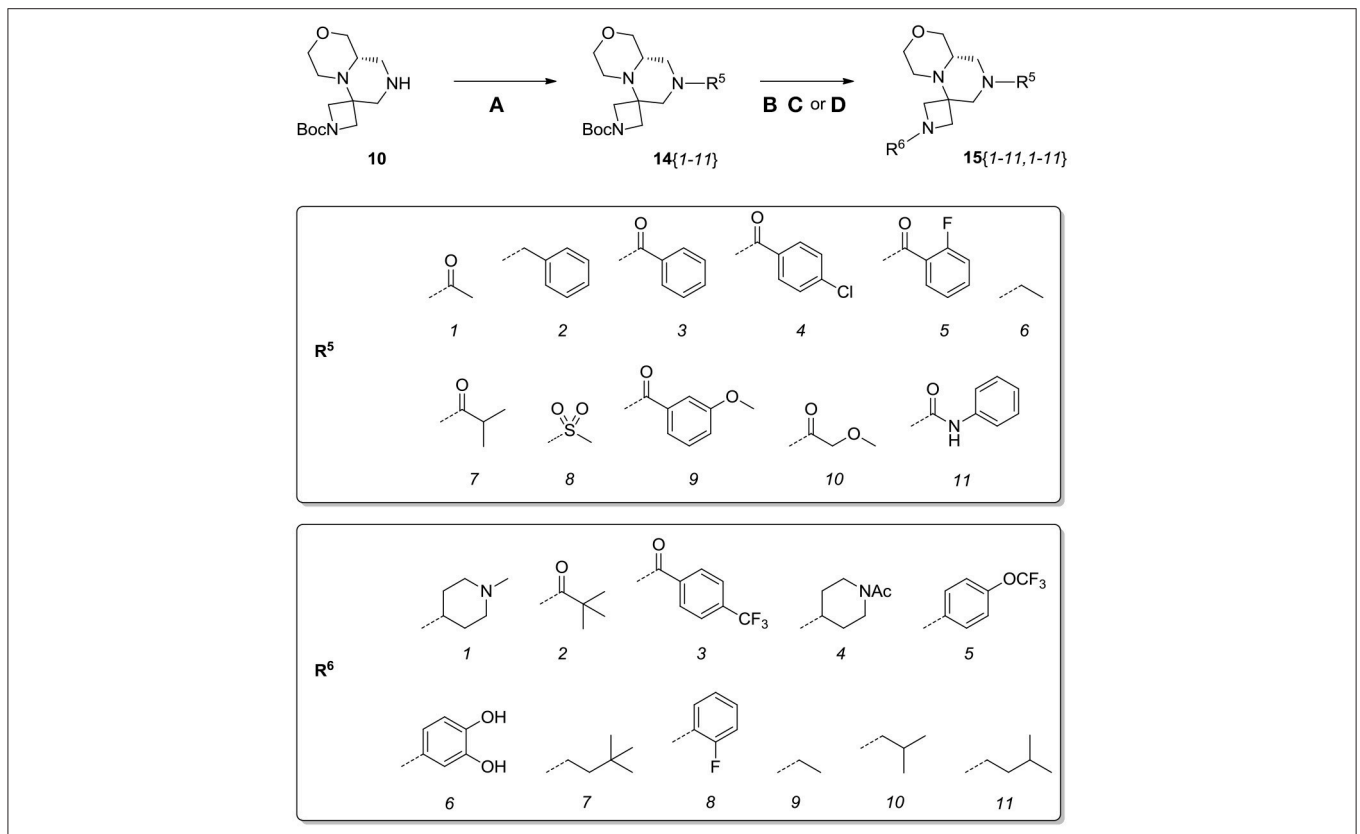

SCHEME 8 | Synthesis of library **15**. Reagents and conditions: **(A)** acyl chloride (or sulfonyl chloride or isocyanate), Et_3N, DCM, rt; **(B)** acyl chloride or sulfonyl chloride, Et_3N, DCM or **(C)** isocyanate, DCM or **(D)** aldehyde/ketone, borane-Me_2S complex, DCM.

TABLE 3 | HPLC-UV purities of library members **15**{*1–11*,*1–11*}.

R_6\R_5	1	2	3	4	5	6	7	8	9	10	11
1											
2											
3											
4											
5											
6											
7											
8											
9											
10											
11											

Purity >90% >75% >50%

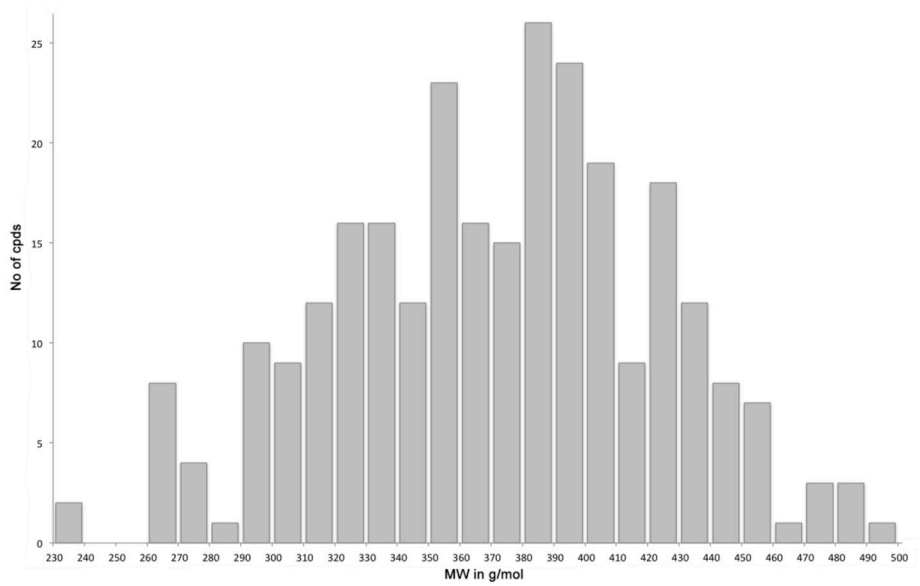

FIGURE 1 | Molecular weight distribution of library members.

EXPERIMENTAL PART

General Remarks

NMR spectra were recorded at 300 MHz (^{1}H) and 75 MHz (^{13}C) and the chemical shifts (δ) are expressed in parts per million relative to tetramethylsilane (TMS) as internal standard (0.00 ppm). Coupling constants are reported in hertz. Unless otherways stated, NMR acquisitions were performed at 295 K and $CDCl_3$ was used as solvent.

Following methods were used for the LC/MS spectra (Shimadzu MS2020) of the final compounds:

Method A: a linear gradient was used starting with 5 mM ammonium hydrogen carbonate buffer containing ammonia (pH 10.4), ending with MeOH containing 5 mM ammonium hydrogen carbonate buffer at a flow rate of 1.2 mL/min.

Method B: a linear gradient was used starting with 5 mM ammonium formiate buffer containing 0.1% formic acid, ending with MeOH/ACN/ammonium formiate buffer containing 0.1% formic acid (0.5:0.5:1, v/v/v) at a flow rate of 0.7 mL/min.

Method C: a linear gradient was used starting with 5 mM ammonium formiate buffer containing 0.1% formic acid, ending with MeOH/ACN/ammonium formiate buffer containing 0.1% formic acid (0.5:0.5:1, v/v/v) at a flow rate of 0.7 mL/min and at a oven temperature of 60°C.

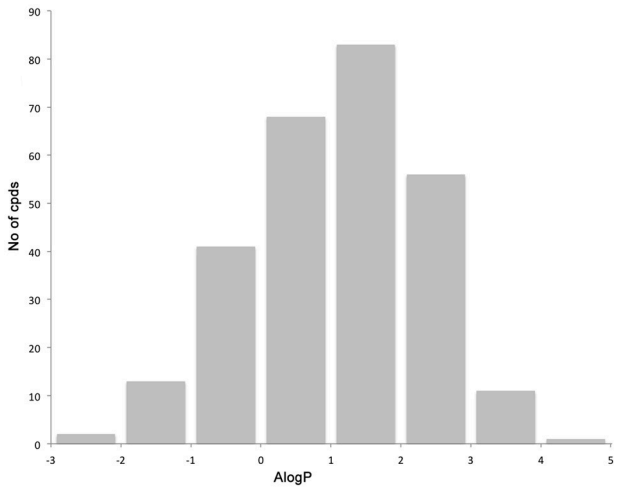

FIGURE 2 | Distribution of the partition coefficient AlogP.

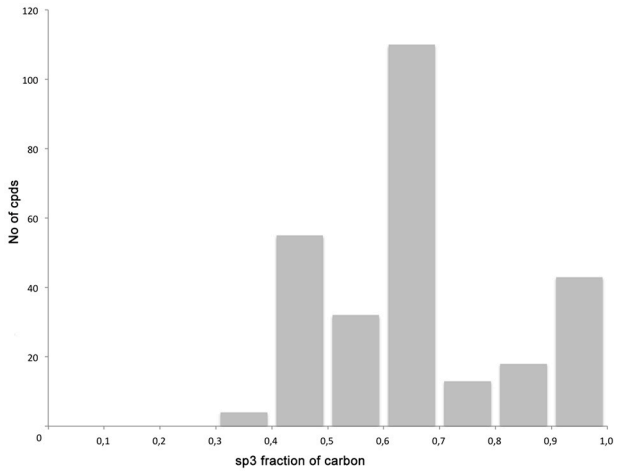

FIGURE 3 | Degree of carbon sp3 fraction.

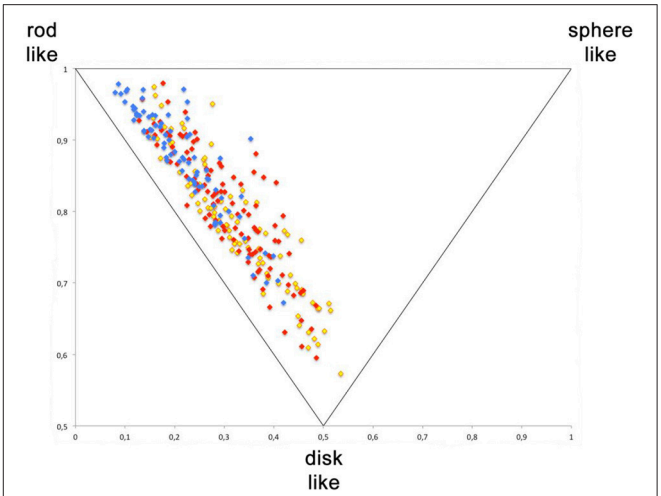

FIGURE 4 | Principle moment of inerta (PMI) analysis. Yellow—library 6, red—library 15, blue—library 13.

All final products with a purity below 90% (UV 215 nm) were purified with preparative HPLC (Knauer K1800 pumps, fitted with a Knauer K2500 UV detector and a Sedere Sedex 75 ELSD). Basic compounds were purified with a Gemini NX column (50 mm × 21.2 mm, 5 μm) using a fitted gradient systems for each compound [solvent A: H_2O, 1%NH_3 (aq., 26%)/solvent B: MeOH, 1%NH3(aq., 26%)] at a flow rate of 35 mL/min. Neutral compounds were purified with a Phenomenex LunaC8 column (50 mm × 25 mm, 5 μm) using a fitted gradient system for each compound (solventA: H_2O, 0.1% AS/solvent B: acetonitrile, 0.1% AS) at a flow rate of 70 mL/min.

HR-MS analyses were carried out on a Synapt G2 QToF mass spectrometer. MS signals were acquired from 50 to 1,200 m/z in ESI positive ionization mode. Reactions were monitored by TLC. TLC analyses were carried out on silica gel plates (thickness = 0.25 mm), viewed at UV (λ = 254 nm) and developed with iodine vapors or Hanessian stain (dipping into a solution of $(NH_4)_4MoO_4{\cdot}4H_2O$ (21 g) and $Ce(SO_4)_2{\cdot}4H_2O$ (1 g) in H_2SO_4 (31 mL) and H_2O (469 mL) and warming). Column chromatographies were performed with the "flash" methodology alternatively using 220–400 mesh silica, grade I alumina or 60–100 mesh Florisil. Solvents employed as eluents and for all other routinary operations, as well as anhydrous solvents and all reagents used were purchased from commercial suppliers and employed without any further purification.

Synthesis of Scaffolds 4, 9, and 10

(7′R,8a′S)-*tert*-butyl 2′-benzyl-7′-hydroxy-1′,3′-dioxohexahydro-*1′H*-spiro[azetidine-3,4′-pyrrolo[1,2-*a*]pyrazine]-1-carboxylate **2**

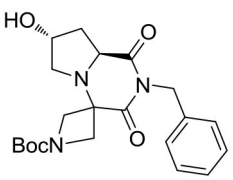

Trans 4-hydroxy-L-proline (3.0 g, 23 mmol) was dissolved in methanol (30 mL) within a pressure flask together with *tert*-butyl-3-oxoazetidine-1-carboxylate (3.9 g, 23 mmol) and benzyl isocyanide (2.7 mL, 23 mmol). The flask was then sealed, warmed up to 65°C and left stirring for 6 days. The solution was then allowed to cool down and the solvent removed in vacuo. Crude material was diluited with dichloromethane and washed with 5% sodium bicarbonate solution and brine. The organic layer was dried over sodium sulfate, filtered and concentrated under reduced pressure.

The crude material was dissolved in acetonitrile (30 mL) and DBU (0.34 mL, 2.3 mmol) was added under vigorous stirring at room temperature. After complete consumption of the Ugi adduct the solution was diluted with dichloromethane

and washed with saturated ammonium chloride, 5% sodium bicarbonate and brine. The organic layer was dried over sodium sulfate, filtered, concentrated under reduced pressure and purified by flash chromatography (PE/EA 1:1 +2% MeOH), yielding 4.2 g of product (10 mmol, 45% yield) as a yellow foam.

^{1}H NMR: 7.35–7.22 (m, 5H), 4.94 (s, 2H), 4.58 (d, J = 8.8 Hz, 1H), 4.43 (m, 1H), 4.14 (d, J = 8.6 Hz, 1H), 3.87 (m, 3H), 2.93 (qd, J = 10.1, 3.6 Hz, 2H), 2.53 (dt, J = 14.0, 6.5 Hz, 1H), 2.44 (d, J = 5.5 Hz, 1H), 2.28 (ddd, J = 14.0, 8.0, 1.7 Hz, 1H), 1.44 (s, 9H).

^{13}C NMR: 171.75, 171.30, 156.11, 136.60, 128.80, 128.70, 127.86, 80.56, 69.31, 58.58, 58.46, 55.89, 54.98 (broad), 54.31 (broad), 43.19, 38.71, 28.44.

HR-MS (m/z): $[M+H]^+$ calcd for $C_{21}H_{28}N_3O_5$, 402.2023; found, 402.2015.

(7′R,8a′S)-*tert*-butyl 2′-benzyl-7′-hydroxyhexahydro-*1′H*-spiro[azetidine-3,4′-pyrrolo[1,2-*a*]pyrazine]-1-carboxylate **3**

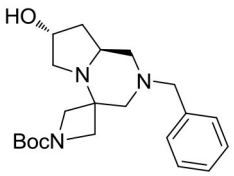

Cyclic imide (2.3 g, 5.7 mmol) was dissolved in THF (25 mL) under nitrogen atmosphere at room temperature. The solution was cooled down to 0°C and borane-dimethylsulfide complex (2 M solution in THF, 14.3 mL, 28.7 mmol) was slowly added in two aliquots with 1 h interval. Once the addition was complete the reaction was warmed up to 60°C and left stirring overnight.

The reaction was then cooled down to 0°C again and methanol (40 mL) was added dropwise in 1 h, then the reaction was left stirring for 1 day to allow complete decomposition of boranes. The solvents were then removed under reduced pressure and the crude material was purified by flash chromatography (PE/EA 4:6) affording the product (1.7 g, 4.7 mmol) in 82% yield as a colorless oil.

^{1}H NMR: 7.36–7.23 (m, 5H), 4.48 (m, 1H), 4.18–4.03 (d, J = 9.3 Hz, 1H), 3.89 (d, J = 9.3 Hz, 1H), 3.68–3.64 (m, 2H), 3.57–3.40 (m, 4H), 2.97–2.81 (m, 2H), 2.70 (m, 1H), 2.52 (dd, J = 9.7, 4.3 Hz, 1H), 2.11 (d, J = 10.8 Hz, 1H), 1.79 (t, J = 10.2 Hz, 1H), 1.74–1.64 (m, 2H), 1.43 (s, 9H).

^{13}C NMR: 156.13, 138.24, 128.94, 128.48, 127.32, 79.70, 69.45, 62.88, 62.51, 60.90, 57.20, 55.66, 55.61, 55.07, 39.32, 30.02, 28.54.

HR-MS (m/z): $[M+H]^+$ calcd for $C_{21}H_{32}N_3O_3$, 374.2438; found, 374.2435.

(7′R,8a′S)-*tert*-butyl 7′-hydroxyhexahydro-*1′H*-spiro[azetidine-3,4′-pyrrolo[1,2-*a*]pyrazine]-1-carboxylate **4**

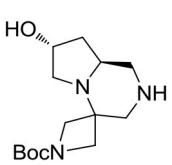

The reaction was performed in a Parr Shaker Hydrogenation apparatus. *N*-benzyl tertiary amine (3.8 g, 10 mmol) was dissolved im methanol (50 mL) under argon atmosphere and 10% Pd/C (0.6 g) was added. The inert atmosphere was then replaced by hydrogen gas (55 psi) and the suspension mechanically shaken for 2 days. Hydrogen atmosphere was then removed, the solution was filtered over a short celite pad and concentrated under reduced pressure. The crude material was recovered in quantitative yield and used for the final acylations without further purification.

^{1}H NMR: 4.52–4.43 (m, 1H), 4.09 (d, J = 9.3 Hz, 1H), 3.93 (d, J = 9.6 Hz, 1H), 3.66 (d, J = 9.0 Hz, 1H), 3.60–3.50 (m, 2H), 3.09 (d, J = 12.0 Hz, 1H), 3.04 (dd, J = 11.7, 2.1 Hz, 1H), 2.71 (dd, J = 12.0, 1.8 Hz, 1H), 2.60–2.35 (m, 3H), 1.80–1.60 (m, 2H), 1.45 (s, 9H).

^{13}C NMR: 156.51, 79.80, 68.92, 58.63, 56.52, 56.20, 55.79, 54.28, 50.44, 39.48, 30.00, 28.54.

HR-MS (m/z): $[M+H]^+$ calcd for $C_{14}H_{26}N_3O_3$, 284.1969; found, 284.1953.

Synthesis of Scaffold 9

(R)-*tert*-butyl 8-benzyl-6,6-dimethyl-7,9-dioxohexahydro-*1H*-pyrazino[1,2-*a*]pyrazine-2(*6H*)-carboxylate

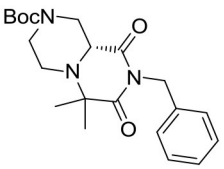

(R)-4-(*tert*-butoxycarbonyl)piperazine-2-carboxylic acid (5.8 g, 25 mmol) was dissolved in methanol (50 mL) within a pressure flask together with acetone (3.5 mL, 50 mmol) and benzyl isocyanide (2.9 mL, 24 mmol). The flask was then sealed, warmed up to 65°C and left stirring for 7 days. The solution was then allowed to cool down and the solvent removed in vacuo. Crude material was diluited with dichloromethane and washed with 5% sodium bicarbonate solution and brine. The organic layer was dried over sodium sulfate, filtered and concentrated under reduced pressure.

The crude material was dissolved in acetonitrile (20 mL) and DBU (0.37 mL, 2.5 mmol) was added under vigorous stirring at room temperature. After complete consumption of the Ugi adduct the solution was diluted with dichloromethane and washed with saturated ammonium chloride, 5% sodium bicarbonate and brine. The organic layer was dried over sodium sulfate, filtered, concentrated under reduced pressure and purified by flash chromatography (PE/EA 1:1), yielding 3.6 g of product (9.4 mmol, 39% yield) as a yellow foam.

^{1}H NMR: 7.34–7.20 (m, 5H), 4.98 (d, J = 14.0 Hz, 1H), 4.89 (d, J = 14.0 Hz, 1H), 4.44 (broad d, J = 13.0 Hz, 1H), 3.93 (d, J = 13.0 Hz, 1H), 3.39 (dd, J = 9.3, 3.7 Hz, 1H), 3.15–2.75 (m, 3H), 2.39 (td, J = 10.9, 3.2 Hz, 1H), 1.52 (s, 3H), 1.47 (s, 9H), 1.22 (s, 3H).

^{13}C NMR: 174.46, 169.42, 154.41, 136.84, 128.60, 128.53, 127.61, 80.47, 61.12, 57.35, 45.52, 44.39, 43.21, 28.50, 23.98, 16.87.

HR-MS (m/z): $[M+H]^+$ calcd for $C_{21}H_{30}N_3O_4$, 388.2231; found, 388.2212.

(S)-*tert*-butyl 8-benzyl-6,6-dimethylhexahydro-*1H*-pyrazino[1,2-*a*]pyrazine-2(*6H*)-carboxylate

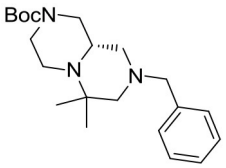

Cyclic imide (2.3 g, 5.9 mmol) was dissolved in THF (26 mL) under nitrogen atmosphere at room temperature. The solution was cooled down to 0°C and borane-dimethylsulfide complex (2 M solution in THF, 15.0 mL, 29.5 mmol) was slowly added in two aliquots with 1 h interval. Once the addition was complete the reaction was warmed up to 60°C and left stirring overnight.

The reaction was then cooled down to 0°C again and methanol (40 mL) was added dropwise in 1 h, then the reaction was left stirring for 1 day to allow complete decomposition of boranes. The solvents were then removed under reduced pressure and the crude material was purified by flash chromatography (PE/EA 7:3) affording the product (1.6 g, 4.5 mmol) in 76% yield as a colorless oil.

^{1}H NMR: 7.40–7.10 (m, 5H), 4.15–3.75 (broad m, 2H), 3.46 (d, J = 14.0 Hz, 1H), 3.37 (d, J = 14.0 Hz, 1H), 3.00–2.30 (series of m, 6H), 2.18 (td, J = 11.8, 2.9 Hz, 1H), 1.96 (d, J = 13.5 Hz, 1H), 1.76 (t, J = 10.5 Hz, 1H), 1.44 (s, 9H), 1.08 (s, 3H), 1.02 (s, 3H).

^{13}C NMR: 154.62, 138.67, 128.79, 128.33, 127.07, 79.71, 66.18, 62.84, 57.34, 53.99, 53.65, 47.50 (broad), 44.58, 44.00 (broad), 28.56, 26.61, 16.05.

HR-MS (m/z): $[M+H]^+$ calcd for $C_{21}H_{34}N_3O_2$, 360.2646; found, 360.2628.

(S)-*tert*-butyl 6,6-dimethylhexahydro-*1H*-pyrazino[1,2-*a*]pyrazine-2(*6H*)-carboxylate **9**

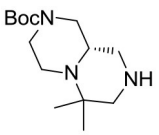

The reaction was performed in a Parr Shaker Hydrogenation apparatus. *N*-benzyl tertiary amine (3.0 g, 8.3 mmol) was dissolved im methanol (35 mL) under argon atmosphere and 10% Pd/C (0.4 g) was added. The inert atmosphere was then replaced by hydrogen gas (55 psi) and the suspension mechanically shaken for 2 days. Hydrogen atmosphere was then removed, the solution was filtered over a short celite pad and concentrated under reduced pressure. The crude material was recovered in quantitative yield and used for the final acylations without further purification.

^{1}H NMR: 4.25–3.75 (broad m, 2H), 3.00–2.30 (series of m, 6H), 2.00–1.60 (m, 3H), 1.49 (s, 9H), 1.09 (s, 3H), 1.04 (s, 3H). *NH is missing*.

^{13}C NMR: 154.53, 79.69, 68.49, 59.24, 55.31, 53.66, 53.23, 46.47, 44.39, 28.45, 26.63, 16.20.

HR-MS (m/z): $[M+H]^+$ calcd for $C_{14}H_{28}N_3O_2$, 270.2176; found, 270.2178.

Synthesis of Scaffold 10

(R)-*tert*-butyl 8′-benzyl-7′,9′-dioxohexahydro-*1′H*-spiro[azetidine-3,6′-pyrazino[2,1-*c*][1,4]oxazine]-1-carboxylate

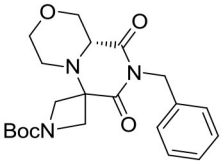

(R)-Morpholine-2-carboxylic acid hydrochloride (6.4 g, 38 mmol) was dissolved in methanol (70 mL) within a pressure flask together with *tert*-butyl-3-oxoazetidine-1-carboxylate (6.5 g, 38 mmol), benzyl isocyanide (4.6 mL, 38 mmol) and triethylamine (10.6 mL, 76 mmol). The flask was then sealed, warmed up to 65°C and left stirring for 10 days. The solution was then allowed to cool down and the solvent removed in vacuo. Crude material was diluted with ethyl acetate and washed with 5% sodium bicarbonate solution and brine. The organic layer was dried over sodium sulfate, filtered and concentrated under reduced pressure.

The crude material was purified by flash chromatography (PE/EA 7:3), yielding 11 g of product (28 mmol, 73% yield) as a yellow foam.

^{1}H NMR: 7.33–7.22 (m, 5H), 5.04 (d, J = 13.5 Hz, 1H), 4.92 (d, J = 13.8 Hz, 1H), 4.57 (d, J = 8.8 Hz, 1H), 4.35–4.20 (m, 1H), 4.10 (d, J = 8.6 Hz, 1H), 3.95–3.65 (m, 5H), 3.47 (broad t, J = 3.5 Hz, 1H), 2.75–2.50 (m, 2H), 1.45 (s, 9H).

^{13}C NMR: 170.53, 168.75, 156.04, 136.47, 128.93, 128.71, 127.88, 80.54, 66.34, 66.23, 66.15, 60.47, 55.97, 53 (broad), 44.15, 43.09, 28.42.

HR-MS (m/z): $[M+H]^+$ calcd for $C_{21}H_{28}N_3O_5$, 402.2023; found, 402.2001.

(S)-*tert*-butyl 8′-benzylhexahydro-*1′H*-spiro[azetidine-3,6′-pyrazino[2,1-*c*][1,4]oxazine]-1-carboxylate

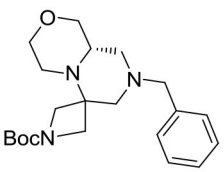

Cyclic imide (6.2 g, 15.4 mmol) was dissolved in THF (80 mL) under nitrogen atmosphere at room temperature. The solution was cooled down to 0°C and borane-dimethylsulfide complex (2 M solution in THF, 38.6 mL, 77 mmol) was slowly added in two aliquots with 1 h interval. Once the addition was complete the reaction was warmed up to 60°C and left stirring overnight.

The reaction was then cooled down to 0°C again and methanol (80 mL) was added dropwise in 1 h, then the reaction was left stirring for 1 day to allow complete decomposition of boranes. The solvents were then removed under reduced pressure and the crude material was purified by flash chromatography (PE/EA 4:6) affording the product (5.0 g, 13.4 mmol) in 87% yield as a colorless oil.

^{1}H NMR: 7.35–7.20 (m, 5H), 4.12 (broad d, J = 9.0 Hz, 1H), 3.94 (d, J = 9.6 Hz, 1H),), 3.87 (broad d, J = 11.1 Hz, 1H), 3.70–3.10 (series of m, 7H), 2.90 (t, J = 9.7 Hz, 2H), 2.60–2.40

(m, 3H), 2.18 (d, J = 10.8 Hz, 1H), 1.80–1.70 (m, 1H), 1.42 (s, 9H).

^{13}C NMR: 155.97, 137.46, 128.59, 128.16, 127.07, 79.26, 69.25, 66.93, 62.35, 61.92, 56.09, 54.79, 53.71, 53.61, 51 (broad), 44.84, 28.19.

HR-MS (m/z): $[M+H]^+$ calcd for $C_{21}H_{32}N_3O_3$, 374.2438; found, 374.2420.

(S)-*tert*-butyl hexahydro-*1′H*-spiro[azetidine-3,6′-pyrazino[2,1-*c*][1,4]oxazine]-1-carboxylate **10**

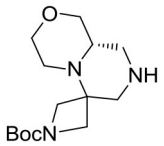

N-benzyl tertiary amine (4.5 g, 12 mmol) was dissolved im ethanol (80 mL) under argon atmosphere and 10% Pd/C (0.75 g) was added. The inert atmosphere was then replaced by hydrogen gas (balloon, atmospheric pressure) and the suspension left stirring at 60°C for 2 days. Hydrogen atmosphere was then removed, the solution was filtered over a short celite pad and concentrated under reduced pressure. The crude material was recovered in quantitative yield and used for the final acylations without further purification.

^{1}H NMR: 4.16 (dd, J = 9.0, 1.5 Hz, 1H), 3.98 (d, J = 9.6 Hz, 1H), 3.92 (broad d, J = 11.4 Hz, 1H), 3.75–3.60 (m, 3H), 3.45 (d, J = 9.9 Hz, 1H), 3.25–3.10 (m, 2H), 2.93 (dt, J = 11.7, 1.8 Hz, 1H), 2.88 (dd, J = 14.1, 1.8 Hz, 1H), 2.80–2.68 (m, 1H), 2.61 (td, J = 11.4, 3.3 Hz, 1H), 2.50–2.38 (m, 2H), 1.44 (s, 9H).

^{13}C NMR: 156.23, 80.25, 68.72, 68.55, 67.13, 55.02, 54 (broad), 52.63, 51 (broad), 44.22, 28.42.

HR-MS (m/z): $[M+H]^+$ calcd for $C_{14}H_{26}N_3O_3$, 284.1969; found, 284.1960.

(6R,9aS)-*tert*-butyl 8-benzyl-6-(hydroxymethyl)-6-methyl-hexahydro-*1H*-pyrazino[1,2-*a*]pyrazine-2(*6H*)-carboxylate **11**

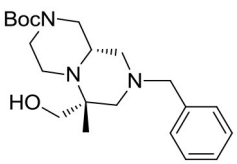

After Ugi reaction and DBU cyclization, performed as described above, the resulting cyclic imide (4.0 g, 9.9 mmol) was dissolved in THF (45 mL) under nitrogen atmosphere at room temperature. The solution was cooled down to 0°C and borane-dimethylsulfide complex (2 M solution in THF, 25.0 mL, 49.7 mmol) was slowly added in two aliquots with 1 h interval. Once the addition was complete the reaction was warmed up to 60°C and left stirring overnight.

The reaction was then cooled down to 0°C again and methanol (45 mL) was added dropwise in 1 h, then the reaction was left stirring for 1 day to allow complete decomposition of boranes. The solvents were then removed under reduced pressure and the crude material was purified by flash chromatography (PE/EA 1:1) affording the product (2.1 g, 5.6 mmol) in 57% yield as a colorless oil.

^{1}H NMR: 7.40–7.10 (m, 5H), 4.10–3.70 (broad m, 2H), 3.47 (d, J = 13.3 Hz, 1H), 3.37 (d, J = 13.3 Hz, 1H), 3.15–2.60 (series of m, 6H), 2.47 (broad t, J = 6.4 Hz, 1H), 2.43 (dd, J = 11.2, 1.8 Hz, 1H), 2.34 (d, J = 11.2, Hz, 1H), 2.23 (td, J = 11.7, 2.9 Hz, 1H), 1.73 (t, J = 11.3 Hz, 1H + –OH overlapped, 1H), 1.45 (s, 9H), 1.02 (s, 3H).

^{13}C NMR: 154.56, 138.38, 128.86, 128.40, 127.21, 79.97, 64.95, 62.93, 61.61, 57.51, 56.79, 53.76, 47.50 (broad), 45.00 (broad), 44.49, 28.54, 14.06.

HR-MS (m/z): $[M+H]^+$ calcd for $C_{21}H_{34}N_3O_3$, 376.2595; found, 376.2578.

General Conditions for Introduction of the First Diversomer

Acylation Reaction

Method A

Compound **4**, **9** or **10** (1.0 mmol) was dissolved in dry DCM (5 mL) under nitrogen and the carboxylic acid (1.1 mmol) was added. The solution was then cooled to 0°C and TBTU (1.1 mmol) and DIPEA (1.5 mmol) were added. The reaction was allowed to warm up to room temperature and left stirring under nitrogen overnight. The solution was then diluted with aqueous ammonium chloride and extracted twice with ethyl acetate. The organic phase was anhydrified over sodium sulfate, concentrated and purified by flash chromatography.

Method B

Compound **4**, **9** or **10** (1.0 mmol) was dissolved in dry DCM (5 mL) under nitrogen and the acyl (or sulfonyl) chloride (1.0 mmol) and triethylamine (1.5 mmol) were added. The reaction was left stirring under nitrogen overnight. The solution was then diluted with aqueous sodium carbonate and extracted twice with ethyl acetate. The organic phase was anhydrified over sodium sulfate, concentrated and purified by flash chromatography.

Method C

Compound **9** or **10** (1.0 mmol) was dissolved in dry DCM (5 mL) under nitrogen and the isocyanate (1.0 mmol) and triethylamine (1.5 mmol) were added. The reaction was left stirring under nitrogen overnight. The solution was then diluted with aqueous sodium bicarbonate and extracted twice with DCM. The organic phase was dired over sodium sulfate, concentrated and purified by flash chromatography.

Reductive Amination Reaction

Compound **4** (1.0 mmol) was dissolved in MeOH and the aldehyde/ketone (1.2 mmol) and Borane-Pyridine complex (2 mmol) were added followed by one drop od 0.5 M HCl. The reaction was left stirring overnight. The solution was then poured over an SCX-cartridge and eluted with MeOH until no impurity could be detected anymore. Then the cartridge was eluted with 5 mL ammonia in MeOH (2–3 M) and the resulting solution was

evaporated to dryness. The remaining residue was purified by flash chromatography.

General Conditions for the Introduction of the Second Diversomer

Boc Cleavage

The Boc-protected compound was dissolved in HCl/MeOH (1.5 M) and the mixture was stirred at rt until completion (usually 1–2 h). The solvent was evaporated, the remainder was dried and used for the next steps withiut further purification.

Acylation Reaction

Acid chlorides

To a solution of the starting material (usually 50–80 mg) in CH_2Cl_2 were added 500 mg Poly(4-vinylpyridine) and the acid chloride. The mixture was agitated at rt for 16 h. After completion (as indicated by TLC-monitoring) the mixture was filtrated. To the filtrate was added half saturated $NaHCO_3$ solution, the mixture was agitated for 30 min, then the phases were separated and the aqueous phase was extracted once again with CH_2Cl_2. The combined organic phases were dried over Na_2SO_4 and the solvent was evaporated.

Isocyanates

To a solution of the starting material (usually 50–80 mg) in CH_2Cl_2 were added 500 mg Poly(4-vinylpyridine) and the isocyanate (1.05 equiv.) The mixture was agitated at rt for 16 h. After completion (as indicated by TLC-monitoring) the mixture was filtrated and the solvent was evaporated.

Sulfonyl chlorides

To a solution of the starting material (usually 50–80 mg) in CH_2Cl_2/Py (3/7, v:v) was added the sulfonyl chloride (5 equiv.) at 0°C. The mixture was agitated at rt for 16 h. After completion (as indicated by TLC-monitoring) the solvent was evaporated. The residue was redissolved in CH_2Cl_2 and extracted with saturated $NaHCO_3$ solution. The organic phase was dried over Na_2SO_4 and the solvent was evaporated.

Reductive Amination Reaction

To a solution of the free amine *19* in 2 ml dry MeOH were added 2 equivalents of the aldehyde or ketone, 2.5 equivalents of the borane-pyridine complex, 1 drop 0.5 M HCl and stirring was continued at rt overnight. LC/MS-check! After completion of the reaction the solution was poured over a SCX-cartridge (Phenomenex, Strata SCX, 0,6 mmol/g) and eluted with methanol until no impurity could be detected anymore. Then the cartridge was eluted with ca. 8 M methanolic ammonia solution. After removal of the solvent in a turbovap the remaining residue was finally evaporated to dryness in a Rotary Vacuum Concentrator (Christ, Germany; 40°C, 6 h) and subjected to analysis.

Analytical Data for Selected Library Members

Compound 6{*3,4*}

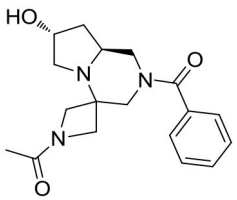

^{1}H NMR ($CDCl_3$, 70°C): 7.47–7.33 (m, 5H), 4.74–4.27 (m, 2H), 4.26–3.90 (m, 3H), 3.87–3.56 (m, 2H), 3.55–3.43 (m, 1H), 2.95 (d, J = 12.9 Hz, 1H), 2.79–2.4 (m, 3H), 2.40–2.05 (broad m, 1H), 1.85 (s, 3H), 1.81–1.56 (m, 2H).

^{13}C NMR ($CDCl_3$, 70°C): 171.11, 170.99, 135.72, 130.20, 128.82, 127.29, 69.04, 56.35, 55.79, 55.51, 55.26, 53.93, 52.20, 49.86, 39.18, 19.02.

HR-MS (m/z): $[M+H]^+$ calcd for $C_{18}H_{24}N_3O_3$, 330.1812; found, 330.1836.

Compound 6{*4,5*}

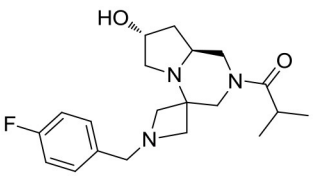

^{1}H NMR: 7.30–7.17 (m, 2H), 7.05–6.90 (m, 2H), 4.92 (d, J = 12.9 Hz, 0.4H), 4.63 (d, J = 12.6 Hz, 0.6H), 4.47 (broad s, 1H), 4.23 (d, J = 12.7 Hz, 0.6H), 3.87 (d, J = 12.1 Hz, 0.4H), 3.60 (s, 2H), 3.57–3.36 (m, 1H), 3.27–2.84 (m, 5H), 2.84–2.15 (m, 5H), 1.86–1.63 (m, 2H), 1.21–1.04 (m, 6H).

The spectrum was not recorded at 70°C because azetidine Hs collapsed.

^{13}C NMR ($CDCl_3$, 70°C): 176.20, 162.33 (d, J = 245 Hz), 134.25, 129.98 (d, J = 7.8 Hz), 115.25 (d, J = 21.2 Hz), 69.46, 62.21, 60.08, 56.74, 56.28, 55.33, 54.48, 39.54, 30.34, 19.86, 19.51.

CH_2S of azetidine ring could only be detected in the HSQC analysis at 53 and 45 ppm.

HR-MS (m/z): $[M+H]^+$ calcd for $C_{20}H_{29}FN_3O_2$, 362.2238; found, 362.2246.

Compound 13{*8,1*}

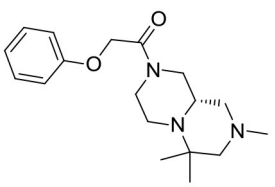

^{1}H NMR (DMSO-d_6, 90°C): 7.32–7.23 (m, 2H), 6.98–6.91 (m, 3H), 4.76 (s, 2H), 4.25–3.80 (m, 2H), 2.90 (broad d, J = 11.4 Hz, 2H), 2.77 (broad d, J = 10.5 Hz, 2H), 2.56–2.48 (m, 2H), 2.20 (s, 3H), 2.17–2.05 (m, 1H), 1.96 (broad d, J = 10.8 Hz, 1H), 1.74 (broad t, J = 9.6 Hz, 1H), 1.04 (s, 3H), 1.03 (s, 3H).

^{13}C NMR (DMSO-d_6, 90°C): 165.20, 157.72, 128.82, 120.56, 114.44, 66.73, 66.11, 57.54, 53.03, 52.62, 45.06, 43.75, 25.64, 20.34, 15.27 (one peak is missing).

HR-MS (m/z): $[M+H]^+$ calcd for $C_{18}H_{28}N_3O_2$, 318.2176; found, 318.2164.

Compound 13{*6,2*}

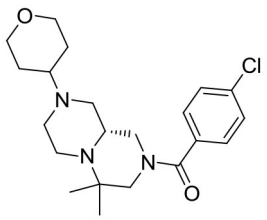

^{1}H NMR ($CDCl_3$, 70°C): 7.36 (d, J = 8.7, 2H), 7.32 (d, J = 8.7, 2H), 3.98 (dm, J = 10.5 Hz, 2H), 3.98–3.50 (very broad m, 1H), 3.33 (td, J = 11.7, 2.1 Hz, 2H), 2.95–2.20 (series of m, 9H), 1.88 (t, J = 9.5, 1H), 1.75–1.65 (m, 2H), 1.53 (qd, J = 12.1, 4.9, 3H), 1.06 (s, 3H), 0.98 (s, 3H).

^{13}C NMR ($CDCl_3$, 70°C): 169.46, 135.96, 134.65, 128.93, 128.82, 67.49 (2C), 61.03, 54.13, 53.30, 53.09, 49.73, 44.89, 29.93, 29.82, 25.98, 14.45.

HR-MS (m/z): $[M+H]^+$ calcd for $C_{21}H_{31}ClN_3O_2$, 392.2099; found, 392.2094.

Compound 15{*6,3*}

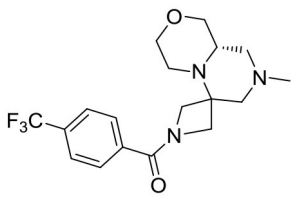

^{1}H NMR: 7.76 (d, J = 8.2 Hz, 2H), 7.66 (d, J = 8.2 Hz, 2H), 4.41 (d, J = 9.7 Hz, 1H), 4.26 (d, J = 10.8 Hz, 1H), 3.97 (d, J = 9.7 Hz, 1H), 3.90 (broad d, J = 11.2 Hz, 1H), 3.73 (d, J = 10.8 Hz, 1H), 3.71–3.58 (m, 2H), 3.21 (dd, J = 11.1, 9.6, Hz, 2H), 3.00–2.87 (m, 2H), 2.62–2.44 (m, 3H), 2.24 (s, 3H), 2.24–2.19 (m, 1H), 1.75 (t, J = 10.9 Hz, 1H).

^{13}C NMR: 169.01, 137.01, 133.21 (q, J = 32.8 Hz), 128.50, 125.58 (q, J = 3.8 Hz), 123.94 (q, J = 272.5 Hz), 69.76, 67.40, 64.54, 57.21, 56.16, 55.22, 55.14 (very broad), 54.06 (very broad), 46.13, 45.22.

HR-MS (m/z): $[M+H]^+$ calcd for $C_{18}H_{23}F_3N_3O_2$, 370.1737; found, 370.1746.

Compound 15{*8,4*}

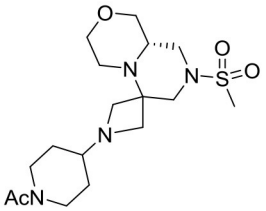

^{1}H NMR ($CDCl_3$, 70°C): 4.05–3.85 (m, 3H), 3.73 (dd, J = 11.1, 3.0 Hz, 1H), 3.63 (td, J = 11.0, 2.5 Hz, 2H), 3.42 (dt, J = 10.8, 2.6 Hz, 1H), 3.35–3.05 (m, 6H), 3.00–2.90 (m, 1H), 2.89 (d, J = 8.1 Hz, 1H), 2.80 (d, J = 12 Hz, 1H), 2.76 (s, 3H), 2.67–2.55 (m, 2H), 2.48 (t, J = 10.8 Hz, 1H), 2.35 (tt, J = 7.7, 3.7 Hz, 1H), 2.04 (s, 3H), 1.70–1.55 (m, 2H), 1.40–1.20 (m, 2H).

^{13}C NMR ($CDCl_3$, 70°C): 168.88, 69.14, 67.55, 62.36, 56.57 (broad), 56.43, 54.04 (broad), 53.92, 53.72, 46.15, 45.36, 44.03 (broad), 39.17 (broad), 34.99, 29.51 (broad), 28.66 (broad), 21.32.

HR-MS (m/z): $[M+H]^+$ calcd for $C_{17}H_{31}N_4O_4S$, 387.2061; found, 387.2052.

AUTHOR CONTRIBUTIONS

All authors listed have made a substantial, direct and intellectual contribution to the work, and approved it for publication.

SUPPLEMENTARY MATERIAL

The Supplementary Material for this article can be found online at: https://www.frontiersin.org/articles/10.3389/fchem.2018.00369/full#supplementary-material

REFERENCES

Basso, A., Banfi, L., and Riva, R. (2010). A marriage of convenience: combining the power of isocyanide-based multicomponent reactions with the versatility of (hetero)norbornene chemistry. *Eur. J. Org. Chem.* 2010, 1831–1841. doi: 10.1002/ejoc.200901438

Basso, A., Banfi, L., Riva, R., and Guanti G. (2004). U-4C-3CR versus U-5C-4CR and stereochemical outcomes using suitable bicyclic β-amino acid derivatives as bifunctional components in the Ugi reaction. *Tetrahedron Lett*. 45, 587–590. doi: 10.1016/j.tetlet.2003.10.193

Basso, A., Banfi, L., Riva, R., and Guanti, G. (2005). A novel highly selective chiral auxiliary for the asymmetric synthesis of l- and d-α-amino acid derivatives via a multicomponent Ugi reaction. *J. Org. Chem*. 70, 575–579. doi: 10.1021/jo048389m

Colomer, I., Empson, C. J., Craven, P., Owen, Z., Doveston, R. G., Churcher, I., et al. (2016). A divergent synthetic approach to diverse molecular scaffolds: assessment of lead-likeness using LLAMA, an open-access computational tool. *Chem. Commun*. 52, 7209–7212. doi: 10.1039/C6CC03244C

Dawidowski, M., Herold, F., Wilczek, M., Turlo, J., Chodkowski, A., Gomolka, A., et al. (2012). Synthesis of bicyclic 2,6-diketopiperazines via a three-step sequence involving an Ugi five-center, four-component reaction. *Tetrahedron* 68, 8222–8230. doi: 10.1016/j.tet.2012.07.064

Dawidowski, M., Sobczak, S., Wilczek, M., Kulesza, A., and Turło, J. (2014). Expanding the substrate scope of ugi five-center, four-component reaction (U-5C-4CR): ketones as coupling partners for secondary amino acids. *Mol. Divers*. 18, 61–77. doi: 10.1007/s11030-013-9488-0

Demharter, A., Hörl, W., Herdtweck, E., and Ugi, I. (1996). Synthesis of chiral 1,1′-iminodicarboxylic acid derivatives from α-amino acids, aldehydes, isocyanides, and alcohols by the diastereoselective five-center–four-component reaction. *Angew. Chem. Int. Ed.* 35, 173–175.

Dömling, A. (2006). Recent developments in isocyanide based multicomponent reactions in applied chemistry. *Chem. Rev*. 106, 17–89. doi: 10.1021/cr0505728

Dömling, A., and Ugi, I. (2000). Multicomponent reactions with isocyanides. *Angew. Chem. Int. Ed.* 39, 3168–3210. doi: 10.1002/1521-3773(20000915)39:183.0.CO;2-U

Fischer, P. M. (2003). Diketopiperazines in peptide and combinatorial chemistry. *J. Peptide Sci*. 9, 9–35. doi: 10.1002/psc.446

Giustiniano, M., Basso, A., Mercalli, V., Massarotti, A., Novellino, E., Tron, G. C., et al. (2017). To each his own: isonitriles for all flavors. *Chem. Soc. Rev*. 46, 1295–1357. doi: 10.1039/C6CS00444J

Kim, Y. B., Choi, E. H., Keum, G., Kang, S. B., Lee, D. H., Koh, H. Y., et al. (2001). An efficient synthesis of morpholin-2-one derivatives using glycolaldehyde dimer by the Ugi multicomponent reaction. *Org. Lett*. 3, 4149–4152. doi: 10.1021/ol016716w

Koopmanschap, G., Ruijter, E., and Orru, R. V. (2014). Isocyanide-based multicomponent reactions towards cyclic constrained peptidomimetics. *Beilstein J. Org. Chem*. 10, 544–598. doi: 10.3762/bjoc.10.50

Lipinski, C. A., Lombardo, F., Dominy, B. W., and Feeney, P. (2001). Experimental and computational approaches to estimate solubility and permeability in drug discovery and development settings. *J. Adv. Drug Del. Rev*. 46, 3–26. doi: 10.1016/S0169-409X(00)00129-0

Liu, H., and Dömling, A. (2009). One-pot synthesis of highly functionalized seleno amino acid derivatives. *Chem. Biol. Drug Des*. 74, 302–308. doi: 10.1111/j.1747-0285.2009.00854.x

Mandai, H., Irie, S., Mitsudo, K., and Suga, S. (2011). Studies on the synthesis of DMAP derivatives by diastereoselective Ugi reactions. *Molecules* 16, 8815–8832. doi: 10.3390/molecules16108815

Mimura, R., Kitamori, A., Ikeda, A., Masuda, T., Nakano, K., Kotsuki, H., et al. (2015). Biomimetic approaches employing the Ugi five-center four-component reaction for synthesis of the right-hand portion of halichonadin Q and the central part of halichonadin M. *Synthesis* 47, 3043–3048. doi: 10.1055/s-0034-1380438

Orru, R. V. A., and de Greef, M. (2003). Recent advances in solution-phase multicomponent methodology for the *Synthesis* of heterocyclic compounds. *Synthesis* 2003, 1471–1499. doi: 10.1055/s-2003-40507

Park, S. J., Keum, G., Kang, S. B., Koh, H. Y., Kim, Y., and Lee, D. H. (1998). A facile synthesis of N-carbamoylmethyl-α-aminobutyrolactones by the Ugi multicomponent condensation reaction. *Tetrahedron Lett*. 39, 7109–7112. doi: 10.1016/S0040-4039(98)01509-3

Perrotta, E., Altamura, M., Barani, T., Bindi, S., Giannotti, D., Harmat, N. J., et al. (2001). 2,6-Diketopiperazines from amino acids, from solution-phase to solid-phase organic synthesis. *J. Comb. Chem*. 3, 453–460. doi: 10.1021/cc0000904

Touré, B. B., and Hall, D. G. (2009). Natural product synthesis using multicomponent reaction strategies. *Chem. Rev*. 109, 4439–4486. doi: 10.1021/cr800296p

Ugi, I., Demharter, A., Hörl, W., and Schmid, T. (1996). Ugi reactions with trifunctional α-amino acids, aldehydes, isocyanides and alcohols. *Tetrahedron* 52, 11657–11664.

Zimmer, R., Ziemer, A., Gruner, M., Brudgam, I., Hartl, H., and Reissig, H. U. (2001). Siloxycyclopropanes in Ugi four-component reaction: a new method for the synthesis of highly substituted pyrrolidinone derivatives. *Synthesis* 11, 1649–1658. doi: 10.1055/s-2001-16762

Conflict of Interest Statement: JS and CM are employed by AnalytiCon Discovery GmbH.

The remaining authors declare that the research was conducted in the absence of any commercial or financial relationships that could be construed as a potential conflict of interest.

frontiers in Chemistry

ORIGINAL RESEARCH
published: 24 August 2018
doi: 10.3389/fchem.2018.00376

A Five-Component Biginelli-Diels-Alder Cascade Reaction

*Taber S. Maskrey, Madeline C. Frischling, Mikhaila L. Rice and Peter Wipf**

Department of Chemistry, University of Pittsburgh, Pittsburgh, PA, United States

A new multi-component condensation was discovered during the reaction of a urea, β-keto ester, and formaldehyde. In the presence of catalytic indium bromide, a Biginelli dihydropyrimidinone intermediate was further converted to a five-component condensation product through a formal hetero Diels-Alder reaction. The product structure was confirmed by NMR and NOE analysis, and the proposed stepwise mechanism was supported by the reaction of the Biginelli intermediate with ethyl 2-methylene-3-oxobutanoate.

Keywords: Biginelli reaction, dihydropyrimidinone, multi-component condensation, 5-CC, hetero Diels-Alder reaction, $InBr_3$

OPEN ACCESS

Edited by:
Andrea Basso,
Università di Genova, Italy

Reviewed by:
Alessandro Massi,
University of Ferrara, Italy
Gian Cesare Tron,
Università degli Studi del Piemonte Orientale, Italy

****Correspondence:***
Peter Wipf
pwipf@pitt.edu

Specialty section:
This article was submitted to Organic Chemistry, a section of the journal Frontiers in Chemistry

Received: *26 June 2018*
Accepted: *03 August 2018*
Published: *24 August 2018*

Citation:
Maskrey TS, Frischling MC, Rice ML and Wipf P (2018) A Five-Component Biginelli-Diels-Alder Cascade Reaction. Front. Chem. 6:376. doi: 10.3389/fchem.2018.00376

INTRODUCTION

Dihydropyrimidinones (DHPMs) represent an attractive class of biologically active small molecules. DHPMs have been shown to have neuroprotective, antiparasitic, antiviral, antitumor, anti-inflammatory, and anticancer activities (de Fátima et al., 2015). Monastrol, for example, is one of the most studied DHPMs based on its antiproliferative activity (**Figure 1**). In 1999, monastrol was found to disrupt mitosis (Mayer et al., 1999; Kapoor et al., 2000). Subsequently, several potent analogs with increased anticancer potency have also been synthesized (Ragab et al., 2017).

The DHPM structure is the product of a reaction between a urea, β-keto ester, and an aldehyde, commonly termed the Biginelli reaction. The creation of a structurally diverse library of pharmacologically active compounds is an attractive possibility with this three-component condensation (Wan and Pan, 2012). As part of our studies on the preparation of bioactive DHPMs, in particular heat shock protein 70 (Hsp70) antagonists and agonists such as MAL3-101 and MAL1-271 (**Figure 1**), we explored the scope of Biginelli reactions in solution, fluorous media, and on solid support, and developed analogs with potent anticancer, antiviral, and neuroprotective properties (Wipf and Cunningham, 1995; Studer et al., 1997; Huryn et al., 2011; Manos-Turvey et al., 2016).

Standard Biginelli reactions frequently use catalytic amounts of Brønsted acids, such as hydrochloric acid (HCl) (Nagarajaiah et al., 2016). Various Lewis acid catalysts, including $InCl_3$ (Ranu et al., 2000), $FeCl_3$ (Lu and Bai, 2002), $BF_3{\bullet}OEt_2$ (Hu et al., 1998), $ZnCl_2$ (Sun et al., 2004), $GaCl_3$ (Yuan et al., 2017), and $InBr_3$ have also been used successfully (Phucho et al., 2009). While working to advance the scope of our own DHPM library, we noted the use of 10% $InBr_3$ as a catalyst at reflux in ethanol for 7 h to produce DHPMs (Fu et al., 2002; Martins et al., 2004). We decided to explore these reaction conditions further as they gave good yields even with formaldehyde as a reaction component. Initially, we hoped to be able to introduce substituents at the 4-position of the DHPM ring through an oxidative photochemical reaction related to the previously reported Friedel-Crafts amidoalkylation with the visible light catalyst, $Ru(bpy)_3Cl_2$ (Dai et al., 2012) (**Figure 2**). However, we found that $InBr_3$ conditions promoted a new five-component condensation with formaldehyde, and decided to first investigate the scope of this process.

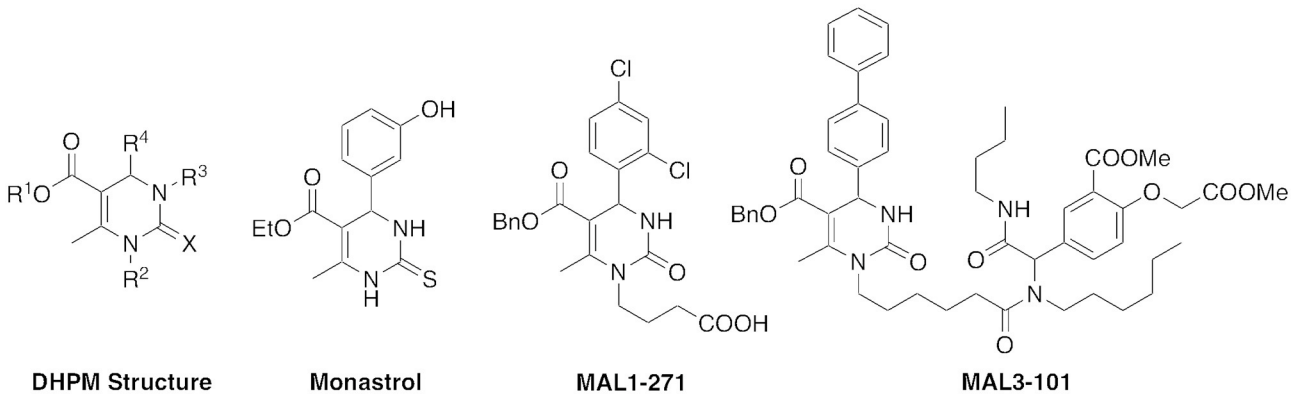

FIGURE 1 | DHPM structure and biologically active analogs.

RESULTS AND DISCUSSION

The originally reported $InBr_3$ reaction conditions utilized an excess of urea and equal equivalents of β-keto ester and aldehyde. For our initial test reactions, we chose *N,N′*-dimethylurea as the limiting reagent. The reaction of *N,N′*-dimethylurea, 1.8 equivalents of ethyl acetoacetate as the β-keto ester, and 3 equivalents of formaldehyde in 95% ethanol at reflux for 7 h yielded not only the expected DHPM product **1A** but also a higher molecular weight product that we did not anticipate (**Figure 3**). Through NMR and NOE analyses, we were able to assign its fused bicyclic structure as **1B**. We hypothesized that this secondary product occurred through a five-component condensation reaction, and an *in situ* formal hetero Diels-Alder reaction of the expected DHPM Biginelli intermediate was in agreement with the product structure.

Prior reports of the product of a Biginelli reaction being utilized as a dienophile in a hetero Diels-Alder reaction are rare. Sharma and coworkers demonstrated the reaction of an isolated Biginelli heterocycle with *N*-arylidine-*N′*-methylformamidines and *N*-arylidine guanidine in THF (Sharma et al., 2005). Our present synthesis represents the first one pot reaction to form these highly functionalized bicyclic products from readily available precursors.

We subsequently explored a range of reaction conditions in an attempt to improve overall yield and selectivity (**Figure 3**). For these optimizations, we used our original reaction components *N,N′*-dimethylurea, ethyl acetoacetate, and formaldehyde (**Table 1**). The traditional Brønsted acid catalyst, HCl, gave no conversion with formaldehyde (entry 2). We experimented with other Lewis acids (entries 3–6) to catalyze the reaction but saw no conversion with $FeCl_3$ or $ZnCl_2$. Conversion was modest with both $InCl_3$ and $AlCl_3$. Increasing the proportions of the β-keto ester and the aldehyde to 2.5 and 5 equivalents, respectively, improved the yield of both products **1A** and **1B** (entry 7). However, increasing or decreasing the reactant concentration (entries 8 and 9) did not improve the overall yield. Doubling the reaction time to 14.5 h also did not increase the conversion to product **1B** (entry 10 vs. entry 7). After a shortened reaction time of 2.0 h, only product **1A** was isolated in 28% yield (entry 11). Accordingly, entry 7 represented our optimized conditions: 1 equivalent of urea, 2.5 equivalents of β-keto ester, 5.0 equivalents of aldehyde, and 0.1 equivalents of $InBr_3$ at reflux conditions in ethanol (0.2 M) for 7 h provided 45% of DHPM **1A** and 48% of pyranopyrimidinone **1B**.

We then used these optimized conditions to further explore the scope of the reaction (**Table 2**). Formaldehyde was used as the aldehyde component in all reactions since preliminary trials with other aldehydes and ketones were not successful in producing any fused bicycles **B**. We also used symmetrical ureas exclusively to avoid possible regioisomers (exploratory reactions confirmed a lack of regioselectivity with unsymmetrical ureas; for example, while 1-methylurea and 1-(4-methoxyphenyl)-3-methylurea provided both the Biginelli DHPM and the Diels-Alder products, we were unable to separate the regioisomers formed in an approximately 1:1 ratio). Curiously, the reaction with the *N,N′*-dimethylthiourea stopped at the Biginelli product **2A**, which was isolated in 61% yield (entry 2). Methyl acetoacetate with thiourea **2** (entry 3) also gave similar results, but product **3A** was formed in lower yield, likely due to *trans*-esterification with ethanol. Utilizing benzyl acetoacetate, we were able to isolate both Biginelli (**4A**, **5A**) and five-component condensation products (**4B**, **5B**) in good overall yields with the urea and thiourea derivatives (entries 4 and 5). However, the yield of the five-component condensation Diels-Alder product **4B** was considerably higher with the urea derivative than the pyranopyrimidinethione **5B** resulting from the thiourea. With allyl acetoacetate and *N,N′*-dimethylurea, we were able to isolate the five-component condensation product **6B**, but not the corresponding Biginelli intermediate, as it proved unstable. We also attempted to replace the traditional β-keto ester with 5,5-dimethyl-1,3-cyclohexanedione (dimedone) to probe the feasibility of adding an additional ring in the hetero Diels-Alder reaction (**Figure 4**). Unfortunately, with both *N,N′*-dimethylurea and its thiourea equivalent, we were only able to isolate Biginelli products **7A** and **8A**, in significantly lower yields than for the β-keto ester conversions.

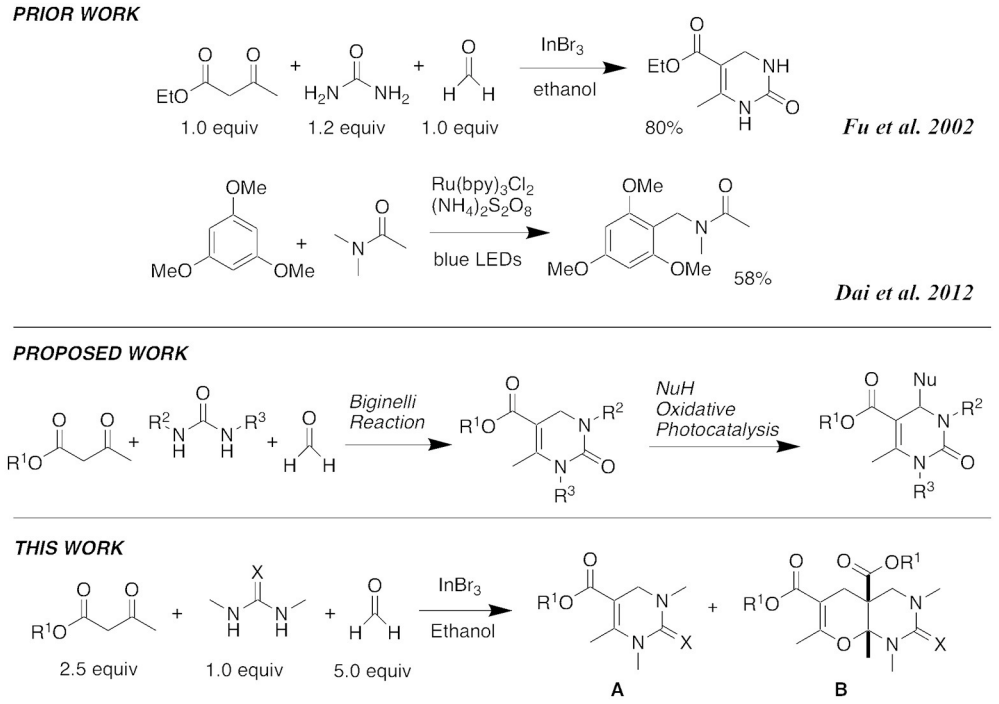

FIGURE 2 | Literature precedence and synthetic plans.

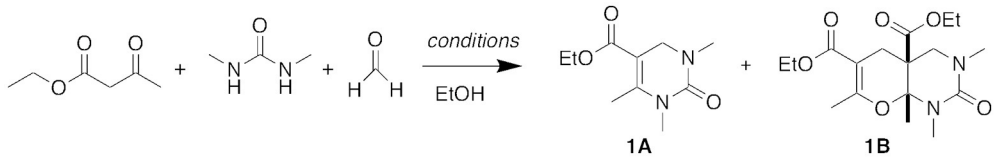

FIGURE 3 | Five-component condensation reaction. For conditions, see **Table 1**.

To confirm our hypothesis that the five-component condensation product formed through a hetero Diels-Alder reaction with the DHPM (Biginelli) intermediate, we reacted Biginelli product **1A** with ethyl 2-methylene-3-oxobutanoate (**Figure 5**). After stirring in sulfolane at room temperature for 18 h, we isolated the corresponding hetero Diels-Alder Product, **1B**, in 11% yield. We were also able to repeat this conversion with the Biginelli intermediate **5A** to form the hetero Diels-Alder Product **9B**.

Interestingly, when the five-component condensation product **1B** was subjected to Krapcho dealkylation conditions with LiCl in DMSO, we isolated the DHPM product, **1A**, in 87% yield, presumable through a retro Diels-Alder reaction (**Figure 6**) (Krapcho et al., 1967).

Figure 7 illustrates our proposed mechanism for the five-component condensation reaction. In the presence of a Lewis acid, condensation of the urea with the aldehyde and subsequent loss of water generates a sufficiently reactive electrophile for attack by the β-keto ester, which then undergoes cyclization to give **1A**. The excess β-keto ester and formaldehyde react to form a methylene group at the α-position, and this electrophile then undergoes a hetero Diels-Alder reaction with the intermediate DHPM **1A** to provide the fused heterocyclic **1B** as a single stereoisomer. We determined the configuration of the methyl group to be *cis* to the ester at the two quaternary ring fusion atoms by converting the ester to the primary alcohol **10** with $LiBH_4$, and then using a NOE analysis to confirm that the methyl group protons showed a >10% percent double resonance enhancement with the newly formed CH_2 protons.

CONCLUSIONS

We have discovered and optimized experimental conditions for a novel one pot, five-component condensation reaction with a β-keto ester, urea, and formaldehyde. The reaction appears to proceed through an intermediate DHPM (Biginelli) product. The DHPM then reacts with the condensation product of the β-keto ester and formaldehyde through a

TABLE 1 | Investigation of reaction time, concentration, equivalents, and catalyst with formaldehyde, *N,N′*-dimethylurea, and ethyl acetoacetate (**Figure 3**).

Entry	Urea (equiv)	Ester (equiv)	Aldehyde (equiv)	Catalyst (equiv)	Time (h)	Concentration (M)	A (% Yield)	B (% Yield)
1	1	1.8	3	$InBr_3$ (0.1)	7	0.2	10	26
2	1	1.8	3	HCl (1.0)	7	0.5	0	0
3	1	1.8	3	$InCl_3$ (0.1)	7	0.3	23	25
4	1	1.8	3	$AlCl_3$ (0.1)	7	0.3	3	14
5	1	1.8	3	$FeCl_3$ (0.2)	7	0.2	0	0
6	1	1.8	3	$ZnCl_2$ (0.2)	7	0.3	0	0
7	1	2.5	5	$InBr_3$ (0.1)	7	0.2	45	48
8	1	2.5	5	$InBr_3$ (0.1)	7	1.0	55	37
9	1	2.5	5	$InBr_3$ (0.1)	7	0.05	38	27
10	1	2.5	5	$InBr_3$ (0.1)	14.5	0.2	41	36
11	1	2.5	5	$InBr_3$ (0.1)	2	0.2	28	0

formal hetero Diels-Alder reaction. While the scope of this new process is still limited to formaldehyde and symmetrical *N,N′*-dialkylated ureas, it provides easy access to bicyclic ring systems that were previously inaccessible through a single transformation.

MATERIALS AND METHODS

General

All reagents were obtained commercially unless otherwise noted. All glassware was dried in an oven at 140°C for 2 h prior to use. Reactions were monitored by TLC analysis (EMD Millipore pre-coated silica gel 60 F254 plates, 250 μM layer thickness) and visualization was accomplished with a 254 nM UV light or staining with a PMA solution (5 g of phosphomolybdic acid in 100 mL of 95% EtOH), p-anisaldehyde solution (2.5 mL of p-anisaldehyde, 2 mL of AcOH, and 3.5 mL of conc. H_2SO_4 in 100 mL of 95% EtOH), or a $KMnO_4$ solution (1.5 g of $KMnO_4$ and 1.5 g of K_2CO_3 in 100 mL of a 0.1% NaOH solution). Some purification by chromatography was performed using a SiO_2 Büchi flash chromatography system. $^1H/^{13}C$ NMR spectra were recorded on either a Bruker Avance 300/75 MHz, Bruker Avance 400/100 MHz, Bruker Avance 500/135 MHz, or Bruker Avance 600/150 MHz instruments. Chemical shifts were reported in parts per million with the residual solvent peak used as the internal standard ($^1H/^{13}C$: $CDCl_3$, 7.26, 77.0 ppm; CD_3OD, 3.31, 49.3 ppm; DMSO, 2.50, 39.5 ppm). Chemical shifts were tabulated as follows: chemical shift, multiplicity (s = singlet, d = doublet, t = triplet, q = quarter, dd = doublet of doublet, dt = doublet of triplet, dq = doublet of quartet, m = multiplet, b = broad, app = apparent), coupling constants, and integration. All 1D NMR spectra were processed using Bruker Topspin NMR. IR spectra were obtained on an Identity IR-ATR spectrometer. Melting points (uncorrected) were determined using a Mel-Temp instrument. HRMS data were obtained on a Thermo Scientific Exactive HRMS coupled to a Thermo Scientific Accela HPLC system using a 2.1 x 50 mm 3.5 μm Waters XTerra C18 column eluting with MeCN/H_2O containing 0.1% formic acid.

TABLE 2 | Reaction scope with formaldehyde, *N,N′*-dimethyl(thio)urea (X=O,S), and alkyl (R^1) acetoacetates. For products A and B, see **Figure 2**.

No.	R^1	X	A (% Yield)	B (% Yield)
1	Ethyl	O	45	48
2	Ethyl	S	61	0
3	Methyl	S	31	0
4	Benzyl	O	12	73
5	Benzyl	S	61	32
6	Allyl	O	0	21

General 5-Component Condensation Reaction Procedure

Representative procedure for **ethyl 1,3,6-trimethyl-2-oxo-1,2,3,4-tetrahydropyrimidine-5-carboxylate (1A) and diethyl(4a*SR*,8a*RS*)-1,3,7,8a-tetramethyl-2-oxo-1,3,4,8a-tetrahydro-2*H*-pyrano[2,3-*d*]pyrimidine-4a,6(5*H*)-dicarboxylate (1B)**. A solution of ethyl acetoacetate (1.21 mL, 9.43 mmol, 2.5 equiv), paraformaldehyde (0.478 g, 15.3 mmol, 5 equiv), and *N,N′*-dimethylurea (0.456 g, 5.07 mmol, 1 equiv) in 95% ethanol (25 mL) was stirred at room temperature for 10 min. Indium(III) bromide (0.180 g, 0.507 mmol, 0.1 equiv) was added and the reaction mixture was heated under reflux for 7 h, cooled to room temperature, filtered through basic Al_2O_3 (EtOAc) and concentrated under reduced pressure. The residue was purified by chromatography on SiO_2 (hexanes/EtOAc, 3:1 to 1:3) to afford **1A** (0.481 g, 2.26 mmol, 45%) as a light yellow wax and **1B** (0.855 g, 2.41 mmol, 48%) as a yellow oil. This procedure was followed for all products in **Table 2** and **Figure 4**, and spectral properties are presented below.

Ethyl 1,3,6-trimethyl-2-oxo-1,2,3,4-tetrahydropyrimidine-5-carboxylate (1A). IR (ATR) 2981.1, 2908.3, 1672.9, 1622.7, 1414.1, 1262.5, 1204.0, 1077.4, 1026.8, 749.3 cm^{-1}; ^1H NMR (400 MHz, CD_3OD) δ 4.16 (q, J = 7.1 Hz, 2 H), 4.01 (d, J = 1.1 Hz, 2 H), 3.17 (s, 3 H), 2.92 (s, 3 H), 2.46 (t, J = 1.3 Hz, 3 H), 1.28 (t, J = 7.1 Hz, 3 H); ^{13}C NMR (100 MHz, CD_3OD) δ 165.9, 154.8, 150.8, 98.3, 59.8, 48.5, 34.2, 29.8, 14.8, 13.2; HRMS (HESI) *m/z* calcd for $C_{10}H_{17}N_2O_3$ $[M+H]^+$ 213.1234, found 213.1234.

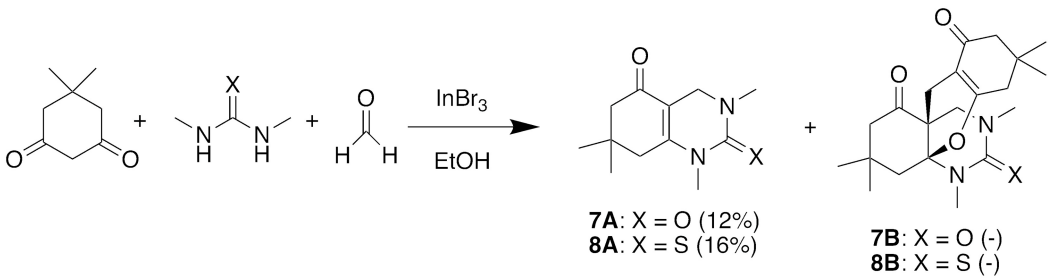

FIGURE 4 | Attempted five-component condensation reaction with a cyclic 1,3-diketone.

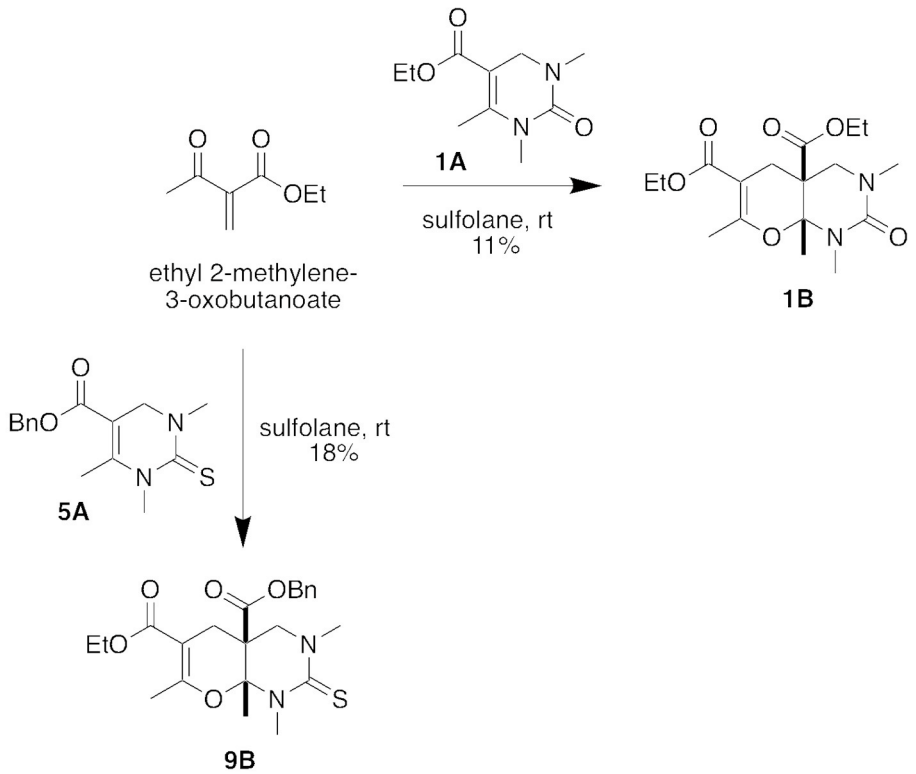

FIGURE 5 | Stepwise conversions of intermediate DHPM (Biginelli) products in a hetero Diels-Alder reaction.

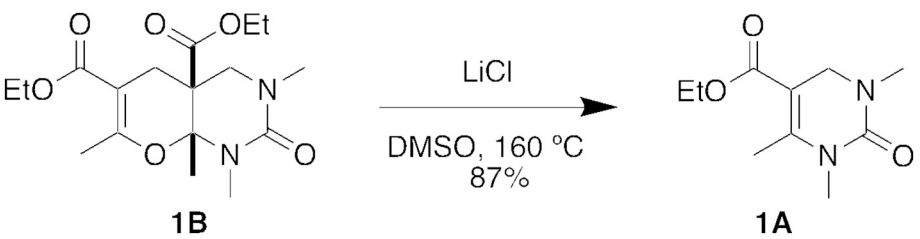

FIGURE 6 | Retro Diels-Alder reaction under Krapcho dealkylation conditions.

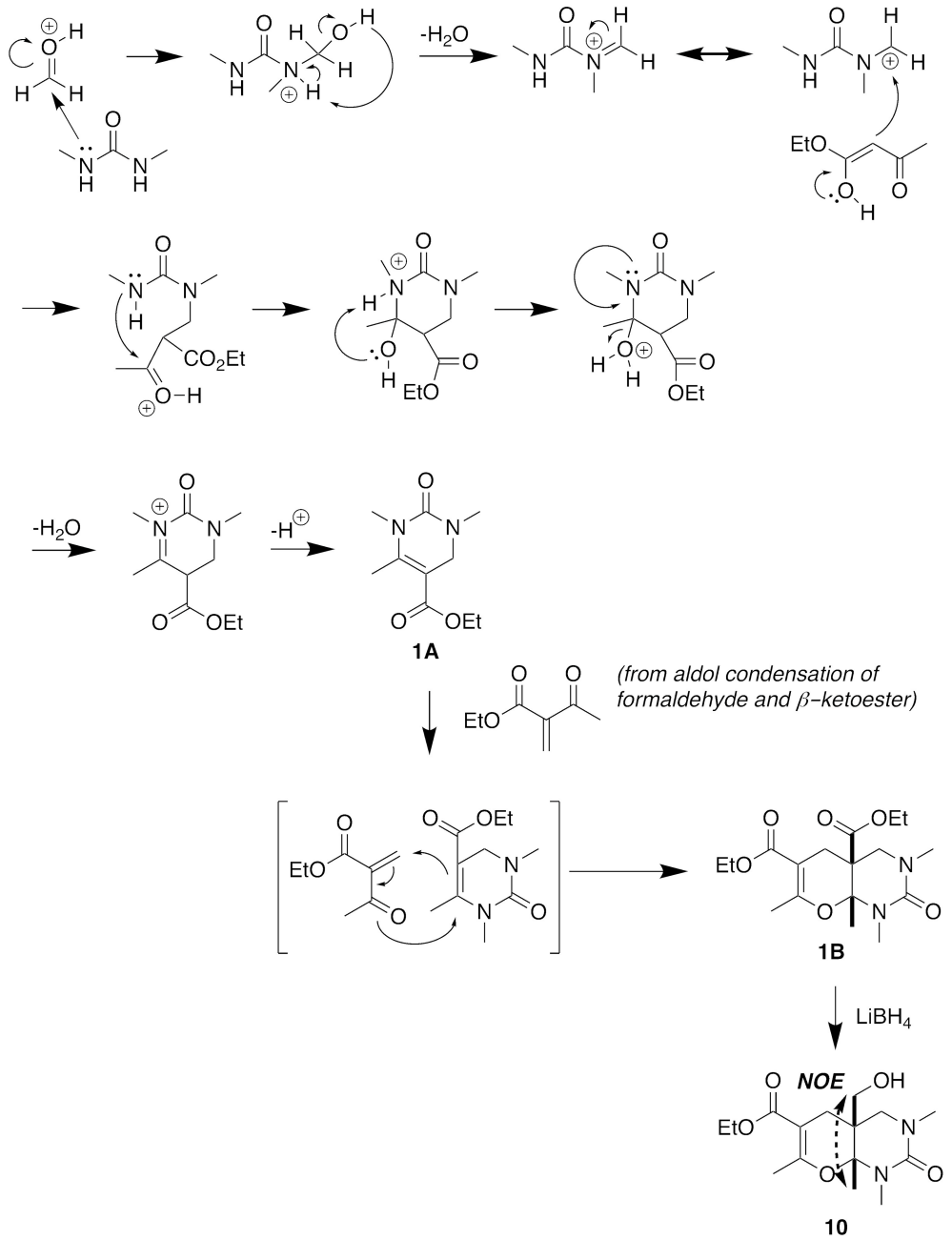

FIGURE 7 | Proposed mechanism of five-component condensation.

Diethyl(4a*SR*,8a*RS*)-1,3,7,8a-tetramethyl-2-oxo-1,3,4,8a-tetrahydro-2*H*-pyrano[2,3-*d*]pyrimidine-4a,6(5*H*)-dicarboxylate (1B). IR (ATR) 2987.8, 2931.8, 1705.4, 1629.0, 1498.5, 1442.6, 1343.8, 1233.9, 1086.6, 1041.9, 984.1, 870.4, 844.3, 753.0 cm^{-1}; ^1H NMR (400 MHz, CD_3OD) δ 4.22–4.14 (m, 4 H), 3.53 (d, J = 12.7 Hz, 1 H), 3.30 (d, J = 12.7 Hz, 1 H), 2.95 (s, 3 H), 2.92 (s, 3 H), 2.69 (dq, J = 17.8, 1.7 Hz, 1 H), 2.45 (dq, J = 17.8, 1.6 Hz, 1 H), 2.24 (t, J = 1.6 Hz, 3 H), 1.61 (s, 3 H), 1.28 (t, J = 7.2 Hz, 3 H), 1.25 (t, J = 7.2 Hz, 3 H); ^{13}C NMR (100 MHz, CD_3OD) δ 170.6, 167.2, 160.2, 154.9, 99.8, 87.8, 61.4, 59.9, 49.3, 44.0, 34.9, 27.6, 27.5, 19.5, 18.5, 13.5, 13.1; HRMS (HESI) *m/z* calcd for $C_{17}H_{27}N_6O_2$ $[M+H]^+$ 355.1864, found 355.1862.

Ethyl 1,3,6-trimethyl-2-thioxo-1,2,3,4-tetrahydropyrimidine-5-carboxylate (2A). IR (ATR) 2978.4, 1670.0, 1636.5, 1524.6, 1442.6, 1356.9, 1267.4, 1207.8, 1168.6, 1140.7, 1088.5, 1015.8 cm^{-1}; ^1H NMR (400 MHz, $CDCl_3$) δ 4.20 (q, J = 7.1 Hz, 2 H), 4.06 (d, J = 1.0 Hz, 2 H), 3.55 (s, 3 H), 3.42 (s, 3 H), 2.45 (t, J = 1.0 Hz, 3 H), 1.30 (t, J = 7.1 Hz, 3 H); ^{13}C

NMR (100 MHz, $CDCl_3$) δ 180.8, 165.3, 149.2, 101.3, 60.5, 47.9, 42.9, 37.9, 16.2, 14.3; HRMS (HESI) *m/z* calcd for $C_{10}H_{17}N_2O_2S$ $[M+H]^+$ 229.1005, found 229.1004.

Methyl 1,3,6-trimethyl-2-thioxo-1,2,3,4-tetrahydropyrimidine-5-carboxylate (3A). IR(ATR) 2929.7, 2828.8, 1698.0, 1619.2, 1516.3, 1459.9, 1425.5, 1366.5, 1317.3, 1261.1, 1169.4, 1091.3, 990.9, 803.2, 765.3 cm^{-1}; ^{1}H-NMR (400 MHz, $CDCl_3$) δ 4.09 (s, 2 H), 3.77 (s, 3 H), 3.58 (s, 3 H), 3.45 (s, 3 H), 2.48 (s, 3 H); ^{13}C NMR (100 MHz, $CDCl_3$) δ 180.8, 165.7, 149.6, 101.0, 51.6, 47.9, 42.9, 37.9, 16.3; HRMS (HESI) *m/z* calcd for $C_9H_{15}N_2O_2S$ $[M+H]^+$ 215.0849, found 215.0848.

Benzyl 1,3,6-trimethyl-2-oxo-1,2,3,4-tetrahydropyrimidine-5-carboxylate (4A). IR (ATR) 2933.0, 1662.6, 1554.5, 1485.5, 1450.1, 1192.9, 1127.6, 1077.3, 1027.0, 691.5 cm^{-1}; ^{1}H-NMR (300 MHz, CD_3OD) δ 7.37–7.34 (m, 5 H), 5.17 (s, 2 H), 4.04 (bd, J = 1.2 Hz, 2 H), 3.17 (s, 3 H), 2.91 (s, 3 H), 2.47 (t, J = 1.2 Hz, 3 H); ^{13}C NMR (75 MHz, $CDCl_3$) δ 180.8, 165.0, 149.9, 136.0, 128.6, 128.3, 128.1, 101.8, 66.3, 47.9, 42.9, 37.9, 16.4; HRMS (HESI) *m/z* calcd for $C_{15}H_{19}N_2O_3$ $[M+H]^+$ 275.1390, found 275.1388.

Dibenzyl(4a*SR*,8a*RS*)-1,3,7,8a-tetramethyl-2-oxo-1,3,4,8a-tetrahydro-2*H*-pyrano[2,3-*d*]pyrimidine-4a,6(5*H*)-dicarboxylate (4B). IR (ATR) 2937.4, 2881.5, 1712.9, 1629.0, 1506.0, 1448.2, 1379.3, 1347.6, 1232.0, 1077.3, 982.3, 883.5, 756.7 cm^{-1}; ^{1}H NMR (300 MHz, CD_3OD) δ 7.35–7.32 (m, 10 H), 5.19, 5.15 (AB, J = 16.4 Hz, 2 H), 5.15 (s, 2 H), 3.54 (d, J = 12.9 Hz, 1 H), 3.27 (d, J = 12.9 Hz, 1 H), 2.90 (s, 3 H), 2.84 (s, 3 H), 2.73 (dq, J = 17.8, 1.6 Hz, 1 H), 2.48 (dq, J = 17.8, 1.6 Hz, 1 H), 2.20 (t, J = 1.6 Hz, 3 H), 1.54 (s, 3 H); ^{13}C NMR (100 MHz, $CDCl_3$) δ 170.6, 167.0, 161.2, 154.1, 136.2, 135.0, 128.6, 128.5 (2C), 128.1 (2C), 128.0, 99.6, 87.6, 67.3, 66.0, 49.7, 44.1, 35.7, 28.1, 27.8, 20.7, 19.7; HRMS (HESI) *m/z* calcd for $C_{27}H_{31}N_2O_6$ $[M+H]^+$ 479.2177, found 479.2176.

Benzyl 1,3,6-trimethyl-2-thioxo-1,2,3,4-tetrahydropyrimidine-5-carboxylate (5A). IR (ATR) 2933.7, 1712.9, 1629.0 1450.1, 1358.8, 1254.4, 1215.2, 1163.0, 1094.1, 1066.1, 1028.8, 734.4 cm^{-1}; ^{1}H-NMR (600 MHz, $CDCl_3$) δ 7.39–7.32 (m, 5 H), 5.19 (s, 2 H), 4.08 (d, J = 1.0 Hz, 2 H), 3.55 (s, 3 H), 3.41 (s, 3 H), 2.47 (d, J = 1.0 Hz, 3 H); ^{13}C NMR (150 MHz, $CDCl_3$) δ 180.8, 165.0, 149.9, 136.0, 128.6, 128.30, 128.17, 100.9, 66.3, 47.9, 43.0, 38.0, 16.4; HRMS (HESI) *m/z* calcd for $C_{15}H_{19}N_2O_2S$ $[M+H]^+$ 291.1162, found 291.1160.

Dibenzyl(4a*SR*,8a*RS*)-1,3,7,8a-tetramethyl-2-thioxo-1,3,4,8a-tetrahydro-2*H*-pyrano[2,3-*d*]pyrimidine-4a,6(5*H*)-dicarboxylate (5B). IR (ATR) 2933.7, 1712.9, 1629.0, 1450.1, 1340.1, 1232.0, 1215.2, 1077.3, 1002.8, 995.3, 734.4, 695.2 cm^{-1}; ^{1}H NMR (300 MHz, $CDCl_3$) δ 7.35–7.32 (m, 10 H), 5.19–5.08 (m, 4 H), 3.79 (d, J = 13.6 Hz, 1 H), 3.39 (s, 3 H), 3.34 (s, 3 H), 3.31 (d, J = 13.5 Hz, 1H), 2.63 (dd, J = 17.8, 1.5 Hz, 1 H), 2.36 (dd, J = 17.8, 1.5 Hz, 1 H), 2.23 (t, J = 1.5 Hz, 3 H), 1.51 (s, 3 H); ^{13}C NMR (100 MHz, CD_3OD) δ 178.3, 169.0, 166.8, 160.1, 136.4, 135.4, 128.3, 128.2 (2C), 128.1 (2C), 128.0, 127.9 (2C), 127.8, 101.1, 86.5, 68.0, 67.1, 65.7, 51.5, 43.1, 42.7, 34.1, 26.0, 20.2, 18.1, 13.9; HRMS (HESI) *m/z* calcd for $C_{27}H_{31}N_2O_5S$ $[M+H]^+$ 495.1948, found 495.1945.

Diallyl(4a*SR*,8a*RS*)-1,3,7,8a-tetramethyl-2-oxo-1,3,4,8a-tetrahydro-2*H*-pyrano[2,3-*d*]pyrimidine-4a,6(5*H*)-dicarboxylate (6B). IR (ATR) 2934.3, 1728.4, 1709.3, 1646.5, 1500.4, 1444.8, 1410.4, 1345.0, 1234.1, 1213.6, 1102.4, 1081.7, 1039.7, 986.7, 881.9, 753.5 cm^{-1}; ^{1}H NMR (400 MHz, DMSO-*d6*) δ 6.00–5.84 (m, 2 H), 5.32–5.21 (m, 4 H), 4.61 (dd, J = 16.0 Hz, 4.0 Hz, 4 H), 3.51 (d, J = 12.4 Hz, 1 H), 3.22 (d, J = 12.4 Hz, 1 H), 2.80 (s, 3 H), 2.68 (s, 3 H), 2.66 (d, J = 17.6 Hz, 1 H), 2.40 (d, J = 17.6 Hz, 1 H), 2.20 (s, 3 H), 1.52 (s, 3 H); ^{13}C NMR (100 MHz, DMSO-*d6*) δ 170.5, 166.6, 160.6, 153.8, 133.5, 132.5, 118.1, 118.0, 99.9, 88.1, 65.8, 64.7, 49.3, 44.2, 35.7, 28.3, 27.7, 20.7, 19.7; HRMS (HESI) *m/z* calcd for $C_{19}H_{27}N_2O_6$ $[M+H]^+$ 379.1864, found 379.1862.

1,3,7,7-Tetramethyl-4,6,7,8-tetrahydroquinazoline-2,5(1*H*,3*H*)-dione (7A). IR (ATR) 2960.4, 2890.4, 1722.3, 1620.5, 1574.3, 1438.2, 1380.7, 1268.3, 1224.5, 1127.4, 1079.6, 1006.6 cm^{-1}; ^{1}H NMR (400 MHz, $CDCl_3$) δ 4.04 (s, 2 H), 3.20 (s, 3 H), 2.98 (s, 3 H), 2.39 (s, 2 H), 2.24 (s, 2 H), 1.11 (s, 6 H); ^{13}C NMR (100 MHz, $CDCl_3$) δ 194.3, 153.5, 153.2, 105.6, 49.2, 45.6, 40.2, 35.8, 32.8, 30.4, 28.6; HRMS (HESI) *m/z* calcd for $C_{12}H_{19}N_2O_2$ $[M+H]^+$ 223.1441, found 223.1440.

1,3,7,7-Tetramethyl-2-thioxo-2,3,4,6,7,8-hexahydroquinazolin-5(1*H*)-one (8A). IR (ATR) 2950.5, 2922.5, 2868.5, 1724.1, 1629.0, 1450.1, 1261.8, 1215.2, 1127.6, 1064.3, 982.3 cm^{-1}; ^{1}H NMR (400 MHz, $CDCl_3$) δ 4.12 (s, 2 H), 3.60 (s, 3 H), 3.44 (s, 3 H), 2.43 (s, 2 H), 2.26 (s, 2 H), 1.11 (s, 6 H); ^{13}C NMR (100 MHz, $CDCl_3$) δ 194.6, 180.1, 151.0, 107.4, 49.3, 45.8, 43.8, 40.6, 37.4, 33.1, 28.6; HRMS (HESI) *m/z* calcd for $C_{12}H_{19}N_2OS$ $[M+H]^+$ 239.1213, found 239.1211.

Diels-Alder Reaction of DHPM Intermediate to Form 5-Component Condensation Product:

Ethyl 2-methyl-3-oxo-2-(phenylthio)butanoate. A stirred solution of N-chlorosuccinimide (6.21 g, 45.1 mmol) in CH_2Cl_2 (66 mL) was treated with thiophenol (0.40 mL, 3.8 mmol) and heated to reflux. After the reaction mixture changed color from yellow to orange, indicating the initiation of the reaction, additional thiophenol (4.24 mL, 41.2 mmol) was added dropwise to maintain a gentle reflux. The mixture was then allowed to cool to RT. After 1 h, the mixture was further cooled to 4°C on an ice bath, and ethyl 2-methylacetoacetate (6.81 mL, 46.7 mmol) was added over a 30 min period. After warming to RT and stirring for an additional 30 min, HCl was removed by bubbling nitrogen through the product solution and the solvent was removed under reduced pressure. The residue was suspended in petroleum ether (44 mL) and filtered. The resulting solid filtrate was washed with 5 portions (44 mL each) of petroleum ether. The combined organic fractions were combined and concentrated to give ethyl 2-methyl-3-oxo-2-(phenylthio)butanoate (11.6 g, 46.1 mmol) as a dark yellow liquid in quantitative yield with a small impurity. This product was used for the next step without further purification: ^{1}H NMR (400 MHz, $CDCl_3$) δ 7.51–7.30 (m, 5 H), 4.28–4.19 (m, 2 H), 2.37 (s, 3 H), 1.49 (s, 3 H), 1.32–1.26 (m, 3 H).

Ethyl 2-methyl-3-oxo-2-(phenylsulfinyl)butanoate. A solution of MCPBA (4.89 g, 19.8 mmol) in CH_2Cl_2 (51 mL) was added dropwise to a cold (0°C) solution of ethyl 2-methyl-3-oxo-2-(phenylthio)butanoate (5.01 g, 19.9 mmol) in CH_2Cl_2

(51 mL). The reaction mixture was stirred for 50 min, filtered through a plug of neutral Al_2O_3 (CH_2Cl_2), and concentrated under reduced pressure to yield ethyl 2-methyl-3-oxo-2-(phenylsulfinyl)butanoate (5.31 g, 19.8 mmol, 98%) as a yellow liquid that was used for the next step without further purification: IR (ATR) 1,030 cm^{-1}.

Ethyl 2-methylene-3-oxobutanoate. A solution of ethyl 2-methyl-3-oxo-2-(phenylsulfinyl)butanoate (5.21 g, 19.4 mmol) in sulfolane (8 mL) was heated at 60°C and 0.1 mm Hg in a Kugelrohr distillation setup for 2 h. The collection vial was cooled to −78°C in a dry ice bath. The tube was vented with nitrogen gas, and the first distillate of ethyl 2-methylene-3-oxobutanoate was collected as a colorless liquid (0.66 g). The distillation was repeated with the remaining solution at 90°C for 1 h and 110°C for 1 h to give a second batch of ethyl 2-methylene-3-oxobutanoate together with residual sulfolane (1.22 g), for an overall yield of 68% (1.87 g, 13.2 mmol). Characteristic signals for ethyl 2-methylene-3-oxobutanoate: ^{1}H NMR (300 MHz, $CDCl_3$) δ 6.44 (d, J = 0.9 Hz, 1 H), 6.41 (d, J = 0.9 Hz, 1 H), 4.30 (q, J = 7.2 Hz, 2 H), 2.43 (s, 3 H), 1.33 (t, J = 7.2 Hz, 3 H).

(Diethyl(4a*SR*,8a*RS*)-1,3,7,8a-tetramethyl-2-oxo-1,3,4,8a-tetrahydro-2*H*-pyrano[2,3-*d*]pyrimidine-4a,6(5*H*)-dicarboxylate (1B). Ethyl 1,3,6-trimethyl-2-oxo-1,2,3,4-tetrahydropyrimidine-5-carboxylate (**1A**, 0.096 g, 0.45 mmol) was added to ethyl 2-methylene-3-oxobutanoate containing residual sulfolane (0.244 g, 1.72 mmol). The reaction mixture was stirred at room temperature for 18 h and then concentrated under reduced pressure. The residue was purified by gradient chromatography on SiO_2 (hexanes/EtOAc, 4:1 to 1:1) to afford **1B** (0.0682 g, 0.192 mmol, 11%) as a yellow oil that was spectroscopically identical to **1B** previously obtained in the one-pot Biginelli-Diels-Alder reaction.

4a-Benzyl 6-ethyl (4a*SR*,8a*RS*)-1,3,7,8a-tetramethyl-2-thioxo-1,3,4,8a-tetrahydro-2*H*-pyrano[2,3-*d*]pyrimidine-4a,6(5*H*)-dicarboxylate (9B). Benzyl 1,3,6-trimethyl-2-thioxo-1,2,3,4-tetrahydropyrimidine-5-carboxylate (**5A**, 0.043 g, 0.15 mmol) was added to ethyl 2-methylene-3-oxobutanoate containing residual sulfolane (0.021 g, 0.15 mmol). The mixture was stirred at room temperature for 18 h. Another 5 equivalents of ethyl 2-methylene-3-oxobutanoate containing residual sulfolane (0.105 g, 0.738 mmol) was added and the reaction mixture was stirred at room temperature for an additional 48 h. The mixture was concentrated under reduced pressure and the resulting residue was purified by chromatography on SiO_2 (hexanes/EtOAc, 4:1 to 2:1) to afford **9B** (0.0113 g, 0.0261 mmol, 18%) as a yellow oil: IR (ATR) 2974.7, 2933.7, 1705.4, 1643.9, 1524.6, 1450.1, 1340.1, 1232.0, 1077.3, 734.4, 700.8 cm^{-1}; ^{1}H NMR (400 MHz, $CDCl_3$) δ 7.34–7.25 (m, 5 H), 5.15, 5.12 (AB, J = 12.0 Hz, 2 H), 4.19–4.08 (m, 2 H), 3.78 (d, J = 13.6 Hz, 1 H), 3.38 (s, 3 H), 3.32–3.28 (m, 4 H), 2.60–2.55 (m, 1 H), 2.35–2.29 (m, 1 H), 2.20 (t, J = 1.6 Hz, 3 H), 1.48 (s, 3 H), 1.27–1.23 (m, 3 H); ^{13}C NMR (100 MHz, CDCl3): δ 178.5, 170.0, 166.9, 159.6, 134.9, 128.7, 128.6, 128.1, 101.3, 86.1, 67.6, 61.7, 60.3, 52.2, 43.9, 43.1, 34.9, 21.5, 19.2, 14.3, 14.0; HRMS (HESI) *m/z* calcd for $C_{22}H_{29}N_2O_5S$ $[M+H]^+$ 433.1792, found 433.1788.

Conversion of 5-Component Condensation Product to DHPM Under Krapcho Conditions

Ethyl 1,3,6-trimethyl-2-oxo-1,2,3,4-tetrahydropyrimidine-5-carboxylate (1A). A mixture of diethyl (4a*SR*,8a*RS*)-1,3,7,8a-tetramethyl-2-oxo-1,3,4,8a-tetrahydro-2*H*-pyrano[2,3-*d*]pyrimidine-4a,6(5*H*)-dicarboxylate (**1B**, 0.050 g, 0.14 mmol), LiCl (0.016 g, 0.37 mmol), DMSO (2 mL), and water (4 drops) was heated at 160°C and the reaction was monitored by TLC analysis (2:1, hexanes:EtOAc). After 4 h, the reaction mixture was cooled to room temperature and extracted with EtOAc. The organic layer was dried ($MgSO_4$), filtered, and concentrated to yield ethyl 1,3,6-trimethyl-2-oxo-1,2,3,4-tetrahydropyrimidine-5-carboxylate (**1A**, 0.026 g, 0.12 mmol, 87%) as a light yellow oil that was spectroscopically identical to **1A** previously obtained in the one-pot Biginelli-Diels-Alder reaction.

Structural Confirmation by Conversion to Alcohol

Ethyl (4a*RS*,8a*RS*)-4a-(hydroxymethyl)-1,3,7,8a-tetramethyl-2-oxo-1,3,4,4a,5,8a-hexahydro-2*H*-pyrano[2,3-*d*]pyrimidine-6-carboxylate (10). A mixture of 4 M $LiBH_4$ in THF (0.16 mL, 0.63 mmol) and diethyl (4a*SR*,8a*RS*)-1,3,7,8a-tetramethyl-2-oxo-1,3,4,8a-tetrahydro-2*H*-pyrano[2,3-*d*]pyrimidine-4a,6(5*H*)-dicarboxylate (**1B**, 150 mg, 0.42 mmol) in Et_2O (2.1 mL) was heated at 35°C for 3 h. The reaction was monitored by TLC analysis (2:1, EtOAc:hexanes). After 3 h, the reaction mixture was quenched with 1 M HCl with ice-cooling. The solution was diluted with water and extracted with CH_2Cl_2 (3 × 5 mL). The organic layer was dried ($MgSO_4$), filtered, and concentrated under reduced pressure to yield **10** (0.0794 g, 0.254 mmol, 60%) as white solid: Mp 114.8–116.9°C; IR (ATR) 3367.1, 2923.7, 1702.4, 1621.6, 1506.7, 1445.3, 1406.9, 1377.5, 1346.8, 1291.2, 1250.2, 1159.3, 1110.5, 985.0, 884.9, 838.9, 753.7 cm^{-1}; ^{1}H NMR (400 MHz, DMSO) δ 5.01 (t, J = 5.4 Hz, 1 H), 4.08 (q, J = 7.2 Hz, 2 H), 3.42 (dd, J = 10.8, 5.2 Hz, 1 H), 3.27 (dd, J = 10.8, 5.2 Hz, 1 H), 3.12 (d, J = 12.0 Hz, 1 H), 2.94 (d, J = 12.0 Hz, 1 H), 2.81 (s, 3 H), 2.80 (s, 3 H), 2.32 (bd, J = 16.4 Hz, 1 H), 2.15 (s, 3 H), 2.13 (bd, J = 16.4 Hz, 1 H), 1.37 (s, 3 H), 1.21 (t, J = 7.2 Hz, 3 H); ^{13}C NMR (100 MHz, DMSO) δ 167.6, 159.9, 154.3, 100.0, 89.9, 62.1, 59.9, 48.7, 37.6, 35.9, 28.1, 27.1, 19.8, 19.7, 14.8; HRMS (HESI) *m/z* calcd for $C_{15}H_{25}N_2O_5$ $[M+H]^+$ 313.1758, found 313.1759.

AUTHOR CONTRIBUTIONS

TM, MF, and MR worked on the presented work under the guidance of PW. The manuscript was written by TM and PW with input from all authors.

ACKNOWLEDGMENTS

The authors would like to thank Jessica M. Williams for her contributions during the preliminary reaction screening efforts. The authors also thank Boehringer-Ingelheim Pharmaceuticals Inc., Ridgefield CT, for discretionary funding of this project.

REFERENCES

Dai, C., Meschini, F., Narayanam, J. M. and Stephenson, C. R. (2012). Friedel–crafts amidoalkylation via thermolysis and oxidative photocatalysis. *J. Organ. Chem.* 77, 4425–4431. doi: 10.1021/jo300162c

de Fátima, Â., Braga, T. C., da S. Neto, L., Terra, B. S., Oliveira, B. G., da Silva, D. L., et al. (2015). A mini-review on biginelli adducts with notable pharmacological properties. *J. Adv. Res.* 6, 363–673. doi: 10.1016/j.jare.2014.10.006

Fu, N., Y., Yuan, Y. F., Cao, Z., Wang, S. W., Wang, J. T., and Peppe, C. (2002). Indium(III) bromide-catalyzed preparation of dihydropyrimidinones: improved protocol conditions for the Biginelli reaction. *Tetrahedron* 58, 4801–4807. doi: 10.1016/S0040-4020(02)00455-6

Hu, E. H., Sidler, D. R., and Dolling, U.-H. (1998). Unprecedented catalytic three component one-pot condensation reaction:an efficient synthesis of 5-alkoxycarbonyl-4-aryl-3,4-dihydropyrimidin-2(1*H*)-ones. *J. Organ. Chem.* 63, 3454–3457. doi: 10.1021/jo970846u

Huryn, D. M., Brodsky, J. L., Brummond, K. M., Chambers, P. G., Eyer, B., Ireland, A. W., et al. (2011). Chemical methodology as a source of small-molecule checkpoint inhibitors and heat shock protein 70 (Hsp70) modulators. *Proc. Natl. Acad. Sci. U.S.A.* 108, 6757–6762. doi: 10.1073/pnas.1015251108

Kapoor, T. M., Mayer, T. U., Coughlin, M. L., and Mitchison, T. J. (2000). Probing spindle assembly mechanisms with monastrol, a small molecule inhibitor of the mitotic kinesin, Eg5. *J. Cell Biol.* 150, 975–988. doi: 10.1083/jcb.150.5.975

Krapcho, A. P., Glynn, A. G., and Grenon, B. J. (1967). The decarbethoxylation of geminal dicarbethoxy compounds. *Tetrahedron Lett.* 8, 215–217. doi: 10.1016/S0040-4039(00)90519-7

Lu, J., and Bai, Y. (2002). Catalysis of the Biginelli reaction by ferric and nickel chloride hexahydrates. One-pot synthesis of 3,4-dihydropyrimidin-2(1*H*)-ones. *Synthesis* 4, 466–470. doi: 10.1055/s-2002-20956

Manos-Turvey, A., Al-Ashtal, H. A., Needham, P. G., Hartline, C. B., Prichard, M. N., Wipf, P., et al. (2016). Dihydropyrimidinones and -thiones with improved activity against human polyomavirus family members. *Bioorg. Med. Chem. Lett.* 26, 5087–5091. doi: 10.1016/j.bmcl.2016.08.080

Martins, M. A. P., Teixeira, M. V. M., Cunico, W., Scapin, E., Mayer, R., Pereira, C. M. P., et al. (2004). Indium(III) bromide catalyzed one-pot synthesis of trichloromethylated tetrahydropyrimidinones. *Tetrahedron Lett.* 45, 8991–8994. doi: 10.1016/j.tetlet.2004.10.048

Mayer, T. U., Kapoor, T. M., Haggarty, S. J., King, R. W., Schreiber, S. L., and Mitchison, T. J. (1999). Small molecule inhibitor of mitotic spindle bipolarity identified in a phenotype-based screen. *Science* 286, 971–974. doi: 10.1126/science.286.5441.971

Nagarajaiah, H., Mukhopadhyay, A., and Moorthy, J. N. (2016). Biginelli reaction: an overview. *Tetrahedron Lett.* 57, 5135–5149. doi: 10.1016/j.tetlet.2016.09.047

Phucho, I. T., Nongpiur, A., Tumtin, S., Nongrum, R., and Nongkhlaw, R. L. (2009). Recent progress in the chemistry of dihydropyrimidinones. *Rasayan J. Chem.* 2, 662–676.

Ragab, F. A. F., Abou-Seri, S. M., Abdel-Aziz, S. A., Alfayomy, A. M., and Aboelmagd, M. (2017). Design, synthesis and anticancer activity of new monastrol analogues bearing 1,3,4-oxadiazole moiety. *Eur. J. Med. Chem.* 138, 140–151. doi: 10.1016/j.ejmech.2017.06.026

Ranu, B. C., Hajra, A., and Jana, U. (2000). Indium(III) chloride-catalyzed one-pot synthesis of dihydropyrimidinones by a three-component coupling of 1,3-dicarbonyl compounds, aldehydes, and urea: an improved procedure for the Biginelli reaction. *J. Organ. Chem.* 65, 6270–6272. doi: 10.1021/jo000711f

Sharma, P., Kumar, A., Rane, N., and Gurram, V. (2005). Hetero Diels–Alder reaction: a novel strategy to regioselective synthesis of pyrimido[4,5-d]pyrimidine analogues from Biginelli derivative. *Tetrahedron* 61, 4237–4248. doi: 10.1016/j.tet.2005.02.066

Studer, A., Jeger, P., Wipf, P., and Curran, D. P. (1997). Fluorous Synthesis: fluorous protocols for the Ugi and Biginelli multicomponent condensations. *J. Organ. Chem.* 62, 2917–2924.

Sun, Q., Wang, Y. Q., Ge, Z. M., Cheng, T. M., and Li, R. T. (2004). A highly efficient solvent-free synthesis of dihydropyrimidinones catalyzed by zinc chloride. *Synthesis* 7, 1047–1051. doi: 10.1002/chin.200437148

Wan, J. P., and Pan, Y. (2012). Recent advance in the pharmacology of dihydropyrimidinone. *Mini Rev. Med. Chem.* 12, 337–349. doi: 10.2174/138955712799829267

Wipf, P., and Cunningham, A. (1995). A solid phase protocol of the Biginelli dihydropyrimidine synthesis suitable for combinatorial chemistry. *Tetrahedron Lett.* 36, 7819–7822. doi: 10.1016/0040-4039(95)01660-A

Yuan, H., Zhang, K., Xia, J., Hu, X., and Yuan, S. (2017). Gallium (III) chloride-catalyzed synthesis of 3,4-dihydropyrimidinones for Biginelli reaction under solvent-free conditions. *Cogent Chem.* 3:1318692. doi: 10.1080/23312009.2017.1318692

Conflict of Interest Statement: The authors declare that the research was conducted in the absence of any commercial or financial relationships that could be construed as a potential conflict of interest.

frontiers in Chemistry

REVIEW
published: 20 November 2018
doi: 10.3389/fchem.2018.00557

Post-Ugi Cyclization for the Construction of Diverse Heterocyclic Compounds: Recent Updates

Jitender Bariwal[1], *Rupinder Kaur*[2], *Leonid G. Voskressensky*[3] *and Erik V. Van der Eycken*[3,4]*

[1] Shiva Institute of B. Pharmacy, Bilaspur, India, [2] Department of Pharmaceutical Chemistry, ISF College of Pharmacy, Moga, India, [3] Laboratory for Organic & Microwave-Assisted Chemistry, University of Leuven, Leuven, Belgium, [4] Peoples' Friendship University of Russia (RUDN University), Moscow, Russia

Multicomponent reactions (MCRs) have proved as a valuable tool for organic and medicinal chemist because of their ability to introduce a large degree of chemical diversity in the product in a single step and with high atom economy. One of the dominant MCRs is the Ugi reaction, which involves the condensation of an aldehyde (or ketone), an amine, an isonitrile, and a carboxylic acid to afford an α-acylamino carboxamide adduct. The desired Ugi-adducts may be constructed by careful selection of the building blocks, opening the door for desired post-Ugi modifications. In recent times, the post-Ugi transformation has proved an important synthetic protocol to provide a variety of heterocyclic compounds with diverse biological properties. In this review, we have discussed the significant advancements reported in the recent literature with the emphasis to highlight the concepts and synthetic applications of the derived products along with critical mechanistic aspects.

Keywords: Post-Ugi modifications, heterocycles, multicomponent reactions, MCR, post-Ugi cyclization

OPEN ACCESS

Edited by:
Andrea Basso,
Università di Genova, Italy

Reviewed by:
Valentine Nenajdenko,
Lomonosov Moscow State University, Russia
Marta Meazza,
University of Southampton, United Kingdom

***Correspondence:**
Erik V. Van der Eycken
erik.vandereycken@kuleuven.be

Specialty section:
This article was submitted to Organic Chemistry, a section of the journal Frontiers in Chemistry

Received: *25 July 2018*
Accepted: *29 October 2018*
Published: *20 November 2018*

Citation:
Bariwal J, Kaur R, Voskressensky LG and Van der Eycken EV (2018) Post-Ugi Cyclization for the Construction of Diverse Heterocyclic Compounds: Recent Updates. Front. Chem. 6:557. doi: 10.3389/fchem.2018.00557

INTRODUCTION

Multicomponent reactions (MCRs) are considered as privileged one-pot processes involving a sequential combination of at least three reagents in the same pot (Ramon and Yus, 2005). The MCRs have found their usefulness and influence in Diversity-Oriented Synthesis (DOS) particularly in the field of medicinal chemistry (Biggs-Houck et al., 2010). The combinatorial compound libraries play a vital role for achieving the goal of DOS providing large compound libraries with reduced synthetic steps and with increased molecular complexity (Bariwal et al., 2010).

From the past two decades, the Ugi four-component reaction (Ugi-4CR) has offered one of the most investigated reaction route for generating multifunctional adducts, owing to the mildness of the reaction conditions, the wide application and the high variability (four diversity points) associated with it (Ugi and Steinbrückner, 1961; Ugi, 1962). More importantly, the Ugi-adduct can be manipulated by careful selection of the starting components (amine, acid, isonitrile, and aldehyde/ketone). Synthesis of the desired heterocycle can be achieved by performing a post-Ugi transformation on the exclusively designed Ugi-adduct (Sharma et al., 2015). The efficiency of post-Ugi transformation is further enhanced by manipulating the Ugi-adducts in a regioselective manner to provide access to complex heterocycles in a domino fashion (Li et al., 2016) (**Scheme 1**).

There are several reports for the transformations of the Ugi-adducts to diverse heterocyclic systems including Ugi-Heck, Ugi-ring opening metathesis, Ugi-intramolecular arylation,

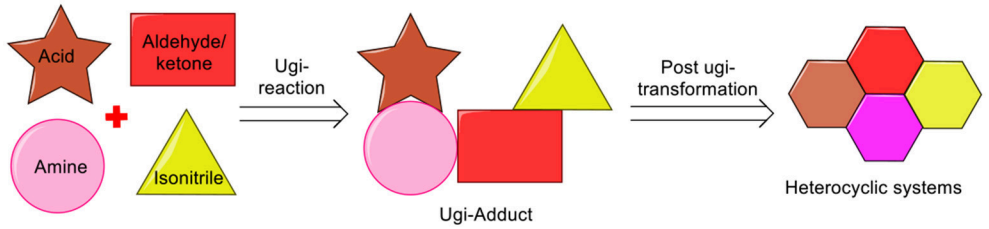

SCHEME 1 | Ugi multicomponent reaction and post Ugi transformation to heterocyclic system.

post-Ugi-cascades, and metal/ligand regio-, chemoselectivity switch, which has been reviewed by us recently (Sharma et al., 2015) and others (Hulme and Dietrich, 2009; Kaïm and Grimaud, 2010, 2014; Koopmanschap et al., 2014; Xiuming et al., 2017). During the last few years, noteworthy progress in the post-Ugi-transformations has taken place as is evident from the substantial number of reports. We have carefully selected the prime literature reports where Ugi-adducts have been cyclized to generate a variety of heterocyclic systems. The present review mainly covers the literature reports on post-Ugi-modifications appeared after the year 2014. However, we have included few other important reports before the year 2014 and were not discussed in previous reviews. We have grouped these reports based on the structural complexity of the product after cyclization. For more clarity, we have started the discussion with the construction of the small heterocyclic systems to larger, and then followed by fused systems after post-Ugi-cyclization as given below:

1. Four-membered heterocycles
2. Five-membered heterocycles
3. Six-membered heterocycles
4. Fused heterocycles
   - 4.1 Five-membered heterocycles fused with five-membered heterocyclic systems
   - 4.2 Five-membered heterocycles fused with six-membered carbocyclic systems
   - 4.3 Five-membered heterocycles fused with six-membered heterocyclic systems
   - 4.4 Five-membered heterocycles fused with medium sized heterocyclic systems
   - 4.5 Six-membered heterocycles fused with six-membered carbocyclic systems
   - 4.6 Seven-membered heterocycles fused with six-membered carbocyclic systems
   - 4.7 Nine-membered heterocycles fused with five-membered heterocycles
5. Tricyclic fused heterocycles
6. Spiro-polyheterocycles

FOUR-MEMBERED HETEROCYCLES

2-Azetidinones, known as β-lactams, are well known antimicrobial agents and are important synthetic intermediates for vitamins, alkaloids, and β-amino acids. Van der Eycken et al. (Li et al., 2015b) have developed a diversity-oriented post-Ugi intramolecular cyclization of Ugi-adducts **2a** to give access to α-methylene β-lactams **2b** in moderate to excellent yields using $InCl_3$ as a catalyst in toluene at 120°C with α,β-unsaturated γ-lactams **2c** as a minor product (**Scheme 2**). Under the optimized conditions, the intramolecular cyclization reaction proceeded smoothly to give α-methylene β-lactams utilizing a variety of substituents on the Ugi-adducts. Ugi-adducts (**2d** and **2e**) prepared from 1-trityl-1*H*-imidazole-4-carbaldehyde and 4-methylthiazole-2-carbaldehyde provided the corresponding alkylidene-β-lactams **2f** in good yields. However, Ugi-adduct derived from imidazo[1,2-*a*]pyridine-3-carbaldehyde or from benzaldehyde failed to cyclized under these conditions. Moreover, the use of Ugi-adducts derived from 4-pentynoic acid did not provide the desired alkylidene-β-lactam.

Interestingly, switching the catalyst to $AlCl_3$, provided exclusive access to the unsaturated γ-lactams **2g** in moderate to excellent yields. Under the optimized conditions, the Ugi-adducts obtained from substituted imidazo[1,2-*a*]pyridine-2-carbaldehydes provided moderate to good yields, whereas 1-trityl-1*H*-imidazole-4-carbaldehyde derived Ugi-adduct provided a low product yield (20% only). In addition, Ugi-adducts **2a** prepared from imidazo[1,2-*a*]pyridine-2-carbaldehyde and 2-butynoic acid, underwent the $InCl_3$-catalyzed Michael addition reaction ($InCl_3$ (10 mol%) in DCE at 120°C for 12 h) and provided exclusive access to γ-lactam **2h** in good to excellent yields, even with a bulky substituent such as a phenyl group on the alkyne.

FIVE-MEMBERED HETEROCYCLES

Shiri et al. (2014) have reported a selective synthesis for a series of novel indolyl based γ-lactams **3b** by cyclization of Ugi-adducts **3a** in the presence of K_2CO_3 in DMF at 100°C within few hours (**Scheme 2**). Under the optimum conditions, adducts derived from activated anilines underwent the reaction smoothly and gave access to the corresponding lactams in moderate to good yields. However, synthesis of Ugi-adducts using deactivated anilines met with failure. Benzyl aniline derived Ugi-adduct also afforded the desired *N*-benzyl lactam in excellent yield, whereas benzaldehyde-derived Ugi-adduct required modified conditions (KOH (1.0 equiv) DMF, 100°C, 10h) to provide access to the γ-lactam in moderate yield. Bulky t*ert*-butyl isocyanide-derived

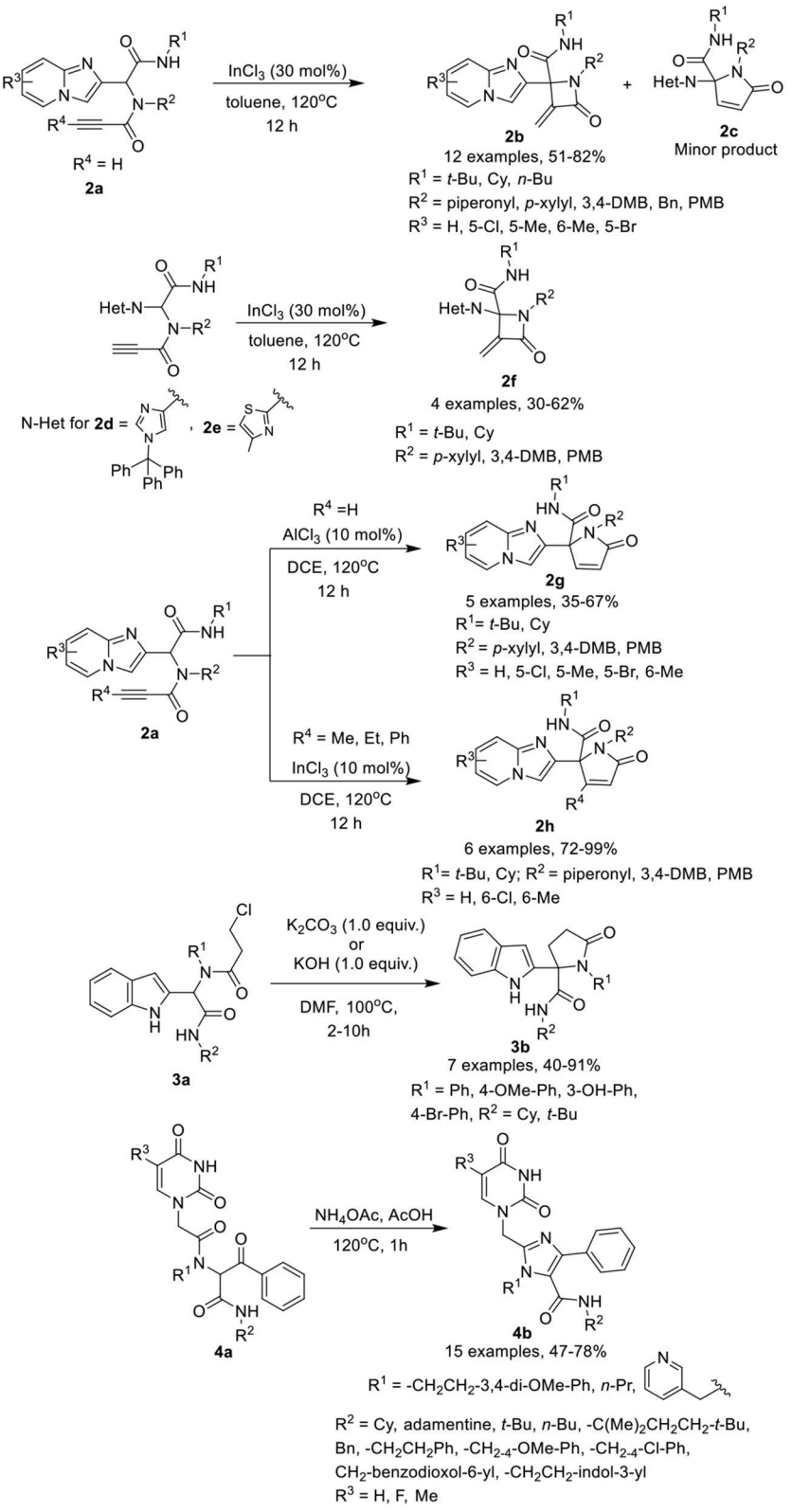

SCHEME 2 | Synthesis of fused α-methylene β-lactams **2b, 2f**, α,β-unsaturated γ-lactams **2g, 2h**, indolyl based γ-lactams **3b** and tetra-substituted Imidazoles **4b**.

Ugi-adduct significantly reduced the product yield compared to the cyclohexyl substituted substrate.

Dömling et al. (Madhavachary et al., 2018) have developed a new, facile one-pot synthetic approach for the synthesis of uracil/thymine-containing tetra-substituted imidazoles **4b** by cyclizing Ugi-adducts **4a** with NH_4OAc in AcOH at 120°C in moderate to excellent yields (**Scheme 2**). Under the optimized conditions, a variety of substituted isocyanides, aliphatic, and aromatic amines and uracil derived acetic acids were found suitable for the reaction and provided good to excellent product yields. From this small library, products obtained from 5-fluorouracil and 5-methyluracil acetic acids are interesting analogs of the marketed drugs Retrovir and Tegafur and were obtained in only two synthetic steps.

SIX-MEMBERED HETEROCYCLES

Balalaie et al. (2017a) have developed a facile post-Ugi-transformation to cyclize Ugi-adducts **5a** to 2,5-diketopiperazines **5b** in good to excellent yields in the presence of triphenylphosphine as catalyst in ethanol at 80°C (**Scheme 3**). Under the optimized conditions, various Ugi-adducts derived from aldehydes and anilines bearing electron-withdrawing and electron-releasing substituents performed well to give the desired products in good to high yields, except with thiophene-2-carbaldehyde and 2-iodo substituted aniline which were obtained in moderate yields. Adducts derived from isocyanides bearing cyclohexyl or ethyl ester underwent the reaction smoothly. However, with *tert*-butyl bearing isocyanide, acetonitrile as solvent was required to furnish the corresponding 2,5-diketopiperazines in moderate yields. The post-Ugi cyclization reaction proceeds by nucleophilic addition of triphenylphosphine to the active alkyne group followed by the proton transfer from amide NH as shown in [**A**]. The nucleophilic addition of nitrogen results in the formation of cyclized intermediate [**B**], followed by PPh_3 elimination furnishing the desired 2,5-diketopiperazines **5b**.

Halimehjani and Sharifi (2017) have reported a simple approach to synthesize functionalized piperazine 2,5-diones **6b** via intramolecular aza-Michael addition reaction of Ugi-adducts **6a** in the presence of NaH in THF at rt (**Scheme 3**). Under the optimized conditions, the reaction proceeds smoothly and provides high product yields with excellent diastereoselectivity.

FUSED HETEROCYCLES

Five-Membered Heterocycles Fused With Five-Membered Heterocyclic Systems

Li et al. (He et al., 2017) have developed a facile post-Ugi gold(I)-catalyzed domino dearomatization/*ipso*-cyclization/aza-Michael cascade reaction of diverse Ugi-adducts **7a** to gain access to the functionalized tetracyclic benzo[*e*]pyrrolo[2,3-*c*]indole-2,4,7(5*H*)-triones **7b** in good yields and with unique diastereoselectivities. The reaction gave best results when $Au(PPh_3)OTf$ was used as a catalyst in $CHCl_3$ at 70°C (**Scheme 4**). Under the optimized conditions, a variety of Ugi-adducts **7a** prepared from diversely substituted amines, isocyanides and acids bearing electron-withdrawing or electron-donating groups performed well to give the desired products in good to excellent yields. Interestingly, Ugi-adducts derived from isonitriles bearing a bulky substituent did not significantly affected the reaction yield. The substrates comprising a terminal alkyne also gave the *exo*-dig products in moderate to good yields. The gold(I)-catalyzed domino dearomatization/*ipso*-cyclization/aza-Michael sequence proceeded by *in situ* formation of a cationic gold(I) species which is followed by nucleophilic attack by the C-4 position of the 1-naphthol (5-*exo*-dig fashion) as shown in intermediate [**A**]. This leads to the formation of the spirocarbocyclic intermediate [**B**]. This generated the tetracyclic scaffold *via* aza-Michael addition facilitated by π-activation by the cationic gold species.

Five-Membered Heterocycles Fused With Six-Membered Carbocyclic Systems

Sharada et al. (Sagar et al., 2015) have described a $FeCl_3$ catalyzed post-Ugi cyclization protocol for cyclization of α-amino amidines **8a**, generated *via* an Ugi-3CR using silica gel as promoter, to construct amidino substituted indazoles **8b** in good to high yields in DMF at 120°C (**Scheme 4**). Under the optimized conditions, a variety of amidino substituted indazoles were prepared where the electronic nature of substituents on the various Ugi-components did not hamper the reaction and provided good product yields.

Van der Eycken et al. (Ambasana et al., 2014) have reported a solvent switchable metal-free [4 + 2] cycloaddition reaction *via* C^2_{sp}-H functionalization of the Ugi-adduct, *N*-propynylphenyl propiolamide **9f** (prepared by reacting aldehyde **9a**, amine **9b**, 2-alkynoic acid **9c** and isonitrile **9d**), to access the *N*-substituted benzo[*f*]isoindolone **9e** or benzo[*e*]isoindolone **9g** in excellent yields and with good regioselectivity. The cyclization reaction to access the benzo[*e*]isoindolones **9g** gave best results in toluene at 150°C. However, the use of a polar-protic solvent alone, or with toluene as co-solvent, resulted in an increased formation of benzo[*f*]isoindolone **9e**. Interestingly, use of *n*-BuOH as a solvent in a one-pot reaction for Ugi-4CR and ring closure reaction, provided access to selective formation of **9e** over **9g** (**Scheme 4**). Under the optimized conditions, Ugi-adducts generated from a broad range of aromatic aldehydes, isonitriles and acids performed well to furnish the benzo[*f*]isoindolones **9e** in excellent yields. However, a low yield of **9e** was observed when aliphatic aldehyde- such as valeraldehyde- derived Ugi-adducts were used in the reaction, whereas use of Ugi-adduct derived from phenyl propargylamine did not underwent the reaction. Further, variedly substituted benzo[*e*]isoindolones **9g** were prepared in moderate to high yields under the optimized conditions from Ugi-adducts derived from differently substituted aldehydes, acids and isonitriles. Importantly, an electron-withdrawing group on the acids improves the yields, while the use of an electron deficient aldehyde and electron rich acid provides low product yields. Interestingly, employing *o*-substituted acid derived Ugi-adduct under the optimized conditions led to the formation of product **9g** as a single isomer.

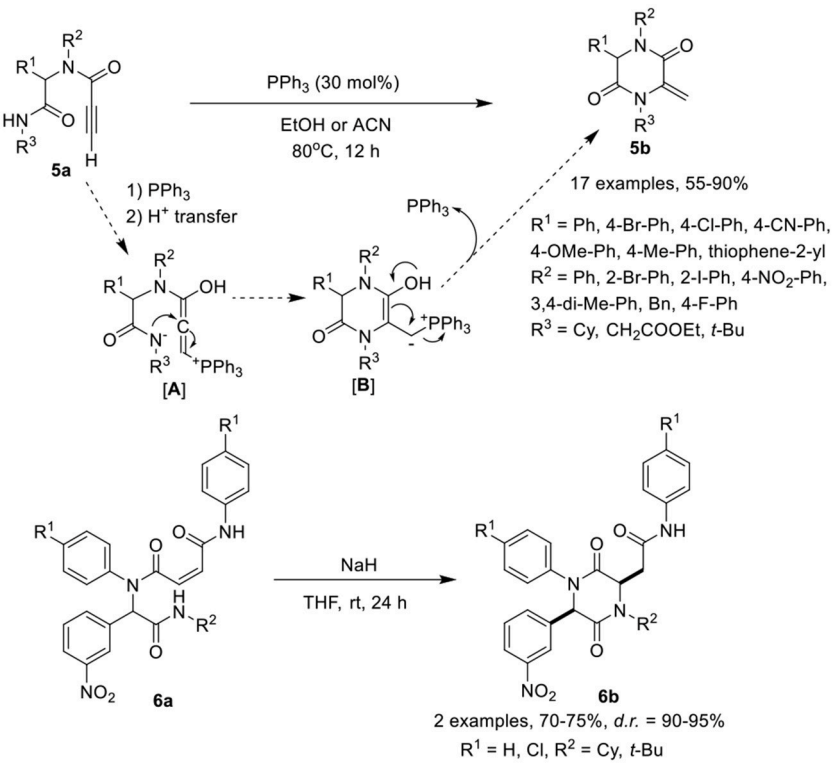

SCHEME 3 | Synthesis of arylidence 2,5-diketopiperazines **5b** and piperazine 2,5-dione **6b.**

Five-Membered Heterocycles Fused With Six-Membered Heterocyclic Systems

González-Zamora et al. (Zamudio-Medina et al., 2015) have described a one-pot, Ugi-4CR for the synthesis of cyclic analogs of hexamethylenebis(3-pyridine)amide (HMBPA) **10e** in low yields. After reaction of diamine **10a**, aldehydes **10b,** and isocyanoacetamides **10c**, cycloaddition and ring opening reaction with maleic anhydride **10d** was performed under MW irradiation using $Sc(OTf)_3$ as a catalyst in benzene (**Scheme 5**). Under the optimized conditions, different isocyanoacetamides and aldehydes furnished the corresponding products **10e** in low yields. During this one-pot synthetic operation, six new chemical bonds were formed.

Van der Eycken et al. (Li et al., 2015a) have developed a facile catalyst-controlled regioselective process for post-Ugi intramolecular hydroarylation reaction to provide access to heterocycles such as pyrroloazepinones **11b**, pyrrolopyridinones **11c**, and benzothienopyridines **11d** in high yields. The intramolecular hydroarylation of Ugi-adduct **11a** furnished the desired pyrroloazepinone **11b** and pyrrolopyridinone **11c** in a nearly 1:1 ratio when $Au(PPh_3)Cl$ and AgOTf were used as a catalytic system at 50°C in $CDCl_3$. Switching the catalyst to $AgSbF_6$ in $CDCl_3$ at 70°C provided exclusive access to pyrroloazepinones **11b** in excellent yields (**Scheme 5**). Other silver and gold salts such as AgOTf, $AgBF_4$, $AgNTf_2$, $AuCl_3$, or AuCl also provided product in moderate to good yield. Interestingly, the use of $InCl_3$ as catalyst in $CDCl_3$, resulted in a switch of selectivity and afforded the pyrrolopyridinones **11c** in excellent yields. Ugi-adducts prepared from aliphatic *n*-butylamine or bulky alkyne substituents, such as phenyl, were not found suitable under these conditions resulting in unstable pyrrolopyridinones. On the other hand, for the pyrroloazepinone **11b**, diversely substituted Ugi-adducts performed well and provided good product yields. However, a bulky phenyl substituent on the alkyne, resulted in a drastic reduction of the product yield, whereas a terminal alkyne afforded the corresponding product in moderate yields. An electron-donating substituent on the carboxamide moiety provided excellent product yields in both cases. In addition, the *exo*-dig cyclization of the benzothiophene comprised Ugi-adducts was also performed in the presence of $IPrAuNTf_2$ as catalyst in DCE at 70°C, affording the selective benzothienopyridines **11d** in excellent yields, whereas $Au(PPh_3)OTf$ provided the products in moderate yield and $InCl_3$, $AgSbF_6$, or $AuCl_3$ did not work for this conversion. Under the optimized conditions, a variety of Ugi-adducts obtained from acids and isonitriles were well tolerated. However, a bulky phenyl substituent on the alkyne failed to give the corresponding product, whereas electron-donating substituents on the amines proved beneficial in this reaction.

Peshkov et al. (Trang et al., 2015) have developed a one-pot base-promoted post-Ugi carbocyclization of Ugi-adduct **12a** with cleavage of the isocyanide-originated amide moiety, to provide facile access to 6,7-dihydro-5*H*-pyrrolo[3,4-*b*]pyridin-5-ones **12b** in high yields when performed under inert atmosphere at 110°C in DMF. However, when this reaction was performed

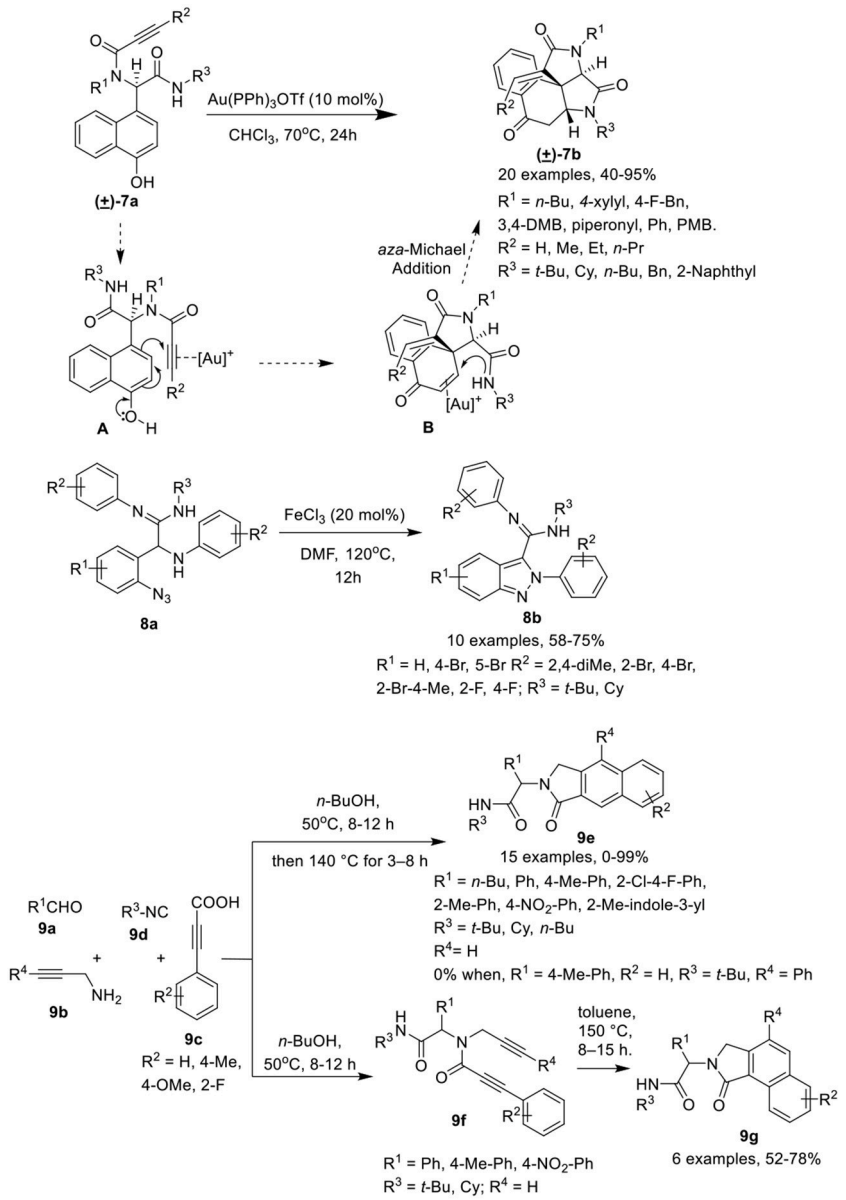

SCHEME 4 | Synthesis of azaspiro tetracyclic scaffolds **7b**, amidino substituted indazoles **8b** and *N*-substitutednenzo*[e]*-or *[f]*isoindolones **9e,g**.

under air atmosphere, the oxidized 7-hydroxy-6,7-dihydro-5*H*-pyrrolo[3,4-*b*]pyridin-5-one **12c** was obtained (**Scheme 6**). Adducts derived from a diverse array of aromatic amines as well as several aromatic and heteroaromatic aldehydes were found suitable in both inert and aerobic conditions, provided the desired products in good to moderate yields. However, aliphatic amines drastically reduced the product yield for both normal **12b** and oxidized product **12c**. Interestingly, the use of butylamine resulted in a poor yield of normal product **12b** and failed to give the oxidized product **12c**. In general, the yields for the non-oxidized products **12b** were higher than for the oxidized ones **12c**.

Srivastava et al. (Ghoshal et al., 2017) have reported an efficient and divergent one-pot sequential Ugi-4CR of amino acetaldehyde acetals **13a**, ketone **13b** or aldehydes **13c**, alkynoic acids **13d,** and isocyanides **13e** in ethanol and subsequent acid-mediated Povarov-type reaction followed by treatment with substituted anilines **13f** and H_2SO_4 to afford the fused quinolines **13g**, and **13h** in moderate to excellent yields at rt (**Scheme 6**). Under the optimized conditions, a diverse array of anilines bearing electron-rich as well as electron-deficient substituents were well tolerated in the Povarov-type reaction. However, heteroaromatic amines afforded the corresponding product in low yield. Interestingly, electron-deficient anilines

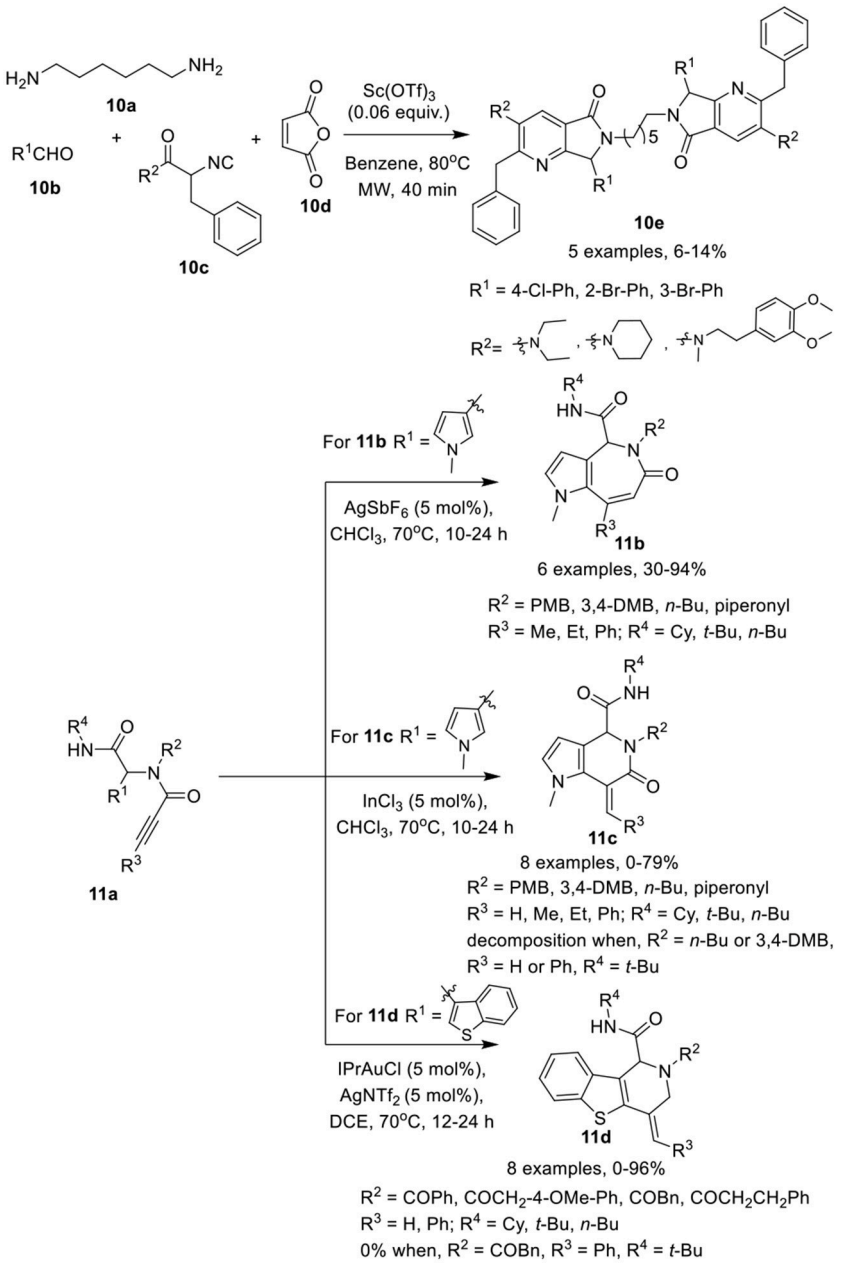

SCHEME 5 | Synthesis of cyclic analogs of HMBPA 10e, pyrroloazepinones **11b**, pyrroloazepinones **11c**, and benzothienopyridines **11d**.

such as 2-iodo-4-nitroaniline provided dihydro-2,3-dihydro-1*H*-pyrrolo[3,4-*b*]quinolin-1-ones (DHPQ) as a minor product which after oxidation, afforded the desired product in low yield. Among the isocyanides, *tert*-butylisocyanide and cyclohexylisocyanide were suitable, whereas the use of naphthylisocyanide led to the formation of the desired product in poor yield. For the acid counterpart, phenylpropiolic acid and other alkynoic acids were found suitable in the reaction resulting in good product yields. A diverse array of aromatic aldehydes bearing electron-rich or electron-deficient groups, as well as, aliphatic aldehydes were found suitable in this reaction, affording the corresponding products in moderate to excellent yields. Importantly, the acidic proton in the Ugi-adduct did not interfere in the Povarov-type reaction. Under these conditions, unprotected propiolamides also provided access to the corresponding products *via* Povarov-type reaction in moderate yields.

Van der Eycken et al. (He et al., 2018) have developed an efficient gold(I)-catalyzed post-Ugi domino dearo matization/*ipso*-cyclization/Michael sequence of Ugi-adduct

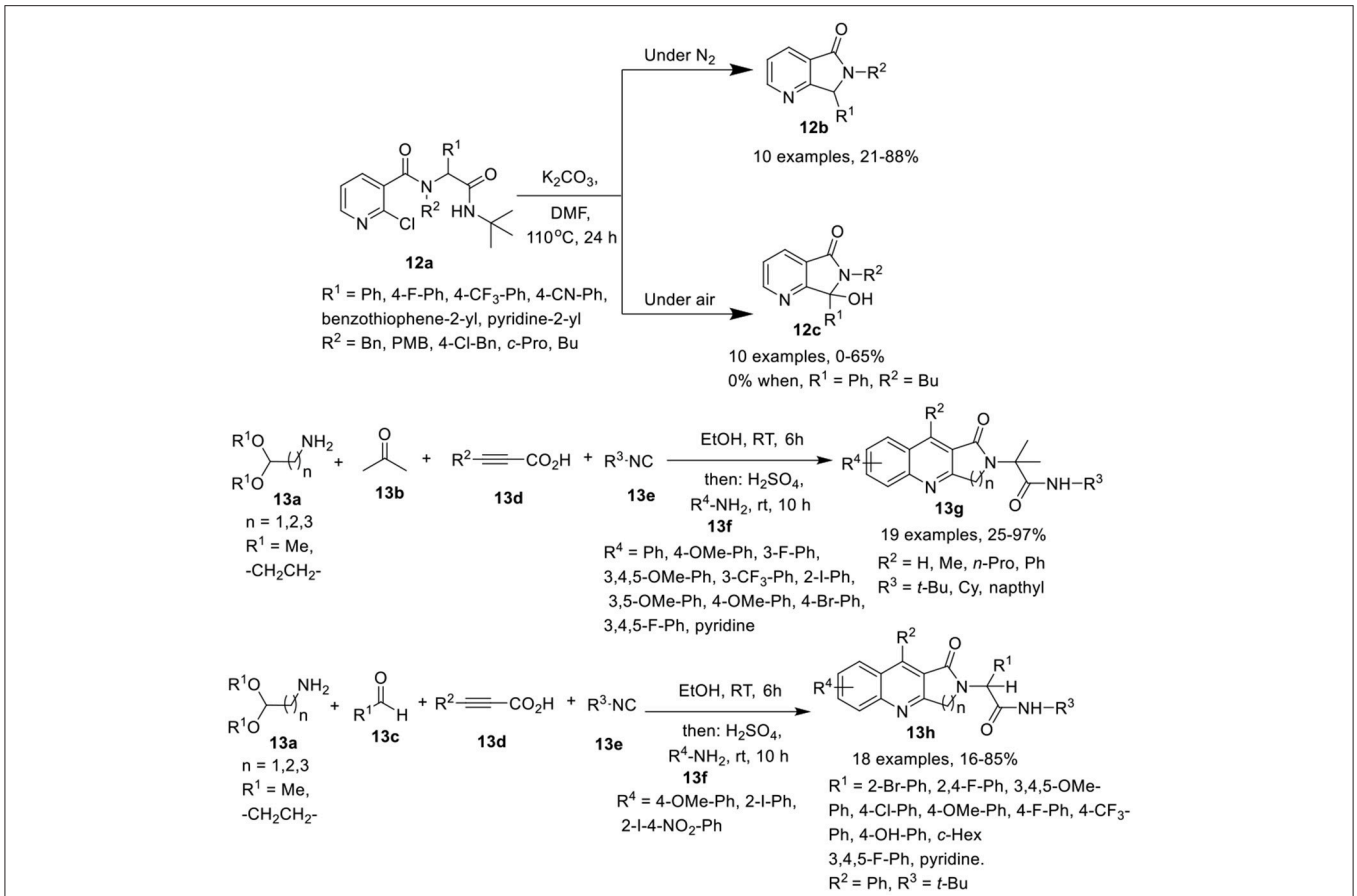

SCHEME 6 | Synthesis of 6,7-dihydro-5*H*-pyrrolo[3,4-*b*]pyridine-5-ones **12b** and the oxidized product **12c** and fused quinolones **13g** and **13h**.

14a that provided access to various (hetero)-arene-annulated tricyclic heterocycles **14b** in moderate to good yields with excellent chemo-, regio-, and diastereoselectivity. The reaction for the synthesis of indole-annulated tricyclic heterocycle **14b** proceeded smoothly utilizing IPrAuCl and AgOTf as catalytic system in $CDCl_3$ at rt (**Scheme 7**). Under the optimal conditions, Ugi-adducts derived from aliphatic and aromatic isonitriles underwent the reaction smoothly and provided good product yields. Bulky alkyne substrates provided good product yields, whereas Ugi-adducts bearing a terminal alkyne did not performed well. Electron-donating as well as electron-withdrawing substituents on the indole ring were well tolerated and provided high yields. A strong electron-withdrawing benzenesulfonyl group on the indole nitrogen atom drastically reduced the C3 nucleophilicity, resulting in the need of high temperature (115°C) to perform the reaction in excellent yield. In contrast to Ugi-adducts derived from *ortho*-substituted 4-aminophenols, *meta*-substituted 4-aminophenols afforded low yields. Pyrrole-containing Ugi-adducts **15a** gave access to the corresponding pyrrole-fused polyheterocycles **15b** in good yields under the optimized conditions. In addition, different Ugi-adducts derived from various heteroaromatic aldehydes led to diverse (hetero)-arene-annulated tricyclic heterocycles in moderate to good yields using the modified conditions. The use of Ugi-adducts derived from benzofuran-2-carbaldehyde, 1-phenyl-1*H*-pyrazole-5-carboxaldehyde, and benzo[*b*]thiophene-3-carbaldehyde resulted in the formation of a mixture of heteroarene-annulated tricycle **15c** and spirocarbocyclic product **15d** in moderate to good yields upon heating at 115°C. Furthermore, Ugi-adducts derived from electron-rich aromatic aldehydes (hydroxy- and alkoxy-substituted benzaldehydes) when used in this domino process underwent the reaction smoothly in $CHCl_3$ at 70°C to afford the benzene-annulated tricyclic heterocycles **15e** in moderate to good yields. The pyrrolidine-substituted benzene provided the benzene-annulated tricycle in high yield at rt, whereas, piperidine- or morpholine-substituted benzaldehydes afforded the benzene-annulated tricycles **15f** in DCE at 115°C in low yields. Interestingly, when these reactions were performed at rt, only the spirocarbocyclic products were obtained (**Scheme 7**). The reaction proceeds by *in situ* generation of cationic gold(I) species that π-activates the alkyne group in the Ugi-adducts to give intermediate [**A**], which is subsequently attacked by the nucleophilic phenol in a 5-*endo*-dig fashion to afford spirocarbocyclic intermediate [**B**]. Subsequent Michael addition of the intermediate

cyclohexadienone with the C3 position of the indole, results in the formation of the indole-annulated tricyclic heterocycle **14b** (**Scheme 7**).

Krasavin et al. (Golubev and Krasavin, 2017) have developed an efficient synthetic protocol to access sterically encumbered tricyclic peptidomimetics **16b** *via* intramolecular nucleophilic substitution reaction of Joullie-Ugi-adduct **16a** in the presence of NaH in THF at 50°C in good to excellent yields (**Scheme 8**). Under the optimized conditions, bulky substituents on the amide nitrogen such as *tert*-butyl or mesityl, did not affect the reaction and provided good product yields. The remaining substituents on the Joullie-Ugi-adducts **16a** did not affect the reaction output significantly. These tricyclic peptidomimetics may be useful as small molecule-ligands for peptidergic biological targets, including G-protein coupled receptors.

VenkataPrasad et al. (VenkataPrasad et al., 2017) have developed an efficient and facile post-Ugi condensation approach to access the pyrrolo[2,3-*c*]pyridines **17b** in excellent yields, using 50 mol% PTSA in methanol at 50°C (**Scheme 8**). Under the optimized conditions, diversely substituted Ugi-adducts **17a** provided the desired products, in moderate to excellent yields. Use of Ugi-adducts bearing CF_3 on the aniline or on the phenyl glyoxylic acid, provided the respective pyrrolo[2,3-*c*]pyridones in excellent yields. However, use of NO_2-substituted aniline did not provided the Ugi-adduct, whereas Ugi-adducts derived from phenylglyoxalic acid bearing a NO_2-group failed to cyclize under the optimized conditions. The reaction proceeds *via* protonation of α-keto group of the Ugi-adduct, followed by the electrophilic addition on the pyrrole ring to give intermediate [**A**], which subsequently underwent dehydration to afford the desired compound *via* intermediate [**B**]. This approach has many advantages including practical simplicity, high atom economy and short reaction time.

Sieburth et al. (Srinivasulu et al., 2018) have developed a serendipitous one-pot protocol for the diastereoselective construction of tricyclic chromenopyrroles **18b** from Ugi-adducts **18a** in moderate to good yields, using $ZnBr_2$ as catalyst in DCE under MW irradiation (**Scheme 8**). Under the optimized conditions, Ugi-adducts **18a** derived from variously substituted methylamines and phenylacetic acids were found well tolerable and afforded the desired products in moderate to good yields. However, the use of benzylamine derived Ugi-adducts provided low product yields. Substitutions on the nitrogen of the Ugi-adduct have little effect on the product output and provided good product yields. Ugi-adducts derived from 2-indole carboxylic acid also gave moderate product yields. Additionally, the Ugi-adducts prepared from *D*- and *L*-phenylalanine and *L*-3,4-dimethoxyphenylalanine underwent the reaction smoothly and furnished the corresponding products as a mixture of diastereomers in moderate yields, in spite of steric hindrance of the amine. The reaction proceeds through the coordination of $ZnBr_2$ that catalyzes the *O*-acylation by the tertiary amide [**A**], followed by rearrangement of the resultant tetrahedral intermediate [**B**]. Abstraction of the benzylic proton led to the formation of azomethine ylide [**C**]. Subsequent intramolecular [3 + 2]-cyclization delivered the highly strained intermediate [**D**], which undergoes expulsion of carbon dioxide and 1,4-proton migration to give the desired chromenopyrrole **18b**.

Five-Membered Heterocycles Fused With Medium-Sized Heterocyclic Systems

Van der Eycken et al. (Li et al., 2014b) have developed an efficient copper-catalyzed post-Ugi intramolecular Ullmann-coupling strategy to give access to 4*H*-benzo[*f*]imidazo[1,4]diazepin-6-ones **19b** in moderate to good yields using Cs_2CO_3 as a base in DMSO at 100°C under MW irradiation (**Scheme 9**). Under the optimized conditions, Ugi-adducts **19a** derived from diversely substituted aromatic acids and amines were found suitable for this reaction and gave access to the corresponding products in moderate to high yields. Use of Ugi-adducts obtained from C-2 or C-5 substituted imidazole-4-carbaldehyde did not underwent the reaction and resulted in the decomposition of the starting Ugi-adduct, whereas Ugi-adducts assembled from imidazole-2-carbaldehyde furnished the corresponding products in moderate to high yields. The reaction takes place through the formation of intermediate [**A**] *via* coordination of copper(I) iodine with the amine of the Ugi-adduct **19a**, which subsequently inserts into the aryl iodine bond, followed by reductive elimination of the resultant intermediate [**B**] generating 4*H*-benzo[*f*]imidazo[1,4]diazepin-6-one **19b**.

Modha et al. (Vachhani et al., 2015) have developed a post-Ugi regioselective intramolecular carbocyclization approach to afford diversely substituted indoloazepinones **20b** and indoloazocinones **20d** in good to excellent yields, using $Au(PPh_3)SbF_6$ as catalyst in $CDCl_3$ at 50°C (**Scheme 9**). Under the optimized conditions, *endo*-dig cyclization afforded the indoloazepinones **20b** in good to excellent yields. Ugi-adducts **20a** derived from aliphatic or aromatic aldehydes were well tolerated. Similarly, bulky substituents on the alkyne such as ethyl, isopropyl, and aryl underwent the reaction smoothly. However, the Ugi-adduct derived from a *tert*-butyl substituted alkyne, failed to afford the corresponding cyclized product. Interestingly, the Ugi-adduct derived from a terminal alkyne, provided the 6-*exo*-dig product. Additionally, intramolecular hydroarylation of Ugi-adducts **20c** under the optimized conditions afforded the indoloazocinones **20d** in good yields except the *tert*-butyl substituted alkyne. The regioselective intramolecular carbocyclization reaction was believed to progress through π-coordination of the cationic gold with the alkyne [**A**], followed by nucleophilic attack by the 3-position of the indole on the π-activated internal alkyne, in an *endo*-dig fashion, in contrast to the terminal alkyne (*exo*-dig fashion). Intermediate [**B**] was formed, which subsequently underwent a 1,2-shift and after deprotonation and protodeauration led to the formation of the indoloazepinone.

Hulme et al. (Medda et al., 2015) have developed a facile and concise route for post-condensation modifications of Ugi-azide adducts **21a** to give the imidazotetrazolodiazepinones **21d** in modest to excellent yields. The reaction proceeds by treatment of tetrazole **21a** with an excess of isocyanate **21b** in ethanol at rt, followed by ring closure of the resultant hydantoin **21c** with TFA in DCE under MW irradiation at 150°C, furnishing the

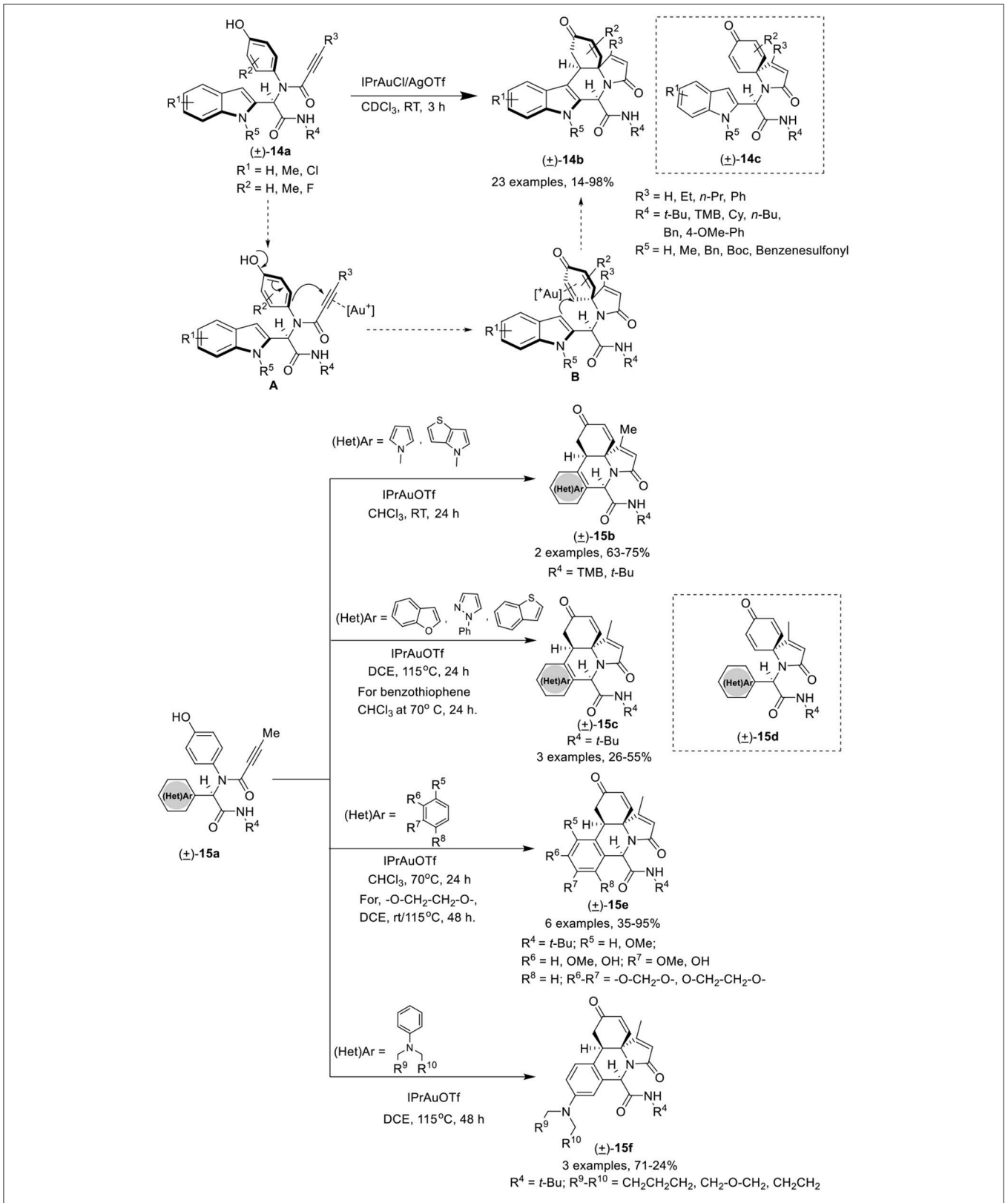

SCHEME 7 | Synthesis of indole-annulated tricyclic heterocycle **14b** and diverse (hetero)-arene-annulated tricyclic heterocycle **15b-f**.

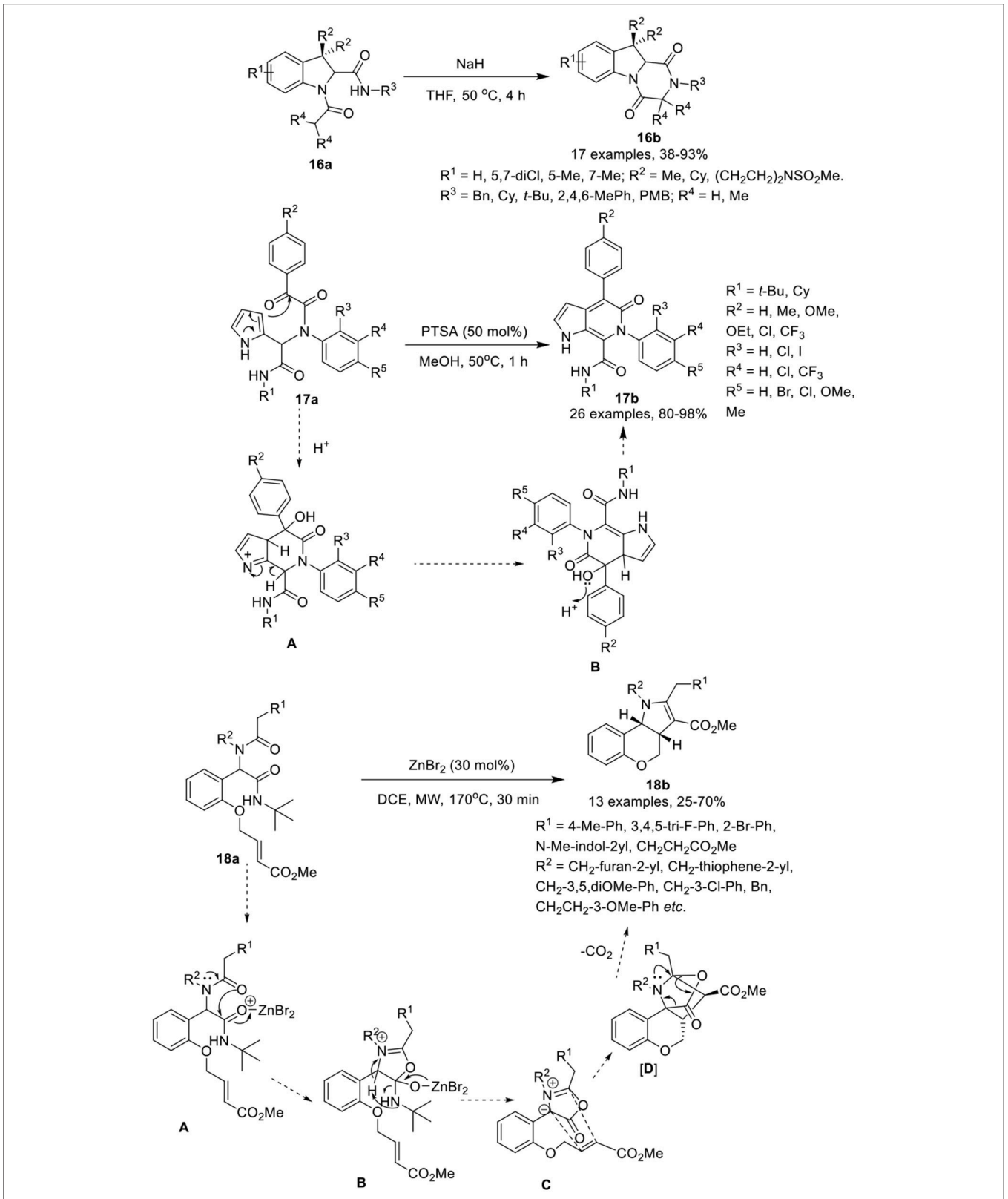

SCHEME 8 | Synthesis of substituted tetrahydropyrazino[1,2-*a*]indole-1,4-diones **16b**, pyrrolo[2,3-c]pyridines **17b** and tricyclic chromenopyrroles **18b**.

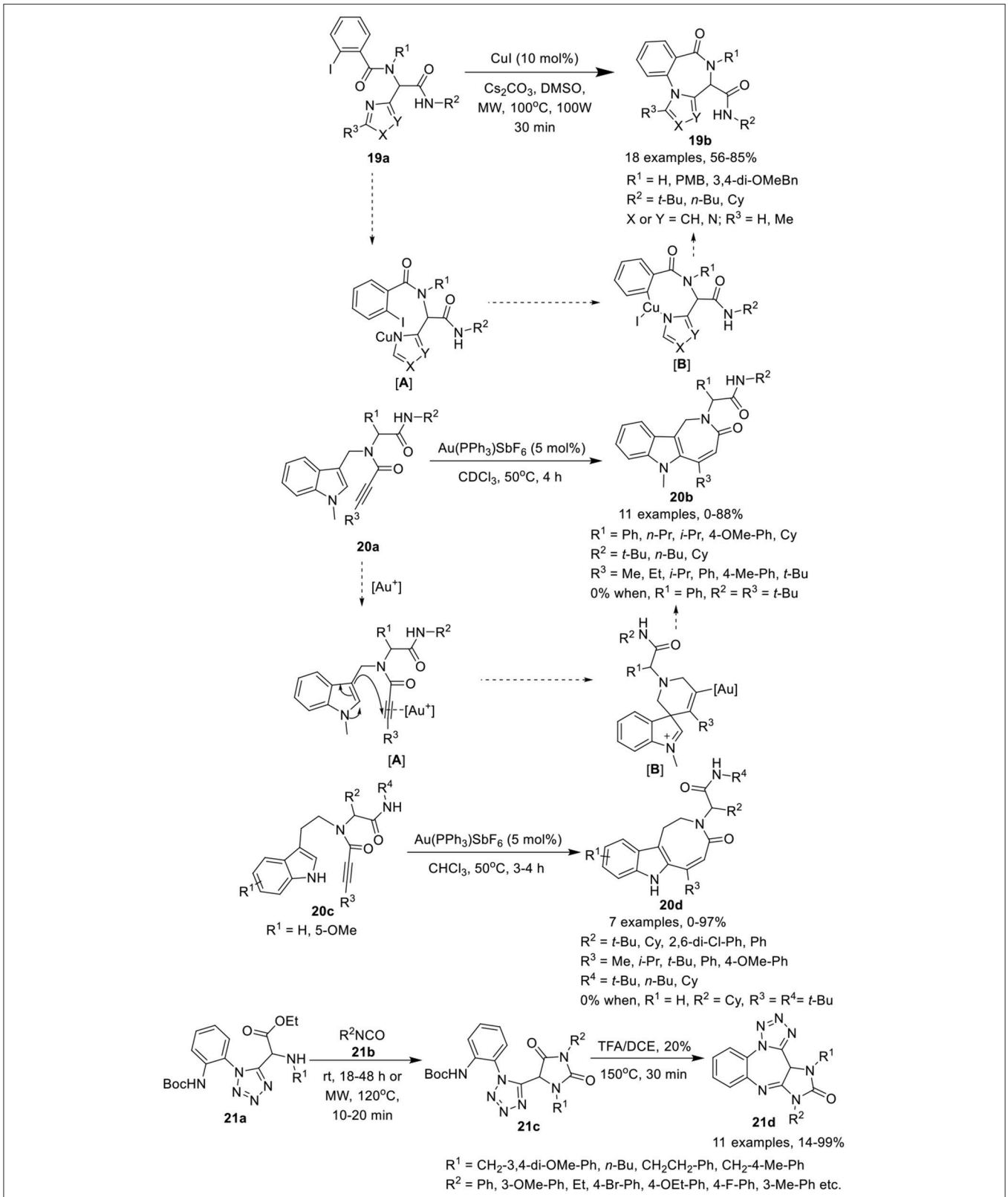

SCHEME 9 | Synthesis of 4*H*-benzo[*f*]imidazo[1,4]diazepin-6-ones **19b,** indoloazepinones **20b** and indoloazocinones **20d,** and imidazo-tetrazolodiazepinones **21d.**

desired imidazotetrazolodiazepinones **21d** (**Scheme 9**). Under the optimized conditions, diversely substituted Ugi-azide adducts **21a** afforded the hydantoin products **21c** in modest to high yields. Adducts derived from isocyanates bearing a 3-methoxyphenyl or an ethyl substituent yielded the desired hydantoin under MW irradiation at a slightly lower temperature of 120°C. Ugi-adducts bearing aliphatic substituents were well tolerated, affording the desired products in higher yields compared to adducts with aromatic substituents. Ring closure and acid-mediated Boc-removal proceeded smoothly under MW irradiation to afford the corresponding products in modest to excellent yields.

Balalaie et al. (Balalaie et al., 2017b) have reported a diversity-oriented access to isoxazolino-benzazepines **22b** and isoxazolo-benzazepines **22d** in good to excellent yields and with high diastereoselectivities (≈95) *via* post-Ugi heteroannulation reaction involving intramolecular 1,3-dipolar cycloaddition of 2-((hydroxyimino)methyl)benzoic acid **22a** and **22c**, respectively. The nitrile oxide reacted with alkenes or alkynes in the presence of sodium hypochlorite (NaOCl) in DCM at rt (**Scheme 10**). Under the optimized conditions, Ugi-adducts derived from aldehydes bearing electron-donating or electron-withdrawing groups provided isoxazolino- and isoxazolo-benzazepines in good to high yields and with high diastereoselectivities. The use of aliphatic aldehydes in both reactions provided low product yields. Ugi-adducts derived from bulky *tert*-butyl isonitriles provided reduced product yields compared to cyclohexyl isonitrile derivatives. The reaction takes place through the chlorination of the oxime group in the Ugi-adduct to chloroxime [**A**], followed by removal of the proton from OH by *in situ*-generated NaOH, and loss of the chloride group resulting in the formation of nitrile oxide [**B**]. Subsequent intramolecular 1,3-dipolar cycloaddition of nitrile oxide with the alkene or alkyne group afforded the corresponding product.

Six-Membered Heterocycles Fused With Six-Membered Carbocyclic Systems

Ding et al. (Wang et al., 2016) have developed a sequential Ugi condensation/Wittig reaction of phosphonium salt **23a** to give access to 1,2-dihydroisoquinolines **23c** in moderate yields in a one-pot fashion. Ugi-adducts **23b** prepared from

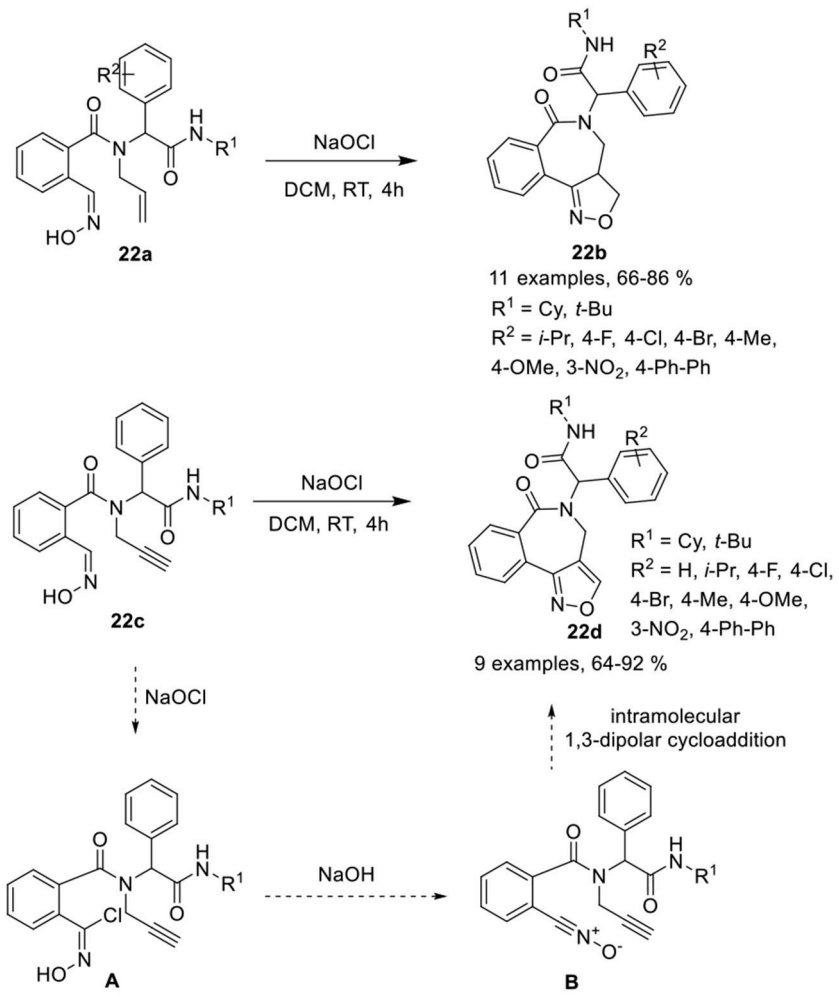

SCHEME 10 | Synthesis of isoxazolino-benzazepines **22b** and isoxazolo-benzazepines **22d.**

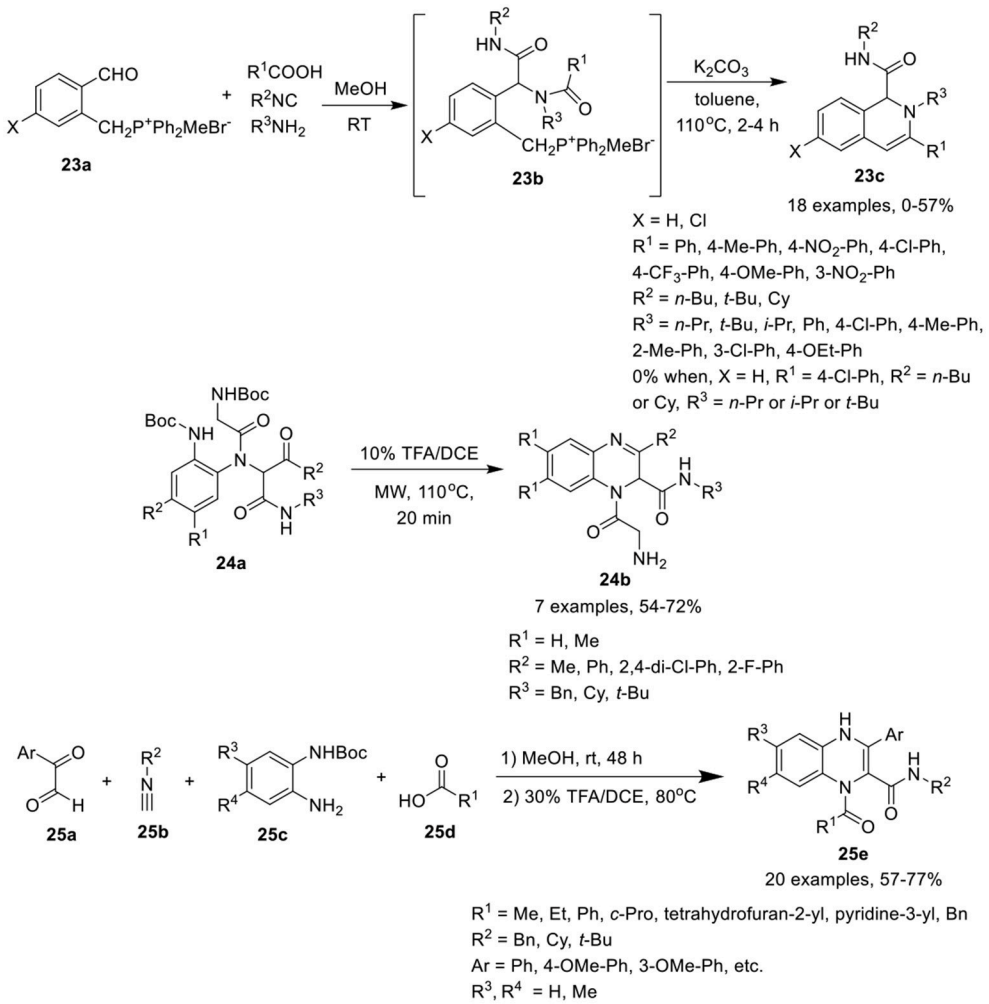

SCHEME 11 | Synthesis of 1,2-dihydroisoquinolines **23c,** quinoxalines **24b** and quinoxalines **25e.**

phosphonium salt **23a** underwent intramolecular Wittig reaction in the presence of K_2CO_3 in toluene under reflux conditions (**Scheme 11**). The reaction proceeded smoothly when formic acid or aromatic acids were utilized as acid components. Bulky substituent derived from *t*-butyl isonitrile and aromatic amines were well tolerated under the optimized conditions. However, adducts derived from aliphatic amines failed to afford the desired products. The substituents on the phosphonium salt **23b** did not influence the product yield.

Chen et al. (Li et al., 2017) have utilized a facile Ugi/deprotection/cyclization (UDC) strategy, followed by a nucleophilic aromatic substitution reaction to give access to diverse quinoxalines **24b** in moderate to good yields under MW irradiation (**Scheme 11**). The reaction proceeded smoothly using diversely substituted Ugi-adducts, providing good yields by deprotection and cyclization of Ugi-adducts **24a** using TFA in DCE under MW irradiation at 110°C. Ugi-adducts derived from differently substituted diamines, isonitriles and aromatic aldehydes were found to be well tolerated under the optimized conditions.

Sotelo et al. (Azuaje et al., 2014) have developed a concise one-pot Ugi-based approach to access the quinoxalines **25e** in excellent yields by Ugi-4CR of glyoxals **25a**, isocyanides **25b**, mono-Boc protected phenylenediamines **25c,** and acids **25d** in methanol at rt, followed by Boc-removal using 30% TFA/DCE at 80°C, and subsequent cyclization (**Scheme 11**). A variety of substituents on all the four building blocks for the Ugi reaction were well tolerated. Bulky substituents on carboxylic acids or isocyanides afforded high yields. However, substitution on the mono-Boc protected phenylenediamines slightly reduced the yield. Further, aromatic acids were better tolerated than aliphatic acids.

Seven-Membered Heterocycles Fused With Six-Membered Carbocyclic Systems

Dai et al. (Shi et al., 2016) have developed an efficient MW-assisted intramolecular Ullmann etherification of Ugi-adducts

26a and **26c** using CuI alone or in combination with *N*,*N*-dimethylglycine HCl (DMG·HCl) as catalyst, in the presence of Cs_2CO_3 in dioxane, to give access dibenz[*b*,*f*][1,4]oxazepin-11(10*H*)ones **26b** and dibenz[*b*,*f*][1,4]oxazepin-11(10*H*)-carboxamides **26d** in good to excellent yields and with excellent chemoselectivity (**Scheme 12**). Under the optimized conditions, most of the reactions proceed smoothly in the absence of ligand under MW irradiation, whereas addition of DMG.HCl as a ligand improves the product yields significantly. Substrates derived from bulky anilines such as 2-naphthylamine, were well tolerated and afforded high product yields. Importantly, for thienyl containing Ugi-adducts, addition of DMG.HCl as ligand was found essential to access the corresponding product. The reaction exhibited excellent chemoselectivity under MW irradiation at elevated temperature. Ugi substrate derived from variety of amines, isocyanides, aldehydes and acids were found well tolerated, providing the products in excellent yields. Interestingly, under these reaction conditions, preference for intramolecular Ullmann etherification was observed over intramolecular Goldberg amidation.

Sharma et al. (Singh et al., 2018) have reported a catalyst-controlled selective intramolecular 7-*endo*-dig and 6-*exo*-dig post-Ugi cyclization of Ugi-adducts **27a** to afford the benzoxazepinones **27b** and benzoxazinones **27c,** respectively, with high regioselectivity. The cyclization of Ugi-product **27a** was performed using $Pd(CH_3CN)_4(BF_4)_2$ as catalyst in toluene facilitated the formation of benzoxazepinones **27b** in high yields with exclusive 7-*endo*-dig selectivity. However, switching the catalyst to 5 mol% of Echavarren's gold(I) catalyst [JohnPhosAu-(CH_3CN)]SbF_6 in DCE resulted in the preferential formation of benzoxazinones **27c** in high yields with 7-*exo*-dig selectivity (**Scheme 12**). Under the optimized conditions for the formation of benzoxazepinones and benzoxazinones, Ugi-adducts derived from various alkynes, isonitriles, aldehydes, and amines underwent the reaction smoothly with high selectivity. Several adducts derived from aldehydes bearing electron-donating or electron-withdrawing substituents underwent the reaction smoothly and yielded the corresponding products in moderate to excellent yields. However, adducts from aldehydes bearing an electron-withdrawing substituent such as cyano, bromo, and bis-amide afforded relatively lower yields for 7-*endo* dig cyclization. No specific electronic effect was observed for the cyclization of Ugi-adducts derived from different isocyanides and 2-aminophenol and afforded the corresponding benzoxazepinones and benzoxazinones in good to high yields. However, Ugi-adducts derived from phenyl substituted alkynes bearing electron-donating groups afforded the corresponding products in slightly lower yields.

Nine-Membered Heterocycles Fused With Five-Membered Heterocycles

Van der Eycken et al. (Li et al., 2014a) have reported an efficient gold-catalyzed intramolecular hydroarylation reaction of Ugi-adduct **28a** for the regioselective construction of the fused nine-membered ring in benzo[*b*]pyrrolo[2,1-*i*][1,5]diazonin-7(6*H*)-ones **28b** in good to excellent yields using 10 mol% $Au(PPh_3)OTf$ in $CDCl_3$ at 50°C (**Scheme 12**). Under the optimized reaction conditions, Ugi-adducts derived from diversely substituted alkynes, isocyanides, aldehydes, and amines were found compatible and underwent the intramolecular hydroarylation reaction smoothly, providing access to the corresponding benzo[*b*]pyrrolo[2,1-*i*][1,5]diazonin-7(6*H*)-ones **28b** in good yields. Ugi-adducts from bulky phenyl-substituted alkynes or terminal alkynes afforded moderate product yields. Cyclization of the Ugi-adduct bearing an indole moiety (from aldehyde component) resulted in decomposition of the Ugi-adduct.

Tricyclic Fused Heterocycles

Jida et al. (Barlow et al., 2016) have developed an efficient, diversity-oriented, one-pot approach to access amino-benzotriazolodiazocine-bearing dipeptides **29c** in good to high yields and with good diastereoselectivity. This catalyst-free reaction of an azidoaniline **29a**, an isocyanide, an aldehyde and a *Boc*-propargylglycine **29b**, proceeded well in methanol at rt and was followed by a thermal azide-alkyne Huisgen cycloaddition reaction at 70°C (**Scheme 13**). Variedly substituted azidoanilines were well tolerated and afforded the corresponding products in good yields without any influence on the diastereoselectivity. Aldehydes were preferred over ketones under the optimum conditions for Ugi reaction. Among differently substituted isocyanides, *t*-Bu-substituted isocyanides yielded the corresponding products in 24 h. However, benzyl- and cyclohexyl-substituted isocyanides required extended reaction times for completion of the reaction. An isomer **29f** with different triazole orientation was obtained in high yield when Boc-*β*-azido-*L*-alanine **29e** and commercially available ethynyl aniline **29d** were used in place of the functionalized azidoanilines **29a** and Boc-*L*-propargylamine **29b**.

Balalaie et al. (Balalaie et al., 2017c) have reported an expedient synthesis of pyranoquinolines **30b** *via* $InCl_3$-catalyzed post-Ugi intramolecular hydroamidation of alkyne containing Ugi-adduct **30a** in toluene at 100°C (**Scheme 13**). The reaction proceeded smoothly under the optimized conditions and accommodated a wide range of Ugi-adducts irrespective of the positional and electronic influence of the substituents, providing the pyranoquinolines in good to excellent yields. The reaction proceeded *via* π-activation of the triple bond using $InCl_3$ and delivered intermediate **A**. The 6-*exo*-dig that led to the pyran ring was preferred over the 7-*endo*-dig cyclization (that should result in the oxepine ring). Nucleophilic addition of the amide oxygen to the internal carbon of the triple bond led to the formation of the desired product through intermediate **B**.

SPIRO-POLYHETEROCYCLES

Ghandi et al. (2015) have developed a one-pot Ugi metal-free intramolecular bisannulation reaction of 2-chloroquinoline-3-carbaldehydes **31a**, with amines **31b**, acids **31d**, or **31e** and isocyanide **31c** to give access to spiro[isoindoline-1,3′-pyrrolo[2,3-*b*]quinoline]-2′,3(1′*H*)-diones **31f** and their aza-analogs, spiro[pyrrolo[2,3-*b*]quinoline-3,7′-pyrrolo[3,4-*b*]pyridine]-2,5′(1*H*,6′*H*)-diones **31g**, in good to high yields,

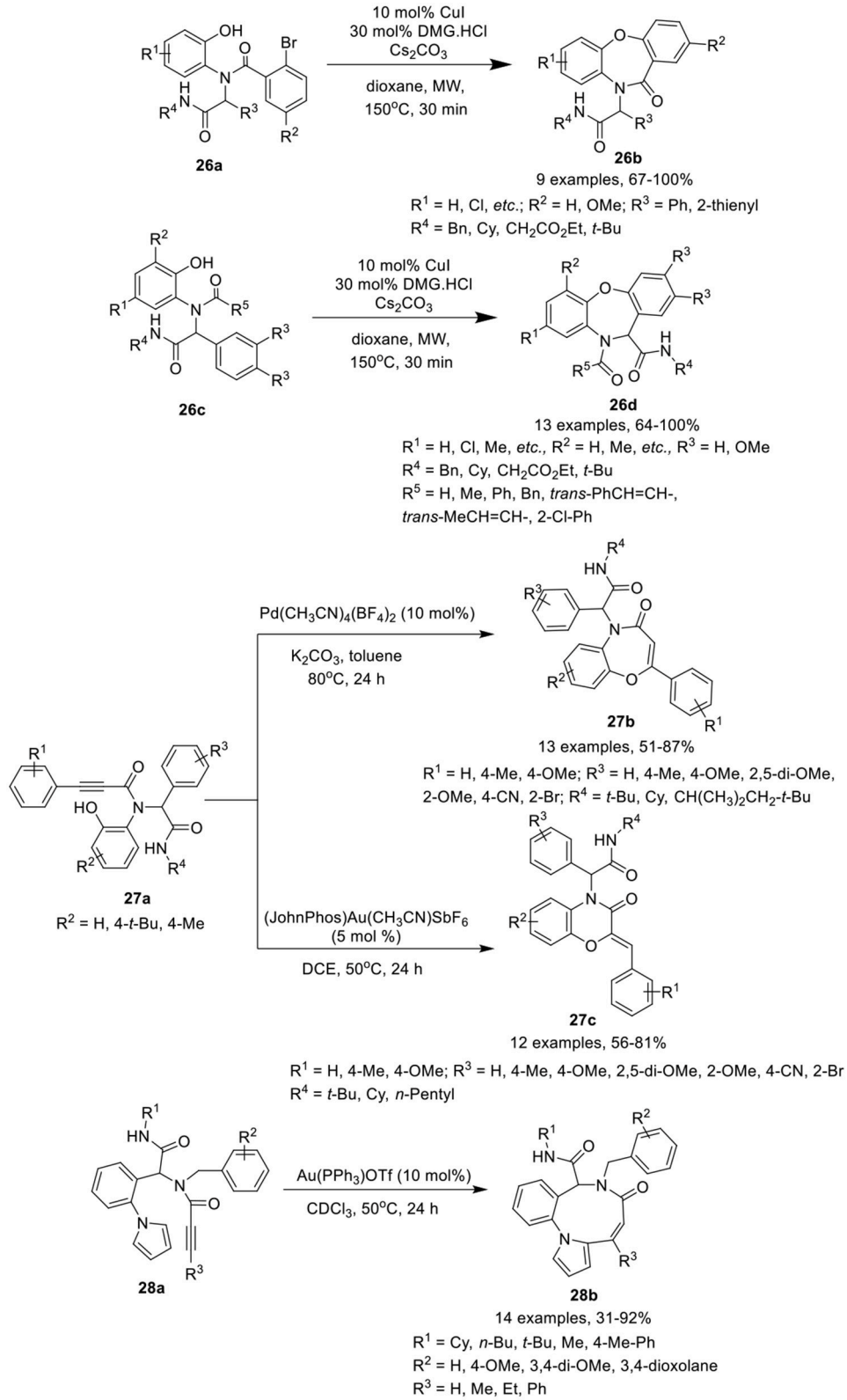

SCHEME 12 | Synthesis of dibenz[*b*,*f*][1,4]oxazepin-11(10*H*)once **26b** and dibenze[b,f][1,4]oxazepin-11(10*H*)-carboxamides **26d**, benzoxazepinones **27b** and benzoxazinones **27c**, and benzo[*b*]pyrrole[2-1-*i*][1,5]diazonin-7(6*H*)-once **28b**.

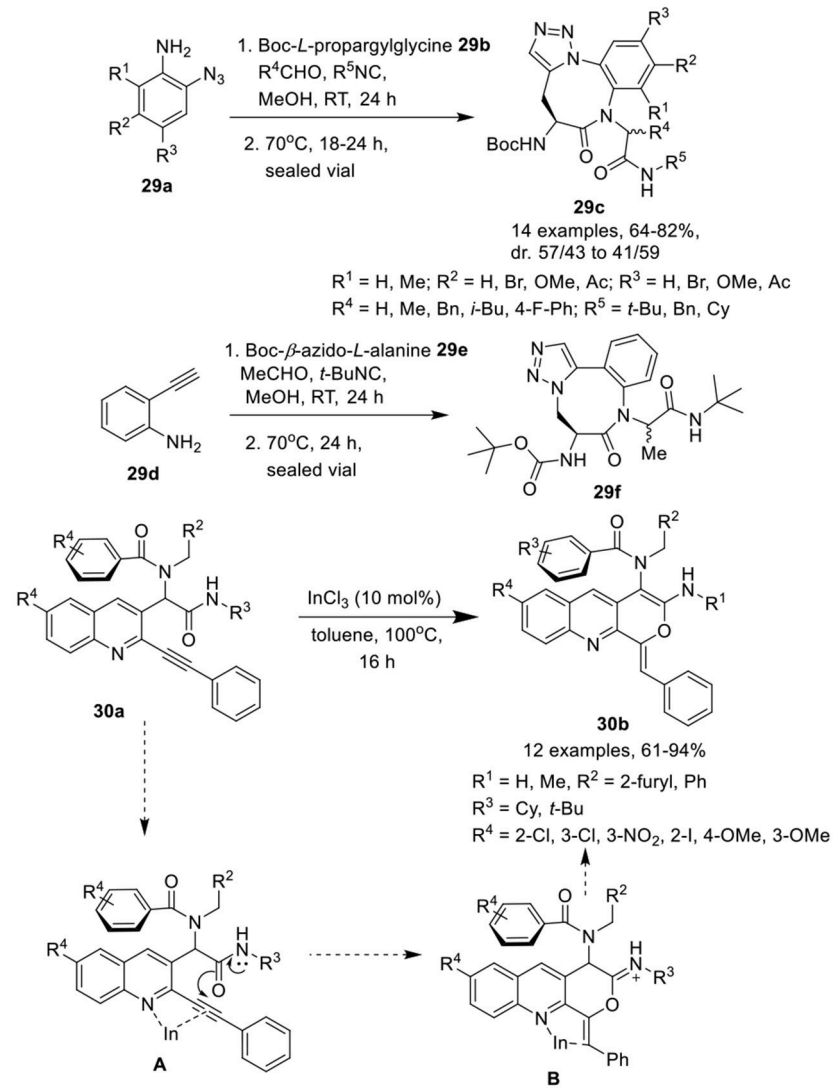

SCHEME 13 | Synthesis of amino-benzotriazocine-bearing dipeptides **29c, 29f** and tricyclic pyranoquinolines **30b**.

using Cs_2CO_3 as base in DMF at 120°C for 2 h (**Scheme 14**). Under the optimized conditions, adducts derived from aliphatic amines provided access to the corresponding products in high yields compared to aromatic amines. Easy cyclization in high yields was achieved for sterically hindered amides, such as 2,4,4-trimethylpentyl amide, suggested insensitive of the reaction to steric hindrance around the amide. Among the aldehydes, unsubstituted or modest electron-donating methyl substituted aldehydes resulted in higher product yields, compared to aldehydes bearing a stronger electron-donating methoxy group. The present approach is very attractive providing molecular diversity and synthetic simplicity with high atom economy.

Sharma et al. (Li et al., 2016) have reported an efficient and diversity-oriented ligand-controlled intramolecular palladium-catalyzed domino post-Ugi Buchwald–Hartwig/Aldol reaction sequence for the construction of (spiro)polyheterocycles **32b** and **32c** using $Pd(OAc)_2$ as catalyst and XantPhos or BINAP as ligand under basic conditions of Cs_2CO_3 in toluene at 120°C (**Scheme 14**). A variety of Ugi-adducts **32a** derived from 2-acetyl benzoic acid, afforded the spiro[indoline-3,3′-isoquinoline]-diones **32b** in modest to excellent yields and with moderate diastereoselectivity. Diversely substituted aromatic aldehydes bearing electron-donating or electron-withdrawing groups were well tolerated. Particularly, fluorine substitution at the *o*- or *m*-position of the aldehydes yielded the corresponding products with good diastereoselectivity. A bulky substituent such as a *tert*-butyl amide on the Ugi-adduct has a significant effect on the reaction outcome, resulting in the formation of polycyclic **32c** as a side product. Interestingly, a switch of ligand from XantPhos to BINAP resulted in the regioselective synthesis of tetrahydrobenzofuro-isoquinoline **32c** in high yields, using a mixture of toluene and methanol (1.95: 0.05 mL)

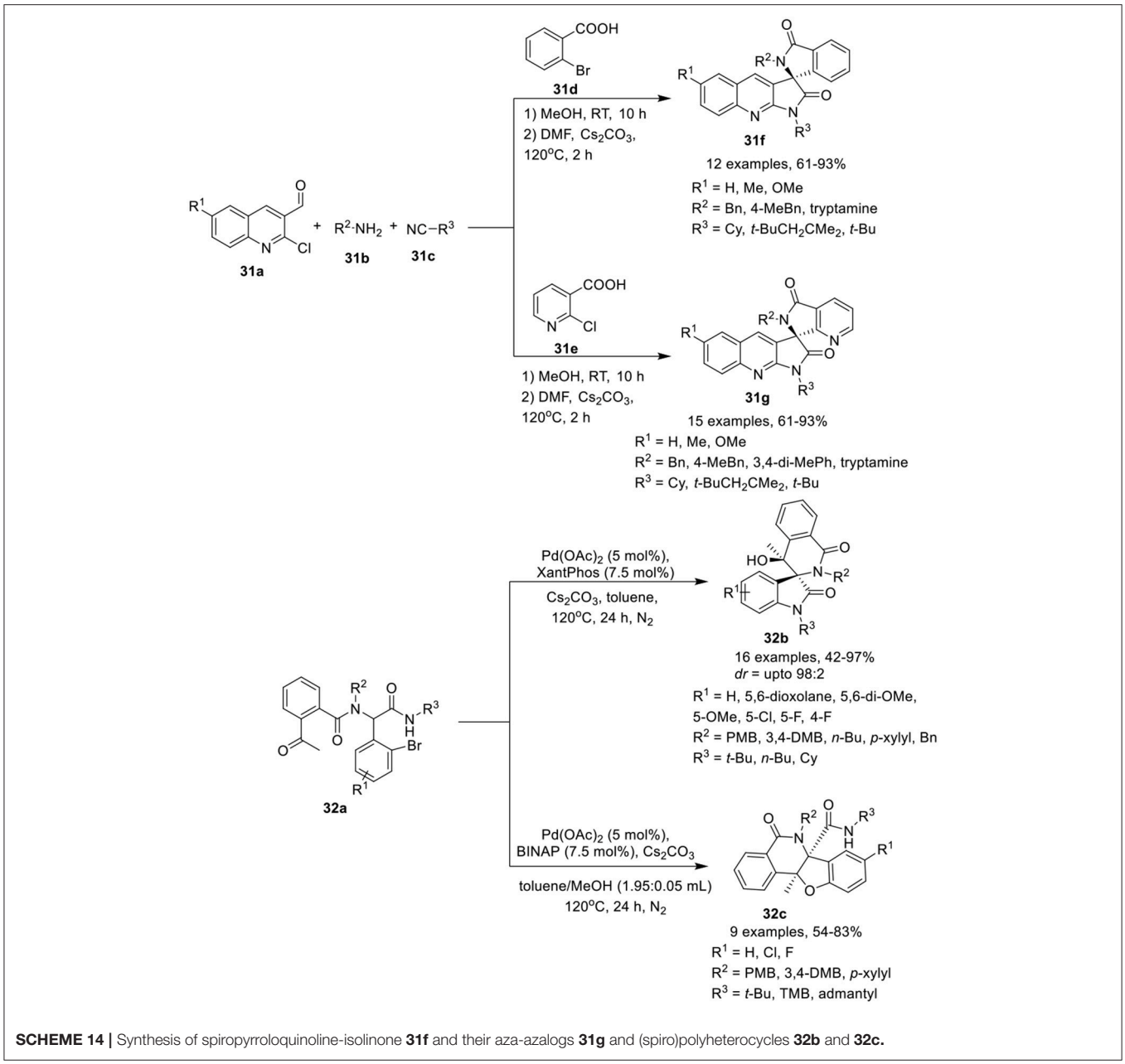

SCHEME 14 | Synthesis of spiropyrroloquinoline-isolinone **31f** and their aza-azalogs **31g** and (spiro)polyheterocycles **32b** and **32c.**

at 120°C. Interestingly, regioselective cyclization for this reaction was only observed with a bulky secondary amide group bearing a *tert*-butyl, a 1,1,3,3-tetramethyl butyl or an adamantyl group. However, linear and cyclic amides led to the formation of a mixture of spirocyclic and polycyclic products.

Sharma et al. (2014) have reported a facile post-Ugi domino Buchwald–Hartwig/Michael reaction of Ugi-adduct **33a** to give access to functionalized spiro[indoline-3,2′-pyrrole]-2,5′-diones **33b** in low to excellent yields using $Pd(OAc)_2$ (5 mol %) as catalyst, Xantphos (7.5 mol %) as ligand, and Cs_2CO_3 as base in toluene at 120 °C (**Scheme 15**). Halogen substituted aromatic aldehydes have a significant effect on the reaction outcome as the Ugi-adduct derived from *o*-iodo substituted benzaldehyde afforded the product in higher yields than its chloro substituted counterpart. Electron-donating or electron-withdrawing substituents at the *o*, *m*, or *p*-position of the aryl ring of the aldehydes were well tolerated. The reactions proceeded smoothly with Ugi-adducts obtained from aliphatic isonitriles. However, the use of aromatic isonitriles provided low product yields. Interestingly, Ugi-adducts obtained from propiolic acid did not provided the desired spiro-product. Additionally, use of α,β-unsaturated acids (instead of 2-alkynoic acids) resulted in spirooxindoles in good yields with adequate diastereoselectivities. Ugi-adducts derived from differently substituted amines were well tolerated.

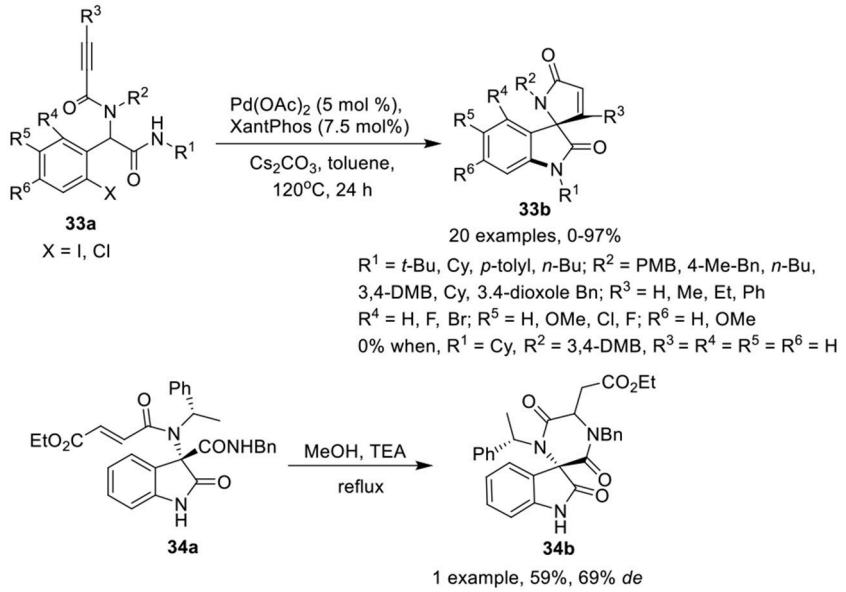

SCHEME 15 | Synthesis of spiro[indoline-3,2′-pyrrole]-2,5′-diones **33b** and spiro-diketopiperazines **34b.**

Silvani et al. (Lesma et al., 2014) have developed an intramolecular aza-Michael reaction for the post-Ugi cyclization of chiral 3,3-disubstituted 3-aminooxindole **34a** to access the spiro-diketopiperazine **34b** in moderate yield and good diastereoselectivity (**Scheme 15**). The spiro-diketopiperazine scaffold has received great recognition as pharmacologically active peptidomimetic.

CONCLUSION

In conclusion, we have demonstrated the wide-spread application of the Ugi reaction for the synthesis of heterocyclic compounds, where careful selection of the starting building blocks provided the appropriate functionality for post-Ugi modifications. We have discussed various recent reports where a variety of heterocyclic systems were successfully synthesized starting from simple four, five or six-membered heterocycles to fused heterocycles and spirocyclized complex molecules. During the post-Ugi transformation, we have witnessed the application of various metallic salts of palladium, gold, indium, copper, zinc, scandium, iron and aluminum, leading to the successful transformation of appropriately substituted Ugi-adducts to heterocyclic systems. The use of modern medicinal chemistry tools such as microwave irradiation has also been successfully applied in post-Ugi transformations. Interestingly, the use of chiral ligands such as BINAP, XantPhos, and triphenylphosphine has provided stereoselectivity and chemoselectivity in such transformations. We anticipate that this review would provide in-depth understanding of the chemistry and applications of post-Ugi transformations for the synthesis of variety of heterocyclic systems. New heterocyclic systems with interesting biological activity are expected from the post-Ugi transformation in the near future.

AUTHOR CONTRIBUTIONS

JB and RK collected the publications related to this review article, wrote the first draft of the manuscript and made subsequent corrections. EV and LV completed critical literature analysis and checked subsequent manuscript drafts.

ACKNOWLEDGMENTS

We acknowledge the support of Shiva Institute of B. Pharmacy and RUDN University Program 5-100.

REFERENCES

Ambasana, P. A., Vachhani, D. D., Galli, M., Jacobs, J., Van Meervelt, L., Shah, A. K., et al. (2014). Solvent switchable cycloaddition: a (one-pot) metal-free approach towards N-substituted benzo[*e*]- or [*f*]isoindolones via Csp2-H functionalization. *Org. Biomol. Chem.* 12, 8861–8865. doi: 10.1039/C4OB01644K

Azuaje, J., Maatougui, E. A., Garcia-Mera, X., and Sotelo, E. (2014). Ugi-based approaches to quinoxaline libraries. *ACS Comb. Sci.* 16, 403–411. doi: 10.1021/CO500036N

Balalaie, S., Kejani, R. R., Ghabraie, E., Darvish, F., Rominger, F., Hamdan, F., et al. (2017a). Diastereoselective synthesis of functionalized diketopiperazines through post-transformational reactions. *J. Org. Chem.* 82, 12141–12152. doi: 10.1021/acs.joc.7b01855

Balalaie, S., Mirzaie, S., Nikbakht, A., Hamdan, F., Rominger, F., Navari, R., et al. (2017b). Indium-catalyzed intramolecular hydroamidation of alkynes: an exo-dig cyclization for the synthesis of pyranoquinolines through post-transformational reaction. *Org. Lett*. 19, 6124–6127. doi: 10.1021/acs.orglett.7b02603

Balalaie, S., Shamakli, M., Nikbakht, A., Alavijeh, N. S., Rominger, F., Rostamizadeh, S., et al. (2017c). Direct access to isoxazolino and isoxazolo benzazepines from 2-((hydroxyimino)methyl)benzoic acid via a post-Ugi heteroannulation. *Org. Biomol. Chem*. 15, 5737–5742. doi: 10.1039/C7OB01142C

Bariwal, J. B., Trivedi, J. C., and Van der Eycken, E. V. (2010). "Microwave Irradiation and Multicomponent Reactions," in *Synthesis of Heterocycles via Multicomponent Reactions II*, eds. R. V. A. Orru and E. Ruijter (Berlin; Heidelberg: Springer Berlin Heidelberg), 169–230.

Barlow, T. M., Jida, M., Guillemyn, K., Tourwe, D., Caveliers, V., and Ballet, S. (2016). Efficient one-pot synthesis of amino-benzotriazolodiazocinone scaffolds via catalyst-free tandem Ugi-Huisgen reactions. *Org. Biomol. Chem*. 14, 4669–4677. doi: 10.1039/C6OB00438E

Biggs-Houck, J. E., Younai, A., and Shaw, J. T. (2010). Recent advances in multicomponent reactions for diversity-oriented synthesis. *Curr. Opin. Chem. Biol*. 14, 371–382. doi: 10.1016/j.cbpa.2010.03.003

Ghandi, M., Zarezadeh, N., and Abbasi, A. (2015). One-pot synthesis of spiropyrroloquinoline-isoindolinone and their aza-analogs via the Ugi-4CR/metal-free intramolecular bis-annulation process. *Org. Biomol. Chem*. 13, 8211–8220. doi: 10.1039/C5OB01095K

Ghoshal, A., Yugandhar, D., Nanubolu, J. B., and Srivastava, A. K. (2017). An efficient one-pot synthesis of densely functionalized fused-quinolines via sequential Ugi4CC and acid-mediated povarov-type reaction. *ACS Comb. Sci*. 19, 600–608. doi: 10.1021/acscombsci.7b00095

Golubev, P., and Krasavin, M. (2017). Sterically constrained and encumbered: an approach to the naturally occurring peptidomimetic tetrahydropyrazino1,2-*a*]indole-1,4-dione core. *Eur. J. Org. Chem*. 2017, 1740–1744. doi: 10.1002/ejoc.201700152

Halimehjani, A. Z., and Sharifi, M. (2017). Synthesis of a novel category of Ugi adducts using succinic acid, succinic anhydride and maleic anhydride and their application in post-Ugi reactions for synthesis of functionalized piperazine 2,5-diones. *Tetrahedron* 73, 5778–5783. doi: 10.1016/j.tet.2017.08.028

He, Y., Li, Z., Robeyns, K., Van Meervelt, L., and Van der Eycken, E. V. (2018). A gold-catalyzed domino cyclization enabling rapid construction of diverse polyheterocyclic frameworks. *Angew. Chem. Int. Ed*. 57, 272–276. doi: 10.1002/anie201710592

He, Y., Li, Z., Tian, G., Song, L., Van Meervelt, L., and Van der Eycken, E. V. (2017). Gold-catalyzed diastereoselective domino dearomatization/ipso-cyclization/aza-Michael sequence: a facile access to diverse fused azaspiro tetracyclic scaffolds. *Chem. Commun*. 53, 6413–6416. doi: 10.1039/C7CC03152A

Hulme, C., and Dietrich, J. (2009). Emerging molecular diversity from the intramolecular Ugi reaction: iterative efficiency in medicinal chemistry. *Mol. Divers*. 13, 195–207. doi: 10.1007/s11030-009-9111-6

Kaïm, L. E., and Grimaud, L. (2010). Ugi–Smiles couplings: new entries to N-aryl carboxamide derivatives. *Mol. Divers*. 14, 855-867. doi: 10.1007/s11030-009-9175-3

Kaïm, L. E., and Grimaud, L. (2014). The Ugi-smiles and passerini-smiles couplings: a story about phenols in isocyanide-based multicomponent reactions. *Eur. J. Org. Chem*. 35, 7749–7762. doi: 10.1002/ejoc.201402783

Koopmanschap, G., Ruijter, E., and Orru, R. V. A. (2014). Isocyanide-based multicomponent reactions towards cyclic constrained peptidomimetics. *Beilstein J. Org. Chem*. 10, 544–598. doi: 10.3762/bjoc.10.50

Lesma, G., Meneghetti, F., Sacchetti, A., Stucchi, M., and Silvani, A. (2014). Asymmetric Ugi 3CR on isatin-derived ketimine: synthesis of chiral 3,3-disubstituted 3-aminooxindole derivatives. *Beilstein J. Org. Chem*. 10, 1383–1389. doi: 10.3762/BJOC.10.141

Li, Y., Lei, J., Xu, J., Tang, D., Chen, Z., Zhu, J., et al. (2017). A facile method for building fused quinoxaline-quinolinones via an acidless post-Ugi cascade reaction. *Chinese Chem Lett*. 28, 541–545. doi: 10.1016/j.cclet.2016.10.027

Li, Z., Kumar, A., Sharma, S. K., Parmar, V. S., and Van der Eycken, E. V. (2015a). Catalyst-controlled exo/endo selectivity in a post-Ugi intramolecular hydroarylation: synthesis of pyrrolopyridinones, pyrroloazepinones, and benzothienopyridines. *Tetrahedron* 71, 3333–3342. doi: 10.1016/j.tet.2015.03.103

Li, Z., Kumar, A., Vachhani, D. D., Sharma, S. K., Parmar, V. S., and Van der Eycken, E. V. (2014a). Regioselective synthesis of diversely substituted diazoninones through a post-Ugi gold-catalyzed intramolecular hydroarylation process. *Eur. J. Org. Chem*. 2014, 2084–2091. doi: 10.1002/ejoc.201301507

Li, Z., Legras, L., Kumar, A., Vachhani, D. D., Sharma, S. K., Parmar, V. S., et al. (2014b). Microwave-assisted synthesis of 4*H*-benzo[f]imidazo[1,4]diazepin-6-ones via a post-Ugi copper-catalyzed intramolecular Ullmann coupling. *Tetrahedron Lett*. 55, 2070–2074. doi: 10.1016/j.tetlet.2014.02.023

Li, Z., Sharma, N., Sharma, U. K., Jacobs, J., Van Meervelt, L., and Van der Eycken, E. V. (2016). Ligand-controlled product selectivity in palladium-catalyzed domino post-Ugi construction of (spiro)polyheterocycles. *Chem. Commun*. 52, 5516–5519. doi: 10.1039/C6CC00784H

Li, Z., Sharma, U. K., Liu, Z., Sharma, N., Harvey, J. N., and Van der Eycken, E. V. (2015b). Diversity-oriented synthesis of β-lactams and γ-lactams by Post-Ugi nucleophilic cyclization: lewis acids as regioselective switch. *Eur. J. Org. Chem*. 2015, 3957–3962. doi: 10.1002/ejoc.201500270

Madhavachary, R., Zarganes-Tzitzikas, T., Patil, P., Kurpiewska, K., Kalinowska-Tluscik, J., and Dömling, A. (2018). Synthesis of highly substituted imidazole uracil containing molecules via Ugi-4CR and passerini-3CR. *ACS Comb. Sci*. 20, 192–196. doi: 10.1021/acscombsci.7b00145

Medda, F., Martinez-Ariza, G., and Hulme, C. (2015). A facile and concise route toward the synthesis of novel imidazo-tetrazolodiazepinones via post-condensation modifications of the Ugi-azide adduct. *Tetrahedron Lett*. 56, 5295–5298. doi: 10.1016/j.tetlet.2015.07.083

Ramon, D. J., and Yus, M. (2005). Asymmetric multicomponent reactions (AMCRs): the new frontier. *Angew. Chem. Int. Ed. Engl*. 44, 1602–1634. doi: 10.1002/anie.200460548

Sagar, A., Babu, V. N., and Sharada, D. S. (2015). Silica gel promoted environment-friendly synthesis of α-amino amidines and regioselective transformation of α-amino amidines into amidino substituted indazoles. *RSC Adv*. 5, 29066–29071. doi: 10.1039/C5RA02491A

Sharma, N., Li, Z., Sharma, U. K., and Van der Eycken, E. V. (2014). Facile access to functionalized spiro[indoline-3,2′-pyrrole]-2,5′-diones via post-Ugi domino Buchwald-Hartwig/Michael reaction. *Org. Lett*. 16, 3884–3887. doi: 10.1021/Ol5019079

Sharma, U. K., Sharma, N., Vachhani, D. D., and Van der Eycken, E. V. (2015). Metal-mediated post-Ugi transformations for the construction of diverse heterocyclic scaffolds. *Chem. Soc. Rev*. 44, 1836–1860. doi: 10.1039/C4CS00253A

Shi, J., Wu, J., Cui, C., and Dai, W. (2016). Microwave-Assisted intramolecular ullmann diaryl etherification as the post-ugi annulation for generation of dibenz[*b,f*][1,4]oxazepine Scaffold. *J. Org. Chem*. 81, 10392–10403. doi: 10.1021/acs.joc.6b01398

Shiri, M., Mirpour-Marzoni, S. Z., Bozorgpour-Savadjani, Z., Soleymanifard, B., and Kruger, H. G. (2014). Base-catalyzed cyclization of Ugi-adducts to substituted indolyl based γ-lactams. *Monatsh Chem*. 145, 1947–1952. doi: 10.1007/s00706-014-1271-0

Singh, K., Malviya, B. K., Roy, T. K., Mithu, V. S., Bhardwaj, V. K., Verma, V. P., et al. (2018). Catalyst-controlled structural divergence: selective intramolecular 7-*endo*-dig and 6-*exo*-dig Post-Ugi cyclization for the synthesis of benzoxazepinones and benzoxazinones. *J. Org. Chem*. 83, 57–68. doi: 10.1021/acs.joc.7b02123

Srinivasulu, V., Sieburth, S. M., El-Awady, R., Kariem, N. M., Tarazi, H., O'Connor, M. J., et al. (2018). Post-Ugi cascade transformations for accessing diverse chromenopyrrole collections. *Org. Lett*. 20, 836–839. doi: 10.1021/acs.orglett.7b03986

Trang, T. T. T., Peshkov, A. A., Jacobs, J., Van Meervelt, L., Peshkov, V. A., and Van der Eycken, E. V. (2015). Post-Ugi carbocyclization/fragmentation sequence for the synthesis of 6,7-dihydro-5*H*-pyrrolo3,4-*b*]pyridin-5-ones. *Tetrahedron Lett*. 56, 2882–2886. doi: 10.1016/j.tetlet.2015.03.092

Ugi, I. (1962). The α-addition of immonium ions and anions to isonitriles accompanied by secondary reactions. *Angew. Chem. Int. Ed. Engl*. 1, 8–21. doi: 10.1002/anie.196200081

Ugi, I., and Steinbrückner, C. (1961). Isonitrile, II. Reaktion von Isonitrilen mit Carbonylverbindungen, Aminen und Stickstoffwasserstoffsäure. *Chem. Ber*. 94, 734–742. doi: 10.1002/cber.19610940323

Vachhani, D. D., Kumar, A., Modha, S. G., Sharma, S. K., Parmar, V. S., and Van der Eycken, E. V. (2015). Diversely substituted indoloazepinones and indoloazocinones: a post-ugi gold-catalyzed regioselective carbocyclization approach. *Synthesis* 47, 1337–1347. doi: 10.1055/s-0034-1379894

VenkataPrasad, J., Krishnamurthy, S., Moriguchi, T., and Tsuge, A. (2017). Efficient synthesis of novel pyrrolo2,3-*c*]pyridone derivatives using the Ugi four-component reaction followed by condensation reaction. *New J. Chem*. 41, 97–107. doi: 10.1039/C6NJ02569B

Wang, L., Guan, Z., and Ding, M. (2016). One-pot synthesis of 1*H*-isochromenes and 1,2-dihydroisoquinolines by a sequential isocyanide-based multicomponent/Wittig reaction. *Org. Biomol. Chem*. 14, 2413–2420. doi: 10.1039/C5OB02405F

Xiuming, L., Xueshun, J., and Liang, Y. (2017). Recent progress on post-Ugi reaction. *Chin. J. Org. Chem*. 37, 2237-2249. doi: 10.6023/cjoc201704026

Zamudio-Medina, A., Garca-González, M. C., Gutierrez-Carrillo, A., and González-Zamora, E. (2015). Synthesis of cyclic analogues of hexamethylenebis(3-pyridine)amide (HMBPA) in a one-pot process. *Tetrahedron Lett*. 56, 627–629. doi: 10.1016/j.tetlet.2014.12.018

Conflict of Interest Statement: The authors declare that the research was conducted in the absence of any commercial or financial relationships that could be construed as a potential conflict of interest.

frontiers in Chemistry

REVIEW
published: 13 November 2018
doi: 10.3389/fchem.2018.00527

Aminoazole-Based Diversity-Oriented Synthesis of Heterocycles

*Maryna V. Murlykina [1], Alisa D. Morozova [1], Ievgen M. Zviagin [1], Yana I. Sakhno [1], Sergey M. Desenko [1,2] and Valentyn A. Chebanov [1,2]**

[1] Department of Organic and Bioorganic Chemistry, State Scientific Institution "Institute for Single Crystals", National Academy of Sciences of Ukraine (NAS), Kharkiv, Ukraine, [2] Chemistry Faculty, Karazin Kharkiv National University, Kharkiv, Ukraine

The comprehensive review contains the analysis of literature data concerning reactions of heterocyclization of aminoazoles and demonstrates the application of these types of transformations in diversity-oriented synthesis. The review is oriented to wide range of chemists working in the field of organic synthesis and both experimental and theoretical studies of nitrogen-containing heterocycles.

OPEN ACCESS

Edited by:
Andrea Basso, Università di Genova, Italy

Reviewed by:
Thomas J. J. Müller, Heinrich-Heine-Universität Düsseldorf, Germany
Tatiana Besset, UMR6014 Chimie Organique, Bioorganique Réactivité et Analyse (COBRA), France

***Correspondence:**
Valentyn A. Chebanov
chebanov@isc.kh.ua

Specialty section:
This article was submitted to Organic Chemistry, a section of the journal Frontiers in Chemistry

Received: *28 June 2018*
Accepted: *11 October 2018*
Published: *13 November 2018*

Citation:
Murlykina MV, Morozova AD, Zviagin IM, Sakhno YI, Desenko SM and Chebanov VA (2018) Aminoazole-Based Diversity-Oriented Synthesis of Heterocycles. Front. Chem. 6:527. doi: 10.3389/fchem.2018.00527

Keywords: aminoazole, diversity-oriented synthesis, heterocycle, heterocyclization reaction, multicomponent reaction, microwave-assisted organic synthesis, ultrasonication, click-chemistry

INTRODUCTION

Heterocyclic compounds are backbone of drug design–about 80% of the known small molecule drugs belong to this type of substances and among them 60% relates to nitrogen containing heterocycles (Kombarov et al., 2010; Vitaku et al., 2014; Taylor et al., 2016). On the other hand, heterocyclic compounds play important role in other branches of science and are the base of all living organisms. Therefore, study of the appropriate field of organic chemistry is a very important challenge that has been attracting attention of numerous scientific groups for last decades and stimulating for detailed study of the topic including the search for novel and development of known synthetic methods.

One of the important pathways to nitrogen containing heterocycles is reactions of aminoazoles (two-component, one-pot, multicomponent, etc.) being efficient mono-, bi- and polynucleophiles with different electrophiles. The presence of several alternative reaction centers in aminoazoles often makes them useful reagents in controlled multidirectional interactions providing the possibility to synthesize diverse chemotypes of final products (see some examples in **Figure 1**). Such approach is widely used in the modern heterocyclic chemistry and some books and reviews have been already published in this field (Desenko, 1995; Chebanov and Desenko, 2006, 2012, 2014; Chebanov et al., 2008a, 2010; Moderhack, 2011; Sedash et al., 2012; Tkachenko and Chebanov, 2016; Aggarwal and Kumar, 2018), however, many of them deal with particular problems of aminoazole chemistry and actually during long period no comprehensive analysis of the problem has been made.

Thus, the present review is devoted to diversity-oriented reactions of heterocyclization involving aminoazoles as a key reagent. It presents analysis of literature mainly from 2010 till present and three main types of such reactions are discussed: multicomponent reactions including application of condition-based divergence strategy for the control of their directions; two-component heterocyclizations and one-pot cascade processes; "click"-chemistry concerning azoles and aminoazoles.

MAIN PART

Multicomponent Reactions of Aminoazoles Involving Cyclic CH-Acids

Multicomponent reactions (MCRs) involving aminoazoles and aldehydes with cyclic CH-acids (different ketones, 1,3-diketones, Meldrum's acid etc.) are similar to the classic Hantzsch or Biginelly condensations. In early publications they had often resulted in the formation of mixtures of positional and regioisomers, therefore, some efficient methods for tuning chemo- and regioselectivity of such multicomponent heterocyclizations, including Condition-based divergence strategy to switch their directions by simple variation of the reaction conditions (solvent, temperature, method of activation–microwave irradiation (MW) and ultrasonication (US), catalyst, etc), were found and developed (Desenko, 1995; Chebanov and Desenko, 2006, 2012; Chebanov et al., 2008a, 2010; Ruijter et al., 2011).

Varying temperature and catalyst allowed authors (Chebanov et al., 2007b, 2008b) to switch the heterocyclization of aromatic aldehydes **1**, 1,3-cyclohexanedione (**2a**) or dimedone (**2b**) with 5-amino-3-arylpyrazoles **3** between two directions with the formation of pyrazoloquinolinenones **6** (EtOH-Et_3N, MW, 150°C, 15 min) and pyrazoloquinazolinones **7** (EtOH, US, r.t., 30 min) being the products of thermodynamically and kinetically controlled reactions, respectively. Non-classical activation methods led to the reduction in time; moreover, applying microwave activation allowed to carry out the transformations at higher temperatures in comparison with standard heating, thus, additionally favoring reaction regioselectivity in case of thermodynamically controlled pathway (**Figure 2**).

In the process of optimization, the new multicomponent reaction was found: *t*-BuOK being a stronger nucleophile then Et_3N attacked the carbonyl group of cyclic 1,3-diketone moiety in the intermediate which resulted in the ring opening and recyclization with the formation of quinolizinones **8**. Later on the greener methodology of obtaining pyrazoloquinolinenones **6** was elaborated using microwave synthesis in water (170°C, 10 min; Andriushchenko et al., 2011). Similar to compounds **6** pyrazoloquinolinenones **9** were synthesized even without solvent using L-proline as a catalyst (MW, 110°C, 15 min; Bhattacharjee et al., 2016).

The analogous to heterocycles **7** linear quinazolinones **10** were obtained on the basis of 3-amino-1,2,4-triazole (**5a**) applying the great variety of conditions (only the endocyclic aminogroup in the position 2 took part in the condensation; Puligoundla et al., 2013; Petrov and Kasatochkin, 2014; Sompalle et al., 2016; Vibhute et al., 2017a,b). It should be noted, that in all cases tetrahydroderivatives **6**–**10** were formed. However, Petrov and Kasatochkin (2014) oxidized partially hydrogenated pyrimidine ring of **10** to obtain compounds **11** using ceric ammonium nitrate (CAN) in acetone. Later on the compounds **11** were synthesized in the three-component reaction of **1**, **2a** and **5a** in water under microwave irradiation also with application of CAN (**Figure 2**; Sompalle and Roopan, 2016).

Linear tetrahydroquinazolinones of type **10** had been also formed in condensations involving 5-amino-4-aryl-1,2,3-triazole and 5-amino-*N*-aryl-1,2,3-triazole-4-carboxamide (Gladkov et al., 2010), 5-aminotetrazole (Shen et al., 2013; Gein et al., 2015; Kour et al., 2017), 2-aminobenzimidazole (Puligoundla et al., 2013; Maleki et al., 2015), 2-aminoindazole moiety (Palaniraja and Roopan, 2015; Shinde and Jeong, 2016), methyl 5-amino-pyrazole-4-carboxylate (Lipson et al., 2010) and 5-amino-pyrazole-4-carbonitrile (Lipson et al., 2010), 4-aryl-5-aminopyrazole (Petrov and Kasatochkin, 2014). It should be noted, that *N*-unsubstituted 5-amino-1,2,3-triazole-4-carboxamide showed the same behavior and the products of reaction involving carboxamide aminogroup were not separated (Gladkov et al., 2012, 2013).

One of the first angular-structured heterocycles **14** was formed in the ABB′ type multicomponent reaction of 3-amino-1,2,4-triazole (**5a**) (X = CH) and two equivalents of cyclohexanone **12** ($n = 2$) and described by Desenko et al. (1990; **Figure 2**). When 5-amino-1,2,3-triazole-4-carboxamide (**13**) was introduced into the same condensation linear compounds **15** with other positional orientation of ketone moieties were obtained. The same heterocycles were synthesized in the reaction with cyclopentanone **12** ($n = 1$; Gladkov et al., 2012). However, cycloheptanone (**12**) ($n = 3$) did not react in a multicomponent procedure, therefore, corresponding spiroheterocycles of type **15** were got by the stepwise protocol through the synthesis of cycloheptalidenecycloheptanone [using two equivalents of ketone **12** ($n = 3$)] and further cyclization with 5-amino-1,2,3-triazole-4-carboxamide (**13**). It's worth noting that in case of other ketones **12** ($n = 0, 1, 2$) compounds of type **15** were formed both by the stepwise and by the multicomponent protocols (**Figure 2**; Gladkov et al., 2012).

ABC type multicomponent cyclization of 5-aminotetrazole (**5b**) (X = N), different aromatic and heteroaromatic aldehydes **1** and ketones **12** ($n = 2$–4) under heating without solvent afforded only one linear isomer **16** (Matveeva et al., 2013), while the same reaction involving 3-amino-1,2,4-triazole (**5a**) (X = CH) resulted in formation of the mixture of isomeric cycloalkatriazolopyrimidines **17** and **18** (**Figure 2**; Matveeva et al., 2015). The analogous to compounds **16** linear tetrahydrobenzo[*h*]tetrazoloquinazolines were yielded in the condensation of the reagents **1**, **5b** with α-tetralone acting as CH-acid (Kantin and Krasavin, 2016).

When 1-ethyl-4-piperidinone (**19**) was used as a CH-acid in the condensation with two equivalents of aromatic aldehyde **1** and 3-amino-1,2,4-triazole (**5a**) or 5-aminotetrazole (**5b**) or (2-aminobenzimidazole) upon heating (MeCN-I_2, Δ, 100°C) 1,2,3,4-tetrahydro-pyrido[4,3-*d*]tetrazolo[1,5-*a*]pyrimidines **20** bearing *in situ* oxidized triazolopyrimidine system were formed (**Figure 2**; Farghaly et al., 2015).

The condensations involving 5-amino-3-methyl-1-phenylpyrazole (**21**) afforded fused heteroaromatic azolopyridines. Thus, the variation of acid-base properties of the reaction medium led to the change in a sequence of elementary stages in multicomponent reaction involving 5-amino-3-methyl-1-phenylpyrazole (**21**), cyclopentanone (**12a**) and aromatic aldehydes **1** that allowed to switch the reaction

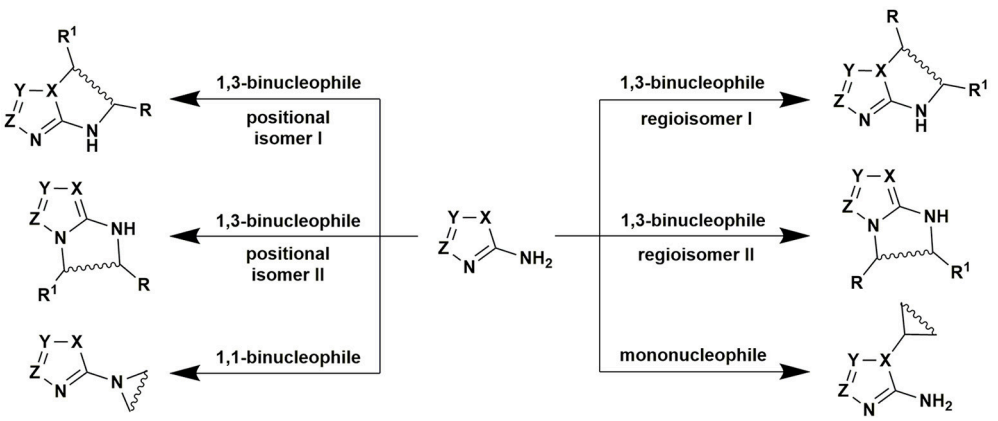

FIGURE 1 | Diversity of heterocyclizations involving aminoazoles.

between two alternative directions and selectively got positional isomers–angular pyrazolopyridines **23** ($n = 1$; Wang et al., 2011) and linear heterocycles **24**. Another authors (Jiang et al., 2011; Chen et al., 2015) described fused pyrazolopyridines **23** with $n =$ 2–4, 8 (**Figure 3**).

Several publications deal with condensations of the reagents **1** and **21** with 1,3-diketones [dimedone (**2b**) (Karnakar et al., 2012; Wang and Shi, 2012), indane-1,3-dione (**22a**) (Quiroga et al., 2008; Shi et al., 2009) and furane-2,4-dione (**22b**) (Shi et al., 2009)] resulting in the formation of heteroaromatic derivatives **26**–**28**. It's interesting that under the same conditions (H_2O-$InCl_3$, Δ) Khurana et al. (2012) obtained dihydropyrazolopyridines **25** only from 1,3-cyclohexanedione (**2a**), whereas in case of indane-1,3-dione (**22a**) and furane-2,4-dione (**22b**) heteroaromatic compounds **27**, **28** were formed (**Figure 3**).

Similar to heterocycles **23** angular products **33** (DMF-MeOH, Δ; Lipson et al., 2015) and **34** (HOAc-TFA, MW, 140°C; Jiang et al., 2011) were also got in the condensation with 5-amino-3-methylpyrazole (**4**) and 5-amino-3-hydroxypyrazole (**29**), while the transformations involving 5-amino-4-arylpyrazoles **32** afforded pyrazolopyrimidines **38** (HOAc, Δ; **Figure 3**; Petrov and Kasatochkin, 2013).

An exhaustive review on the properties of 5-aminopyrazoles as precursors in design and synthesis of fused pyrazoloazines being published yet (Aggarwal and Kumar, 2018) describes the reaction of 5-amino-3-methyl-1-phenylpyrazole (**21**) and aromatic aldehydes **1** with 4-hydroxycoumarin, where 3 types of possible products (4,7-dihydropyrazolo[3,4-*b*]pyridine-, aromatized pyrazolo[3,4-*b*]pyridine derivatives and the product of C–O bond cleavage from cyclic ester) were formed depending on the type of solvent and temperature. MCRs of 1-aryl-3-indolyl-5-aminopyrazoles, cyclic β-diketones (dimedone, cyclopentanedione, indane-1,3-dione) and aromatic aldehydes also gave dihydro- and aromatized pyrazolo[3,4-*b*]pyridine derivatives, what is more, dihydropyrazolo[3,4-*b*]pyridines formed could be transformed into their heteroaromatized analogs by prolonged heating in acetonitrile with DDQ (2,3-dichloro-5,6-dicyanobenzoquinone).

It should be noted, that reactions with chroman-4-one (**22d**), thiochroman-4-one (**22e**) or 3,4-dihydronaphthalen-1(2*H*)-one (**22f**) (EtOH-*t*-BuOK, Δ) despite of the origin or position of the substituent in pyrazole afforded only heteroaromatized "classical" Biginelly-type pyrazolopyrimidines **39** and **40** (Saikia et al., 2014). Condensations of 1,3-diketones with 3-substituted 5-aminopyrazoles **3** and **4** also led exclusively to linear dihydropyrazolopyridinones **35** (Hatti et al., 2015) and **36**, **37** (Lipson et al., 2015), correspondingly (**Figure 3**).

Using 5-aminopyrazoles **41** bearing carboxamide fragment in the fourth position in condensations with 1,3-cyclohexanediones **2a,b** and aromatic aldehydes **1** led to widening the scope of target compounds whereas varying reaction parameters and applying non-classical methods of activation (ultrasonication and microwave irradiation) allowed to switch cyclizations between several directions (**Figure 4**; Chebanov et al., 2012b).

Thus, condensation of starting reagents **1**, **2a,b**, and **41** upon heating or MW irradiating in DMF or ultrasonication in HOAc at room temperature always afforded tricyclic dihydropyrimidines **42**. Addition of catalytic amounts of hydrochloric acid resulted in switching the reaction to another direction and yielding positionally isomeric angular compounds **43**. Implementation of the third route with the formation of acrydindiones **44** occurred upon increasing the temperature and introducing the double excess of diketone **2** (Chebanov et al., 2012b).

Meldrum's acid is also widely used as a building block for the synthesis of azoloazine systems. A significant contribution to the study of the condensations involving aminoazoles and aldehydes with Meldrum's acid was made by Lipson's group (**Figure 4**; Lipson and Gorobets, 2009). It was established, that in some cases these multicomponent reactions afforded positional isomers. For example, condensations involving 3-amino-5-methylthio-1,2,4-triazole (**46**) gave 5-pyrimidinones **50a** or 7-pyrimidinones **50b** with impurities of **50a** depending on solvent and catalyst (Lipson and Gorobets, 2009).

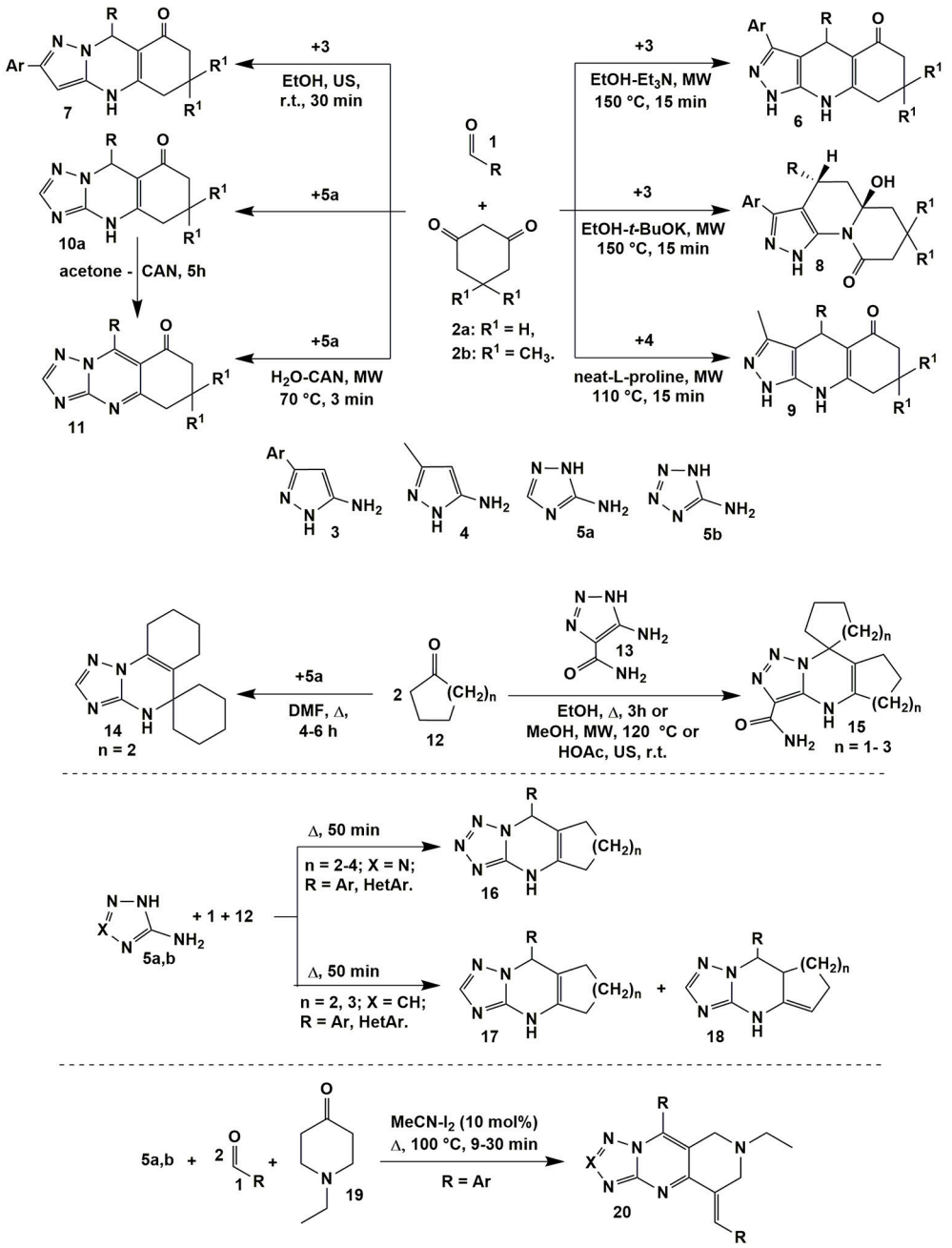

FIGURE 2 | Examples of the condensations involving α-aminoazoles, aldehydes and cyclic carbonyl compounds.

The opposite situation was observed in case of 3,5-diamino-1,2,4-triazole (**47**): 5-pyrimidinones **51a** were obtained only in mixture with isomers **51b**. At the same time the latter compounds **51b** were isolated in a pure state after changing DMF to methanol or isopropanol (Lipson and Gorobets, 2009). When 3-amino-1,2,4-triazole **5a** (Lipson and Gorobets, 2009) took part in the condensation with compounds **1** and **45** only 5-pyrimidinones **49a** were isolated while the reaction involving 2-aminobenzimidazole **48** (Sheibani et al., 2012) afforded only 7-pyrimidinones **54b** (**Figure 4**).

Condensations of 5-amino-3-methylpyrazole (**4**) (Lipson and Gorobets, 2009; Zhong et al., 2013) or 5-amino-3-methyl-*N*-phenylpyrazole (**21**) (Shi et al., 2011) with aldehydes **1** or arylglyoxals (Petrova et al., 2014) and Meldrum's acid **45** under various conditions gave 5-pyrimidinones **52a** and **53a,** correspondingly (**Figure 4**); similar heterocycles were obtained from 2-aminobenzothiazole (Arya et al., 2012).

An interesting one-pot four-component reaction was described by Shaabani et al. (2015): [1,2,4]triazolo[1,5-*a*]pyrimidine-6-carboxamide derivatives **56** were synthesized

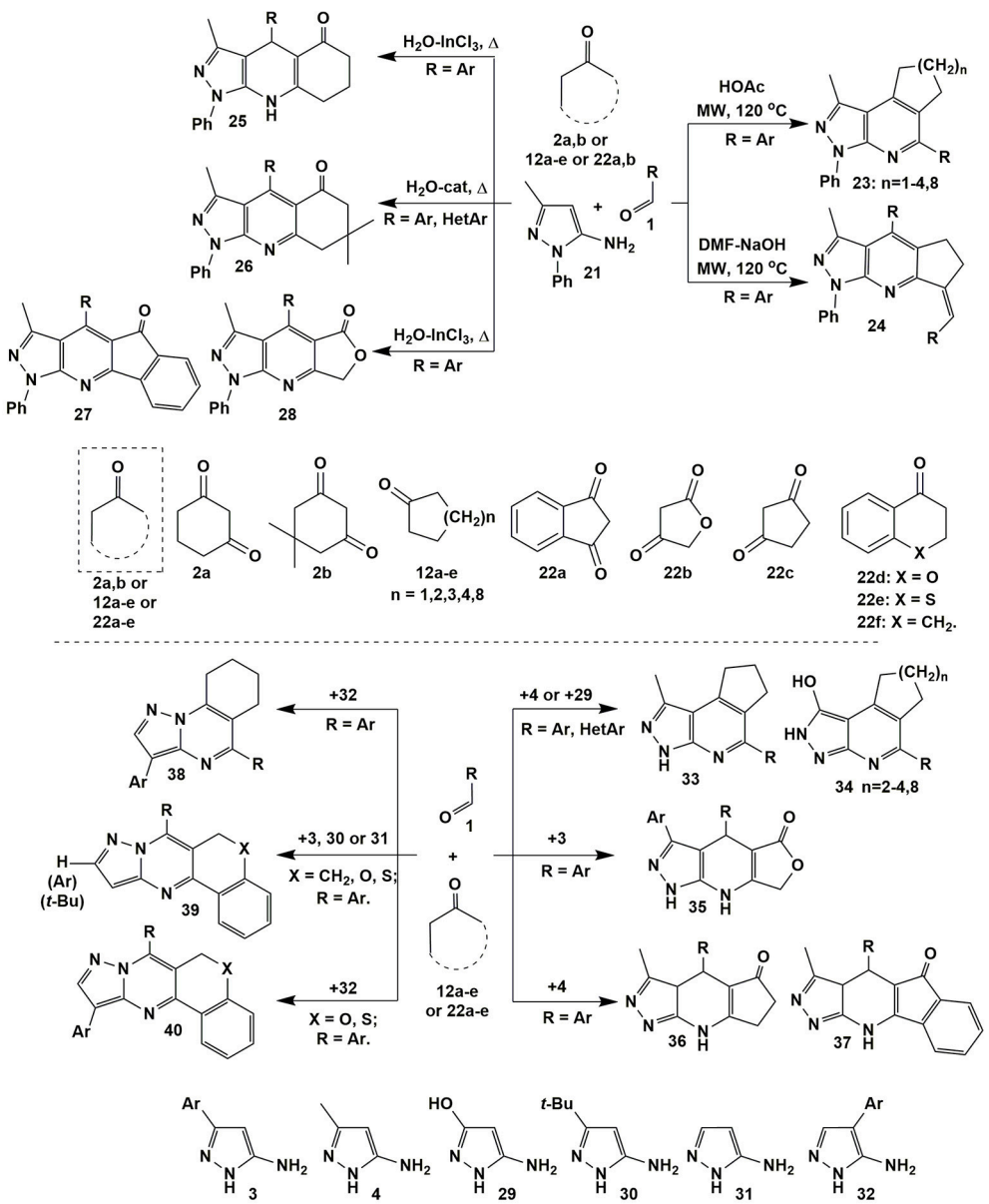

FIGURE 3 | Examples of heterocyclization reactions involving 5-aminopyrazoles, aldehydes and cyclic active methylene compounds.

via reaction of primary aliphatic or aromatic amines **55** and 2,2,6-trimethyl-4*H*-1,3-dioxin-4-one (**45b**) (heating under solvent-free conditions, 150°C, 30 min) followed by the subsequent condensation with 3-amino-1,2,4-triazole (**5a**) and aliphatic or aromatic aldehydes **1** (H_2O-*p*-TSA, Δ, 3.5–4.5 h; **Figure 4**).

The presence of four non-equivalent reaction centers in 1,2-diamino-4-phenylimidazole (**57**) makes possible new alternative reaction routes with electrophilic reagents. Due to the lower nucleophilicity of exocyclic amino groups in comparison with endocyclic CH-group, 1,2-diaminoimidazoles in the reactions with α,β-unsaturated ketones, their mono- and dibromo derivatives, with aroylacrylic acids, and in the three-component reactions with aldehydes and Meldrum's acid formed not triazepine fragments but pyridazine and pyrimidine systems fused with azole cycle (Lipson et al., 2012). This fact was also confirmed in the multicomponent reaction involving 1,3-cyclohexanediones **2a,b** upon boiling in DMF (1 h) or methanol (2 h) which resulted in the formation of dihydroimidazo[1,5-*b*]cinnolinones **58**. Only in case of 4-nitrobenzaldehyde **1** the short-term boiling the compounds **1**, **2** and **57** in DMF led to the formation of heteroaromatic derivatives **59** (**Figure 5**; Lipson et al., 2012).

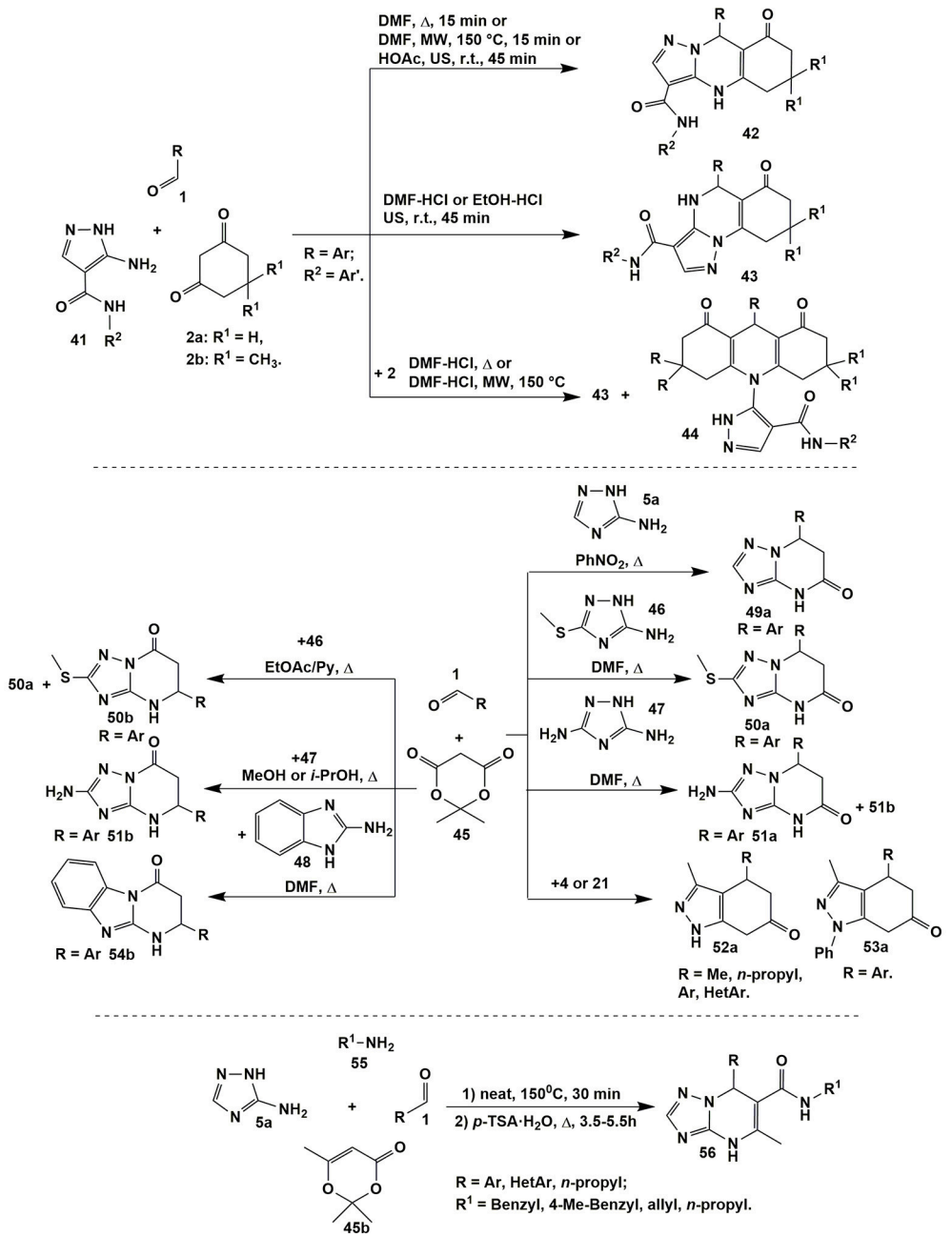

FIGURE 4 | Examples of azoloazines synthesis via reactions involving 5-aminopyrazole-4-carboxamides of 3-amino-1,2,4-triazoles derivatives.

N-Unsubstituted 2-aminoimidazole exhibited similar properties (lower nucleophilicity of exocyclic aminogroup than endocyclic reaction centers) in the reactions with aromatic aldehydes and different CH-acids (dimedone, barbituric acid), but instead of cyclic products the treatments yielded Michael adducts (with participation of CH-center in the position 3; Andriushchenko et al., 2013). On the other hand, the formation of Mannich bases in the similar reactions involving 2-aminothiazole indicates on the higher reactivity of its exocyclic NH_2-group in comparison with the endocyclic nucleophilic centers (Ghatole et al., 2015).

There is contradictory data in the literature about three-component reactions involving 5-amino-3-methyl(aryl)isoxazole **60** and aromatic aldehydes **1** with various 1,3-diketones. Thus, Tu et al. (2009) carried out that condensations under microwave irradiation at 120°C in water and synthetized isoxazolo[5,4-*b*]pyridines **61–63**. Surprisingly, heterocyclization involving

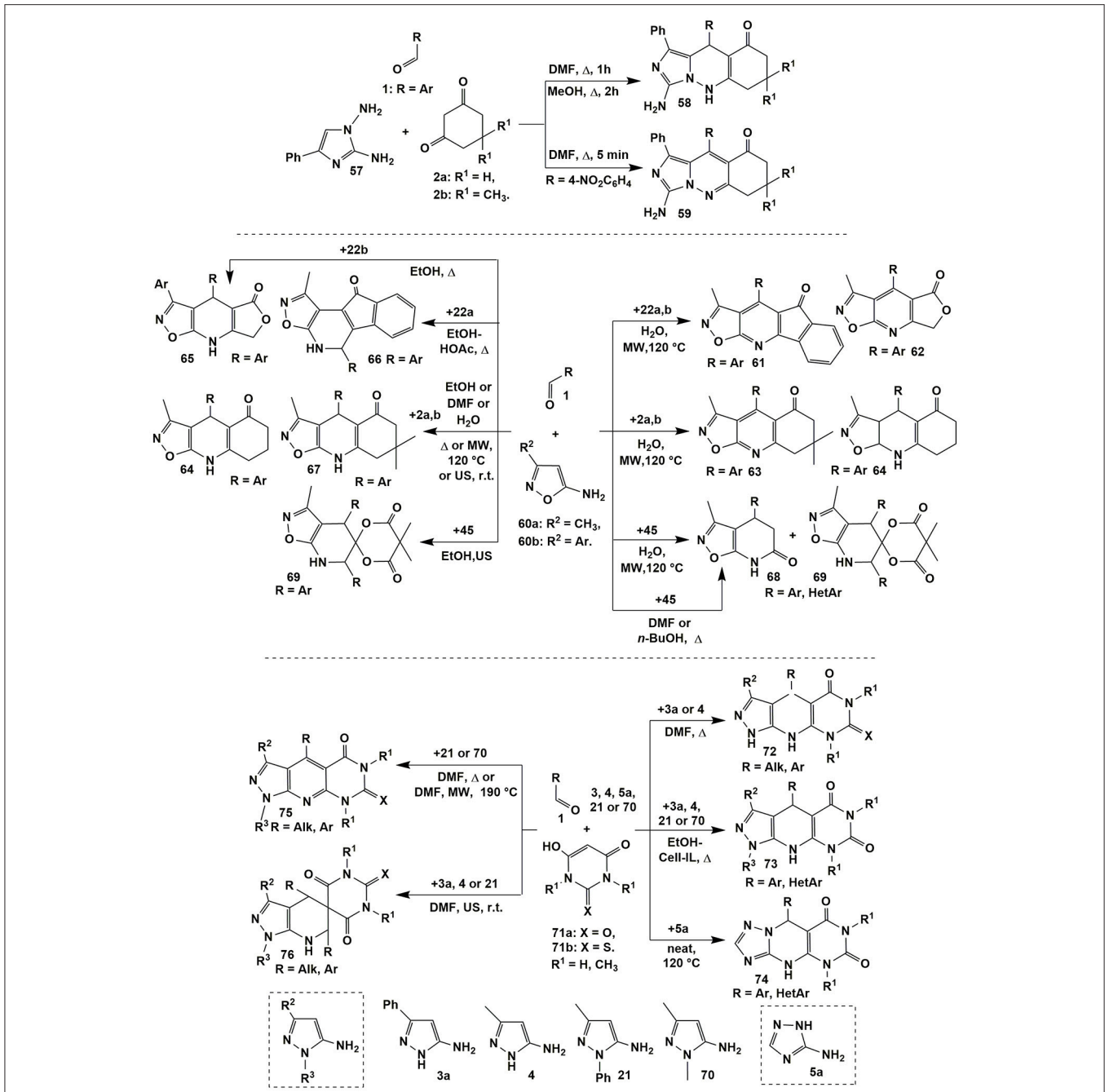

FIGURE 5 | Diversity of compounds generated by using the conditions based divergence strategy.

1,3-cyclohexanedione (**2a**) under the same conditions led to dihydroderivatives **64** (**Figure 5**).

Later on Muravyova et al. (2013) carried out wide screening of the reaction conditions and found that in all cases including those ones described in the work of Tu et al. (2009) [in the model reactions with 1,3-cyclohexanedione (**2a**) and dimedone (**2b**)] dihydroisoxazole[5,4-*b*]pyridines **64** and **67**, respectively, had been formed. Annulated with furane-2,4-dione moiety dihydroisoxazolo[5,4-*b*]pyridines **65** were yielded upon boiling the starting materials in EtOH (Kamal et al., 2011). Hamama et al. (2012) managed to synthesize angular heterocycles **66** on the basis of indane-1,3-dione (**22a**) [EtOH-HOAc (15:1), Δ], however, we suggest that there is not enough data proving the structure of compounds **66** (**Figure 5**).

When Meldrum's acid was used, different compounds—4,7-dihydroisoxazolo[5,4-*b*]pyridine-6(5*H*)-ones **68** (6–9 min) or

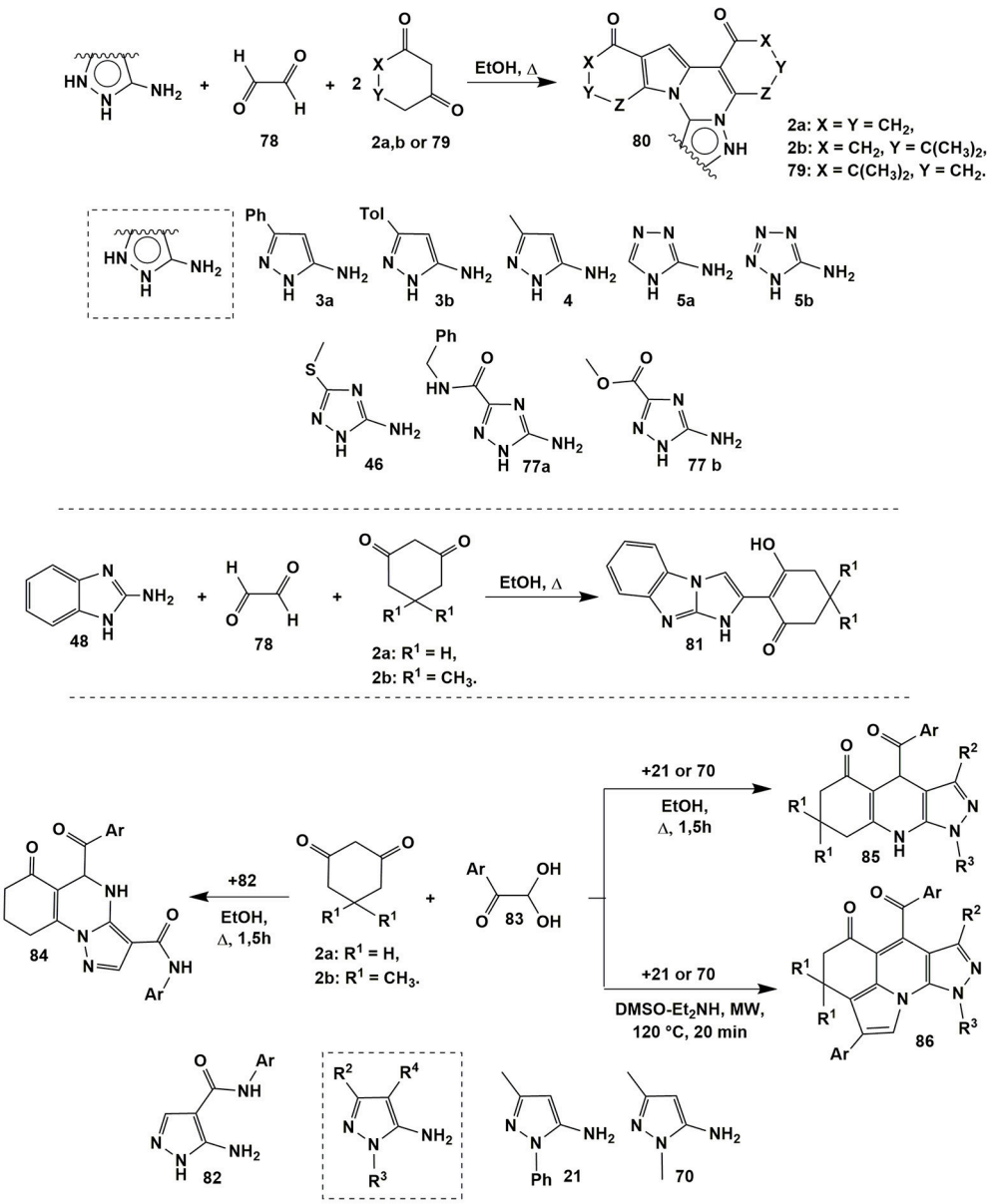

FIGURE 6 | MCRs involving glyoxales derivatives acting as carbonyl compounds.

spiroheterocycles **69** (9–13 min) were got under almost the same conditions by Tu et al. in two consecutive publications (Tu et al., 2009; Ma et al., 2010). Later on Morozova et al. (2017) reproduced the synthesis of compounds **68** and **69** under the same conditions, however, all the attempts gave only the mixtures of compounds **68** and **69** or heterocycles **69** were isolated in the lower yields than in the previous work (Tu et al., 2009). Therefore, Morozova et al. (2017) studied in details the reactions of 5-amino-3-methylisoxazole (**60a**) and aromatic aldehydes **1** with Meldrum's acid (**45**) and developed the preparative methodologies for selective synthesis of the products **68** (boiling in DMF or *n*-BuOH) and **69** (ultrasonication in EtOH).

The detailed study of the reactions of 5-aminopyrazoles (**3a**, **4**, **21**, and **70**) with aromatic aldehydes **1** and barbituric acids **71** (a: X = O, b: X = S) showed that varying temperature and type of R^3-substituent in 5-aminopyrazole were the main factors of switching the direction to produce different final compounds (Muravyova et al., 2009). Thus, in case of pyrazoles **3a** and **4** (R^3 = H) boiling the reagents in DMF led to dihydropyrazolopyridopyrimidines **72** (Muravyova et al., 2009) whereas pyrazoles **70** and **21** bearing methyl or aryl R^3-substituents (both of electron donor and acceptor origin) afforded heteroaromatized derivatives **75** (Muravyova et al., 2009). It's interesting to note that Satasia et al. (2014) got

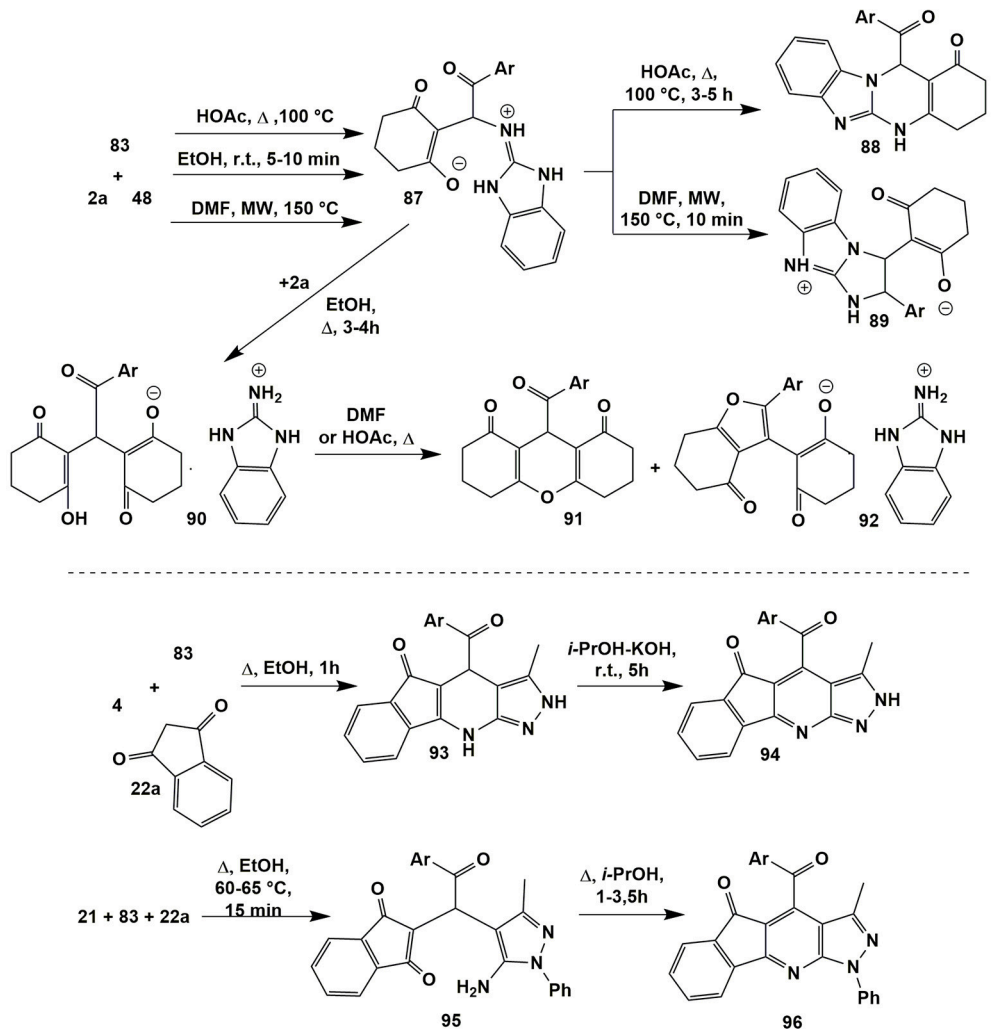

FIGURE 7 | Condensations of α-aminoazoles involving arylglyoxales and cyclic CH-acids.

dihydropyrazolopyridopyrimidines **73** in case of all the pyrazoles (R^3 = H, Ph) under refluxing the starting materials in ethanol with adding cellulose supported ionic liquid (Cell-IL) (**Figure 5**).

Similar to heterocycles **75** other heteroaromatic compounds were synthesized earlier by the group of Shi (Shi et al., 2008) in the reaction of 5-amino-3-methyl-1-phenylpyrazole (**21**), aromatic aldehydes **1** and barbituric acids **71a** (R^1 = H, CH_3; H_2O-*p*-TSA, MW, 140°C) whereas the condensation involving thiobarbituric acids **71b** (R^1 = H; neat-*p*-TSA, MW, 100°C) afforded corresponding dihydropyrazolopyridopyrimidines of type **73** (El-Emary and El-Mohsen, 2012). Later on dihydropyridopyrimidines **74** were synthesized starting from 3-amino-1,2,4-triazole (**5a**) (Karami et al., 2015a) and 2-aminobenzimidazole (Kaur G. et al., 2015).

Ultrasonication at room temperature of compounds **1** and **71** with 5-aminopyrazoles **3a**, **4** or **21** afforded new spiroheterocyclic systems **76** (Muravyova et al., 2009) that had not been formed in the previously described reactions with 1,3-diketones. Analogous reactions involving 5-amino-3-methylisoxazole were studied in several works. After wide screening the reaction conditions similar to compounds **76** spiroheterocycles were the only product obtained in the condensation of 5-amino-3-methylisoxazole (**60a**) with aromatic aldehydes **1** and barbituric acids **71** under MW irradiation in water (9–13 min; Jiang et al., 2012) or by ultrasonication in ethanol (r.t., 2 h; Morozova et al., 2017).

Replacing 5-amino-3-methylisoxazole (**60a**) with isomeric 3-amino-5-methylisoxazole did not contribute to the formation of new heterocyclic fragments: it didn't react with aldehydes and barbituric acids or Meldrum's acid (arylidene derivatives were yielded); heating 3-amino-5-methylisoxazole with aldehydes and Meldrum's acid in DMF or ethanol afforded only its acylated derivative (Morozova et al., 2017). Such a reactivity of 3-amino-5-methylisoxazole is consistent with other literature data, which describes its chemical behavior in the synthesis of pyrrolones (Ryabukhin et al., 2012), in the Hantzch (Rajanarendar et al., 2011b) and Betti (Shafiee et al., 2012) reactions as well as

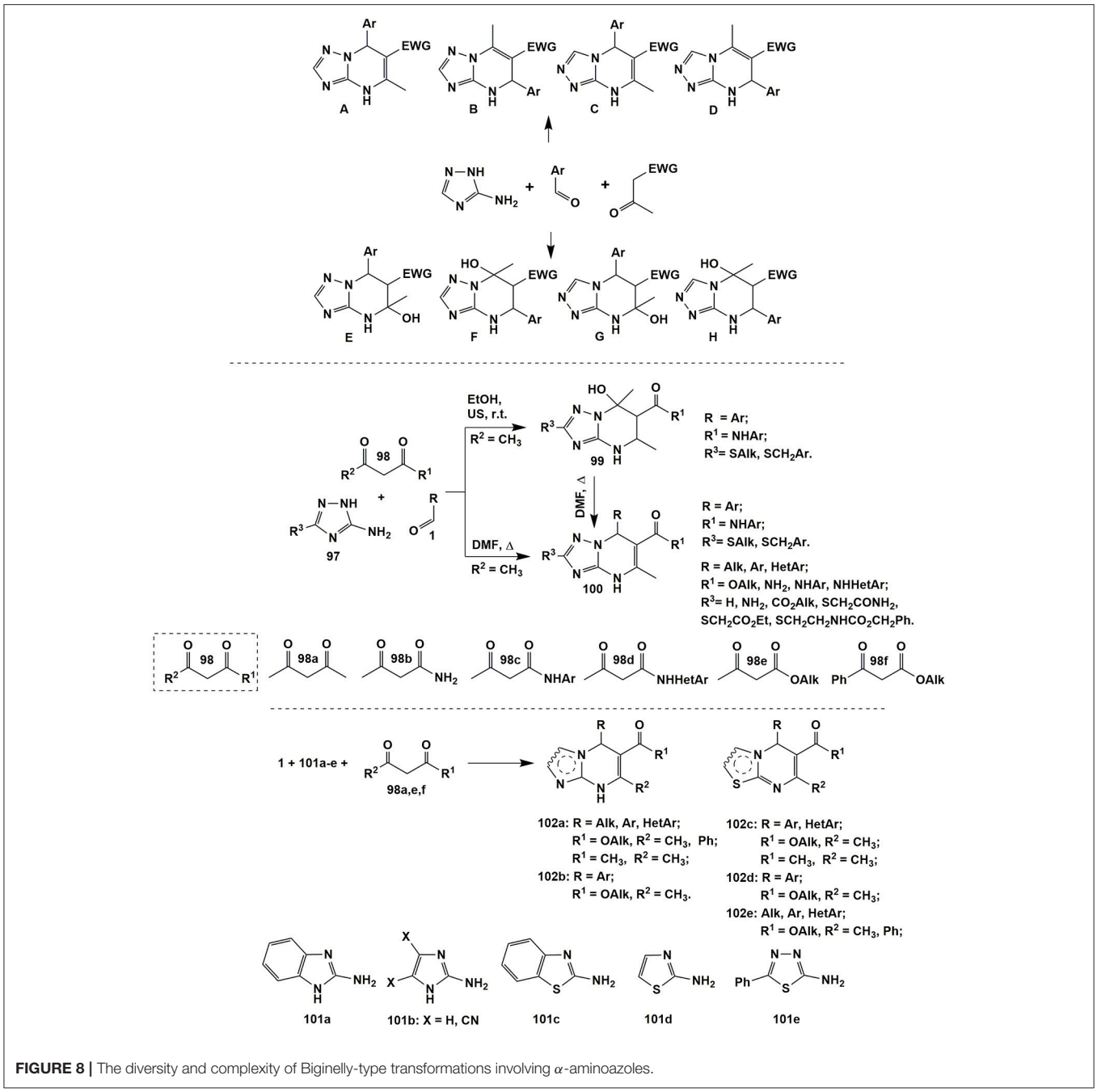

FIGURE 8 | The diversity and complexity of Biginelly-type transformations involving α-aminoazoles.

in four-component condensation with formation of imidazole moiety (Rajanarendar et al., 2011a).

When glyoxales and arylglyoxales were used instead of aldehydes in multicomponent reactions, some additional reaction pathways could be implemented. Thus, Petrova et al. (2013b) studied the condensations of wide spectrum of aminoazoles (**3a**, **3b**, **4**, **5a**, **5b**, **46**, **77a**, and **77b**) with glyoxales **78** and 1,3-diketones **2a,b** or **79** upon refluxing in ethanol (for 30–40 min in case of 5-aminopyrazoles; 2.5–3 h in case of 1,2,4-triazoles and for 10 h in case of 5-aminotetrazole) and obtained the novel heterocyclic system–indolo[1,2-*c*]polycyclic compounds **80** (**Figure 6**) instead of the expected 4,5,6,7,8,9-hexahydro-8-oxoazolo[5,1-*b*]quinazoline-9-carbaldehyde derivatives (similar to compounds **7** or **10**, see **Figure 2**).

In case of 2-aminobenzimidazole **48** its condensation with glyoxal **78** and 1,3-diketones **2a,b** under the same conditions led to the formation of benzo[*d*]imidazo[1,2-*a*]benzimidazoles **81** containing only one cyclohexanedione fragment in their structure (**Figure 6**; Petrova et al., 2013b).

When arylglyoxals **83** had been introduced into condensation with 5-aminopyrazoles **82** having arylcarboxamide group in the fourth position, angular pyrazoloquinazolinones **84** (similar to

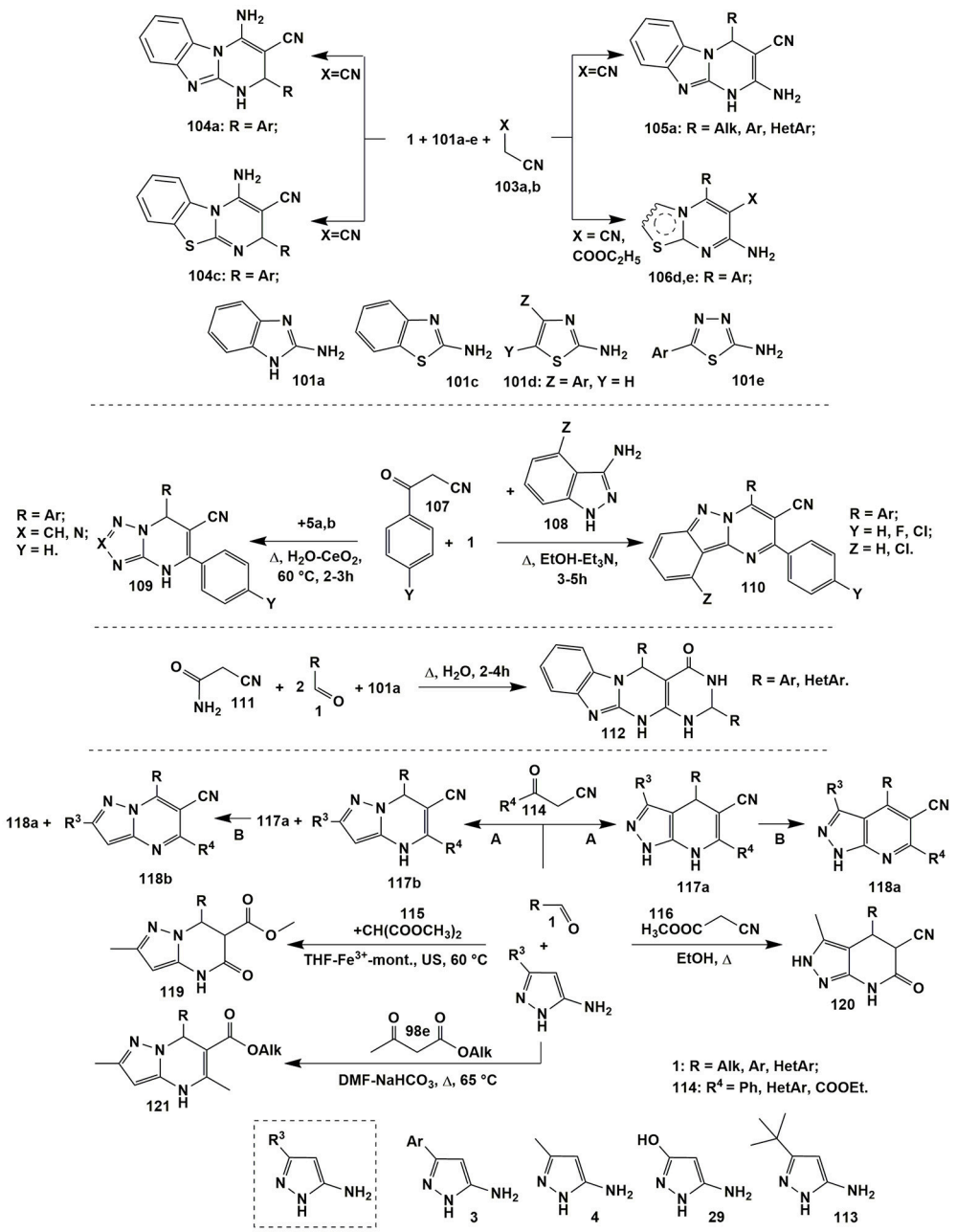

FIGURE 9 | Examples of cyclizations involving α-aminoazoles, aldehydes and non-cyclic carbonyl compounds.

compounds **43**, **Figure 4**) were formed under refluxing in EtOH (**Figure 6**; Petrova et al., 2013a). Other 1- and 3-substituted 5-aminopyrazoles **21** and **70** (R^4 = H) in the condensation with compounds **2a,b** and **83** under the same conditions gave expected pyrazoloquinolinenones **85**. Applying microwave irradiation in DMSO-Et_2NH (120°C, 20 min) to the mixture of diketones **2a,b**, pyrazoles **21** or **70** and two equivalents of arylglyoxals **83** afforded an elegant four-component domino reaction leading to polycyclic compounds **86** (Wang et al., 2015b; **Figure 6**).

A multicomponent reaction involving 2-aminobenzimidazole (**48**), cyclohexanedione (**2a**) and arylglyoxales **83** was thoroughly studied by Petrova et al. (2015b); all the compounds including intermediates were isolated in individual form, characterized and their structures were proven with the help of X-Ray analysis (**Figure 7**).

It was established that the reaction of the reagents **2a**, **48**, and **83** in ethanol at room temperature for 5–10 min yielded Michael adduct **87** that remained stable upon latter refluxing in primary alcohols. However, after adding the second equivalent of cyclohexanedione (**2a**) and further prolonged refluxing the reaction mixture in ethanol salts **90** were isolated. All the attempts to convert them into the products of condensation with

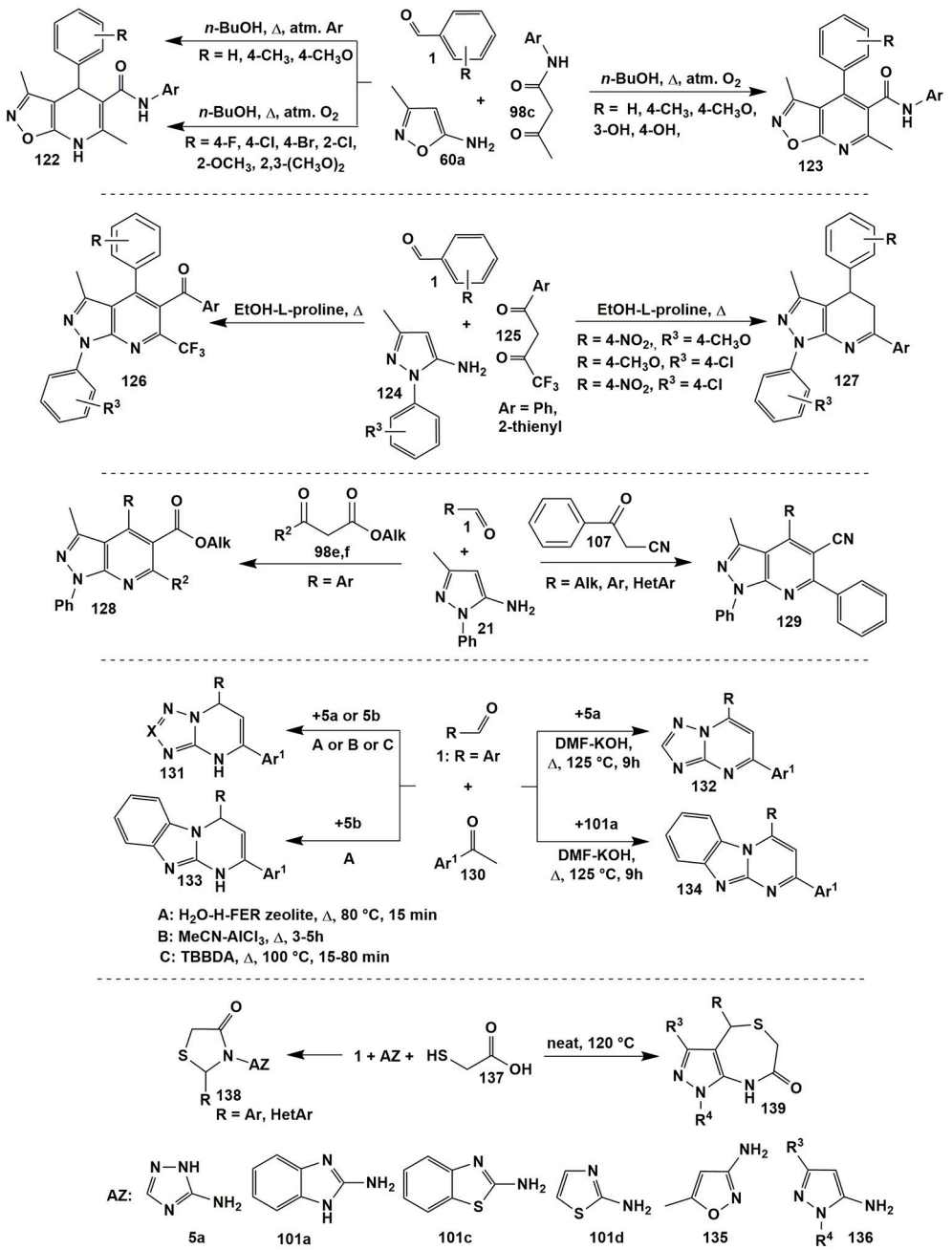

FIGURE 10 | MCRs involving α-aminoazoles, aldehydes and non-cyclic carbonyl compounds.

2-aminobenzimidazole (**48**) upon refluxing in DMF or acetic acid or fusion under neat conditions were unsuccessful. In all cases the mixtures of xanthenediones **91** and salts **92** were obtained.

The authors (Petrova et al., 2015b) established that Michael adduct **87** had been also formed after heating the starting reagents in acetic acid at 100°C; after longer heating, they turned into condensed quinazolinones **88**. Microwave irradiation of the starting reagents **2a**, **48**, and **83** in DMF (150°C) afforded to get heterocycles **89** as the main products (**Figure 7**).

Linear pyrazolopyridinones **93** (Petrova et al., 2015a) were synthesized by the condensation involving 5-amino-3-methyl-pyrazole (**4**) and arylglyoxales **83** with indane-1,3-dione (**22a**) upon short-term heating in ethanol. Further prolonged treatment of compounds **93** at room temperature in isopropanol with the addition of KOH led to their transformation into heteroaromatic derivatives **94**. When the authors (Petrova et al., 2015a) applied 5-aminopyrazole **21** containing an aryl substituent in the first position, in the

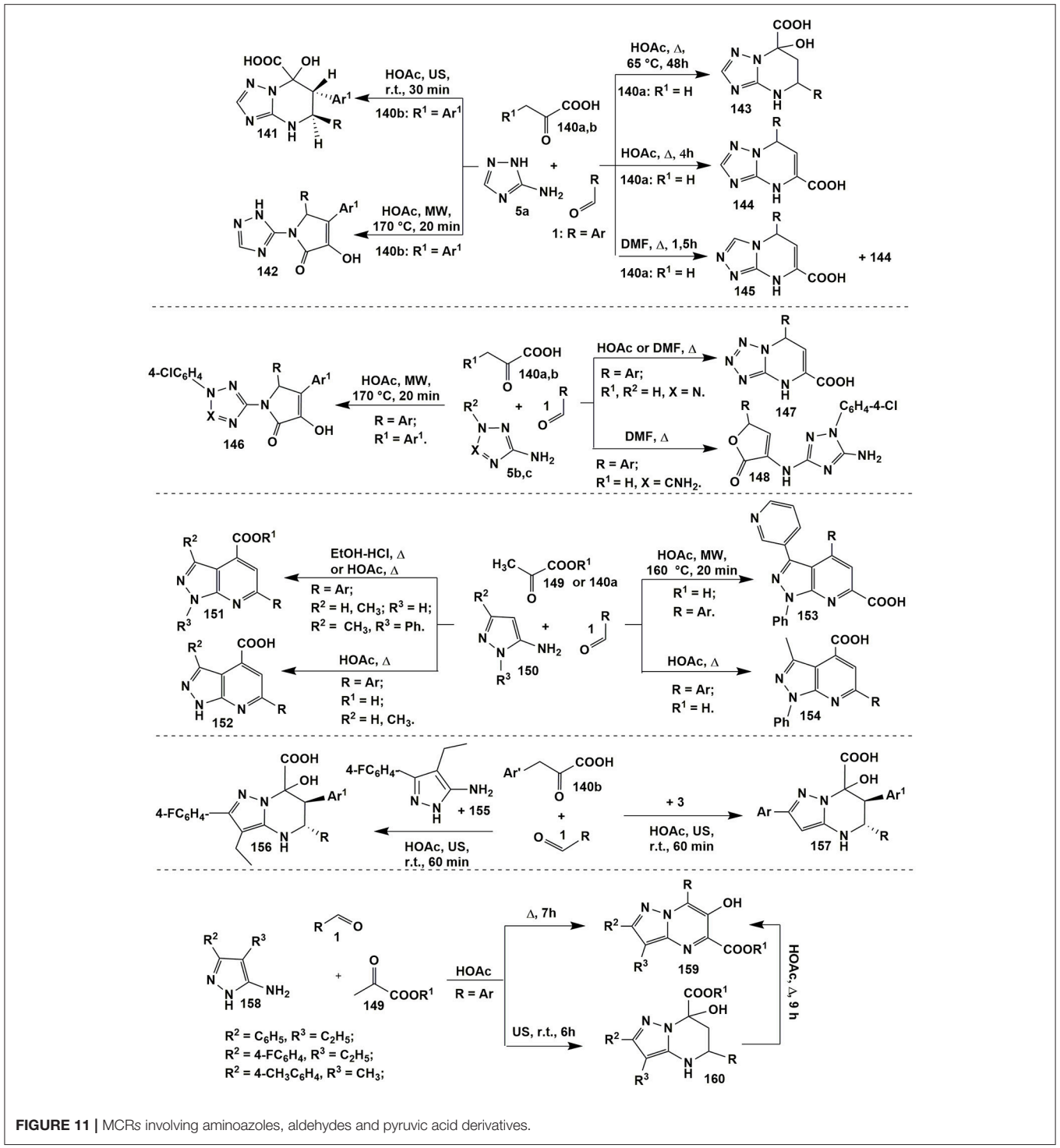

FIGURE 11 | MCRs involving aminoazoles, aldehydes and pyruvic acid derivatives.

reaction with compounds **83** and **22a** in ethanol (60–65°C, 15 min) the Michael adduct **95** was initially isolated. Further prolonged boiling the compound **95** in isopropanol led directly to heteroaromatic derivatives **96** whereas dihydroindeno[1,2-*b*]pyrazolo[4,3-*e*]pyridinones of type **93** failed to be found (**Figure 7**).

Multicomponent Reactions of Aminoazoles Involving Non-cyclic CH-Acids

Multicomponent reactions of aminoazoles and carbonyl compounds often involve such CH-acids as enolizable ketones, 1,3-dicarbonyl compounds (acetoacetic acid and its derivatives, 1,3-diketones, ketosulfones), 1,2-dicarbonyl

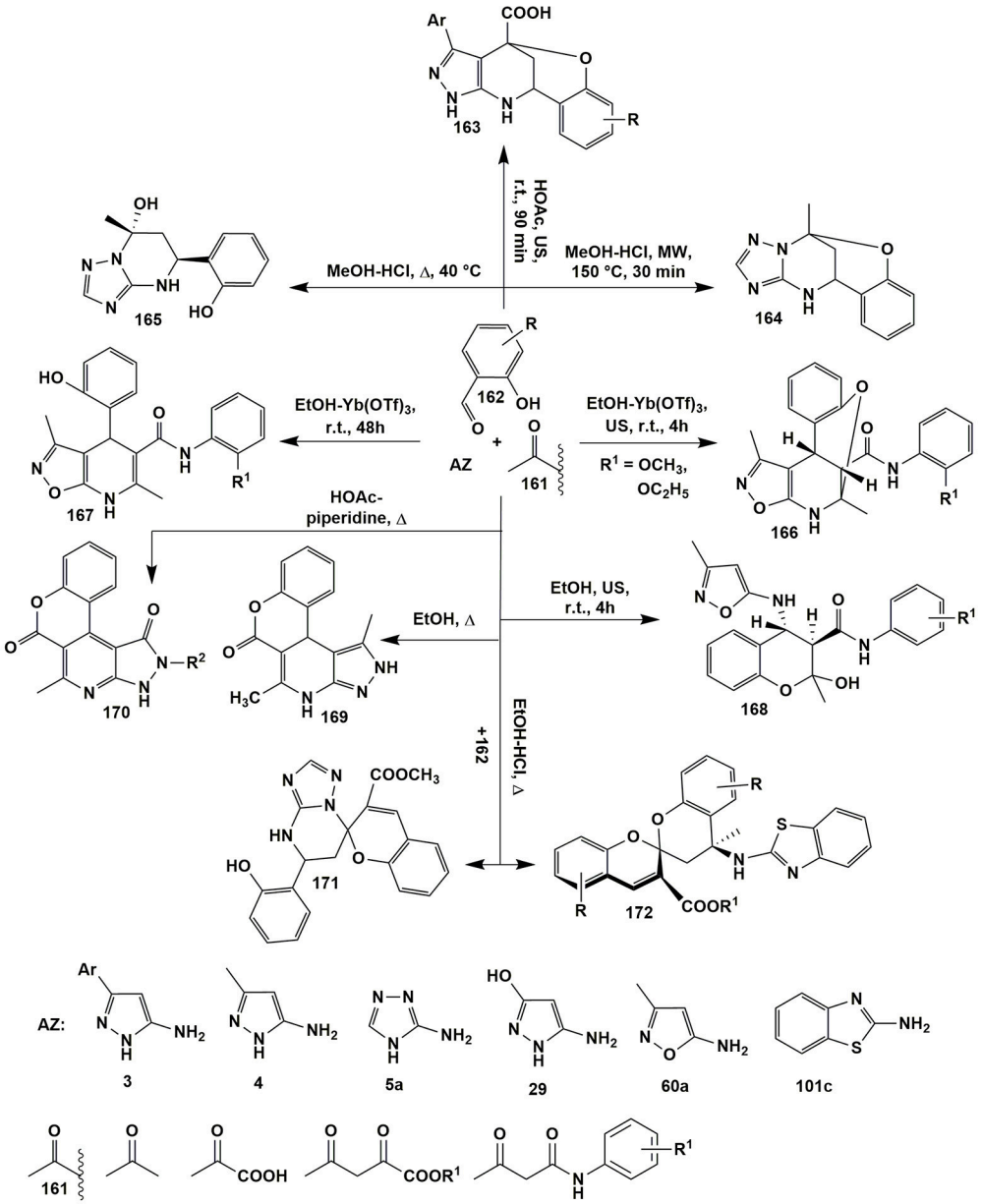

FIGURE 12 | Some post-cyclizations serving as an additional source of molecular diversity in MCRs involving salicylic aldehydes, aminoazoles and active methylene compounds.

compounds (pyruvic acid and its derivatives), malonic acid and its derivatives, cyanoacetamide etc.

Recently published review by Sedash et al. (2012) clearly illustrates the diversity and complexity of MCRs of aminoazoles, carbonyl compounds and non-cyclic CH-acids on the example of the Biginelly-type transformations involving 3-amino-1,2,4-triazoles as 1,3-binucleophiles. It was shown that the stepwise character of the MCRs themselves and polyfunctional character of that 1,3-binucleophile could lead to at least eight possible products **A–H** from one set of the starting reagents usually depending on the reaction conditions (and sometimes specific structure of the starting reagents themselves). The pairs **A-B**, **C-D**, **E-F**, and **G-F** could be considered as positional isomers whereas the pairs **A-C**, **B-D**, **E-G**, and **F-H**–as regioisomers. As a consequence of such diversity of the possible reaction products their structural elucidation often becomes problematic (**Figure 8**).

The authors (Sedash et al., 2012) explored the literature dealing with this type of reactions and concluded that the existing data about the structure of the reaction products **A–H** was not always comprehensive and found that most of the literature sources concerning Biginelli-like MCRs involving 3-amino-1,2,4-triazoles had described structure **A** as the most usual product under quite harsh conditions and different

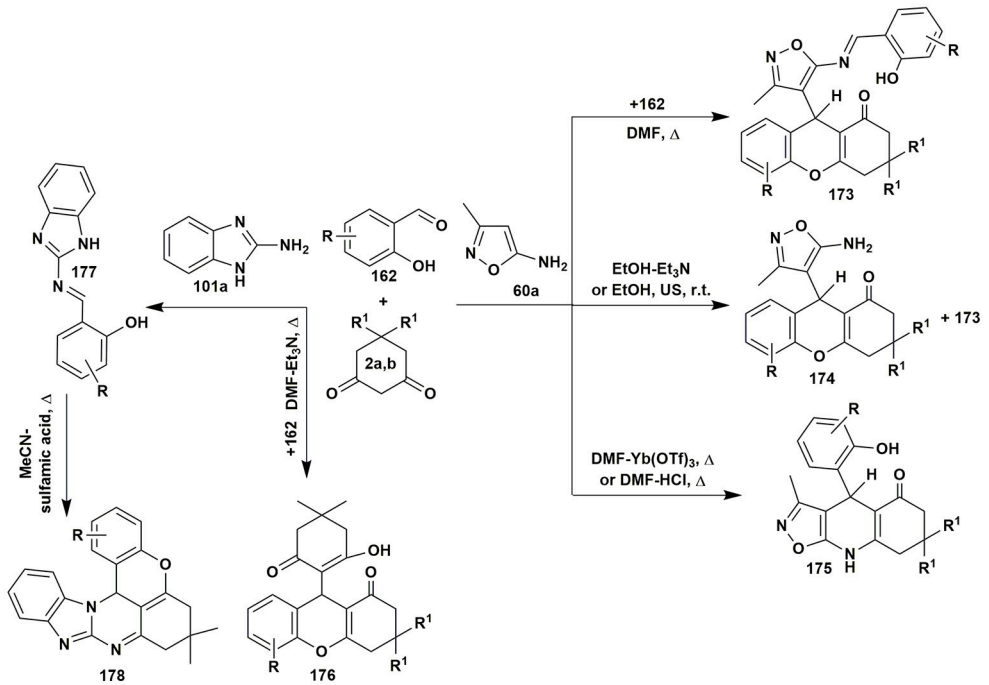

FIGURE 13 | Condition-based divergence strategy in MCRs of aminoazoles with salicylic aldehydes and cyclic active methylene compounds.

reagents (acetophenone, ethyl and methyl esters of acetoacetic acid and its fluorinated derivatives, substituted amides of acetoacetic acids, pyruvic acid, 1-(methylsulfonyl)propan-2-one and 2-(methylsulfonyl)-1-phenylethanone, aliphatic ketones). The structure **C** was sometimes reported as a side product accompanying the formation of the main product **A** (in the reactions with pyruvic acid or methyl acetoacetate). Only the condensation involving acetylpyrazole derivative afforded compound of structure **C** as the only product (Ali et al., 2016). Tetrahydroderivatives of type **F** were described in the reactions under mild conditions (with phenylpyruvic acid or ethyl acetoacetate). Products of **E**-type could be obtained on the basis of fluorinated esters of acetoacetic acid and further converted into **A**-type heterocycles thus being the products of kinetically and thermodynamically controlled reactions. The products of structure **B** could be formed when two molecules of acetophenone (or cyclohexanone, see compound **14**, **Figure 2**) reacted with 3-amino-1,2,4-triazole derivatives. The products **D** were not obtained by Biginelli-like MCRs, they could be synthesized using other approaches whereas products of structure **G** and **H** were not described at all (**Figure 8**; Sedash et al., 2012).

The conclusions of Sedash et al. about preferential formation of compounds with the structure of type **A** in the multicomponent reactions involving 3-amino-1,2,4-triazole were confirmed by the subsequent publications of other authors: 4,7-dihydroazolo[1,5-*a*]pyrimidines were synthesized from 3-amino-1,2,4-triazole or 5-aminotetrazole, aromatic aldehydes and acetone, α-acetyl-butyrolactone, acetylacetone or acetoacetic acid derivatives (Ryabukhin et al., 2011; Gein et al., 2012, 2014; Kumari et al., 2012; Li et al., 2012; Liu et al., 2012b; Rajua et al., 2012; Ghorbani-Vaghei et al., 2013; El Rady, 2014; Haleel et al., 2014; Bhatt et al., 2015; Adrom et al., 2016; Komykhov et al., 2016, 2017; Gümüş et al., 2017b; Kour et al., 2017; Maleki et al., 2017).

An example illustrating the dependence of the reaction direction on the conditions is given in work of Muravyova et al. (2011) Varying temperature and using ultrasonic activation allowed to switch MCR involving acetoacetamides **98b** (R^1 = NHAr, R^2 = CH_3), aromatic aldehydes **1** and substituted 3-amino-1,2,4-triazole **97** (R^3 = SAlk, SCH_2Ar) between kinetically- and thermodynamically-controlled directions and selectively obtain tetrahydro- or dihydroderivatives **99** or **100**, correspondingly. Later on Wang et al. (2015a) expanded the list of dihydropyrimidines **100** by using other substituted triazoles **97** (R^3 = H, NH_2, CO_2Alk, SCH_2CONH_2, $SCH_2CO_2C_2H_5$, $SCH_2CH_2NHCO_2CH_2Ph$) and acetoacetic acid derivatives **98** (R^1 = OAlk, NH_2, NHAr, NHHetAr, R^2 = CH_3; **Figure 8**).

It is worth noting that the analogous behavior of 5-aminopyrazoles substituted in the fourth position with electron-withdrawing groups [CN, CO_2CH_3, $CONH_2$ (Muravyova et al., 2011)] in the condensations being similar to the described above and leading to tetrahydro- and dihydropyrimidines of types **99** and **100** as well.

Dihydropyrimidine systems **102a–e** (**Figure 8**) were also formed in condensation of acetoacetic acid and its derivatives (or acetylacetone) **98** with 2-aminobenzimidazole (**101a**) [under

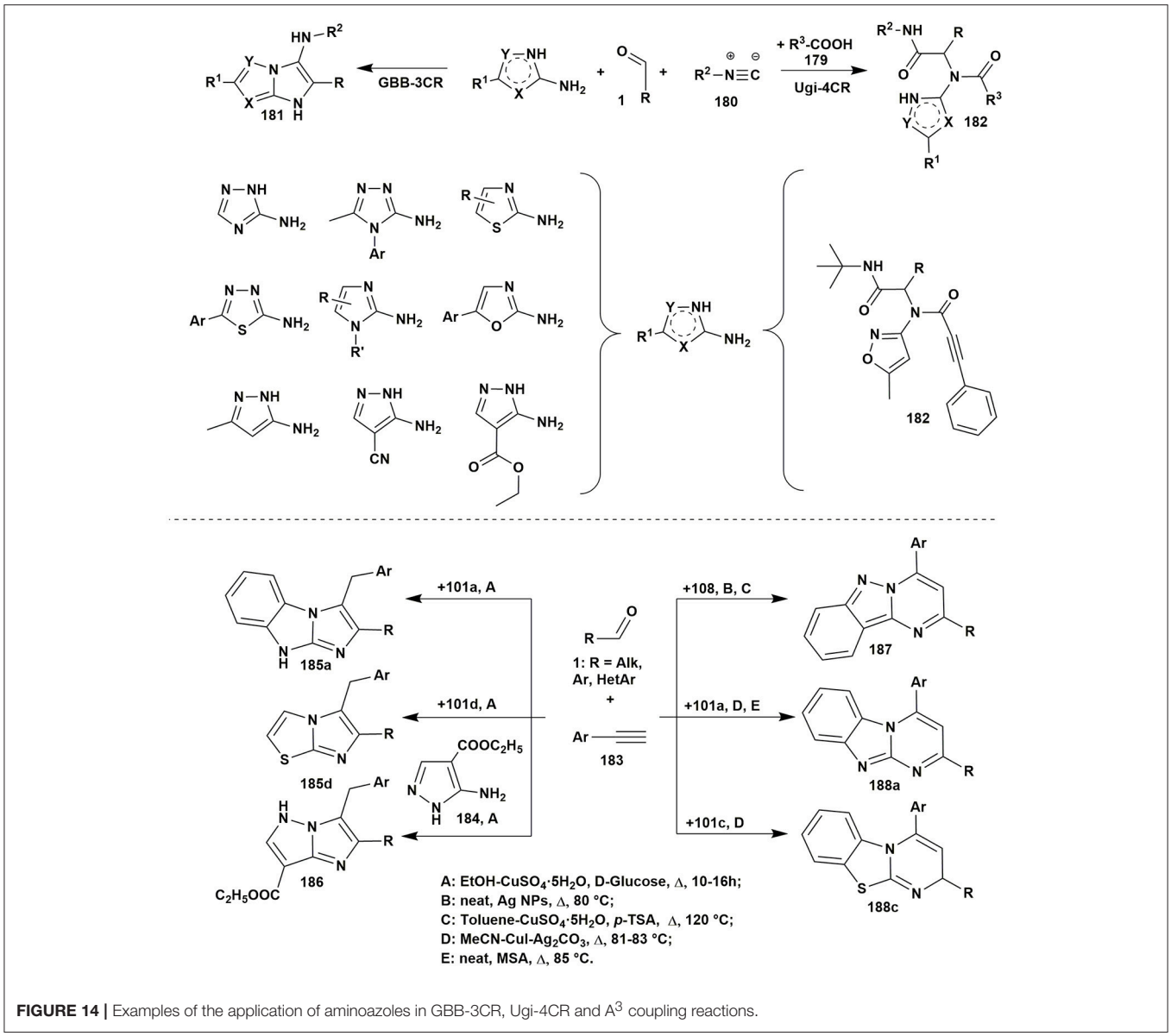

FIGURE 14 | Examples of the application of aminoazoles in GBB-3CR, Ugi-4CR and A^3 coupling reactions.

neat conditions-ionic liquid catalyzed, US, 50°C (Reddy et al., 2016) etc. (Ryabukhin et al., 2011; Shaterian et al., 2014; Kaur N. et al., 2015; Abedini et al., 2016; Dam et al., 2016)], 2-aminoimidazoles **101b** [DMF-$(CH_3)_3SiCl$, US, r.t. (Ryabukhin et al., 2011)], 2-aminobenzothiazole (**101c**) (MeOH-HCl, Δ (Chikhale et al., 2015) etc. (Zhao et al., 2013; Atar et al., 2014; Shaterian et al., 2014; Moradi et al., 2015), 2-aminothiazole **101d** [HOAc, MW, 80°C (Zhao et al., 2013) etc. (Batool et al., 2016; Dam et al., 2016; Tan et al., 2016)] and 2-amino-1,3,4-thiadiazole **101e** (HOAc, MW, 65°C; Zhao et al., 2014).

It should be noted, that Thorat et al. (2013) obtained imidazopyrimidines (EtOH-ionic liquid catalyzed, r.t.) with another positional orientation of substituents than in compounds **102b**. However, there was not enough data (2D NMR experiments or X-Ray analysis) proving that structure while the structure of azolopyrimidines **102** was proven with the help of X-Ray analysis in cases of heterocycles **102d** (Zhao et al., 2013) and **102e** (Zhao et al., 2014).

Formation of pyrimidines **105a** and **106d,e** was also observed in the reactions with the CH-acids **103**: malononitrile (**103a**) (X = CN) or ethyl 2-cyanoacetate (**103b**) (X = $COOC_2H_5$). The condensation of aldehydes **1**, malononitrile (**103a**) and 2-aminobenzimidazole (**101a**) under the variety of conditions [neat, poly(vinylpyrrolidonium) perchlorate catalyzed, 100°C (Abedini et al., 2016); neat-*p*-TSA(10%), 80°C (Reddy et al., 2014b); EtOH-Fe_3O_4@IM, Δ (Hemmati et al., 2016); PEG-H_2O (4:1), Δ (Survase et al., 2017)] afforded dihydrobenzo[4,5]imidazo[1,2-*a*]pyrimidines **105a**. When 2-aminothiazoles **101d** and 2-amino-1,3,4-thiadiazoles **101e** reacted with aldehydes **1** and malononitrile (**103a**) or ethyl 2-cyanoacetate (**103b**), [EtOH-H_2O, MW, 100°C (Sahi and Paul, 2016)] pyrimidines **106d,e** were isolated (**Figure 9**).

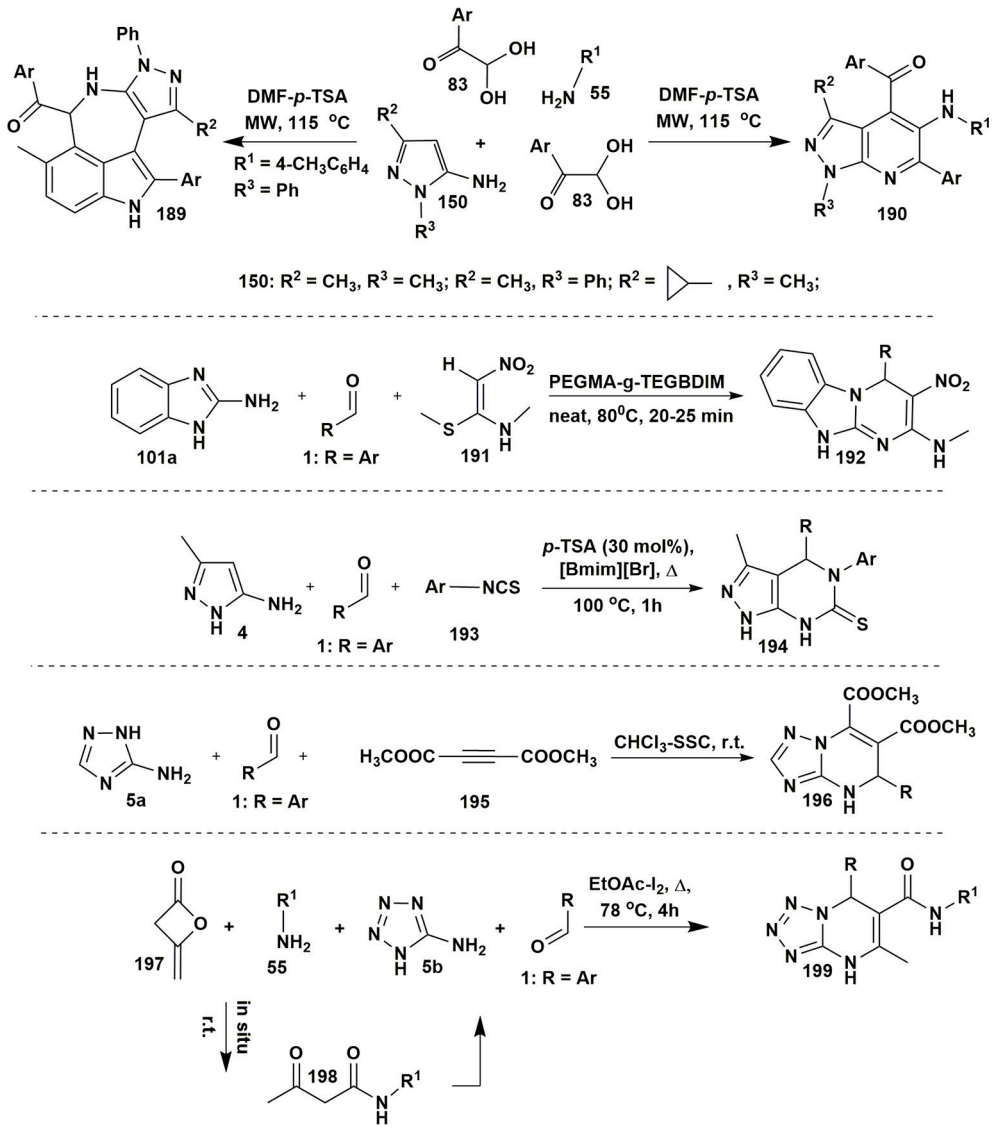

FIGURE 15 | Examples of other MCRs involving aminoazoles.

On the other hand, a lot of earlier publications stated that the MCR of malononitrile (**103a**) or ethyl 2-cyanoacetate (**103b**) and aromatic aldehydes **1** with 2-aminobenzimidazole (**101a**) or 2-aminobenzothiazole (**101c**) afforded the products **104a** (EtOH-alum, 70°C (Karimi and Bayat, 2011); H_2O, Δ (Risley et al., 2014); neat with alkyl disulfamic acid functionalized magnetic nanoparticles, 90°C (Bodaghifard et al., 2016) and **104c** [MeCN-MgO, Δ (Sheibani and Babaie, 2013)] with the other positional orientation than in heterocycles **105a** and **106d,e**. Since a lot of authors provided no sufficient experiment to prove the stated structures the data described above was contradictory. For example, some publications operate with 2D NMR studies: Hemmati et al. (2016) observed NOE between the signals of pyrimidine CH and aromatic benzimidazole protons and indicated on the structure **105a**, whereas Karimi and Bayat (2011) didn't observe such NOE correlation and suggested the formation of isomeric structure **104a**. Some authors on the basis of references for similar compounds having the results of the X-Ray analysis indicated on the formation of isomer **104a** as well.

Similar to compounds **106** heteroaromatized pyrazolopyridines were obtained in the condensations of malononitrile (**103a**) and arylglyoxals **83** both with 5-amino-3-methyl(aryl)-1-phenylpyrazole and *N*-unsubstituted 5-amino-3-methylpyrazole (Petrova et al., 2016).

A facile and efficient cascade reaction of 3-oxo-3-arylpropanenitrile **107** and aromatic aldehydes **1** with substituted 1*H*-indazol-3-amines **108** upon refluxing in EtOH-Et_3N medium (3–5 h) under metal-free conditions afforded pyrimido[1,2-*b*]indazole-3-carbonitrile derivatives **110** (Li et al., 2017) while their dihydro analogs **109** (Suresh et al., 2016) were synthesized

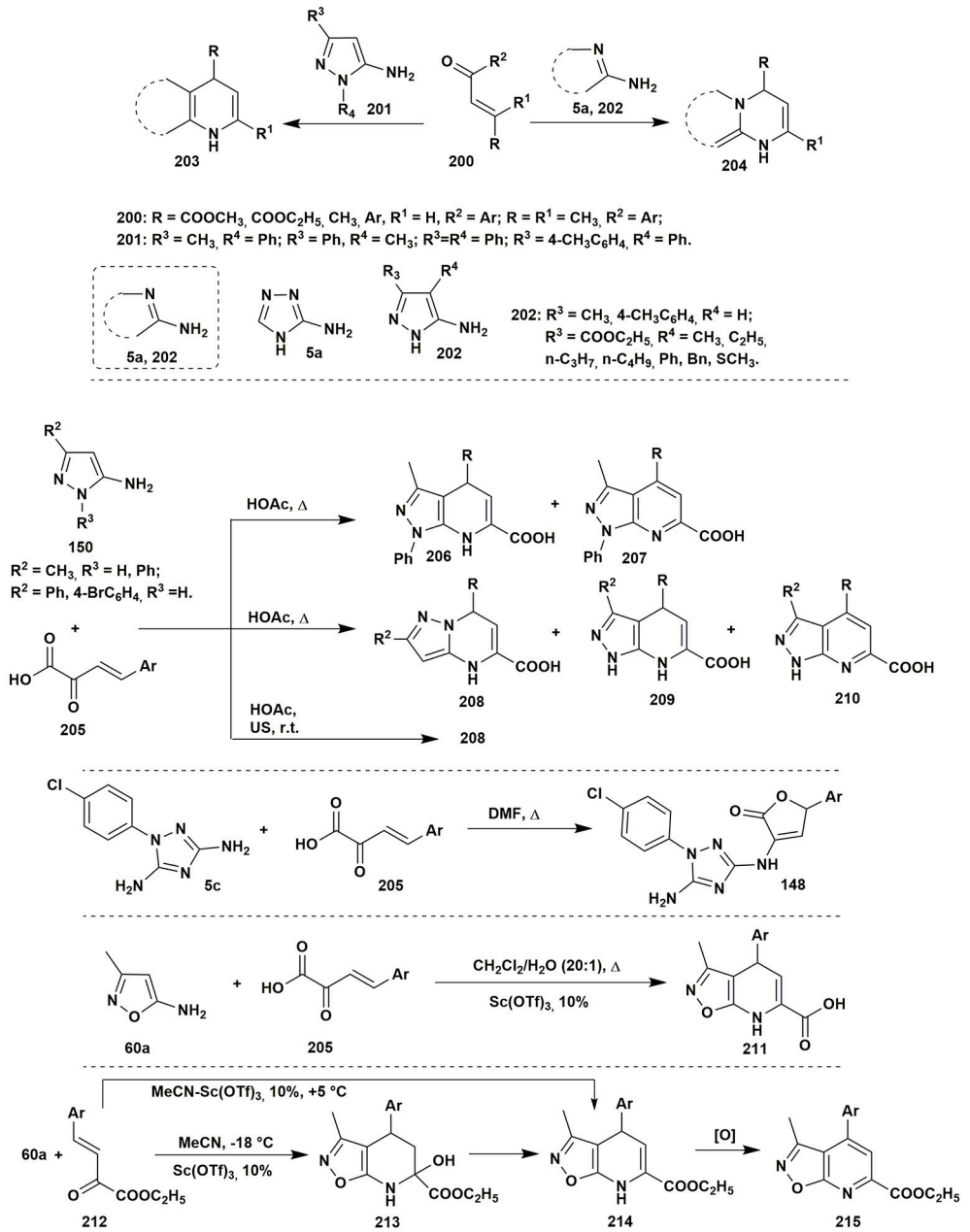

FIGURE 16 | Examples of two-component heterocyclizations of the aminoazoles with α,β-unsaturated carbonyl compounds.

in the condensation of the starting reagents **1** and **107** with 3-amino-1,2,4-triazole (**5a**) (X = CH) or 5-aminotetrazole (**5b**) (X = N) under heating in water with adding of nano CeO_2 catalyst (60°C, 2–3 h). Tetracyclic derivatives **112** were formed in the reaction involving 2-cyanoacetamide (**111**) with 2-aminobenzimidazole (**101a**) and aldehydes **1** followed by the further cyclization with the second equivalent of aldehyde **1** by heating in water for 2–4 h (Liu et al., 2012a) or at room temperature in polyethylene glycol for 1 h (**Figure 9**; Reddy et al., 2014a).

The introduction of 1- and 4-unsubstituted 5-aminopyrazoles (**3**, **4**, **29** or **113**) to the reactions with aldehydes and CH-acids enables the formation of the regioisomers. Thus, 4,7-dihydropyrazolopyridines **117a** were the products of condensation of 5-aminopyrazoles **3, 4** or **29** and aldehydes **1** with substituted 3-oxopropanenitriles **114** (A: DMF-Et_3N, Δ). The volatile substances were removed from the reaction mixture and the residue was oxidized with sodium nitrite in acetic acid (B), which resulted in isolation of pyrazolopyridines **118a** (Hill, 2016). Regioisomeric pyrazolopyrimidines **117b**

were formed under the same conditions when 5-aminopyrazoles contained a sufficiently large substituent R^3 at position 3 (for example, *tert*-butyl in compound **113**) which complicated the electrophilic aromatic substitution with the participation of the C4 nucleophilic center in the aminopyrazole **113** and led to cyclization into compounds **117b**. The authors (Hill, 2016) also discovered the steric influence of an aldehyde component **1** on the ratio of products **118a** and **118b** in the mixture (**Figure 9**). Analogous to heterocycles **117a** dihydropyrazolopyridines were isolated as a result of heating the compounds **1**, **4** and **114** in ethanol with adding Fe(III)-montmorillonite (Mamaghani et al., 2013).

When methyl cyanoacetate **116** was introduced into the reaction with compounds **1** and **4** under refluxing in ethanol (Mahdavinia and Rahmati, 2015) or ethanol with *p*-TSA (Rahmati, 2010) 6-oxo-4,5,6,7-tetrahydro-2*H*-pyrazolo[3,4-*b*]pyridines **120** were obtained. Isomeric pyrazolopyrimidinones **119** (Hossein Nia et al., 2014) were isolated in the condensation involving dimethyl malonate **115** under ultrasonication in THF with adding of Fe^{3+}-montmorillonite (**Figure 9**). Cyclizations involving acetoacetic acid derivative **98e** proceeded involving endocyclic amino group of 5-aminopyrazole **4** with the formation of dihydropyrimidines **121** (Finlay et al., 2012, 2013).

Steric and electronic effects of a substituent R in aldehyde **1** significantly influenced the ability to oxidation of dihydropyrimidine cycle in the condensations involving 5-amino-3-methylisoxazole (**60a**) and aromatic aldehydes **1** with *N*-arylacetoacetamides **98c**. Thus, under identical conditions (*n*-BuOH, Δ, oxygen of air) dihydropyridines **122** were isolated only in case of *para*-halogeno- and *ortho*-substituted aldehydes **1**. The authors (Tkachenko et al., 2014b) associate this with the electronic influence of the halogenaryl moiety or the steric effect of *ortho*-substituents, which complicates the oxidation of heterocycles **122** to **123**. In case of other aldehydes such conditions led to the formation of heteroaromatized systems **123**. Only carrying out the reaction in the argon atmosphere afforded isolation of dihydropyridines **122** (except hydroxy-substituted ones). However, blowing oxygen through their ethanol solutions led to the transformation of compounds **122** to **123** (**Figure 10**).

The influence of substituents on the direction of a reaction involving asymmetric 1,3-diketones **125**, aromatic aldehydes **1** and 5-amino-1-aryl-3-methylpyrazoles **124** was also significant. The regioselectivity of the formation of aromatic pyrazolopyridines **126** was caused by a greater electrophilicity of $COCF_3$ than COAr-carbonyl group. However, for some combinations of substituents in 5-aminopyrazole **124** and aldehyde **1** dihydropyrazolopyridines **127** without trifluoroacetyl moiety were formed (**Figure 10**; Gunasekaran et al., 2013).

When 5-amino-3-methyl-1-phenylpyrazole (**21**) reacted with aldehydes **1** and other CH-acids (acetoacetic acid derivatives), e.g., **98e,f** (Fan et al., 2016), 3-oxo-3-phenylpropanenitrile **107** (Huang et al., 2011; Rahmati and Khalesi, 2012) heteroaromatic pyrazolopyridines **128** (similar to compounds **126**) and **129** (similar to compounds **118a**, **Figure 8**) were formed (**Figure 10**).

When acetophenones **130** were used as CH-acids in condensations with aldehydes **1** and different aminoazoles [3-amino-1,2,4-triazole (**5a**), 5-aminotetrazole (**5b**), 2-aminobenzimidazole (**101a**), 5-aminopyrazole and 3-aminoindazole] two types of products were formed–azolopyrimidines of types **132** (Palaniraja et al., 2016a) and **134** (Palaniraja et al., 2016a) or their dihydroanalogues **131** (Ghorbani-Vaghei et al., 2013; Hassaneen and Farghaly, 2015; Kour et al., 2017) and **133** (Hassaneen and Farghaly, 2015; **Figure 10**).

Conditions for the obtaining thiazolidin-4-ones **138** from aldehydes **1**, different aminoazoles and thioglycolic acid (**137**) were dependent on the origin of aminoazole. Thus, for 3-amino-1,2,4-triazole **5a** (Ebrahimi, 2016) the cyclization was performed under solvent-free conditions with addition of ammonium persulfate as a catalyst (Δ, 90°C, 1 h); for 2-aminobenzimidazole (**101a**) (Kumar et al., 2013) and 2-aminobenzothiazole (**101c**) (Kumar et al., 2013)–in toluene with addition of $HClO_4$-SiO_2 catalyst (Δ, 100°C, 3–6 h); for 2-aminothiazole (**101d**) (Wu et al., 2014)–in toluene (Δ, 140°C) and for 3-amino-5-methylisoxazole (**135**) (Murugesan et al., 2014)–in toluene (Δ, 140°C, ∼24 h). Application of 1- and 3-substituted 5-aminopyrazoles **136** (Abonia, 2014) with the reagents **1** and **137** under solvent-free conditions and self-catalysis with thioglycolic acid (**137**) afforded cyclic pyrazolo[3,4-*e*][1,4]thiazepin-7(4*H*)-ones **139** to be isolated (**Figure 10**).

A special attention should be also paid to the multicomponent reactions of aminoazoles and aromatic aldehydes with pyruvic acid and its derivatives, especially because of the ambiguity in the realization of directions of such processes. Chebanov's group (Chebanov et al., 2005, 2007a, 2012a; Sakhno et al., 2008, 2010, 2011, 2015) contributed a lot to studying both stepwise and MCR reactions involving pyruvic acid and aminoazoles and showed that their chemo- and regioselectivity, positional orientation of the substituents in the final products significantly depend on the reaction parameters and structure of the starting reagents.

Thus, in the heterocyclizations involving 3-amino-1,2,4-triazole (**5a**) and aromatic aldehydes **1** with pyruvic acid (**140a**) (R^1 = H) dihydrotriazolopyrimidines **144** (Chebanov et al., 2005) with the same positional orientation as for acetoacetic acid reaction (heterocycle **100**, **Figure 8**) were formed (HOAc, Δ, 4 h). When compounds **1**, **5a**, and **140a** were refluxed in DMF dihydrotriazolopyrimidine **144** was obtained in a mixture with regioisomer **145** (which was impossible to isolate in a pure state). Later on it was found that prolonged heating of compounds **1**, **5a**, and **140a** (HOAc, Δ, 65°C, 48 h) also afforded tetrahydroderivatives **143** (Murlykina et al., 2015) that could be converted into dihydropyrimidines **144** after refluxing in HOAc for 4 h (**Figure 11**).

Temperature regime was also crucial in the condensations involving arylpyruvic acid **140b** (R^1 = Ar): (Sakhno et al., 2008, 2010; Murlykina et al., 2015), tetrahydropyrimidines **141** were yielded under the room temperature conditions (HOAc, US, r.t., 30 min) while pyrrolones **142** were obtained at elevated temperatures (HOAc, MW, 170°C, 20 min). Authors also carried out the transformation of compounds **141** into **142** (HOAc, MW, 170°C, 40 min) and proved the formation of compounds **141**

and **142** under kinetic or thermodynamic control, respectively (**Figure 11**).

Heterocyclizations involving 5-aminopyrazolecarboxamides (Chebanov et al., 2007a) under the same conditions afforded products of types **141**, **142** and **144** that again indicated on the similar behavior of substituted in the position 4 pyrazoles and 3-amino-1,2,4-triazole that had been already mentioned for the condensations with acetoacetic acid derivatives (see **Figure 8**).

In the contrary, the behavior of 5-aminotetrazole (**5b**) (X = N, R^2 = H) and 1-(4-chlorophenyl)-3,5-diamino-1,2,4-triazole (**5c**) (X = CNH_2, R^2 = 4-ClC_6H_4) was somewhat different. Application of the same conditions (HOAc or DMF, Δ) or (EtOAc-I_2, Δ) (Zeng et al., 2011) for the condensation of aldehydes **1**, pyruvic acid (**140a**) and 5-aminotetrazole (**5b**) gave the analogous to compounds **144** dihydrotetrazolopyrimidines **147** (Chebanov et al., 2005) while in case of 1-(4-chlorophenyl)-3,5-diamino-1,2,4-triazole (**5c**)–furanones **148** (Sakhno et al., 2011). Pyrrolones **146** (Sakhno et al., 2008) were the high-temperature products of the condensations involving both aminoazoles **5b** and **5c** with arylpyruvic acids [as in case of 3-amino-1,2,4-triazole (**5a**)]. All the attempts to isolate dihydropyrimidine acids of type **147** on the basis of 3,5-diaminotriazole **5c** were unsuccessful that was explained (Sakhno et al., 2011) by the loss of aromaticity in azole cycle during the formation of the fused fragment (**Figure 11**).

A large number of pyrrolones was also synthesized by Ryabukhin et al. (2012) in the reactions of ethyl 2,4-dioxo-4-arylbutanoates with aldehydes and 2-aminobenzothiazole, 2-aminothiazole, 2-amino-1,3,4-thiadiazole, 5-amino-1,2,4-thiadiazole, 3-amino-5-methylisoxazole, 3-amino-4-methyl-1,2,5-oxadiazole.

Condensation of pyruvic acid (**140a**) or its esters **149** and aldehydes **1** with 5-amino-3-aryl(alkyl)pyrazoles **150** afforded heteroaromatic pyrazolopyridine acids **152** (Cowen et al., 2016) and **154** (Chebanov et al., 2007a) (HOAc, Δ), their esters **151** [HOAc, Δ (Chebanov et al., 2007a) or EtOH-HCl, Δ (Dias et al., 2007)], correspondingly. It's interesting to note, that in case of 5-amino-1-phenyl-3-(pyridine-3-yl)-1*H*-pyrazole El-Borai et al. (2012) obtained pyrazolopyridines **153** (HOAc, MW, 160°C, 20 min) with different positional orientation of substituents than in the products **151**, **152**, **154** (**Figure 11**).

Introduction of arylpyruvic acid **140b** into the same high-temperature reaction yielded no pyrrolone of type **142** but led to the tarring the reaction mixture. Only reducing temperature together with applying ultrasonic activation allowed to synthesize tetrahydropyrazolopyrimidines **156** and **157** (Murlykina et al., 2013; similar to compounds **141**) in cases of 4-ethyl-5-amino-3-(4-fluorophenyl)pyrazole **155** and 5-amino-3-aryl-pyrazole **3** (HOAc, US, r.t., 60 min; **Figure 11**).

The analogous tetrahydropyrazolopyrimidines **160** (Sakhno et al., 2018) were synthesized in the reaction of 3-aryl-4-alkyl-substituted 5-aminopyrazoles **158** and aromatic aldehydes **1** with alkyl pyruvates **149** in acetic acid at room temperature. At the same time refluxing compounds **1**, **149** and **158** in acetic acid for 7 h led to the formation of a pyrimidine ring followed by an oxidative heteroaromatization process which gave 6-hydroxy-substituted alkyl pyrazolopyrimidine-5-carboxylates **159** (Sakhno et al., 2018). That was explained by disproportionation process; it was confirmed by carrying out this reaction in the inert atmosphere (where neither dihydropyrazolopyrimidine nor the compound without a hydroxyl group was observed). As it was expected, heterocycles **160** were transformed into heteroaromatic derivatives **159** upon boiling in acetic acid for 9 h (**Figure 11**).

Post-cyclizations can serve as an additional source of molecular diversity in the MCR*s*. They occur, for example, when salicylaldehyde is used in the MCR*s*. Thus, Gorobets et al. (2010) by varying temperature in the MCR of salicylaldehyde **162** with acetone (**161**) and 3-amino-1,2,4-triazole (**5a**) yielded both bridged benzoxadiazocines **164** (MeOH-HCl, MW, 150°C, 30 min) and tetrahydroderivatives **165** (CH_3OH-HCl, Δ, 40°C). Later on several groups (Kondratiuk et al., 2016; Gümüş et al., 2017a; Komykhov et al., 2017; Aydemir et al., 2018) studied the aspects of these transformations in details. It's interesting, that condensation involving 5-amino-3-arylpyrazoles **3**, salicylaldehydes **162** and pyruvic acid (**140a**), unlike the MCR with 3-amino-1,2,4-triazole (**5a**), afforded bridged benzoxazocines **163** at room temperature (HOAc, US, 90 min) whereas microwave heating at 150°C led to heteroaromatized pyrazolopyridines of type **152** (**Figure 12**).

Varying the conditions of the reaction and structures of the starting reagents afforded to synthesize three different classes of compounds **166**–**168** from the same reagents (Tkachenko et al., 2014a). Ultrasonication of 5-amino-3-methylisoxazole (**60**), *N*-aryl-3-oxobutanamide (**161**) and salicylaldehyde (**162**) afforded *N*-aryl-4-(3-methylisoxazole-5-ylamino)chromane-3-carboxamides **168**. Stirring *N*-aryl-3-oxobutanamides **161** with R^1 = 2-CH_3O- or 2-C_2H_5O- and compounds **162** and **60** in the presence of $Yt(OTf)_3$ redirected the condensation toward the formation of dihydroisoxazolopyridines **167**, whereas ultrasonication led to benzoxazocines **166**. This was almost an exceptional case when the replacement of the usual stirring by ultrasonic activation under other identical conditions led to the formation of different compounds (**Figure 12**; Tkachenko et al., 2014a).

It's worth to note, that in case of other substituted *N*-aryl-3-oxobutanamides **161** (R^1 = 2-OH, 2-CH_3, 2-Cl, 3-Cl) only heterocycles **167** were isolated both with the help of mechanical stirring and under ultrasonication. The authors (Tkachenko et al., 2014a) suppose that the direction leading to benzoxazocines **166** is favored by the formation of 3-coordinated complex of $Yt(OTf)_3$ with NH- and $CH_3O(C_2H_5O)$-groups of carboxamide fragment and OH-group of intermediate tetrahydroisoxazolopyridine. In turn, ultrasound supplies to the reaction system a sufficient amount of energy that is needed for nucleophilic substitution and bridged moiety formation (**Figure 12**).

o-Hydroxyl group of aldehyde **162** can also participate in the formation of lactones of types **169** (Svetlik et al., 2010) and **170** (Frolova et al., 2011), that were synthesized in the condensation of salicylaldehyde (**162**), 5-aminopyrazoles **4** or **29** and acetoacetic acid esters **161**. Heterocyclization of compound **161** with a double excess of salicylaldehyde (**162**) and 3-amino-1,2,4-triazole (**5a**) or 2-aminobenzothiazole (**101c**) gave spiroheterocycles **171** (Světlík and Kettmann, 2011) and **172**

(Svetlík et al., 2014); 2-aminobenzimidazole reacted with an exocyclic amino-group as a mononucleophile (**Figure 12**).

In the multicomponent reaction of 5-amino-3-methylisoxazole (**60a**) and salicylaldehydes **162** with 1,3-cyclohexanediones **2** Muravyova et al. (2013) synthesized several heterocycles **173–175** depending on the conditions. In case of 2-aminobenzimidazole (**101a**) condensation with the reagents **2** and **162** under the different conditions (heating in toluene with addition of K_2CO_3 or heating in chloroform with addition of sulfamic acid) resulted exclusively in xanthene-1-ones **176**. Only the stepwise transformation involving the preliminary synthetized imine **177** with dimedone (**2b**) afforded tetrahydrobenzo[4,5]imidazo[2,1-*b*]chromeno[4,3,2-*de*]quinazolines **178** (Saeedi et al., 2011; **Figure 13**).

Other Multicomponent Reactions of Aminoazoles

Isocyanide-based reactions may be separated into an individual large group and certainly should be described in special reviews, a lot of brilliant examples of which have already been published (Dömling and Ugi, 2000; Banfi et al., 2010; Ruijter et al., 2011; Dömling et al., 2012; Cioc et al., 2014; Koopmanschap et al., 2014; Devi et al., 2015; Zarganes-Tzitzikas et al., 2015; Shaaban and Abdel-Wahab, 2016). As it's recognized the classical components of the Ugi four-component reaction (Ugi-4CR) are aliphatic or aromatic amines and aldehydes, carboxylic acids and substituted isocyanides, that are generally well responsive to the formation of Ugi products at room or slightly elevated temperatures (Dömling and Ugi, 2000; Dömling, 2006). Groebke-Blackburn-Bienaymé three-component reaction (GBB-3CR) usually undergoes with participation of 2-aminoazines or 2-aminoazoles, aromatic or aliphatic aldehydes and substituted isocyanides. Brønsted or Lewis acids are often used in GBB-3CR (sometimes in Ugi-4CR) for activation of intermediate imine. Almost all the types of solvents (including water and ionic liquids) and catalysts, different temperature regimes (conventional or microwave heating) were studied in GBB-3CR (**Figure 14**; Devi et al., 2015).

There are a lot of examples of using aminoazoles as an amine component in GBB-3CR resulting in the formation of heterocycles like **181**. The most studied ones are the processes involving 3-amino-1,2,4-triazoles (Bienaymé and Bouzid, 1998; Tyagi et al., 2012; Urich et al., 2013; Aouali et al., 2015), 2-amino(benzo)thiazoles (Bienaymé and Bouzid, 1998; Guchhait and Madaan, 2009, 2010; Guchhait et al., 2009; Al-Tel et al., 2010; Akritopoulou-Zanze et al., 2011; Baviskar et al., 2011; Burchak et al., 2011; Hieke et al., 2012; Tyagi et al., 2012; Vidyacharan et al., 2014; Martinez-Ariza et al., 2015; Ansari et al., 2016; Shaabani and Hooshmand, 2016; Shao et al., 2017), 2-amino-1,3,4-thiadiazoles (Krasavin et al., 2008; Guchhait and Madaan, 2009; Guchhait et al., 2009; Wadhwa et al., 2015), 2-amino(benz)imidazoles (Lee et al., 2013; Pereshivko et al., 2013). GBB-3CR involving 2-aminooxazoles (Bienaymé and Bouzid, 1998) led to the formation of imidazoazoles while involving 1,2,5-oxadiazole-3,4-diamine (Kysil et al., 2010) gave oxadiazolopyrazines. Groebke condensations of 5-aminopyrazoles (5-amino-3-methylpyrazole, 5-aminopyrazole-4-carbonitrile, ethyl 5-aminopyrazole-4-carboxylate) are described in the following publications (Bienaymé and Bouzid, 1998; Guchhait and Madaan, 2009; Guchhait et al., 2009; Baviskar et al., 2011; Rahmati and Kouzehrash, 2011; Rahmati et al., 2013; Demjén et al., 2014; Murlykina et al., 2017).

Although there are a lot of variations and modifications known for the Ugi-4CR there is only one example of using aminoazole as an amine component in this reaction, which includes the treatment of 3-amino-5-methylisoxazole, aromatic aldehydes, phenylpropiolic acid and *tert*-butylisocyanide with formation of Ugi-product **182** (**Figure 14**; Murlykina et al., 2017).

Several publications deal with A^3 coupling reactions between aromatic aldehydes **1**, aryl acetylenes **183** and aminoazoles resulting in the formation of two types of products–via multicomponent assembly reaction through 6-endo-dig (heterocycles **187**, **188**) or through 5-exo-dig cyclization (heterocycles **185**, **186**). Thus, imidazoazoles **185a,d** and **186** were synthesized via method A [EtOH-$CuSO_4{\cdot}5H_2O$, D-glucose, Δ, 10–16 h (Guchhait et al., 2012)] on the basis of 2-aminobenzimidazole (**101a**), 2-aminothiazole (**101d**) and ethyl 5-aminopyrazole-4-carboxylate (**184**) via A^3-coupling reaction followed with 5-exo-dig cycloisomerization and prototropic shift (**Figure 14**).

At the same time, coupling involving 2-aminobenzimidazole (**101a**) (or 2-aminobenzothiazole **101c**) under other conditions [MeCN-CuI-Ag_2CO_3, Δ, 81–83°C (Kumar et al., 2014)] or [neat, MSA (molybdate sulfuric acid), Δ, 85°C (Shinde and Jeong, 2015)] led to formation of the benzimidazolopyrimidines **188a** (or benzothiazolopyrimidines **188c**). Carrying out the reaction involving 1*H*-indazol-3-amine (**108**) under neat conditions [Ag NPs (nanoparticles), Δ, 80°C (Balwe et al., 2017)] or in toluene [$CuSO_4{\cdot}5H_2O$, *p*-TSA Δ, 120°C (Palaniraja et al., 2016b)] resulted in multicomponent assembly reaction through 6-endo-dig cyclization and formation of pyrimido[1,2-*b*]indazoles **187** (**Figure 15**).

A four-component strategy for the selective synthesis of fused azepino[5,4,3-*cd*]indoles **189** and pyrazolo[3,4-*b*]pyridines **190** was elaborated by Jiang et al. (2014). The direction of multicomponent reaction involving 1,3-substituted 5-aminopyrazoles **150** and amines **55** with two equivalents of arylglyoxals **83** (DMF-*p*-TSA, MW, 115°C) was dependent on the electronic effects of arylglyoxals and aromatic amines (**Figure 15**).

Reddy et al. (2017) developed a highly active and stable heterogeneous POEGMA-g-TEGBDIM (polyethylene glycol methacrylate-grafted tetraethyleneglycol-bridged dicationic imidazolium-based IL) catalyst for the synthesis of substituted benzo[4,5]imidazo[1,2-*a*]pyrimidine heterocycles **192** upon solvent-free conditions (80°C) from 2-aminobenzimidazole (**101c**), aromatic aldehydes **1** and (*E*)-*N*-methyl-1-(methylthio)-2-nitroethenamine (**191**) (**Figure 15**).

A synthetic pathway to access fused pyrazolo[3,4-*d*]pyrimidine-6(7*H*)-thiones **194** by the three-component reaction of 5-amino-3-methylpyrazole (**4**), aldehydes **1** and

arylisothiocyanates **193** in an ionic liquid in the presence of catalytic amounts of *p*-TSA was elaborated by Safaei et al. (2012; **Figure 15**).

Application of heterogeneous solid base, silica sodium carbonate (SSC) as a catalyst allowed isolation of dimethyl 4,5-dihydrotriazolopyrimidine-6,7-dicarboxylates **196** in the MCR of dimethyl acetylenedicarboxylate (**195**) with **1** and **5a**. The authors (Karami et al., 2015b) suggested that the base favors the formation of an intermediate product of condensation between nucleophilic NH in the position 2 of 3-amino-1,2,4-triazole (**5a**) and electrophilic CH-center of dimethyl acetylenedicarboxylate (**195**) followed by the attack of aldehyde **1**, cyclization and dehydration (**Figure 15**).

In some cases, synthesis of starting materials for MCRs is also a difficult task. For example, the formation of acetoacetamide building-block by synthetic methods is an expensive and difficult procedure. Therefore, to avoid laborious stage of acetoacetamide synthesis, as a continuation of the work of Shaabani et al. (2009) four-component procedure for obtaining *N*,7-disubstituted-5-methyl-4,7-dihydrotetrazolo[1,5-*a*]pyrimidine-6-carboxamides **199** (Zeng et al., 2012) was elaborated. It consisted of the reaction of primary amines **198**, diketene **197**, 5-aminotetrazole (**5b**) and aldehydes **1** (EtOAc-I_2, Δ, 78°C, 4 h). In this MCR acetoacetamide was formed *in situ* by the addition of amine to diketene molecule (**Figure 15**).

Two-Component Condensations of Aminoazoles

To the best of our knowledge the condensations of aminoazoles with α,β-unsaturated carbonyl compounds **200** could be performed as one of the simplest and effective ways to the diverse azoloazine systems, such as **203**, **204**, since this type of starting materials usually contains alternative nucleophilic and electrophilic reaction centers. The most utilized α,β-unsaturated carbonyl compounds in such reactions are chalcones or cinnamic acid derivatives. The condensations of the enones with aminoazoles could be performed in various solvents within wide range of the temperatures and with application of different types of catalysis (Kolos et al., 2011; Yoshida et al., 2011; Orlov and Sidorenko, 2012; **Figure 16**).

Two-component heterocyclizations of the aminoazoles could be considered as convergent procedures concerning the corresponding multicomponent synthesis, or as independent transformations. Thus, in the previous section of the review it was shown that multicomponent heterocyclizations of the pyruvic acid derivatives with α-aminoazoles and carbonyl compounds could be applied for the synthesis of diverse heterocyclic systems. However, preliminary condensation of the pyruvic acid with aromatic aldehyde gives arylidenepyruvic acids **205** and their further reaction with 5-aminopyrazoles **150** in comparison to the multicomponent procedure allows to obtain different regioisomers **208**, **209** (Chebanov et al., 2007a, 2012a). At the same time, in the article (Sakhno et al., 2011) it was shown that the two-component condensation of arylidenepyruvic acid **205** and 1-(4-chlorophenyl)-3,5-diamino-1,2,4-triazole (**5c**) in DMF resulted in the formation of the same furanones **148** as in the corresponding MCR, however, in smaller yields (**Figure 16**).

The opposite pattern was observed in case of the 5-amino-3-methylisoxazole (**60a**) (Morozova et al., 2016). Multicomponent condensation of this aminoazole, pyruvic acid and aromatic aldehyde resulted in the decomposition of the initial amine due to the low stability of the isoxazole moiety in the acidic media. Application of the two-component procedure, via preliminary synthesis of unsaturated acids **205**, under $Sc(OTf)_3$ catalysis in CH_2Cl_2:H_2O (20:1) allowed to isolate compound **211** in low yields. An unexpected result was obtained when the unsaturated acid was replaced by the corresponding ethyl ester **212**: the condensation of the starting reagents in MeCN containing $Sc(OTf)_3$ at −18°C resulted in the formation of tetrahydroisoxazolopyridine system **213**. Typically, such compounds cannot be isolated due to the fast water elimination with the formation of dihydropyridine rings. Indeed, the condensation at higher temperatures led to the formation of dihydropyridine **214**, which was further spontaneously oxidized (**Figure 16**).

The condensation of ethyl arylidenepyruvate **212** with 5-aminopyrazoles **158** in acetic acid without additional catalyst (Sakhno et al., 2018) had a different character and allowed to isolate both pyrazolopyrimidines **159** (under heating) and dihydropyrazolopyrimidines **216** (at room temperature) having OH-group in position 6 (**Figure 17**). The yields of the product **159** for this two-component condensation were better in comparison to the multicomponent procedure (**Figure 11**).

3-Methoxalylchromone (**218**) containing hidden α,β-unsaturated fragment exhibited properties being similar to the derivatives of arylidenepyruvic acid: its condensation with different α-aminoazoles **21, 217a–c** resulted in the formation of azoloazines **219** under refluxing in acetic acid or heating in DMF-TMSCl at 80–100°C (Mkrtchyan et al., 2010). Another group studied the condensation of ethyl 5,5,5-trichloro-3-[(dimethylamino)methylene]-2,4-dioxopentanoate (**220**) with 2-aminothiazole or 2-aminobenzimidazole **101a,d**. The starting β-enaminodiketone has two nonequivalent carbonyl groups; however, the condensation with aminoazole is selective through the influence of the trichloromethyl group adjacent to the reaction's site. Nucleophilic attack of the carbonyl carbon atom by the lone electron pair of the endocyclic nitrogen resulted in the elimination of the trichloromethyl group and in the formation of corresponding thiazolo[3,2-*a*]pyrimidinone and pyrimido[1,2-*a*]benzimidazole **221** (Campos et al., 2017; **Figure 17**).

The application of 1,3-dielectrophiles in the azoloazine synthesis is not limited to the enones. β-Dicarbonyl compounds, for example, derivatives of acetylacetone **98** and acetoacetate **225** (Marjani et al., 2015) are used for the formation of the pyrimidine ring with substituents in positions 4 and 6. The asymmetric β-dicarbonyl compounds can produce positional isomers, but often the reactions give only one compound. The aminoazoles with pyrrole N-atom in the α-position to the NH_2-group are most often used as 1,3-binucleophiles (Gujjar et al., 2011; Ivachtchenko et al., 2011; Gege et al., 2012; Patnaik et al., 2012; **Figure 17**).

Among reactions involving β-diketones there is rather interesting condensation of 5-aminopyrazole **158** and dehydroacetic acid **227** (Aggarwal et al., 2014). It was found that the reaction did not stop on the formation of **228**: the presence of the reactive toward 5-aminopyrazole acetylacetone fragment induced further condensation with the second molecule of the amine **158** that gave bis(pyrazolo[1,5-*a*]pyrimidinyl)-7-ones **229** (**Figure 18**).

Despite the fact that compounds containing 4*H*-chromen-4-one moiety don't have real 1,3-dicarbonyl fragment in the presence of alkali in the reaction mixture the ring-opening process with the generation of the corresponding 1,3-dicarbonyl compound takes place (Zhang et al., 2011). In such way 7-diphenylpyrazolo[1,5-*a*]pyrimidine derivatives **232** were synthesized by the condensation of isoflavone **230** and 3-aminopyrazole (**31**) in MeOH-MeONa in moderate to good yields (**Figure 18**).

Resembling condensation of chromone-3-carboxylic acid (**233**) and aminopyrazole **21** in acetic acid gave chromeno[4,3-*b*]pyrazolo[4,3-*e*]pyridin-6(10*H*)-one **237** as the major product of the condensation. However, side decarboxylation of the intermediate **234** following with further condensation resulted in the formation of traces of pyrazolo[3,4-*b*]pyridine **239** (Miliutina et al., 2017). The intermediate **238** was isolated in low yields when the reaction was stopped after 1 h at 60°C (**Figure 18**).

Quite interesting heterocyclizations of 5-aminotetrazole were reported by Goryaeva et al. (2015): heterocyclization of 5-aminotetrazole (**5b**) and 2-ethoxymethylidene-3-oxo esters **240**, depending on the ester type and/or the condition, could give 2-azidopyrimidines **241** or tetrazolo[1,5-*a*]pyrimidines **242**. The starting materials under refluxing in EtOH or 1,4-dioxane didn't react completely even after long duration of the treatment and resulted in the formation of inseparable mixtures. Carrying out the reaction in the 2,2,2-trifluoroethanol (TFE) gave 2-azidopyrimidines **241** due to the opening of the tetrazole ring. At the same time, 4-methyl-2-azidopyrimidine was not stable and converted into the **242** even while standing as solid on air. The synthesis of the substance **242** could be carried out in EtOH at r.t. from 5-aminotetrazole (**5b**) and ester **240**, the presence of the **241** was indicated by TLC in the reaction mixture, which allows to assume that the reaction could pass through the formation of azide (**Figure 19**).

Despite the fact that the condensation of 5-aminotetrazole (**5b**) with the fluorinated reagents in 1,4-dioxane resulted in the mixtures of compounds, the presence of the catalytic amounts of sodium acetate led to the formation of azide **241** with further elimination of the nitrogen and nitrenes that gave ethyl 2-amino-4-(polyfluoroalkyl)pyrimidine-5-carboxylates **243**. In case of the CF_3-substituted ester the formation of the side product **244** was observed as well. On the other hand, 2-benzoyl-3-ethoxyprop-2-enoate in the condensation with 5-aminotetrazole in TFE under reflux yielded the mixture of compounds **245** and **246** due to the decomposition of the initial ester and the formation of the reacting ethyl benzoylacetate. Application of 2-ethoxymethylidene malonate **240** under refluxing in EtOH allowed to isolate ethyl-7-hydroxytetrazolo[1,5-*a*]pyrimidine-6-carboxylate **247**. Thus, depending on the substituent in 2-ethoxymethylidene-3-oxo esters different tetrazolopyrimidines or pyrimidines were obtained (**Figure 19**).

Acetoacetic esters may be easily replaced by malonic ester or sodium nitromalonaldehyde monohydrate (Ren et al., 2012). The malonic esters **248** were used as efficient starting materials for the synthesis of the azoloazines **249** substituted in the position 5 (Saito et al., 2011; **Figure 20**).

The condensations of α-dicarbonyl compounds could be carried out with α-diamines as well. An interesting publication was presented by Willer et al. (2012) dealing with short synthetic route to [1,2,5]oxadiazolo[3,4-*b*]pyrazine moiety. The reaction of diamine **250** and glyoxal or pyruvic aldehyde **251** under mild conditions (45°C, 45 min) yielded 5,6-dihydroxy-4,5,6,7-tetrahydro[1,2,5]oxadiazolo[3,4-*b*]pyrazine **252** (R = H; conversion 96%) or its unstable analog **252** ($R = CH_3$). Isolation of the pure compound **252** was made by lyophilization or by carrying out the reaction at 20°C. Further pyrolysis on the silica gel gave target [1,2,5]oxadiazolo[3,4-*b*]pyrazines **253** in low yields (10–33%; **Figure 20**).

Fusco et al. (2016) applied the condensation between α-diamines **254** and α-diketones **255a–e** to obtain triazolo[4,3-*b*][1,2,4]triazines **256** in 25–95% yield (the lowest yield for a system with two diketone moieties). An analogous result was obtained for 1,2,5-thiadiazole-3,4-diamine **257** (Planells et al., 2014; **Figure 20**).

The article published by Lauro et al. (2017) presented the possibility to apply hem-diols instead of α-diketones. The condensation of amine **250** with the selected 2,2-dihydroxy-1*H*-indene-1,3(2*H*)-diones **260** gave compounds **261** in moderate yields (**Figure 20**).

Diaminoazoles can be applied not only for synthesis of six-membered heterocycles: the condensation of isatin (**262**) and 1,2,5-oxadiazole-3,4-diamine (**250**) in the boiling acetonitrile gave 4,6-dihydrospiro(imidazo[4,5-*c*][1,2,5]oxadiazol-5,3′-indol)-2′(1′*H*)-one **263** (Gurevich et al., 2011; **Figure 20**).

Very unusual application of selenium dioxide as a carbonyl compound in the condensation with 1,2,5-thiadiazole-3,4-diamine (**257**) giving [1,2,5]selenadiazolo[3,4-*c*][1,2,5]thiadiazole (**264**) was described (Konstantinova et al., 2015). As the side reaction an exchange of the sulfur of the thiadiazole was observed: that also allowed to isolate [1,2,5]selenadiazolo[3,4-*c*][1,2,5]selenadiazole (**265**). The formation of compound **265** as the major product of the heterocyclization could happen in DMF at 100°C (**Figure 20**).

The acylation of the vicinal diamines by the acetic anhydride under reflux could give the new azole ring. Thus, Centore et al. (2017) applied the reaction of 3,4-diamino-1,2,4-triazole (**266**) with acetic anhydride to obtain [1,2,4]triazolo[3,2-*c*][1,2,4]triazole (**267**) without isolation of non-cyclic products of acylation (**Figure 21**).

The condensations of aminoazoles with carbonyl compounds are not limited to the vicinal amines. The azoles with an amide group next to the amine one also can be used as the reagents for the synthesis of pyrimidinones, but the condensation should be promoted by catalysts. Mulakayala et al. (2012) showed that

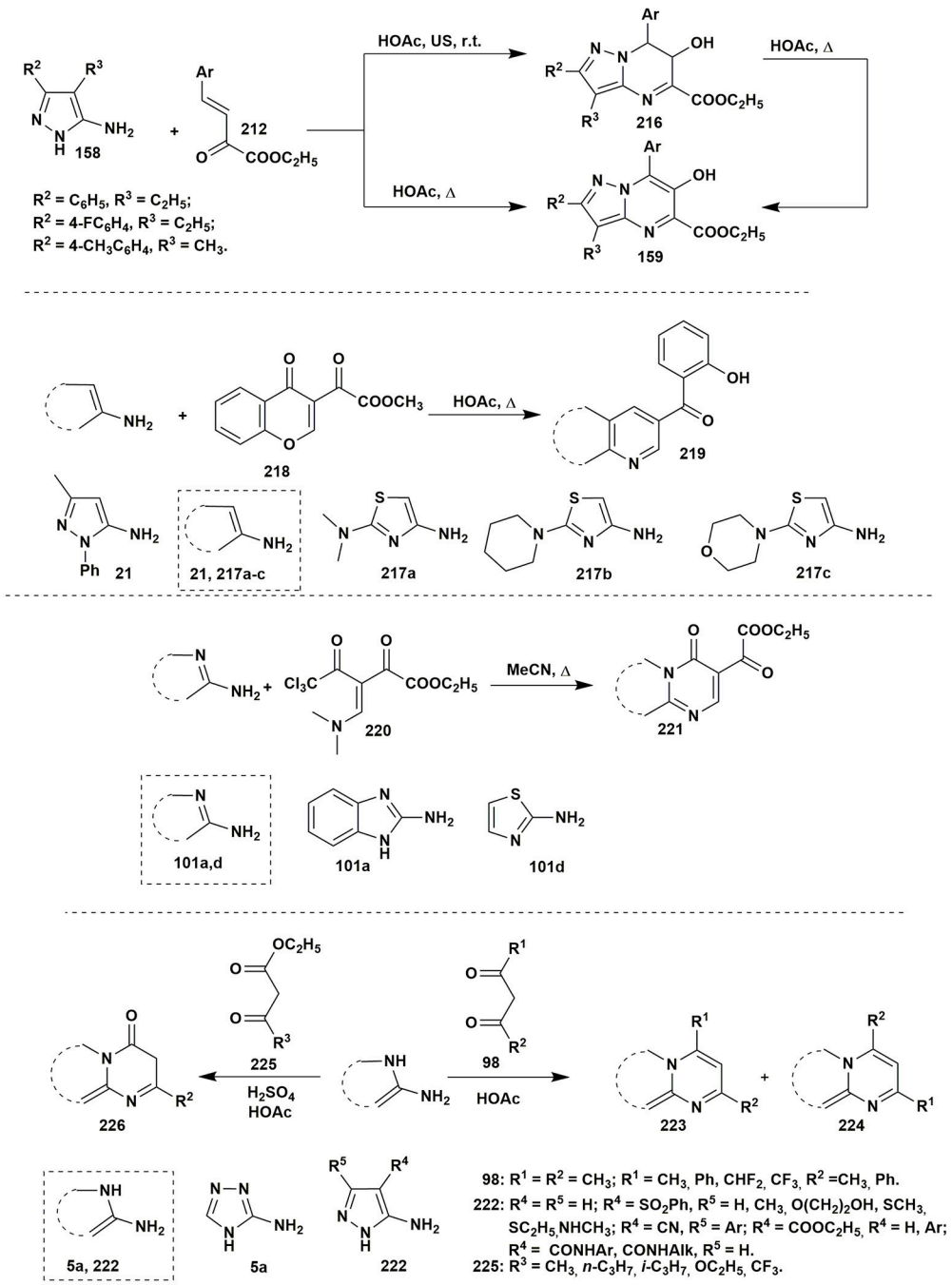

FIGURE 17 | Examples of the application of 1,3-dielectrophiles in the azoloazine synthesis.

condensation between 4-amino-1*H*-pyrazole-5-carboxamide (**268**) and aromatic aldehydes **1** occured without Lewis acid neither at room temperature nor under refluxing, however, the presence of the catalytic amounts of $InCl_3$ promoted the cyclocondensation. Among the studied solvents, the best result was observed in case of MeCN (10% mol of the catalyst) at room temperature. Variation of the solvents (MeOH, *i*-PrOH, EtOAc, CH_2Cl_2, $CHCl_3$) or Lewis acids ($AlCl_3$, $TiCl_4$, BF_3-OEt_2, $FeCl_3$, $CuCl_2$) led to the yields decreasing. Later on another method for synthesis of the similar 1,6-dihydro-7*H*-pyrazolo[4,3-*d*]pyrimidin-7-one (**270**) was performed (Mohammed et al., 2015). Metal-free condensation of aromatic ketones **269** with azole **268** was induced by the molecular iodine (10% mol) with oxygen in DMSO at 110°C and resulted in the formation of the Schiff bases but not the oxidation of the acetophenone to the 2-oxo-2-arylacetaldehyde that was observed in case

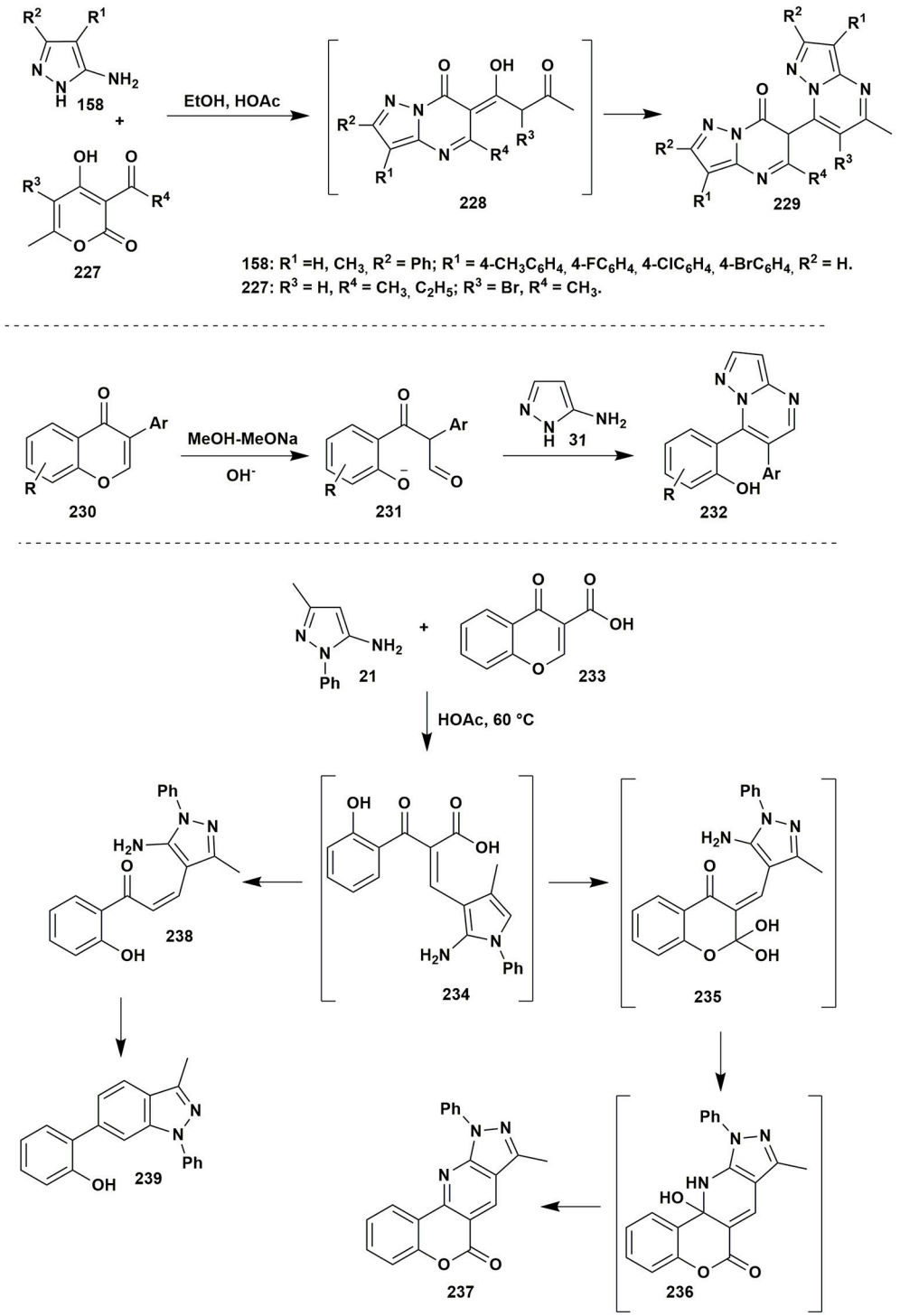

FIGURE 18 | Two-component condensations of aminoazoles with carbonyl compounds containing pyrone moiety.

of 110% I_2 excess. Continuous heating promoted further intermolecular condensation with the formation of 1,6-dihydro-7*H*-pyrazolo[4,3-*d*]pyrimidin-7-one **270**. Attempts to expand the range of the substrates have shown that aliphatic ketones couldn't be used as the reagents; N-substituted amides also did not undergo the condensation under such conditions. Application of the $K_2S_2O_8$ in acetonitrile–water mixture (1:1) at the room temperature (Hudwekar et al., 2017) allowed to apply the procedure not only for carbonyl compounds, but also for benzylamines or benzyl alcohol via their *in situ*

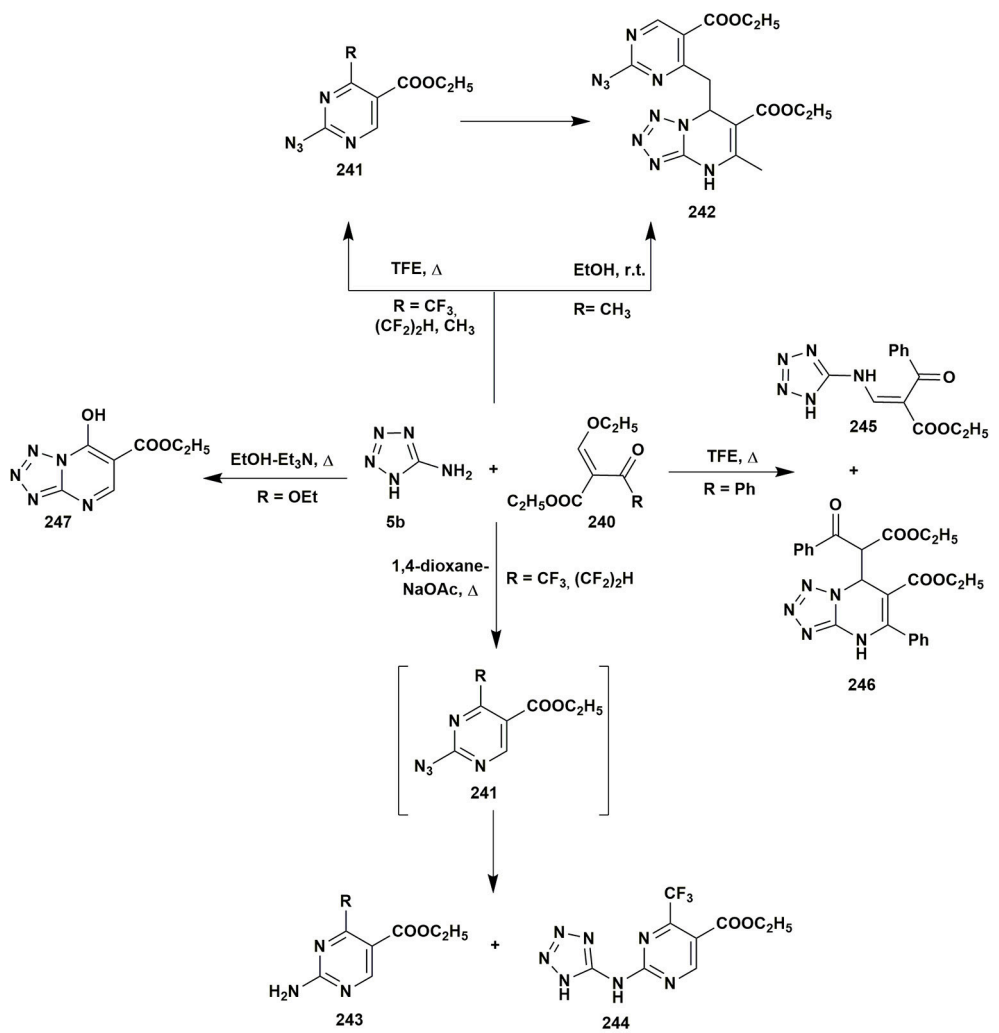

FIGURE 19 | Heterocyclizations of 5-aminotetrazole and 2-ethoxymethylidene-3-oxo esters.

oxidation. The formation of 1,5-dihydro-4*H*-pyrazolo[3,4-*d*]pyrimidin-4-ones **273** was also observed in the reaction of 5-amino-1*H*-pyrazole-5-carboxamide **271** and methyl phenylacetate (**272**) in EtOH-EtONa (Tintori et al., 2015; **Figure 21**).

The construction of the azoloazine ring may be performed by using other types of reactive groups in the β-position to the amino group of aminoazole. For example, 5-amino-1*H*-pyrazole-4-carbonitrile (**274**) reacted with formamide (**275**) under microwave irradiation at 200°C with the formation of 1*H*-pyrazolo[3,4-*d*]pyrimidin-4-amine (**276**) (Todorovic et al., 2011). The condensation of the benzamidine **278** proceeded in a similar way (Makarov et al., 2015; **Figure 21**).

An interesting result was obtained in the condensation of 1-phenyl-5-(1*H*-pyrrol-1-yl)-1*H*-pyrazol-4-amine (**280**) with CDI in 1,4-dioxane or with CS_2 in pyridine under refluxing that gave pyrazolo[4,3-*e*]pyrrolo[1,2-*a*]pyrazine systems **281**, **282** (Farghaly and El-Kashef, 2011; **Figure 22**).

Two component heterocyclization of aminoazoles **101f–h** and phenacyl bromide **283** or its aliphatic analogs was reported in numerous publications as a simple way to synthesize fused imidazoles **284**: imidazolo[2,1-*b*]benzothiazole (Chandak et al., 2013), imidazo[2,1-*b*][1,3,4]thiadiazole (Copin et al., 2016) were obtained under refluxing in EtOH, CCl_4, MeCN. It should be noted, that the formation of uncyclized reaction products is often observed due to the protonation of the exocyclic amino group to form hydrobromic acid salts (Kamal et al., 2010; **Figure 22**).

2-Chloroacetyl chloride (**286**) in glacial acetic acid and 2-chloroacetonitrile (**288**) in DMF-KOH also could be applied in such type of heterocyclizations with the formation of 3,5-dihydro-4*H*-imidazol-4-ones **287** and 4*H*-imidazol-5-amines **289** (Rateb, 2014; Soliman et al., 2014; **Figure 22**).

Reactions of aminoazoles and β-halogen containing carbonyl compounds were reported as a way for the synthesis of angular fused heterocyclic systems. The copper catalyzed synthesis of

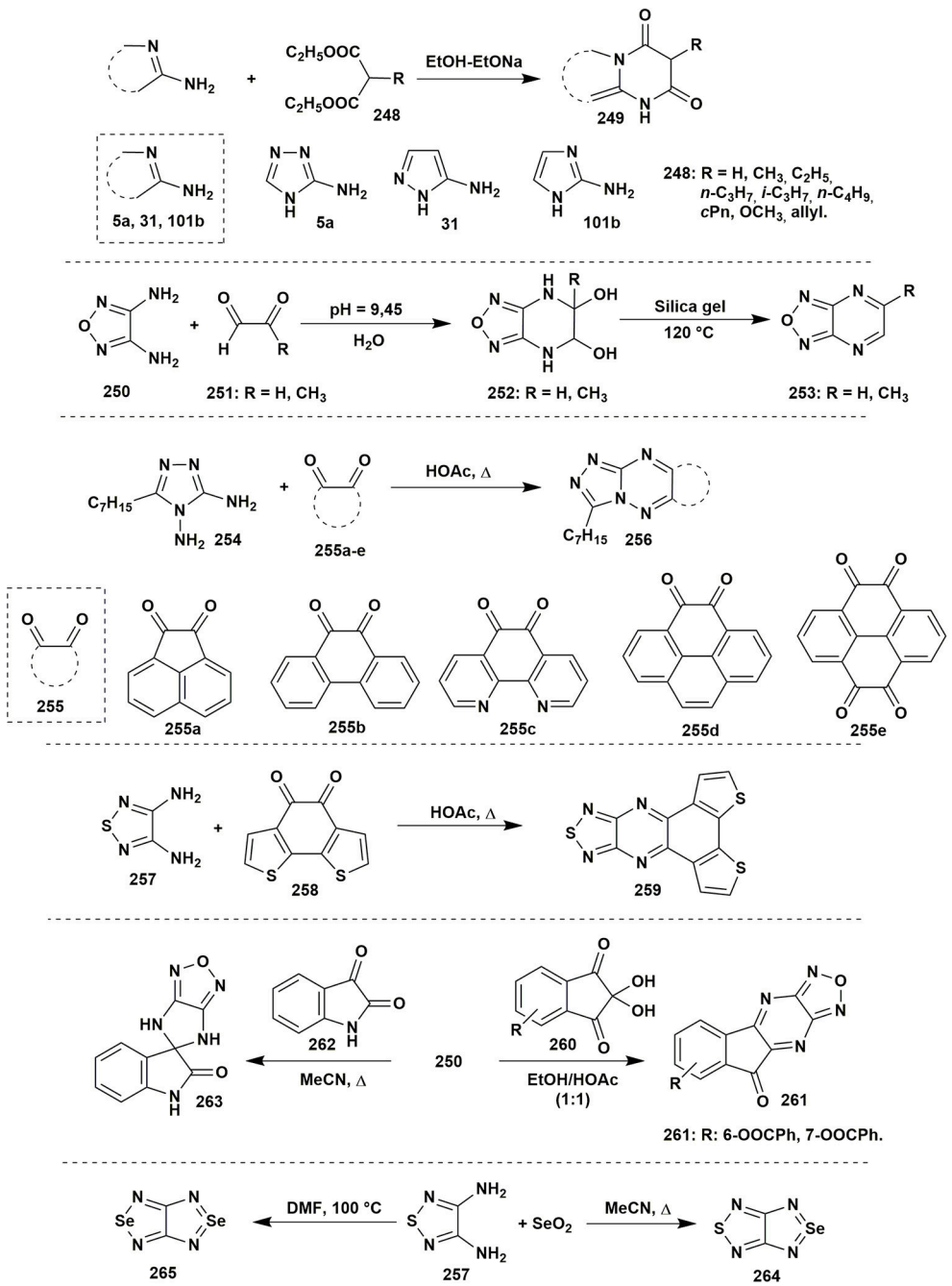

FIGURE 20 | Some two-component transformations of aminoazoles with malonic esters, glyoxals derivatives, hem-diols, isatin, or selenium dioxide.

the pyrazolo[1,5-*a*]quinazolines **293** was published by Gao et al. The most promising results were obtained in the system DMF-CuI-K_2CO_3 while other types of alkali media gave the worth results. It was found, that the application of the CuI, additionally stabilized by ethylenediamine was the most effective (Gao et al., 2014; **Figure 23**).

On the other hand, Nue et al. showed that 2-F and 2-NO_2-derivatives **294** may be also applied in such reactions. Simple heating of the starting reagents in dry DMF-Cs_2CO_3 yielded angular heterocycles **295**. Unlike previous authors, application of the K_2CO_3 instead of Cs_2CO_3 gave worth results. The absence of the molecular sieves decreased the yield of the target [1,2,4]triazolo[1,5-*a*]quinazoline **295** from 84 to 74%. Monitoring the reaction mixture by HRMS showed the presence of the Schiff base, that could be one of the intermediates of the heterocyclization (Fang et al., 2014; Niu et al., 2014; **Figure 23**).

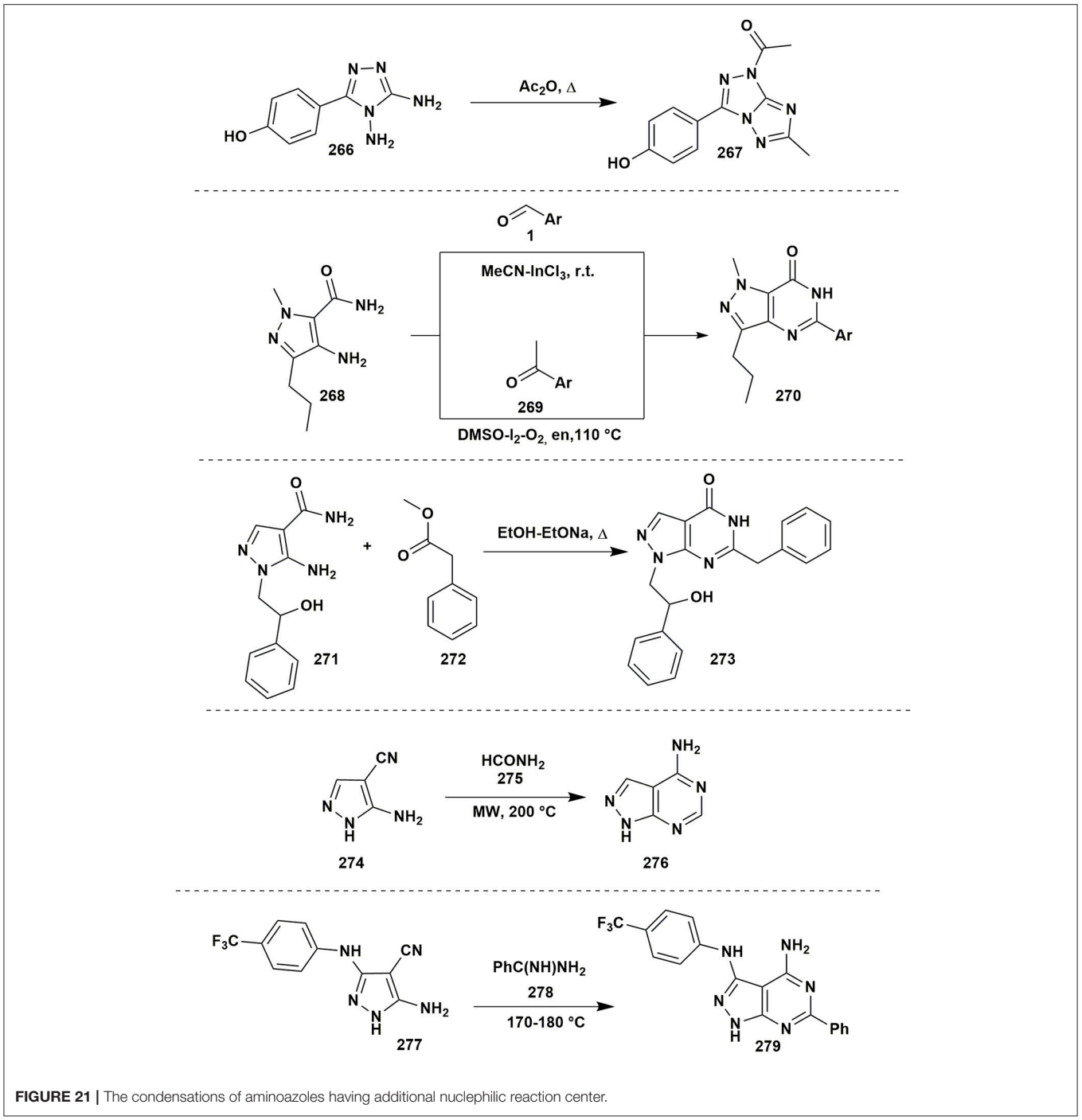

FIGURE 21 | The condensations of aminoazoles having additional nuclephilic reaction center.

Hedidi et al. reported the copper catalyzed synthesis of pyrido[2,3-*e*]pyrimidines **297** (Hedidi et al., 2017). The attempts to obtain the target compounds via simple heating of the reagents **5a, 31, 101a**, and **296** with Cs_2CO_3 in DMF, as it had been reported in Niu et al. (2014), were unsuccessful while application of the procedure reported by Gao et al. (2014) allowed to fix their traces. The best results were observed in the system DMSO-CuI-K_3PO_4 without any ligand (**Figure 23**).

3-Amino-5-methylisoxazole was sometimes considered as a 1,3-binucleophile reacting with the preservation of the isoxazole moiety. However, in some cases establishing structures of the compounds synthesized without X-Ray data was not sufficient (Rajanarendar et al., 2016; Diyanatizadeh and Yavari, 2017). Sometimes the structures of final compounds were assigned similarly with the pyrazole-containing compounds, which in our opinion may be incorrect due to the possibility of isoxazole ring opening. For instance, the condensations of 3-amino-5-methylisoxazole (**298**) with arylisothiocyanate **193** with further Boulton—Katritzky rearrangement result in the formation of the 1,2,4-thiadiazoles

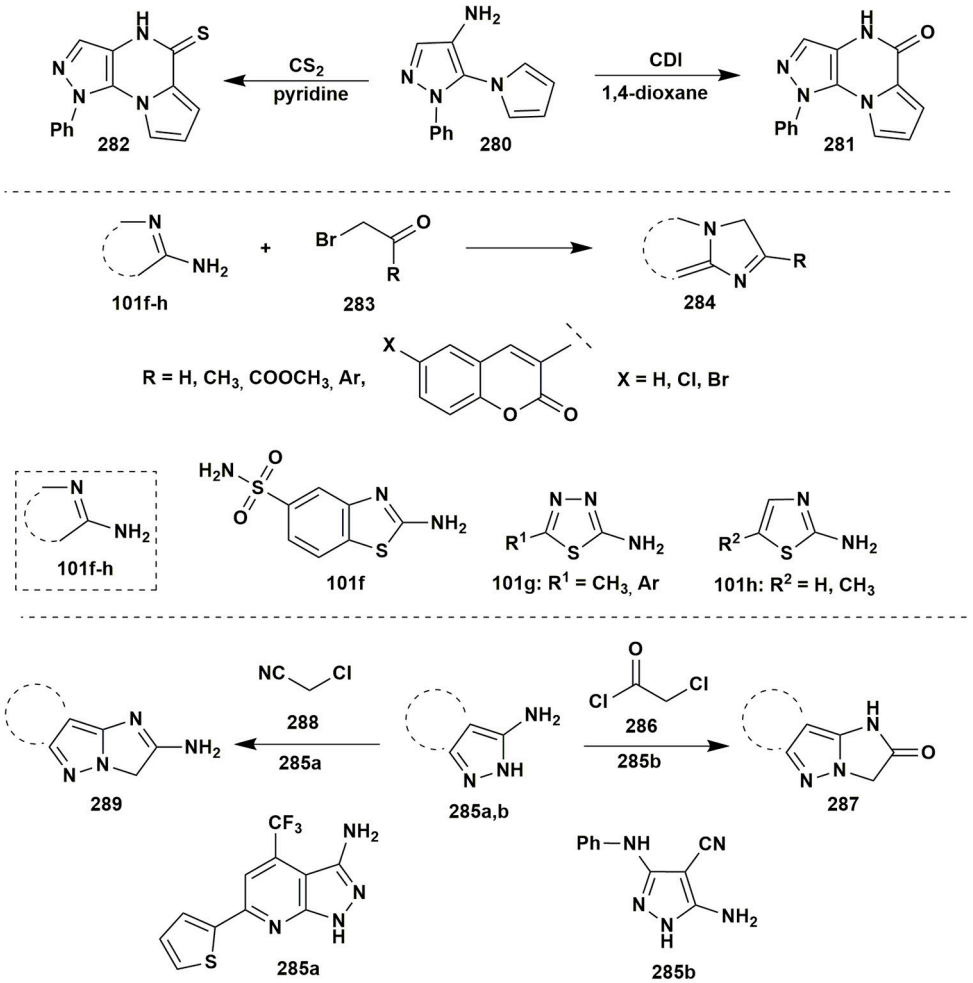

FIGURE 22 | Other examples of two-component reactions involving aminoazles.

300 (Pokhodylo and Shyyka, 2014; Proshin et al., 2014; **Figure 24**).

Thus, two component reactions involving aminoazoles and substrates of various origins allow forming diverse azoloazine, azinoazine and other heterocyclic systems. The substrates for condensations are not limited to 1,3-dielectrophiles or carbonyl compounds although they constitute the overwhelming majority of typical reagents.

Click Chemistry Concerning Azoles and Aminoazoles

Click chemistry, by B. Sharpless definition (Kolb et al., 2001), describes reactions that are wide in scope, suitable for most substrates, stereospecific, have high yields and low amount of side products, the latter can be removed without application of chromatography methods. The process itself needs to be conducted in mild conditions, the reactants–to be readily available, the solvent–to be easily removed or absent, and the product–to be effortlessly separated from the reaction mixture. The concept of click chemistry perfectly goes along with the principles of green chemistry and with diversity oriented synthesis due to the possibility to build different types of molecular skeleton and may be used for synthesis and further modification of aminoazoles as well.

Talking about click chemistry, azide-alkyne cycloaddition is always the first thought, but the authors of the term (Kolb et al., 2001) also include to the massive of click reactions the following:

- [3 + 2], [4 + 2] and [4 + 1] cycloadditions, Diels-Alder reaction, in particular;
- Nucleophilic addition, oxirane and aziridine ring opening;
- Some heterocyclization reactions
- Reactions of carbonyl compounds: azomethine derivatives formation, epoxidation, Michael reaction.

The most obvious reason for the development of this field of study is the minimization of efforts for obtaining the final product by means of resource economy. The advantages of click chemistry are useful for the purposes of pharmacology

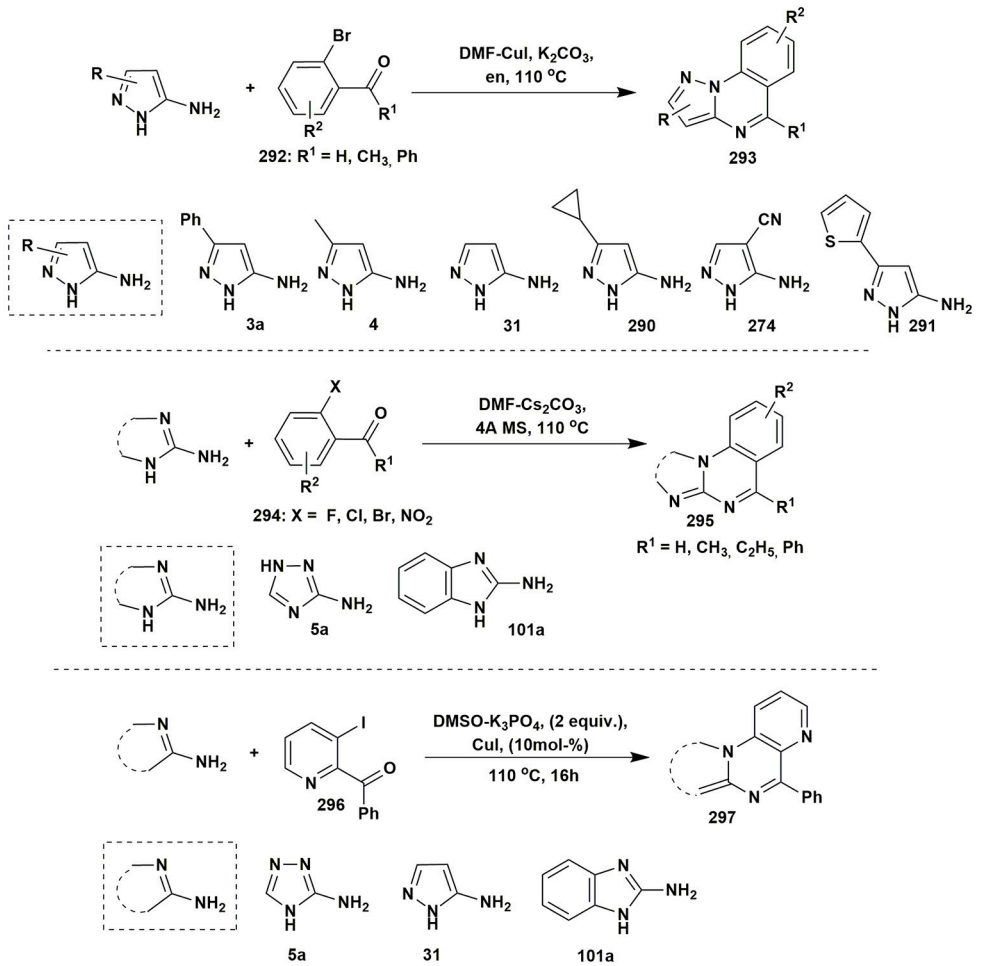

FIGURE 23 | Reactions of aminoazoles and β-halogen containing aromatic carbonyl compounds.

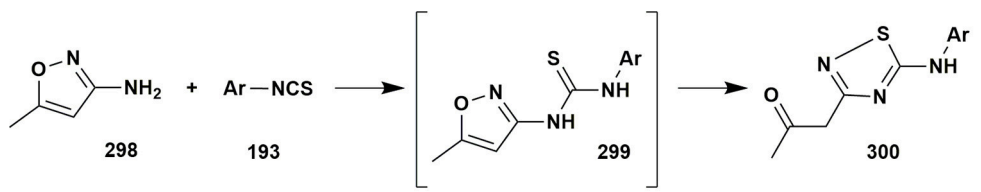

FIGURE 24 | Boulton–Katritzky rearrangement in the reactions of 3-amino-5-methylisoxazole with arylisothiocyanates.

and medicinal chemistry (Choi et al., 2006; He et al., 2016). Wastelessness and bioorthogonality of this reaction type promoted its implementation into medicinal chemistry and caused, for example, development of new molecules for contrast identification of cancer cells (Lee et al., 2014), RNA and DNA molecules, proteins (Shieh et al., 2015), etc.

Although, as it was mentioned, the most popular first thought about click-chemistry is the Cu(I)-assisted synthesis of 1,2,3-triazoles, in this part of the review we will focus on the procedures with different starting reactants rather than publications discussing new catalysts for the reaction of azide and alkyne.

The pre-click triazole-forming cycloaddition reactions were well-known in the nineteenth century, but were very inconvenient as they required long-term heating in closed vessels, thus, could be in no way characterized as "click" reactions. As an example, one of those methods (Michael, 1893) included addition of 2-phenyl-*2H*-triazirine (**301**) to dimethyl

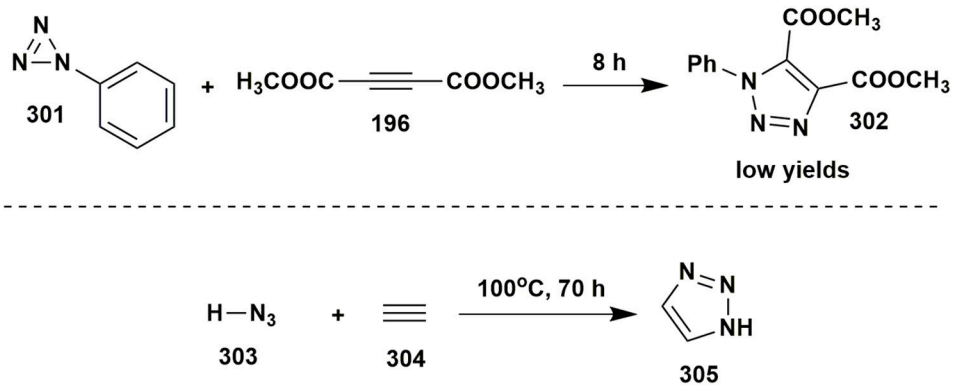

FIGURE 25 | First attempts for 1,2,3-triazole moiety synthesis.

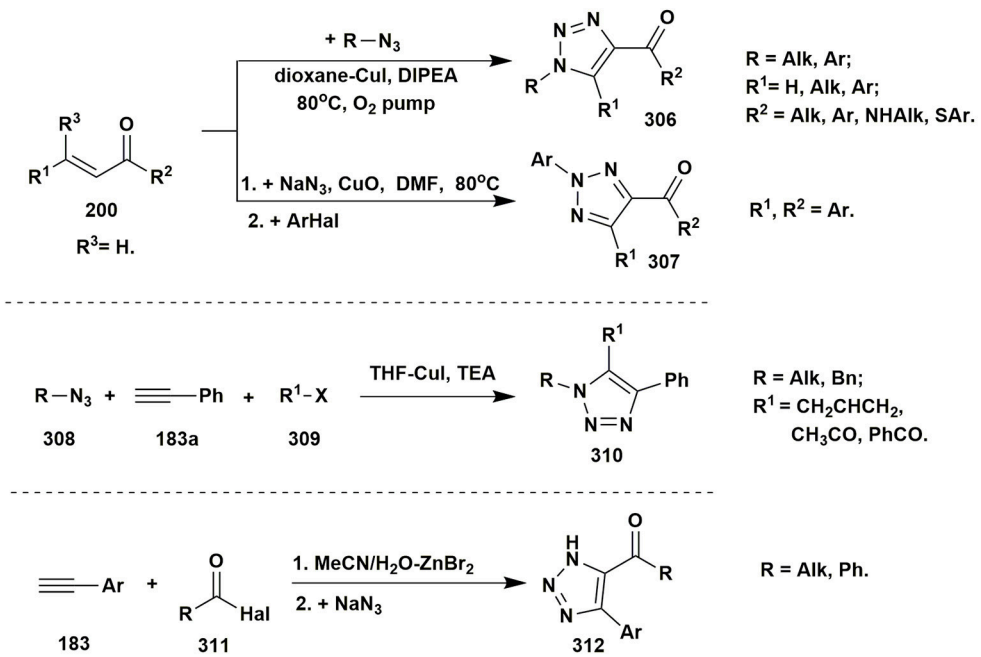

FIGURE 26 | Azide-based cycloaddition in synthesis of 4-acyl-1,2,3-triazoles.

acetylenedicarboxylate (**195**) in molten form and the product **302** was formed in low yields (**Figure 25**).

The first azide-alkyne reaction involved transformation of hydrogen azide (**303**) and acetylene (**304**) in ethanol-acetone mixture in a closed vessel for 70 h (Dimroth and Fester, 1910). Such unfriendly reaction conditions closed the door to 1,2,3-triazole (**305**) synthesis and research of the properties of these heterocycles for decades (**Figure 25**). It should be noted, that the original paper (Dimroth and Fester, 1910) can be hardly found in the journal, though there exists a plenty of references in many papers and theses.

Unarguably, the simplest method to obtain 1,2,3-triazole fragment is copper-catalyzed 1,3-dipolar azide-alkyne cycloaddition (CuAAC), firstly described by Meldal (Tornøe et al., 2002) and Sharpless (Rostovtsev et al., 2002) groups. Its mechanism was studied and published by Worrell et al. (2013), and mechanistic data was thoroughly reviewed by Berg and Straub (2013). Needless to say, CuAAC is highly progressing and, thus, popular object of research, described in a great number of papers and reviews (Hein and Fokin, 2010; Berg and Straub, 2013), and a plenty of other publications are devoted to this reaction in different subtopics, including solid-phase (Castro et al., 2016), green (Shirame and Bhosale, 2018), solvent-free (Tireli et al., 2017) syntheses.

Cu(I) only shows its great catalytic activity with terminal alkynes as reactants (Liang and Astruc, 2011). For non-terminal

alkynes catalysts on the basis of platinum metals are known, such as ruthenium (Boren et al., 2008; Johansson et al., 2016) and palladium (Kamijo et al., 2002). Metal-free azide-alkyne cycloadditions and photoclick reactions are also known and intensively studied (Rodríguez-Rodríguez et al., 2015; Singh et al., 2016; Jalani et al., 2017).

Regardless of the novelty of CuAAC method it has quickly become the most popular procedure for the synthesis of 1,2,3-triazole derivatives. Variations were also invented for preparation of these heterocycles from alkenes. For instance, Janreddy et al. (2013) report successful cycloaddition of organic azides **308** to α,β-unsaturated ketones **200**, such as vinyl ketones and chalcones, in an oxidative atmosphere of pure oxygen. As an oxidant CuO can also be employed, as a more convenient reagent than gaseous oxygen (**Figure 26**). In another paper, the triazole ring was also arylated by aryl halides without separation to obtain triazoles **307** (Zhang et al., 2012).

1,2,3-Triazole fragments were also obtained by multicomponent ways. For example, Wu et al. (2005) reported reaction of organic azide **308** and terminal alkyne **183** in the presence of Cu(I) salts and following cleavage of C-Cu bond in an Ullmann-like reaction by an alkylating agent **309**, which resulted in 1,4,5-substituted triazole **310** (**Figure 26**).

Another multicomponent approach (**Figure 26**) included consecutive reaction of terminal alkyne **183** with acyl halide **311**, and then with sodium azide with application of zinc bromide, which served as a catalyst for both steps of the process (Keivanloo et al., 2013).

Another type of click reactions–syntheses of tetrazoles–were carried out even more than a century ago (Pinner, 1894; Dimroth and Merzbacher, 1910), but those tries took a lot of time and energy, requiring 40 h-long refluxing in ethanol, heating in a sealed vial under high pressure etc. Such methods were reviewed by Benson (1947).

Only the second half of XX century contributed easier and faster procedure of tetrazole fragment formation. An end-of-the-century review was published in 1994 (Wittenberger, 1994) and included latest advances in synthesis, functionalization and applications of these heterocycles.

Three-component reactions of primary amines **55** of various origin, including aminoazoles, orthoformic ester **313** and sodium azide leading to 1-substituted tetrazoles **315** (**Figure 27**) was thoroughly studied by Gaponik group and their followers (Gaponik et al., 1985, 1990; Voitekhovich et al., 2005, 2013). One of the latest and most complete reviews was presented in Grigoriev et al. (2017).

Isonitriles **180** were shown to react with trimethylsilylazide in the presence of hydrochloric acid (Jin et al., 2004), forming 1-substituted tetrazoles **315**. Arylisothiocyanates **193** in the reaction with sodium azide form 5-thiotetrazoles **314**, which could be oxidized to 1-aryltetrazoles **315** by hydrogen peroxide, chromium trioxide and other oxidizers (Joule and Mills, 2010; **Figure 27**).

Synthesis of C-substituted tetrazoles **317** is more widely studied, and the number of methods for their preparation is larger. A Lewis acid-assisted reaction of organic nitriles **316** and sodium azide is probably the most popular (**Figure 28**).

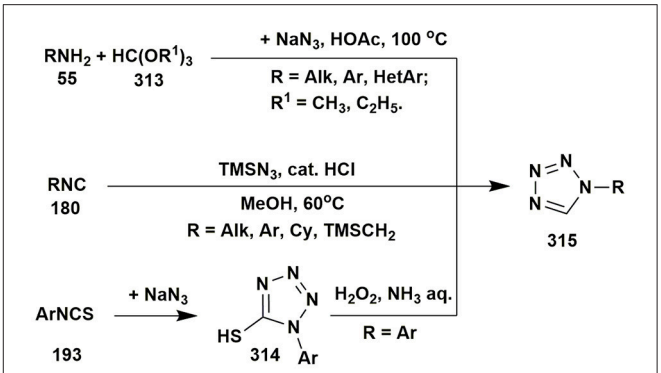

FIGURE 27 | Syntheses of N-substituted tetrazoles.

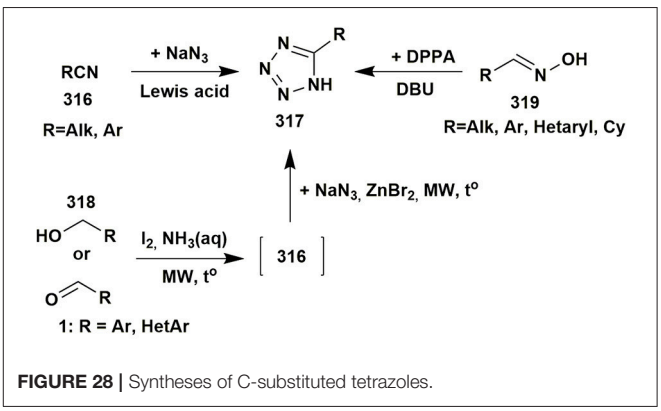

FIGURE 28 | Syntheses of C-substituted tetrazoles.

Yields were reported to be as high as 90% for benzonitriles in the presence of $ZrOCl_2$, but using zinc salts became a classic procedure (Galante and Somerville, 1996).

Nitriles **316**, reactive toward [3 + 2]-cycloaddition reactions with azide, can be formed *in situ* from primary alcohols **318** or aldehydes **1** by oxidation with iodine in aqueous ammonia under microwave irradiation (Shie and Fang, 2007; **Figure 28**). Tetrazoles **317** were reported to be separated in high yields in such procedure.

Diphenylphosphorazidate (DPPA) served as a reactant in conversion of aldoximes **319** to 5-substituted tetrazoles **317** (**Figure 28**), making the publication (Ishihara et al., 2018) different from other methods employing aldoximes as initial compounds by the relative safety of the procedure, which excludes explosive azide sources and heavy metals.

5-Aryl-1-substituted tetrazoles **321** can also be obtained via click reactions. The method (Kaim et al., 2011) suggests mixing of isonitriles **180** with bromine and sodium azide in acetonitrile; arylboric acid with Suzuki catalysts are introduced to the reaction mixture without separation of an intermediate product **320**.

Other method of preparation of 1,5-disubstituted tetrazoles **323** can include one-pot transformation of an alkene **322**, *N*-bromosuccinimide, nitriles and trimethylsilane azide, catalyzed by triflates and is reported by Hajra et al. (2007). Yields appeared to be higher when zinc triflate was used (**Figure 29**).

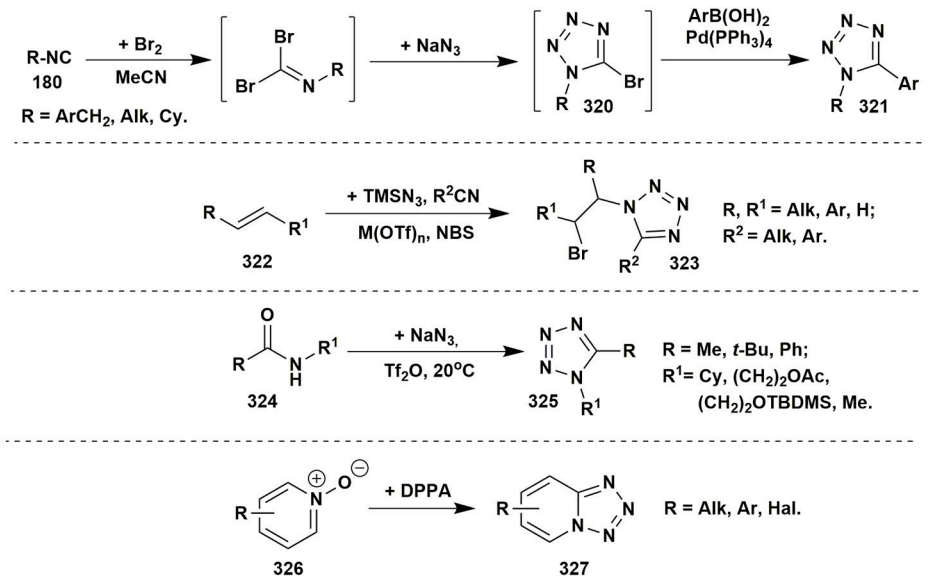

FIGURE 29 | Syntheses of disubstituted tetrazoles.

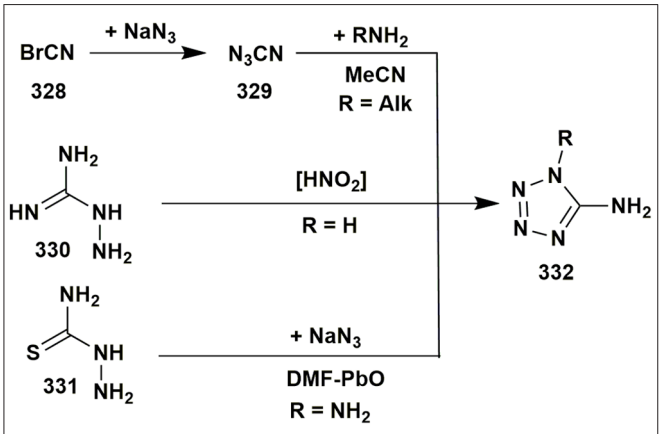

FIGURE 30 | Syntheses of 5-aminotetrazoles.

Methods of preparation of tetrazole **325** starting from carboxamides **324** are also known. In this case, amide group needs to be activated, for example, by trifluorosulfonic acid anhydride (Thomas, 1993) and then [3 + 2]-cycloaddition of azide proceeds (**Figure 29**).

Tetrazolopyridine **327** synthesis was described by Keith (2006). Pyridine N-oxides **326** were allowed to react with phosphorylazides in hot pyridine as a solvent. Various phosphorylazides were tested, but diphenylphosphorazidate (DPPA) proved to be the most convenient source of azide group (**Figure 29**).

1-Alkyl-5-aminotetrazoles **332** can be obtained by reaction of cyanazide **329** and primary amines, which form intermediate amidoylazide with subsequent cyclization in acetonitrile-water mixture (Joo and Shreeve, 2008; **Figure 30**).

5-Aminotetrazole (**5b**) (**332** R = H) was synthesized by nitrosation of aminoguanidine (**330**) and following heterocyclization of the intermediate with high yields (Kurzer and Godfrey, 1963; **Figure 30**). 5-Molar nitric acid needs to be considered as a hazard in this synthesis.

1,5-Diaminotetrazole (**332**) (R = NH_2) was formed by heating thiosemicarbazide (**331**) suspension in dry DMF with ammonium chloride, lead(II) oxide and sodium azide (Gaponik and Karavai, 1984). Only freshly obtained red modification of PbO proved to be useful in this reaction (**Figure 30**).

CONCLUSIONS

In summary, comprehensive analysis of the literature concerning the topic of the present review demonstrates that reactions involving aminoazoles as key reagents possess a high potential for diversity-oriented synthesis and open up effective and convenient pathways to numerous types of final heterocyclic compounds. Classical two-component and stage-by-stage procedures as well as multicomponent reactions of aminoazoles allow to synthesize diverse five-, six- and seven-membered heterocycles using a limited set of reagents the most common of which are α,β-unsaturated carbonyl and carboxyl compounds, cyclic and non-cyclic CH-acids, aldehydes, ketones and diketones of different origin. Additional benefits may be obtained by application of such innovative approaches as microwave- and ultrasonic-assisted organic synthesis, methods of click-chemistry, using special catalysts etc. The compounds synthesized from aminoazoles are useful as building-blocks for further construction of complex heterocyclic systems, as promising objects of medicinal-oriented chemistry to search for

the novel drug-like substances and as components of functional materials.

AUTHOR CONTRIBUTIONS

YS and SD collected most publications related to this review article and sorted them. MM analyzed the literature and wrote the chapter about multicomponent reactions. AM analyzed the literature and wrote the chapter about two-component reactions. IZ analyzed the literature and wrote the chapter about click-chemistry. VC developed the concept of the review, co-wrote and corrected the manuscript.

FUNDING

Authors thank National Academy of Sciences of Ukraine for financial support in the frame of the projects Development of methods of synthesis of novel chemotypes of drug-like nitrogen containing heterocyclic compounds (0116U001209) and Development of methodology of click-chemistry for the creation of components for novel chelating materials (0117U001280) and President of Ukraine for financial support in the frame of the project Multicomponent isocyanide-based reactions of functionalized starting reagents and post-transformations of the compounds synthesized (F-78/205-2018).

REFERENCES

Abedini, M., Shirini, F., Mousapour, M., and Jolodar, O. G. (2016). Poly(vinylpyrrolidonium) perchlorate catalyzed one-pot synthesis of tricyclic dihydropyrimidine derivatives. *Res. Chem. Intermed.* 42, 6221–6229. doi: 10.1007/s11164-016-2456-4

Abonia, R. (2014). Solvent-free and self-catalyzed three-component synthesis of diversely substituted pyrazolo[1,4]thiazepinones of potential antitumor activity. *Curr. Org. Synth.* 11, 773–786. doi: 10.2174/15701794116661403270020 45

Adrom, B., Hazeri, N., Lashkari, M., and Maghsoodlou, M. T. (2016). Multicomponent facile synthesis of highly substituted [1,2,4]triazolo[1,5-*a*] pyrimidines. *J. Chem. Res.* 40, 458–460. doi: 10.3184/174751916X14664307728623

Aggarwal, R., and Kumar, S. (2018). 5-Aminopyrazole as precursor in design and synthesis of fused pyrazoloazines. *Beilstein J. Org. Chem.* 14, 203–242. doi: 10.3762/bjoc.14.15

Aggarwal, R., Rani, C., Kumar, R., Garg, G., and Sharma, J. (2014). Synthesis of new bi(pyrazolo[1,5-*a*]pyrimidinyl)-7-one derivatives from dehydroacetic acid and its analogues as antibacterial agents. *Arkivoc* 2014, 120–134. doi: 10.3998/ark.5550190.p008.089

Akritopoulou-Zanze, I., Wakefield, B. D., Gasiecki, A., Kalvin, D., Johnson, E. F., Kovar, P., et al. (2011). Scaffold oriented synthesis. Part 4: Design, synthesis and biological evaluation of novel 5-substituted indazoles as potent and selective kinase inhibitors employing heterocycle forming and multicomponent reactions. *Bioorganic Med. Chem. Lett.* 21, 1480–1483. doi: 10.1016/j.bmcl.2011.01.001

Ali, K. A., Ragab, E. A., Abdelghafar, H. S., and Farag, A. M. (2016). Facile synthetic approaches for new series of pyrazole-4-carbonitrile derivatives. *Res. Chem. Intermed.* 42, 3553–3566. doi: 10.1007/s11164-015-2231-y

Al-Tel, T. H., Al-Qawasmeh, R. A., and Voelter, W. (2010). Rapid assembly of polyfunctional structures using a one-pot five- and six-component sequential Groebke-Blackburn/Ugi/Passerini process. *Eur. J. Org. Chem.* 5586–5593. doi: 10.1002/ejoc.201000808

Andriushchenko, A. Y., Desenko, S. M., Chernenko, V. N., and Chebanov, V. A. (2011). Green and efficient synthesis of pyrazolo[3,4-*b*]quinolin-5-ones derivatives by microwave-assisted multicomponent reaction in hot water medium. *J. Heterocycl. Chem.* 48, 365–367. doi: 10.1002/jhet.586

Andriushchenko, A. Y., Saraev, V. E., Shishkina, S. V., Shishkin, O. V., Musatov, V. I., Desenko, S. M., et al. (2013). Unusual direction of three-component reactions involving 2-amino-4-arylimidazoles and carbonyl compounds leading to Knoevenagel-Michael adducts. *Arkivoc* 2013, 61–80. doi: 10.3998/ark.5550190.0014.306

Ansari, A. J., Sharma, S., Pathare, R. S., Gopal, K., Sawant, D. M., and Pardasani, R. T. (2016). Solvent-free multicomponent synthesis of biologically-active fused-imidazo heterocycles catalyzed by reusable $Yb(OTf)_3$ under microwave irradiation. *ChemistrySelect* 1, 1016–1021. doi: 10.1002/slct.201600241

Aouali, M., Mhalla, D., Allouche, F., El Kaim, L., Tounsi, S., Trigui, M., et al. (2015). Synthesis, antimicrobial and antioxidant activities of imidazotriazoles and new multicomponent reaction toward 5-amino-1-phenyl[1,2,4]triazole derivatives. *Med. Chem. Res.* 24, 2732–2741. doi: 10.1007/s00044-015-1322-z

Arya, A. K., Gupta, S. K., and Kumar, M. (2012). A domino protocol for the efficient synthesis of structurally diverse benzothiazolylquinoline-2,5-diones and their spiro analogues. *Tetrahedron Lett.* 53, 6035–6038. doi: 10.1016/j.tetlet.2012.08.099

Atar, A. B., Jeong, Y. S., and Jeong, Y. T. (2014). Iron fluoride: The most efficient catalyst for one-pot synthesis of 4*H*-pyrimido[2,1-*b*]benzothiazoles under solvent-free conditions. *Tetrahedron* 70, 5207–5213. doi: 10.1016/j.tet.2014.05.094

Aydemir, E., Kansiz, S., Gumus, M. K., Gorobets, N. Y., and Dege, N. (2018). Crystal structure and Hirshfeld surface analysis of 7-ethoxy-5-methyl-2-(pyridin-3-yl)-11,12-dihydro-5,11-methano[1,2,4]triazolo[1,5-*c*][1,3,5]benzoxadiazocine. *Acta Crystallogr. Sect. E Crystallogr. Commun.* 74, 367–370. doi: 10.1107/S2056989018002621

Balwe, S. G., Shinde, V. V., Rokade, A. A., Park, S. S., and Jeong, Y. T. (2017). Green synthesis and characterization of silver nanoparticles (Ag NPs) from extract of plant *Radix Puerariae*: an efficient and recyclable catalyst for the construction of pyrimido[1,2-*b*]indazole derivatives under solvent-free conditions. *Catal. Commun.* 99, 121–126. doi: 10.1016/j.catcom.2017.06.006

Banfi, L., Basso, A., and Riva, R. (2010). "Synthesis of heterocycles through classical Ugi and Passerini reactions followed by secondary transformations involving one or two additional functional groups," in *Synthesis of Heterocycles via Multicomponent Reactions I*, eds R. V. A. Orru, and E. Ruijter (Berlin; Heidelberg: Springer-Verlag), 1–39.

Batool, I., Saeed, A., Qureshi, I. Z., Kalsoom, S., and Razzaq, A. (2016). Synthesis, molecular docking and biological evaluation of new thiazolopyrimidine carboxylates as potential antidiabetic and antibacterial agents. *Res. Chem. Intermed.* 42, 1139–1163. doi: 10.1007/s11164-015-2078-2

Baviskar, A. T., Madaan, C., Preet, R., Mohapatra, P., Jain, V., Agarwal, A., et al. (2011). N-fused imidazoles as novel anticancer agents that inhibit catalytic activity of topoisomerase IIα and induce apoptosis in G1/S phase. *J. Med. Chem.* 54, 5013–5030. doi: 10.1021/jm200235u

Benson, F. R. (1947). The chemistry of the tetrazoles. *Chem. Rev.* 41, 1–61. doi: 10.1021/cr60128a001

Berg, R., and Straub, B. F. (2013). Advancements in the mechanistic understanding of the copper-catalyzed azide–alkyne cycloaddition. *Beilstein J. Org. Chem.* 9, 2715–2750. doi: 10.3762/bjoc.9.308

Bhatt, J. D., Chudasama, C. J., and Patel, K. D. (2015). Pyrazole clubbed triazolo[1,5-*a*]pyrimidine hybrids as an anti-tubercular agents: synthesis, *in vitro* screening and molecular docking study. *Bioorganic Med. Chem.* 23, 7711–7716. doi: 10.1016/j.bmc.2015.11.018

Bhattacharjee, D., Kshiar, B., and Myrboh, B. (2016). L-Proline as an efficient enantioinduction organo-catalyst in the solvent-free

synthesis of pyrazolo[3,4-*b*]quinoline derivatives via one-pot multi-component reaction. *RSC Adv.* 6, 95944–95950. doi: 10.1039/C6RA22429F

Bienaymé, H., and Bouzid, K. (1998). A new heterocyclic multicomponent reaction for the combinatorial synthesis of fused 3-aminoimidazoles. *Angew. Chem. Int. Ed. Engl.* 37, 2234–2237. doi: 10.1002/(SICI)1521-3773(19980904)37:16<2234::AID-ANIE2234>3.0.CO;2-R

Bodaghifard, M. A., Faraki, Z., and Karimi, A. R. (2016). Mild synthesis of mono-, bis- and tris 1,2-dihydrobenzo[4,5]imidazo[1,2-*a*]pyrimidine derivatives using alkyl disulfamic acid functionalized magnetic nanoparticles. *Curr. Org. Chem.* 20, 1648–1654. doi: 10.2174/1385272820666160218233729

Boren, B. C., Narayan, S., Rasmussen, L. K., Zhang, L., Zhao, H., Lin, Z., et al. (2008). Ruthenium-catalyzed azide–alkyne cycloaddition: scope and mechanism. *J. Am. Chem. Soc.* 130, 8923–8930. doi: 10.1021/ja0749993

Burchak, O. N., Mugherli, L., Ostuni, M., Lacapère, J. J., and Balakirev, M. Y. (2011). Combinatorial discovery of fluorescent pharmacophores by multicomponent reactions in droplet arrays. *J. Am. Chem. Soc.* 133, 10058–10061. doi: 10.1021/ja204016e

Campos, P. T., Rodrigues, L. V., Belladona, A. L., Bender, C. R., Bitencurt, J. S., Rosa, F. A., et al. (2017). Regiochemistry of cyclocondensation reactions in the synthesis of polyazaheterocycles. *Beilstein J. Org. Chem.* 13, 257–266. doi: 10.3762/bjoc.13.29

Castro, V., Rodríguez, H., and Albericio, F. (2016). CuAAC: an efficient click chemistry reaction on solid phase. *ACS Comb. Sci.*18, 1–14. doi: 10.1021/acscombsci.5b00087

Centore, R., Manfredi, C., Capobianco, A., Volino, S., Ferrara, M. V., Carella, A., et al. (2017). Solid state separation and isolation of tautomers of fused-ring triazolotriazoles. *J. Org. Chem.* 82, 5155–5161. doi: 10.1021/acs.joc.7b00380

Chandak, N., Bhardwaj, J. K., Sharma, R. K., and Sharma, P. K. (2013). Inhibitors of apoptosis in testicular germ cells: Synthesis and biological evaluation of some novel IBTs bearing sulfonamide moiety. *Eur. J. Med. Chem.* 59, 203–208. doi: 10.1016/j.ejmech.2012.11.015

Chebanov, V. A., and Desenko, S. M. (2006). Dihydroazines based on α,β-unsaturated ketones reactions. *Curr. Org. Chem.* 10, 297–317. doi: 10.2174/138527206775473904

Chebanov, V. A., and Desenko, S. M. (2012). Multicomponent heterocyclization reactions with controlled selectivity (review). *Chem. Heterocycl. Compd.* 48, 566–583. doi: 10.1007/s10593-012-1030-2

Chebanov, V. A., and Desenko, S. M. (2014). Switchable multicomponent heterocyclizations for diversity oriented synthesis. *Divers. Oriented Synth.* 1, 43–63. doi: 10.2478/dos-2014-0003

Chebanov, V. A., Desenko, S. M., and Gurley, T. W. (2008a). *Azaheterocycles Based on α,β-Unsaturated Carbonyls*. Berlin; Heidelberg: Springer-Verlag.

Chebanov, V. A., Gura, K. A., and Desenko, S. M. (2010). "Aminoazoles as key reagents in multicomponent heterocyclizations," in *Synthesis of Heterocycles via Multicomponent Reactions I*, eds R. V. A. Orru, and E. Ruijter (Berlin; Heidelberg: Springer-Verlag), 41–84.

Chebanov, V. A., Sakhno, Y. I., and Desenko, S. M. (2012a). High regioselective ultrasonic-assisted synthesis of 2,7-diaryl-4,7-dihydropyrazolo[1,5-*a*]pyrimidine-5-carboxylic acids. *Ultrason. Sonochem.* 19, 707–709. doi: 10.1016/j.ultsonch.2011.08.003

Chebanov, V. A., Sakhno, Y. I., Desenko, S. M., Chernenko, V. N., Musatov, V. I., Shishkina, S. V., et al. (2007a). Cyclocondensation reactions of 5-aminopyrazoles, pyruvic acids and aldehydes. Multicomponent approaches to pyrazolopyridines and related products. *Tetrahedron* 63, 1229–1242. doi: 10.1016/j.tet.2006.11.048

Chebanov, V. A., Sakhno, Y. I., Desenko, S. M., Shishkina, S. V., Musatov, V. I., Shishkin, O. V., et al. (2005). Three-component procedure for the synthesis of 5-aryl-5,8-dihydroazolo[1,5-*a*]pyrimidine-7-carboxylic acids. *Synthesis*, 2597–2601. doi: 10.1055/s-2005-872073

Chebanov, V. A., Saraev, V. E., Desenko, S. M., Chernenko, V. N., Knyazeva, I. V., Groth, U., et al. (2008b). Tuning of chemo- and regioselectivities in multicomponent condensations of 5-aminopyrazoles, dimedone, and aldehydes. *J. Org. Chem.* 73, 5110–5118. doi: 10.1021/jo800825c

Chebanov, V. A., Saraev, V. E., Desenko, S. M., Chernenko, V. N., Shishkina, S. V., Shishkin, O. V., et al. (2007b). One-pot, multicomponent route to pyrazoloquinolizinones. *Org. Lett.* 9, 1691–1694. doi: 10.1021/ol070411l

Chebanov, V. A., Saraev, V. E., Shishkina, S. V., Shishkin, O. V., Musatov, V. I., and Desenko, S. M. (2012b). Controlled switching of multicomponent heterocyclizations of 5-amino-N-arylpyrazole-4-carboxamides, 1,3-cyclohexanediones, and aldehydes. *Eur. J. Org. Chem.* 2012, 5515–5524. doi: 10.1002/ejoc.201200669

Chen, Z., Shi, Y., Shen, Q., Xu, H., and Zhang, F. (2015). Facile and efficient synthesis of pyrazoloisoquinoline and pyrazolopyridine derivatives using recoverable carbonaceous material as solid acid catalyst. *Tetrahedron Lett.* 56, 4749–4752. doi: 10.1016/j.tetlet.2015.06.044

Chikhale, R., Thorat, S., Pant, A., Jadhav, A., Thatipamula, K. C., Bansode, R., et al. (2015). Design, synthesis and pharmacological evaluation of pyrimidobenzothiazole-3-carboxylate derivatives as selective L-type calcium channel blockers. *Bioorganic Med. Chem.* 23, 6689–6713. doi: 10.1016/j.bmc.2015.09.009

Choi, W. J., Shi, Z. D., Worthy, K. M., Bindu, L., Karki, R. G., Nicklaus, M. C., et al. (2006). Application of azide–alkyne cycloaddition 'click chemistry' for the synthesis of Grb2 SH2 domain-binding macrocycles. *Bioorganic Med. Chem. Lett.* 16, 5265–5269. doi: 10.1016/j.bmcl.2006.08.004

Cioc, R. C., Ruijter, E., and Orru, R. V. A. (2014). Multicomponent reactions: advanced tools for sustainable organic synthesis. *Green Chem.* 16, 2958–2975. doi: 10.1039/c4gc00013g

Copin, C., Buron, F., and Routier, S. (2016). Palladium-catalyzed amination of C-5 bromoimidazo[2,1-*b*]-[1,3,4]-thiadiazoles. *Eur. J. Org. Chem.* 2016, 1958–1962. doi: 10.1002/ejoc.201600145

Cowen, S. D., Russell, D., Dakin, L. A., Chen, H., Larsen, N. A., Godin, R., et al. (2016). Design, synthesis, and biological activity of substrate competitive SMYD2 inhibitors. *J. Med. Chem.* 59, 11079–11097. doi: 10.1021/acs.jmedchem.6b01303

Dam, B., Pal, A. K., and Gupta, A. (2016). Nano-Fe_3O_4@silica sulfuric acid as a reusable and magnetically separable potent solid acid catalyst in Biginelli-type reaction for the one-pot multicomponent synthesis of fused dihydropyrimidine derivatives: a greener NOSE and SFRC approach. *Synth. Commun.* 46, 275–286. doi: 10.1080/00397911.2015.1135955

Demjén, A., Gyuris, M., Wölfling, J., Puskás, L. G., and Kanizsai, I. (2014). Facile synthesis of 1*H*-imidazo[1,2-*b*]pyrazoles via a sequential one-pot synthetic approach. *Beilstein J. Org. Chem.* 10, 2338–2344. doi: 10.3762/bjoc.10.243

Desenko, S. M. (1995). Dihydroazolopyrimidines with a nodal nitrogen atom: Synthesis, reactions, tatutomerism (review). *Chem. Heterocycl. Compd.* 31, 125–136. doi: 10.1007/BF01169665

Desenko, S. M., Orlov, V. D., and Estrada, K. (1990). Formation of derivatives of 1,2,4-triazoloquinazolines in the reactions of 3-amino-1,2,4-triazoles with cyclohexanone. *Chem. Heterocycl. Compd.* 26, 839–840. doi: 10.1007/BF00509729

Devi, N., Rawal, R. K., and Singh, V. (2015). Diversity-oriented synthesis of fused-imidazole derivatives via Groebke-Blackburn-Bienayme reaction: a review. *Tetrahedron* 71, 183–232. doi: 10.1016/j.tet.2014.10.032

Dias, L. R. S., Santos, M. B., De Albuquerque, S., Castro, H. C., De Souza, A. M. T., Freitas, A. C. C., et al. (2007). Synthesis, *in vitro* evaluation, and SAR studies of a potential antichagasic 1*H*-pyrazolo[3,4-*b*]pyridine series. *Bioorganic Med. Chem.* 15, 211–219. doi: 10.1016/j.bmc.2006.09.067

Dimroth, O., and Fester, G. (1910). Triazole and tetrazole from hydrazoic acid (Engl. Transl.). *Berichte Dtsch. Chem. Gesellschaft* 43, 2219–2223.

Dimroth, O., and Merzbacher, S. (1910). Synthese von Tetrazolen aus Arylaziden. *Berichte Dtsch. Chem. Gesellschaft* 43, 2899–2904. doi: 10.1002/cber.19100430350

Diyanatizadeh, M. H., and Yavari, I. (2017). Synthesis of spiro heterocyclic systems from 2-(3-oxoisobenzofuran-1(3*H*)-ylidene)malononitrile and binucleophiles. *J. Chem. Res.* 41, 330–332. doi: 10.3184/174751917X14944355549159

Dömling, A. (2006). Recent developments in isocyanide-based multicomponent reactions in applied chemistry. *Chem. Rev.* 106, 17–89. doi: 10.1021/cr0505728

Dömling, A., and Ugi, I. (2000). Multicomponent reactions with isocyanides. *Angew. Chem. Int. Ed. Engl.* 39, 3168–3210. doi: 10.1002/1521-3773(20000915)39:18<3168::AID-ANIE3168>3.0.CO;2-U

Dömling, A., Wang, W., and Wang, K. (2012). Chemistry and biology of multicomponent reactions. *Chem. Rev.* 112, 3083–3135. doi: 10.1021/cr100233r

Ebrahimi, S. (2016). One-pot synthesis of 1,3-thiazolidin-4-one using ammonium persulfate as catalyst. *J. Sulfur Chem.* 5993, 1–6. doi: 10.1080/17415993.2016.1223298

El Rady, E. A. (2014). Three-component uncatalyzed eco-friendly reactions for one-pot synthesis of 4,7-dihydro[1,2,4]triazolo[1,5-*a*]pyrimidine derivatives. *J. Heterocycl. Chem.* 51, 869–875. doi: 10.1002/jhet.1771

El-Borai, M. A., Rizk, H. F., Abd-Aal, M. F., and El-Deeb, I. Y. (2012). Synthesis of pyrazolo[3,4-*b*]pyridines under microwave irradiation in multi-component reactions and their antitumor and antimicrobial activities–part 1. *Eur. J. Med. Chem.* 48, 92–96. doi: 10.1016/j.ejmech.2011.11.038

El-Emary, T. I., and El-Mohsen, S. A. (2012). Multi-component one-pot synthesis and antimicrobial activities of 3-methyl-1,4-diphenyl-7-thioxo-4,6,8,9-tetrahydro-pyrazolo[5,4-*b*]pyrimidino[5,4-*e*]pyridine-5-one and related derivatives. *Molecules* 17, 14464–14483. doi: 10.3390/molecules171214464

Fan, L., Yao, C., and Shu, M. (2016). Three-component synthesis of new *o*-hydroxyphenyl-substituted pyrazolo[3,4-*b*]pyridines promoted by $FeCl_3$. *Heterocycl. Commun.* 22, 63–67. doi: 10.1515/hc-2015-0234

Fang, S., Niu, X., Yang, B., Li, Y., Si, X., Feng, L., et al. (2014). One-Pot synthesis of benzo[4,5]imidazo[1,2-*a*]quinazoline derivatives via facile transition-metal-free tandem process. *ACS Comb. Sci.* 16, 328–332. doi: 10.1021/co500001u

Farghaly, A.-R., and El-Kashef, H. (2011). Pyrazoles and pyrazolo[4,3-*e*]pyrrolo[1,2-*a*]pyrazines II. *J. Heterocycl. Chem.* 48, 678–683. doi: 10.1002/jhet.581

Farghaly, T., S., Shawali, A. M. H., Abbas, E. A., and Abdel-hafez, N. (2015). A facile synthesis of new polyazaheterocycles via one-pot three-components condensation reaction and study of their reactions with nitrilimines. *Curr. Org. Synth.* 12, 95–101. doi: 10.2174/1570179411666140806005524

Finlay, H. J., Jiang, J., Caringal, Y., Kover, A., Conder, M. L., Xing, D., et al. (2013). Triazolo and imidazo dihydropyrazolopyrimidine potassium channel antagonists. *Bioorganic Med. Chem. Lett.* 23, 1743–1747. doi: 10.1016/j.bmcl.2013.01.064

Finlay, H. J., Lloyd, J., Vaccaro, W., Kover, A., Yan, L., Bhave, G., et al. (2012). Discovery of ((*S*)-5-(methoxymethyl)-7-(1-methyl-1*H*-indol-2-yl)-2-(trifluoromethyl)-4,7-dihydro pyrazolo[1,5-*a*]pyrimidin-6-yl)((*S*)-2-(3-methylisoxazol-5-yl)pyrrolidin-1-yl)methanone as a potent and selective I_{Kur} inhibitor. *J. Med. Chem.* 55, 3036–3048. doi: 10.1021/jm201386u

Frolova, L. V., Malik, I., Uglinskii, P. Y., Rogelj, S., Kornienko, A., and Magedov, I., V (2011). Multicomponent synthesis of 2,3-dihydrochromeno[4,3-*d*]pyrazolo[3,4-*b*]pyridine-1,6-diones: a novel heterocyclic scaffold with antibacterial activity. *Tetrahedron Lett.* 52, 6643–6645. doi: 10.1016/j.tetlet.2011.10.012

Fusco, S., Maglione, C., Velardo, A., Piccialli, V., Liguori, R., Peluso, A., et al. (2016). N-rich fused heterocyclic systems: synthesis, structure, optical and electrochemical characterization. *Eur. J. Org. Chem.* 2016, 1772–1780. doi: 10.1002/ejoc.201501283

Galante, R. J., and Somerville, N. J. (1996). *Method of Synthesizing Sterically Hindered 5-Substituted-1H-Tetrazoles From Nitriles Using a Lewis Acid and an Azide*. U.S. Patent No 5502191. Madison, NJ: U.S. American Cyanamid Company.

Gao, L., Song, Y., Zhang, X., Guo, S., and Fan, X. (2014). Copper-catalyzed tandem reactions of 2-bromobenzaldehydes/ketones with aminopyrazoles toward the synthesis of pyrazolo[1,5-*a*]quinazolines. *Tetrahedron Lett.* 55, 4997–5002. doi: 10.1016/j.tetlet.2014.07.028

Gaponik, P. N., and Karavai, V. P. (1984). Synthesis and properties of 1,5-diaminotetrazole. *Chem. Heterocycl. Compd.* 20, 1388–1391. doi: 10.1007/BF00505966

Gaponik, P. N., Karavai, V. P., Davshko, I. E., Degtyarik, M. M., and Bogatikov, A. N. (1990). Synthesis and properties of phenylenebis-1*H*-tetrazoles. *Chem. Heterocycl. Compd.* 26, 1274–1278. doi: 10.1007/BF00476984

Gaponik, P. N., Karavai, V. P., and Grigor'ev, Y. V. (1985). Synthesis of 1-substituted tetrazoles by heterocyclization of primary amines, orthoformic ester, and sodium azide. *Chem. Heterocycl. Compd.* 21, 1255–1258. doi: 10.1007/BF00515224

Gege, C., Bao, B., Bluhm, H., Boer, J., Gallagher, B. M., Korniski, B., et al. (2012). Discovery and evaluation of a non-Zn chelating, selective matrix metalloproteinase 13 (MMP-13) inhibitor for potential intra-articular treatment of osteoarthritis. *J. Med. Chem.* 55, 709–716. doi: 10.1021/jm201152u

Gein, V. L., Kazantseva, M. I., Zamaraeva, T. M., Gein, L. F., and Slepukhin, P. A. (2015). Synthesis of 9-aryl-5,6,7,9-tetrahydrotetrazolo[5,1-*b*]quinazolin-8(4*H*)-ones. *Russ. J. Gen. Chem.* 85, 1984–1986. doi: 10.1134/S1070363215080332

Gein, V. L., Zamaraeva, T. M., Nosova, N. V., Vakhrin, M. I., and Slepukhin, P. A. (2012). Synthesis of N-substituted 7-aryl-5-methyl-4,7-dihydrotetrazolo[1,5-*a*]pyrimidine-6-carboxamides. *Russ. J. Org. Chem.* 48, 419–422. doi: 10.1134/S107042801203013X

Gein, V. L., Zamaraeva, T. M., and Vakhrin, M. I. (2014). Synthesis of N,7-diaryl-5-methyl-4,7-dihydro-1,2,4-triazolo[1,5-α]pyrimidine-6-carboxamides. *Russ. J. Gen. Chem.* 84, 82–85. doi: 10.1134/S1070363214010125

Ghatole, A. M., Lanjewar, K. R., Gaidhane, M. K., and Hatzade, K. M. (2015). Evaluation of substituted methyl cyclohexanone hybrids for anti-tubercular, anti-bacterial and anti-fungal activity: facile syntheses under catalysis by ionic liquids. *Spectrochim. Acta Part A Mol. Biomol. Spectrosc.* 151, 515–524. doi: 10.1016/j.saa.2015.06.035

Ghorbani-Vaghei, R., Toghraei-Semiromi, Z., Amiri, M., and Karimi-Nami, R. (2013). One-pot synthesis of tetrazolo[1,5-*a*]pyrimidines under solvent-free conditions. *Mol. Divers.* 17, 307–318. doi: 10.1007/s11030-013-9435-0

Gladkov, E. S., Desenko, S. M., Konovalova, I. S., Groth, U., Shishkin, O. V., Vashchenko, E. V., et al. (2013). Microwave-assisted and ultrasonic-assisted three-component heterocyclization of 4-amino-5-carboxamido-1,2,3-triazole, thiopyran-3-one-1,1-dioxide, and aromatic aldehydes. *J. Heterocycl. Chem.* 50, E189–E192. doi: 10.1002/jhet.1503

Gladkov, E. S., Gura, K. A., Sirko, S. M., Desenko, S. M., Groth, U., and Chebanov, V. A. (2012). Features of the behavior of 4-amino-5-carboxamido-1,2,3-triazole in multicomponent heterocyclizations with carbonyl compounds. *Beilstein J. Org. Chem.* 8, 2100–2105. doi: 10.3762/bjoc.8.236

Gladkov, E. S., Sirko, S. N., Shishkina, S. V., Shishkin, O. V., Knyazeva, I. V., Desenko, S. M., et al. (2010). Efficient multicomponent synthesis of highly substituted [1,2,3]triazolo[1,5-*a*]pyrimidines. *Monatshefte Chemie Chem. Mon.* 141, 773–779. doi: 10.1007/s00706-010-0326-0

Gorobets, N. Y., Sedash, Y. V., Ostras, K. S., Zaremba, O. V., Shishkina, S. V., Baumer, V. N., et al. (2010). Unexpected alternative direction of a Biginelli-like multicomponent reaction with 3-amino-1,2,4-triazole as the urea component. *Tetrahedron Lett.* 51, 2095–2098. doi: 10.1016/j.tetlet.2010.02.045

Goryaeva, M. V., Burgart, Y. V., Ezhikova, M. A., Kodess, M. I., and Saloutin, V. I. (2015). The reactions of 2-ethoxymethylidene-3-oxo esters and their analogues with 5-aminotetrazole as a way to novel azaheterocycles. *Beilstein J. Org. Chem.* 11, 385–391. doi: 10.3762/bjoc.11.44

Grigoriev, Y. V., Voitekhovich, S. V., Karavai, V. P., and Ivashkevich, O. A. (2017). Synthesis of tetrazole and its derivatives by heterocyclization reaction involving primary amines, orthoesters, and azides. *Chem. Heterocycl. Compd.* 53, 670–681. doi: 10.1007/s10593-017-2108-7

Guchhait, S. K., Chandgude, A. L., and Priyadarshani, G. (2012). $CuSO_4$ – glucose for *in situ* generation of controlled Cu(I)–Cu(II) bicatalysts: multicomponent reaction of heterocyclic azine and aldehyde with alkyne, and cycloisomerization toward synthesis of N-fused Imidazoles. *J. Org. Chem.* 77, 4438–4444. doi: 10.1021/jo3003024

Guchhait, S. K., and Madaan, C. (2009). An efficient, regioselective, versatile synthesis of N-fused 2- and 3-aminoimidazoles via Ugi-type multicomponent reaction mediated by zirconium(IV) chloride in polyethylene glycol-400. *Synlett* 2009, 628–632. doi: 10.1055/s-0028-1087915

Guchhait, S. K., and Madaan, C. (2010). Towards molecular diversity: dealkylation of tert-butyl amine in Ugi-type multicomponent reaction product establishes tert-butyl isocyanide as a useful convertible isonitrile. *Org. Biomol. Chem.* 8, 3631–3634. doi: 10.1039/c0ob00022a

Guchhait, S. K., Madaan, C., and Thakkar, B. S. (2009). A highly flexible and efficient Ugi-type multicomponent synthesis of versatile N-fused aminoimidazoles. *Synthesis* 2009, 3293–3300. doi: 10.1055/s-0029-1216916

Gujjar, R., El Mazouni, F., White, K. L., White, J., Creason, S., Shackleford, D. M., et al. (2011). Lead optimization of aryl and aralkyl amine-based triazolopyrimidine inhibitors of plasmodium falciparum dihydroorotate dehydrogenase with antimalarial activity in mice. *J. Med. Chem.* 54, 3935–3949. doi: 10.1021/jm200265b

Gümüş, M. K., Gorobets, N. Y., Sedash, Y. V., Chebanov, V. A., and Desenko, S. M. (2017a). A modified Biginelli reaction toward oxygen-bridged tetrahydropyrimidines fused with substituted 1,2,4-triazole ring. *Chem. Heterocycl. Compd.* 53, 1261–1267. doi: 10.1007/s10593-018-2204-3

Gümüş, M. K., Gorobets, N. Y., Sedash, Y. V., Shishkina, S. V., and Desenko, S. M. (2017b). Rapid formation of chemical complexity via

a modified Biginelli reaction leading to dihydrofuran-2(3*H*)-one spiro-derivatives of triazolo[1,5-*a*]pyrimidine. *Tetrahedron Lett.* 58, 3446–3448. doi: 10.1016/j.tetlet.2017.07.071

Gunasekaran, P., Indumathi, S., and Perumal, S. (2013). L-Proline-catalyzed three-component domino reactions in the regioselective synthesis of novel densely functionalized pyrazolo[3,4-*b*]pyridines. *RSC Adv.* 3, 8318–8325. doi: 10.1039/c3ra00136a

Gurevich, P. A., Sattarova, L. F., Petrovskiy, A. S., Frolova, N. A., Strunin, B. P., and Musin, R. Z. (2011). Interaction of spiro-heterocyclic oxindole system with sodium diformylimide. *Chem. Heterocycl. Compd.* 46, 1527–1530. doi: 10.1007/s10593-011-0703-6

Hajra, S., Sinha, D., and Bhowmick, M. (2007). Metal triflate catalyzed reactions of alkenes, NBS, nitriles, and $TMSN_3$: synthesis of 1,5-disubstituted tetrazoles. *J. Org. Chem.* 72, 1852–1855. doi: 10.1021/jo062432j

Haleel, A., Arthi, P., Reddy, N. D., Veena, V., Sakthivel, N., Arun, Y., et al. (2014). DNA binding, molecular docking and apoptotic inducing activity of nickel(II), copper(II) and zinc(II) complexes of pyridine-based tetrazolo[1,5-*a*]pyrimidine ligands. *RSC Adv.* 4, 60816–60830. doi: 10.1039/C4RA11197D

Hamama, W. S., Ibrahim, M. E., and Zoorob, H. H. (2012). Efficient regioselective synthesis and potential antitumor evaluation of isoxazolo[5,4-*b*]pyridines and related annulated compounds. *Arch. Pharm.* 345, 468–475. doi: 10.1002/ardp.201100258

Hassaneen, H. M. E., and Farghaly, T. A. (2015). A simple, convenient, one-pot synthesis of dihydro-azolopyrimidines, DFT calculation, and NMR determination by using H-ferrierite zeolite as catalyst. *J. Heterocycl. Chem.* 52, 1154–1161. doi: 10.1002/jhet.2152

Hatti, I., Sreenivasulu, R., Jadav, S. S., Jayaprakash, V., Kumar, C. G., and Raju, R. R. (2015). Synthesis, cytotoxic activity and docking studies of new 4-aza-podophyllotoxin derivatives. *Med. Chem. Res.* 24, 3305–3313. doi: 10.1007/s00044-015-1375-z

He, X. P., Zeng, Y. L., Zang, Y., Li, J., Field, R. A., and Chen, G. R. (2016). Carbohydrate CuAAC click chemistry for therapy and diagnosis. *Carbohydr. Res.* 429, 1–22. doi: 10.1016/J.CARRES.2016.03.022

Hedidi, M., Maillard, J., Erb, W., Lassagne, F., Halauko, Y. S., Ivashkevich, O. A., et al. (2017). Fused systems based on 2-aminopyrimidines: synthesis combining deprotolithiation-*in situ* zincation with N-arylation reactions and biological properties. *Eur. J. Org. Chem.* 2017, 5903–5915. doi: 10.1002/ejoc.201701004

Hein, J. E., and Fokin, V., V (2010). Copper-catalyzed azide-alkyne cycloaddition (CuAAC) and beyond: new reactivity of copper(I) acetylides. *Chem. Soc. Rev.* 39, 1302–1315. doi: 10.1039/b904091a

Hemmati, B., Javanshir, S., and Dolatkhah, Z. (2016). Hybrid magnetic Irish moss/Fe_3O_4 as a nano-biocatalyst for synthesis of imidazopyrimidine derivatives. *RSC Adv.* 6, 50431–50436. doi: 10.1039/C6RA08504K

Hieke, M., Rödl, C. B., Wisniewska, J. M., La Buscató, E., Stark, H., Schubert-Zsilavecz, M., et al. (2012). SAR-study on a new class of imidazo[1,2-*a*]pyridine-based inhibitors of 5-lipoxygenase. *Bioorganic Med. Chem. Lett.* 22, 1969–1975. doi: 10.1016/j.bmcl.2012.01.038

Hill, M. D. (2016). A multicomponent approach to highly substituted 1*H*-pyrazolo[3,4-*b*]pyridines. *Synthesis* 48, 2201–2204. doi: 10.1055/s-0035-1562230

Hossein Nia, R., Mamaghani, M., Shirini, F., and Tabatabaeian, K. (2014). A convenient one-pot three-component approach for regioselective synthesis of novel substituted pyrazolo[1,5-*a*]pyrimidines using Fe^{+3}-montmorillonite as efficient catalyst. *J. Heterocycl. Chem.* 51, 363–367. doi: 10.1002/jhet.1576

Huang, Z., Hu, Y., Zhou, Y., and Shi, D. (2011). Efficient one-pot three-component synthesis of fused pyridine derivatives in ionic liquid. *ACS Comb. Sci.* 13, 45–49. doi: 10.1021/co1000162

Hudwekar, A. D., Reddy, G. L., Verma, P. K., Gupta, S., Vishwakarma, R. A., and Sawant, S. D. (2017). Transition metal-free single step approach for arylated pyrazolopyrimidinones and quinazolinones using benzylamines/benzylalcohols/benzaldehydes. *ChemistrySelect* 2, 4963–4968. doi: 10.1002/slct.201700896

Ishihara, K., Kawashima, M., Matsumoto, T., Shioiri, T., and Matsugi, M. (2018). A practical synthesis of 5-substituted 1*H*-tetrazoles from aldoximes employing the azide anion from diphenyl phosphorazidate. *Synthesis* 50, 1293–1300. doi: 10.1055/s-0036-1591851

Ivachtchenko, A. V., Golovina, E. S., Kadieva, M. G., Koryakova, A. G., Mitkin, O. D., Tkachenko, S. E., et al. (2011). 2-Substituted 5,6-dimethyl-3-phenylsulfonyl-pyrazolo[1,5-*a*]pyrimidines: New series of highly potent and specific serotonin 5-HT6 receptor antagonists. *Eur. J. Med. Chem.* 46, 1189–1197. doi: 10.1016/j.ejmech.2011.01.038

Jalani, H. B., Karagöz, A. Ç., and Tsogoeva, S. B. (2017). Synthesis of substituted 1,2,3-triazoles via metal-free click cycloaddition reactions and alternative cyclization methods. *Synthesis* 49, 29–41. doi: 10.1055/s-0036-1588904

Janreddy, D., Kavala, V., Kuo, C. W., Chen, W. C., Ramesh, C., Kotipalli, T., et al. (2013). Copper(I)-catalyzed aerobic oxidative azide-alkene cycloaddition: an efficient synthesis of substituted 1,2,3-triazoles. *Adv. Synth. Catal.* 355, 2918–2927. doi: 10.1002/adsc.201300344

Jiang, B., Liu, Y.-P., and Tu, S.-J. (2011). Facile three-component synthesis of macrocyclane-fused pyrazolo[3,4-*b*]pyridine derivatives. *Eur. J. Org. Chem.* 2011, 3026–3035. doi: 10.1002/ejoc.201100127

Jiang, B., Ma, N., Wang, X. H., Tu, S. J., and Li, G. (2012). Microwave-assisted multicomponent reaction in water: highly stereoselective synthesis of pyrimidinespiroisoxazolo[5,4-*b*]pyridine derivatives. *Heterocycles* 84, 765–774. doi: 10.3987/COM-11-S(P)53

Jiang, B., Ye, Q., Fan, W., Wang, S. L., Tu, S. J., and Li, G. (2014). Four-component strategy for selective synthesis of azepino[5,4,3-*cd*]indoles and pyrazolo[3,4-*b*]pyridines. *Chem. Commun.* 50, 6108–6111. doi: 10.1039/C4CC00740A

Jin, T., Kamijo, S., and Yamamoto, Y. (2004). Synthesis of 1-substituted tetrazoles via the acid-catalyzed [3 + 2] cycloaddition between isocyanides and trimethylsilyl azide. *Tetrahedron Lett.* 45, 9435–9437. doi: 10.1016/j.tetlet.2004.10.103

Johansson, J. R., Beke-Somfai, T., Said Stålsmeden, A., and Kann, N. (2016). Ruthenium-catalyzed azide alkyne cycloaddition reaction: scope, mechanism, and applications. *Chem. Rev.* 116, 14726–14768. doi: 10.1021/acs.chemrev.6b00466

Joo, Y. H., and Shreeve, J. M. (2008). 1-Substituted 5-aminotetrazoles: syntheses from CNN_3 with primary amines. *Org. Lett.* 10, 4665–4667. doi: 10.1021/ol8019742

Joule, J. A., and Mills, K. (2010). *Heterocyclic Chemistry*. *5th Edn*. Chichester, UK: Wiley-Blackwell.

Kaim, L., El Grimaud, L., and Patil, P. (2011). Three-component strategy toward 5-membered heterocycles from isocyanide dibromides. *Org. Lett.* 13, 1261–1263. doi: 10.1021/ol200003u

Kamal, A., Dastagiri, D., Ramaiah, M. J., Reddy, J. S., Bharathi, E. V., Srinivas, C., et al. (2010). Synthesis of imidazothiazole-chalcone derivatives as anticancer and apoptosis inducing agents. *ChemMedChem* 5, 1937–1947. doi: 10.1002/cmdc.201000346

Kamal, A., Suresh, P., Mallareddy, A., Kumar, B. A., Reddy, P. V., Raju, P., et al. (2011). Synthesis of a new 4-aza-2,3-didehydropodophyllotoxin analogues as potent cytotoxic and antimitotic agents. *Bioorganic Med. Chem.* 19, 2349–2358. doi: 10.1016/j.bmc.2011.02.020

Kamijo, S., Jin, T., Huo, Z., and Yamamoto, Y. (2002). Regiospecific synthesis of 2-allyl-1,2,3-triazoles by palladium-catalyzed 1,3-dipolar cycloaddition. *Tetrahedron Lett.* 43, 9707–9710. doi: 10.1016/S0040-4039(02)02206-2

Kantin, G. P., and Krasavin, M. (2016). Reaction of α-tetralone, 1*H*-tetrazol-5-amine, and aromatic aldehydes upon microwave irradiation – a convenient method for the synthesis of 5,6,7,12-tetrahydrobenzo[*h*]tetrazolo[5,1-*b*]quinazolines. *Chem. Heterocycl. Compd.* 52, 918–922. doi: 10.1007/s10593-017-1985-0

Karami, B., Farahi, M., and Banaki, Z. (2015a). A new protocol for catalyst-free regioselective synthesis of 5,9-dihydropyrimido[5,4-*e*][1,2,4]triazolo[1,5-*a*]pyrimidine-6,8(4*H*,7*H*)-diones. *Synlett* 26, 741–744. doi: 10.1055/s-0034-1379953

Karami, B., Farahi, M., and Banaki, Z. (2015b). A novel one-pot method for highly regioselective synthesis of triazoloapyrimidinedicarboxylates using silica sodium carbonate. *Synlett* 26, 1804–1807. doi: 10.1055/s-0034-1380677

Karimi, A. R., and Bayat, F. (2011). Mono- and bis-pyrimido[1,2-*a*]benzimidazoles: alum catalyzed regioselective three- or pseudo five-component reaction of 2-aminobenzimidazole with aldehyde and malononitrile. *Lett. Org. Chem.* 8, 631–636. doi: 10.2174/157017811799304368

Karnakar, K., Narayana Murthy, S., Ramesh, K., Satish, G., Nanubolu, J. B., and Nageswar, Y. V. D. (2012). Polyethylene glycol (PEG-400): An efficient

and recyclable reaction medium for the synthesis of pyrazolo[3,4-*b*]quinoline derivatives. *Tetrahedron Lett.* 53, 2897–2903. doi: 10.1016/j.tetlet.2012.03.135

Kaur, G., Raj, T., Kaur, N., and Singh, N. (2015). Pyrimidine-based functional fluorescent organic nanoparticle probe for detection of *Pseudomonas aeruginosa*. *Org. Biomol. Chem.* 13, 4673–4679. doi: 10.1039/C5OB00206K

Kaur, N., Kaur, K., Raj, T., Kaur, G., Singh, A., Aree, T., et al. (2015). One-pot synthesis of tricyclic dihydropyrimidine derivatives and their biological evaluation. *Tetrahedron* 71, 332–337. doi: 10.1016/j.tet.2014.11.039

Keith, J. M. (2006). One-step conversion of pyridine *N*-oxides to tetrazolo[1,5-*a*]pyridines. *J. Org. Chem.* 71, 9540–9543. doi: 10.1021/jo061819j

Keivanloo, A., Bakherad, M., Taheri, S. A. N., and Samangooei, S. (2013). One-pot synthesis of 4,5-disubstituted 1,2,3-(NH)-triazoles by silica supported-zinc bromide in the aerobic condition. *Comptes Rendus Chim.* 16, 239–243. doi: 10.1016/j.crci.2012.11.007

Khurana, J. M., Chaudhary, A., Nand, B., and Lumb, A. (2012). Aqua mediated indium(III) chloride catalyzed synthesis of fused pyrimidines and pyrazoles. *Tetrahedron Lett.* 53, 3018–3022. doi: 10.1016/j.tetlet.2012.04.001

Kolb, H. C., Finn, M. G., and Sharpless, K. B. (2001). Click chemistry: diverse chemical function from a few good reactions. *Angew. Chemie Int. Ed.* 40, 2004–2021. doi: 10.1002/1521-3773(20010601)40:11<2004::AID-ANIE2004>3.0.CO;2-5

Kolos, N. N., Kovalenko, L. U., and Borovskoy, V. A. (2011). Reactions of 3-aroylacrylates with α-aminoazoles. *Chem. Heterocycl. Compd.* 47, 983–988. doi: 10.1007/s10593-011-0864-3

Kombarov, R., Altieri, A., Genis, D., Kirpichenok, M., Kochubey, V., Rakitina, N., et al. (2010). BioCores: identification of a drug/natural product-based privileged structural motif for small-molecule lead discovery. *Mol. Divers.* 14, 193–200. doi: 10.1007/s11030-009-9157-5

Komykhov, S. A., Bondarenko, A. A., Musatov, V. I., Diachkov, M. V., Gorobets, N. Y., and Desenko, S. M. (2017). (5*S*,7*R*)-5-aryl-7-methyl-4,5,6,7-tetrahydro-[1,2,4]triazolo[1,5-*a*]pyrimidin-7-ols as products of three-component condensation. *Chem. Heterocycl. Compd.* 53, 378–380. doi: 10.1007/s10593-017-2059-z

Komykhov, S. A., Tkachenko, I. G., Musatov, V. I., Diachkov, M. V., Chebanov, V. A., and Desenko, S. M. (2016). Multicomponent synthesis in water of 7-unsubstituted 4,7-dihydro- 1,2,4-triazolo[1,5-*a*]pyrimidines and their antimicrobial and antifungal activity. *Arkivoc* 2016, 277–287. doi: 10.3998/ark.5550190.p009.610

Kondratiuk, M., Gorobets, N., Sedash, Y., Gümüş, M., and Desenko, S. (2016). 5-(5-Bromo-2-hydroxy-3-methoxyphenyl)-7-methyl-4,5,6,7-tetrahydro[1,2,4]triazolo[1,5-*a*]pyrimidin-7-ol. *Molbank* 2016:M898. doi: 10.3390/M898

Konstantinova, L. S., Knyazeva, E. A., Nefyodov, A. A., Camacho, P. S., Ashbrook, S. E. M., Woollins, J. D., et al. (2015). Direct synthesis of fused 1,2,5-selenadiazoles from 1,2,5-thiadiazoles. *Tetrahedron Lett.* 56, 1107–1110. doi: 10.1016/j.tetlet.2015.01.106

Koopmanschap, G., Ruijter, E., and Orru, R. V. (2014). Isocyanide-based multicomponent reactions towards cyclic constrained peptidomimetics. *Beilstein J. Org. Chem.* 10, 544–598. doi: 10.3762/bjoc.10.50

Kour, P., Singh, V. P., Khajuria, B., Singh, T., and Kumar, A. (2017). Al(III) chloride catalyzed multi-component domino strategy: Synthesis of library of dihydrotetrazolo[1,5-*a*]pyrimidines and tetrahydrotetrazolo[1,5-*a*]quinazolinones. *Tetrahedron Lett.* 58, 4179–4185. doi: 10.1016/j.tetlet.2017.09.052

Krasavin, M., Tsirulnikov, S., Nikulnikov, M., Kysil, V., and Ivachtchenko, A. (2008). Poorly reactive 5-piperazin-1-yl-1,3,4-thiadiazol-2-amines rendered as valid substrates for Groebke-Blackburn type multi-component reaction with aldehydes and isocyanides using TMSCl as a promoter. *Tetrahedron Lett.* 49, 5241–5243. doi: 10.1016/j.tetlet.2008.06.113

Kumar, A., Kumar, M., Maurya, S., and Khanna, R. S. (2014). Regioselective synthesis of fused imidazo[1,2-*a*]pyrimidines via intramolecular C–N bond formation/6-*endo-dig* cycloisomerization. *J. Org. Chem.* 79, 6905–6912. doi: 10.1021/jo5007762

Kumar, D., Sonawane, M., Pujala, B., Jain, V. K., Bhagat, S., and Chakraborti, A. K. (2013). Supported protic acid-catalyzed synthesis of 2,3-disubstituted thiazolidin-4-ones: enhancement of the catalytic potential of protic acid by adsorption on solid supports. *Green Chem.* 15, 2872–2884. doi: 10.1039/c3gc41218k

Kumari, K., Raghuvanshi, D. S., and Singh, K. N. (2012). An expeditious synthesis of tetrahydro-1,2,4-triazolo[5,1-*b*]quinazolin-8(4*H*)-ones and dihydro-1,2,4-triazolo[1,5-*a*]pyrimidines. *Org. Prep. Proced. Int.* 44, 460–466. doi: 10.1080/00304948.2012.715062

Kurzer, F., and Godfrey, L. E. A. (1963). Syntheses of heterocyclic compounds from aminoguanidine. *Angew. Chemie Int. Ed.* 2, 459–476. doi: 10.1002/anie.196304591

Kysil, V., Khvat, A., Tsirulnikov, S., Tkachenko, S., Williams, C., Churakova, M., et al. (2010). General multicomponent strategy for the synthesis of 2-amino-1,4-diazaheterocycles: scope, limitations, and utility. *Eur. J. Org. Chem.* 2010, 1525–1543. doi: 10.1002/ejoc.200901360

Lauro, G., Manfra, M., Pedatella, S., Fischer, K., Cantone, V., Terracciano, S., et al. (2017). Identification of novel microsomal prostaglandin E2 synthase-1 (mPGES-1) lead inhibitors from fragment virtual screening. *Eur. J. Med. Chem.* 125, 278–287. doi: 10.1016/j.ejmech.2016.09.042

Lee, C.-H., Hsu, W.-S., Chen, C.-H., and Sun, C.-M. (2013). A telescoping synthesis of chimeric polyheterocycles through a piperidine- mediated multicomponent reaction. *Eur. J. Org. Chem.* 2013, 2201–2208. doi: 10.1002/ejoc.201201645

Lee, S., Koo, H., Na, J. H., Han, S. J., Min, H. S., Lee, S. J., et al. (2014). Chemical tumor-targeting of nanoparticles based on metabolic glycoengineering and click chemistry. *ACS Nano* 8, 2048–2063. doi: 10.1021/nn406584y

Li, L., Xu, H., Dai, L., Xi, J., Gao, L., and Rong, L. (2017). An efficient metal-free cascade process for the synthesis of 4-arylpyrimido[1,2-*b*]indazole-3-carbonitrile derivatives. *Tetrahedron* 73, 5358–5365. doi: 10.1016/j.tet.2017.07.035

Li, T., Yao, C., Yu, C., Wang, X., and Tu, S.-J. (2012). Ionic liquid-mediated one-pot synthesis of 5-(trifluoromethyl)-4,7-dihydrotetrazolo[1,5-*a*]pyrimidine derivatives. *Synth. Commun.* 42, 2728–2738. doi: 10.1080/00397911.2011.566460

Liang, L., and Astruc, D. (2011). The copper(I)-catalyzed alkyne-azide cycloaddition (CuAAC) "click" reaction and its applications. An overview. *Coord. Chem. Rev.* 255, 2933–2945. doi: 10.1016/j.ccr.2011.06.028

Lipson, V. V., Borodina, V. V., Zemlyanaya, N. I., Shirobokova, M. G., Musatov, V. I., Shishkina, S. V., et al. (2015). Domino reactions of 3-methyl-5-aminopyrazole with aryl(hetaryl)aldehydes, cyclopentanone, cyclopentan-1,3-dione, and 1,3-indanedione. *Russ. J. Org. Chem.* 51, 697–704. doi: 10.1134/S1070428015050206

Lipson, V. V., and Gorobets, N. Y. (2009). One hundred years of Meldrum's acid: advances in the synthesis of pyridine and pyrimidine derivatives. *Mol. Divers.* 13, 399–419. doi: 10.1007/s11030-009-9136-x

Lipson, V. V., Svetlichnaya, N. V., Borodina, V. V., Shirobokova, M. G., Shishkina, S. V., Shishkin, O. V., et al. (2010). Cascade cyclization of 3(5)-aminopyrazoles with aromatic aldehydes and cyclohexanediones. *Russ. J. Org. Chem.* 46, 1388–1298. doi: 10.1134/S1070428010090216

Lipson, V. V., Svetlichnaya, N. V., Shirobokova, M. G., Musatov, V. I., Shishkin, O. V., and Shishkina, S. V. (2012). Cascade cyclization of 1,2-diamino-4-phenylimidazole with aromatic aldehydes and cyclohexanediones. *Russ. J. Org. Chem.* 48, 273–277. doi: 10.1134/S1070428012020182

Liu, J., Lei, M., and Hu, L. (2012a). A catalyst-free reaction in water: synthesis of benzo[4,5]imidazo[1,2-*a*]pyrimido[4,5-*d*]pyrimidin-4(1*H*)-one derivatives. *Green Chem.* 14, 2534–2539. doi: 10.1039/C2GC35745C

Liu, J., Lei, M., and Hu, L. (2012b). Thiamine hydrochloride (VB_1): as an efficient promoter for the one-pot synthesis of benzo[4,5]imidazo[1,2-*a*]pyrimidine and [1,2,4]triazolo[1,5-*a*] pyrimidine derivatives in water medium. *Green Chem.* 14, 840–846. doi: 10.1039/C2GC16499J

Ma, N., Jiang, B., Zhang, G., Tu, S., Wever, W., and Li, G. (2010). New multicomponent domino reactions (MDRs) in water: highly chemo-, regio- and stereoselective synthesis of spiro{[1,3]dioxanopyridine}-4,6-diones and pyrazolo[3,4-*b*]pyridines. *Green Chem.* 12, 1357–1361. doi: 10.1039/c0gc00073f

Mahdavinia, G. H., and Rahmati, A. (2015). Silica sulfuric acid as a solid acid catalyzed synthesis of 4,5,6,7-tetrahydro-2*H*-pyrazolo[3,4-*b*]pyridine-5-carbonitriles and 1,4-diaryl-4,5-dihydro-3-methyl-1*H*-pyrazolo[3,4-*b*]pyridine-6(7*H*)-ones. *Rev. Roum. Chim.* 60, 1025–1032.

Makarov, V. A., Braun, H., Richter, M., Riabova, O. B., Kirchmair, J., Kazakova, E. S., et al. (2015). Pyrazolopyrimidines: potent inhibitors targeting

the capsid of rhino- and enteroviruses. *ChemMedChem* 10, 1629–1634. doi: 10.1002/cmdc.201500304

Maleki, A., Aghaei, M., and Ghamari, N. (2015). Synthesis of benzimidazolo[2,3-*b*]quinazolinone derivatives via a one-pot multicomponent reaction promoted by a chitosan-based composite magnetic nanocatalyst. *Chem. Lett.* 44, 259–261. doi: 10.1246/cl.141074

Maleki, A., Ravaghi, P., Aghaei, M., and Movahed, H. (2017). A novel magnetically recyclable silver-loaded cellulose-based bionanocomposite catalyst for green synthesis of tetrazolo[1,5-*a*]pyrimidines. *Res. Chem. Intermed.* 43, 5485–5494. doi: 10.1007/s11164-017-2941-4

Mamaghani, M., Tabatabaeian, K., Bayat, M., Nia, R. H., and Rassa, M. (2013). Regioselective synthesis and antibacterial evaluation of a new class of substituted pyrazolo[3,4-*b*]pyridines. *J. Chem. Res.* 37, 494–498. doi: 10.3184/174751913X13735444714766

Marjani, A. P., Khalafy, J., Salami, F., and Ezzati, M. (2015). The synthesis of new pyrazolo[1,5-*a*]pyrimidine derivatives. *Arkivoc* 2015, 277–286. doi: 10.3998/ark.5550190.p009.062

Martinez-Ariza, G., Nunez-Rios, J., Lee, Y.-S., and Hulme, C. (2015). Acetyl cyanide as a cyanide source in a tandem catalyst-free modified Groebke–Blackburn–Bienaymé [4 + 1]-cycloaddition-Strecker cascade. *Tetrahedron Lett.* 56, 1038–1040. doi: 10.1016/j.tetlet.2014.12.127

Matveeva, A. A., Matikenova, A. A., Anis'kov, A. A., and Kriven'ko, A. P. (2015). One-pot synthesis of isomeric cycloalkatriazolopyrimidines. *Russ. J. Org. Chem.* 51, 378–381. doi: 10.1134/S107042801503015X

Matveeva, A. A., Poplevina, N. V., Borisova, N. O., and Kriven'ko, A. P. (2013). Three-component synthesis of tetrazolopyrimidines annelated by C_6 to C_8 carbocycles. *Chem. Heterocycl. Compd.* 48, 1877–1879. doi: 10.1007/s10593-013-1224-2

Michael, A. (1893). Ueber die Einwirkung von Diazobenzolimid auf Acetylendicarbonsäuremethylester. *J. Prakt. Chem.* 48, 94–95. doi: 10.1002/prac.18930480114

Miliutina, M., Janke, J., Chirkina, E., Hassan, S., Ejaz, S. A., Khan, S. U., et al. (2017). Domino reactions of chromone-3-carboxylic acids with aminoheterocycles: synthesis of heteroannulated pyrido[2,3-*c*]coumarins and their optical and biological activity. *Eur. J. Org. Chem.* 2017, 7148–7159. doi: 10.1002/ejoc.201701276

Mkrtchyan, S., Iaroshenko, V. O., Dudkin, S., Gevorgyan, A., Vilches-Herrera, M., Ghazaryan, G., et al. (2010). 3-Methoxalylchromone — a novel versatile reagent for the regioselective purine isostere synthesis. *Org. Biomol. Chem.* 8, 5280–5284. doi: 10.1039/c0ob00379d

Moderhack, D. (2011). N-hydroxy- and N-aminotetrazoles and their derivatives – synthesis and reactions. *Heterocycles* 83, 1435–1487. doi: 10.3987/REV-11-693

Mohammed, S., Vishwakarma, R. A., and Bharate, S. B. (2015). Iodine catalyzed oxidative synthesis of quinazolin-4(3*H*)-ones and pyrazolo[4,3-*d*]pyrimidin-7(6*H*)-ones via amination of sp^3 C–H bond. *J. Org. Chem.* 80, 6915–6921. doi: 10.1021/acs.joc.5b00989

Moradi, A., Heydari, R., and Maghsoodlou, M. T. (2015). Agar: a novel, efficient, and biodegradable catalyst for the one-pot three-component and green synthesis of 2,3-dihydroquinazolin-4(1*H*)-one, 4*H*-pyrimidobenzothiazole and 2-aminobenzothiazolomethylnaphthol derivatives. *Res. Chem. Intermed.* 41, 7377–7391. doi: 10.1007/s11164-014-1818-z

Morozova, A. D., Muravyova, E. A., Desenko, S. M., Musatov, V. I., Yedamenko, D. V., and Chebanov, V. A. (2016). Heterocyclization reactions of 3-methylisoxazol-5-amine with pyruvic acid derivatives using classical and non-classical methods of activation. *Chem. Heterocycl. Compd.* 52, 934–942. doi: 10.1007/s10593-017-1989-9

Morozova, A. D., Muravyova, E. A., Shishkina, S. V., Vashchenko, E. V., Sen'ko, Y. V., and Chebanov, V. A. (2017). Diversity-oriented multicomponent heterocyclizations involving derivatives of 3(5)-aminoisoxazole, aldehydes and meldrum's or *N*,*N*′-dimethylbarbituric acid. *J. Heterocycl. Chem.* 54, 932–943. doi: 10.1002/jhet.2656

Mulakayala, N., Kandagatla, B., Ismail Rapolu, R. K., Rao, P., Mulakayala, C., et al. (2012). $InCl_3$-catalysed synthesis of 2-aryl quinazolin-4(3*H*)-ones and 5-aryl pyrazolo[4,3-*d*]pyrimidin-7(6*H*)-ones and their evaluation as potential anticancer agents. *Bioorganic Med. Chem. Lett.* 22, 5063–5066. doi: 10.1016/j.bmcl.2012.06.003

Muravyova, E. A., Desenko, S. M., Rudenko, R. V., Shishkina, S. V., Shishkin, O. V., Sen'ko, Y. V., et al. (2011). Switchable selectivity in multicomponent heterocyclizations of acetoacetamides, aldehydes, and 3-amino-1,2,4-triazoles/5-aminopyrazoles. *Tetrahedron* 67, 9389–9400. doi: 10.1016/j.tet.2011.09.138

Muravyova, E. A., Shishkina, S. V., Musatov, V. I., Knyazeva, I. V., Shishkin, O. V., Desenko, S. M., et al. (2009). Chemoselectivity of multicomponent condensations of barbituric acids, 5-aminopyrazoles, and aldehydes. *Synthesis* 2009, 1375–1385. doi: 10.1055/s-0028-1088024

Muravyova, E. A., Tkachenko, V. V., Desenko, S. M., Sen'ko, Y. V., Müller, T. J. J., Vashchenko, E. V., et al. (2013). Behavior of 5-amino-3-methylisoxazole in multicomponent heterocyclizations with carbonyl compounds under thermal heating and non-classical conditions. *Arkivoc* 2013, 338–371. doi: 10.3998/ark.5550190.p008.093

Murlykina, M. V., Kornet, M. N., Desenko, S. M., Shishkina, S. V., Shishkin, O. V., Brazhko, A. A., et al. (2017). New tricks of well-known aminoazoles in isocyanide-based multicomponent reactions and antibacterial activity of the compounds synthesized. *Beilstein J. Org. Chem.* 13, 1050–1063. doi: 10.3762/bjoc.13.104

Murlykina, M. V., Sakhno, Y. I., Desenko, S. M., Konovalova, I. S., Shishkin, O. V., Sysoiev, D. A., et al. (2013). Features of switchable multicomponent heterocyclizations of salicylic aldehydes and 5-aminopyrazoles with pyruvic acids and antimicrobial activity of the reaction products. *Tetrahedron* 69, 9261–9269. doi: 10.1016/j.tet.2013.08.055

Murlykina, M. V., Sakhno, Y. I., Desenko, S. M., Shishkina, S. V., Shishkin, O. V., Sysoiev, D. O., et al. (2015). Study of the chemoselectivity of multicomponent heterocyclizations involving 3-amino-1,2,4-triazole and pyruvic acids as key reagents, and biological activity of the reaction products. *Eur. J. Org. Chem.* 2015, 4481–4492. doi: 10.1002/ejoc.201500469

Murugesan, V., Makwana, N., Suryawanshi, R., Saxena, R., Tripathi, R., Paranjape, R., et al. (2014). Rational design and synthesis of novel thiazolidin-4-ones as non-nucleoside HIV-1 reverse transcriptase inhibitors. *Bioorganic Med. Chem.* 22, 3159–3170. doi: 10.1016/j.bmc.2014.04.018

Niu, X., Yang, B., Fang, S., Li, Y., Zhang, Z., Jia, J., et al. (2014). An efficient one-pot synthesis of 1,2,4-triazoloquinoxalines. *Tetrahedron* 70, 4657–4660. doi: 10.1016/j.tet.2014.05.029

Orlov, V. D., and Sidorenko, D. Y. (2012). Carbo[3 + 3] cyclocondensation reactions. A new method for the synthesis of tetrahydropyrazolo[1,5-*b*]quinazolines and tetrahydropyrazolo[4,5-*b*]quinolines. *Chem. Heterocycl. Compd.* 48, 650–657. doi: 10.1007/s10593-012-1039-6

Palaniraja, J., Mohana Roopan, S., Mokesh Rayalu, G., Abdullah Al-Dhabi, N., and Valan Arasu, M. (2016a). A metal-free regioselective multicomponent approach for the synthesis of free radical scavenging pyrimido-fused indazoles and their fluorescence studies. *Molecules* 21:1571. doi: 10.3390/molecules21111571

Palaniraja, J., and Roopan, S. M. (2015). Iodine-mediated synthesis of indazolo-quinazolinones via a multi-component reaction. *RSC Adv.* 5, 8640–8646. doi: 10.1039/C4RA13779E

Palaniraja, J., Roopan, S. M., and Rayalu, G. M. (2016b). One-pot synthesis of highly functionalized pyrimido[1,2-*b*]indazoles via 6-endo-dig cyclization. *RSC Adv.* 6, 24610–24616. doi: 10.1039/C6RA02596J

Patnaik, S., Zheng, W., Choi, J. H., Motabar, O., Southall, N., Westbroek, W., et al. (2012). Discovery, structure–activity relationship, and biological evaluation of noninhibitory small molecule chaperones of glucocerebrosidase. *J. Med. Chem.* 55, 5734–5748. doi: 10.1021/jm300063b

Pereshivko, O. P., Peshkov, V. A., Ermolat'ev, D. S., and Van Der Eycken, E. V. (2013). Fast Assembly of 1*H*-Imidazo[1,2-*a*]imidazol-5-amines via Groebke–Blackburn–Bienaymé reaction with 2-aminoimidazoles. *Synlett* 24, 351–354. doi: 10.1055/s-0032-1317986

Petrov, A. A., and Kasatochkin, A. N. (2013). Synthesis of 6,7,8,9-Tetrahydropyrazolo[1,5-*a*]quinazolines containing a 5-phenylamine fragment. *Russ. J. Org. Chem.* 49, 1250–1252. doi: 10.1134/S1070428013080307

Petrov, A. A., and Kasatochkin, A. N. (2014). Convenient synthesis of 6,7-dihydroazolo[5,1-*b*]quinazolin-8(5*H*)-one derivatives. *Russ. J. Org. Chem.* 50, 1485–1495. doi: 10.1134/S1070428014100145

Petrova, O. N., Lipson, V. V., Zamigailo, L. L., Shirobokova, M. G., Musatov, V. I., Baumer, V. N., et al. (2015a). Synthesis and chemical properties of 4-aroyl-3-methyl-4,10-dihydroindeno[1,2-*b*]pyrazolo-[4,3-*e*]pyridin-5-ones. *Russ. J. Org. Chem.* 51, 1597–1605. doi: 10.1134/S1070428015110147

Petrova, O. N., Lipson, V. V., Zamigajlo, L. L., Shirobokova, M. G., Musatov, V. I., and Dmitrienko, D. A. (2016). Domino reactions of pyrazol-5-amines

with arylglyoxals and malononitrile. *Russ. J. Org. Chem.* 52, 1168–1172. doi: 10.1134/S1070428016080121

Petrova, O. N., Zamigailo, L. L., Shirobokova, M. G., Shishkina, S. V., Shishkin, O. V., Musatov, V. I., et al. (2013a). Cyclocondensation of 3(5)-aminopyrazoles with arylglyoxals and cyclohexane-1,3-diones. *Chem. Heterocycl. Compd.* 49, 955–967. doi: 10.1007/s10593-013-1332-z

Petrova, O. N., Zamigajlo, L. L., Gella, I. M., Musatov, V. I., Shishkina, S. V., Shishkin, O. V., et al. (2014). Three-component synthesis of 4-aroyl-2(1),4,5,7-tetrahydropyrazolo[3,4-*b*]pyridin-6-ones and their properties. *Chem. Heterocycl. Compd.* 50, 514–527. doi: 10.1007/s10593-014-1502-7

Petrova, O. N., Zamigajlo, L. L., Ostras, K. S., Shishkina, S. V., Shishkin, O. V., Borisov, A. V., et al. (2015b). Multicomponent reaction of 2-aminobenzimidazole, arylglyoxals, and 1,3-cyclohexanedione. *Chem. Heterocycl. Compd.* 51, 310–319. doi: 10.1007/s10593-015-1700-y

Petrova, O. N., Zamigajlo, L. L., Shishkina, S. V., Shishkin, O. V., Musatov, V. I., Borisov, A. V., et al. (2013b). A facile one-pot highly chemo- and regioselective synthesis of the novel heterocyclic system indolo[1,2-*c*]azolo[1,5-*a*]quinazoline-8,10-dione. *Tetrahedron* 69, 11185–11190. doi: 10.1016/j.tet.2013.10.073

Pinner, A. (1894). Ueber die Einwirkung von Hydrazin auf Imidoäther. *Berichte Dtsch. Chem. Gesellsch.* 27, 984–1009. doi: 10.1002/cber.189402701207

Planells, M., Nikolka, M., Hurhangee, M., Tuladhar, P. S., White, A. J. P., Durrant, J. R., et al. (2014). The effect of thiadiazole out-backbone displacement in indacenodithiophene semiconductor polymers. *J. Mater. Chem. C* 2, 8789–8795. doi: 10.1039/C4TC01500B

Pokhodylo, N. T., and Shyyka, O. Y. (2014). 1-(5-(*R*-Amino)-1,2,4-thiadiazol-3-yl)propan-2-ones: convenient ketomethylenic reagents for the Gewald and Dimroth reactions. *J. Heterocycl. Chem.* 51, 1487–1490. doi: 10.1002/jhet.1719

Proshin, A. N., Serkov, I. V., Petrova, L. N., and Bachurin, S. O. (2014). 5-Amino-3-(2-aminopropyl)-1,2,4-thiadiazoles as the basis of hybrid multifunctional compounds. *Russ. Chem. Bull.* 63, 1148–1152. doi: 10.1007/s11172-014-0563-1

Puligoundla, R. G., Karnakanti, S., Bantu, R., Kommu, N., Kondra, S. B., and Nagarapu, L. (2013). A simple, convenient one-pot synthesis of [1,2,4]triazolo/benzimidazolo quinazolinone derivatives by using molecular iodine. *Tetrahedron Lett.* 54, 2480–2483. doi: 10.1016/j.tetlet.2013.02.099

Quiroga, J., Cobo, D., Insuasty, B., Abonía, R., Cruz, S., Nogueras, M., et al. (2008). Regioselective three-component synthesis of novel indeno[1,2-*b*]pyrazolo[4,3-*e*]pyridines-fused derivatives of 4-azafluorenone alkaloid. *J. Heterocycl. Chem.* 45, 155–159. doi: 10.1002/jhet.5570450116

Rahmati, A. (2010). Synthesis of 4-aryl-3-methyl-6-oxo-4,5,6,7-tetrahydro-2*H*-pyrazolo[3,4-*b*]pyridine-5-carbonitrile via a one-pot, three-component reaction. *Tetrahedron Lett.* 51, 2967–2970. doi: 10.1016/j.tetlet.2010.03.109

Rahmati, A., Eskandari-Vashareh, M., and Alizadeh-Kouzehrash, M. (2013). Synthesis of 3-(benzylideneamino)-2-phenyl-5*H*-imidazo[1,2-*b*]pyrazole-7-carbonitriles via a four-component condensation reaction. *Tetrahedron* 69, 4199–4204. doi: 10.1016/j.tet.2013.03.103

Rahmati, A., and Khalesi, Z. (2012). Catalyst free synthesis of fused pyrido[2,3-*d*]pyrimidines and pyrazolo[3,4-*b*]pyridines in water. *Chinese Chem. Lett.* 23, 1149–1152. doi: 10.1016/j.cclet.2012.08.009

Rahmati, A., and Kouzehrash, M. (2011). Synthesis of N-alkyl-2-aryl-5*H*-imidazo[1,2-*b*]pyrazol-3-amines by a three-component condensation reaction. *Synthesis* 2011, 2913–2920. doi: 10.1055/s-0030-1260154

Rajanarendar, E., Murthy, K. R., and Reddy, M. N. (2011a). A mild and efficient four component one-pot synthesis of 2,4,5-triphenyl-(1*H*-1-imidazolyl)isoxazoles catalyzed by ceric ammonium nitrate. *Indian J. Chem.* 50B, 926–930.

Rajanarendar, E., Reddy, M. N., and Raju, S. (2011b). An efficient one-pot synthesis of isoxazolyl polyhydroquinolines via Hantzsch condensation using L-proline as catalyst. *Indian J. Chem.* 50B, 751–755.

Rajanarendar, E., Thirupathaiah, K., Ramakrishna, S., and Nagaraju, D. (2016). A convenient and facile Hantzsch synthesis of aryl imidazo[1,2-*b*]Isoxazolyl-N-aryl thiazol amines. *J. Heterocycl. Chem.* 53, 1983–1989. doi: 10.1002/jhet.2518

Rajua, C., Kalaipriyab, M., Umaa, R., Sridhar, R., and Ramakrishna, S. (2012). Pyridinium trifluoro acetate mediated synthesis of 3,4-dihydropyrimidin-2(1H)-ones and tetrazolo[1,5-*a*]pyrimidine-6-carboxylates. *Curr. Chem. Lett.* 1, 27–34. doi: 10.5267/j.ccl.2011.12.004

Rateb, N. M. (2014). Synthesis of pyrido[2′,3′:3,4]pyrazolo[1,5-*a*]pyrimidine, pyrido[2′,3′:3,4]pyrazolo[5,1-*c*][1,2,4]triazine, and pyrazolyl oxadiazolylthieno[2,3-*b*]pyridine derivatives. *J. Heterocycl. Chem.* 51, 1349–1356. doi: 10.1002/jhet.1799

Reddy, M. V., Byeon, K. R., Park, S. H., and Kim, D. W. (2017). Polyethylene glycol methacrylate-grafted dicationic imidazolium-based ionic liquid: heterogeneous catalyst for the synthesis of aryl-benzo[4,5]imidazo[1,2-*a*]pyrimidine amines under solvent-free conditions. *Tetrahedron* 73, 5289–5296. doi: 10.1016/j.tet.2017.07.025

Reddy, M. V., Kim, J. S., Lim, K. T., and Jeong, Y. T. (2014a). Polyethylene glycol (PEG-400): an efficient green reaction medium for the synthesis of benzo[4,5]imidazo[1,2-*a*]pyrimido[4,5-*d*]pyrimidin-4(1*H*)-ones under catalyst-free conditions. *Tetrahedron Lett.* 55, 6459–6462. doi: 10.1016/j.tetlet.2014.09.135

Reddy, M. V., Oh, J., and Jeong, Y. T. (2014b). *p*-Toluenesulfonic acid-catalyzed one-pot synthesis of 2-amino-4-substituted-1,4-dihydrobenzo[4,5]imidazolo[1,2-*a*]pyrimidine-3-carbonitriles under neat conditions. *Comptes Rendus Chim.* 17, 484–489. doi: 10.1016/j.crci.2013.08.007

Reddy, M. V., Reddy, A. V. S., and Jeong, Y. T. (2016). Di-n-butyl ammonium chlorosulfonate ionic liquids as an efficient and recyclable catalyst for the synthesis of 1,4-dihydrobenzo[4,5]imidazo[1,2-*a*]pyrimidine-3-carboxylates under solvent-free ultrasound irradiation. *Res. Chem. Intermed.* 42, 4893–4906. doi: 10.1007/s11164-015-2328-3

Ren, L., Laird, E. R., Buckmelter, A. J., Dinkel, V., Gloor, S. L., Grina, J., et al. (2012). Potent and selective pyrazolo[1,5-*a*]pyrimidine based inhibitors of B-RafV600E kinase with favorable physicochemical and pharmacokinetic properties. *Bioorganic Med. Chem. Lett.* 22, 1165–1168. doi: 10.1016/j.bmcl.2011.11.092

Risley, V. A., Henry, S., Kosyrikhina, M. V., Manzanares, M. R., Payan, I., Downer, C. D., et al. (2014). 4-Amino-2-aryl-3-cyano-1,2-dihydropyrimido-[1,2-*a*]benzimidazoles and their pyrimidine analogs as new anticancer agents. *Chem. Heterocycl. Compd.* 50, 185–194. doi: 10.1007/s10593-014-1460-0

Rodríguez-Rodríguez, M., Gras, E., Pericàs, M. A., and Gómez, M. (2015). Metal-free intermolecular azide-alkyne cycloaddition promoted by glycerol. *Chem. A Eur. J.* 21, 18706–18710. doi: 10.1002/chem.201503858

Rostovtsev, V. V., Green, L. G., Fokin, V. V., and Sharpless, K. B. (2002). A stepwise Huisgen cycloaddition process: copper(I)-catalyzed regioselective "ligation" of azides and terminal alkynes. *Angew. Chemie Int. Ed.* 41, 2596–2599. doi: 10.1002/1521-3773(20020715)41:14<2596::AID-ANIE2596>3.0.CO;2-4

Ruijter, E., Scheffelaar, R., and Orru, R. V. A. (2011). Multicomponent reaction design in the quest for molecular complexity and diversity. *Angew. Chemie Int. Ed.* 50, 6234–6246. doi: 10.1002/anie.201006515

Ryabukhin, S. V., Panov, D. M., Plaskon, A. S., and Grygorenko, O. O. (2012). Approach to the library of 3-hydroxy-1,5-dihydro-2*H*-pyrrol-2-ones through a three-component condensation. *ACS Comb. Sci.* 14, 631–635. doi: 10.1021/co300082t

Ryabukhin, S. V., Plaskon, A. S., Boron, S. Y., Volochnyuk, D. M., and Tolmachev, A. A. (2011). Aminoheterocycles as synthons for combinatorial Biginelli reactions. *Mol. Divers.* 15, 189–195. doi: 10.1007/s11030-010-9253-6

Saeedi, M., Beheshtiha, Y. S., Heravi, M. M., and Oskooie, H. A. (2011). Synthesis of novel tetrahydro[4,5]imidazo[2,1-*b*]chromeno[4,3,2-*de*] quinazoline and benzothiazol-2-ylaminoxanthenone derivatives. *Heterocycles* 83, 1831–1841. doi: 10.3987/COM-11-12201

Safaei, S., Mohammadpoor-Baltork, I., Khosropour, A. R., Moghadam, M., Tangestaninejad, S., and Mirkhani, V. (2012). Regioselective multi-component synthesis of 1*H*-pyrazolo[3,4-*d*]pyrimidine-6(7*H*)-thiones. *Mol. Divers.* 16, 591–600. doi: 10.1007/s11030-012-9391-0

Sahi, S., and Paul, S. (2016). Synthesis and biological evaluation of quinolines, thiazolo[3,2-*a*]pyrimidines, thiadiazolo[3,2-*a*]pyrimidines and triazolo[3,4-*b*][1,3,4]thiadiazepines as antimicrobial agents. *Med. Chem. Res.* 25, 951–969. doi: 10.1007/s00044-016-1540-z

Saikia, P., Kaishap, P. P., Prakash, R., Shekarrao, K., Gogoi, S., and Boruah, R. C. (2014). A facile one-pot synthesis of 7-substituted pyrazolo[1,5-*a*]pyrimidines by base induced three-component reaction. *Tetrahedron Lett.* 55, 3896–3900. doi: 10.1016/j.tetlet.2014.05.021

Saito, T., Obitsu, T., Minamoto, C., Sugiura, T., Matsumura, N., Ueno, S., et al. (2011). Pyrazolo[1,5-*a*]pyrimidines, triazolo[1,5-*a*]pyrimidines

and their tricyclic derivatives as corticotropin-releasing factor 1 (CRF1) receptor antagonists. *Bioorganic Med. Chem.* 19, 5955–5966. doi: 10.1016/j.bmc.2011.08.055

Sakhno, Y. I., Desenko, S. M., Shishkina, S. V., Shishkin, O. V., Musatov, V. I., and Chebanov, V. A. (2011). Unusual direction of cyclocondensation of 1-(4-chlorophenyl)-3,5-diamino-1,2,4-triazole, pyruvic acid, and aldehydes. *Synthesis* 1120–1124. doi: 10.1055/s-0030-1258468

Sakhno, Y. I., Desenko, S. M., Shishkina, S. V., Shishkin, O. V., Sysoyev, D. O., Groth, U., et al. (2008). Multicomponent cyclocondensation reactions of aminoazoles, arylpyruvic acids and aldehydes with controlled chemoselectivity. *Tetrahedron* 64, 11041–11049. doi: 10.1016/j.tet.2008.09.089

Sakhno, Y. I., Kozyryev, A. V., Desenko, S. M., Shishkina, S. V., Musatov, V. I., Sysoiev, D. O., et al. (2018). Features of two- and multicomponent heterocyclization reactions involving 3,4-disubstituted 5-aminopyrazoles and alkyl pyruvates. *Tetrahedron* 74, 564–571. doi: 10.1016/j.tet.2017.12.031

Sakhno, Y. I., Murlykina, M. V., Morozova, A. D., Kozyryev, A. V., and Chebanov, V. A. (2015). Heterocyclization reactions of pyruvic acids and aminoazoles with controlled chemoselectivity. *French Ukrainian J. Chem.* 3, 1–20. doi: 10.17721/fujcV3I2P1-20

Sakhno, Y. I., Shishkina, S. V., Shishkin, O. V., Musatov, V. I., Vashchenko, E. V., Desenko, S. M., et al. (2010). Diversity oriented heterocyclizations of pyruvic acids, aldehydes and 5-amino-N-aryl-1*H*-pyrazole-4-carboxamides: catalytic and temperature control of chemoselectivity. *Mol. Divers.* 14, 523–531. doi: 10.1007/s11030-010-9226-9

Satasia, S. P., Kalaria, P. N., and Raval, D. K. (2014). Catalytic regioselective synthesis of pyrazole based pyrido[2,3-*d*] pyrimidine-diones and their biological evaluation. *Org. Biomol. Chem.* 12, 1751–1758. doi: 10.1039/b000000x

Sedash, Y. V., Gorobets, N. Y., Chebanov, V. A., Konovalova, I. S., Shishkin, O. V., and Desenko, S. M. (2012). Dotting the i's in three-component Biginelli-like condensations using 3-amino-1,2,4-triazole as a 1,3-binucleophile. *RSC Adv.* 2, 6719–6728. doi: 10.1039/c2ra20195j

Shaaban, S., and Abdel-Wahab, B. F. (2016). Groebke–Blackburn–Bienaymé multicomponent reaction: emerging chemistry for drug discovery. *Mol. Divers.* 20, 233–254. doi: 10.1007/s11030-015-9602-6

Shaabani, A., and Hooshmand, S. E. (2016). Choline chloride/urea as a deep eutectic solvent/organocatalyst promoted three-component synthesis of 3-aminoimidazo-fused heterocycles via Groebke–Blackburn–Bienayme process. *Tetrahedron Lett.* 57, 310–313. doi: 10.1016/j.tetlet.2015.12.014

Shaabani, A., Seyyedhamzeh, M., Ganji, N., Hamidzad Sangachin, M., and Armaghan, M. (2015). One-pot four-component synthesis of highly substituted [1,2,4]triazolo[1,5-*a*]pyrimidines. *Mol. Divers.* 19, 709–715. doi: 10.1007/s11030-015-9604-4

Shaabani, A., Seyyedhamzeh, M., Maleki, A., Behnam, M., and Rezazadeh, F. (2009). Synthesis of fully substituted pyrazolo [3,4-*b*]pyridine-5-carboxamide derivatives via a one-pot four-component reaction. *Tetrahedron Lett.* 50, 2911–2913. doi: 10.1016/j.tetlet.2009.03.200

Shafiee, M., Khosropour, A. R., Mohammadpoor-Baltork, I., Moghadam, M., Tangestaninejad, S., and Mirkhani, V. (2012). An efficient, expeditious, and diastereoselective one-pot pseudo-five-component reaction for the synthesis of new bis-Betti bases under catalyst-free conditions. *Tetrahedron Lett.* 53, 3086–3090. doi: 10.1016/j.tetlet.2012.04.037

Shao, T., Gong, Z., Su, T., Hao, W., and Che, C. (2017). A practical and efficient approach to imidazo[1,2-*a*]pyridine-fused isoquinolines through the post-GBB transformation strategy. *Beilstein J. Org. Chem.* 13, 817–824. doi: 10.3762/bjoc.13.82

Shaterian, H. R., Fahimi, N., and Azizi, K. (2014). New applications of phosphoric acid supported on alumina (H_3PO_4-Al_2O_3) as a reusable heterogeneous catalyst for preparation of 2,3-dihydroquinazoline-4(1*H*)-ones, 2*H*-indazolo[2,1-*b*]phthalazinetriones, and benzo[4,5]imidazo[1,2-*a*]pyrimidines. *Res. Chem. Intermed.* 40, 1879–1898. doi: 10.1007/s11164-013-1087-2

Sheibani, H., and Babaie, M. (2013). Three-component synthesis of 4-amino-2-aryl-2*H*-pyrimido-[1,2-*b*][1,3]benzazole-3-carbonitriles and 4*H*-pyrimido-[2,1-*b*][1,3]benzazoles in the presence of magnesium oxide and 12-tungstophosphoric acid as catalysts. *Russ. Chem. Bull.* 62, 2202–2208. doi: 10.1007/s11172-013-0319-3

Sheibani, H., Saidi, K., and Lakaei, M. (2012). Three-component one-pot synthesis of 4-aryl-2,3-dihydropyrimido[1,2-*a*]benzimidazol-2-ones catalyzed by L-proline. *J. Heterocycl. Chem.* 49, 1386–1390. doi: 10.1002/jhet

Shen, S., Zhang, H., Yu, C., Yao, C., Li, T., Qin, B., et al. (2013). Solvent-free combinatorial synthesis of tetrazolo[1,5-*a*]thiopyrano[3,4-*d*]pyrimidine derivatives. *Res. Chem. Intermed.* 39, 1799–1806. doi: 10.1007/s11164-012-0714-7

Shi, C.-L., Chen, H., and Shi, D.-Q. (2011). An efficient one-pot synthesis of pyrazolo[3,4-*b*]pyridinone derivatives catalyzed by L-proline. *J. Heterocycl. Chem.* 48, 351–354. doi: 10.1002/jhet.573

Shi, D.-Q., Yang, F., and Ni, S.-N. (2009). A facile synthesis of furo[3,4-*e*]pyrazolo[3,4-*b*]pyridine-5(7*H*)-one derivatives via three-component reaction in ionic liquid without any catalyst. *J. Heterocycl. Chem.* 46, 469–476. doi: 10.1002/jhet.103

Shi, F., Zhou, D., Tu, S., Li, C., Cao, L., and Shao, Q. (2008). Pot, atom and step economic synthesis of fused three heterocyclic ring compounds under microwave irradiation in water. *J. Heterocycl. Chem.* 45, 1305–1310. doi: 10.1002/jhet.5570450508

Shie, J.-J., and Fang, J.-M. (2007). Microwave-assisted one-pot tandem reactions for direct conversion of primary alcohols and aldehydes to triazines and tetrazoles in aqueous media. *J. Org. Chem.* 72, 3141–3144. doi: 10.1021/jo0625352

Shieh, P., Dien, V. T., Beahm, B. J., Castellano, J. M., Wyss-Coray, T., and Bertozzi, C. R. (2015). CalFluors: a universal motif for fluorogenic azide probes across the visible spectrum. *J. Am. Chem. Soc.* 137, 7145–7151. doi: 10.1021/jacs.5b02383

Shinde, V. V., and Jeong, Y. T. (2015). Molybdate sulfuric acid (MSA): an efficient solid acid catalyst for the synthesis of diversely functionalized fused imidazo[1,2-*a*]pyrimidines under solvent-free conditions. *New J. Chem.* 39, 4977–4986. doi: 10.1039/C5NJ00516G

Shinde, V. V., and Jeong, Y. T. (2016). Sonochemical FeF_3 catalyzed three-component synthesis of densely functionalized tetrahydroindazolo[3,2-*b*]quinazoline under solvent-free conditions. *Tetrahedron Lett.* 57, 3795–3799. doi: 10.1016/j.tetlet.2016.07.031

Shirame, S. P., and Bhosale, R. B. (2018). "Green approach in click chemistry," in *Green Chemistry*, eds H. E. M. Saleh and M. Kolle (London: InTech).

Singh, M. S., Chowdhury, S., and Koley, S. (2016). Advances of azide-alkyne cycloaddition-click chemistry over the recent decade. *Tetrahedron* 72, 5257–5283. doi: 10.1016/J.TET.2016.07.044

Soliman, A. M. M., El-Remaily, M. A. E.-A. A. A., Sultan, A. A., and Abdel-Ghany, H. (2014). Synthesis of some novel imidazopyrazole and pyrazolopyrimidine derivatives. *J. Heterocycl. Chem.* 51, 1476–1481. doi: 10.1002/jhet.1701

Sompalle, R., Arunachalam, P., and Roopan, S. M. (2016). Conventional spectroscopic identification of N-alkylated triazolo-quinazolinones and its antioxidant, solvatochromism studies. *J. Mol. Liq.* 224, 1348–1357. doi: 10.1016/j.molliq.2016.10.124

Sompalle, R., and Roopan, S. M. (2016). Microwave assisted synthesis of ring junction heterocyclic antioxidants. *Res. Chem. Intermed.* 42, 5353–5366. doi: 10.1007/s11164-015-2371-0

Suresh, L., Kumar, P. S. V., Vinodkumar, T., and Chandramouli, G. V. P. (2016). Heterogeneous recyclable nano-CeO_2 catalyst: efficient and eco-friendly synthesis of novel fused triazolo and tetrazolo pyrimidine derivatives in aqueous medium. *RSC Adv.* 6, 68788–68797. doi: 10.1039/C6RA16307F

Survase, D., Bandgar, B., and Helavi, V. (2017). Polyethylene glycol-promoted synthesis of pyrimido[1,2-*a*]benzimidazole and pyrano[2,3-*c*]pyrazole derivatives in water. *Synth. Commun.* 47, 680–687. doi: 10.1080/00397911.2017.1278774

Světlík, J., and Kettmann, V. (2011). The chameleon-like behaviour of 3-amino-1,2,4-triazole in the Biginelli reaction: unexpected formation of a novel spiroheterocyclic system. *Tetrahedron* 52, 1062–1066. doi: 10.1016/j.tetlet.2010.12.051

Svetlík, J., Pronayova, N., Svor, L., and Frecer, V. (2014). A complicated path of salicylaldehyde through the Biginelli reaction: a case of unexpected spiroketalization. *Tetrahedron* 70, 8354–8360. doi: 10.1016/j.tet.2014.09.003

Svetlik, J., Veizerová, L., Mayer, T. U., and Catarinella, M. (2010). Monastrol analogs: A synthesis of pyrazolopyridine, benzopyranopyrazolopyridine, and oxygen-bridged azolopyrimidine derivatives and their biological screening.

Bioorganic Med. Chem. Lett. 20, 4073–4076. doi: 10.1016/j.bmcl.2010.05.085

Tan, S. H., Chuah, T. S., and Chia, P. W. (2016). An improved protocol on the synthesis of thiazolo [3,2-*a*]pyrimidine using ultrasonic probe irradiation. *J. Korean Chem. Soc.* 60, 245–250. doi: 10.5012/jkcs.2016.60.4.245

Taylor, A. P., Robinson, R. P., Fobian, Y. M., Blakemore, D. C., Jones, L. H., and Fadeyi, O. (2016). Modern advances in heterocyclic chemistry in drug discovery. *Org. Biomol. Chem.* 14, 6611–6637. doi: 10.1039/C6OB00936K

Thomas, E. W. (1993). The conversion of secondary amides to tetrazoles with trifluoromethanesulfonic anhydride and sodium azide. *Synthesis* 1993, 767–768. doi: 10.1055/s-1993-25934

Thorat, V. V., Dake, A. S., Deshmukh, U. S., Rasokkiyam, E., Farees Uddin, M., and Pawar, R. P. (2013). Ionic liquid mediated synthesis of novel tetrahydroimidazo[1,2-*a*]pyrimidine-6-carboxylate derivatives. *Lett. Org. Chem.* 10, 178–184. doi: 10.2174/1570178611310030006

Tintori, C., La Sala, G., Vignaroli, G., Botta, L., Fallacara, A. L., Falchi, F., et al. (2015). Studies on the ATP binding site of Fyn kinase for the identification of new inhibitors and their evaluation as potential agents against tauopathies and tumors. *J. Med. Chem.* 58, 4590–4609. doi: 10.1021/acs.jmedchem.5b00140

Tireli, M., Maračić, S., Lukin, S., Kulcsár, M. J., Žilić, D., Cetina, M., et al. (2017). Solvent-free copper-catalyzed click chemistry for the synthesis of *N*-heterocyclic hybrids based on quinoline and 1,2,3-triazole. *Beilstein J. Org. Chem.* 13, 2352–2363. doi: 10.3762/bjoc.13.232

Tkachenko, V. V., and Chebanov, V. A. (2016). Reactions of 3(5)-aminoisoxazoles using classical methods of activation, microwave irradiation, and ultrasonication. *Chem. Heterocycl. Compd.* 52, 866–886. doi: 10.1007/s10593-017-1980-5

Tkachenko, V. V., Muravyova, E. A., Desenko, S. M., Shishkin, O. V., Shishkina, S. V., Sysoiev, D. O., et al. (2014a). The unexpected influence of aryl substituents in n-aryl-3-oxobutanamides on the behavior of their multicomponent reactions with 5-amino-3-methylisoxazole and salicylaldehyde. *Beilstein J. Org. Chem.* 10, 3019–3030. doi: 10.3762/bjoc.10.320

Tkachenko, V. V., Muravyova, E. A., Shishkina, S. V., Shishkin, O. V., Desenko, S. M., and Chebanov, V. A. (2014b). Study of three-component reactions between 5-amino-3-methylisoxazole, n-arylamides of acetoacetic acid, and aromatic aldehydes. *Chem. Heterocycl. Compd.* 50, 1166–1176. doi: 10.1007/s10593-014-1578-0

Todorovic, N., Awuah, E., Shakya, T., Wright, G. D., and Capretta, A. (2011). Microwave-assisted synthesis of N1- and C3-substituted pyrazolo[3,4-*d*]pyrimidine libraries. *Tetrahedron Lett.* 52, 5761–5763. doi: 10.1016/j.tetlet.2011.08.103

Tornøe, C. W., Christensen, C., and Meldal, M. (2002). Peptidotriazoles on solid phase: [1,2,3]-triazoles by regiospecific copper(I)-catalyzed 1,3-dipolar cycloadditions of terminal alkynes to azides. *J. Org. Chem.* 67, 3057–3064. doi: 10.1021/jo011148j

Tu, S. J., Zhang, X. H., Han, Z. G., Cao, X. D., Wu, S. S., Yan, S. et al. (2009). Synthesis of isoxazolo[5,4-*b*]pyridines by microwave-assisted multi-component reactions in water. *J. Comb. Chem.* 11, 428–432. doi: 10.1021/cc800212v

Tyagi, V., Khan, S., Bajpai, V., Gauniyal, H. M., Kumar, B., and Chauhan, P. M. S. (2012). Skeletal diverse synthesis of N-fused polycyclic heterocycles via the sequence of ugi-type MCR and CuI-catalyzed coupling/tandem Pictet–Spengler reaction. *J. Org. Chem.* 77, 1414–1421. doi: 10.1021/jo202255v

Urich, R., Wishart, G., Kiczun, M., Richters, A., Tidten-Luksch, N., Rauh, D., et al. (2013). *De novo* design of protein kinase inhibitors by *in silico* identification of hinge region-binding fragments. *ACS Chem. Biol.* 8, 1044–1052. doi: 10.1021/cb300729y

Vibhute, S., Jamale, D., Undare, S., Valekar, N., Kolekar, G., and Anbhule, P. (2017a). An efficient, one-pot three components synthesis of [1,2,4] triazoloquinazolinone derivatives using anthranilic acid as green catalyst. *Res. Chem. Intermed.* 43, 4561–4574. doi: 10.1007/s11164-017-2896-5

Vibhute, S., Jamale, D., Undare, S., Valekar, N., Patil, K., Kolekar, G., et al. (2017b). A bio-oriented anthranilic acid catalyzed synthesis of quinazolin-8(4*H*)-one derivatives: evaluation by green chemistry metrics. *Synth. Commun.* 47, 1747–1757. doi: 10.1080/00397911.2017.1348526

Vidyacharan, S., Shinde, A. H., Satpathi, B., and Sharada, D. S. (2014). A facile protocol for the synthesis of 3-aminoimidazo-fused heterocycles via the Groebke–Blackburn–Bienayme reaction under catalyst-free and solvent-free conditions. *Green Chem.* 16, 1168–1175. doi: 10.1039/c3gc42130a

Vitaku, E., Smith, D. T., and Njardarson, J. T. (2014). Analysis of the structural diversity, substitution patterns, and frequency of nitrogen heterocycles among U.S. FDA Approved Pharmaceuticals. *J. Med. Chem.* 57, 10257–10274. doi: 10.1021/jm501100b

Voitekhovich, S. V., Ivashkevich, O. A., and Gaponik, P. N. (2013). Synthesis, properties, and structure of tetrazoles: certain achievements and prospects. *Russ. J. Org. Chem.* 49, 635–654. doi: 10.1134/S1070428013050011

Voitekhovich, S. V., Vorob'ev, A. N., Gaponik, P. N., and Ivashkevich, O. A. (2005). Synthesis of new functionally substituted 1-*R*-tetrazoles and their 5-amino derivatives. *Chem. Heterocycl. Compd.* 41, 999–1004. doi: 10.1007/s10593-005-0267-4

Wadhwa, P., Kaur, T., and Sharma, A. (2015). The first catalyst and solvent-free synthesis of 2-arylimidazo[2,1-*b*][1,3,4]thiadiazoles: a comparative assessment of greenness. *RSC Adv.* 5, 44353–44360. doi: 10.1039/C5RA06747B

Wang, H., Lee, M., Peng, Z., Blázquez, B., Lastochkin, E., Kumarasiri, M., et al. (2015a). Synthesis and evaluation of 1,2,4-triazolo[1,5-*a*]pyrimidines as antibacterial agents against *Enterococcus faecium*. *J. Med. Chem.* 58, 4194–4203. doi: 10.1021/jm501831g

Wang, H.-Y., and Shi, D.-Q. (2012). Three-component one-pot synthesis of pyrazolo[3,4-*b*]quinolin-5(6*H*)-one derivatives in aqueous media. *J. Heterocycl. Chem.* 49, 212–216. doi: 10.1002/jhet.781

Wang, J. J., Feng, X., Xun, Z., Shi, D. Q., and Huang, Z. B. (2015b). Multicomponent strategy to pyrazolo[3,4-*e*]indolizine derivatives under microwave irradiation. *J. Org. Chem.* 80, 8435–8442. doi: 10.1021/acs.joc.5b01314

Wang, S. L., Liu, Y. P., Xu, B. H., Wang, X. H., Jiang, B., and Tu, S. J. (2011). Microwave-assisted chemoselective reaction: a divergent synthesis of pyrazolopyridine derivatives with different substituted patterns. *Tetrahedron* 67, 9417–9425. doi: 10.1016/j.tet.2011.09.081

Willer, R. L., Storey, R. F., Campbell, C. G., Bunte, S. W., and Parrish, D. (2012). A re-examination of the reaction of 3,4-diamino[1,2,5]oxadiazole with glyoxal. *J. Heterocycl. Chem.* 49, 919–925. doi: 10.1002/jhet.1054

Wittenberger, S. J. (1994). Recent developments in tetrazole chemistry. A review. *Org. Prep. Proced. Int.* 26, 499–531. doi: 10.1080/00304949409458050

Worrell, B. T., Malik, J. A., and Fokin, V. V. (2013). Direct evidence of a dinuclear copper intermediate in Cu(I)-catalyzed azide-alkyne cycloadditions. *Science* 340, 457–460. doi: 10.1126/science.1229506

Wu, J., Yu, L., Yang, F., Li, J., Wang, P., Zhou, W., et al. (2014). Optimization of 2-(3-(arylalkyl amino carbonyl) phenyl)-3-(2-methoxyphenyl)-4-thiazolidinone derivatives as potent antitumor growth and metastasis agents. *Eur. J. Med. Chem.* 80, 340–351. doi: 10.1016/j.ejmech.2014.04.068

Wu, Y. M., Deng, J., Li, Y., and Chen, Q. Y. (2005). Regiospecific synthesis of 1,4,5-trisubstituted-1,2,3-triazole via one-pot reaction promoted by copper(I) salt. *Synthesis*, 1314–1318. doi: 10.1055/s-2005-861860

Yoshida, M., Mori, A., Morimoto, S., Kotani, E., Oka, M., Notoya, K., et al. (2011). Novel and potent calcium-sensing receptor antagonists: discovery of (5*R*)-N-[1-ethyl-1-(4-ethylphenyl)propyl]-2,7,7-trimethyl-5-phenyl-4,5,6,7-tetrahydropyrazolo[1,5-*a*]pyrimidine-3-carboxamide monotosylate (TAK-075) as an orally active bone anabolic agent. *Bioorganic Med. Chem.* 19, 1881–1894. doi: 10.1016/j.bmc.2011.02.001

Zarganes-Tzitzikas, T., Chandgude, A. L., and Dömling, A. (2015). Multicomponent reactions, union of MCRs and beyond. *Chem. Rec.* 15, 981–996. doi: 10.1002/tcr.201500201

Zeng, L.-Y., Ji, F., and Cai, C. (2012). Four-component tandem reaction to synthesize dihydrotetrazolopyrimidinyl carbamides. *J. Heterocycl. Chem.* 49, 237–241. doi: 10.1002/jhet.698

Zeng, L.-Y., Ren, Y.-M., and Cai, C. (2011). Iodine-catalyzed, multicomponent, one-pot synthesis of 5-aryl-5,8-dihydrotetrazolo[1,5-*a*]pyrimidine-7-carboxylic acids. *Synth. Commun.* 41, 3635–3643. doi: 10.1080/00397911.2010.519842

Zhang, Y., Li, X., Li, J., Chen, J., Meng, X., Zhao, M., et al. (2012). CuO-promoted construction of *N*-2-aryl-substituted-1,2,3-triazoles via azide-chalcone oxidative cycloaddition and post-triazole arylation. *Org. Lett.* 14, 26–29. doi: 10.1021/ol202718d

Zhang, Z.-T., Ma, Y.-Q., Liang, Y., Xue, D., and He, Q. (2011). An efficient one-pot synthesis of diarylpyrazolo[1,5-*a*]pyrimidine from isoflavones. *J. Heterocycl. Chem.* 48, 279–285. doi: 10.1002/jhet.546

Zhao, B., Jiang, L.-L., Liu, Z., Deng, Q.-G., Wang, L.-Y., Song, B., et al. (2013). A microwave assisted synthesis of highly substituted 7-methyl-5*H*-thiazolo[3,2-*a*]pyrimidine-6-carboxylate derivatives via one-pot reaction of aminothiazole, aldehyde and ethyl acetoacetate. *Heterocycles* 87, 2093–2102. doi: 10.3987/COM-13-12797

Zhao, B., Xu, Y., Deng, Q. G., Liu, Z., Wang, L. Y., and Gao, Y. (2014). One-pot, three component synthesis of novel 5*H*-[1,3,4]thiadiazolo[3,2-*a*]pyrimidine-6-carboxylate derivatives by microwave irradiation. *Tetrahedron Lett.* 55, 4521–4524. doi: 10.1016/j.tetlet.2014.06.073

Zhong, X., Dou, G., and Wang, D. (2013). Polyethylene glycol (PEG-400): an efficient and recyclable reaction medium for the synthesis of pyrazolo[3,4-*b*]pyridin-6(7*H*)-one derivatives. *Molecules* 18, 13139–13147. doi: 10.3390/molecules181113139

Conflict of Interest Statement: The authors declare that the research was conducted in the absence of any commercial or financial relationships that could be construed as a potential conflict of interest.

frontiers in Chemistry

ORIGINAL RESEARCH
published: 21 December 2018
doi: 10.3389/fchem.2018.00642

Synthesis and Evaluation of a New Type of Small Molecule Epigenetic Modulator Containing Imidazo[1,2-*b*][1,2,4]triazole Motif

Fan Wu[1†], *Jing Zhang*[1†], *Erchang Shang*[1], *Junzhi Zhang*[1], *Xiang Li*[2], *Bing Zhu*[2] *and Xiaoguang Lei*[1*]

[1] *Beijing National Laboratory for Molecular Sciences, Key Laboratory of Bioorganic Chemistry and Molecular Engineering of Ministry of Education, Department of Chemical Biology, Peking-Tsinghua Center for Life Sciences, College of Chemistry and Molecular Engineering, Peking University, Beijing, China,* [2] *National Laboratory of Biomacromolecules, Institute of Biophysics, Chinese Academy of Sciences, Beijing, China*

Epigenetic modifications such as DNA methylation is important for many cellular processes, such as cell differentiation and cell death. The disorder of epigenetic state is closely related to human diseases, especially cancers. DNA methylation is a well-characterized epigenetic modification which is related to gene silencing and is considered as a repressive epigenetic mark. DNA methylation caused gene repression can be derepressed by chemical agents. Small molecules targeting DNA methyltransferases, histone deacetylases, and other regulatory factors can activate genes silenced by DNA methylation. However, more and more studies have shown that histone deacetylation is not the only downstream event of DNA methylation. Some additional, unknown mechanisms that promote DNA methylation-mediated gene silencing may exist. Recently, through high-throughput screening using a 308,251-member chemical library to identify potent small molecules that derepress an EGFP reporter gene silenced by DNA methylation, we identified seven hit compounds that did not directly target bulk DNA methylation or histone acetylation. Three of them (LX-3, LX-4, LX-5) were proven to selectively activate the p38 MAPK pathway in multiple cell types. In order to identify the exact cellular targets of these compounds, we turn to work on the SAR study of LX-3 by constructing a structurally diverse chemical library based on the imidazo[1,2-*b*][1,2,4]triazole core structure via diversity-oriented synthesis. Our work provides a general approach to efficiently access diverse heterocyclic molecules with interesting epigenetic modulation activities.

Keywords: epigenetics, DNA methylation, gene silence, structure activity relationship, p38 MAPK pathway, Imidazo[1, 2-*b*][1, 2, 4]triazole

OPEN ACCESS

Edited by:
Seung Bum Park,
Seoul National University, South Korea

Reviewed by:
Wei Zhang,
University of Massachusetts Boston, United States
Claudia Ferroni,
Italian National Research Council, Italy

****Correspondence:***
Xiaoguang Lei
xglei@pku.edu.cn

[†]These authors have contributed equally to this work

Specialty section:
This article was submitted to Organic Chemistry, a section of the journal Frontiers in Chemistry

Received: *06 September 2018*
Accepted: *11 December 2018*
Published: *21 December 2018*

Citation:
Wu F, Zhang J, Shang E, Zhang J, Li X, Zhu B and Lei X (2018) Synthesis and Evaluation of a New Type of Small Molecule Epigenetic Modulator Containing Imidazo[1,2-b][1,2,4]triazole Motif. Front. Chem. 6:642. doi: 10.3389/fchem.2018.00642

INTRODUCTION

DNA methylation is a well-characterized epigenetic modification which is related to gene silence (Cedar, 1988; Bird, 2002; Bestor et al., 2015). Studies have shown that abnormal DNA methylation is associated with many diseases, including cancers, neurodegenerative diseases and heart failure. It can be observed that the overall methylation level of tumor genome is low, while the methylation

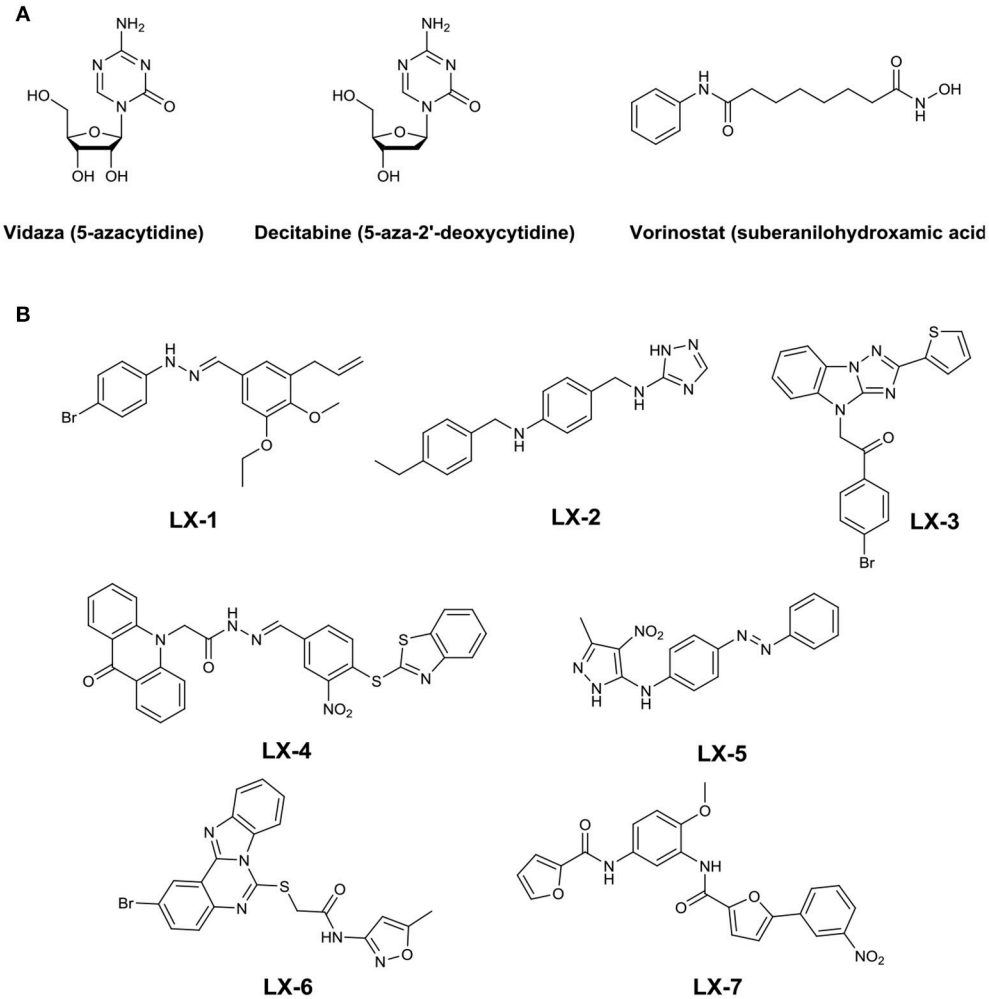

FIGURE 1 | (A) Three anticancer drugs approved by FDA targeting epigenetic pathways. **(B)** Structures of seven hit compounds.

level is high at the promoter regions of tumor suppressor genes (Esteller, 2008). On the other hand, many neurological diseases, including fragile X syndrome, Friedreich's ataxia and spinal muscular atrophy are associated with hypermethylation on the promoter regions of certain genes (Verkerk et al., 1991; Lefebvre et al., 1995; Campuzano et al., 1996). Unlike mutations, DNA methylations are reversible. It is possible to re-express DNA-methylated genes and to rescue their functionality by using small molecules to reactivate genes silenced by DNA methylation (Taunton et al., 1996).

Early studies have shown that gene silencing was caused by DNA methyltransferases (DNMTs) and methyl-CpG(5′-Cytosine-phosphate-Guanine-3′) -binding domain proteins (MBDs) which can recruit histone deacetylases (HDACs) (Bird, 2002). Enzymes involved in this process have been identified as potential therapeutic targets. Chemical tools to modulate the functions of these proteins have been identified mainly for DNMTs and HDACs. For example, azacytidine (Vidaza) and 5-aza-2′-deoxycytidine (decitabine), inhibitors of DNMTs, have been approved as effective treatments for the myelodysplastic syndrome and leukemia. And the small molecule inhibitor of HDACs, Vorinostat (suberanilohydroxamic acid), has been approved by the Food and Drug Administration for the treatment of cutaneous T-cell lymphoma (**Figure 1A**) (Byrd et al., 2005; O'Connor et al., 2006; Garcia et al., 2010).

Accordingly, the studies on the relationship between DNA methylation and gene silencing is an important direction in the field of epigenetics. Although DNA methylation in the promoter region can inhibit the expression of the gene, it is not the major cause of gene silencing. Changes in chromatin structure resulted from a series of downstream events of DNA are the primary cause of gene silencing. DNA methylation recruits methylated CpG to recognize MBD and then HDAC, which catalyzes the deacetylation of chromatin nucleosomes in this region, makes chromatin compact. Compact chromatin rejects transcription related proteins, giving rise to gene silencing (Robertson and Wolffe, 2000).

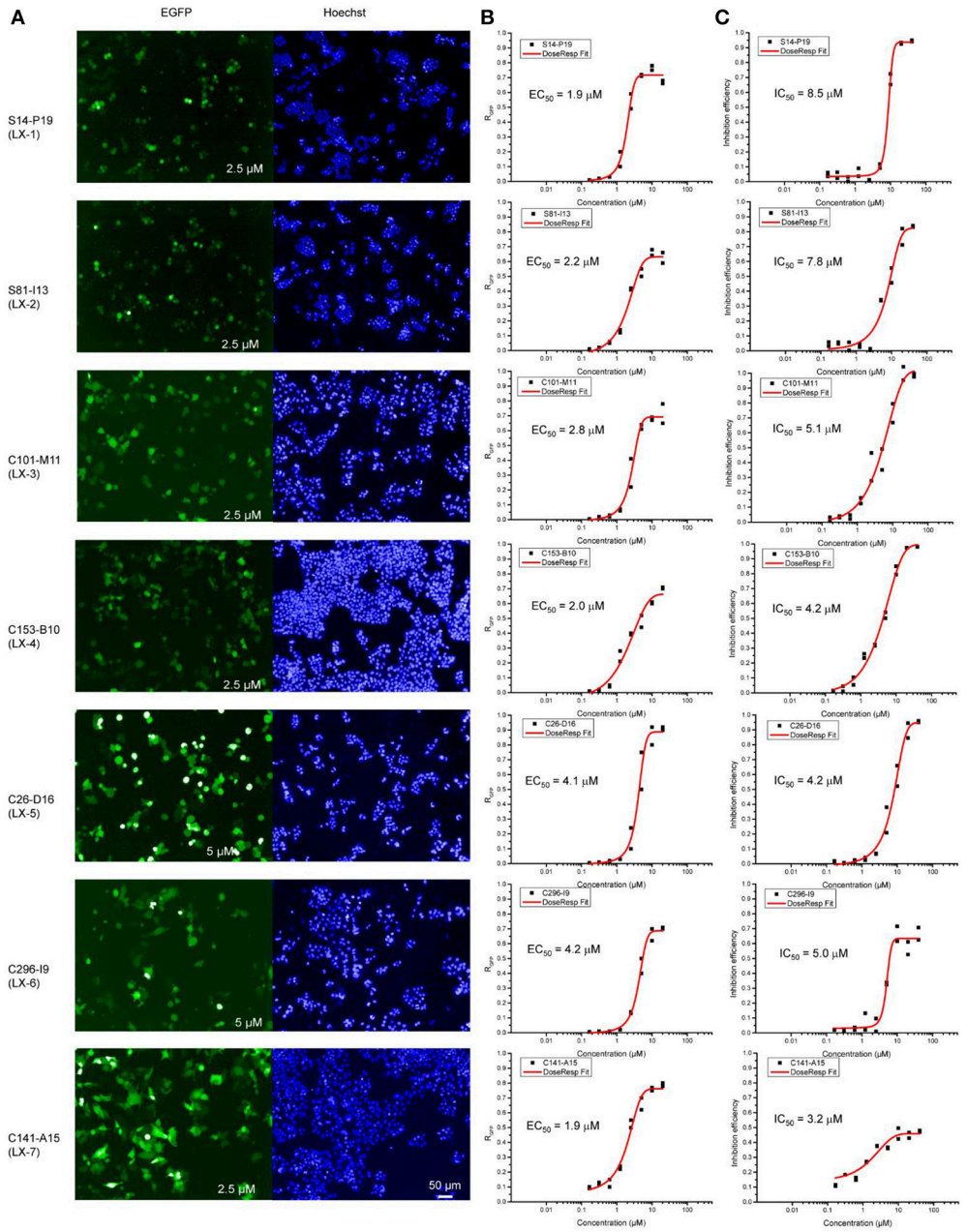

FIGURE 2 | Opera confocal images **(A)**, Dose-response curve **(B)**, and lethality curve **(C)** of B2-17 cells for compound LX-1 to LX-7. The concentration used is indicated in corner of images. The EC_{50} and IC_{50} of each compound are displayed.

However, this model is not complete. First, HDAC inhibitors cannot activate many DNA methylated silencing genes. In addition, HDAC inhibitor and DNA methyltransferases inhibitor showed certain complementary synergistic effect. This leads us to speculate that there may be a parallel downstream event of DNA methylation distinct from histone deacetylation. The discovery of these unknown signaling pathways may reveal a deeper understanding for DNA methylation mediated gene silencing. In order to serve the purpose of further understanding the detailed mechanism of DNA methylation-dependent gene silencing, we plan to identify novel compounds. While not directly relating to the inhibition of DNMTs and HDACs, those compounds should be able to derepress certain genes repressed by DNA methylation.

To identify novel small molecules targeting gene repression, we devised an image-based high-throughput screening system using the engineered HEK 293 F cell (termed as B2-17 cells) as report cell line. A chemical library containing 308,251 small molecules was screened in this system. Purposed for unbiased compound screening, this library had been used in a variety of studies (Sun et al., 2012; Wang et al., 2013; Dong et al.,

2015; Li et al., 2016). Hundred and fifty eight compounds which reactivated reporter genes in more than half of cells were selected as hits. Next, we performed titration experiments for all these hits in the B2-17 cell line. The efficacy of each compound was evaluated by its maximal percentage of $EGFP^+$ cells in the dose-response curve (maximal R_{GFP}) and relative half maximal effect concentration (EC_{50}). The toxicity of the hits was also tested in parallel, measured by number of viable cells in each treatment. The assay is based on quantitative analysis of ATP, an indicator of metabolically active cells. For each compound, we calculated the relative half maximal growth inhibitory concentration (IC50), based on the abovementioned assay.

Seven compounds (LX-1 to LX-7) (**Figure 1B**) was identified following the criteria: maximal R_{GFP} >60% (good response rate), EC_{50} <5 μM (good efficacy), and IC_{50} >3 μM (less toxic) (**Figure 2**), and the proof of absence of those compounds in DNA methylation or histone deacetylation levels were confirmed by subsequent biological evaluations(Dong et al., 2018; Li et al., 2018). Their relative half maximal effect concentrations (EC_{50}) are 1.9, 2.2, 2.8, 2.0, 4.1, 4.2, and 1.9 μM respectively, while the relative half maximal growth inhibitory concentration (IC_{50}) in turn are 8.5, 7.8, 5.1, 4.2, 4.2, 5.0, and 3.2 μM respectively (**Table 1**). The majority of genes upregulated by compound LX-3, LX-4, and LX-5 overlapped with each other, suggesting that these compounds may function through the same pathway. Results from Gene Ontology (GO) enrichment analysis suggested that the DNA derepression effect of compound LX-3, LX-4, and LX-5 are likely to functionalize via the activation of the MAPKs pathway and its downstream transcription factors. Further study shows these compounds selectively activate the p38 MAPK pathway, which is capable of activating the methylated EGFP reporter gene.

TABLE 1 | Bioactivity data for seven lead compounds.

No.	EC_{50} (μM)	Maximal R_{GFP}%	IC_{50} (μM)
LX-1	1.9	72	8.5
LX-2	2.2	67	7.8
LX-3	2.8	79	5.1
LX-4	2.0	68	4.2
LX-5	4.1	89	4.2
LX-6	4.2	71	5.0
LX-7	1.9	79	3.2

In general, these results show that LX-3, LX-4, and LX-5 are related with p38 MAPK pathway as agonists, but the exact targets of these compounds are elusive. In order to generate more potent and selective compounds to develop effective chemical probes for target identification, LX-3 that possessed novel structure and potent activity was herein chosen as our lead compound for the following structure-activity relationship (SAR) studies.

Diversity-oriented synthesis (DOS) has proven to be a successful strategy for the rapid access to structurally diverse chemical libraries (Galloway et al., 2010). A DOS library was designed based on the central imidazo[1,2-*b*][1,2,4]triazole (**Figure 2**). Around it, compound LX-3 can be divided into three parts (labeled as A–C respectively). A is a benzene ring, which is fused with the imidazole of the central structure. The right side of this molecule is connected with the thiophene ring (B) at the 2-position, and the bottom part is connected with 4′-bromoacetophenone (C) at the 4-position. The aromatic ring of C and the imidazo[1,2-*b*][1,2,4]triazole are connected by a two-carbon unit (Linker). There was no efficient synthetic strategy for such novel heterocyclic structure. Recently we developed an efficient synthetic strategy for [1,2,4]triazolo[1,5-*a*]benzazole type scaffold (Shang et al., 2016). As shown in **Scheme 1**, the synthesis of the key intermediate **4** is taken as an example. Commercially available materials **1** and **2** were assembled to afford guanidine compound **3** (78% yield) under the catalysis of tin tetrachloride. And under the condition of NCS and potassium *tert*-butanol, the [1,2,4]triazolo[1,5-*a*]benzazole type scaffold was obtained in high yield. Here, for the synthesis

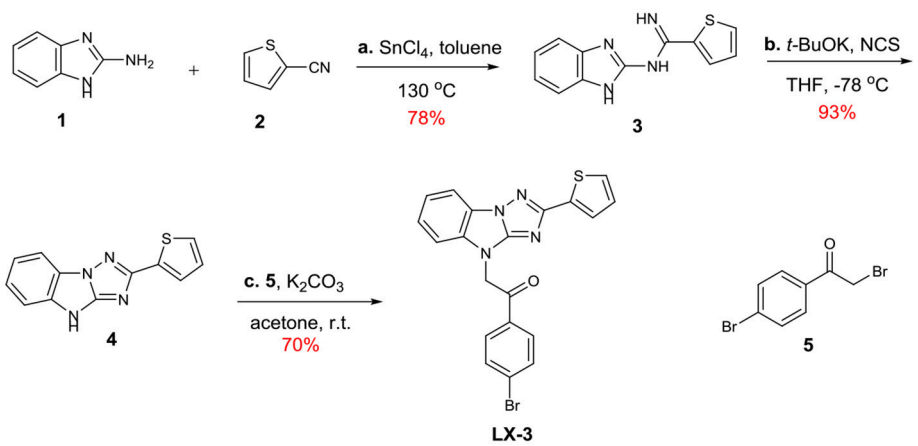

SCHEME 1 | Synthesis of the hit compound **LX-3**. General conditions: (a) $SnCl_4$, toluene, 130 °C (b) *t*-BuOK, NCS, THF, −78°C (c) K_2CO_3, acetone, r.t. *t*-BuOK = Potassium tert-butoxide NCS = N-chlorosuccinimide.

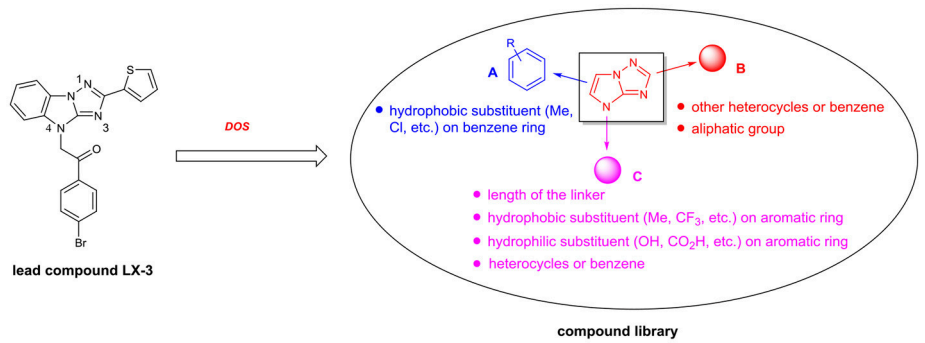

FIGURE 3 | Structural analysis and design for the SAR study of the hit compound LX-3.

of the lead compound **LX-3**, **4** was further reacted with 2,4′-dibromoacetophenone **5** using potassium carbonate to provide the desired product smoothly. This convergent strategy was applied to install diverse A, B and C units to afford a DOS library for SAR study of **LX-3**.

In terms of molecular hydrophobicity of **LX-3**, the [1,2,4]triazolo[1,5-*a*]benzazole is mainly hydrophobic (**Figure 3**), while nitrogen atoms at 1- and 3-positions are potential hydrogen bond acceptors. The B and C are also hydrophobic, so the overall hydrophobicity of this molecule is very high. The carbonyl group can act as a potential hydrogen bond acceptor. For the structural diversification of C, we can replace the bromine atom by a variety of hydrophobic or hydrophilic groups, such as other halogens, hydroxyl groups, carboxyl groups, etc. These functional groups can also be launched at different positions of the benzene ring. In addition, the benzene ring can be replaced by other heterocycles to evaluate the effect on the bioactivity. We can also modify the length of the linker of C. For the structural diversification of B, substituents can be introduced at different positions of the thiophene, such as methyl and chlorine atoms. The thiophene can also be replaced by other heterocycles, phenyl group or aliphatic group. The SAR of A can be investigated by introducing different hydrophobic substituents to the benzene.

MATERIALS AND METHODS

General Information

^{1}H NMR spectra were recorded on Brucker ARX 400 MHz or DRX 500 MHz spectrometer at ambient temperature with $CDCl_3$ or DMSO-d6 or CD_3OD as the solvent unless otherwise stated. Chemical shifts are reported in parts per million relative to chloroform or DMSO (1H, δ 7.26 for $CDCl_3$, 2.50 for DMSO-d6, 3.31 for CD_3OD). Data for ^{1}H NMR are reported as follows: chemical shift, integration, multiplicity (s = singlet, d = doublet, t = triplet, q = quartet, m = multiplet) and coupling constants. High-resolution mass spectra were obtained at Peking University Mass Spectrometry Laboratory using a Bruker APEX Flash chromatography. Flash chromatography was performed using 200–300 mesh silica gel. Yields refer to chromatographically and spectroscopically pure materials unless otherwise stated. Dichloromethane, dichloroethane, acetonitrile, and dimethyl formamide were distilled from calcium hydride; tetrahydrofuran was distilled from sodium/benzophenone ketyl prior to use. Reagents were purchased at the highest commercial quality and used without further purification unless otherwise stated. All reactions were carried out in oven-dried glassware under an argon atmosphere with dry solvents unless otherwise noted. The compound library consisted of 5 sub-libraries purchased from Maybridge, Enamine, Specs, Chemdiv, and WXTD.

Synthesis

N-(1H-benzo[d]imidazol-2-yl)thiophene-2-carboximidamide 3

General procedure A: A mixture of 1 (133.2 mg, 1 mmol), 2 (109.1 mg, 1 mmol) and anhydrous tin tetrachloride (1 M in dichloromethane, 3 mL, 3 mmol) in a sealed tube was heated at 130°C under argon for 24 h. The mixture was then stirred at room temperature and dispersed into the ethyl acetate. The obtained ethyl acetate solution was poured into the ice cold aq. 20% NaOH gradually, and the resulting mixture was extracted with ethyl acetate (20 mL × 3). The organic layers were combined together, washed with water, brine, and dried over Na_2SO_4 successively. After evaporation of the solvent under reduced pressure, the residue was subjected to column chromatography on silica gel column chromatography (PE/EtOAc = 1/1) to provide the 3 as a white powder (189.0 mg, 78%).

^{1}H NMR (400 MHz, DMSO-d6) δ 11.93 (br, 1H), 10.27 (br, 1H), 8.68 (br, 1H), 7.93 (dd, J = 4.0 Hz, 1.2 Hz, 1H), 7.76 (dd, J = 4.0 Hz, 1.2 Hz, 1H), 7.45-7.48 (m, 1H), 7.23-7.27 (m, 1H), 7.19-7.22 (m, 1H), 7.09∼7.04 (m, 2H).

HRMS (ESI) $[M + H]^+$ calculated for $C_{12}H_{11}N_4S$: 243.0695, found: 243.0670.

2-(thiophen-2-yl)-4H-benzo[4,5]imidazo[1,2-b][1,2,4]triazole 4

General procedure B: To a flame-dried 10 mL flask with a magnet, was added the amidine 3 (24.2 mg, 0.1 mmol) and KO*t*Bu (44.8 mg, 0.4 mmol) under argon. The flask was cooled in a dry ice-acetone bath, and THF (2 mL) was then added with stirring. After 1 h stirring at same temperature, a solution of N-chlorosuccinimide (NCS) (16.0 mg, 0.12 mmol) in THF

(2 mL) was added and the result mixture was stirred until it finished by TLC monitor (about 0.5∼1 h). The reaction was then quenched with saturated aqueous NH_4Cl (1 mL) and moved to room temperature. The system was diluted with ethyl acetate, washed with water, brine and dried over Na_2SO_4 successively. The dried solution was concentrated in vacuo to 2 mL, filtrated and washed with a small amount of ethyl acetate to obtain a large portion of the final product. The mother liquid was then purified by a short silica gel column chromatography (PE/EtOAc = 1/2) to provide another portion of the final product. The two portions were combined together to afford 4 as a white powder (22.3 mg, 93%).

^{1}H NMR (400 MHz, DMSO-d6) δ 12.45 (br, 1H), 7.84 (d, J = 8 Hz, 1H), 7.70 (dd, J = 4 Hz, 0.8 Hz, 1H), 7.65 (dd, J = 4 Hz, 0.8 Hz, 1H), 7.56 (d, J = 8 Hz, 1H), 7.34-7.40 (m, 1H), 7.30-7.32 (m, 1H), 7.19 (dd, J = 8 Hz, 4 Hz, 1H).

HRMS (ESI) $[M + H]^+$ calculated for $C_{12}H_9N_4S$: 241.0540, found: 241.0542.

1-(4-bromophenyl)-2-(2-(thiophen-2-yl)-4H-benzo[4,5] imidazo[1,2-b][1,2,4]triazol-4-yl)ethan-1-one LX-3

General procedure C: To a flame-dried 10 mL flask with a magnet, potassium carbonate (55.3 mg, 0.4 mmol) was added to the anhydrous acetone solution (5 mL) of 4 (24.0 mg, 0.1 mmol) and bromide 5 (30.6 mg, 0.11 mmol). The reaction mixture was stirred overnight, diluted with water and extracted with ethyl acetate. Washed with brine and then dried over Na_2SO_4. filtered and concentrated in vacuo to give a crude oil, which was purified by silica gel column chromatography (PE/EtOAc = 1/2) to afford compound LX-3 as a white powder (30.6 mg, 70%).

^{1}H NMR (400 MHz, $CDCl_3$) δ 7.93 (d, J = 8.4 Hz, 2H), 7.90–7.85 (m, 1H), 7.77 (d, J = 3.5 Hz, 1H), 7.70 (d, J = 8.4 Hz, 2H), 7.38 (d, J = 5.0 Hz, 1H), 7.37–7.30 (m, 2H), 7.22–7.17 (m, 1H), 7.15–7.11 (m, 1H), 5.66 (s, 2H);

^{13}C NMR (151 MHz, $CDCl_3$) δ 190.0, 161.3, 134.9, 134.5, 132.8, 132.5, 129.9, 129.6, 127.8, 126.8, 126.6, 124.7, 124.0, 122.4, 111.3, 110.6, 49.6.

HRMS (ESI) $[M + H]^+$ calculated for $C_{20}H_{14}BrN_4OS$: 437.0066, found: 437.0081.

1-phenyl-2-(2-(thiophen-2-yl)-4H-benzo[4,5] imidazo[1,2-b][1,2,4]triazol-4-yl)ethan-1-one 7a

According to the general procedure C, the reaction was finished in 12 h.

White powder,1.0 mg, yield 67% **^{1}H NMR** (400 MHz, $CDCl_3$) δ 8.08 (d, J = 8.4 Hz, 2H), 7.88 (d, J = 4.8 Hz, 1H), 7.77 (dd, J = 4.0, 1.6 Hz, 1H), 7.67 (t, J = 5.6 Hz, 1H), 7.57 (t, J = 8.4 Hz, 2H), 7.38–7.33 (m, 3H), 7.23–7.20 (m, 1H), 7.13–7.11 (m, 1H), 5.72 (s, 2H).

1-(4-methoxyphenyl)-2-(2-(thiophen-2-yl)-4H-benzo[4,5] imidazo[1,2-b][1,2,4]triazol-4-yl)ethan-1-one 7b

According to the general procedure C, the reaction was finished in 12 h.

White powder,1.1 mg, yield 58% **^{1}H NMR** (400 MHz, $CDCl_3$) δ 8.04 (d, J = 8.9 Hz, 2H), 7.89–7.84 (m, 1H), 7.77 (dd, J = 3.6, 1.0 Hz, 1H), 7.37 (dd, J = 5.0, 1.0 Hz, 1H), 7.34–7.29 (m, 2H), 7.23–7.18 (m, 1H), 7.12 (dd, J = 4.9, 3.7 Hz, 1H), 7.01 (d, J = 8.9 Hz, 2H), 5.66 (s, 2H), 3.91 (s, 3H);

^{13}C NMR (151 MHz, CDCl3) δ 189.1, 164.5, 161.2, 154.5, 135.2, 134.6, 130.6, 127.7, 127.2, 126.7, 126.6, 124.6, 124.0, 122.2, 114.3, 111.2, 110.8, 55.6, 49.4.

HRMS (ESI) $[M + H]^+$ calculated for $C_{21}H_{17}N_4O_2S$: 389.1067, found: 389.1075.

1-(4-nitrophenyl)-2-(2-(thiophen-2-yl)-4H-benzo[4,5] imidazo[1,2-b][1,2,4]triazol-4-yl)ethan-1-one 7c

According to the general procedure C, the reaction was finished in 12 h.

Yellow powder,1.4 mg, yield 20% **^{1}H NMR** (400 MHz, $CDCl_3$) δ 8.40 (d, J = 8.6 Hz, 2H), 8.25 (d, J = 8.7 Hz, 2H), 7.92–7.83 (m, 1H), 7.77 (d, J = 3.5 Hz, 1H), 7.43–7.32 (m, 3H), 7.23–7.18 (m, 1H), 7.16–7.09 (m, 1H), 5.73 (s, 2H).

^{13}C NMR (151 MHz, $CDCl_3$) δ 189.8, 161.3, 154.3, 151.1, 138.4, 134.8, 134.4, 129.4, 127.8, 126.9, 126.7, 124.7, 124.3, 124.2, 122.6, 111.4, 110.5, 50.1.

HRMS (ESI) $[M + H]^+$ calculated for $C_{20}H_{14}N_5O_3S$: 404.0812, found: 404.0802.

methyl 4-(2-(2-(thiophen-2-yl)-4H-benzo[4,5] imidazo[1,2-b][1,2,4]triazol-4-yl)acetyl)benzoate 7d

According to the general procedure C, the reaction was finished in 24 h.

White powder,7.1 mg, yield 30% **^{1}H NMR** (400 MHz, $CDCl_3$) δ 8.21 (d, J = 8.4 Hz, 2H), 8.13 (d, J = 8.3 Hz, 2H), 7.91 – 7.86 (m, 1H), 7.77 (d, J = 3.6 Hz, 1H), 7.40–7.33 (m, 3H), 7.23–7.19 (m, 1H), 7.15–7.11 (m, 1H), 5.73 (s, 2H), 3.98 (s, 3H).

^{13}C NMR (151 MHz, $CDCl_3$) δ 189.9, 164,3, 159.0, 143.6, 142.7, 138.9, 134.3, 128.8, 128.5, 128.1, 127.4, 125.1, 124.1, 123.9, 123.2, 122.6, 111.9, 110.0, 51.6, 50.3.

HRMS (ESI) $[M + H]^+$ calculated for $C_{22}H_{17}N_4O_3S$: 417.1016, found: 417.1015;

2-(2-(thiophen-2-yl)-4H-benzo[4,5] imidazo[1,2-b][1,2,4]triazol-4-yl)-1-(4-(trifluoromethyl)phenyl)ethan-1-one 7e

According to the general procedure C, the reaction was finished in 12 h.

White powder,1.1 mg, yield 17% **^{1}H NMR** (400 MHz, $CDCl_3$) δ 8.19 (d, J = 8.2 Hz, 2H), 7.88 (dd, J = 5.3, 3.9 Hz, 1H), 7.83 (d, J = 8.3 Hz, 2H), 7.77 (dd, J = 3.6, 1.1 Hz, 1H), 7.39 (dd, J = 5.0, 1.1 Hz, 1H), 7.34 (dd, J = 6.3, 2.7 Hz, 2H), 7.22–7.18 (m, 1H), 7.13 (dd, J = 5.0, 3.7 Hz, 1H), 5.72 (s, 2H);

^{13}C NMR (151 MHz, CDCl3) δ 190.2, 161.3, 154.4, 136.7, 134.9, 134.5, 128.6, 127.8, 126.8, 126.6, 126.2, 126.2, 124.7, 124.1, 122.5, 111.3, 110.5, 49.9.

HRMS (ESI) $[M + H]^+$ calculated for $C_{21}H_{14}F_3N_4OS$: 427.0835, found: 427.0837.

1-(2,4-difluorophenyl)-2-(2-(thiophen-2-yl)-4H-benzo[4,5]imidazo[1,2-b][1,2,4]triazol-4-yl)ethan-1-one 7f

According to the general procedure C, the reaction was finished in 12 h at 40°C.

White powder,5.0 mg, yield 44% **^{1}H NMR** (400 MHz, $CDCl_3$) δ 8.06 (dd, J = 15.0, 8.3 Hz, 1H), 7.91–7.86 (m, 1H), 7.76 (d, J = 3.5 Hz, 1H), 7.35 (dt, J = 14.9, 5.4 Hz, 3H), 7.19 (dd, J = 5.3, 3.8 Hz, 1H), 7.14–7.10 (m, 1H), 7.09–6.99 (m, 2H), 5.61 (d, J = 3.9 Hz, 2H).

^{13}C NMR (151 MHz, CDCl3) δ 187.7, 142.7, 142.2, 135.0, 134.6, 133.3, 133.2, 127.7, 126.7, 126.6, 124.6, 123.9, 122.3, 113.2, 113.1, 111.3, 110.4, 105.0, 53.1.

HRMS (ESI) $[M + H]^+$ calculated for $C_{20}H_{13}F_2N_4OS$: 395.0773, found: 395.0768;

1-(perfluorophenyl)-2-(2-(thiophen-2-yl)-4H-benzo[4,5] imidazo[1,2-b][1,2,4]triazol-4-yl)ethan-1-one 7g

According to the general procedure C, the reaction was finished in 12 h at 40°C.

White powder,2.0 mg, yield 22% **^{1}H NMR** (400 MHz, $CDCl_3$) δ 7.88 (dd, J = 6.1, 3.1 Hz, 1H), 7.77 (dd, J = 3.6, 1.0 Hz, 1H), 7.41–7.34 (m, 3H), 7.21 (dd, J = 6.2, 3.0 Hz, 1H), 7.13 (dd, J = 5.0, 3.7 Hz, 1H), 5.52 (s, 2H).

HRMS (ESI) $[M + H]^+$ calculated for $C_{20}H_{10}F_5N_4OS$: 449.0490, found: 449.0491;

1-(thiazol-2-yl)-2-(2-(thiophen-2-yl)-4H-benzo[4,5] imidazo[1,2-b][1,2,4]triazol-4-yl)ethan-1-one 9a

According to the general procedure C, the reaction was finished in 12 h.

White powder,3.8 mg, yield 57% **^{1}H NMR** (400 MHz, $CDCl_3$) δ 8.15 (d, J = 3.0 Hz, 1H), 7.93–7.87 (m, 1H), 7.84 (d, J = 3.0 Hz, 1H), 7.77 (d, J = 3.6 Hz, 1H), 7.41–7.30 (m, 3H), 7.24 (d, J = 4.3 Hz, 1H), 7.16–7.09 (m, 1H), 5.92 (s, 2H);

^{13}C NMR (151 MHz, $CDCl_3$) δ 184.9, 163.6, 161.4, 145.4, 134.6, 135.0, 127.7, 127.5, 126.7, 126.6, 124.7, 124.0, 122.3, 111.3, 110.4, 49.6.

HRMS (ESI) $[M + H]^+$ calculated for $C_{17}H_{12}N_5OS_2$: 366.0478, found: 366.0470.

1-(furan-2-yl)-2-(2-(thiophen-2-yl)-4H-benzo[4,5] imidazo[1,2-b][1,2,4]triazol-4-yl)ethan-1-one 9b

According to the general procedure C, the reaction was finished in 12 h.

White powder,1.9 mg, yield 14% **^{1}H NMR** (400 MHz, $CDCl_3$) δ 7.87 (dd, J = 5.9, 3.2 Hz, 1H), 7.81–7.76 (m, 1H), 7.70 (d, J = 1.0 Hz, 1H), 7.42 (d, J = 3.6 Hz, 1H), 7.39–7.37 (m, 1H), 7.33 (dt, J = 7.4, 3.7 Hz, 2H), 7.12 (dd, J = 4.9, 3.7 Hz, 1H), 6.65 (dd, J = 3.6, 1.7 Hz, 1H), 5.57 (s, 2H);

^{13}C NMR (151 MHz, CDCl3) δ 185.0, 147.4, 127.7, 126.7, 126.6, 124.6, 124.0, 122.8, 122.3, 121.8, 118.7, 113.0, 111.9, 111.2, 110.7, 109.5, 53.4.

HRMS (ESI) $[M + H]^+$ calculated for $C_{18}H_{13}N_4O_2S$: 349.0754, found: 349.0751.

1-(thiophen-2-yl)-2-(2-(thiophen-2-yl)-4H-benzo[4,5] imidazo[1,2-b][1,2,4]triazol-4-yl)ethan-1-one 9c

According to the general procedure C, the reaction was finished in 12 h.

White powder,2.0 mg, yield 17% **^{1}H NMR** (400 MHz, $CDCl_3$) δ 7.99 (d, J = 3.6 Hz, 1H), 7.87 (dd, J = 5.9, 3.0 Hz, 1H), 7.78 (d, J = 4.3 Hz, 2H), 7.41 – 7.31 (m, 3H), 7.29 (d, J = 3.3 Hz, 1H), 7.23 (d, J = 4.3 Hz, 1H), 7.16–7.09 (m, 1H), 5.61 (s, 2H);

^{13}C NMR (151 MHz, $CDCl_3$) δ 189.9, 158.5, 147.9, 142.5, 141.6, 134.8, 134.0, 125.2, 124.3, 124.0, 122.9, 122.1, 120.6, 118.5, 110.8, 110.1, 49.5.

HRMS (ESI) $[M + H]^+$ calculated for $C_{18}H_{13}N_4OS2$: 365.0525, found: 365.0532.

1-(pyridin-4-yl)-2-(2-(thiophen-2-yl)-4H-benzo[4,5] imidazo[1,2-b][1,2,4]triazol-4-yl)ethan-1-one 9d

According to the general procedure C, the reaction was finished in 12 h.

Yellow powder, 6.6 mg, yield 88% **^{1}H NMR** (400 MHz, $CDCl_3$) δ 8.91 (d, J = 5.8 Hz, 2H), 7.91–7.82 (m, 3H), 7.79–7.75 (m, 1H), 7.41–7.31 (m, 3H), 7.21–7.16 (m, 1H), 7.13 (dd, J = 4.9, 3.7 Hz, 1H), 5.69 (s, 2H);

^{13}C NMR (151 MHz, $CDCl_3$) δ 190.9, 161.3, 151.4, 139.8, 134.8, 134.4, 127.8, 126.9, 126.7, 124.7, 124.1, 122.6, 120.9, 111.4, 110.4, 49.9.

HRMS (ESI) $[M + H]^+$ calculated for $C_{19}H_{13}N_5OS$: 360.0914, found: 360.0904.

1-(4-bromophenyl)-2-(6,7-dimethyl-2-(thiophen-2-yl)-4H-benzo[4,5]imidazo[1,2-b][1,2,4]triazol-4-yl)ethan-1-one 14a

According to the general procedure C, the reaction was finished in 12 h.

White powder,11.1 mg, yield 92% **^{1}H NMR** (400 MHz, $CDCl_3$) δ 7.92 (d, J = 8.5 Hz, 2H), 7.74 (dd, J = 3.6, 0.9 Hz, 1H), 7.69 (d, J = 8.5 Hz, 2H), 7.64 (s, 1H), 7.36 (dd, J = 5.0, 0.9 Hz, 1H), 7.11 (dd, J = 4.9, 3.7 Hz, 1H), 6.94 (s, 1H), 5.60 (s, 2H), 2.38 (s, 3H), 2.34 (s, 3H);

^{13}C NMR (151 MHz, $CDCl_3$) δ 189.5, 153.7, 146.3, 142.5, 134.8, 133.5, 132.0, 131.1, 129.8, 129.0, 128.2, 127.1, 123.8, 119.1, 116.4, 111,0, 49.5, 18.1, 17.5.

HRMS (ESI) $[M + H]^+$ calculated for $C_{22}H_{18}BrN_4OS$: 465.0379, found: 465.0377.

1-(4-bromophenyl)-2-(6,7-dimethyl-2-(thiazol-2-yl)-4H-benzo[4,5] imidazo[1,2-b][1,2,4]triazol-4-yl)ethan-1-one 14b

According to the general procedure C, the reaction was finished in 12 h.

White powder,2.7 mg, yield 29% **^{1}H NMR** (400 MHz, $CDCl_3$) δ 7.94 (dd, J = 12.9, 5.8 Hz, 3H), 7.70 (d, J = 8.4 Hz, 3H), 7.42 (d, J = 3.0 Hz, 1H), 6.99 (s, 1H), 5.65 (s, 2H), 2.41 (s, 3H), 2.36 (s, 3H).

^{13}C NMR (151 MHz, $CDCl_3$) δ 190.1, 154.3, 144.0, 141.1, 133.6, 132.7, 131.5, 131.0, 129.7, 127.3, 125.9, 123.0, 118.7, 116.4, 111,3, 50.1, 17.9, 16.7.

HRMS (ESI) $[M + H]^+$ calculated for $C_{21}H_{17}BrN_5OS$: 466.0332, found: 466.0326.

2-(7-bromo-2-(thiophen-2-yl)-4H-benzo[4,5] imidazo[1,2-b][1,2,4]triazol-4-yl)-1-(4-bromophenyl)ethan-1-one 17a

According to the general procedure C, the reaction was finished in 6 h.

White powder,4.2 mg, yield 24% **^{1}H NMR** (400 MHz, $CDCl_3$) δ 8.03 (s, 1H), 7.93 (d, J = 8.5 Hz, 2H), 7.76 (d, J = 3.6 Hz, 1H), 7.71 (d, J = 8.5 Hz, 2H), 7.47 – 7.43 (m, 1H), 7.39 (d, J = 5.0 Hz, 1H), 7.15 – 7.10 (m, 1H), 7.07 (d, J = 8.7 Hz, 1H), 5.65 (s, 2H);

HRMS (ESI) $[M + H]^+$ calculated for $C_{20}H_{13}Br_2N_4OS$: 514.9171, found: 514.9159.

2-(7-bromo-2-(5-bromothiophen-2-yl)-4H-benzo[4,5] imidazo[1,2-b][1,2,4]triazol-4-yl)-1-(4-bromophenyl)ethan-1-one 17c

According to the general procedure C, the reaction was finished in 4 h.

White powder,3.0 mg, yield 15% **^{1}H NMR** (500 MHz, $CDCl_3$) δ 8.02 (d, J = 1.6 Hz, 1H), 7.92 (d, J = 8.5 Hz, 2H), 7.71 (d, J = 8.5 Hz, 2H), 7.49 (d, J = 3.9 Hz, 1H), 7.45 (dd, J = 8.6, 1.7 Hz, 1H), 7.08 (d, J = 4.1 Hz, 1H), 7.06 (s, 1H), 5.62 (s, 2H).

^{13}C NMR (151 MHz, $CDCl_3$) δ 189.5, 135.7, 132.7, 132.6, 130.7, 130.1, 129.6, 127.3, 127.1, 126.9, 125.5, 125.3, 115.2, 114.5, 114.3, 113.0, 111.9, 49.7.

HRMS (ESI) $[M + H]^+$ calculated for $C_{20}H_{12}Br_3N_4OS$: 592.8276, found: 592.8277.

1-(4-bromophenyl)-2-(7-chloro-2-(thiophen-2-yl)-4H-benzo[4,5]imidazo[1,2-b][1,2,4]triazol-4-yl)ethan-1-one 19

To a solution of 16a (3.0 mg, 0.0094 mmol) in DMF was added CuCl (1.9 mg, 0.0188 mmol), the reaction was stirred at 160°C for 6 h, then cooled to r.t.. Ethyl acetate was added and the resulting solution was stirred with saturated aq. NH_4Cl/ $NH_3{\cdot}H_2O$ (9:1) solution for 15 min. Then extracted with ethyl acetate. The organic layer was dried over Na_2SO_4, filtered and concentrated in vacuo to yield the crude product and used directly in next step.

According to the general procedure C, the reaction was finished in 5 h.

White powder,1.5 mg, 34% **^{1}H NMR** (400 MHz, $CDCl_3$) δ 7.93 (d, J = 8.6 Hz, 2H), 7.88 (d, J = 1.9 Hz, 1H), 7.76 (d, J = 2.6 Hz, 1H), 7.71 (d, J = 8.6 Hz, 2H), 7.40 (d, J = 5.0 Hz, 1H), 7.31 (dd, J = 8.7, 1.9 Hz, 1H), 7.12 (dd, J = 8.6, 4.5 Hz, 2H), 5.65 (s, 2H);

HRMS (ESI) $[M + H]^+$ calculated for $C_{20}H_{13}BrClN_4OS$: 470.9676, found: 470.9666.

1-(4-bromophenyl)-2-(2-phenyl-4H-benzo[4,5] imidazo[1,2-b][1,2,4]triazol-4-yl)ethan-1-one 22a

According to the general procedure C, the reaction was finished in 12 h.

White powder,41.1 mg, yield 54% **^{1}H NMR** (400 MHz, $CDCl_3$) δ 8.22–8.16 (m, 2H), 7.96 (d, J = 8.5 Hz, 2H), 7.92–7.86 (m, 1H), 7.71 (d, J = 8.5 Hz, 2H), 7.45 (ddd, J = 8.5, 7.7, 2.2 Hz, 3H), 7.38–7.30 (m, 2H), 7.24–7.19 (m, 1H), 5.68 (s, 2H).

^{13}C NMR (151 MHz, CDCl3) δ 190.2, 165.5, 154.7, 135.0, 132.9, 132.5, 131.7, 129.7, 129.5, 128.6, 126.7, 124.0, 122.3, 111.3, 110.6, 100.0, 49.7.

HRMS (ESI) $[M + H]^+$ calculated for $C_{22}H_{16}BrN_4O$: 431.0502, found: 431.0492.

1-(4-bromophenyl)-2-(2-(2-methoxyphenyl)-4H-benzo[4,5] imidazo[1,2-b][1,2,4]triazol-4-yl)ethan-1-one 22b

According to the general procedure C, the reaction was finished in 12 h.

White powder,10.4 mg, yield 87% **^{1}H NMR** (400 MHz, $CDCl_3$) δ 8.00–7.90 (m, 4H), 7.69 (d, J = 8.6 Hz, 2H), 7.42 (dd, J = 11.7, 4.0 Hz, 1H), 7.34 (dd, J = 6.4, 2.8 Hz, 2H), 7.23–7.19 (m, 1H), 7.06 (dd, J = 12.1, 4.7 Hz, 2H), 5.68 (s, 2H), 3.98 (s, 3H);

^{13}C NMR (151 MHz, $CDCl_3$) δ 190.0, 159.4, 158.0, 141.3, 133.6, 131.4, 131.0, 129.5, 128.9, 128.2, 127.8, 124.0, 123.8, 122.9, 121.3, 120.5, 110.4, 109.6, 53.4, 49.3.

HRMS (ESI) $[M + H]^+$ calculated for $C_{23}H_{18}BrN_4O_2$: 461.0608, found: 461.0600.

1-(4-bromophenyl)-2-(2-(thiazol-2-yl)-4H-benzo[4,5] imidazo[1,2-b][1,2,4]triazol-4-yl)ethan-1-one 22c

According to the general procedure C, the reaction was finished in 12 h.

White powder,1.3 mg, yield 77% **^{1}H NMR** (400 MHz, $CDCl_3$) 7.97 (t, J = 1.2 Hz, 1H), 7.94–7.92 (m, 3H), 7.71 (d, J = 6.8 Hz, 2H), 7.44 (t, J = 1.6 Hz, 1H), 7.40–7.38 (m, 2H), 7.26–7.24 (m, 1H), 5.71 (s, 3H).

1-(4-bromophenyl)-2-(2-(3-methylthiophen-2-yl)-4H-benzo[4,5] imidazo[1,2-b][1,2,4]triazol-4-yl)ethan-1-one 22d

According to the general procedure C, the reaction was finished in 12 h.

White powder,3.7 mg, yield 83% **^{1}H NMR** (400 MHz, $CDCl_3$) δ 7.95 (d, J = 8.4 Hz, 2H), 7.90 – 7.85 (m, 1H), 7.70 (d, J = 8.4 Hz, 2H), 7.33 (t, J = 3.6 Hz, 3H), 7.23 – 7.18 (m, 1H), 6.95 (d, J = 5.0 Hz, 1H), 5.66 (s, 2H), 2.69 (s, 3H).

^{13}C NMR (151 MHz, $CDCl_3$) δ 190.2, 142.1, 138.0, 134.9, 132.9, 132.5, 131.6, 129.9, 129.7, 128.3, 125.3, 124.8, 123.98, 122.28, 121.0, 111.38, 110.6, 49.7, 29.7, 15.9.

HRMS (ESI) $[M + H]^+$ calculated for $C_{21}H_{16}BrN_4OS$: 451.0223, found: 451.0224.

1-(4-bromophenyl)-2-(2-(pyridin-2-yl)-4H-benzo[4,5] imidazo[1,2-b][1,2,4]triazol-4-yl)ethan-1-one 22e

According to the general procedure C, the reaction was finished in 12 h.

White powder,2.7 mg, yield 54% **^{1}H NMR** (400 MHz, $CDCl_3$) δ 8.76 (d, J = 4.4 Hz, 1H), 8.24 (d, J = 7.9 Hz, 1H), 7.97–7.90 (m, 3H), 7.81 (t, J = 7.7 Hz, 1H), 7.70 (d, J = 8.4 Hz, 2H), 7.40–7.31 (m, 3H), 7.23 (dd, J = 6.0, 3.1 Hz, 1H), 5.72 (s, 2H);

^{13}C NMR (151 MHz, CDCl3) δ 190.0, 150.2, 150.0, 147.4, 136.7, 135.4, 132.8, 132.5, 129.9, 129.6, 124.8, 124.4, 124.0, 122.4, 121.8, 111.6, 110.7, 49.7.

HRMS (ESI) $[M + H]^+$ calculated for $C_{21}H_{15}BrN_5O$: 432.0454, found: 432.0468.

2-(2-benzyl-4H-benzo[4,5]imidazo[1,2-b][1,2,4] triazol-4-yl)-1-(4-bromophenyl)ethan-1-one 22f

According to the general procedure C, the reaction was finished in 12 h.

White powder,1.7 mg, yield 64% **^{1}H NMR** (400 MHz, CDCl3) δ 7.90 (d, J = 8.6 Hz, 2H), 7.81 (d, J = 9.1 Hz, 1H), 7.65 (d, J = 8.6 Hz, 2H), 7.39 (d, J = 7.0 Hz, 2H), 7.34–7.28 (m, 5H), 7.19–7.17 (m, 1H), 5.58 (s, 2H), 4.20 (s, 2H).

1-(4-bromophenyl)-2-(2-(tert-butyl)-4H-benzo[4,5] imidazo[1,2-b][1,2,4]triazol-4-yl)ethan-1-one 22g

According to the general procedure C, the reaction was finished in 12 h.

White powder,8.2 mg, yield 57% **^{1}H NMR** (400 MHz, $CDCl_3$) δ 7.92 (d, J = 7.0 Hz, 2H), 7.79 (dd, J = 4.9, 2.3 Hz, 1H), 7.65 (d, J = 6.9 Hz, 2H), 7.27 (s, 1H), 7.25 (s, 1H), 7.19–7.10 (m, 1H), 5.60 (s, 2H), 1.43 (s, 9H);

^{13}C NMR (151 MHz, $CDCl_3$) δ 190.4, 176.1, 134.7, 132.9, 132.4, 129.8, 129.7,124.8, 123.5, 121.9, 111.0, 110.4, 49.7, 34.1, 29.7.

HRMS (ESI) $[M + H]^+$ calculated for $C_{20}H_{20}BrN_4O$: 411.0815, found: 411.0804.

1-(4-bromophenyl)-2-(2-(5-(p-tolyl)thiophen-2-yl)-4H-benzo[4,5]imidazo[1,2-b][1,2,4]triazol-4-yl)ethan-1-one 25

To a mixture of 16b (14.4 mg, 0.034 mmol), 23 (9.3 mg, 0.069 mmol), $Pd(OAc)_2$ (0.4 mg, 0.0017 mmol), PPh_3 (1.8 mg, 0.0069

mmol) were added ethanol and toluene. The mixture was then treated with sat. aq. $NaHCO_3$. The reaction was heated at 80°C for 8 h then 100°C for 5 h. Then the reaction was cooled and concentrated in vacuo to yield the crude product and used directly in next step.

According to the general procedure C, the reaction was finished in 12 h.

White powder,8.0 mg, yield 65% **^{1}H NMR** (400 MHz, $CDCl_3$) δ 7.93 (d, J = 8.4 Hz, 2H), 7.89–7.85 (m, 1H), 7.70 (dd, J = 6.1, 4.8 Hz, 3H), 7.56 (d, J = 8.1 Hz, 2H), 7.36–7.31 (m, 2H), 7.29 (d, J = 3.8 Hz, 1H), 7.23–7.17 (m, 3H), 5.66 (s, 2H), 2.38 (s, 3H);

^{13}C NMR (151 MHz, $CDCl_3$) δ 190.0, 145.8, 137.8, 135.0, 132.9, 132.8, 132.5, 131.3, 129.9, 129.7, 129.6, 127.5, 125.7, 124.7, 124.0, 123.2, 122.3, 111.3, 110.6, 49.7, 21.2.

HRMS (ESI) $[M + H]^+$ calculated for $C_{27}H_{20}BrN_4OS$: 527.0536, found: 527.0542.

5-(4-(2-(4-bromophenyl)-2-oxoethyl)-4H-benzo[4,5]imidazo[1,2-b][1,2,4]triazol-2-yl)thiophene-2-carbonitrile 27

To a solution of 16b (7.2 mg, 0.0172 mmol) in DMF was added CuCN (4.6 mg, 0.0515 mmol), the reaction was stirred at 160°C for 6 h, then cooled to r.t.. Diluted with water and the resulting solution was stirred with saturated aq. NH_4Cl/ $NH_3{\bullet}H_2O$ (9:1) solution for 15 min. Then extracted with ethyl acetate. The organic layer was dried over Na_2SO_4, filtered and concentrated in vacuo to yield the crude product and used directly in next step.

According to the general procedure C, the reaction was finished in 12 h.

White powder,4.9 mg, yield 61% **^{1}H NMR** (400 MHz, $CDCl_3$) δ 7.94 (d, J = 8.6 Hz, 2H), 7.74 – 7.70 (m, 3H), 7.61 (d, J = 4.0 Hz, 1H), 7.49 (d, J = 8.6 Hz, 1H), 7.38 (dd, J = 6.0, 3.3 Hz, 2H), 6.99 (d, J = 4.6 Hz, 1H), 5.67 (s, 2H);

HRMS (ESI) $[M + H]^+$ calculated for $C_{21}H_{13}BrN_5OS$: 462.0019, found: 462.0020.

1-(4-bromophenyl)-2-(2-(5-chlorothiophen-2-yl)-4H-benzo[4,5] imidazo[1,2-b][1,2,4]triazol-4-yl)ethan-1-one 29

To a solution of 16b (6.5 mg, 0.016 mmol) in DMF was added CuCl (7.7 mg, 0.078 mmol), the reaction was stirred at 160°C for 6 h, then cooled to r.t.. Ethyl acetate was added and the resulting solution was stirred with saturated aq. NH_4Cl/ $NH_3{\bullet}H_2O$ (9:1) solution for 15 min. Then extracted with ethyl acetate. The organic layer was dried over Na_2SO_4, filtered and concentrated in vacuo to yield the crude product and used directly in next step.

According to the general procedure C, the reaction was finished in 12 h.

White powder,7.6 mg, yield 32% **^{1}H NMR** (400 MHz, $CDCl_3$) δ 7.94 (d, J = 8.4 Hz, 2H), 7.89–7.83 (m, 1H), 7.71 (d, J = 8.4 Hz, 2H), 7.52 (d, J = 3.9 Hz, 1H), 7.40–7.32 (m, 2H), 7.23–7.17 (m, 1H), 6.93 (d, J = 3.9 Hz, 1H), 5.65 (s, 2H);

^{13}C NMR (151 MHz, $CDCl_3$) δ 189.9, 135.0, 133.1, 132.7, 132.5, 131.4, 129.9, 129.7, 126.9, 125.7, 125.2, 124.6, 124.2, 122.5, 111.3, 110.6, 49.60.

HRMS (ESI) $[M + H]^+$ calculated for $C_{20}H_{13}BrClN_4OS$: 470.9676, found: 470.9662

1-(4-hydroxyphenyl)-2-(2-(thiophen-2-yl)-4H-benzo[4,5]imidazo[1,2-b][1,2,4]triazol-4-yl)ethan-1-one 7h

To a solution of 7b (4.3 mg, 0.011 mmol) in 0.8 mL of CH_2Cl_2 at 0°C was added BBr_3 (1.0 M in CH_2Cl_2, 55 μL, 0.055 mmol) dropwise. The resulting solution was stirred for 14 h from 0 to 15°C gradually and quenched with saturated aqueous Na_2CO_3 (5 mL). The mixture was extracted with $CHCl_3$/*i*-PrOH (3/1) three times, and the combined organic layers were dried over anhydrous Na_2SO_4, filtered and concentrated in vacuo. Flash chromatography (THF/DCM = 3/97) provided 7 h (4.1 mg, 34%) as a white solid.

^{1}H NMR (400 MHz, $CDCl_3$) δ 7.91 (d, J = 4.7 Hz, 1H), 7.80 (d, J = 3.4 Hz, 1H), 7.63 (d, J = 8.8 Hz, 2H), 7.42 – 7.35 (m, 4H), 7.14 – 7.12 (m, 1H), 6.90 (d, J = 8.5 Hz, 2H), 5.54 (s, 2H);

HRMS (ESI) $[M + H]^+$ calculated for $C_{20}H_{15}N_4O_2S$: 375.0910, found: 375.0913.

1-(4-aminophenyl)-2-(2-(thiophen-2-yl)-4H-benzo[4,5]imidazo[1,2-b][1,2,4]triazol-4-yl)ethan-1-one 7i

Methanol solution of 7c (7.9 mg, 0.0196 mmol) and 5% Pd/C (1.6 mg) was stirred vigorously for 10 h under H_2 atmosphere. The insoluble material was removed by filtration through celite, the filtrate was concentrated in vacuo. Flash chromatography (MeOH/DCM = 3/97) provided 7i (1.2 mg, 16%) as a light yellow solid.

^{1}H NMR (400 MHz, $CDCl_3$) δ 7.89 (d, J = 8.2 Hz, 3H), 7.77 (s, 1H), 7.37 (d, J = 4.7 Hz, 1H), 7.31 (s, 2H), 7.23 (s, 1H), 7.12 (s, 1H), 6.70 (d, J = 8.2 Hz, 2H), 5.61 (s, 2H), 4.31 (s, 2H).

4-(2-(2-(thiophen-2-yl)-4H-benzo[4,5]imidazo[1,2-b][1,2,4]triazol-4-yl)acetyl)benzoic acid 7j

To a solution of 7d (4.3 mg, 0.0103 mmol) in a mixture of methanol (0.1 mL), water (0.1 mL) and THF (0.3 ml) was added LiOH (4.3 mg, 0.103 mmol) and refluxed for 1 h. After the reaction mixture cold to room temperature, 1M HCl was added, and extracted with EtOAc. The extracted organic layer was dried over anhydrous Na_2SO_4, concentrated in vacuo. Flash chromatography (MeOH/DCM = 3/97) provided 7j (4.2 mg, 36%) as a white solid.

^{1}H NMR (400 MHz, CD_3OD) δ 8.23 (d, J = 2.8 Hz, 4H), 7.88 (t, J = 4.8 Hz, 1H), 7.75–7.74 (m, 1H), 7.53 (dd, J = 5.2, 1.2 Hz, 2H), 7.42 (t, J = 4.8, 2H), 7.16–7.14 (m, 1H), 6.03 (s, 2H).

^{13}C NMR (151 MHz, $CDCl_3$) δ 190.3, 163.7, 158.4, 145.3, 142.6, 138.1, 133.0, 127.2, 125.9, 125.3, 124.5, 123.9, 123.8, 123.2, 122.7, 121.5, 111.6, 110.0, 51.9.

HRMS (ESI) $[M + H]^+$ calculated for $C_{21}H_{15}N_4O_3S$: 403.0859, found: 403.0857;

General procedure D: To a solution of 22c (1.0 eq) in DMF (0.33 M) was added DIPEA (7.0 eq) and stirred for 1 h. In a separate flask 30 (2.0 eq), EDCI (3.0 eq), HOBt (3.0 eq), and DMF (1.0 M) are mixed and stirred for 1 h. The contents of the second flask are transferred via canula into the first flask and the reaction is allowed to stirred for 24 h. The reaction was diluted with EtOAc /THF (10/1) and

washed with saturated aqueous NH_4Cl and brine. The organic layer was dried over Na_2SO_4, filtered and concentrated in vacuo to yield the crude product. The crude product was purified by flash chromatography (PE/EtOAc = 2/1) to yield the product.

(4-bromophenyl) (2-(thiazol-2-yl)-4H-benzo[4,5] imidazo[1,2-b][1,2,4]triazol-4-yl)methanone 31a

According to the general procedure D, the reaction was finished in 24 h.

White powder,3.9 mg, yield 25% **^{1}H NMR** (400 MHz, $CDCl_3$) δ 8.43–8.36 (m, 1H), 7.88–7.83 (m, 3H), 7.72 (d, J = 8.6 Hz, 2H), 7.63 (dd, J = 3.6, 1.1 Hz, 1H), 7.53–7.44 (m, 2H), 7.36 (dd, J = 5.0, 1.1 Hz, 1H), 7.08 (dd, J = 5.0, 3.7 Hz, 1H).

HRMS (ESI) $[M + H]^+$ calculated for $C_{19}H_{12}BrN_4OS$: 422.9910, found: 422.9911.

2-(4-bromophenyl)-1-(2-(thiazol-2-yl)-4H-benzo[4,5] imidazo[1,2-b][1,2,4]triazol-4-yl)ethan-1-one 31b

According to the general procedure D, the reaction was finished in 24 h.

White powder,2.1 mg, yield 52% **^{1}H NMR** (400 MHz, $CDCl_3$) δ 8.50 (d, J = 7.7 Hz, 1H), 7.85 (dd, J = 3.6, 1.1 Hz, 1H), 7.83–7.78 (m, 1H), 7.50 (d, J = 8.4 Hz, 2H), 7.48–7.42 (m, 3H), 7.40 (d, J = 8.4 Hz, 2H), 7.17 (dd, J = 5.0, 3.7 Hz, 1H), 4.75 (s, 2H).

HRMS (ESI) $[M + H]^+$ calculated for $C_{20}H_{14}BrN_4OS$: 437.0066, found: 437.0065.

3-(4-bromophenyl)-1-(2-(thiazol-2-yl)-4H-benzo[4,5] imidazo[1,2-b][1,2,4]triazol-4-yl)propan-1-one 31c

According to the general procedure D, the reaction was finished in 24 h.

White powder,12.8 mg yield 57% **^{1}H NMR** (400 MHz, DMSO-d_6) δ 8.44 (dd, J = 6.4, 2.7 Hz, 1H), 7.92 (dd, J = 6.2, 2.8 Hz, 1H), 7.79–7.69 (m, 2H), 7.62–7.46 (m, 4H), 7.38 (d, J = 8.4 Hz, 2H), 7.22 (dd, J = 4.9, 3.7 Hz, 1H), 3.66 (t, J = 7.6 Hz, 2H), 3.09 (t, J = 7.6 Hz, 2H).

^{13}C NMR (151 MHz, CDCl3) δ 169.9, 161.6, 139.0, 133.7, 132.1, 131.6, 130.4, 130.3, 127.8, 127.4, 127.2, 125.8, 125.6, 125.4, 120.3, 118.1, 110.7, 38.4, 29.6.

HRMS (ESI) $[M + H]^+$ calculated for $C_{21}H_{16}BrN_4OS$: 451.0223, found: 451.0219.

General procedure for bromination: To a mixture of 4 (1.0 eq) in $CHCl_3$ (0.1 M), was added N-bromosuccinimide (NBS) (1.03 eq). The reaction was stirred at r.t. for 4 h. Then the reaction was quenched with saturated aq. $NaHCO_3$ and extracted with ethyl acetate, the organic layer was dried over Na_2SO_4, filtered and concentrated in vacuo to yield the crude product. The residue was redissolved in CH_2Cl_2. Et_3N (2.5 eq) and $(Boc)_2O$ (3.7 eq) was added sequentially. The resulting reaction mixture was stirred at r.t. overnight then concentrated and purified by flash chromatography (PE/ CH_2Cl_2 = 7/3) to yield the product.

tert-butyl7-bromo-2-(thiophen-2-yl)-4H-benzo[4,5] imidazo[1,2-b] [1,2,4]triazole-4-carboxylate 16a

According to the general procedure for bromination, the reaction was finished in 12 h.

White powder,9.3 mg, yield 7%**^{1}H NMR** (400 MHz, CDCl3) δ 8.02 (d, J = 8.8 Hz, 1H), 7.95 (d, J = 1.9 Hz, 1H), 7.58 (d, J = 3.9 Hz, 1H), 7.53 (dd, J = 8.8, 1.9 Hz, 1H), 7.07 (d, J = 3.9 Hz, 1H), 1.75 (s, 9H).

tert-butyl2-(5-bromothiophen-2-yl)-4H-benzo[4,5] imidazo[1,2-b] [1,2,4]triazole-4-carboxylate 16b

According to the general procedure for bromination, the reaction was finished in 12 h.

White powder,23.1 mg, yield 17% **^{1}H NMR** (400 MHz, CDCl3) δ 8.14 (dd, J = 5.8, 3.2 Hz, 1H), 7.82–7.77 (m, 1H), 7.59 (d, J = 3.9 Hz, 1H), 7.46 – 7.39 (m, 2H), 7.07 (d, J = 3.9 Hz, 1H), 1.76 (s, 10H).

tert-butyl7-bromo-2-(5-bromothiophen-2-yl)-4H-benzo[4,5] imidazo[1,2-b][1,2,4]triazole-4-carboxylate 16c

According to the general procedure for bromination, the reaction was finished in 12 h.

White powder,70.7 mg, yield 44% **^{1}H NMR** (400 MHz, $CDCl_3$) δ 8.02 (d, J = 8.8 Hz, 1H), 7.95 (d, J = 1.9 Hz, 1H), 7.58 (d, J = 3.9 Hz, 1H), 7.53 (dd, J = 8.8, 1.9 Hz, 1H), 7.07 (d, J = 3.9 Hz, 1H), 1.75 (s, 9H).

Compound Effective Assay

Procedure for cell culture and establishment of the reporter cell line were reported in our previously published paper (Li et al., 2018).

Before plating cells, 384-well plates (ViewPlate, PerkinElmer) were coated with PDL (poly-D-lysine, Sigma). For each well, 1,300 B2-17 cells were plated by using a Matrix Wellmate microplate dispenser (Thermo Scientific). Then, 0.25 μL of compound was added to each well by using a versatile pipetting robot, the Biomek FX workstation (Beckman Coulter), to give a final compound concentration of 5 μM. After treatment for 72 h, the cell nuclei were stained by Hoechst 33342 (Sigma) before imaging.

The cells were imaged with Opera LX (PerkinElmer, three views per well by using 10 x (air) objective lens). Images were analyzed with the Columbus system, the mean percentage of EGFP+ cells (RGFP) was obtained to extrapolate the number of EGFP expressing cells and Hoechst-stained nuclei.

For the titration assay, the positive compounds were diluted in DMSO at concentrations ranging from 0.625 to 4 mM. Then, the B2-17 cells were treated by gradient compound and imaged as described before.

For each compound, a dose-response series was generated by using Origin 6.0 Pro software. The dot plot was fit by a DoseResp curve and then the EC50 was calculated.

Viability Assays

HEK 293 F cells were plated in 384-well, flat-bottom, tissue culture dishes (Corning) and treated with compounds, incubated 3 days, and assayed for viability using the CellTiter-Glo Luminescent Cell Viability Assay (Promega) according to the manufacturer's protocol. The absorbance at 490 and 650 nm (reference) was measured with an EnSight plate reader (Perkin Elmer). Data were normalized to the untreated control (100% viability). Each treatment was tested in two independent assays, each containing 3 replicates. The titration-viability curves of each compound were also generated by using Origin 6.0 Pro software.

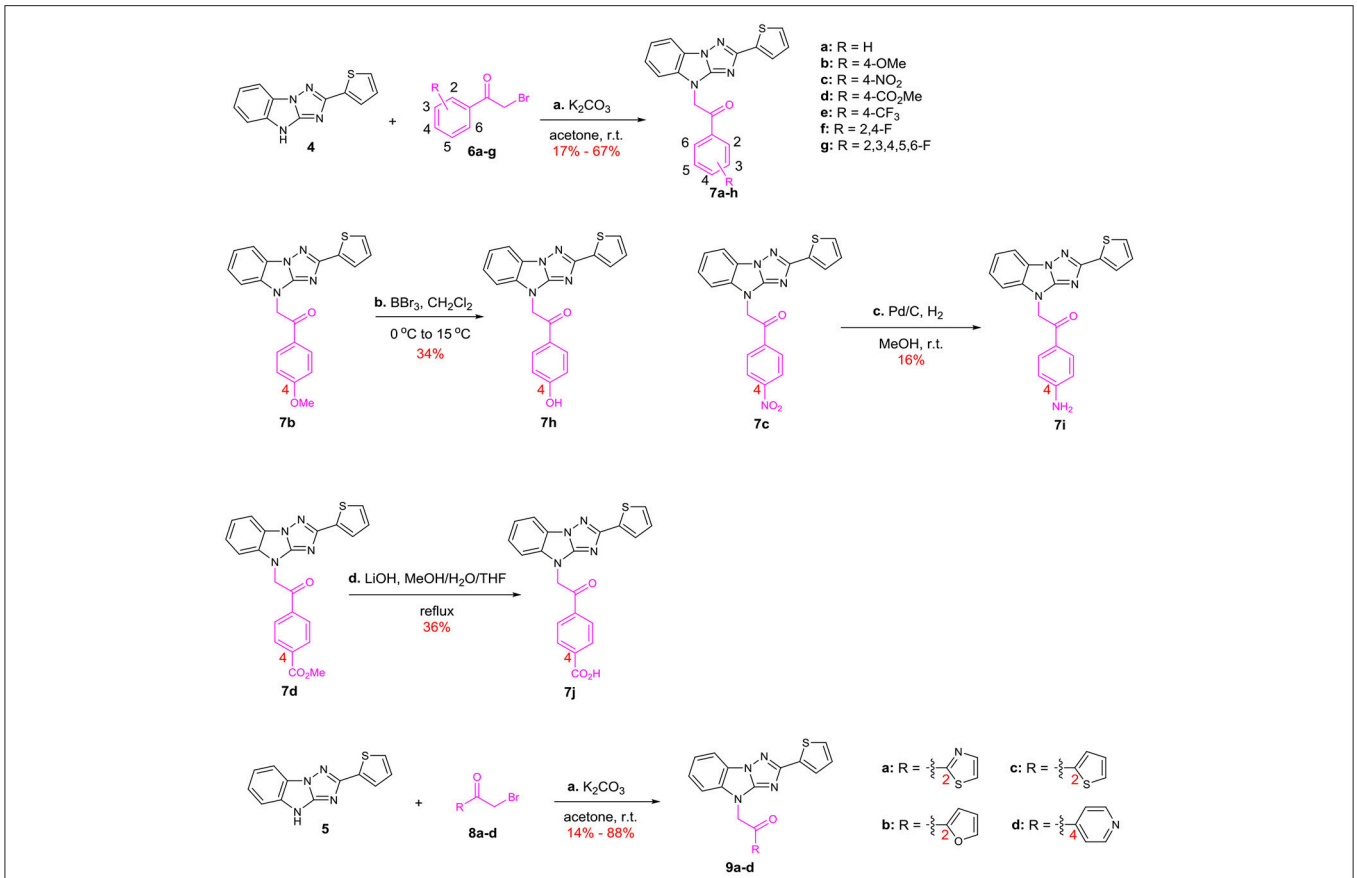

SCHEME 2 | Syntheses of the C-modified analogs: (a) K_2CO_3, acetone, r.t. (b) BBr_3, CH_2Cl_2, 0–15°C (c) Pd/C, H_2, MeOH, r.t. (d) LiOH, MeOH/H_2O/THF, reflux.

RESULTS AND DISCUSSION

We started with the structural diversification of C. The syntheses of C analogs are described in **Scheme 2**. N-alkylation of key intermediate **4** with bromide **6** bearing different substituents on the benzene ring provided **7a**-**g**, including unsubstituted, 4-OMe, 4-NO_2, 4-CO_2Me, 4-CF_3, 2,4-F and 2,3,4,5,6-F groups. Similarly, N-alkylation with 2-bromo-1-heterocyclic ethanone **8a-d** afforded skeletons **9a-d** with various heterocyclic substituents, including 2-thiazolyl, 2-furyl, 2-thiophenyl and 4-pyridyl groups. Meanwhile, methoxyl substituted compound **7b** was demethylated by using BBr_3 to provide phenolic compound **7h**. The nitro group of **7c** was reduced to afford aniline **7i**, and 4-benzoic acid **7j** was derived from methyl ester **7d** by hydrolysis using LiOH.

The syntheses of A analogs are summarized in **Scheme 3**. Both 6,7-dimethyl-2-thiophenyl (**14a**) and 6,7-dimethyl-2-thiazolyl (**14b**) analogs were synthesized using the method we describe in **Scheme 1**, where building blocks were changed correspondingly (**10** and **11a**-**b**). To prepare 7-halogenated analogs, the key intermediate **4** was brominated using NBS, but the regioselectivity for this reaction was not good, which provided **15a**-**c** as a mixture. Due to the similar polarity of these three compounds, it was difficult to separate them. Fortunately, after the imidazole of **15a**-**c** was protected with Boc, the generated compounds **16a**-**c** were easily separated. **16a**-**c** was then deprotected and alkylated with 2,4′-dibromoacetophenone **5** to give analogs **17a**-**c**, respectively. In addition, **16a** was chlorinated by using CuCl, and the subsequent substitution reaction provided **19**.

The structural diversification of B is summarized in **Scheme 4**. **22a**-**g**, whose B were phenyl, 2-methoxyphenyl, 2-thiazolyl, 3-methylthiophen-2-yl, 2-pyridyl, benzyl and *tert*-butyl groups, were prepared through the same 2-step procedures. Then **16b** was utilized as a key intermediate for the synthesis of **25**, **27** and **29**. Suzuki coupling of **16b** and subsequent N-alkylation reaction provided analog **25**. **27**and **39** were obtained through cyanation and chlorination reactions followed by N-alkylation reaction.

Finally, modifications of the length of the linker are summarized in **Scheme 5**. **4** were condensed with acids **30a**-**c** by using EDCI and HOBt afford amides **31a**-**c**, which bearing one- to three-carbon linker**.**

After constructing the DOS library containing over 30 compounds based on the central imidazo[1,2-*b*][1,2,4]triazole of **LX-3**, we set out to investigate the bioactivities of those compounds using the same screening method as we used on LX-1 to LX-7 to compare with the lead compound LX-3(**Compound effective assay and Viability assays**). The C analogs were

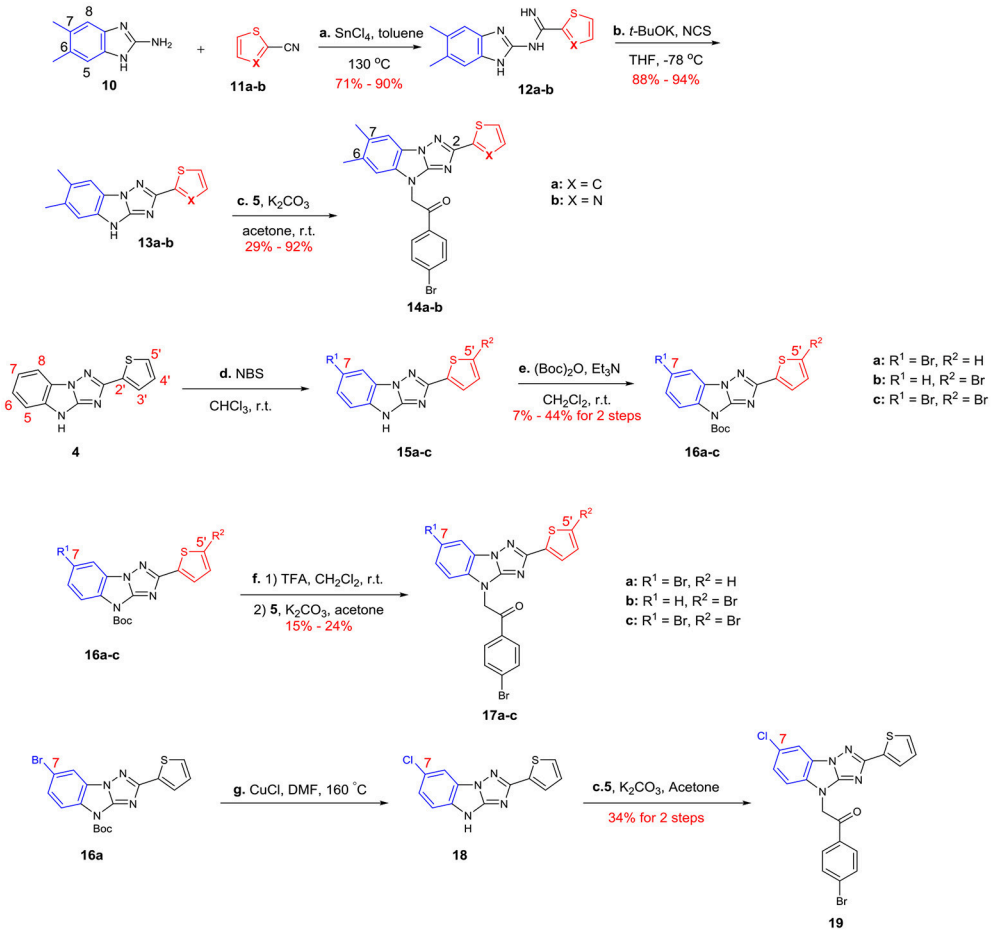

SCHEME 3 | Syntheses of the A-modified analogs: (a) $SnCl_4$, toluene, 130°C (b) *t*-BuOK, NCS, THF, −78°C (c) K_2CO_3, acetone, r.t. (d) NBS, $CHCl_3$, r.t. (e) $(Boc)_2O$, Et_3N, CH_2Cl_2, r.t. (f) 1) TFA, CH_2Cl_2, r.t. 2) 6, K_2CO_3, acetone (g) CuCl, DMF, 160°C NBS = N-Bromosuccinimide $(Boc)_2O$ = Di-tert-butyl dicarbonate Et_3N = Triethylamine TFA = Trifluoroacetic acid.

first evaluated (**Table 2**). Interestingly, we found that bromine atoms were important for activity, since when bromine atoms were removed (compound **7a**), the activity of derepressing the EGFP reporter gene silenced by DNA methylation was lost. When the bromine atoms were replaced with other hydrophobic substituent such as methoxy group (compound **7b**), nitro group (compound **7c**) or hydrophilic groups such as hydroxyl group (compound **7h**), amino group (compound **7i**) and carboxyl group (compound **7j**), the activity was decreased to some extent. However, hydrophobic groups were more beneficial, because when the carboxyl group (compound **7j**) was protected as methyl ester (compound **7d**), the activity was significantly increased (EC_{50} = 2.4 μM). Compound **7d** showed even better activity and less toxicity (IC_{50} = 10.2 μM) than the hit compound **LX-3**. When we continued to replace bromine atoms with other halogen or halogen containing groups, such as trifluoromethyl groups (compound **7e**), the activity remained the same. However, when halogen atoms (compounds **7f** and **7g**) were introduced into the 2-, 4- position (*ortho)* or 3-, 5- position (*meta)*, the potency was significantly decreased. Next, the effect of replacement of C benzene ring with different heterocyclic rings (compound **9a-d**) including thiazole, furan, thiophene and pyridine was also evaluated. It was found that the activity was comparable when the thiophene ring was introduced, even though the maximal R_{GFP} (40%) was lower than **LX-3**, while other heterocycles caused reduced activity to varying degrees.

Then, we focused on the structure-activity relationship of A (**Table 3**). When hydrophobic groups, such as halogens and methyl group were installed at the 6- or 7-position (compounds **14a**, **17a**, **19**), the activities were significantly decreased. Moreover, we found that the water solubility of these derivatives decreased a lot. However, when B was replaced with thiazole (**14b** vs. **14a**), the solubility significantly increased and the activity was comparable with the hit compound **LX-3**.

Next, we evaluated the effect of B on the activity of derepressing the EGFP reporter gene silenced by DNA methylation (**Table 4**). When the thiophene ring was replaced by benzene ring or substituted benzene ring (compound **22a**,**b**) the activity decreased significantly or even disappeared, indicating

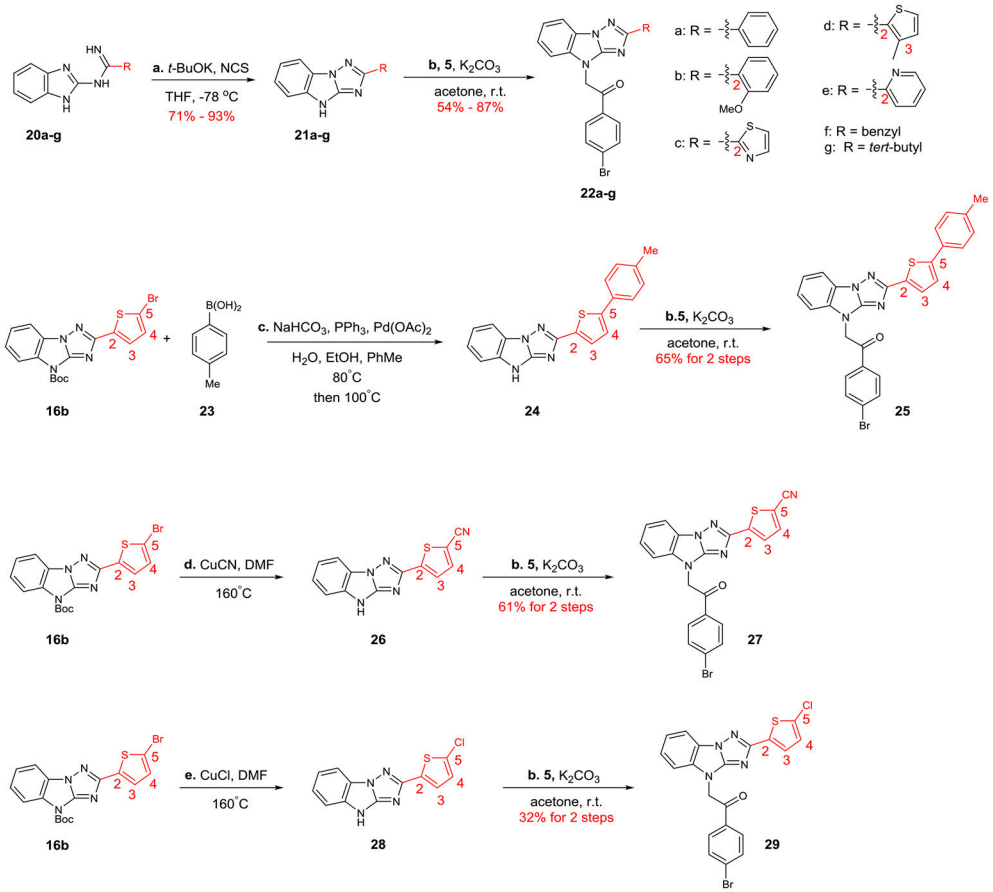

SCHEME 4 | Syntheses of the B-modified analogs: (a) *t*-BuOK, NCS, THF, −78°C (b) K_2CO_3, acetone, r.t. (c) $NaHCO_3$, PPh_3, $Pd(OAc)_2$, H_2O, EtOH, PhMe, 80°C; then 100°C (d) CuCN, DMF, 160°C (e) CuCl, DMF, 160°C.

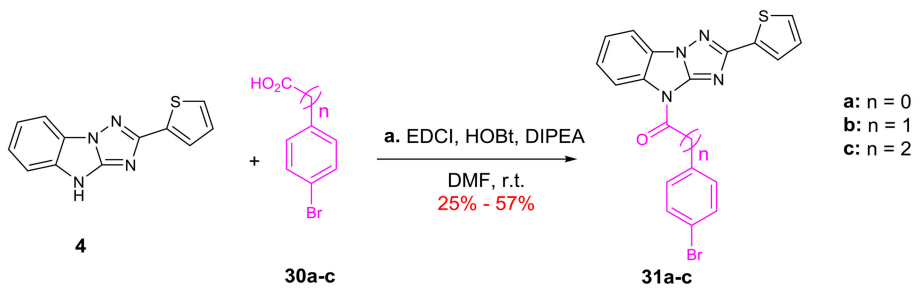

SCHEME 5 | Change of the length for the C linker: (a) EDCI, HOBt, DIPEA, DMF, r.t. EDCI = 1-(3-Dimethylaminopropyl)-3-ethylcarbodiimide HOBt = 1-Hydroxybenzotriazole DIPEA = N,N-Diisopropylethylamine.

that it was not feasible to replace B with aryl groups. Other heterocyclic rings, including thiazole and pyridine were also evaluated. Pyridine led to the loss of activity, while thiazole could slightly reduce activity (EC_{50} = 4.5 μM). Further replacing thiophene with benzyl (compound **22f**) or *tert*-butyl group (compound **22g**) also significantly decreased or even lost the activity (maximal R_{GFP} was <22%). Therefore, we further evaluated the effect of different substituents on thiophene ring. When methyl group was introduced to thiophene 3-position (**22d**), the activity disappeared. The introduction of aryl ring (compound **25**) and cyano group (compound **27**) at the 5-position of thiophene resulted in significant decrease or disappearance of activity, while the introduction of chlorine atom (compound **29**) resulted in little reduction of potency. This indicates that the substitution of 3- or 5-position on thiophene ring cannot improve the activity.

TABLE 2 | SAR of the substitutions on C.

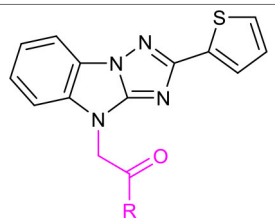

No.	R	EC_{50} (μM)	Maximal R_{GFP}%	IC_{50} (μM)
LX-3		2.8	79	5.1
7a	phenyl	–	7	1.9
7b	4-methoxyphenyl	6.2	23	3.1
7c	4-nitrophenyl	14.9	41	11.9
7d	4-(methoxycarbonyl)phenyl	2.4	73	10.2
7e	4-trifluoromethyphenyl	3.7	81	4.7
7f	2,4-difluorophenyl	–	16	17.8
7g	2,3,4,5,6-pentafluorophenyl	–	10	1.1
7h	4-hydroxyphenyl	5.8	56	16.7
7i	4-aminophenyl	–	19	5.3
7j	4-carboxyphenyl	–	7	4.8
9a	2-thiazolyl	4.7	30	8.7
9b	2-furyl	–	6.6	–
9c	2-thiophenyl	2.3	40	4.9
9d	4-pyridyl	13.6	35	6.5

TABLE 3 | SAR of the substitutions on A.

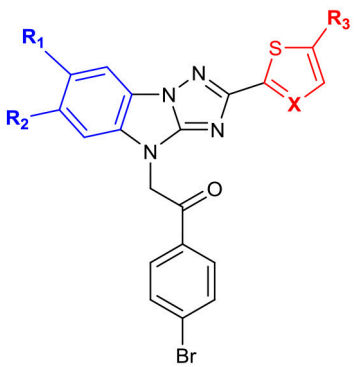

No.	R_1	R_2	R_3	X	EC_{50} (μM)	Maximal R_{GFP}%	IC_{50} (μM)
LX-3					2.8	79	5.1
14a	CH_3	CH_3	H	C	28.0	26	3.9
14b	CH_3	CH_3	H	N	3.4	58	2.1
17a	Br	H	H	C	19.4	41	6.6
17c	Br	H	Br	C	21.8	28	3.8
19	Cl	H	H	C	14.9	63	14.3

We also evaluate the effect of the linker of C (**Table 5**). First, we reduced the two-carbon unit to a single-carbon unit (compound **31a**) and found that its activity of derepressing the

TABLE 4 | SAR of the substitutions on B.

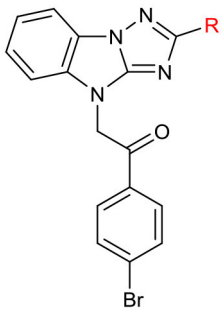

No.	R	EC_{50} (μM)	Maximal R_{GFP}%	IC_{50} (μM)
LX-3		2.8	79	5.1
22a	phenyl	–	6%	4.4
22b	2-methoxyphenyl	6.8	21	3.3
22c	2-thiazolyl	4.5	48	5.3
22d	3-methylthiophen-2-yl	–	19	12.3
22e	2-pyridyl	–	6	2.8
22f	benzyl	6.4	22	4.7
22g	*tert*-butyl	–	10	8.3
25	5-(4-tolyl)thiophen-2-yl	29.9	61	10.9
27	5-cyanothiophen-2-yl	–	6	–
29	5-chlorothiophen-2-yl	8.9	83	13.63

TABLE 5 | SAR of the linkers on C.

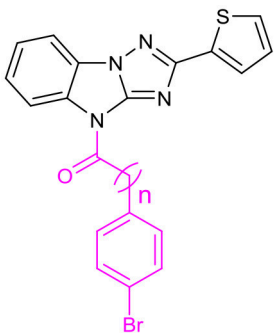

No.	n	EC_{50} (μM)	Maximal R_{GFP} %	IC_{50} (μM)
LX-3		2.8	79	5.1
31a	0	–	4.0	7.8
31b	1	–	6.0	11.5
31c	2	–	9.0	15.9

DNA methylation silenced genes disappeared. The loss of activity can also be caused by exchanging relative location of the carbonyl and methylene groups (compound **31b**) or by increasing the carbon chain (compound **31c**). These results suggest that the two carbon units in the linker section are necessary for the activity, and that the carbonyl group must be on the side close to C.

Based on the above structural modification and biological evaluation of each part of the hit compound **LX-3**, we can conclude and draw the structure-activity relationship diagram

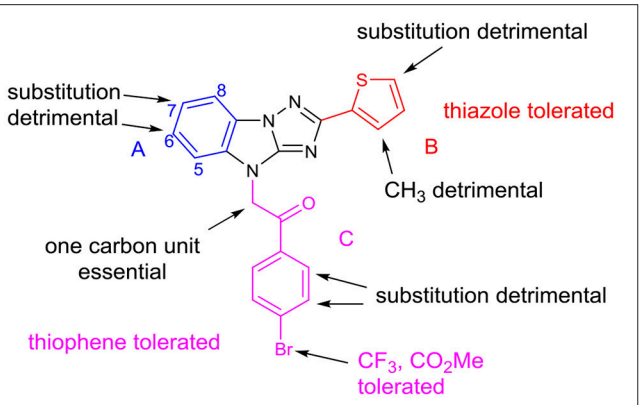

FIGURE 4 | Summary of SAR.

(**Figure 4**). First, for A, 6- and 7-substitution will result in the reduced activity. And when B is thiazole, the 7-hydrophobic small group substitution is tolerable. Secondly, for B, replacing thiophene with thiazole slightly affects the activity, but when the 3- or 5-position of thiophene is substituted, the activity decreased. In C, when the bromine atoms were replaced by hydrophobic trifluoromethyl group or the methyl carboxylate, activity was retained well. Introducing substituents to the *ortho* or *meta* position of halogen significantly reduced the activity. When the benzene ring was replaced by thiophene ring, the activity was slightly reduced.

CONCLUSION

Three small molecules, LX-3, LX-4, and LX-5, are identified utilizing high through put screening. Capable of activating a DNA methylation-repressed reporter gene, the activity can be achieved without any direct impact on DNA methylation machinery or factors downstream to DNA methylation. The derepression effect of compound LX-3, LX-4, and LX-5 functions through the activation of p38 MAPK pathway. Though capable of being activated by a number of extracellular stimuli (anisomycin, UV light, LPS, TNF-α, other cytokines and growth factors; Ono and Han, 2000; Chang and Karin, 2001; Zarubin and Jiahuai, 2005), p38 MAPK cannot be selectively activated. This lack of selectivity comes from the ability of p38 and diverse MAPKs module, especially c-jun N-terminal Kinases (JNK) module, to respond to similar stimuli. For example, anisomycin activates both p38 and JNK (Laird, 2003). Thus, an agonist that can selectively activate the p38 pathway is currently lacking. Deeper understanding of MAPKs is needed due to their involvement in many cellular processes, in which they are activated by diverse upstream stimuli(Meehan et al., 1992; Eden et al., 1998; De Smet et al., 1999). Compound(s) with specificity would serve this purpose well by facilitating the study toward individual pathways involving MAPKs. In our previous work (Li et al., 2018), we have already proved that Compound LX-3, LX-4 and LX-5 could selectively activate the p38 MAPK pathway in multiple cell types, these compounds can serve as a useful tool to discriminate the p38 module from other MAPK modules, thus they will hopefully play a role in the future applications.

However, with the exact targets of these compounds remaining to be known, futher optimization of our identified lead compounds is necessary. Through a series of modular syntheses based on the central imidazo[1,2-*b*][1,2,4]triazole structure of LX-3, a DOS library consisting of more than 30 derivatives was obtained. The SAR of A, B, C, and linker parts of the hit compound LX-3 was systematically evaluated, and the overall structure-activity diagrams were obtained. Through these endeavors, an analog, compound **7d** with slightly better activity of derepressing the EGFP reporter gene silenced by DNA methylation and less toxicity was identified. This work provides a general approach to efficiently access diverse heterocyclic molecules with interesting epigenetic modulation activities and set up a foundation for the subsequent design of chemical probes to identify the cellular targets of these lead compounds.

AUTHOR CONTRIBUTIONS

FW and JZ synthesized all of the compounds with the help of ES and JuZ. XL and BZ performed the biological evaluations of these compounds. XL supervised this work and wrote the paper with the help of FW and JZ.

ACKNOWLEDGMENTS

Financial support from the National Key Research and Development Program of China (2017YFA0505200), National High Technology Project 973 (2015CB856200), NNSFC (21625201, 21561142002, 21661140001, and 21521003) is gratefully acknowledged.

REFERENCES

Bestor, T. H., Edwards, J. R., and Boulard, M. (2015). Notes on the role of dynamic DNA methylation in mammalian development. *Proc. Natl. Acad. Sci. U.S.A.* 112,6796–6799. doi: 10.1073/pnas.1415301111

Bird, A. (2002). DNA methylation patterns and epigenetic memory. *Genes Dev*. 16, 6–21. doi: 10.1101/gad.947102

Byrd, J. C., Marcucci, G., Parthun, M. R., Xiao, J. J., Klisovic, R. B., Moran, M., et al. (2005). A phase 1 and pharmacodynamic study of depsipeptide (FK228) in chronic lymphocytic leukemia and acute myeloid leukemia. *Blood* 105,959–967. doi: 10.1182/blood-2004-05-1693

Campuzano, V., Montermini, L., Moltò, M. D., and Pianese, L., et al. (1996). Friedreich's ataxia: autosomal recessive disease caused by an intronic GAA triplet repeat expansion. *Science* 271:1423. doi: 10.1126/science.271.5254.1423

Cedar, H. (1988). DNA methylation and gene activity. *Cell* 53, 3–4. doi: 10.1016/0092-8674(88)90479-5

Chang, L., and Karin, M. (2001). Mammalian MAP kinase signalling cascades. *Nature*. 410, 37–40. doi: 10.1038/35065000

De Smet, C., Lurquin, C., Lethé, B., Martelange, V., and Boon, T. (1999). DNA methylation is the primary silencing mechanism for a set of germ line-and tumor-specific genes with a CpG-rich promoter. *Mol. Cell. Biol.* 19, 7327–7335. doi: 10.1128/MCB.19.11.7327

Dong, Q., Li, X., Wang, C. Z., Xu, S., Yuan, G., Shao, W., et al. (2018). Roles of the CSE1L-mediated nuclear import pathway in epigenetic silencing. *Proc. Natl. Acad. Sci. U.S.A.* 112, 6796–6799. doi: 10.1073/pnas.1800505115

Dong, T., Li, C., Wang, X., Dian, L., Zhang, X., Li, L., et al. (2015). Ainsliadimer A selectively inhibits IKKα/β by covalently binding a conserved cysteine. *Nat. Commun.* 6:6522. doi: 10.1038/ncomms7522

Eden, S., Hashimshony, T., Keshet, I., Cedar, H., and Thorne, A. (1998). DNA methylation models histone acetylation. *Nature* 394, 842–842. doi: 10.1038/29680

Esteller, M. (2008). Epigenetics in cancer. *N. Engl. J. Med.* 358,1148–1159. doi: 10.1056/NEJMra072067

Galloway, W. R. J. D., Isidro-Llobet, A., and Spring, D. R. (2010). Diversity-oriented synthesis as a tool for the discovery of novel biologically active small molecules. *Nat. Commun.* 1:80. doi: 10.1038/ncomms1081

Garcia, J. S., Jain, N., and Godley, L. A. (2010). An update on the safety and efficacy of decitabine in the treatment of myelodysplastic syndromes. *Onco. Targets Ther.* 3,1–13. doi: 10.2147/OTT.S7222

Laird, P. W. (2003). The power and the promise of DNA methylation markers. *Nat. Rev. Cancer* 3, 253–266. doi: 10.1038/nrc1045

Lefebvre, S., Bürglen, L., Reboullet, S., Clermont, O., Burlet, P., Viollet, L., et al. (1995). Identification and characterization of a spinal muscular atrophy-determining gene. *Cell* 80, 155–165. doi: 10.1016/0092-8674(95)90460-3

Li, D., Li, C., Li, L., Chen, S., Wang, L., Li, Q., et al. (2016). Natural product kongensin A is a non-canonical HSP90 inhibitor that blocks RIP3-dependent necroptosis. *Cell Chem. Biol.* 23, 257–266. doi: 10.1016/j.chembiol.2015.08.018

Li, X., Shang, E., Dong, Q., Li, Y., Zhang, J., Xu, S., et al. (2018). Small molecules capable of activating DNA methylation–repressed genes targeted by the p38 mitogen-activated protein kinase pathway *J. Biol. Chem*. 293, 7423–7436. doi: 10.1074/jbc.RA117.000757.

Meehan, R., Lewis, J. D., and Bird, A. P. (1992). Characterization of MeCP2, a vertebrate DNA binding protein with affinity for methylated DNA. *Nucleic Acids Res.* 20, 5085–5092. doi: 10.1093/nar/20.19.5085

O'Connor, O. A., Heaney, M. L., and Schwartz, L. (2006). Clinical experience with intravenous and oral formulations of the novel histone deacetylase inhibitor suberoylanilide hydroxamic acid in patients with advanced hematologic malignancies *J. Clin. Oncol.* 24, 166–173. doi: 10.4081/hmr.v1i8.297

Ono, K., and Han, J. (2000). The p38 signal transduction pathway activation and function. *Cell Signal.* 12, 1–13. doi: 10.1016/S0898-6568(99)00071-6

Robertson, K. D., and Wolffe, A. P. (2000). DNA methylation in health and disease. *Nat. Rev. Genet.* 1,11–19. doi: 10.1038/35049533

Shang, E., Zhang, J., Bai, J., Wang, Z., Li, X., Zhu, B., et al. (2016). Syntheses of [1,2,4]triazolo[1,5-a]benzazoles enabled by the transition-metal-free oxidative N–N bond formation. *Chem. Commun.* 52, 7028-—7031. doi: 10.1039/c6cc01976e

Sun, L., Wang, H., Wang, Z., He, S., Chen, S., Liao, D., et al. (2012). Mixed lineage kinase domain-like protein mediates necrosis signaling downstream of RIP3 kinase. *Cell* 148, 213–227. doi: 10.1016/j.cell.2011.11.031

Taunton, J., Hassig, C. A., and Schreiber, S. L. (1996). A mammalian histone deacetylase related to the yeast transcriptional regulator Rpd3p. *Science* 272, 408–411. doi: 10.1126/science.272.5260.408

Verkerk, A. J., Pieretti, M., Sutcliffe, J. S., Fu, Y. H., Kuhl, D. P., Pizzuti, A., et al. (1991). Identification of a gene (FMR-1) containing a CGG repeat coincident with a breakpoint cluster region exhibiting length variation in fragile X syndrome. *Cell* 65, 905–914. doi: 10.1016/0092-8674(91)90397-H

Wang, G., Wang, X., Yu, H., Wei, S., Williams, N., Holmes, D. L., et al. (2013). Small-molecule activation of the TRAIL receptor DR5 in human cancer cells. *Nat. Chem. Biol.* 9, 84–89. doi: 10.1038/nchembio.1153

Zarubin, T., and Jiahuai, H. (2005). Activation and signaling of the p38 MAP kinase pathway. *Cell Res.* 15, 11–18. doi: 10.1038/sj.cr.7290257

Conflict of Interest Statement: The authors declare that the research was conducted in the absence of any commercial or financial relationships that could be construed as a potential conflict of interest.

frontiers in Chemistry

ORIGINAL RESEARCH
published: 27 November 2018
doi: 10.3389/fchem.2018.00579

Diversity-Oriented Synthesis and Optical Properties of Bichromophoric Pyrrole-Fluorophore Conjugates

*Oliver Grotkopp, Bernhard Mayer and Thomas J. J. Müller**

Institut für Organische Chemie und Makromolekulare Chemie, Heinrich-Heine-Universität Düsseldorf, Düsseldorf, Germany

The mild reaction conditions of the palladium-copper coupling-isomerization reaction open a highly convergent, chromogenic route to blue emissive pyrroles in the sense of a consecutive four-component reaction. By virtue of this strategy a phenol derivative can be readily accessed, which can be transformed in a level-2 transformation to a library of bichromophoric pyrrol-fluorophore conjugates by facile alkylation with fluorophore halides. The photophysics of the underlying blue emitter derivative and the conjugates is studied by absorption and emission spectroscopy, furnishing intramolecular energy transfer at short distances as well as competing fluorescence quenching. In some cases partial energy transfer results in the occurrence of dual emission, for instance seen as magenta-rose emission arising from blue and red orange luminescence. The experimental photophysical studies are rationalized by DFT and TD-DFT calculations.

Keywords: absorption, bichromophores, DFT, emission, energy transfer, level-2 functionalization, multicomponent reaction, pyrrole

OPEN ACCESS

Edited by:
Lisa Moni,
Università di Genova, Italy

Reviewed by:
Fabio De Moliner,
University of Edinburgh,
United Kingdom
Eddy Sotelo,
Universidade de Santiago de Compostela, Spain

****Correspondence:***
Thomas J. J. Müller
thomasjj.mueller@hhu.de

Specialty section:
This article was submitted to Organic Chemistry, a section of the journal Frontiers in Chemistry

Received: *10 September 2018*
Accepted: *06 November 2018*
Published: *27 November 2018*

Citation:
Grotkopp O, Mayer B and Müller TJJ (2018) Diversity-Oriented Synthesis and Optical Properties of Bichromophoric Pyrrole-Fluorophore Conjugates. Front. Chem. 6:579. doi: 10.3389/fchem.2018.00579

INTRODUCTION

A particularly interesting aspect of functional organic materials (Müller and Bunz, 2007) is based on inter- and intra-molecular interactions of chromophores, eventually, as multichromophore systems (Bazan, 2007). Non-conjugatively ligated multichromophores will not interact in the electronic ground state, if rigidified orientations and intramolecular aggregation are excluded, but their interaction occurs after photonic excitation, i.e., in the electronically excited states. Luminescence as an excited state phenomenon is particularly intriguing because it bears an enormous potential of application, ranging from fundamental science in molecular photonics (for reviews, see e.g., Fox, 1999; Garnier, 1999; Tour, 2000; Carroll and Gorman, 2002; Coropceanu et al., 2007; Shirota and Kageyama, 2007; Walzer et al., 2007) to illumination technology by OLED (organic light emitting diodes) (for reviews, see e.g., Müllen and Scherf, 2006; Park et al., 2011; Thejo Kalayani and Dhoble, 2012; Li, 2015). For modulation of emission colors not only is relevant for environment sensitive mapping of cellular compartments and structures (Klymchenko, 2017), but also in white light generation (Yuan et al., 2013) in the sense of additive color mixing. Most crucial in this context is avoidance of energy transfer cross-talk that proceeds within Förster radii. At usual concentration two chromophores emit independently in solution (Sarkar et al., 2016). Likewise this effect can also be achieved by embedding in micelles, organic or hybrid matrices (For recent examples of photochromic and multichromophoric emitters embedded in micelles or matrices, see e. g., Findlay et al., 2014; Shi et al., 2015; Bälter et al., 2016; Joshi et al., 2016; Börgardts and Müller, 2017; Pallavi et al., 2018). Far more challenging, however, is the conceptual design of unimolecular bi- or multichromophores capable of polychromic emission (for reviews on organic white light emitting

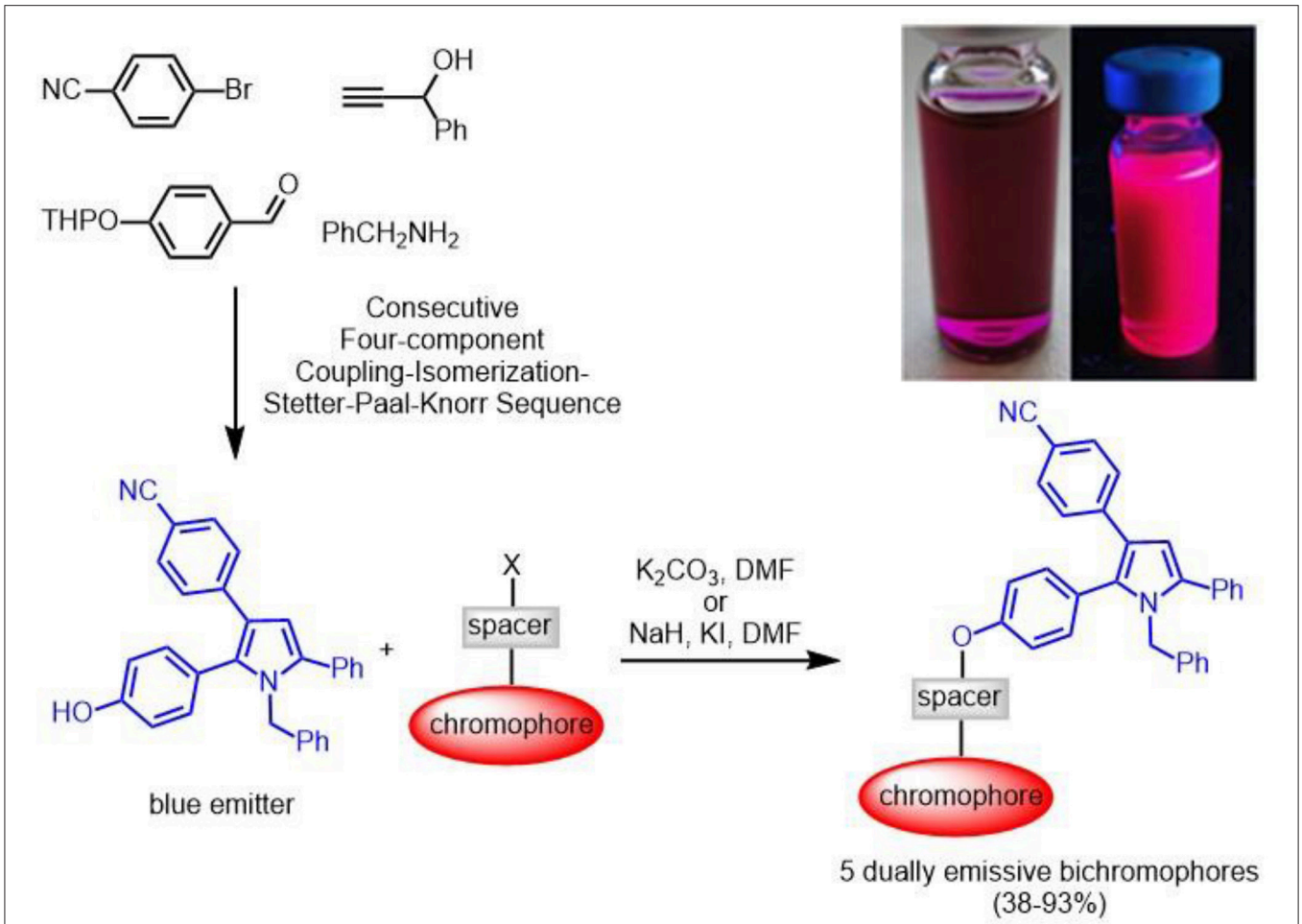

Graphical Abstract| Concise two-step pyrrole-based non-conjugated emissive bichromophores by four-component pyrrole synthesis and nucleophilic substitution.

devices and materials, see Mukherjee and Thilagar, 2014, 2015; Wu and Ma, 2016). In this case the occurrence of dual (or even polychromic) emission has to operate at intramolecular chromophore-chromophore distances around 1 nm, where excited state resonance energy transfer is ultrafast (for a detailed study on a umbelliferone–alizarin bichromophore, see Lapini et al., 2014). The control of energy transfer cross-talk of the constituting luminophores has to be modulated by partial and frustrated energy transfer (Klymchenko et al., 2003, 2007). While frustrated energy transfer unimolcular bichromophores operated by ESIPT (excited state intramolecular proton transfer) have been disclosed (for representative small molecule emitters operated by frustrated and partial energy transfer by ESIPT, see e.g., Park et al., 2009; Kwon et al., 2013; Benelhadj et al., 2014), we reasoned linear and angular geometrical orientation in emissive bichromophores might be achieved by level-2 functionalization of a blue emitter with several bathochromically emitting chromophores should lead to dually solution emissive unimolecular bichromophores.

Diversity-oriented syntheses of dyes (for reviews on diversity-oriented syntheses of π-systems, see Briehn and Bäuerle, 2002; Müller, 2007; Müller and D'Souza, 2008; de Moliner et al., 2017) in a one-pot fashion have become an attractive tool for designing and optimizing chromophores. In this context, we have predominantly been focusing on developing chromogenic multicomponent syntheses of functional chromophores (Levi and Müller, 2016b), fluorophores (**Figure 1**) (Levi and Müller, 2016a; Riva et al., 2016), and aggregation-induced emissive chromophores (Müller, 2016; Merkt and Müller, 2018).

Several years ago we disclosed a consecutive four-component synthesis of blue-emissive pyrroles by a coupling-isomerization-Stetter-Paal-Knorr sequence (Braun et al., 2001; Braun and Müller, 2004). Herein, we report concise two step syntheses of a selection of bichromophoric pyrrole-fluorophore conjugates based upon the MCR pyrrole synthesis and its level two functionalization with a second redshifted emissive chromophore via Williamson ether synthesis or sulfonate formation. The electronic properties are conducted with absorption and

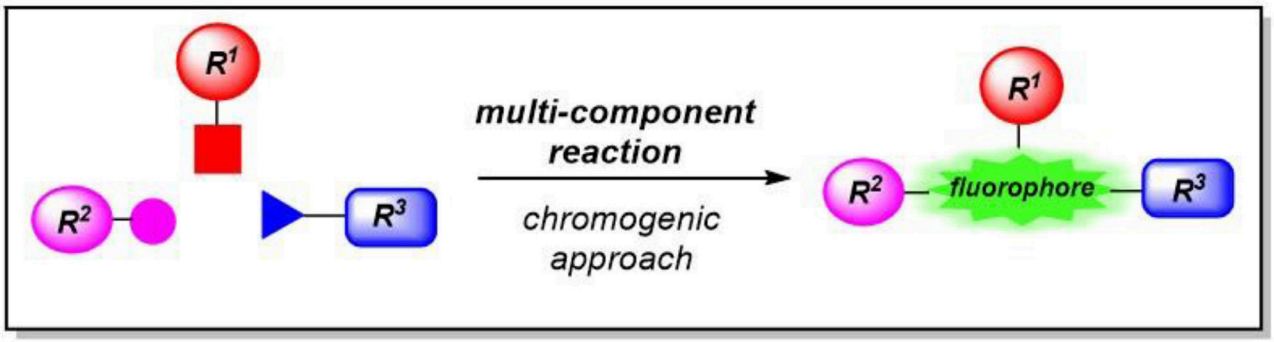

FIGURE 1 | Diversity oriented syntheses of fluorophores by chromogenic multi-component reactions.

fluorescence spectroscopy as well as interpreted in the light of DFT and TD DFT calculations.

RESULTS AND DISCUSSION

Synthesis

First attempts to employ the four-component coupling-isomerization-Stetter-Paal-Knorr pyrrole synthesis (Braun et al., 2001; Braun and Müller, 2004) to introduce the second chromophore in a one-pot fashion failed, predominantly due to solubility issues. Therefore, we envisioned that a phenol containing pyrrole might ideally serve for a post MCR ligation by etherification or esterification. Therefore, performing the four-component pyrrole synthesis with THP-protected *para*-hydroxybenzaldehyde gave rise to the formation of 4-(1-benzyl-2-(4-hydroxy-phenyl)-5-phenyl-1*H*-pyrrol-3-yl)benzonitrile (**1**) after isolation and chromatographic purification in 26% (**Scheme 1**). Under the acidic conditions of the terminal Paal-Knorr cyclocondensation the THP group is cleaved to give the free phenol.

Absorption spectroscopy of phenol **1** reveals a longest wavelength absorption maximum at 319 nm and an additional absorption band at 275 nm. Upon excitation at the longest wavelength maximum a broad intense emission at 442 nm is found with a relative fluorescence quantum yield Φ_F of 0.11, i.e., in a comparable magnitude as other benzonitrile substituted pyrroles (Braun and Müller, 2004) (vide infra). With this intensively blue emissive building block in hand the stage was set for the synthesis of luminescent bichromophores in the sense of a level-2 functionalization.

The reference luminophore **2**, a methyl ether derivative, was synthesized by etherification of phenol **1** with methyl iodide in 68% yield. Halide functionalized luminophores **3** (Aathimanikandan et al., 2005) and **5** (Kucherak et al., 2010), **6** (Lord et al., 2010), and **7** (Lord et al., 2010) (some also containing alkyl spacers) were prepared according to literature protocols (dansyl chloride was purchased and used as received) and submitted to base mediated Williamson ether synthesis or sulfonylation with phenol **1** to give bichromophores **8–12** in moderate to excellent yield (**Scheme 2**). While the bromides **3** and **5**, dansyl chloride **4** and methyl iodide react smoothly with potassium carbonate as a base, for the chlorides **6** and **7**, Finkelstein conditions with potassium iodide have to applied, which work best in these cases with sodium hydride as a base.

The ^{1}H and ^{13}C NMR and mass spectra (MALDI-TOF and HRMS) unambiguously confirm the successful ligation of the **1** with the second chromophores **3–7** as well as methyl iodide, and thereby the structures of pyrrole reference chromophore **2** and the bichromophores **8–12**.

Photophysical Properties and Electronic Structure

Upon excitation with a handheld UV lamp the pyrrole reference chromophore **2** and all bichromophores **8–12** luminesce, indicating that the photonic excitation is neither completely quenched by internal conversion nor by electron transfer into long-lived charge separated states arising from photoinduced intramolecular electron transfer (PIET) (Kavarnos, 1993). This prompted us to study the absorption and emission spectra of the luminophores **2** and **8–12** in more detail (**Table 1**).

The absorption spectra of all bichromophores **8–12** behave essentially additively with respect to the underlying subchromophores. This is quantitatively demonstrated by comparison of the UV/Vis spectrum of the pyrrole-anthracene bichromophore **8** and the sum spectra of the reference chromophores **2** (pyrrole) and 9-methyl anthracene (anthracene) (for spectral details, see **Supplementary Material**). As expected, in the electronic ground state, from where photonic excitation starts, the two subchromophores essentially neither interact nor form aggregates at the concentrations investigated. However, in the excited state, as studied by fluorescence spectroscopy, in some cases a cooperative behavior exists, which is also dependent on the excited subchromophore.

Upon excitation of the pyrrole-anthracene bichromophore **8** at the absorption bands of the anthracene chromophore at 260, 367, and 387 nm clearly the emission bands of anthracene with vibrational resolution are detected (for spectral details, see **Supplementary Material**). However, upon excitation at the pyrrole absorption bands at 317 and 330 nm exclusively the

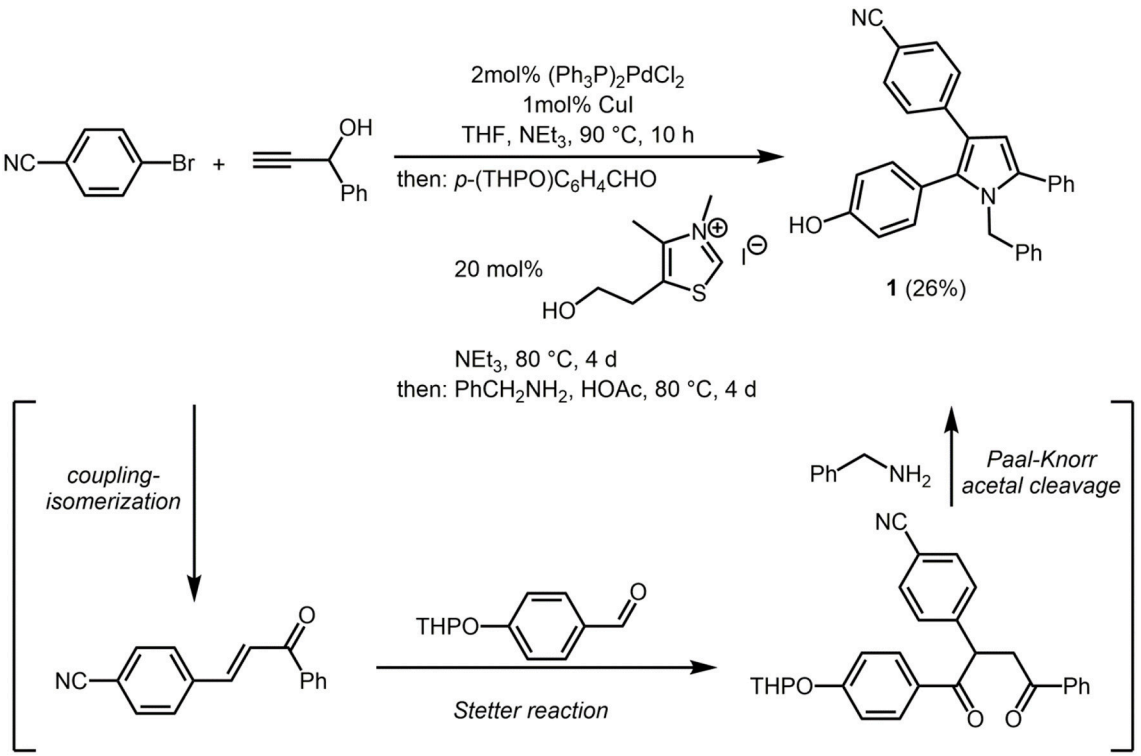

SCHEME 1 | Consecutive four-component coupling-isomerization-Stetter-Paal-Knorr synthesis of 4-(1-benzyl-2-(4-hydroxy-phenyl)-5-phenyl-1*H*-pyrrol-3-yl)benzonitrile (**1**).

pyrrole typical structureless emission band at 443.5 nm appears (**Figure 2**). The separate excitations of the discrete absorption bands of the subchromophores in bichromophore **8** are not accompanied by energy transfer from the donor (pyrrole) to the acceptor (anthracene). Although the fluorescence quantum yield Φ_f of 0.09 accounts for a significant energy dissipation upon excitation of the anthracene moiety, the lack of overlap of the absorption band of the acceptor with the emission band of the donor and, hence, the absence of energy transfer suggests that in bichromophore **8** are not electronically coupled.

In the other bichromophores **9**–**12** bearing redshifted absorptions of the acceptor chromophores the situation of the emission characteristics changes (for spectral details, see **Supplementary Material**).

The absorption bands of the dansyl-pyrrole (**9**), the Nile red-pyrrole (**10**), and the quinoxalinyl-styryl-pyrrole (**12**) bichromophores clearly possess significant energy transfer characteristics, where the selective excitation of the pyrrole donor chromophore with its emission band more (**10**, **12**) or less (**9**) overlaps with the absorption bands of the corresponding acceptor chromophores. The efficiency of the energy transfer Φ_{EnT} can be estimated according to the formula (Qing et al., 2011) $\Phi_{EnT} = 1 - \frac{\Phi_{Donor}}{\Phi^0_{Donor}}$, where Φ_{donor} is the measured quantum yield of the (residual) donor emission band of the bichromophore and Φ^0_{donor} is the quantum yield of the donor chromophore. Determination of Φ_{Donor} of the residual pyrrole emission at 445 nm furnishes for bichromophore **12** a quantum yield of the energy transfer Φ_{EnT} of over 0.97. For the dansyl bichromophore **9** Φ_{EnT} can be estimated to be >0.98, while for the Nile red bichromophore **10** no residual emission around 450 nm can be detected, indicating an Φ_{EnT} of unity. However, it has to be kept in mind that an exergonic photoinduced intramolecular electron transfer (PIET) cannot be fully excluded, in particular, since the determined fluorescence quantum yields are relatively low. For the anthryl-pyrrole bichromophore **8** the PIET can be estimated to be endothermic.

Most remarkable, however, are the emission characteristics of the 3-cyano-5,5-dimethylfuran-2(5*H*)-ylidene)malononitrile-styryl bichromophore **11**, where a strong dependence on the excitation wavelength λ_{exc} can be detected. The dichloromethane solution of bichromophore **11** does not show the typical red emission of the acceptor chromophore upon eyesight at excitation with 254 or 365 nm by a handheld UV lamp, but rather a magenta-rose emission with significant intensity (**Figure 3**, top). This mixing emission color between violet ($\lambda_{max,em}$ = 442 nm) and orange red ($\lambda_{max,em}$ = 618 nm) almost matches with the line of purples (Westland, 2003; Broadbent, 2004; Schanda, 2007). The emission spectra at various excitation wavelength clearly reveal that an excitation at 365 nm not only causes an energy transfer from the pyrrole donor to the 3-cyano-5,5-dimethylfuran-2(5*H*)-ylidene)malononitrile-styryl acceptor (**Figure 3**, bottom), which emits at 618 nm, but also an emission of the donor itself at 442 nm. This peculiar behavior can be interpreted in

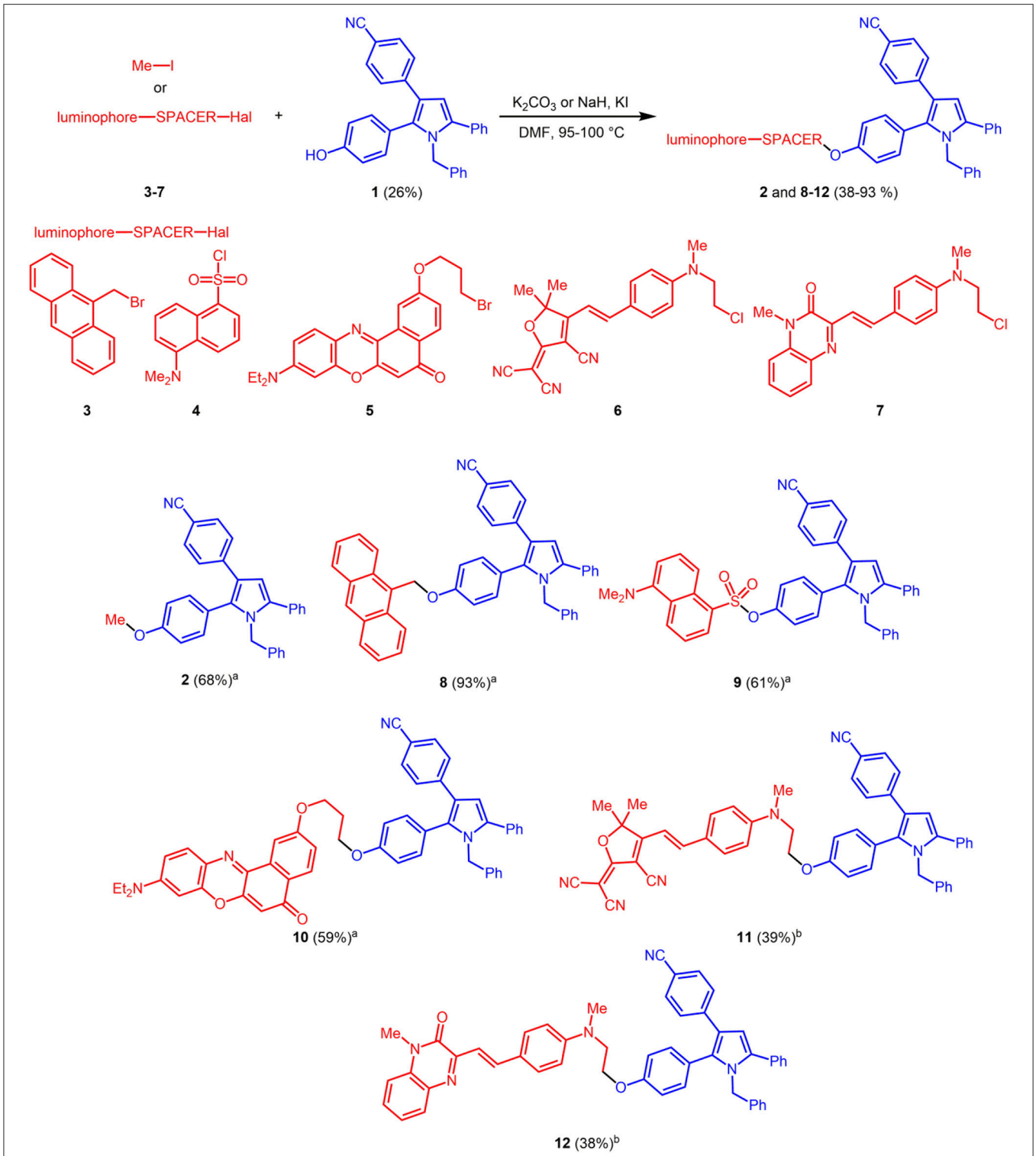

SCHEME 2 | Synthesis of reference pyrrole **2** and fluorescent bichromophores **8**–**12** by base mediated etherification or sulfonylation of phenol **1** (blue emitter) and luminophore derivatives **3–7** (redshifted emitters) or methyl iodide ([a]K_2CO_3; [b]NaH, KI).

the sense of a partial energy transfer (for representative small molecule emitters operated by frustrated and partial energy transfer by ESIPT, see e.g., Park et al., 2009; Kwon et al., 2013; Benelhadj et al., 2014), i.e., a dual emission as a consequence of an excited state communication between donor and acceptor.

TABLE 1 | Selected absorption and emission data of luminophores **2,** reference luminophores, and bichromophores **8–12** [recorded in dichloromethane at concentrations of 10^{-5} M (absorption) and 10^{-7} M (emission) at $T = 293$ K][a].

Compounds	Absorption	Emission	Stokes shift[a]	Emission color[b]
	$\lambda_{max,abs}$ [nm]	$\lambda_{max,em}$ [nm]	$\Delta\tilde{\nu}$ [cm^{-1}]	
	(ε) [L mol^{-1} cm^{-1}]	(Φ_f)		
2	276 (30,600), **316** (20,200)	**445.5** (0.28)[d]	9,200	blue
9-methyl anthracene (Roberts and Yavari, 1981)	332 (4,400), 348 (5,400), 365 (12,900), **385** (11,000)	**388**, 411 (0.36) (Rice et al., 1980)	200	blue
dansyl phenolate (Beyeh et al., 2007)[h]	263 (16,800), **350** (4,600)	**515**	9,200	Green
8	258 (192,800), 315.5 (29,800), 329 (29,600), 367 (18,100), **387** (14,200)	**394**, 415.5, 439.5 (0.09)[c,d] **443.5**[d,e]	500 9,000	Blue
9	266 (54,400), **318** (32,200)	**519** (0.28)[f] 444 (sh)	12,700	Green
10	267.5 (16,200), 294 (7,200), 316 (6,000), **529.5** (10,500)	**596**	2,000	Red
11	302 (34,700), **566** (51,900)	442, **618**[g]	1,500	Purple
12	267 (54,700), **446** (51,700)	445 (<0.01)[d], **551** (0.04)[f]	4,200	Yellow orange

[a] *The absorption maxima employed for calculating the Stokes shifts ($\Delta\tilde{\nu} = 1/\lambda_{max,abs} - 1/\lambda_{max,em}$ [cm^{-1}]) are marked bold face.*
[b] *Emission color upon excitation with a handheld UV lamp ($\lambda_{exc} = 365$ nm).*
[c] *Fluorescence upon excitation at $\lambda_{exc} = 260$, 367, and 387 nm.*
[d] *Determined with 1,9-diphenylanthracene as a standard (cyclohexane, $\Phi_f = 1.00$).*
[e] *Fluorescence upon excitation at $\lambda_{exc} = 317$ and 330 nm.*
[f] *Determined with dansyl glycine as a standard (1,4-dioxane, $\Phi_F = 0.66$).*
[g] *Upon excitation at $\lambda_{exc} = 365$ nm.*
[h] *Recorded in chloroform.*

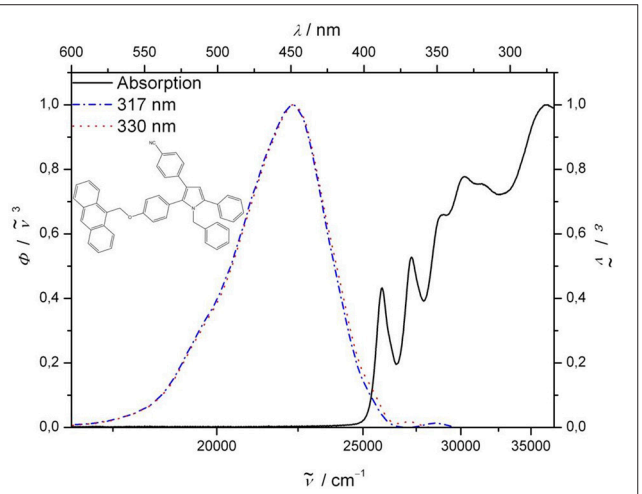

FIGURE 2 | Normalized UV/Vis (solid lines) and emission spectra (dotted: $\lambda_{exc} = 330$ nm; dash-dotted: $\lambda_{exc} = 317$ nm) of bichromophore **8** (recorded in CH_2Cl_2 at $T = 298$ K).

For a deeper understanding of the observed chromophore-chromophore interactions TD-DFT calculations were performed on the pyrrole **2** and the bichromophores **8–12**. The geometries of the electronic ground-state and excited structures were optimized by using Gaussian09 (Frisch et al., 2009) with the B3LYP functional (Lee et al., 1988; Becke, 1993; Kim and Jordan, 1994; Stephens et al., 1994) and the Pople 6-311G** basis set (Krishnan et al., 1980). Since absorption properties were measured in dichloromethane solutions, the polarizable continuum model (PCM) with dichloromethane as a solvent was utilized (Scalmani and Frisch, 2010). All minimum structures were unambiguously assigned by analytical frequency analysis. The optimized structures were then submitted to TD-DFT calculations employing the gradient-corrected exchange and correlation Perdew-Burke-Ernzerhof functionals PBE_1PBE (Adamo and Barone, 1999)/6-311** (Krishnan et al., 1980) with dichloromethane (IEFPCM) (Scalmani and Frisch, 2010) as a solvent.

The blue emissive pyrrole **2** was considered as the model donor chromophore in the bichromophore systems. The TD-DFT calculation of structure **2** revealed, in reasonably good agreement with the experimentally determined longest wavelength absorption band at 316 nm (for detailed calculated transitions, see **Table S1**), a lowest energy transition at 347 nm for the S_1 Franck-Condon absorption, which is represented to 99% as a HOMO → LUMO transition with considerable charge transfer character from the anisyl and phenyl moieties of the pyrrole to the *p*-cyanophenyl acceptor (**Figure 4**). The excitation from the vibrationally excited ground state S_0^* to the relaxed first excited state S_1 translates to the process of fluorescence. The involved HOMO → LUMO transition (99%, $f = 0.2298$, $\lambda_{calc} = 443$ nm, $\lambda_{max,exp} = 446$ nm) almost exactly reverts the electron coefficient density distribution of the absorption.

For further discussion only the absorption characteristics of the bichromophores **8**-**12** were considered (for Jablonski diagrams of the dominant absorption bands, see **Figures S12–S16**). The calculations support the additive nature of the

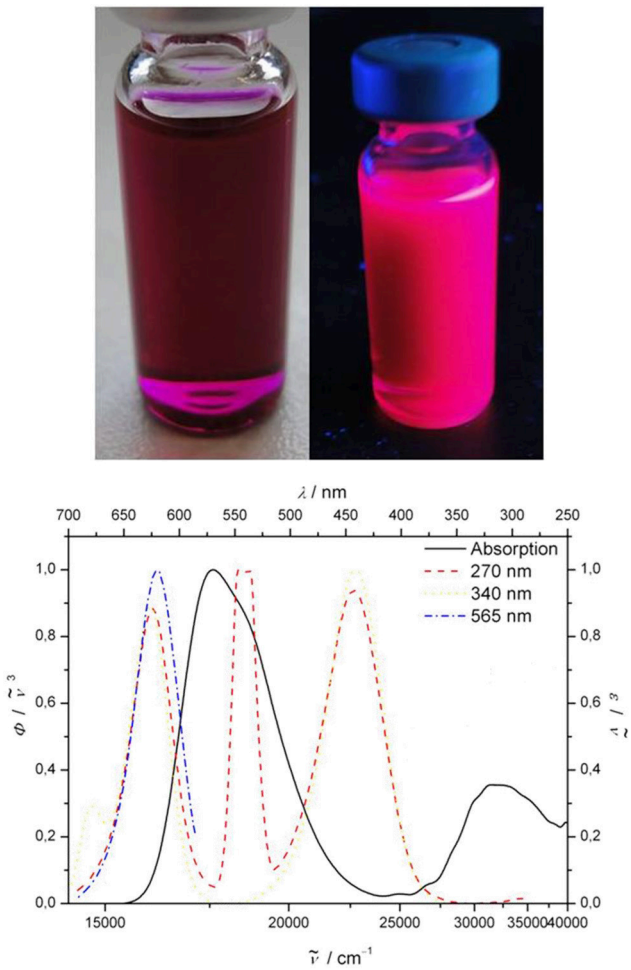

FIGURE 3 | (Top) Dichloromethane solution of bichromophore **11** at day light and under the handheld UV lamp (λ_{exc} = 365 nm). **(Bottom)** Normalized absorption (black solid line) and emission spectra at λ_{exc} = 565 (blue dashed), 340 (yellow dashed), and 270 nm (red dashed) (recorded in dichloromethane at T = 298 K; the intense, second order signal at 540 nm upon excitation at λ_{exc} = 270 nm is its first harmonic).

absorption bands of the constituting chromophores, i.e., all chromophore-chromophore interactions occur in the excited state. As observed experimentally, energy transfer as an envisioned interaction requires sufficient overlap of the emission band of the pyrrole and the absorption band of the corresponding ligated second chromophore. If a dual emission is intended as observed for bichromophore **11**, for creating dual emission color mixing, it becomes obvious that partial energy transfer is more favorable than complete Förster resonance energy transfer.

CONCLUSION

The consecutive four-component coupling-isomerization-Stetter-Paal-Knorr synthesis of blue luminescent pyrrole has been employed to furnish a pyrrole chromophore, which can be successfully ligated in the sense of a level-2 functionalization with emitter chromophores, absorbing at longer wavelengths to give a library of emissive bichromophores. The photophysical data could be quickly assessed by absorption and emission spectroscopy and were rationalized by TD-DFT calculations. While significant overlap of the absorption bands of both chromophores do not reveal a peculiar interaction in the excited state, those bichromophores where the second absorption bands overlap with the pyrrole emission reveal energy transfer characteristics. In the case of the reddish purple chromophore dual emission from the pyrrole and the 3-cyano-5,5-dimethylfuran-2(5*H*)-ylidene)malononitrile-styryl moiety clearly results from partial energy transfer causing a magenta-rose emission with significant intensity. This diversity-oriented synthetic principle now enables a rapid synthetic approach to dually emissive unimolecular bichromophores operating by partial energy transfer. The novel principle can be envisioned to be employed for accessing unimolecular white light emitters for OLED and biophysical analytics. Synthetic and photophysical studies of similar blue-red emitting bichromophores are currently underway.

EXPERIMENTAL

4-(1-Benzyl-2-(4-hydroxyphenyl)-5-phenyl-1*H*-pyrrol-3-yl)benzonitrile (1)

In a screw-cap Schlenk vessel with a magnetic stir bar were placed dry THF (10 mL), *p*-bromo benzonitrile (910 mg, 5.00 mmol), 1-phenylprop-2-yn-1-ol (660 mg, 5.00 mmol), $PdCl_2(PPh_3)_2$ (70 mg, 0.10 mmol), CuI (40 mg, 0.20 mmol), and triethylamine (1.7 mL, 12 mmol) under nitrogen and the mixture was stirred at 90°C (oil bath) for 10 h. Then, after cooling to room temp, 4-(tetrahydro-2*H*-pyran-2-yloxy)benzaldehyde (1.10 g, 5.25 mmol), 3,4-dimethyl-5-(2-hydroxyethyl)-thiazolium iodide (385 mg, 1.35 mmol), and triethylamine (2.5 mL, 18 mmol) were added and the mixture was stirred at 80°C for 4 d. After cooling to room temp acetic acid (10 mL) and benzyl amine (2.6 g, 25 mmol) were added and the reaction mixture was stirred at 80°C for 3 d. After cooling to room temp a saturated aqueous sodium carbonate solution was added, the phases were separated and the aqueous phase was extracted with diethyl ether (3 × 50 mL). The combined organic layers were dried (anhydrous sodium sulfate), filtered and the filtrate was adsorbed on celite® and purified by flash chromatography on silica gel (hexane/ethyl acetate 20:1) to give pyrrole **1** as a colorless solid (554 mg, 26%), Mp 202°C.

^{1}H NMR (500 MHz, $CDCl_3$): δ 5.15 (s, 2 H), 6.7 (m, 3 H), 6.82 (d, ^3J = 8.6 Hz, 2 H), 7.07 (d, ^3J = 8.6 Hz, 2 H), 7.12 (m, 2 H), 7.29 (m, 1 H), 7.36 (m, 3 H), 7.41 (m, 2 H), 7.46 (m, 2 H), 7.52 (m, 2 H), 8.61 (s, 1 H). ^{13}C NMR (126 MHz, $CDCl_3$): δ 49.4 (CH_2), 108.7 (C_{quat}), 109.8 (CH), 116.5 (C_{quat}), 116.6 (CH), 119.8 (C_{quat}), 121.9 (C_{quat}), 124.3 (C_{quat}), 126.7 (CH), 127.7 (CH), 128.2 (CH), 128.3 (CH), 129.1 (CH), 129.4 (CH), 129.7 (CH), 132.7 (CH), 133.3 (CH), 134.2 (C_{quat}), 134.9 (C_{quat}), 136.6 (C_{quat}), 139.9 (C_{quat}), 142.5 (C_{quat}). MALDI-TOF [*m/z* (%)]: 426.0 ([M]$^+$, 100). IR (KBr): $\tilde{\nu}$ [cm^{-1}] = 3,342 (w), 2,229 (m), 1,601 (s), 1,516 (m),

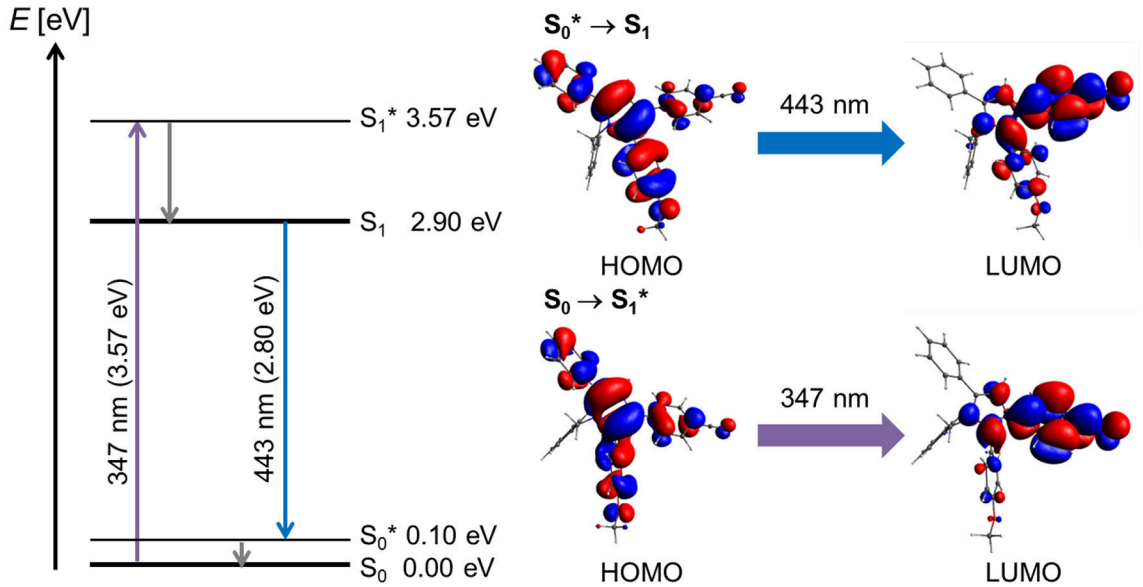

FIGURE 4 | Jablonski diagram of compound **2** and assignment of the FMO-transitions in the longest wavelength absorption band and the emission band [$E(S_0) = 0$ eV; PBE_1PBE 6-311G** IEFPCM CH_2Cl_2, isosurface value at 0.03 a.u.].

TABLE 2 | Alkylation synthesis of pyrrole **2** and bichromophores **8–12**.

Entry	Pyrrole 1	Alkylation substrate	Pyrrole 2 and bichromophores 8–12
1[a]	43 mg (0.1 mmol)	50 mg (0.4 mmol) of methyl iodide	39 mg (68%) of **2**
2[a]	58 mg (0.1 mmol)	27 mg (0.1 mmol) of **3**	57 mg (93%) of **8**
3[a]	44 mg (0.1 mmol)	28 mg (0.1 mmol) of **4**	42 mg (61%) of **9**
4[a]	44 mg (0.1 mmol)	42 mg (0.1 mmol) of **5**	46 mg (59%) of **10**
5[b]	105 mg (0.25 mmol)	96 mg (0.25 mmol) of **6**	70 mg (39%) of **11**
6[b]	105 mg (0.25 mmol)	84 mg (0.25 mmol) of **7**	78 mg (38%) of **12**

[a]*According to variation A.*
[b]*According to variation B.*

1,450 (m), 1,402 (w), 1,338 (m), 1,267 (s), 1,228 (m), 1,172 (m), 1,072 (w), 939 (w), 839 (s). Anal. calcd. for $C_{30}H_{22}N_2O + H_2O$ (426.5 + 18.01): C 81.06, H 5.44, N 6.30; Found: C 81.01, H 5.01, N 6.14. HRMS (ESI) calcd. for $[C_{30}H_{22}N_2O - H]^+$: 425.16484; Found: 425.16485.

General Procedure (GP) for the Synthesis of the Pyrrole Reference Chromophore 2 and Bichromophores 8–12

Variation A: Pyrrole **1** (1.00 equiv), halide **2–4** or methyl iodide (1.00 equiv), K_2CO_3 (2.00 equivs) and dry DMF (5 mL) were placed in a screw-cap Schlenk vessel with a magnetic stir bar under nitrogen (for details, see **Table 2**). The reaction mixture was heated at 100°C for 5 h. After cooling to room temp celite® was added to the reaction mixture and the solvents were removed in vacuo. The residue was purified by flash chromatography on silica gel (hexane/ethyl acetate) to give the pyrrole reference chromophore **2** or bichromophores **8–10**.

Variation B: Pyrrole **1** (1.00 equiv), KI (1.00 equiv), and dry DMF (6 mL) were placed in a screw-cap Schlenk vessel with a magnetic stir bar under nitrogen. The mixture was cooled to 0°C (ice/water bath) and sodium hydride (2.00 equivs) was added. Then, halide **5** or **6** (1.00 equiv) was added and the mixture was allowed to come to room temp. Then, the mixture was stirred at 90°C for 3.5 h (for details, see **Table 2**). After cooling to room temp water (2 mL) was carefully added and the mixture was extracted with ethyl acetate (3 × 25 mL). The combined organic phases were dried (anhydrous sodium sulfate) and the solvents were removed in vacuo. The residue was purified by flash chromatography on silica gel (hexane/ethyl acetate 4:1) to give the bichromophores **11** or **12**.

4-(1-Benzyl-2-(4-methoxyphenyl)-5-phenyl-1H-pyrrol-3-yl)benzonitrile (2)

According to the GP (variation A) compound **2** (30 mg, 68%) was obtained as a colorless solid, Mp 166°C.

^{1}H NMR (300 MHz, $CDCl_3$): δ 3.79 (s, 3 H), 5.05 (s, 2 H), 6.57 (s, 1 H), 6.66 (m, 2 H), 6.81 (d, ^3J = 8.84 Hz, 2 H), 7.07 (d, ^3J = 8.43 Hz, 2 H), 7.12 (m, 2 H), 7.24-7.42 (m, 10 H). ^{13}C NMR (75 MHz, $CDCl_3$): δ 48.6 (CH_2), 55.4 (CH_3), 108.1 (C_{quat}), 109.0 (CH), 114.4 (CH), 119.8 (C_{quat}), 121.5 (C_{quat}), 124.7 (C_{quat}), 126.2 (CH), 127.1 (CH), 127.6 (CH), 127.7 (CH), 128.5 (CH), 128.7 (CH), 129.3 (CH), 132.2 (CH), 132.5 (CH), 133.2 (C_{quat}), 133.6 (C_{quat}), 136.1 (C_{quat}), 139.0 (C_{quat}), 141.4 (C_{quat}), 159.8 (C_{quat}). MALDI-TOF [*m/z* (%)]: 440.05 ([M]$^+$, 100). IR (KBr): $\tilde{\nu}$ [cm^{-1}] = 2,224 (m), 1,601 (s), 1,576 (m), 1,516 (m), 1,489 (m), 1,470 (w), 1,386 (w), 1,354 (m), 1,306 (w), 1,290 (m), 1,253 (s), 1,178 (m), 1,109 (w), 1,028 (m), 1,016 (w), 839 (s), 769 (m), 759 (s), 723 (s), 698 (s). HRMS (ESI) calcd. for [$C_{31}H_{24}N_2O$ + H]$^+$: 441.19614; Found: 441.19728.

4-(2-(4-(Anthracen-9-ylmethoxy)phenyl)-1-benzyl-5-phenyl-1H-pyrrol-3-yl)benzonitrile (8)

According to the GP (variation A) compound **8** (57 mg, 93%) was obtained as a colorless solid, Mp 202°C.

^{1}H NMR (500 MHz, $CDCl_3$): δ 5.10 (s, 2 H), 5.95 (s, 2 H), 6.58 (s, 1 H), 6.71 (d, ^3J = 6.3 Hz, 2 H), 7.05 (m, 2 H), 7.15 (m, 5 H), 7.31 (m, 4 H), 7.38 (m, 2 H), 7.48 (m, 5 H), 7.55 (m, 2 H), 8.05 (d, ^3J = 8.3 Hz, 2 H), 8.28 (d, ^3J = 8.9 Hz, 2 H), 8.53 (s, 1 H). ^{13}C NMR (126 MHz, $CDCl_3$): δ 48.7 (CH_2), 63.1 (CH_2), 108.2 (C_{quat}), 109.2 (CH), 115.5 (CH), 115.5 (CH), 119.8 (C_{quat}), 121.6 (C_{quat}), 124.1 (CH), 125.3 (CH) 125.3 (C_{quat}), 126.2 (CH), 126.8 (C_{quat}), 126.9 (CH), 127.2 (CH), 127.7 (CH), 128.6 (CH), 128.7 (CH), 129.3 (CH), 129.4 (CH), 129.4 (CH), 131.3 (C_{quat}), 131.7 (C_{quat}), 132.2 (CH), 132.7 (CH), 133.2 (C_{quat}), 133.6 (C_{quat}), 136.3 (C_{quat}), 139.0 (C_{quat}), 141.5 (C_{quat}), 159.4 (C_{quat}). MALDI-TOF [*m/z* (%)]: 617.2 ([M+H]$^+$, 60). IR (KBr): $\tilde{\nu}$ [cm^{-1}] = 2,224 (m), 1,603 (m), 1,516 (w), 1,489 (w), 1,450 (w), 1,244 (s), 1,224 (w), 1,175 (m), 1,001 (w), 989 (w), 835 (s), 762 (s), 731 (s), 698 (s). UV/Vis: $\lambda_{max}(\varepsilon)$ (CH_2Cl_2, T = 293 K) = 258 nm (192,800 L mol^{-1} cm^{-1}), 315.5 nm (29,800 L mol^{-1} cm^{-1}), 329 nm (29,600 L mol^{-1} cm^{-1}), 367 nm (18,100 L mol^{-1} cm^{-1}), 387 nm (14,200 L mol^{-1} cm^{-1}). HRMS (ESI) calcd. for [$C_{45}H_{32}N_2O$ + H]$^+$: 617.2586; Found: 617.2577.

4-(1-Benzyl-3-(4-cyanophenyl)-5-phenyl-1H-pyrrol-2-yl)phenyl 5-(dimethylamino)naphthalene-1-sulfonate (9)

According to the GP (variation A) compound **9** (42 mg, 61%) was obtained as a yellow solid, Mp 124°C.

^{1}H NMR (300 MHz, $CDCl_3$): δ 2.90 (s, 6 H), 4.97 (s, 2 H), 6.52 (m, 3 H), 6.80 (d, ^3J = 8.37 Hz, 2 H), 6.93 (d, ^3J = 8.79 Hz, 2 H), 7.08 (m, 5 H), 7.23 (m, 1 H), 7.33 (m, 7 H), 7.44 (dd, ^3J = 7.4 Hz, ^3J = 8.5 Hz, 1 H), 7.64 (dd, ^3J = 7.4 Hz, ^3J = 8.5 Hz, 1 H), 8.06 (dd, ^4J = 1.3 Hz, ^3J = 7.3 Hz, 1 H), 8.44 (d, ^3J = 8.7 Hz, 1 H), 8.62 (d, ^3J = 8.5 Hz, 1 H). ^{13}C NMR (75 MHz, $CDCl_3$): δ 45.7 (CH_3), 48.8 (CH_2), 108.5 (C_{quat}), 109.3 (CH), 116.0 (CH), 119.6 (C_{quat}), 122.2 (C_{quat}), 122.7 (CH), 123.0 (CH), 126.1 (CH), 127.3 (CH), 127.8 (CH), 128.0 (CH), 128.6 (CH), 128.7 (CH), 128.8 (CH), 129.3 (CH), 129.3 (CH), 129.8 (C_{quat}), 130.3 (C_{quat}), 131.0 (C_{quat}), 131.4 (CH), 131.6 (C_{quat}), 132.0 (C_{quat}), 132.1 (CH), 132.3 (CH), 132.5 (CH), 132.8 (C_{quat}), 136.9 (C_{quat}), 138.4 (C_{quat}), 140.9 (C_{quat}), 149.7 (C_{quat}). MALDI-TOF [*m/z* (%)]: 660.17 ([M-H]$^+$, 100). IR (KBr): $\tilde{\nu}$ [cm^{-1}] = 2,924 (w), 2,222 (w), 1,602 (m), 1,570 (w), 1,508 (w), 1,452 (w), 1,369 (s), 1,307 (w), 1,193 (m), 1,174 (s), 1,145 (s), 1,049 (w), 1,018 (w), 943 (w), 860 (s), 844 (s). HRMS (ESI) calcd. for [$C_{42}H_{33}N_3O_3S$ + H]$^+$: 660.23154; Found: 660.23087.

4-(1-Benzyl-2-(4-(3-((9-(diethylamino)-5-oxo-5H-benzo[a]phenoxazin-2-yl)oxy)propoxy)phenyl)-5-phenyl-1H-pyrrol-3-yl)benzonitrile (10)

According to the GP (variation A) compound **10** (46 mg, 59%) was obtained as a red solid, Mp 143°C.

^{1}H NMR (600 MHz, acetone-d_6): δ 1.26 (t, ^3J = 7.1 Hz, 6 H), 2.36 (p, ^3J = 6.2 Hz, 2 H), 3.58 (q, ^3J = 7.1 Hz, 4 H), 4.29 (t, ^3J = 6.2 Hz, 2 H), 4.42 (t, ^3J = 6.2 Hz, 2 H), 5.16 (s, 2 H), 6.12 (s, 1 H), 6.60 (d, ^4J = 2.7 Hz, 1 H), 6.68 (m, 3 H), 6.82 (dd, ^3J = 9.1 Hz, ^4J = 2.8 Hz, 2 H), 6.99 (d, ^3J = 8.8 Hz, 2 H), 7.11 (m, 3 H), 7.17 (d, ^3J = 8.8 Hz, 2 H), 7.27 (dd, ^3J = 8.7 Hz, ^4J = 2.6 Hz, 1 H), 7.31 (m, 1 H), 7.37 (m, 2 H), 7.40 (d, ^3J = 8.7 Hz, 2 H), 7.46 (m, 2 H), 7.53 (d, ^3J = 8.6 Hz, 1 H), 7.58 (d, ^3J = 9.0 Hz, 1 H), 8.08 (d, ^4J = 2.6 Hz, 1 H), 8.11 (d, ^3J = 8.7 Hz, 1 H). ^{13}C NMR (150 MHz, acetone-d_6): δ 12.9 (CH_3), 45.6 (CH_2), 49.0 (CH_2), 65.2 (CH_2), 65.7 (CH_2), 97.1 (CH), 105.4 (CH), 107.6 (CH), 108.8 (C_{quat}), 109.9 (CH), 110.7 (CH), 111.5 (C_{quat}), 115.7 (CH), 118.7 (CH), 119.7 (C_{quat}), 122.1 (C_{quat}), 125.1 (C_{quat}), 125.5 (C_{quat}), 126.6 (C_{quat}), 126.6 (CH), 127.7 (CH), 128.2 (CH), 128.3 (CH), 128.4 (CH), 129.1 (CH), 129.4 (CH), 129.7 (CH), 131.9 (CH), 132.8 (CH), 133.3 (CH), 134.1 (C_{quat}), 134.6 (C_{quat}), 135.0 (C_{quat}), 136.8 (C_{quat}), 139.9 (C_{quat}), 140.4 (C_{quat}), 142.4 (C_{quat}), 147.7 (C_{quat}), 152.0 (C_{quat}), 152.9 (C_{quat}), 160.0 (C_{quat}), 162.5 (C_{quat}), 182.5 (C_{quat}). MALDI-TOF [*m/z* (%)]: 801.3 ([M-H]$^+$, 100). IR (KBr): $\tilde{\nu}$ [cm^{-1}] = 2,965 (w), 2,926 (w), 2,222 (w), 1,732 (w), 1,709 (w), 1,620 (m), 1,595 (s), 1,580 (s), 1,516 (m), 1,495 (m), 1,466 (m), 1,406 (m), 1,339 (m), 1,314 (m), 1,254 (s), 1,223 (m), 1,177 (m), 1,111 (s), 1,080 (m), 1,026 (m), 966 (w), 907 (w), 876 (w), 827 (s), 795 (s). HRMS (ESI) calcd. for [$C_{53}H_{44}N_4O_4$ + H]$^+$: 801.34353; Found: 801.34390.

(E)-2-(4-(4-((2-(4-(1-Benzyl-3-(4-cyanophenyl)-5-phenyl-1H-pyrrol-2-yl)phenoxy)ethyl)(methyl)amino)styryl)-3-cyano-5,5-dimethylfuran-2(5H)-ylidene)malononitrile (11)

According to the GP (variation B) compound **11** (78 mg, 39%) was obtained as a blue solid, Mp 135°C.

^{1}H NMR (300 MHz, $CDCl_3$): δ 1.76 (s, 6 H), 3.22 (s, 3 H), 3.91 (t, ^3J = 5.2 Hz, 2 H), 4.19 (t, ^3J = 5.2 Hz, 2 H), 5.05 (s, 2 H), 6.57 (s, 1 H), 6.66 (dd, ^3J = 6.7 Hz, ^4J = 2.8 Hz, 2 H), 6.79 (m, 5 H), 7.08 (d, ^3J = 8.7 Hz, 2 H), 7.13 (m, 3 H), 7.24–7.39 (m, 7 H), 7.41 (d, ^3J = 8.6 Hz, 2 H), 7.56 (d, ^3J = 9.0 Hz, 2 H), 7.61 (d, ^3J = 16.1 Hz, 1 H). ^{13}C NMR (75 MHz, $CDCl_3$): δ 26.9 (CH_3), 39.8 (CH_3), 48.5 (CH_2), 51.9 (CH_2), 65.4 (CH_2), 97.1 (C_{quat}), 108.0 (C_{quat}), 109.1 (CH), 109.5 (CH), 111.5 (C_{quat}), 112.7 (CH), 114.8 (CH), 119.6 (C_{quat}), 119.65 (C_{quat}), 119.7 (C_{quat}), 119.8 (C_{quat}), 121.6 (C_{quat}), 122.7 (C_{quat}), 125.4 (C_{quat}), 126.0 (CH), 127.1

(CH), 127.6 (CH), 127.7 (CH), 128.5 (CH), 128.7 (CH), 129.2 (CH), 132.1 (CH), 132.3 (CH), 132.6 (CH), 133.0 (C_{quat}), 133.1 (C_{quat}), 136.2 (C_{quat}), 138.9 (C_{quat}), 141.4 (C_{quat}), 148.2 (CH), 152.9 (C_{quat}), 158.4 (C_{quat}), 174.4 (C_{quat}), 176.3 ($C_{quat.}$). MALDI-TOF [*m/z* (%)]: 769.3 ([M-H]$^+$, 100). IR (KBr): $\tilde{\nu}$ [cm^{-1}] = 2,960 (w), 2,222 (m), 1,599 (w), 1,558 (m), 1,516 (s), 1,464 (m), 1,435 (w), 1,371 (s), 1,276 (s), 1,244 (m), 1,190 (m), 1,170 (s), 1,150 (m), 1,105 (m), 1,072 (m), 1,031 (m), 1,016 (m), 966 (w), 937 (w), 839 (m), 815 (m), 795 (m). HRMS (ESI) calcd. for $[C_{51}H_{40}N_6O_2 + Na]^+$: 791.31050; Found: 791.31045.

(E)-4-(1-Benzyl-2-(4-(2-(methyl(4-(2-(4-methyl-3-oxo-3,4-dihydrochinoxalin-2-yl)vinyl)phenyl)amino)ethoxy)phenyl)-5-phenyl-1H-pyrrol-3-yl)benzonitrile (12)

According to the GP (variation B) compound **12** (70 mg, 38%) was obtained as an orange solid, Mp 152°C.

^{1}H NMR (300 MHz, $CDCl_3$): δ 3.12 (s, 3 H), 3.73 (s, 3 H), 3.82 (t, ^3J = 5.6 Hz, 2 H), 4.15 (m, 2 H), 5.06 (s, 2 H), 6.58 (s, 1 H), 6.66 (m, 2 H), 6.75 (d, ^3J = 8.9 Hz, 2 H), 6.8 (d, ^3J = 8.8 Hz, 2 H), 7.07 (d, ^3J = 8.7 Hz, 2 H), 7.26–7.50 (m, 16 H), 7.62 (m, 2 H), 7.85 (dd, ^3J = 8.0 Hz, ^4J = 1.1 Hz, 1 H), 8.11 (d, ^3J = 16.0 Hz, 1 H). ^{13}C NMR (75 MHz, $CDCl_3$): δ 29.3 CH_3, 39.5 (CH_3), 48.5 (CH_2), 51.8 (CH_2), 65.4 (CH_2), 108.0 (C_{quat}), 109.0 (CH), 112.0 (CH), 113.7 (CH), 114.8 (CH), 117.5 (CH), 119.7 (C_{quat}), 121.4 (C_{quat}), 123.9 (CH), 125.0 (C_{quat}), 125.1 (C_{quat}), 126.0 (CH), 127.1 (CH), 127.5 (CH), 127.6 (CH), 128.4 (CH), 128.6 (CH), 129.0 (CH), 129.2 (CH), 129.4 (CH), 129.9 (CH), 132.1 (CH), 132.5 (CH), 132.8 (C_{quat}), 133.1 (C_{quat}), 133.4 (C_{quat}), 133.7 (C_{quat}), 136.1 (C_{quat}), 138.8 (C_{quat}), 131.3 (C_{quat}), 149.8 (C_{quat}), 153.0 (C_{quat}), 155.4 (C_{quat}), 158.7 (C_{quat}). MALDI-TOF [*m/z* (%)]:744.3 ([M-H]$^+$, 100). IR (KBr): $\tilde{\nu}$ [cm^{-1}] = 2,963 (w), 2,928 (w), 2,907 (w), 2,220 (w), 1,651 (w), 1,599 (m), 1,514 (w), 1,489 (w), 1,470 (w), 1,450 (w), 1,412 (w), 1,377 (w), 1,350 (w), 1,317 (w), 1,304 (w), 1,258 (s), 1,179 (m), 1,084 (s), 1,013 (s), 864 (m), 790 (s). HRMS (ESI) calcd. for $[C_{50}H_{41}N_5O_2 + H]^+$: 744.33330; Found: 744.33373.

AUTHOR CONTRIBUTIONS

The project was conceptualized by TM for the Ph.D. thesis of OG, who developed the synthetic approach and conducted the photophysical studies and their evaluation. BM performed all DFT and TD-DFT calculations and assigned the absorption transitions. Based upon the doctoral thesis of OG manuscript was written and corrected by TM and BM.

FUNDING

Fonds der Chemischen Industrie (ad personam funding of TM) and Deutsche Forschungsgemeinschaft (Mu 1088/6-1).

ACKNOWLEDGMENTS

We cordially thank Fonds der Chemischen Industrie and Deutsche Forschungsgemeinschaft (Mu 1088/6-1) for the financial support. Computational support and infrastructure was provided by the Centre for Information and Media Technology (ZIM) at the University of Düsseldorf (Germany).

SUPPLEMENTARY MATERIAL

The Supplementary Material for this article can be found online at: https://www.frontiersin.org/articles/10.3389/fchem.2018.00579/full#supplementary-material

Data Sheet 1 | This Supplementary Information file contains the ^{1}H and ^{13}C NMR spectra of compounds **1**, **2**, **8**–**12**, the absorption and emission spectra of compounds **2**, **8**–**12**, and the data and evaluation of the DFT and TD-DFT calculations on the structures **2**, **8**–**12**.

REFERENCES

Aathimanikandan, S. V., Sandanaraj, B. S., Arges, C. G., Bardeen, C. J., and Thayumanavan, S. (2005). Effect of guest molecule flexibility in access to dendritic interiors. *Org. Lett.* 7, 2809–2812. doi: 10.1021/ol050579b

Adamo, C., and Barone, V. (1999). Toward reliable density functional methods without adjustable parameters: the PBE0 model. *J. Chem. Phys.* 110, 6158–6170. doi: 10.1063/1.478522

Bälter, M., Li, S., Morimoto, M., Tang, S., Hernando, J., Guirado, G., et al. (2016). Emission color tuning and white-light generation based on photochromic control of energy transfer reactions in polymer micelles. *Chem. Sci.* 7, 5867–5871. doi: 10.1039/C6SC01623E

Bazan, G. (2007). Novel organic materials through control of multichromophore interactions. *J. Org. Chem.* 72, 8615–8635. doi: 10.1021/jo071176n

Becke, A. D. (1993). A new mixing of Hartree–Fock and local density-functional theories. *J. Chem. Phys.* 98, 1372–1377. doi: 10.1063/1.464304

Benelhadj, K., Muzuzu, W., Massue, J., Retailleau, P., Charaf-Eddin, A., Laurent, A. D., et al. (2014). White emitters by tuning the excited-state intramolecular proton-transfer fluorescence emission in 2-(2′-Hydroxybenzofuran)benzoxazole Dyes. *Chem. Eur. J.* 20, 12843–12857. doi: 10.1002/chem.201402717

Beyeh, N. K., Aumanen, J., Åhman, A., Luostarinen, M., Mansikkamäki, H., Nissinen, M., et al. (2007). Dansylated resorcinarenes. *New J. Chem.* 31, 370–376. doi: 10.1039/B615772F

Börgardts, M., and Müller, T. J. J. (2017). Energy down converting organic fluorophore functionalized mesoporous silica hybrids for monolith-coated light emitting diodes. *Beilstein J. Org. Chem.* 13, 768–778. doi: 10.3762/bjoc.13.76

Braun, R. U., and Müller, T. J. J. (2004). Coupling-isomerization-stetter and coupling-isomerization-stetter-paal-knorr sequences - a multicomponent approach to furans and pyrroles. *Synthesis* 2004, 2391–2406. doi: 10.1055/s-2004-831192

Braun, R. U., Zeitler, K., and Müller, T. J. J. (2001). A novel one-pot pyrrole synthesis via a coupling-isomerization-stetter-paal-knorr sequence. *Org. Lett.* 3, 3297–3300. doi: 10.1021/ol0165185

Briehn, C. A., and Bäuerle, P. (2002). From solid-phase synthesis of π-conjugated oligomers to combinatorial library construction and screening. *Chem. Commun.* 2002, 1015–1023. doi: 10.1039/b108846g

Broadbent, A. D. (2004). A critical review of the development of the CIE1931 RGB color-matching functions. *Color Res. Appl.* 29, 267–272. doi: 10.1002/col.20020

Carroll, R. L., and Gorman, C. B. (2002). The genesis of molecular electronics. *Angew. Chem. Int. Ed.* 41, 4378–4400. doi: 10.1002/1521-3773(20021202)41:23<4378::AID-ANIE4378>3.0.CO;2-A

Coropceanu, V., Cornil, J., da Silva Filho, D. A., Oliver, Y., Silbey, R., and Brédas, J.-L. (2007). Charge transport in organic semiconductors. *Chem. Rev.* 107, 926–953. doi: 10.1021/cr050140x

de Moliner, F., Kielland, N., Lavilla, R., and Vendrell, M. (2017). Modern synthetic avenues for the preparation of functional fluorophores. *Angew. Chem. Int. Ed.* 56, 3758–3769. doi: 10.1002/anie.201609394

Findlay, N. J., Bruckbauer, J., Inigo, A. R., Breig, B., Arumugam, S., Wallis, D. J., et al. (2014). An organic down-converting material for white-light emission from hybrid LEDs. *Adv. Mater.* 26, 7290–7294. doi: 10.1002/adma.201402661

Fox, M. A. (1999). Fundamentals in the design of molecular electronic devices: long-range charge carrier transport and electronic coupling. *Acc. Chem. Res.* 32, 201–207. doi: 10.1021/ar9600953

Frisch, M. J., Trucks, G. W., Schlegel, H. B., Scuseria, G. E., Robb, M. A., Cheeseman, J. R., et al. (2009). *GAUSSIAN 09 (Revision A.02)*. Wallingford, CT: Gaussian Inc.

Garnier, F. (1999). Organic-based electronics à la carte. *Acc. Chem. Res.* 32, 209–215. doi: 10.1021/ar9800340

Joshi, N. K., Polgar, A. M., Steer, R. P., and Paige, M. F. (2016). White light generation using Förster resonance energy transfer between 3-hydroxyisoquinoline and Nile Red. *Photochem. Photobiol. Sci.* 15, 609–617. doi: 10.1039/C6PP00005C

Kavarnos, G. J. (1993). *Fundamentals of Photoinduced Electron Transfer*. New York, NY: Wiley-VCH Verlag GmbH.

Kim, K., and Jordan, K. D. (1994). Comparison of density functional and MP2 calculations on the water monomer and dimer. *J. Phys. Chem.* 98, 10089–10094. doi: 10.1021/j100091a024

Klymchenko, A. S. (2017). Solvatochromic and fluorogenic dyes as environment-sensitive probes: design and biological applications. *Acc. Chem. Res.* 50, 366–375. doi: 10.1021/acs.accounts.6b00517

Klymchenko, A. S., Pivovarenko, V. G., Ozturk, T., and Demchenko, A. P. (2003). Modulation of the solvent-dependent dual emission in 3-hydroxychromones by substituents. *New J. Chem.* 27, 1336–1343. doi: 10.1039/b302965d

Klymchenko, A. S., Yushchenko, D. A., and Mely, Y. (2007). Tuning excited state intramolecular proton transfer in 3-hydroxyflavone derivative by reaction of its isothiocyanate group with an amine. *J. Photochem. Photobiol. A* 192, 93–97. doi: 10.1016/j.jphotochem.2007.05.009

Krishnan, R., Binkley, J. S., Seeger, R., and Pople, J. A. (1980). Self-consistent molecular orbital methods. XX. A basis set for correlated wave functions. *J. Chem. Phys.* 72, 650–654. doi: 10.1063/1.438955

Kucherak, O. A., Oncul, S., Darwich, Z., Yushchenko, D. A., Arntz, Y., Didier, P., et al. (2010). Switchable nile red-based probe for cholesterol and lipid order at the outer leaflet of biomembranes. *J. Am. Chem. Soc.* 132, 4907–4916. doi: 10.1021/ja100351w

Kwon, J. E., Park, S., and Park, S. Y. (2013). Realizing molecular pixel system for full-color fluorescence reproduction: RGB-Emitting Molecular Mixture Free from Energy Transfer Crosstalk. *J. Am. Chem. Soc.* 135, 11239–11246. doi: 10.1021/ja404256s

Lapini, A., Fabbrizzi, P., Piccardo, M., di Donato, M., Lascialfari, L., Foggi, P., et al. (2014). Ultrafast resonance energy transfer in the umbelliferone–alizarin bichromophore. *Phys. Chem. Chem. Phys.* 16, 10059–10074. doi: 10.1039/C3CP54609H

Lee, C., Yang, W., and Parr, R. G. (1988). Development of the Colle-Salvetti correlation-energy formula into a functional of the electron density. *Phys. Rev. B Condens. Matter Mater. Phys.* 37, 785–789. doi: 10.1103/PhysRevB.37.785

Levi, L., and Müller, T. J. J. (2016a). Multicomponent syntheses of fluorophores initiated by metal catalysis. *Eur. J. Org. Chem.* 2016, 2907–2918. doi: 10.1002/ejoc.201600409

Levi, L., and Müller, T. J. J. (2016b). Multicomponent syntheses of functional chromophores. *Chem. Soc. Rev.* 45, 2825–2846. doi: 10.1039/C5CS00805K

Li, Z. R. (2015). *Organic Light-Emitting Materials and Devices, 2nd Edn*. New York, NY: CRC Press.

Lord, S. J., Conley, N. R., Lee, H.-L. D., Samuel, R., Weber, R., Liu, N., et al. (2010). Azido push–pull fluorogens photoactivate to produce bright fluorescent labels. *J. Phys. Chem. B* 114, 14157–14167. doi: 10.1021/jp907080r

Merkt, F. K., and Müller, T. J. J. (2018). Solid state and aggregation induced emissive chromophores by multi-component syntheses. *Isr. J. Chem.* 58, 889–900. doi: 10.1002/ijch.201800058

Mukherjee, S., and Thilagar, P. (2014). Organic white-light emitting materials. *Dyes Pigm.* 110, 2–27. doi: 10.1016/j.dyepig.2014.05.031

Mukherjee, S., and Thilagar, P. (2015). Recent advances in purely organic phosphorescent materials. *Chem. Commun.* 51, 10988–11003. doi: 10.1039/C5CC03114A

Müllen, K., and Scherf, U. (eds.). (2006). *Organic Light-Emitting Diodes - Synthesis, Properties, and Applications*. Weinheim: Wiley-VCH.

Müller, T. J. J. (2007). "Diversity-oriented synthesis of chromophores by combinatorial strategies and multi-component reactions," in *Functional Organic Materials. Syntheses, Strategies, and Applications*, eds T. J. J. Müller and U. H. F. Bunz (Weinheim: Wiley-VCH), 179–223.

Müller, T. J. J. (2016). "Chapter 6: Multicomponent and domino syntheses of AIE chromophores," in *Aggregation Induced Emission: Materials and Applications,* eds M. Fujiki, B. Z. Tang and B. Liu (Washington, CA: ACS Symposium Series e-book), 85–112.

Müller, T. J. J., and Bunz, U. H. F. (eds.). (2007). *Functional Organic Materials. Syntheses, Strategies, and Applications.* Weinheim: Wiley-VCH.

Müller, T. J. J., and D'Souza, D. M. (2008). Diversity-oriented syntheses of functional π-systems by multicomponent and domino reactions. *Pure Appl. Chem.* 80, 609–620. doi: 10.1351/pac200880030609

Pallavi, P., Sk, B., Ahir, P., and Patra, A. (2018). Tuning the förster resonance energy transfer through a self-assembly approach for efficient white-light emission in an aqueous medium. *Chem. Eur. J.* 24, 1151–1158. doi: 10.1002/chem.201704437

Park, J.-S., Chae, H., Chung, H. K., and Lee, S. I. (2011). Thin film encapsulation for flexible AM-OLED: a review. *Semicond. Sci. Technol.* 26, 034001–034008. doi: 10.1088/0268-1242/26/3/034001

Park, S., Kwon, J. E., Kim, S. H., Seo, J., Chung, K., Park, S.-Y., et al. (2009). A white-light-emitting molecule: frustrated energy transfer between constituent emitting centers. *J. Am. Chem. Soc.* 131, 14043–14049. doi: 10.1021/ja902533f

Qing, Z., Audebert, P., Clavier, G., Mèallat-Renault, R., Mionmandre, F., and Tang, J. (2011). Bright fluorescence through activation of a low absorption fluorophore: the case of a unique naphthalimide–tetrazine dyad. *New J. Chem.* 35, 1678–1682. doi: 10.1039/c1nj20100j

Rice, J., McDonald, D. B., Ng, L.-K., and Yang, N. C. (1980). Effect of viscosity on fluorescence of anthracenes in solution. *J. Chem. Phys.* 73, 4144–4146. doi: 10.1063/1.440648

Riva, R., Moni, L., and Müller, T. J. J. (2016). Multicomponent strategies for the diversity-oriented synthesis of blue emissive heterocyclic chromophores. *Targets Heterocyc. Syst.* 20, 85–112. doi: 10.17374/targets.2017.20.85

Roberts, R. M. G., and Yavari, F. (1981). Kinetics and mechanism of diels-alder additions of tetracyanoethylene to anthracene derivatives-III: effect of substituents on rates and intermediate complex formation. *Tetrahedron* 37, 2657–2662. doi: 10.1016/S0040-4020(01)98972-0

Sarkar, S. K., Kumar, G. R., and Thilagar, P. (2016). White light emissive molecular siblings. *Chem. Commun.* 52, 4175–4178. doi: 10.1039/C6CC00823B

Scalmani, G., and Frisch, M. J. (2010). Continuous surface charge polarizable continuum models of solvation. I. General formalism. *J. Chem. Phys.* 132, 114110. doi: 10.1063/1.3359469

Schanda, J. (2007). *Colorimetry: Understanding the CIE System*. Hoboken, NJ: John Wiley & Sons, Inc.

Shi, N., Guan, Y., Zhang, J., and Wan, X. H. (2015). Multicolor luminescent hybrid assembled materials based on lanthanide-containing polyoxometalates free from energy transfer crosstalk. *RSC Adv.* 5, 34900–34907. doi: 10.1039/C5RA03329B

Shirota, Y., and Kageyama, H. (2007). Charge carrier transporting molecular materials and their applications in devices. *Chem. Rev.* 107, 953–1010. doi: 10.1021/cr050143+

Stephens, P. J., Devlin, F. J., Chabalowski, C. F., and Frisch, M. J. (1994). *Ab initio* calculation of vibrational absorption and circular dichroism spectra using density functional force fields. *J. Phys. Chem.* 98, 11623–11627. doi: 10.1021/j100096a001

Thejo Kalayani, N., and Dhoble, S. J. (2012). Organic light emitting diodes: energy saving lighting technology - A review. *Renew. Sust. Energ. Rev.* 16, 2696–2723. doi: 10.1016/j.rser.2012.02.021

Tour, J. M. (2000). Molecular electronics. Synthesis and testing of components. *Acc. Chem. Res.* 33, 791–804. doi: 10.1021/ar0000612

Walzer, K., Maennig, B., Pfeiffer, M., and Leo, K. (2007). Highly efficient organic devices based on electrically doped transport layers. *Chem. Rev.* 107, 1233–1271. doi: 10.1021/cr050156n

Westland, S. (2003). Review of the CIE system of colorimetry and its use in dentistry. *J. Esthet. Restor. Dent.* 15, S5–S12. doi: 10.1111/j.1708-8240.2003.tb00313.x

Wu, Z., and Ma, D. (2016). Recent advances in white organic light-emitting diodes. *Mater. Sci. Eng. R Rep.* 107, 1–42. doi: 10.1016/j.mser.2016.06.001

Yuan, C., Saito, S., Camacho, C., Irle, S., Hisaki, I., and Yamaguchi, S. (2013). A π-conjugated system with flexibility and rigidity that shows environment-dependent RGB luminescence. *J. Am. Chem. Soc.* 135, 8842–8845. doi: 10.1021/ja404198h

Conflict of Interest Statement: The authors declare that the research was conducted in the absence of any commercial or financial relationships that could be construed as a potential conflict of interest.

The handling editor declared a past co-authorship with one of the authors TM.

Advantages of publishing in Frontiers

OPEN ACCESS
Articles are free to read for greatest visibility and readership

FAST PUBLICATION
Around 90 days from submission to decision

HIGH QUALITY PEER-REVIEW
Rigorous, collaborative, and constructive peer-review

TRANSPARENT PEER-REVIEW
Editors and reviewers acknowledged by name on published articles

Frontiers
Avenue du Tribunal-Fédéral 34
1005 Lausanne | Switzerland

Visit us: www.frontiersin.org
Contact us: info@frontiersin.org | +41 21 510 17 00

REPRODUCIBILITY OF RESEARCH
Support open data and methods to enhance research reproducibility

DIGITAL PUBLISHING
Articles designed for optimal readership across devices

FOLLOW US
@frontiersin

IMPACT METRICS
Advanced article metrics track visibility across digital media

EXTENSIVE PROMOTION
Marketing and promotion of impactful research

LOOP RESEARCH NETWORK
Our network increases your article's readership